

# Solid-phase microextraction as sample preparation method for metabolomics

by

Dajana Vuckovic

A thesis  
presented to the University of Waterloo  
in fulfillment of the  
thesis requirement for the degree of  
Doctor of Philosophy  
in  
Chemistry

Waterloo, Ontario, Canada, 2010

© Dajana Vuckovic 2010

## **AUTHOR'S DECLARATION**

I hereby declare that I am the sole author of this thesis. This is a true copy of the thesis, including any required final revisions, as accepted by my examiners.

I understand that my thesis may be made electronically available to the public.

## Abstract

The main objective of the emerging field of metabolomics is the analysis of all small molecule metabolites present in a particular living system in order to provide better understanding of dynamic processes occurring in living systems. This type of studies is of interest in various fields including systems biology, medicine and drug discovery. The main requirements for sample preparation methods used in global metabolomic studies are lack of selectivity, incorporation of a metabolism quenching step and good reproducibility. The efficiency of metabolism quenching and stability of analytes in selected biofluid or tissue dictate how accurately the analytical results represent true metabolome composition at the time of sampling. However, complete quenching of metabolism is not easily accomplished, so sample preparation can significantly affect metabolome's composition and the quality of acquired metabolomics data. In this research, the feasibility of the use of solid-phase microextraction (SPME) in direct extraction mode for global metabolomic studies of biological fluids based on liquid chromatography-mass spectrometry (LC-MS) was investigated for the first time.

Initial research presented in this thesis focused on resolving several outstanding issues regarding the use of SPME for the analysis of biological fluids. SPME was not simultaneously capable to provide high-sample throughput and high degree of automation when coupled to LC-MS. This was successfully addressed through the development and evaluation of a new robotic station based on a 96-well plate format and an array of 96 SPME fibres. The parallel format of extraction and desorption allowed increased sample throughput of >1000 samples/day which represents the highest throughput of any SPME technique to date. This exceeds sample throughput requirements for a typical metabolomics study whereby ~100 samples/day are processed.

SPME can also be used for direct *in vivo* sampling of flowing blood of an animal without the need to isolate a defined sample volume. This format of SPME is particularly attractive for metabolomic studies as it decreases the overall number of steps and also eliminates the need for metabolism quenching step because only small molecular weight species are extracted by the device, whereas large biological macromolecules such as proteins are not extracted by the coating. In current work, *in vivo* SPME sampling was successfully applied for sampling of mice for the first time. The proposed sampling procedure was fully validated against traditional terminal and serial sampling approaches for a pharmacokinetic study of carbamazepine and its metabolite. Excellent agreement of pharmacokinetic parameters such as systemic clearance, steady-state volume of distribution and

terminal half-life was found for all three methods, with no statistically significant differences ( $p > 0.05$ ). The performance of new prototype commercial SPME devices based on hypodermic needle was also evaluated within the context of the study. The availability of such single-use devices with excellent inter-fibre reproducibility ( $< 10\%$  RSD) presents an important step forward in order to gain wider acceptance of *in vivo* SPME sampling.

Finally, existing SPME coatings were not suitable for the simultaneous direct extraction of both hydrophilic and hydrophobic species, which is one of the requirements for a successful global metabolomics study. To address this issue, a systematic study of 40 types of commercially available sorbents was carried out using a metabolite standard test mixture spanning a wide molecular weight (80-777 Da) and polarity range (log P range of -5 to 7.4). The best performance for balanced extraction of species of varying polarity was achieved by (i) mixed-mode coating containing octadecyl or octyl group and benzenesulfonic acid ion exchange group, (ii) polar-enhanced polystyrene-divinylbenzene polymeric coatings and (iii) phenylboronic acid coatings.

The second aspect of the research focused on the evaluation of SPME for a global metabolomics study of human plasma using two complementary LC-MS methods developed on benchtop Orbitrap MS system: reverse-phase method using pentafluorophenyl LC stationary phase and HILIC method using underivatized silica stationary phase. The parameters influencing overall method sensitivity such as voltages, mass ranges and ion inject times into C-trap were optimized to ensure best instrument performance for global metabolomic studies. Orbitrap system provided a powerful platform for metabolomics because of its high resolution and mass accuracy, thus helping to distinguish between metabolites with same nominal mass. The acquisition speed of the instrument at the highest resolution setting was insufficient for use with ultrahigh performance liquid chromatography (UHPLC), so all methods were developed using conventional LC. However, overall metabolite coverage achieved in current study compared well or even exceeded metabolite coverage reported in literature on different LC-MS or UHPLC-MS platforms including time-of-flight, quadrupole time-of-flight and hybrid Orbitrap instruments.

The performance of SPME was fully compared versus traditional methods for global metabolomics (plasma protein precipitation and ultrafiltration). The main findings of this systematic study show that SPME provides improved coverage of hydrophobic metabolites versus ultrafiltration and reduces ionization suppression effects observed with both plasma protein precipitation and ultrafiltration methods. Using SPME,  $< 5\%$  and  $< 20\%$  of peaks showed significant matrix effects in reverse phase

and HILIC methods, respectively and the observed effects were mostly correlated to elution within retention time window of anticoagulant for the majority of metabolites showing this effect. This improves overall quality of collected metabolomics data and can also improve metabolite coverage. For example, the highest number of metabolite features (3320 features) was observed using SPME in combination with negative ESI reverse-phase LC method, while in positive ESI mode plasma protein precipitation with methanol/ethanol mixture provided the most comprehensive metabolite coverage (3245 features versus 1821 features observed for SPME). Method precision of SPME method was excellent as evaluated using median RSD (11-18% RSD) of all metabolites detected. A proof-of-concept *in vivo* SPME study was also performed on mice to study the effects of carbamazepine administration and shows that SPME can be used as successful sample preparation method for global metabolomic studies in combination with unsupervised statistical data analysis techniques. This study highlights important advantages of *in vivo* sampling approaches including the ability to capture short-lived and/or unstable metabolites, to achieve truer representation of the metabolome at the time of sampling than achievable by blood withdrawal methods and the ability to use smaller animal cohorts while obtaining highly-relevant data sets. The experimental results provide new and useful insight into the effects of different sample preparation methods on the collected metabolomics data, and establish both *in vitro* and *in vivo* SPME as a new tool for global LC-MS metabolomics analysis for the first time.

## **Acknowledgements**

I owe my deepest gratitude to my supervisor, Professor Janusz Pawliszyn, for this research opportunity and the perfect balance of support and independence during my studies.

I thank my committee members, Professors Mikkelsen, Gabryelski and Dieckmann for their time and helpful guidance in preparation of this thesis. I would like to extend my sincere gratitude to my external examiner, Professor Novotny, and my internal examiner Professor Servos for invaluable time and commitment to serve on my examination committee.

I extend a sincere thank you to all my colleagues and collaborators throughout the years, with a special acknowledgement to Dr. Pauline McGregor, Dr. Rosa Vatinno, and Ms. Sanja Risticvic who challenged and inspired me throughout the years.

This thesis would never have been possible without heartfelt support of my family and friends. Thank you for your love and understanding on this exciting and demanding journey.

## **Dedication**

To my loving family... your support and encouragement shines through everything I do.

## Table of Contents

AUTHOR'S DECLARATION.....	ii
Abstract.....	iii
Acknowledgements.....	vi
Dedication.....	vii
Table of Contents.....	viii
List of Figures.....	xv
List of Tables.....	xxviii
List of Abbreviations.....	xxxiii
Chapter 1 Introduction.....	1
1.1 Metabolomics, metabonomics and biomarkers.....	1
1.2 Analytical approaches for global metabolomic studies.....	5
1.3 Sample preparation methods for global metabolomic studies by LC-MS.....	8
1.3.1 Sample preparation methods for biofluids.....	8
1.3.2 Sample preparation methods for tissues.....	12
1.3.3 Sample preparation methods for microorganisms.....	12
1.3.4 Importance of sample preparation method selection.....	13
1.4 Introduction to solid-phase microextraction (SPME).....	15
1.4.1 SPME and metabolomics: an overview.....	20
1.5 Research objectives.....	23
Chapter 2 Automation of SPME in 96-well plate format for high-throughput analysis of biological fluids.....	25
2.1 Preamble and introduction.....	25
2.1.1 Preamble.....	25
2.1.2 Introduction.....	26
2.2 Experimental.....	29
2.2.1 Chemicals and materials.....	29
2.2.2 Preparation of buffers and standard solutions.....	29
2.2.3 Preparation of 96-SPME device using pin-tool replicator and PDMS coating.....	30
2.2.4 Preparation of 96-SPME device using 1.55 mm diameter stainless steel wire and coated silica particles.....	30
2.2.5 Description of PAS autosampler for automated SPME.....	32



2.2.6 LC-MS/MS analysis .....	33
2.2.7 SPME procedure during optimization/evaluation experiments .....	34
2.2.8 SPME procedure for high-throughput analysis of benzodiazepines in whole blood.....	34
2.2.9 Data analysis and calculations.....	35
2.3 Results and discussion.....	35
2.3.1 Optimization and evaluation of automated 96-SPME system and PAS autosampler .....	35
2.3.1.1 Optimization of desorption conditions for PDMS coating .....	36
2.3.1.2 Determination of extraction time profile for PDMS coating.....	37
2.3.1.3 Evaluation of inter-fibre and intra-fibre reproducibility of PDMS fibres .....	39
2.3.1.4 Investigation of carryover using PDMS coatings.....	41
2.3.1.5 Investigation of the uniformity of agitation using orbital shaking and PDMS coatings .....	42
2.3.1.6 Investigation of well cross-talk using PDMS coatings.....	43
2.3.1.7 Summary of overall performance of PDMS coatings.....	44
2.3.1.8 SPME coatings based on coated silica particles: influence of particle type on coating properties .....	45
2.3.1.9 Evaluation of inter-fibre and intra-fibre reproducibility for C <sub>18</sub> and RPA coatings .....	46
2.3.1.10 Optimization of acid etching time .....	50
2.3.1.11 Examination of coating surface using scanning electron microscopy (SEM) .....	51
2.3.1.12 Optimization of automated SPME method for benzodiazepines.....	51
2.3.1.13 Summary of coating evaluation results: comparison of PDMS <i>versus</i> RPA coating .	52
2.3.1.14 Comparison of method precision for manual <i>versus</i> automated dispensing of desorption solvent.....	53
2.3.1.15 Comparison of calibration methods.....	54
2.3.1.16 SPME method development using Concept 96: general considerations .....	57
2.3.2 Example application of PAS autosampler: high-throughput analysis of benzodiazepines in whole blood .....	59
2.3.2.1 Evaluation of matrix effects .....	59
2.3.2.2 Linearity, limit of detection (LOD) and limit of quantitation (LOQ).....	61
2.3.2.3 Method accuracy and precision: intra- and inter-day results.....	62
2.3.2.4 Summary of method performance .....	64
2.4 Conclusions and future directions .....	65

2.5 Addendum.....	67
Chapter 3 <i>In vitro</i> evaluation of <i>in vivo</i> SPME devices.....	68
3.1 Preamble and introduction .....	68
3.1.1 Preamble .....	68
3.1.2 Introduction.....	68
3.2 Experimental.....	70
3.2.1 Chemicals and materials .....	70
3.2.2 Preparation of standard solutions.....	71
3.2.3 SPME procedure .....	72
3.2.4 LC-MS/MS analysis.....	73
3.2.5 Data analysis and calculations .....	74
3.2.6 SEM procedure .....	74
3.3 Results and discussion .....	74
3.3.1 Evaluation of extraction efficiency and comparison to commercial CW-TPR coating .....	76
3.3.2 Evaluation of coating thickness: effect on extraction time and inter-fibre reproducibility.	79
3.3.3 Evaluation of carryover.....	82
3.3.4 Selection of coating thickness.....	83
3.3.5 Evaluation of inter-fibre reproducibility .....	84
3.3.6 Evaluation of method linearity.....	86
3.3.7 Evaluation of absolute matrix effects.....	88
3.3.8 Optimization of preconditioning procedure .....	90
3.3.9 Optimization of standard loading procedure.....	92
3.3.10 Studies of coating performance: comparison between lots.....	93
3.4 Conclusions and future directions.....	94
3.5 Addendum.....	95
Chapter 4 <i>In vivo</i> SPME sampling of mice: application to pharmacokinetic studies of carbamazepine and its metabolite .....	97
4.1 Preamble and introduction .....	97
4.1.1 Preamble .....	97
4.1.2 Introduction.....	98
4.2 Experimental.....	102
4.2.1 Chemicals and materials .....	102

4.2.2 <i>In vivo</i> SPME procedure.....	102
4.2.3 <i>In vivo</i> SPME calibration procedure for determination of both free and total CBZ and CBZ-EP concentrations .....	104
4.2.3.1 Determination of $q_0$ .....	104
4.2.3.2 Determination of $n$ and $Q$ .....	105
4.2.3.3 Matrix-free and matrix-matched calibration: determination of $K_{fs} \cdot V_f$ product.....	105
4.2.3.4 Determination of blood to plasma concentration ratios.....	107
4.2.4 <i>In vitro</i> SPME validation.....	108
4.2.5 Terminal cardiac puncture sampling and automated serial sampling using Culex®.....	109
4.2.6 LC-MS/MS analysis .....	110
4.3 Results and discussion.....	111
4.3.1 Summary of SPME method development .....	111
4.3.2 Investigation of suitability of PBS buffer for free concentration determination .....	113
4.3.3 Summary of method validation results.....	113
4.3.4 Evaluation of <i>in vivo</i> performance of prototype SPME assemblies .....	115
4.3.5 Results of <i>in vivo</i> study: pharmacokinetics of CBZ and CBZEP using <i>in vivo</i> SPME .....	117
4.3.6 Results of <i>in vivo</i> study: comparison of <i>in vivo</i> SPME to automated serial and discrete terminal sampling of mice .....	119
4.3.7 Preliminary investigation of suitability of <i>in vivo</i> SPME for global metabolomics .....	125
4.4 Conclusions .....	127
4.5 Addendum .....	128
Chapter 5 Systematic evaluation of SPME extraction phases for metabolomics .....	129
5.1 Preamble and introduction.....	129
5.1.1 Preamble .....	129
5.1.2 Introduction .....	129
5.1.2.1 Overview of LC-MS methods for metabolomics .....	130
5.2 Experimental .....	133
5.2.1 Materials and coatings preparation.....	133
5.2.2 Materials and metabolite standard mixture preparation .....	133
5.2.3 SPME procedure.....	134
5.2.3.1 SPME desorption prior to reverse phase LC-MS (used for analytes of low to intermediate polarity) .....	140

5.2.3.2 SPME desorption prior to HILIC LC-MS (used for polar analytes).....	140
5.2.4 Calculation of correction factors to account for different coating dimensions .....	140
5.2.5 LC-MS analysis .....	143
5.3 Results and discussion .....	147
5.3.1 Development of pentafluorophenyl (PFP) reverse-phase method .....	147
5.3.2 Evaluation of extraction reproducibility .....	147
5.3.3 Comparison of extraction efficiency of various sorbents at pH 7.4.....	151
5.3.4 Dependence of extraction efficiency on pH.....	151
5.3.5 Summary of coating selection and performance .....	160
5.4 Conclusions.....	162
Chapter 6 Development and evaluation of global SPME-LC-MS metabolomics methods on benchtop Orbitrap instrument.....	163
6.1 Preamble and introduction .....	163
6.1.1 Preamble .....	163
6.1.2 Introduction: metabolomics and high-resolution mass spectrometry .....	163
6.1.3 Strategies for improving metabolite coverage in LC-MS metabolomics.....	164
6.2 Experimental.....	166
6.2.1 Materials and reagents .....	166
6.2.2 LC-MS analysis .....	166
6.2.2.1 Reverse-phase LC method using pentafluorophenyl stationary phase.....	167
6.2.2.2 HILIC LC method using aminopropyl stationary phase .....	167
6.2.2.3 HILIC LC method using underivatized silica stationary phase .....	167
6.2.2.4 Summary of optimized MS conditions for all LC methods .....	168
6.2.3 Data processing.....	169
6.2.4 Evaluation of absolute matrix effects.....	169
6.3 Results and discussion .....	169
6.3.1 Comparison of instrumental sensitivity: ion trap <i>versus</i> triple quadrupole <i>versus</i> benchtop Orbitrap.....	169
6.3.2 Development of MS methods on Exactive.....	170
6.3.3 Evaluation of reverse-phase LC-MS method using pentafluorophenyl column .....	173
6.3.4 Evaluation of LC-MS method using amino column for improved separation of sugar compounds .....	177

6.3.5 Evaluation of HILIC LC-MS method on Exactive using underivatized Si column .....	179
6.3.6 Summary of proposed LC-MS methods on Exactive .....	187
6.3.7 Evaluation of global SPME-LC-MS method using pentafluorophenyl LC-MS method...	189
6.3.7.1 Evaluation of extraction time .....	189
6.3.7.2 Evaluation of carryover of SPME method for metabolomics .....	192
6.3.7.3 Evaluation of analyte stability in SPME coating.....	195
6.3.7.4 Comparison of coating performance for the extraction of human plasma for known metabolites.....	196
6.4 Conclusions .....	196
Chapter 7 Metabolomics of human plasma: comparison of <i>in vitro</i> SPME to traditional methods ...	198
7.1 Preamble and introduction.....	198
7.1.1 Preamble .....	198
7.1.2 Introduction: current sample preparation trends for global metabolomics of human plasma .....	198
7.1.3 Challenges with existing sample preparation methods.....	203
7.2 Experimental .....	204
7.2.1 Materials .....	204
7.2.2 SPME sample preparation .....	204
7.2.3 Ultrafiltration (UF) sample preparation.....	205
7.2.4 Plasma protein precipitation with acetonitrile (PP).....	205
7.2.5 Plasma protein precipitation with methanol/ethanol (PM).....	205
7.2.6 LC-MS analysis .....	205
7.2.7 Data processing .....	207
7.3 Results and discussion.....	211
7.3.1 Comparison of sample preparation methods for known identified metabolites .....	211
7.3.2 Global metabolomics - plasma protein precipitation with acetonitrile (PP) results .....	215
7.3.3 Global metabolomics - plasma protein precipitation with methanol/ethanol (PM) results	220
7.3.4 Global metabolomics - ultrafiltration (UF) results .....	227
7.3.5 Global metabolomics - SPME results using mixed-mode coating .....	229
7.3.6 Results for semi-quantitative analysis of identified metabolites using traditional methods .....	237
7.3.7 Comparison of methods: summary.....	240

7.3.8 Global metabolomics: data processing and identification challenges.....	244
7.4 Conclusions.....	246
7.5 Addendum.....	247
Chapter 8 <i>In vivo</i> SPME sampling for global metabolomic studies in mice.....	248
8.1 Preamble and introduction .....	248
8.1.1 Preamble .....	248
8.1.2 Introduction.....	248
8.2 Experimental.....	249
8.2.1 Materials .....	249
8.2.2 Summary of overall experiment design .....	249
8.2.2.1 <i>In vivo</i> SPME sampling.....	251
8.2.2.2 <i>Ex vivo</i> SPME .....	252
8.2.2.3 Ultrafiltration (UF) sample preparation .....	252
8.2.2.4 Plasma protein precipitation with methanol/ethanol (PM) .....	252
8.2.3 LC-MS analysis .....	253
8.2.4 Data processing.....	253
8.3 Results and discussion .....	253
8.3.1 Blank controls .....	253
8.3.2 Quality control (QC) results.....	255
8.3.3 Evaluation of intra-animal variability and reproducibility of <i>in vivo</i> SPME sampling.....	257
8.3.4 Principal component analysis: effect of CBZ dosing.....	258
8.3.5 Principal component analysis: biochemical individuality.....	269
8.3.6 Advantages of <i>in vivo</i> sampling <i>versus</i> blood withdrawal approaches.....	271
8.4 Conclusions.....	278
Chapter 9 Summary and future directions .....	280
9.1 Summary .....	280
9.2 Future directions .....	283
References.....	286

## List of Figures

<b>Figure 1.1</b> Interaction of the different -omes in a cell. Each -ome (except the genome) is a complex function of the other -omes, and the amount of integration increases from the bottom to the top of the Figure. Thus, the metabolome and the fluxome represent integrative functions of the other -omes, and, at the same time, they are closely connected. Exchange with the environment occurs primarily via the metabolome (i.e. between the endometabolome and the exometabolome). Figure reprinted from reference with permission of publisher. <sup>13</sup> .....	2
<b>Figure 1.2</b> Typical workflow of a global metabolomics study. ....	4
<b>Figure 1.3</b> Schematic of SPME procedure using direct extraction mode. (a) Fibre is exposed directly to the sample solution, and analyte of interest is extracted into the coating. (b) Fibre is now exposed to desorption solvent, and the analyte is desorbed from the coating into the solvent solution. Small arrows indicate the direction of mass transfer. ....	16
<b>Figure 2.1</b> Structures of selected benzodiazepines included in evaluation of Concept 96 autosampler. ....	28
<b>Figure 2.2</b> (a) Custom-made multi-fibre SPME device constructed using 1.55 mm stainless steel wires and RPA extraction phase. (b) Photo showing the details of SPME multi-fibre device, 96 multi-well plate and agitator employed in PAS robotic system. ....	31
<b>Figure 2.3</b> Overview of optimized coating procedure using 5- $\mu$ m coated silica particles. ....	32
<b>Figure 2.4</b> Photo showing PAS Concept 96 robotic system. A and B are orbital agitators used for extraction and desorption, C is system controller, D is the arm used to manipulate SPME multi-fibre device, E depicts SPME multi-fibre device, F is syringe arm and G is the arm used for simultaneous nitrogen evaporation from all wells. ....	33
<b>Figure 2.5</b> Optimization of desorption conditions for diazepam using PDMS coating (n=3). Extraction was performed from 100 ng/mL diazepam standard in PBS buffer pH 7.4 for 60 min using agitation of 850 rpm. ....	37

**Figure 2.6** (a) Representative extraction time profiles for the extraction of diazepam from 100 ng/mL standard solution for 6 different fibres and well positions (data for all 96 fibres was collected as discussed in text, but is shown for only 6 fibres for clarity) (b) Dependence of % RSD for the amount extracted of diazepam (n=96 fibres) on the extraction time. .... 38

**Figure 2.7** Amount of diazepam extracted from 1 mL of 100 ng/mL diazepam standard solution using automated multi-fibre SPME (n=96 fibres). .... 40

**Figure 2.8** Evaluation of intra-fibre reproducibility using PDMS coating. The distribution of fibres with given RSD for n=5 independent extractions using the same fibre is shown. The performance of fibres with % RSD exceeding 10 was deemed unacceptable for quantitative analysis. All of the extractions were performed using 100 ng/mL standard solution of diazepam in PBS and optimized SPME conditions. .... 41

**Figure 2.9** Dependence of the amount extracted on well position in two typical experiments. The residual plots for the amount of diazepam extracted by each well of a 96-well plate are shown. Both figures are plotted using the same scale, and 0 position represents the overall mean amount of diazepam extracted (n=96) for the given extraction. .... 43

**Figure 2.10** Plate map indicating well selection for cross-talk experiment. B denotes placement of blank PBS solution in the well and S denotes placement of 300 ng/mL diazepam standard solution in the well..... 44

**Figure 2.11** Evaluation of different coated silica particles for use as SPME extraction phases. The amount shown is the mean amount extracted by 12 fibres tested. The error bars show one standard deviation from the mean. The results for two consecutive extractions are shown as an indication of coating adhesion..... 46

**Figure 2.12** Diagram showing reusability of RPA 5 µm coatings over 14 extractions. The amount extracted of diazepam and oxazepam is shown over time for three representative fibres. Data points for lorazepam and nordiazepam are omitted for clarity. .... 47

**Figure 2.13** (a) Evaluation of the effect of the diameter of stainless steel support on extraction efficiency for diazepam. The bars show the mean amount extracted by batch of 12 fibres, and the error bars show one standard deviation of results (b) Comparison of inter-fibre reproducibility (%)



RSD for the amount extracted) of batches of 12 fibres prepared using different dimensions of stainless steel support.....	49
<b>Figure 2.14</b> Optimization of nitric acid etching time. Batches of 15 fibres (1.55 mm diameter) were prepared using coating procedure described in Experimental except acid etching time was increased from 20 min to 2 hr. The extraction was performed from 100 ng/mL benzodiazepine standard solution using optimized SPME conditions. ....	50
<b>Figure 2.15</b> SEM images of 1.55 mm SPME fibre coated with 5 µm RPA particles and prepared according to procedure described in Experimental. (a) surface morphology using 300x magnification (b) estimation of coating thickness using 600x magnification. ....	51
<b>Figure 2.16</b> Extraction time profile for diazepam, nordiazepam, oxazepam and lorazepam using RPA coating. Extraction conditions: 100 ng/mL benzodiazepine standard in PBS pH 7.4, 850 rpm agitation.....	52
<b>Figure 2.17</b> (a) Comparison of external standard, internal standard and on-fibre standardization (standard-on-the fibre) calibration methods for the use with automated multi-fibre SPME. The dependence of % RSD (n=12 fibres) of the amount extracted on the choice of calibration method is shown. All extractions were performed from 100 ng/mL diazepam standard solution in PBS buffer pH 7.4 using optimal SPME conditions. (b) Comparison of standard-on-fibre <i>versus</i> internal standard calibration for improving intra-fibre reproducibility. The dependence of % RSD (n=5 extractions using each fibre) on the choice of calibration method is shown.....	56
<b>Figure 2.18</b> Overview of parameters which may require optimization during method development of an automated SPME method using Concept 96 robotic station. ....	57
<b>Figure 2.19</b> Overview of automated SPME procedure using Concept 96 robotic station.....	58
<b>Figure 2.20</b> Example extracted ion chromatograms (XIC) of diazepam, nordiazepam, oxazepam and lorazepam in (a) blank whole blood sample and (b) 50 ng/mL benzodiazepine standard in whole blood.....	60
<b>Figure 3.1</b> Overview of desired properties for SPME coatings in bioanalysis. ....	69

**Figure 3.2** Chemical structures of model drugs used in the evaluation of biocompatible coatings (a) carbamazepine, (b) propranolol (c) pseudoephedrine (d) diazepam (e) ranitidine. .... 70

**Figure 3.3** Chemical structures of coatings evaluated in this chapter (a) octadecyl (C<sub>18</sub>) (b) C<sub>16</sub> with an embedded amide group (reverse-phase amide, RPA) and (c) cyanopropyl coating. .... 71

**Figure 3.4** Prototype *in vivo* SPME probe obtained from Supelco Inc. (A) SPME fibre is housed inside commercial hypodermic syringe for protection and for piercing living system or septum of sampling device. (B) Pushing on the plunger exposes SPME coating during extraction and desorption steps. .... 72

**Figure 3.5** Example SEM image acquired using 300x magnification of the surface of biocompatible RPA coating (3 µm particle size). Upper portion of coating was removed on purpose to facilitate the determination of coating thickness as shown in the image (41.4 µm). .... 75

**Figure 3.6** (a) Comparison of the extraction efficiency of RPA, C<sub>18</sub> and cyano coatings (45 µm thickness, n = 10 fibres of each type) for the extraction of various drugs. Extraction conditions: 2 min without agitation from 100 ng/mL drug standard in PBS buffer pH 7.4. Correction factor of 1.6 was applied to CW-TPR data in order to account for different thickness and dimensions of CW-TPR fibre as discussed in text. (b) Effect of sample volume (1.8 mL *versus* 0.25 mL) on the amount of drug extracted from plasma using 45 µm C<sub>18</sub> SPME coating (n=3 fibres per sample volume). Extraction conditions: equilibrium extraction from human plasma spiked with 100 ng/mL drug standard. .... 78

**Figure 3.7** Example extraction time profiles for carbamazepine (a) using C<sub>18</sub> coatings (n = 3 fibres) of 15 µm, 30 µm, 45 µm and 60 µm thickness without agitation (b) using C<sub>18</sub> and RPA coatings of 45 µm thickness (n=3 fibres) using 2400 rpm vortex agitation to enhance mass transfer rates of analyte. .... 81

**Figure 3.8** Comparison of carryover results for carbamazepine using 15 µm and 60 µm C<sub>18</sub> coatings. Extraction conditions: 90 min extraction of 250 ng/mL carbamazepine standard in PBS buffer (n=3 fibres). Desorption conditions: two serial desorptions using conditions stated in figure..... 83

**Figure 3.9** Example calibration curve obtained for extraction of carbamazepine in PBS buffer pH 7.4 in concentration range 1-1000 ng/mL. LOQ of the method was 1 ng/mL. Extraction conditions: 2 min static, C<sub>18</sub> coating. .... 87

**Figure 3.10** Overlaid TIC chromatograms obtained for 20 µL injection of desorption solvent and blank plasma extract in the region of m/z 100-500. The main ions contributing to the peaks observed are marked directly on the chromatogram. Two large peaks with retention times 3-4 min arose from purified water and interfered with the analysis of propranolol..... 90

**Figure 3.11** Investigation of the effect of fibre preconditioning on the amount of analyte extracted using carbamazepine and diazepam as model analytes. Effect of no preconditioning is compared *versus* 30 min preconditioning in purified water *versus* 30 min preconditioning in methanol/water mixture. Extraction conditions: C<sub>18</sub> coating of 45 µm thickness, 2 min static extraction from 100 ng/mL standard in PBS buffer, n=6 fibres per each condition. .... 91

**Figure 3.12** Comparison of the extraction efficiency obtained for eight independent Supelco C<sub>18</sub> lots of coating (n=10 fibres per lot) prepared on different days in April-May 2009. The results for four model analytes: diazepam, lorazepam, nordiazepam and oxazepam are shown. Extraction conditions: equilibrium, extraction from 100 ng/mL drug standard in PBS buffer pH 7.4. .... 93

**Figure 3.13** Recommended workflow for (a) *in vitro* and (b) *in vivo* SPME procedure using prototype biocompatible SPME fibres..... 96

**Figure 4.1** Photograph of the mouse sampling interface shown with an SPME probe assembly inserted through the PRN adapter..... 103

**Figure 4.2** Example selected reaction monitoring chromatogram of 5 ng/mL CBZ and CBZEP validation sample prepared in mouse whole blood with heparin as anticoagulant using SPME-LC-MS/MS method as described in Experimental. .... 111

**Figure 4.3** Results of *in vitro* evaluation of assisted agitation speed. The dependence of the response (chromatographic peak area of CBZ, n=3 determinations) of SPME sampling to a rapid change in CBZ concentration (0 to 50 ng/mL as described in text) and influence of assisted agitation speed (4 *versus* 10 push/pull cycles)..... 112

**Figure 4.4** Whole blood concentration *versus* time profiles obtained by *in vivo* SPME sampling for CBZ (A) and its formed metabolite, CBZEP (B), in seven individual mice (M01 to M07) following the administration of a single *i.v.* dose of 2 mg/kg CBZ. Samples were collected up to 240 min, but

CBZ and CBZEP were not detected in some of the late time point samples as shown in the figure. Y-scale is shown on logarithmic scale. .... 120

**Figure 4.5** Whole blood concentration *versus* time profiles obtained by automated serial sampling for CBZ and its formed metabolite, CBZEP, in three individual mice (M01 to M03) following administration of a single *i.v.* dose of 2 mg/kg of CBZ. This data was collected by NoAB BioDiscoveries and is included for comparison purposes only with permission of authors..... 121

**Figure 4.6** Mean ( $\pm$ SD) concentration *versus* time profiles of CBZ (A) and CBZEP metabolite (B), following 2 mg/kg *i.v.* administration of CBZ to mice. Samples were taken by serial SPME sampling (n=7 mice), by serial automated blood draws (n=3 mice) or by terminal blood draws (3 mice/time point). SPME and serial blood sampling measured whole blood concentrations whereas terminal sampling measured plasma concentrations. SPME analysis was performed at the University of Waterloo, while serial and terminal analysis were performed by NoAB BioDiscoveries and are included only for comparison purposes with permission of authors..... 122

**Figure 4.7** Representative results from a proof of concept *in vivo* SPME metabolomics study. (a) Scores scatter plot indicating good clustering of two sample types 5 min post-dose samples (labelled as 5B and C) and 30 min post-dose samples (labelled as 30 B and C). (b) Loadings scatter plot of PC1 *versus* PC2 illustrating the peaks contributing most to the observed clustering. (c) Example of a score contribution plot showing 30 representative metabolites. In this metabolite subset, metabolites with IDs of 56, 60, 432 and 1980 contribute the most to the observed clustering. (d) pair-wise comparison of selected differentiating peaks based on PCA analysis including observed signal intensity and RSD. .... 127

**Figure 5.1** Structures of metabolites included in metabolite standard test mixture. .... 139

**Figure 5.2** Example chromatogram using reverse phase pentafluorophenyl LC-MS method. .... 144

**Figure 5.3** Example of extraction reproducibility (a) at extraction pH of 7.4 and analysis using reverse phase LC-MS method and (b) at extraction pH of 9.5 and analysis using HILIC LC-MS. ... 148

**Figure 5.4** Comparison of the extraction efficiency of all sorbents for the extraction of 12 selected metabolites at pH 7.4 analyzed using PFP reverse phase method. .... 149

<b>Figure 5.5</b> Comparison of the extraction efficiency of all sorbents for the extraction of seven selected metabolites at pH 7.4 analyzed using HILIC method. ....	150
<b>Figure 5.6</b> Comparison of extraction efficiency of CW-TPR, HRP, FOCUS, PBA,C <sub>8</sub> +B and RPA SPME coatings for the extraction of selected metabolites at pH 7.4.....	154
<b>Figure 5.7</b> Extraction efficiency of selected individual metabolites (histidine, phenylalanine, adenine, progesterone, AMP and β-NAD) at pH 7.4 using all coatings tested.....	156
<b>Figure 5.8</b> Comparison of the extraction efficiency of all sorbents for the extraction of 12 selected metabolites at pH 9.5 analyzed using PFP reverse phase method.....	157
<b>Figure 5.9</b> Dependence of the extraction efficiency of selected metabolites on pH using (a) PBA coating (b) mixed-mode C <sub>8</sub> +B coating and (c) HRP coating. ....	159
<b>Figure 5.10</b> Comparison of three most promising types of coatings for global metabolomic studies for the extraction of representative metabolites at pH 7.4: mixed mode coating, polystyrene divinylbenzene polymer and PBA coating. For mixed mode coating, experimental results for C <sub>8</sub> with benzenesulfonic acid coating from UCT is shown as example. For polystyrene divinylbenzene polymer coating, the results for HRP coating from Macherey Nagel are shown. Correction factor to account for differences in particle size was applied as discussed in text to facilitate the comparison between various coatings. The metabolites are arranged in the order of decreasing polarity (increasing log P value) from left to right to illustrate any trends with respect to analyte polarity. ....	160
<b>Figure 6.1</b> Effect of capillary and tube lens voltage on signal intensity of selected analytes using positive ESI PFP LC-MS method. The capillary and tube lens settings for methods positive 1, 2 and 3 were 27.5 and 100 V, 57.5 and 110 V and 90 and 170 V, respectively. ....	175
<b>Figure 6.2</b> Evaluation of absolute matrix effects using (a) positive and (b) negative ESI reverse-phase LC-MS method with PFP column. Percent signal was calculated as the area obtained in human plasma extract spiked post-extraction <i>versus</i> neat standard at the same concentration level prepared directly in desorption solvent. Percent signal >120% represents ionization enhancement for a given metabolite and % signal <80% represents ionization suppression for a given metabolite. The results are shown for two types of Supelco biocompatible coatings: mixed mode and C <sub>18</sub> coatings. ....	177

**Figure 6.3** Evaluation of absolute matrix effects using negative ESI HILIC LC-MS method with amino column. Percent signal was calculated as the area obtained in human plasma extract spiked post-extraction *versus* neat standard at the same concentration level prepared directly in desorption solvent. Percent signal >120% represents ionization enhancement for a given metabolite and % signal <80% represents ionization suppression for a given metabolite. .... 179

**Figure 6.4** Example XIC of metabolite standard solution prepared at 1 µg/mL in 60% acetonitrile and analyzed using HILIC method with unmodified Si column in negative ESI mode (a) final method using 20 mM effective concentration of buffer and (b) initial method using 5 mM effective concentration of buffer. Only selected metabolites are shown for clarity. .... 181

**Figure 6.5** Evaluation of absolute matrix effects using (a) positive and (b) negative ESI HILIC LC-MS method with underivatized Si column. Percent signal was calculated as the area obtained in human plasma extract spiked post-extraction *versus* neat standard at the same concentration level prepared directly in desorption solvent. Percent signal >120% represents ionization enhancement for a given metabolite and % signal <80% represents ionization suppression for a given metabolite. ... 182

**Figure 6.6** Optimization of MS parameters (capillary temperature, capillary voltage and tube lens voltage) for metabolites using negative ESI HILIC LC-MS method (a) results for very polar metabolites (b) results for metabolites with sufficient retention using reverse phase method – full scale (c) same as in (b) but y-scale zoomed in to show trends for metabolites not well visible in (b). .... 185

**Figure 6.7** The dependence of the amount extracted of known metabolites on extraction time using Supelco mixed-mode fibres (n=3 at each time point). Samples were analyzed using pentafluorophenyl LC-MS method. (a) The results for analytes observed in positive ESI mode. The inset graph shows expanded region to facilitate the comparison of analytes with sub-ng amounts extracted (b) the results for analytes observed in negative ESI. The inset graph shows expanded region to facilitate the comparison of analytes with < 20 ng extracted. .... 191

**Figure 6.8** The dependence of the amount extracted of known metabolites on extraction time. All extractions were performed from human plasma using Supelco mixed-mode fibres (n=3 at each time point). Samples were analyzed using HILIC LC-MS method. The results for analytes observed in negative ionization mode. The inset graph shows full scale for glucose and fructose..... 192

**Figure 6.9** The amount of carryover observed for known metabolites and its dependence on extraction time. All extractions were performed from human plasma using Supelco mixed-mode fibres (n=3 at each time point). Samples were analyzed using pentafluorophenyl LC-MS method. The carryover was evaluated by performing a second desorption using fresh 300  $\mu$ L portion of desorption solvent. The results for analytes observed in (a) positive and (b) negative ionization mode. .... 194

**Figure 6.10** The results of the evaluation of metabolite stability (1-week, -20°C storage) within SPME coating for selected metabolites using n=3 mixed-mode Supelco fibres. .... 195

**Figure 6.11** Comparison of the performance of biocompatible C<sub>18</sub> *versus* biocompatible mixed-mode (C<sub>18</sub> + Benzenesulfonic acid) coating for extraction of human plasma. Extraction was performed using n=3 fibres of each type, for 1440 min and the analysis was performed using negative ESI HILIC LC-MS method. Coating dimensions and thickness were the same so no correction factor was applied. Error bars show one standard deviation from the mean. .... 196

**Figure 7.1** Example results for QC sample analyzed using positive ESI PFP LC-MS method over 48-hr period. .... 207

**Figure 7.2** Dependence of % RSD on signal intensity for n=7 injections of QC sample prepared by mixing aliquots of each sample within the sample set. The sample set was SPME extraction from human plasma using different extraction times. The QC injections were made randomly throughout the sample run over 48-hour period using pentafluorophenyl LC-MS method. Each point represents known metabolite detected in human plasma. (a) results for positive ionization mode (b) results for positive ionization mode: expanded scale to enable comparison of RSD for low signal intensities. (c) results for negative ionization mode (d) results for negative ionization mode: expanded scale to enable comparison of RSD for low signal intensities. .... 208

**Figure 7.3** Data processing procedures for LC-MS-based metabolomics. Chromatographic and spectral data are acquired by high-resolution LC-MS. Subsequent data processing, such as centroiding, deisotoping, filtering, peak recognition, yields a data matrix containing information on sample identity, ion identity (RT and *m/z*) and ion abundance. With appropriate data transformation and scaling, a multivariate model can be established through unsupervised or supervised multivariate data analysis (MDA). The scores plot illustrates the principal or latent components of the model and sample classification, while the loadings plot presents the contribution of each ion to each principal

component of the MDA model. Figure reprinted with permission from Taylor & Francis from review by Chen *et al.*<sup>27</sup> ..... 210

**Figure 7.4** Comparison of method precision (expressed as % RSD for n=7 replicates) obtained for plasma protein precipitation with methanol/ethanol (PM), plasma protein precipitation with acetonitrile (PP), ultrafiltration (UF) and SPME. The samples were prepared using single pooled lot of human plasma with sodium citrate as anti-coagulant using procedures described in Experimental section. Missing bars denote peak not detected by a particular method. (a) Results for the analysis using pentafluorophenyl LC-MS method in positive ESI mode. (b) Results for the analysis using pentafluorophenyl LC-MS method in negative ESI mode. The results for two independent sample sets are shown and denoted as Day 1 and Day 2. .... 212

**Figure 7.5** Taurocholic acid example. Taurocholic acid peak detected using negative ESI pentafluorophenyl LC-MS method in (a) standard mixture (b) human plasma sample prepared using PM (c) human plasma sample prepared using PP (d) human plasma sample prepared using SPME shown on same scale as PM and PP methods (e) human plasma sample prepared using SPME but y-scale zoomed in to better see peak shape (f) number of points obtained across SPME peak (g) human plasma sample prepared using UF shown using y-scale zoomed to the same scale as shown in (e). 215

**Figure 7.6** Total ion count (TIC) chromatograms obtained using negative ESI pentafluorophenyl LC-MS method in (a) human plasma sample prepared using UF (b) human plasma sample prepared using SPME (c) human plasma sample prepared using PP (d) human plasma sample prepared using PM. All TICs are shown on the same scale ( $1 \times 10^8$ ) to facilitate comparison..... 217

**Figure 7.7** Total ion count (TIC) and extracted ion chromatogram (XIC) for tryptophan obtained using negative ESI HILIC LC-MS method in (a) human plasma sample prepared using PM (b) human plasma sample prepared using PP (c) human plasma sample prepared using UF (d) human plasma sample prepared using SPME. All TICs and XIC are shown on the same scale ( $1 \times 10^8$  and  $5 \times 10^5$ , respectively) to facilitate comparison across methods..... 218

**Figure 7.8** (a) Ion map ( $m/z$  versus retention time) for human plasma sample prepared using plasma protein precipitation with acetonitrile (PP) and analyzed using positive ESI pentafluorophenyl LC-MS method. (b) Number of peaks with given % RSD obtained in two independent data sets..... 221



**Figure 7.9** (a) Ion map (*m/z* versus retention time) for human plasma sample prepared using plasma protein precipitation with acetonitrile (PP) and analyzed using negative ESI pentafluorophenyl LC-MS method. (b) Number of peaks with given % RSD obtained in two independent data sets. .... 222

**Figure 7.10** (a) Ion map (*m/z* versus retention time) for human plasma sample prepared using plasma protein precipitation with ethanol/methanol (PM) and analyzed using positive ESI pentafluorophenyl LC-MS method. (b) Number of peaks with given % RSD obtained in two independent data sets.... 223

**Figure 7.11** (a) Ion map (*m/z* versus retention time) for human plasma sample prepared using plasma protein precipitation with ethanol/methanol (PM) and analyzed using negative ESI pentafluorophenyl LC-MS method. (b) Number of peaks with given % RSD obtained in two independent data sets.... 224

**Figure 7.12** Comparison of plasma protein precipitation methods using data collected with (a) positive and (b) negative ESI pentafluorophenyl LC-MS method. Two independent data sets are shown (T0 and T7) acquired a week apart on the same human plasma sample using  $n=7$  independently prepared replicates. The graph shows number of peaks with given area ratio. For peaks with area ratios of 0.8-1.2, two methods can be considered to be equivalent. For peaks with area ratios  $<0.8$  plasma protein precipitation with acetonitrile (PP) yielded better results. For peaks with area ratios  $>1.2$  plasma protein precipitation with methanol/ethanol yielded better results. .... 226

**Figure 7.13** (a) Ion map (*m/z* versus retention time) for human plasma sample prepared using ultrafiltration (UF) and analyzed using positive ESI pentafluorophenyl LC-MS method. (b) Number of peaks with given % RSD obtained in two independent data sets..... 228

**Figure 7.14** (a) Ion map (*m/z* versus retention time) for human plasma sample prepared using ultrafiltration (UF) and analyzed using negative ESI pentafluorophenyl LC-MS method. (b) Number of peaks with given % RSD obtained in two independent data sets..... 229

**Figure 7.15** (a) Ion map (*m/z* versus retention time) for human plasma sample prepared using SPME and analyzed using positive ESI pentafluorophenyl LC-MS method. (b) Number of peaks with given % RSD obtained in two SPME data sets where extraction time was varied from 5 min to overnight. .... 231

**Figure 7.16** (a) Ion map (*m/z* versus retention time) for human plasma sample prepared using SPME and analyzed using negative ESI pentafluorophenyl LC-MS method. (b) Number of peaks with given

% RSD obtained in two SPME data sets where extraction time was varied from 5 min to overnight.  
 ..... 232

**Figure 7.17** Example of three metabolites processed using SIEVE software (a,b) peak showing equilibrium reached trend with no further increases in the amount extracted with increasing extraction time (c,d) peak showing decreasing trend where the amount extracted decreases with increasing extraction time (e,f) peak showing increasing trend where the amount extracted decreases with increasing extraction time. The panels a, c, e show XIC for this metabolite and demonstrate good chromatographic alignment of the peaks. The panels b, d, f show the magnitude of integrated intensity for each extraction time (n=3 extractions per each time point), while label 0 shows the results for blank injection of desorption solvent. .... 234

**Figure 7.18** Dependence of % RSD on signal intensity. Comparison of plasma protein precipitation with acetonitrile (PP) *versus* SPME using pentafluorophenyl method in negative ESI mode..... 236

**Figure 7.19** Example metabolite detected (m/z of 411.0783) by SPME and UF methods, but not by plasma protein precipitation methods. All XICs are shown on the scale of  $5 \times 10^4$  to facilitate comparison between methods. The analysis was performed using negative ESI HILIC LC-MS method. Search of HMDB resulted in four possible hits with mass accuracy of 0.8 ppm (HMDB 00379, 06471, 06355 and 03518) and one hit with mass accuracy of -3.6 ppm (HMDB ID 01451).  
 ..... 242

**Figure 8.1** Overview of animal study employed for comparison of *in vivo* SPME to traditional methods based on blood withdrawal..... 251

**Figure 8.2** TIC of (a) blank SPME fibre (absolute intensity  $9.3 \times 10^7$  counts, run order 66) and (b) blank desorption solvent (absolute intensity  $1.1 \times 10^8$  counts, run order 81) collected using positive ESI LC-MS method with pentafluorophenyl column. .... 254

**Figure 8.3** Signal intensity versus QC run order for selected compounds (a) glucose (b) reduced glutathione (c) progesterone (d) nicotinamide and (e) carbamazepine. .... 257

**Figure 8.4** Comparison of inter-animal versus intra-animal variability (expressed as %RSD) for the set of known metabolites detected using *in vivo* SPME sampling. .... 258

**Figure 8.5** (a) 3D scores plot obtained for *in vivo* SPME sampling of n=4 mice (M5, M6, M7, M8) prior to (T0) and 30-min (T30) post dose. (b) 2D scores plot of the same dataset showing PC1 versus PC2 (c) Loadings scatter plot of PC1 versus PC2 illustrating the peaks contributing most to the observed clustering (d) 2D scores plot of the same dataset showing PC1 versus PC3 (e) Loadings scatter plot of PC1 versus PC3 illustrating the peaks contributing most to the observed clustering. Blank injections are shown, while QC injections are omitted for clarity in all plots. .... 260

**Figure 8.6** (a) 3D scores plot obtained using ultrafiltration (UF) and solvent precipitation (PM) for n=4 mice prior to CBZ dosing (PM and UF) and n=4 mice 30-min post dose (PM CBZ and UF CBZ). (b) 2D scores plot of the same dataset showing PC1 versus PC2 (c) Loadings scatter plot of PC1 versus PC2 illustrating the peaks contributing most to the observed clustering (d) 2D scores plot of the same dataset showing PC1 versus PC3 (e) Loadings scatter plot of PC1 versus PC3 illustrating the peaks contributing most to the observed clustering. Blank injections are shown, while QC injections are omitted for clarity in all plots. .... 262

**Figure 8.7** Plot of principal component 1 (a), 2 (b) and 3 (c) versus observation ID for data set shown in Figure 8.3. .... 265

**Figure 8.8** Individual 3D scores plot obtained using (a) ultrafiltration (UF) and (b) solvent precipitation (PM) for n=4 mice prior to CBZ dosing (PM and UF) and n=4 mice 30-min post dose (PM CBZ and UF CBZ). .... 266

**Figure 8.9** Results of PCA comparing *in vivo* versus *ex vivo* SPME sampling (no CBZ dosing) shown as 2D scores plot of 2 main principal components contributing 51.2% and 19.0% of variance respectively. .... 266

**Figure 8.10** XIC of m/z 662.1019 corresponding to  $\beta$ -NAD for the same mouse sample analyzed using negative ESI reverse phase PFP LC-MS method by (a) PM (b) *in vivo* SPME (c) *ex vivo* SPME (d) UF and (e) injection of authentic metabolite standard containing  $\beta$ -NAD. .... 276

**Figure 8.11** Mass spectrum of (a) authentic  $\beta$ -NAD standard solution dissolved directly in desorption solvent (mass accuracy -2.1 ppm) (b) unknown peak identified for *in vivo* SPME sample shown in Figure 8.10 (mass accuracy 0 ppm). Mass accuracy is calculated using expected accurate mass of  $\beta$ -NAD of 662.1019 for [M-H]<sup>-</sup> in negative ESI mode. .... 277

## List of Tables

<b>Table 1.1</b> Overview of global metabolomics studies using <i>in vivo</i> SPME and GC-MS analysis .....	22
<b>Table 2.1</b> Summary of MS/MS parameters for the analysis of benzodiazepines.....	34
<b>Table 2.2</b> The effect of fibre rinsing on the amount of diazepam extracted and inter-fibre reproducibility using multi-fibre SPME with PDMS coating.....	40
<b>Table 2.3</b> Summary of intra-fibre reproducibility results for 15 fibres coated with RPA 5 µm extraction phase and using 0.81 mm stainless steel support. The results are shown as intra-day and inter-day reproducibility. The effect of the use of lorazepam as internal standard to improve reproducibility is also shown. ....	47
<b>Table 2.4</b> Summary of inter-fibre reproducibility results for 96 fibres coated with RPA 5 µm extraction phase and using 1.55 mm stainless steel support. The effect of the use of lorazepam as internal standard to improve reproducibility is also shown. ....	50
<b>Table 2.5</b> Comparison of performance of PDMS and RPA coatings for the extraction of diazepam.	53
<b>Table 2.6</b> Comparison of method precision (n=96 fibres) of manual pipetting <i>versus</i> automated dispensing. For manual pipetting, standard solution and desorption solvent were placed into wells using air displacement Fisherbrand 100-1000 µL pipette. For automated dispensing experiment, standard solution and desorption solvent were placed into wells using Ultraspense2000.....	54
<b>Table 2.7</b> Results of the evaluation of absolute matrix effects for the analysis of benzodiazepines in whole blood. % signal represents the ratio of the signal of blank whole blood extract spiked post-extraction <i>versus</i> neat standard prepared directly in desorption solvent at the same concentration level.....	61
<b>Table 2.8</b> Automated SPME-LC-MS/MS method validation results: LOQ and linear range. ....	62
<b>Table 2.9</b> Automated SPME-LC-MS/MS method validation results: summary of intra-day accuracy and precision. ....	63

<b>Table 2.10</b> Automated SPME-LC-MS/MS method validation results: summary of accuracy and inter-day reproducibility results. ....	64
<b>Table 2.11</b> Summary of SPME methods reported for analysis of diazepam in plasma, serum or whole blood. ....	65
<b>Table 3.1</b> Summary of analyte properties, MS/MS parameters and LC retention times. ....	73
<b>Table 3.2</b> Comparison of extraction efficiency at equilibrium of proposed biocompatible coatings <i>versus</i> existing commercial CW-TPR coating for compounds of varying polarity. ....	77
<b>Table 3.3</b> Effect of increasing extraction time on the amount extracted and inter-fibre variability. ...	81
<b>Table 3.4</b> Evaluation of inter-fibre reproducibility for three model drugs in three matrices of increasing complexity: PBS, urine and plasma. All extractions were performed using n=10 fibres with 45 µm thickness coating. ....	86
<b>Table 3.5</b> Summary of linearity results obtained for C <sub>18</sub> and RPA coatings in human urine and plasma for diazepam and propranolol. Each point of each calibration set was obtained using different fibre (n=1 determination for each concentration level). ....	88
<b>Table 3.6</b> Evaluation of absolute matrix effects for the analysis of model drugs in human plasma. % signal represents the ratio of the signal of blank plasma extract spiked post-extraction <i>versus</i> neat standard prepared directly in desorption solvent at the same concentration level. ....	89
<b>Table 3.7</b> Effect of sample volume and standard concentration on success of loading procedure. ....	92
<b>Table 4.1</b> Example calibration curves obtained for CBZ and CBZEP in PBS, blood and plasma. ...	106
<b>Table 4.2</b> Determination of whole blood to plasma concentration ratio for CBZ using equilibrium <i>in vitro</i> SPME. ....	108
<b>Table 4.3</b> Summary of validation results for CBZ using SPME with on-fibre standardization. ....	114
<b>Table 4.4</b> Absolute recovery of CBZ and CBZEP at equilibrium in PBS, plasma and whole blood (n=10 concentration levels for CBZ, n=6 concentration levels for CBZEP). ....	114

<b>Table 4.5</b> Results obtained for repeated sampling: probes with red appearance <i>versus</i> new probes used for re-sampling. ....	116
<b>Table 4.6</b> Free concentration (ng/mL) of CBZ in circulating blood of n=7 mice obtained by <i>in vivo</i> SPME sampling. ....	118
<b>Table 4.7</b> Free concentration (ng/mL) of CBZEP in circulating blood of n=7 mice obtained by <i>in vivo</i> SPME sampling. ....	118
<b>Table 4.8</b> Mean ( $\pm$ SD) estimated PK parameters for CBZ following 2 mg/kg <i>i.v.</i> administration of CBZ to mice. Blood was sampled by SPME sampling (n=7 mice) and by serial automated blood draws (n=3 mice) and plasma was sampled by terminal blood draws (n=3 mice/time point). SPME analysis was performed at the University of Waterloo, while serial and terminal blood draw analyses were performed by NoAB BioDiscoveries and are included only for comparison purposes with permission of authors. ....	123
<b>Table 4.9</b> Mean ( $\pm$ SD) estimated PK parameters in blood for the formed metabolite, CBZEP, following 2 mg/kg <i>i.v.</i> bolus administration of CBZ to mice. Blood was sampled by SPME sampling (n=7 mice) and by serial automated blood draws (n=3 mice). SPME analysis was performed at the University of Waterloo, while serial blood draw analysis was performed by NoAB BioDiscoveries and is included only for comparison purposes with permission of authors. ....	123
<b>Table 5.1</b> Summary of SPE sorbents and their properties. ....	135
<b>Table 5.2</b> Physicochemical properties of metabolites included in standard metabolite mixture. ....	137
<b>Table 5.3</b> Determination of correction factors to use during coating comparison. ....	142
<b>Table 5.4</b> Summary of optimized LC-MS parameters. ....	143
<b>Table 5.5</b> Optimization of MS parameters (a) needle voltage, (b) capillary voltage and (c) RF voltage in positive ESI mode for compounds with MW<500. ....	145
<b>Table 5.6</b> Optimization of MS parameters (a) needle voltage, (b) capillary voltage and (c) RF voltage in negative ESI mode for compounds with MW<500. ....	146

<b>Table 5.7</b> Optimization of MS parameters (a) needle voltage, (b) capillary voltage and (c) RF voltage in positive ESI mode for compounds with MW>500.....	146
<b>Table 5.8</b> Dependence of the extraction efficiency of Waters Oasis MAX, MCX, WAX and WCX coatings on sample pH. ....	159
<b>Table 6.1</b> Summary of Exactive MS parameters used for metabolomics.....	168
<b>Table 6.2</b> Comparison of instrumental sensitivity for benzodiazepines based on injections of neat standards using reverse phase C <sub>18</sub> method and positive ESI mode. ....	170
<b>Table 6.3</b> Summary of ions observed and mass accuracy in positive ESI mode during direct infusion of metabolite standard mixture using 5 µL/min flow rate.....	171
<b>Table 6.4</b> Summary of ions observed and mass accuracy in negative ESI mode during direct infusion of metabolite standard mixture using 5 µL/min flow rate.....	172
<b>Table 6.5</b> Summary of LOQs obtained for various metabolites using proposed LC-MS methods on Exactive instrument.....	174
<b>Table 6.6</b> Results of QC sample analysis for known metabolites using negative ESI mode HILIC LC-MS method with aminopropyl column. % signal intensity of QC2 and QC3 is shown with respect to signal intensity observed for QC1 with approximately 10 hr elapsed between each QC sample. Signal intensity observed for QC1 was set to 100%.....	180
<b>Table 6.7</b> Results of QC sample analysis for known metabolites using negative ESI mode HILIC LC-MS method with unmodified Si column. % signal intensity of QC2 and QC3 is shown with respect to signal intensity observed for QC1 with approximately 10 hr elapsed between each QC sample. Signal intensity observed for QC1 was set to 100%.....	186
<b>Table 7.1</b> Overview of global LC-MS metabolomics studies using human plasma or serum.....	202
<b>Table 7.2</b> List of features exhibiting decreasing trend with increasing SPME extraction time.....	235

<b>Table 7.3</b> Summary of metabolite concentrations in human plasma determined using traditional sample preparation methods and comparison to normal concentrations expected in plasma according to the ranges reported in Human Metabolome Database. <sup>243-245</sup> .....	239
<b>Table 7.4</b> Summary of results (metabolite coverage and median RSD) observed for the analysis of technical replicates (n=7) of the same human plasma sample prepared using different sample preparation methods as discussed in experimental and analyzed using reverse-phase PFP LC-MS method. ....	241
<b>Table 8.1</b> List of features contributing to differentiation of UF samples according to CBZ dosing.	268
<b>Table 8.2</b> List of features contributing to differentiation of <i>in vivo</i> SPME samples according to CBZ dosing.....	269
<b>Table 8.3</b> List of features contributing to differentiation of <i>in vivo</i> SPME samples according to biochemical individuality.....	270
<b>Table 8.4</b> List of features observed using <i>in vivo</i> SPME and not observed using <i>ex vivo</i> SPME.....	272
<b>Table 8.5</b> List of features observed using <i>ex vivo</i> SPME and not observed using <i>in vivo</i> SPME.....	278



## List of Abbreviations

a	time constant
A	surface area
ADP	adenosine diphosphate
AGC	automated gain control
AMP	adenosine monophosphate
APCI	atmospheric pressure chemical ionization
ATP	adenosine triphosphate
$\beta$ -NAD	$\beta$ -nicotinamide adenine dinucleotide
$C_0$	initial analyte concentration
$C_{\text{FREE}}$	free (unbound) concentration of analyte
$C_{\text{TOTAL}}$	total (bound + unbound) concentration of analyte
CBZ	carbamazepine
CBZEP	carbamazepine epoxide
CE	capillary electrophoresis
CW-TPR	Carbowax-templated resin
DBT	dibenzothiophene
DIMS	direct infusion mass spectrometry
DVB	divinylbenzene
EDTA	ethylenediaminetetraacetic acid
ESI	electrospray
FDA	Food and Drug Administration
GC	gas chromatography

HBA 3-hydroxybutyric acid

HILIC hydrophilic interaction chromatography

HMDB Human Metabolome Database

HPLC high performance liquid chromatography

ID inner diameter

*i.v.* intravenous

$K_{fs}$  Distribution constant for an analyte between SPME fibre and sample

LC liquid chromatography

LOD limit of detection

Log P log of octanol/water partition coefficient

LOQ limit of quantitation

LLE liquid-liquid extraction

MALDI matrix-assisted laser desorption ionization

MDA multivariate data analysis

MRM multiple reaction monitoring mode

MS mass spectrometer/spectrometry

MW molecular weight

$n$  amount of analyte extracted by SPME fibre

$n_e$  amount of analyte extracted by SPME fibre at equilibrium

NA not available

ND not detected

NR not reported

OD outer diameter

PBA phenylboronic acid

PBS phosphate buffered saline, pH 7.4

PC principal component

PCA principal component analysis

PDMS polydimethylsiloxane

PFP pentafluorophenyl stationary phase

PK pharmacokinetic(s)

PM plasma protein precipitation with methanol

PP plasma protein precipitation with acetonitrile

ppm parts per million

q amount of calibrant desorbed from the fibre

$q_0$  amount of calibrant preloaded on fibre

Q amount of calibrant remaining on the fibre after extraction

QC quality control

QTOF quadrupole time-of-flight mass spectrometer

rpm revolutions per minute

RSD relative standard deviation

RT retention time

SAX strong anion exchange

SCX strong cation exchange

SD standard deviation

SEM scanning electron microscopy

SPE solid phase extraction

SRM selected reaction monitoring mode

SPME solid-phase microextraction

TIC total ion chromatogram

TOF time-of-flight mass spectrometer

UDP uridine diphosphate

UDPG uridine diphosphate glucose

UF ultrafiltration

UHPLC ultrahigh pressure liquid chromatography

t sampling time

$V_f$  volume of fibre coating

$V_s$  sample volume

v/v volume by volume

WAX weak anion exchange

WCX weak cation exchange

XIC extracted ion chromatogram

# Chapter 1

## Introduction

### 1.1 Metabolomics, metabonomics and biomarkers

Metabolomics can be defined as the comprehensive analytical approach to study all low molecular weight species present in a given biological system under study. Metabolome is the collection of all these small molecular weight species (typically defined as <1000 Da or <1500 Da).<sup>1</sup> The data obtained in metabolomics is complementary to data obtained by other “omics” approaches: genomics, transcriptomics and proteomics. The integration of all these types of biological data provides a holistic picture of a living organism as shown in Figure 1.1 and is invaluable within the discipline of systems biology. From historical perspective, metabolomics is both an old and a new field. Chinese doctors used ants for disease diagnosis based on the properties of patient’s urine in 1500-2000 BC, and similar approaches were employed in ancient Egypt and Greece.<sup>2</sup> The modern term of metabolomics was only coined in late 1990’s by Fiehn<sup>3</sup> but first metabolite profiling studies were carried out much earlier (1960-1970s) using gas chromatography-mass spectrometry (GC-MS) and can be classified as metabolomic studies under current terminology.<sup>2,4,5</sup> For instance, Williams discussed the utility of multicomponent analyses as early as 1950s<sup>6</sup>, while the major strides in carrying out such studies experimentally were made by Horning and Horning who even introduced the term “metabolic profiles” for the first time<sup>7,8</sup>. Jellum proposed the idea of finding biomarkers for all possible diseases and conditions once a full inventory of all constituents and their concentrations in biofluids and tissues can be established.<sup>9</sup> Finally, Pauling described the concept of personalized medicine which is currently accepted as one of the driving forces behind “omics” studies.<sup>10</sup> Thus, conceptually the field of metabolomics was born much earlier than given credit for, but the limitations of analytical methods employed could not fulfill the full promise of this novel concept back in 1960 and 1970s. More recently, technological advancements in instrumentation have sparked a flurry of research activity in this area because increased analytical capability enables much more complete global (untargeted) metabolomics studies with the objective of simultaneous analysis of as many metabolites as possible using a particular analytical platform.

Metabolomics approach appears to be particularly promising because metabolites represent endpoints of the molecular pathways perturbed by other “omes”. Thus metabolome defines the

individual phenotype, whereas transcriptomic and proteomic information alone does not reveal individual phenotypes.<sup>4, 11, 12</sup> For example, observed increases in mRNA may not always result in increases in protein expression, and an over-expressed protein may or may not be enzymatically active. The level of each metabolite is dependent not only on the concentration of proteins present within the system but also on processes such as transcription and translation, allosteric regulation of enzymes and the degree and type of protein-protein interactions. Most metabolites also participate in several metabolic pathways, which convolves biological interpretation and makes recent global approaches very attractive. For example, genome-scale models, show that <30% of metabolites are involved in only two reactions while ~12% participate in >10 reactions.<sup>13</sup> Most reactions involve more than one product and substrate, resulting in very tightly connected metabolic networks, which can be sensitive to even small perturbations in proteome.<sup>14</sup> In addition to genetic factors and health

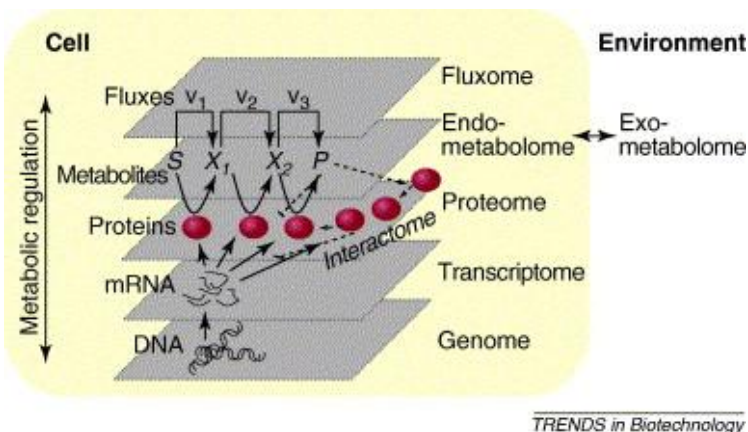


**Figure 1.1 Interaction of the different -omes in a cell. Each -ome (except the genome) is a complex function of the other -omes, and the amount of integration increases from the bottom to the top of the Figure. Thus, the metabolome and the fluxome represent integrative functions of the other -omes, and, at the same time, they are closely connected. Exchange with the environment occurs primarily via the metabolome (i.e. between the endometabolome and the exometabolome). Figure reprinted from reference with permission of publisher.<sup>13</sup>**

status, other factors also contribute to the observed metabolome of an individual and include environment, age, sex, dietary intake and gut microflora thus complicating interpretation of metabolomics data even further.<sup>15</sup> However, recent study of human urine over three-year period supports the idea of unique metabolic phenotype as it was possible to accurately classify urinary profiles belonging to particular individuals despite changes in their diet, gut microflora, lifestyle and

environmental factors.<sup>16</sup> This indicates that genetic factors play important role in an individual's metabolomic phenotype, and that metabolic phenotypes are not extremely variable on the timescale of years for an individual. Of course, additional large-scale longitudinal studies are needed to further elucidate the contributions of various factors to metabolic phenotypes and the stability of metabolic phenotype over an individual's lifetime. In another interesting study, Minami *et al.* successfully used global metabolomics of blood, to accurately predict internal body time in mice.<sup>17</sup> This study provides important resource regarding the number and identity of metabolites which exhibit known circadian rhythms, and shows that the combination of these metabolites can be used to pinpoint exact internal body time due to the presence of highly reproducible oscillating time profiles. The prediction was robust in terms of different strains of mice, sex, age, and feeding conditions and could even detect jet-lag.

The overall workflow of a global metabolomics study is shown in Figure 1.2. The first step of this type of global metabolomics study typically involves differential comparison of several subject or treatment groups (for example: normal *versus* treated, healthy *versus* disease) without *a priori* identification of all metabolites detected. After sample collection, data is processed using appropriate statistical techniques (for example, principal component analysis) in order to isolate a smaller number of potentially relevant metabolites that are believed to differentiate the groups (potential biomarkers).

According to National Institute of Health definition, biomarker is a characteristic that is objectively measured and evaluated as an indicator of normal biological processes, pathogenic processes, or pharmacologic responses to a therapeutic intervention.<sup>18</sup> The main uses of biomarkers in medicine are diagnosis of human disease, assessment of drug efficacy and/or safety and selection of patients with highest probability of benefiting from a particular treatment. After the first step of isolation of potential biomarkers, subsequent experiments focus on their identification and the development of quantitative analytical methods for selected potential biomarkers. In final stage, the utility of biomarker is further investigated/confirmed using large-scale studies on a large number of subjects and the biological explanation for the observed change in biomarker is also researched.

Majority of global metabolomic studies to date deal with the first stage of the process where the goal is to simply isolate potential metabolites of interest (“differentiating metabolites”) and/or improve the analytical methodology employed.<sup>19</sup> The outcomes of such studies cannot be viewed as potential biomarkers as these differentiating species may not be related to the disease of interest, but may be involved in general processes such as inflammation. For example, Koulman *et al.* cite various

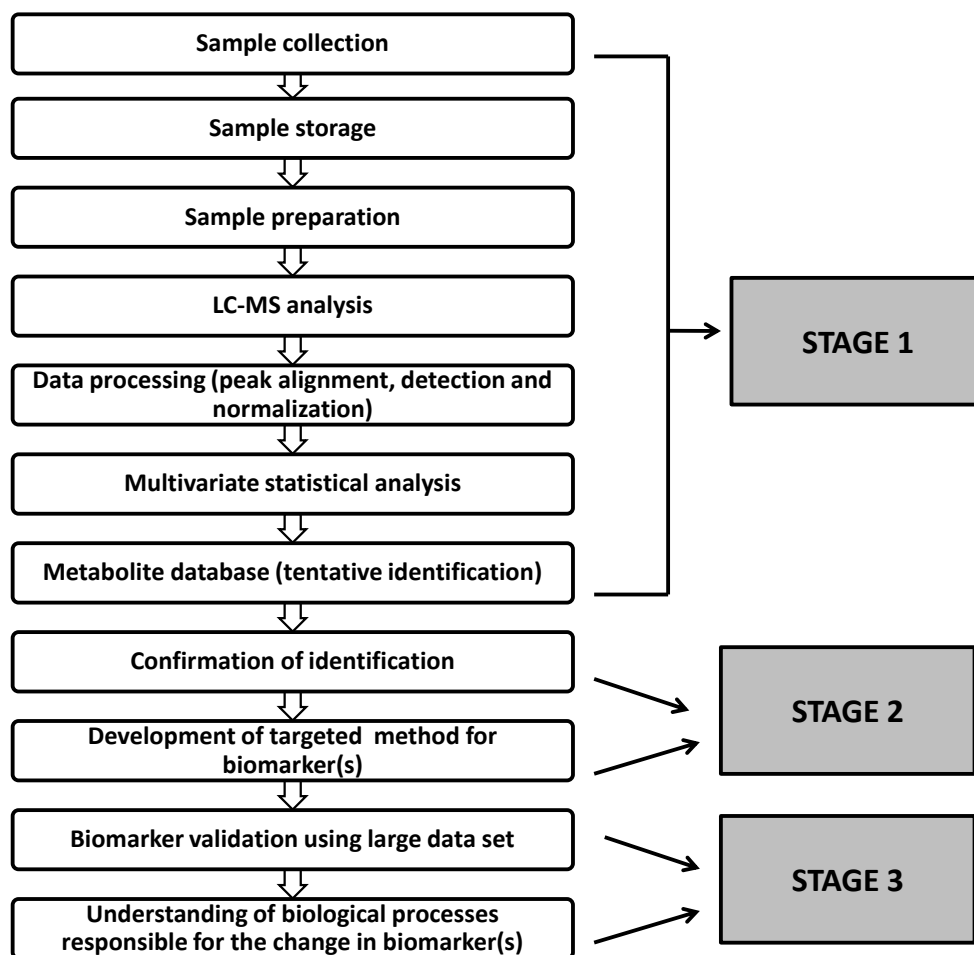


**Figure 1.2** Typical workflow of a global metabolomics study.

studies where glycerophosphatidylcholines are reported as differentiating metabolites in various diseases, but clearly these species are not specific biomarkers of a particular disease, which minimizes their utility in clinical diagnosis.<sup>19</sup> In other words, a clinically useful biomarker must distinguish not only between a healthy and diseased individual, it must also be able to distinguish between the individuals with one particular disease *versus* other diseases. Overall, the difficulties in the initial stage of metabolomic studies have prevented rapid progress in biomarker validation stage with a notable exception of a recent study reporting sarcosine as potential biomarker of prostate cancer.<sup>20</sup> In this study, after isolation of sarcosine as putative biomarker of prostate cancer in urine and confirmation of its elevated levels using targeted GC-MS method in an independent sample set, the authors also show that both the addition of sarcosine and genetic knock-down of enzyme responsible for degradation of sarcosine increase invasiveness of cells. Conversely, the inhibition of



enzyme that produces sarcosine limits prostate cancer invasion. These biological assays provide additional evidence of a mechanistic link between this metabolite and prostate cancer progression, and can also potentially lead to new drugs that target this pathway. This example application shows the potential of global metabolomic studies using liquid chromatography-mass spectrometry (LC-MS). It is generally believed that the use of several biomarkers can provide better predictive value than the use of single biomarker, and it is hoped that the use of global metabolomics approaches can enable the recognition of relevant patterns for sets of biomarkers. However, the discovery of clinically relevant biomarkers is only one type of application of the field of metabolomics.<sup>1, 19</sup> Other applications include understanding of disease<sup>21, 21-23</sup> and other biological processes (growth, aging, stress, etc.); toxicology<sup>24</sup>; effect of nutrition on health<sup>15, 25</sup>; understanding the mechanisms of drug action, metabolism or toxicity<sup>23, 26, 27</sup>; understanding of gene function (functional genomics)<sup>4, 21</sup>; biotechnology and bioengineering<sup>28</sup>; and plant metabolism and breeding<sup>4, 29</sup>.

The main difference between the terms metabolomics and metabonomics is that the goal of metabolomics is quantitative and qualitative analysis of metabolites in a given biological system, whereas the goal of metabonomics is the comparison of metabolite levels in a given system in response to a particular stimulus or treatment.<sup>30, 31</sup> Thus, by definition, the evaluation of normal levels of metabolites in urine, for example, would fall under the category of metabolomics study, while the comparison of metabolome of healthy versus diabetic mice would fall under the category of metabonomics study. In more recent literature, the distinction between the two terms is slowly disappearing, with both terms used interchangeably. In this dissertation, the term metabolomics will be used throughout.

## **1.2 Analytical approaches for global metabolomic studies**

The analytical approaches used in global metabolomic studies are not yet as well-defined as in other “omics” studies and are currently an active area of research. Considering the large number of possible metabolites, their chemical diversity and large range of possible concentrations (estimated 7-9 orders of magnitude<sup>14</sup>), there is no single analytical platform that can claim to achieve full coverage of the entire metabolome. As such, a variety of techniques is employed, with nuclear magnetic resonance (NMR) and mass spectrometry (MS) being the most dominant. NMR is a non-destructive analytical method and also provides the advantages of absolute quantification and identification, good reproducibility, easy sample preparation and high sample throughput. It can be employed both in the solution state and for solid samples such as tissues using high-resolution magic angle spinning.

However, sensitivity of NMR is relatively low, so typical metabolomic studies by NMR are able to accurately determine about 25-100 of most abundant metabolites even when hyphenated with liquid chromatography to reduce sample complexity and improve metabolite coverage.<sup>21, 22, 32</sup> A typical biological fluid sample is expected to contain >1000 metabolites even by most conservative accounts<sup>33, 34</sup>, while Human metabolome project estimates the number of endogenous metabolites in humans to be ~3000<sup>35</sup>. As a result, MS has been employed extensively to increase metabolite coverage and is starting to overtake NMR as the analytical platform of choice for metabolomic studies.

Direct infusion MS (DIMS) has been successfully used for classification and identification of microorganisms<sup>11, 36</sup> and in plant metabolomics<sup>29</sup>. Its advantages are high-throughput with typical analysis times 1-5 min.<sup>14, 37</sup> However, competitive ionization of metabolites can lead to low sensitivity and low metabolite coverage as well as reproducibility issues. Furthermore, structural isomers cannot be differentiated, and data interpretation is complicated due to the presence of multiple ions from the same metabolite species (adducts, fragments or multimers).<sup>37-39</sup> One of the reasons DIMS has been successful in cell and plant metabolomics, but not in other areas, is because cells and plants can be grown with isotopically labelled media (for example <sup>13</sup>C by growing plant using <sup>13</sup>CO<sub>2</sub> in the growth chamber). The fully isotopically-labelled biological material is then used as complex internal or external standard, and offers several advantages including (i) ability to differentiate ions of biological origin versus background and contaminant ions (ii) improved relative quantitation for observed metabolites, as the labelled metabolite can be used to reduce effects of ionization suppression from the data and (iii) improved identification capability because <sup>13</sup>C labelling provides number of C atoms thus reducing number of potential chemical formulas for a given unknown metabolite.<sup>39</sup> High-throughput metabolic profiling strategy using matrix-assisted laser desorption ionization (MALDI) MS has also been proposed.<sup>40, 41</sup> The main advantages of this approach are the use of very small sample volumes (1 μL), better tolerance for the presence of salts within the sample and very rapid analysis time (1.5 min). The formation of multiple adducts such as encountered in electrospray ionization (ESI) is avoided, resulting in easier interpretation of mass spectra. However, only negative ionization mode is feasible due to the limited availability of appropriate matrices for the analysis of small molecular weight compounds without the interference of matrix background and no data on analytical reproducibility is provided, although typical RSDs of >30% can be expected in typical MALDI analysis according to literature.<sup>37</sup> Recently, the utility of the combination of ion mobility and mass spectrometry was also shown for high-throughput metabolomics.<sup>42</sup>

Due to the complexity of biological samples, however, best results are obtained if mass spectrometry is preceded by an appropriate separation step, such as gas chromatography (GC), liquid chromatography (LC) or capillary electrophoresis (CE). The choice of separation technique is primarily dictated by analyte properties, with GC-MS most suitable for volatile and semi-volatile analytes, LC-MS most suitable for polar and non-volatile analytes and CE most suitable for charged analytes. In a recent study investigating potential biomarkers of nephrotoxicity, comparison of GC-MS and LC-MS methods resulted in 547 metabolites detected in kidney tissue and 657 metabolites in urine samples.<sup>43</sup> Among these 30% and 46% respectively were detected by GC-MS, and the remaining were detected by LC-MS. In a similar study on human plasma, approximately 60% of metabolites were detected by LC-MS and 40% by GC-MS, with about 10-15% overlap between the two platforms.<sup>44</sup> A recent systematic study compared several GC, LC and CE-MS platforms (two complementary methods/platform) using a defined mixture of 91 metabolites covering central carbon metabolism, redox metabolism, amino acids and nucleotides.<sup>45</sup> For the analyses on a single platform, LC-MS provided the most comprehensive metabolite coverage with 65 out of total of 75 non-isomeric species detected, whereas CE-MS and GC-MS platforms detected 64 and 42 species, respectively. About 23-33 compounds could be detected using all three platforms depending on the complexity of sample matrix. CE-MS was found the least suitable platform for metabolomics because of poor robustness observed for the analysis of real biological samples.

In comparison to GC-MS, LC-MS does not require derivatization step and can be coupled to fraction collector for further metabolite characterization. One major disadvantage of LC-MS versus GC-MS is the lack of LC-MS libraries which makes compound identification very challenging. The main reason for the lack of libraries, is the variability of ESI which can result in the variation in relative ion abundances due to adduct formation and in-source fragmentation.<sup>37</sup> Due to the variability inherent in both chromatographic and MS steps, LC-MS data are much less robust than NMR data, and comparison between the data acquired on different instruments and even on different days can be very difficult, if not impossible.<sup>23</sup> In order to facilitate comparisons between different data sets collected by different groups, an initiative to standardize the information reported for any metabolomic study has been proposed.<sup>46</sup> These guidelines address all aspects of metabolomics workflow including sample collection, preparation, analysis and data processing to ensure sufficient detail is provided to enable more successful subsequent data interpretation. In terms of sample preparation, the draft guidelines recommend the documentation of addition of buffers and/or internal standards, storage conditions, detailed extraction protocol, any derivatization strategies, description of

all sample containers used during sample handling, and details of any robotics equipment used, as all of these can impact the collected metabolomics data.

### **1.3 Sample preparation methods for global metabolomic studies by LC-MS**

The choice of sample preparation method plays an extremely important role in metabolomic studies because it affects both the metabolite content and data quality.<sup>12, 34, 47</sup> Despite its importance, sample preparation is often an overlooked aspect of metabolomics workflow.<sup>34</sup> An ideal sample preparation method for the metabolomic analysis of biofluids by LC-MS should (i) be non-selective (ii) be simple and fast to prevent metabolite loss and/or degradation during preparation procedure and enable high-throughput (iii) be reproducible and (iv) incorporate metabolism quenching step.<sup>31</sup> Metabolism quenching step aims to stop metabolic processes through the use of low temperatures (cold solvent addition, freezing in liquid nitrogen), addition of acid or fast heating.<sup>14, 41, 45, 48, 49</sup> However, metabolic processes are very fast with timescales  $<1$  s, so the quenching step must be extremely rapid to be fully effective, and can be very difficult to implement for biological samples within appropriate time scale.<sup>14</sup> Quenching step is typically included in most studies on microorganisms, but similar studies on biofluids typically do not employ any quenching step and the analytical data in support of omission of quenching step for biofluids is currently lacking. As such, it is not clear how well the analyzed metabolome reflects the true metabolome at the time of sampling and further research is clearly needed. Furthermore, even when a quenching step is applied, the application of this step can cause inadvertent degradation or loss of some metabolites. Freezing can result in loss of metabolites, while the use of acidic treatments can cause severe degradation of some metabolites, poor overall metabolite coverage and poor compatibility with MS methods.<sup>22</sup> The following sections provide a brief overview of the most common methods employed for metabolomics analysis of biofluids, tissues and microorganisms, while section 7.1 provides a more in-depth discussion of the sample preparation methods employed to date, specifically for the analysis of human plasma.

#### **1.3.1 Sample preparation methods for biofluids**

The most commonly employed method for global metabolomic studies of biofluids by LC-MS is protein precipitation with organic solvent (methanol, acetonitrile, ethanol, acetone or combination thereof), and for urine “dilute-and-shoot” strategy is also often employed.<sup>31</sup> These methods predominate in the field of metabolomics because they are the most unselective, thus providing high metabolite coverage. However, the main issues that are often overlooked or inadequately discussed in

reported precipitation methods are ionization suppression which can occur due to the competitive nature of ESI process and the issues of metabolite loss due to co-precipitation with proteins<sup>50</sup> and/or poor solubility of metabolites in selected solvent. Furthermore, the use of such methods with poor sample clean-up can significantly reduce column lifetime and cause contamination of ion source, thus requiring frequent MS cleaning. In fact, several publications to date advocate metabolomics sample runs of no more than 100 samples to ensure good data quality, with source cleaning between each data set.<sup>51, 52</sup> This is not surprising when the complexity of a typical biological fluid is considered. For example, total protein concentration of blood serum or plasma is 6-8 g/dL, while concentration in urine is significantly less, but still considerable, with approximate concentrations of 50-100 mg/dL.<sup>50</sup>

More recently, few reports of successful use of ultrafiltration<sup>32, 53-55</sup> and solid-phase extraction methods<sup>24, 26, 51, 56</sup> were published. Ultrafiltration is a simple sample preparation procedure where a sample is filtered through a special filter which only allows molecules of certain molecular weight to pass through, and the filtration is achieved through application of pressure or via centrifugation. Filters with molecular weight cutoffs of 3000 Da, 10000 Da and 30000 Da are commonly available. The use of 3000 Da filter can physically separate small molecular weight species from proteins or other macromolecules present in a given sample, and is thus useful for metabolomics. Solid-phase extraction (SPE) uses large amount of sorbent, typically housed in cartridge format, to exhaustively extract an analyte from a given sample. The analyte is subsequently removed from the sorbent using solvent elution. Depending on the sample volume applied on the cartridge and volume of elution solvent used, significant analyte pre-concentration can be achieved using this method. Furthermore, prior to the elution process, cartridge can be washed to remove various interferences which are less strongly bound to the sorbent than the analyte of interest, thus providing better sample clean-up than achievable by simple plasma protein precipitation methods. The main driving force for exploring the use of SPE in LC-MS metabolomics applications is to try and address matrix effects and increase column lifetime and overall method robustness by injecting much cleaner samples. The main disadvantage is that the selection of the sorbent material increases the selectivity of the preparation procedure which can reduce metabolite coverage. For metabolomics applications, the use of C<sub>18</sub> sorbent<sup>51</sup>, the combination of C<sub>18</sub> and polystyrene-divinylbenzene sorbents<sup>56</sup> and the use of divinylbenzene/n-vinylpyrrolidone co-polymer<sup>24, 26</sup> has been proposed. In a recent plant metabolomics study, the combination of strong cation-exchange and anion-exchange sorbent was also successfully employed and found to reduce ionization suppression effects.<sup>39</sup>

One emerging technique in the field of bioanalysis and metabolomics is the dried blood spot sampling.<sup>1</sup> In this approach, small drop of whole blood is placed on filter paper and allowed to dry. This spot is subsequently extracted in solvent prior to analysis. The use of this sampling strategy has proven very successful for neonatal screening using targeted metabolite approach. However, limited data to date exists on the stability of analytes within dried blood spots, and the effect of long-term storage on observed metabolite profile for untargeted studies.<sup>1</sup>

In addition to the choice of sample preparation method, all steps from sample collection to the injection of the sample into LC-MS system can influence the observed metabolite profile. These include choice of anticoagulant, sample processing times and temperatures, degree of hemolysis in the sample, sample storage parameters, clotting times (for serum), age of the sample and the number of freeze-thaw cycles.<sup>47,57</sup> For example, the choice of anticoagulant used during blood collection was found to influence observed metabolic profiles in a recent study.<sup>58</sup> Another study by NMR found differences in energy metabolites depending on clotting time used for human serum.<sup>47</sup> They recommend the use of clotting times up to 35 min on ice, to ensure no compositional changes occur, and immediate centrifugation post-clotting is necessary. For both plasma and serum, exact time to centrifugation is important to eliminate bias in order to minimize metabolism and transport of metabolites between different compartments. Remaining enzymatic activity was found in rat plasma stored refrigerated for prolonged periods, and resulted in increased levels of choline, glycerol, tyrosine and phenylalanine.<sup>59</sup> In another study of the factors influencing the stability of metabolites in cerebrospinal fluid, the authors found that rapid centrifugation and snap-freezing immediately after collection were important to preserve accurate metabolite levels.<sup>60</sup> After delayed storage of 30 and 120 min, numerous metabolites showed significantly elevated levels including glucose and ten amino acids (Thr, Glu, Gly, His, Ser, Ala, Phe, Tyr, Ile and Asn) due to unquenched enzymatic activity. The storage of plasma or urine at ambient conditions can also cause the depletion of easily oxidizable species such as ascorbic acid, adrenaline, noradrenaline and dopamine.<sup>61</sup> Enzymatic conversion of various species can also occur rapidly after sample collection, for example conversion of cytidine into uridine or adenosine into inosine.<sup>61</sup> Another study investigating optimum storage conditions for peptides found clear dependence of peptide recovery for hydrophobic peptides on storage container.<sup>62</sup> Surely, similar results can be expected for some of the more hydrophobic metabolites and this deserves further investigation. These examples show various possible sources of systematic bias which can affect the results of metabolomics analysis especially during statistical analysis of data, and has been identified as a critical threat to biomarker research.<sup>47</sup>

The recommendations based on systematic investigation of bacterial overgrowth in urine included urine centrifugation immediately upon collection, immediate refrigeration and addition of appropriate preservatives such as boric acid or sodium azide prior to long-term storage in freezer.<sup>63</sup> Although this study was performed from proteomics perspective, the presence of bacterial contamination would be expected to have adverse effects on metabolite profiles as well, although this effect has not yet been examined in detail. For the analysis of urine samples, storage at even -80°C was found to impact metabolite levels and pH, with some authors advocating storage for a minimum of 1 week to achieve consistent degradation of urinary components across the cohort.<sup>64</sup> Although such approach can facilitate comparison across samples, it is clear that the analyzed metabolome is not entirely reflective of true metabolome, as the potential metabolites of interest may not be present at the time of analysis while peaks due to degradation may be misidentified as possible features of interest.

In fact, processes occurring prior to sample collection also impact the composition of biofluids collected. For example, dietary intake was found to affect observed profiles in human and animal biofluids.<sup>65, 66</sup> These effects could be minimized in urine by the consumption of standardized diet by subjects on the day prior to the sample collection, but such standardized diet approach did not reduce variability of plasma and salivary metabolomics profiles.<sup>15, 25, 23, 23</sup> Gut flora was also found to have significant impact on metabolomics data, both in human and animal studies, with up to 15-fold differences in some metabolites observed.<sup>23, 25</sup> Obviously, this factor cannot be standardized in human studies, but improved understanding of contributions of gut flora can aid in data interpretation.

More similar studies for collection of specimens for metabolomic studies are needed in order to eliminate bias caused by sampling procedures and to enable comparison of various data sets. For metabolomics analysis, the choice of plasma versus serum could also play an important role since the clotting process needed to obtain serum is carried out at room temperature for 30-60 min, but no relevant studies have been reported to date on how the clotting step impacts the composition of the metabolome.

The need for the standardization of sample collection and storage procedures has been well-recognized in proteomics community because of its documented impact on analytical outcome.<sup>57</sup> This idea is also slowly becoming more accepted in the field of metabolomics. Standardized collection, storage and handling protocols, and ensuring all the samples are treated exactly the same can help alleviate some of these problems, so that truly differential metabolites rather than artifacts are detected during unsupervised statistical analysis. When such proper care is taken, analytical variation

was shown to be smaller than biological variation using both NMR and LC-MS studies.<sup>47, 67</sup> However, the standardization merely ensures that all of the samples are treated exactly the same, thus minimizing the differences between samples due to handling. It does not address how well the composition of the metabolome at the time of the analysis matches the metabolome composition in the living system at the time of sampling. Thus, additional research into best practices to ensure that the analyzed metabolome reflects well the true metabolome is also needed.

### **1.3.2 Sample preparation methods for tissues**

A recent comparison of methods for the extraction of selected target metabolites from muscle tissue found the best performance for boiling water extraction, while boiling ethanol and perchloric acid showed the poorest overall performance.<sup>48</sup> Methods that can simultaneously extract both hydrophilic and lipophilic species, such as chloroform/methanol extraction are also popular but the use of chloroform is problematic in LC-MS necessitating further sample manipulation prior to injection.<sup>22</sup> Sun *et al.* proposed methanol/chloroform/water extraction protocol for the analysis of mouse heart tissue in order to extract both lipophilic and hydrophilic species, and eliminate ionization suppression effects inherent when perchloric acid extraction was used for the same analysis.<sup>41</sup> Williams *et al.* successfully used similar extraction approach for brain samples.<sup>68</sup>

### **1.3.3 Sample preparation methods for microorganisms**

The choice of sample preparation methods for the analysis of cells is also complicated and depends on the type of cells and whether the analysis of intra- or extra-cellular metabolites is of interest.<sup>11, 49</sup> For the analysis of extra-cellular metabolites, the possibility of inadvertent leakage of intracellular metabolites must be examined, while for the analysis of intra-cellular species effective methods of disruption of cell membrane are necessary. Canelas *et al.* compared the efficiency of five commonly used methods for intracellular metabolite extraction (quantitative analysis of 44 metabolites) from yeast cells: hot water extraction, boiling ethanol extraction, chloroform-methanol extraction, acidic acetonitrile-methanol extraction and freezing-thawing cycles in methanol.<sup>69</sup> All of these methods are well-established for extraction of intracellular metabolites, with the first two available since 1950's and the rest of methods introduced as milder alternatives in 1990's. The results show the best performance of boiling ethanol extraction and chloroform-methanol extraction for the majority of metabolites tested (38 out of 44), indicating that these methods meet most of the criteria of ideal metabolomics method for yeast. On the other hand, the results for acidic acetonitrile-methanol and for



freezing-thawing cycles in methanol methods show poorer precision, and significant changes in recovery of phosphorylated metabolites attributed to metabolite loss (solubility issues and accidental co-precipitation) or metabolite conversion during extraction procedure (due to incomplete metabolism quenching). The latter result is particularly interesting as the literature prior to this study reported freezing-thawing method in methanol as the best choice for yeast metabolomics. Hot water extraction generally performed well but evidence of protein degradation was observed which resulted in increase in the levels of relevant amino acids. Although not specifically focused on the development of sample preparation methods, another study reports the potential losses of oxaloacetate, oxalate and glyceraldehyde during sample preparation process and attributes these losses to the incorporation of a drying step within the procedure.<sup>45</sup>

Bolten *et al.* showed that the choice of best sample preparation protocol is organism-dependent and should be properly validated prior to start of any metabolomics study.<sup>49</sup> The common quenching method of cold methanol followed by centrifugation was found to lead to drastic loss of metabolites (>60%) resulting in large errors in determined *in vivo* intracellular levels of metabolites in prokaryotic organisms, while fast filtration worked well for metabolites with low turnover rates, but is not sufficiently rapid for metabolites with high turnover rates. Among the various methods tested, no single method appeared sufficiently universal, and the authors strongly recommend further research into improvement and design of sampling protocols in order to improve the quality of metabolomics data collected. Currently, the one species with commonly accepted sample preparation protocol is yeast and involves cold methanol quenching and boiling ethanol extraction.<sup>45</sup> Energy charge ratio ( $([ATP]+0.5[ADP])/([ATP]+[ADP]+[AMP])$ ) is frequently used to evaluate sample preparation methods.<sup>49, 70</sup> These phosphate species have very fast turnover rates in cells with half lives less than 0.1 seconds, so they can be used to evaluate the efficiency of metabolism quenching step in cell metabolomic studies.<sup>28</sup> The ratio of 0.80-0.95 is expected for a growing cell, but an examination of sample preparation methods reported in literature showed ratios far from expected physiological range (0.16-0.66) indicating that the metabolism was not sufficiently quenched.<sup>49</sup> Although this is just an example of a small subset of metabolites, similarly erroneous results can be expected for other metabolites with high turnover ratios.

#### **1.3.4 Importance of sample preparation method selection**

It is clear from above discussion that the choice of sampling, sample collection and sample preparation strategy plays an important role in the quality of metabolomics data. Clearly, the success

of metabolomics requires further research in this important area in order to provide better understanding of which method should be employed for which type of sample and analysis, and to better understand the shortcomings of the methods employed and thus limitations of the data collected. Without such fundamental studies, the field of LC-MS-based metabolomics can continue to suffer from isolation of “biomarkers” which are subsequently discovered to be artifacts of the analytical procedure. This point was well-illustrated by Canelas *et al.* who showed that even the relative levels of metabolites (up- or down-regulation when comparing two conditions) could be distorted on the basis of sample preparation method selection leading to erroneous conclusions,<sup>69</sup>.

In contrast, for the analysis of human hepatocytes, the source of hepatocytes was the most significant contributor to the variation observed in regulation processes and collected metabolomic data.<sup>71</sup> This is in line with majority of other well-designed studies where technical variability (evaluated by preparation of technical replicates of the same sample) is significantly lower than biological variability. For example, another study used ANOVA to characterize analytical, sample preparation and biological variability within collected data sets, and found analytical < sample preparation < biological regardless of analytical platform employed (GC-MS versus LC-MS).<sup>72</sup>

These examples collectively show that increased validation and understanding of existing sample preparation methods as well as the emergence of new sample preparation techniques for metabolomics is necessary before the potential of metabolomics can be fully exploited. Once these technical aspects are adequately addressed, metabolomic studies can start to generate accurate quantitative data and build appropriate databases which will allow subsequent integration with other “omics” techniques, both of which are crucial to the success of this field as recently reviewed by Nielsen and Oliver.<sup>13</sup>

Given the variety of problems described above, *in vivo* sample preparation and/or analysis becomes an attractive option for its capability to provide a true(r) representation of the metabolome without some of the issues inherent in multi-step sample handling procedures and taking the sample out of its biological milieu.<sup>4</sup> In fact *in vivo* dynamics, for example metabolite fluxes, can only be revealed in intact systems in their natural environment, and steady-state approaches are not sufficient for such analysis.<sup>73</sup>

## 1.4 Introduction to solid-phase microextraction (SPME)

Solid-phase microextraction (SPME) is a non-exhaustive sample preparation method which permits integration of sampling and sample preparation steps. The technique was originally introduced for the extraction of organic species followed by GC analysis<sup>74, 75</sup>, but over the past twenty years the technique has matured with numerous applications spanning environmental, food, pharmaceutical, forensic and clinical fields.<sup>76-78</sup>

The most common format of SPME is fibre geometry, in which a small amount of extracting phase is immobilized on a solid support as shown schematically in Figure 1.3. Other formats of SPME such as thin film, coated stir-bar and coated capillary are also available, and the format of the device can be modified depending on the application requirements. The main steps of SPME procedure are (i) extraction of the analyte by SPME coating from the sample solution and (ii) desorption of the extracted analytes from the coating. The extraction process can be carried out by exposing fibre to the headspace above sample solution (headspace extraction) or by direct contact of the fibre with the sample solution (direct immersion). The former is applicable to volatile and semi-volatile species, while the latter extraction mode can be applied regardless of analyte volatility, and is illustrated in Figure 1.3 (a). The desorption of the analytes from the coating can be carried out (i) thermally by direct insertion of fibre into GC injector or (ii) using appropriate solvent as shown in Figure 1.3 (b). The work described in this thesis deals with the analysis of polar and/or non-volatile species from biological fluids, so direct extraction mode and solvent desorption were utilized throughout this work.

The amount of analyte extracted by SPME depends on the time of contact between sample and extraction phase. If the time of contact is sufficiently long, equilibrium between extraction phase and sample is established. In this case, the amount of analyte extracted is given by Equation 1.1,

$$n_e = \frac{C_0 K_{fs} V_s V_f}{K_{fs} V_f + V_s} \quad \text{Equation 1.1}$$

where  $n$  is the number of moles of analyte extracted,  $C_0$  is the initial analyte concentration in the sample,  $V_s$  is the volume of the sample,  $V_f$  is the volume of fibre coating, and  $K_{fs}$  is the distribution constant between SPME coating and sample matrix defined as the ratio of analyte concentration in the coating  $C_f^\infty$  to the analyte concentration in the sample at equilibrium  $C_s^\infty$  according to Equation 1.2

$$K_{fs} = C_f^\infty / C_s^\infty \quad \text{Equation 1.2}$$

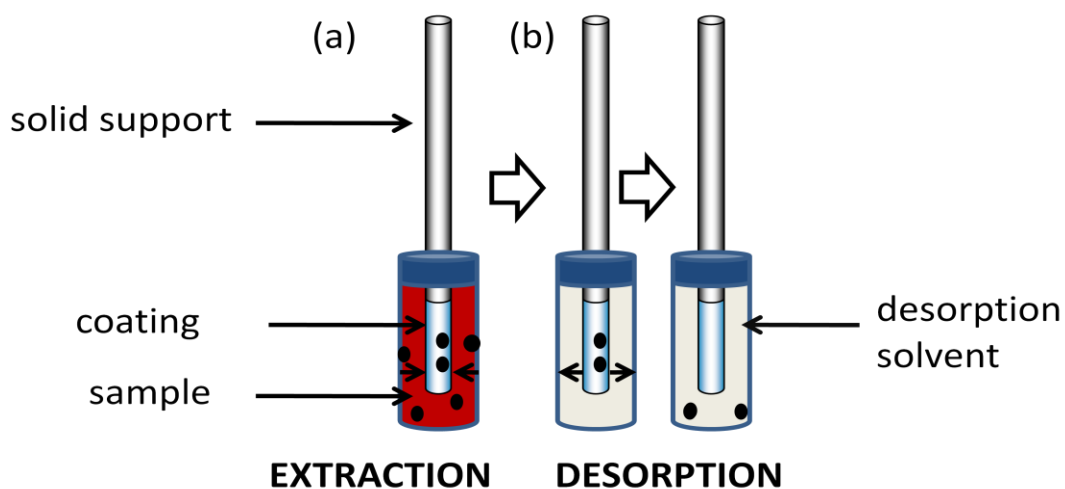


**Figure 1.3 Schematic of SPME procedure using direct extraction mode. (a) Fibre is exposed directly to the sample solution, and analyte of interest is extracted into the coating. (b) Fibre is now exposed to desorption solvent, and the analyte is desorbed from the coating into the solvent solution. Small arrows indicate the direction of mass transfer.**

The magnitude of  $K_{fs}$  depends on the nature of analyte and coating selected for the analysis, but is also impacted by the exact properties of sample matrix such as temperature, pH, addition of organic solvent and ionic strength, so it is important to keep these factors constant during sample analysis.

Microextraction process is considered complete when equilibrium is reached between sample and coating, and increasing the extraction time beyond the time required to reach equilibrium does not result in any further increases in the amount extracted within experimental error. Thus, microextraction methods are considerably different from traditional exhaustive methods of sample preparation such as SPE, because complete extraction of analyte from the sample is not achieved. Only a small portion of analyte is extracted from the sample because the employed volume of extraction phase is typically much smaller than the sample volume. This is in contrast to SPE, where large volume of sorbent is used to ensure exhaustive removal of analyte from the sample.

Equation 1.1 is applicable to absorptive coatings, such as polydimethylsiloxane (PDMS) where analyte can diffuse within the entire coating volume within the time scale of the experiment. In contrast, solid adsorptive coatings such as polypyrrole have limited number of surface sites, and the diffusion coefficient of analyte within the sorbent is too small, so the analytes can only be extracted

by the surface of the coating and not diffuse within the entire volume of the coating. In this case the amount of analyte extracted at equilibrium can be calculated using Equation 1.3,

$$n_e = \frac{C_0 K_{Afs} V_s V_f (C_{f \max} - C_f^\infty)}{V_s + K_{Afs} V_f (C_{f \max} - C_f^\infty)} \quad \text{Equation 1.3}$$

where  $C_{f \max}$  is the maximum concentration of active sites on the coating,  $C_f^\infty$  is the equilibrium concentration of analyte on the fibre, and  $K_{Afs}$  is the analyte's adsorption equilibrium constant rather than partitioning constant described in Equation 1.1. From Equation 1.3, it can be seen that for low analyte concentrations on the fibre (if  $C_f^\infty \ll C_{f \max}$ ), when the number of occupied sites is low, the amount of analyte extracted is linearly proportional to initial sample concentration. However, if analyte concentrations are sufficiently high, saturation of the surface can occur, which results in nonlinear adsorption isotherms. Furthermore, one analyte can be competitively displaced from the coating by other analytes or other competing interferences present in the sample. The likelihood of this occurrence depends on the magnitude of K values of competing interferences as well as their concentration in the matrix.

Furthermore, Equation 1.1 assumes that sample matrix is homogenous and that no headspace is present in the system. For multi-phase systems and heterogeneous samples, this equation can be further modified to Equation 1.4

$$n_e = \frac{K_{fs} V_f C_0 V_s}{K_{fs} V_f + \sum_{i=1}^{i=m} K_{is} V_i + V_s} \quad \text{Equation 1.4}$$

where  $K_{is} = C_i^\infty / C_s^\infty$  is the distribution constant of the analyte between the  $i^{\text{th}}$  phase and the matrix of interest, and the rest of the terms are the same as defined previously. For example,  $i^{\text{th}}$  phase can be headspace, and contribution of this phase should be taken into account for volatile analytes. In complex matrices,  $i^{\text{th}}$  phase can be binding matrix such as proteins present in blood samples. Equation 1.4 has two very important consequences: it shows that the amount of analyte extracted is proportional to unbound analyte concentration and that the exact composition of sample matrix can impact the amount extracted by SPME when dealing with complex heterogeneous samples. The former is an important advantage of SPME over traditional methods, as it enables the use of SPME to determine free (unbound) or total (bound + unbound) concentration of analyte in given sample by performing appropriate calibration in appropriate sample matrices with (for total concentration) and

without (for free concentration) presence of binding matrix. However, from calibration perspective, Equation 1.4 shows that strict control is necessary to ensure calibration samples exactly match the composition of real samples, and that small variations in matrix composition can have adverse effects on method performance.

From theoretical perspective, time required to reach equilibrium is infinite. From practical viewpoint, it is useful to define equilibrium time as the time required to extract 95% of analyte and can be approximated by Equation 1.5

$$t_e = t_{95\%} = 3 \frac{\delta K_{fs} (b - a)}{D_s} \quad \text{Equation 1.5}$$

where  $D_s$  is the diffusion coefficient of the analyte in the sample matrix,  $(b-a)$  is the coating thickness and  $\delta$  is the thickness of boundary layer. The time required to reach equilibrium depends on factors such as agitation conditions, physicochemical properties of analytes and the dimensions of sample matrix and fibre coating. Thus, for best sample throughput, it is recommended to use thin coatings and employ efficient agitation conditions.

The extraction process can be interrupted before equilibrium is reached, and in this case the amount of analyte extracted is based on the timed accumulation of the analyte in the extraction phase and can be calculated using Equation 1.6 proposed by Ai<sup>79</sup>:

$$n = (1 - e^{-at}) \cdot \frac{C_0 K_{fs} V_s V_f}{K_{fs} V_f + V_s} = (1 - e^{-at}) \cdot n_e \quad \text{Equation 1.6}$$

where  $t$  is the extraction time and  $a$  is time constant whose magnitude depends on factors such as mass transfer coefficients, distribution constant, sample volume, and volume and surface area of extraction phase. When equilibrium is reached, Equation 1.6 reduces to Equation 1.1. Clearly, the amount of analyte extracted is the highest at equilibrium, so if highest analytical sensitivity is needed for a particular application, extraction should be performed at equilibrium. However, if analytical sensitivity achievable with short extraction times is sufficient for a given application, pre-equilibrium SPME can be used to increase sample throughput.

Both equations 1.1 and 1.6 show that the amount of analyte extracted is linearly proportional to initial sample concentration, thus enabling quantitative analysis. However, for this linear relationship to hold true in pre-equilibrium case (Equation 1.6), agitation conditions and extraction time must

remain constant. In contrast, the amount of analyte extracted is independent of agitation conditions at equilibrium.

One interesting feature of SPME is that under the conditions of negligible depletion, when  $V_s \gg V_f K_{fs}$ , Equation 1.1 reduces to Equation 1.7, and the amount of analyte extracted by SPME becomes approximately independent of sample volume.

$$n_e = C_0 K_{fs} V_f$$

**Equation 1.7**

This equation is very important from the perspective of integrating sampling and sample preparation, as it indicates that defined sample volume is not necessary for quantitative analysis. This means that sampling can be performed directly on-site (for example, direct on-site sampling of river or lake) or directly within a living system (for example, direct sampling of circulating blood of an animal). This capability of direct *in vivo* sampling makes SPME very attractive from the perspective of the field of metabolomics, as it should enable the capture of true metabolome at the time of sampling.

For *in vivo* SPME applications where temporal resolution is important, such as pharmacokinetic studies, it is not feasible to wait to establish equilibrium between the analyte and extraction phase. In this case, SPME can still be used for quantitative analysis to accurately determine the initial analyte concentration in the living system, but appropriate pre-equilibrium calibration methods need to be employed.<sup>80-83</sup> One such calibration method is called kinetic on-fibre standardization method.<sup>84, 85</sup> This calibration method uses the process of desorption of calibrant from the fibre coating in order to calibrate the process of the extraction of the analyte into the coating. These two processes are symmetric provided the calibrant employed has the same time constant as the analyte of interest. To fulfill this requirement, deuterated analogue of analyte is often employed<sup>86-88</sup>, although other studies have demonstrated that other compounds with similar diffusion properties can also be successfully used.<sup>89</sup> The simultaneous processes of analyte extraction and calibrant desorption are governed by the following equation which is derived from Equation 1.6:

$$\frac{n}{n_e} \bullet \frac{Q}{q_0} = 1$$

**Equation 1.8**

where  $n$  and  $n_e$  are the same as described previously,  $Q$  is the standard remaining on the fibre at time  $t$ , and  $q_0$  is the amount of standard preloaded on the fibre.

However from equation 1.1 we know that the amount of analyte extracted at equilibrium using SPME is a function of distribution coefficient, fibre volume and sample volume. Thus, if these two equations are combined, the initial concentration of analyte in *in vivo* sample is given by following equation, where all the terms are the same as defined previously:

$$C_0 = \frac{nq_0}{q_0 - Q} \cdot \frac{1}{K_{fs} V_f} \quad \text{Equation 1.9}$$

Equation 1.9 shows that it is necessary to determine the product of  $K_{fs} \cdot V_f$  in order to determine initial analyte concentrations in the system under study. This must be accomplished at equilibrium, by performing SPME using a set of calibration standards of known analyte concentration prepared in an appropriate matrix.

Finally, on-fibre standardization method also compensates well for unknown agitation within a living system, such as the unknown or changing blood flow rate over the course of the entire *in vivo* experiment. Such uncontrolled agitation conditions cannot be well replicated and compensated using simple *in vitro* calibration methods.

#### 1.4.1 SPME and metabolomics: an overview

*In vitro* and *in vivo* headspace SPME in combination with GC-MS analysis was previously successfully used for clinical metabolomic studies of volatile and semi-volatile species. The main types of applications reported to date include analysis of (i) disease biomarkers in human breath (ii) human skin emissions and (iii) analysis of cell lines. Soini *et al.* developed a very rapid sampling methodology using commercially available Twister PDMS stir bar for high-throughput metabolomic studies of human skin emissions.<sup>90-92</sup> This device was rolled on 10 cm<sup>2</sup> area of human skin for 10-12 seconds. Rich metabolite profiles and good sampling reproducibility (both intra- and inter-day) were achieved. Two internal standards (7-tridecanone and <sup>13</sup>C-benzyl alcohol) were preloaded in the PDMS devices prior to sampling in order to compensate for small variations in sampling and instrumental responses over time. Long-term reproducibility of 14.3% and 14.7% RSD was achieved for the two internal standards obtained during analysis of total of 960 *in vivo* samples over 3-month period.<sup>90</sup> Riazanskaia *et al.* investigated the use of thin PDMS film geometry for sampling of carcinoma lesions and other skin disorders.<sup>93</sup> Very rich volatile profiles containing >300 peaks were obtained after thermal desorption of the PDMS thin films by GC-MS, and precision of repeated *in vivo* sampling was satisfactory with RSD <20% for selected representative metabolites. In another



study, the use of headspace *in vivo* SPME with specially designed sampling chamber resulted in profiles with >100 peaks.<sup>94</sup> Gallagher *et al.* compared the performance of *in vivo* SPME versus hexane extraction for the analysis of human skin emissions.<sup>95</sup> They tentatively identified a total of 92 compounds: 58 were found using *in vivo* SPME while 49 were found in hexane extracts, indicating that the two techniques are complementary in nature. Higher molecular weight compounds predominated in hexane extracts, while SPME was more suitable for collection of lower molecular weight aldehydes and ketones. SPME was useful to extract five compounds that varied significantly according to age, among which the authors propose dimethylsulphone, benzothiazole and nonanal as biomarkers of aging. In another example, Zimmermann *et al.* were able to identify for the first time methyl dodecanoate, decan-1-ol, heptan-1-ol, 3-methylbutan-1-ol, pentadecan-2-one, nonan-2-one and undecan-2-ol in human cells, indicating SPME can be very useful approach in global metabolomic studies.<sup>96</sup>

Although the above-mentioned studies were able to propose some tentative biomarkers, the data should still be interpreted with caution as it typically relied on small data sets (with the exception of Soini *et al.* study) and requires further biomarker validation. For example, the tentative lung cancer biomarkers proposed by Gaspar *et al.* may not be specific for lung cancer, as they were previously also correlated to breast cancer, indicating that these compounds may be good general markers of oxidative stress rather than specific disease.<sup>97</sup> In another example, Xue *et al.* investigated volatile biomarkers in liver cancer blood using *in vitro* SPME, and suggested hexanal, octane and 1-octen-3-ol as possible biomarkers of liver cancer. However, elevated levels of hexanal were reported in other types of cancer such as lung cancer, leukemia, bone cancer and lymphoma.<sup>102</sup> These examples illustrate that biological interpretation of metabolomics data can be very difficult and requires multi-disciplinary collaboration to interpret and deconvolve observed trends.

In addition to metabolomic studies by GC-MS, the potential of SPME to characterize short-lived and/or unstable species or reaction intermediates has also been demonstrated. For example, SPME was successfully used to elucidate biotransformation pathways of explosives and natural products, biotransformation routes of hydrocarbons such as benzene and biodesulfurization pathway of dibenzothiophene.<sup>103-105, 105-108</sup> For example, SPME was used to propose stepwise desulfurization metabolism of dibenzothiophene (DBT) through formation of DBT-sulfoxide, DBT-sulfone, DBT-sultine, DBT-sultone to the final product of 2-hydroxybiphenyl.<sup>106</sup> SPME was also successfully used

**Table 1.1 Overview of global metabolomic studies using *in vivo* SPME and GC-MS analysis**

Sample type	Extraction mode	Purpose of study	Potential biomarkers	Analytical parameters for selected metabolites	Ref.
Exhaled air	Headspace	Lung cancer	Linear and branched hydrocarbons C <sub>14</sub> -C <sub>24</sub>	RSD 9-26% LOD 0.04-8.0 ng/mL	97
Skin emission	Headspace	Skin emission as fingerprint	Aldehydes, alcohols, esters and long-chain alkanes as biomarkers of seasonal emissions (winter versus summer)	NR	94
Skin emission	Headspace	Normal skin emission baseline	dimethylsulphone, benzothiazole and nonanal as biomarkers of aging no potential biomarkers for gender	NR	95
Skin emission	Headspace	Skin emission as fingerprint	NA Frequency of occurrence of various metabolites examined in emissions of 60 individuals	NR	98
Cancer tissue and bacterial cell culture	Headspace	Early diagnosis of gastric cancer	1-propanol and carbon disulfide	RSD 6-10% LOD 0.6-14 ng/mL	99
Colon cancer cells	Headspace	Understanding of colon cancer	NA New metabolites reported: time methyl dodecanoate, decan-1-ol, hepan-1-ol, 3-methylbutan-1-ol, pentadecan-2-one, nonan-2-one and undecan-2-ol	NR	96
Lung cancer cells and breath	Headspace	Early diagnosis of lung cancer	Styrene, decane, isoprene, benzene, undecane, 1-hexene, hexanal, propyl benzene, 1,2,4-trimethyl benzene, heptanal, methyl cyclopentane	NR	100
Breath	Headspace	Early diagnosis of lung cancer	Alkanes and aromatic hydrocarbons	RSD 3.7-9.8% LOQ 0.04-4.2 ng/mL	101

NR=Not reported, NA= not available

to monitor yeast metabolism during fermentation processes in order to determine optimum fermentation time<sup>109</sup> and to differentiate between toxigenic strains of mycotoxin-producing *Fusarium* fungi.<sup>110</sup> In another study, SPME was used to isolate lilac aldehydes and alcohols for the first time as

metabolic byproducts of fungal biotransformation of linalool.<sup>108</sup> Furthermore, *in vivo* SPME has been extensively applied for study of insect emissions such as semiochemicals and defense chemicals.<sup>111-119</sup> These studies were performed using headspace SPME or direct contact between the fibre and the insect, followed by GC analysis. For example, undecane was isolated as recruitment pheromone in ants which enables long-range intra-species communication when a good supply of food is discovered.<sup>111</sup> In another study, SPME was used to identify for the first time sex pheromone (blend of tetradecanal and pentadecanal) in praying mantid.<sup>115</sup> Prior to the availability of SPME for this type of application, insect sacrifice followed by solvent extraction was employed, and did not permit monitoring of dynamic changes in emissions of semiochemicals over time or changes in emissions upon interactions with other individuals, exposure to environmental stimuli or when limited number of colonies are available. Another interesting study comparing the results of hexane extraction and SPME subsequently showed that the results obtained for hexane extraction were incorrect, and the observed peaks were contaminants rather than true representation of cuticular hydrocarbon secretions.<sup>120</sup> In contrast, the results of SPME were correct. This study effectively illustrates that increased number of steps often involved in traditional sample preparation methods can sometimes lead to inadvertent contamination and erroneous results/conclusions. Finally, metabolomics applications of *in vivo* SPME are not confined to sampling of animals and microorganisms, but SPME has also been successfully applied in plant metabolomics for isolation and monitoring of scent development, wound response, infestation, etc.<sup>121-123</sup> For instance, in a targeted metabolomics study of scent development over time and corresponding circadian rhythms, the performance of *in vivo* and *in vitro* sampling was compared. Using *in vitro* sampling (freezing with liquid N<sub>2</sub> to stop the metabolism), additional peaks attributed to lipid peroxidation were observed indicating the effects of sample preparation method on observed metabolome.<sup>122</sup>

## 1.5 Research objectives

The main research objective of this thesis is to demonstrate for the first time the suitability of SPME in direct extraction format for global metabolomic studies using LC-MS.

The main requirements for a sample preparation method of biofluids were discussed in detail in 1.3 and include (i) speed and simplicity, (ii) high throughput and automation, (iii) efficient extraction of diverse range of metabolites and (iv) the need to quench metabolism. However, SPME methodology required further development in terms of automation and selectivity of extraction before it could be successfully applied to metabolomic studies. Thus, Chapter 2 describes initial work regarding

automation of SPME in 96-well plate format to enable higher sample throughput. Chapters 3 and 4 describe the commercial development of *in vivo* SPME sampling device in collaboration with Supelco Inc. and optimization of *in vivo* SPME procedures including the first application of *in vivo* SPME to mice. The extension of *in vivo* SPME sampling to small rodents such as mice was deemed particularly important from metabolomics perspective, as the advantages of elimination of the need of blood withdrawal are particularly important for such animals where very limited amount of blood is available (<2 mL total blood volume). Mice are often utilized in metabolomic studies of disease models and pharmaceutical discovery<sup>23, 124</sup> and recently it was recommended that all control strains used to generate transgenic or knock-out mice should be used as controls in metabolomic studies on the basis of significant influence of strain on metabolomics data.<sup>21</sup> Such recommendations for increased animal use or the need for longitudinal studies of same animals to monitor metabolic trajectories such as return to healthy metabolic profile after particular treatment or to monitor progress of disease<sup>23, 125</sup> make blood-free approaches such as *in vivo* SPME even more attractive. Chapter 5 discusses the development of SPME coatings suitable for direct extraction of diverse range of metabolites which make up the metabolome, as suitable coatings for this type of application were not previously reported in literature.

Chapter 6 describes the development of the basic SPME methodology suitable for use in metabolomic studies and describes in detail the optimization of LC-MS methods. The latter optimization was very important in order to ensure adequate metabolite coverage, as SPME extracts only small portion of metabolite, so good instrumental sensitivity is of paramount importance. Chapter 7 summarizes the results of a full *in vitro* metabolomics study on human plasma and also compares the performance of SPME to traditional methods of plasma protein precipitation and ultrafiltration. This comparison was useful to place SPME within the context of commonly employed methods and to evaluate whether the developed methodology was sufficient for application during *in vivo* studies in terms of analytical parameters such as sensitivity, precision and metabolite coverage. Chapter 8 describes the successful application of *in vivo* SPME to mice to study the effects of carbamazepine administration in a preliminary proof-of-concept study. Clear advantages of *in vivo* sampling approach *versus* the methods relying on blood withdrawal are demonstrated. Finally, Chapter 9 summarizes the main research findings of current work and proposes future directions and challenges for this type of studies.

## Chapter 2

# Automation of SPME in 96-well plate format for high-throughput analysis of biological fluids

### 2.1 Preamble and introduction

#### 2.1.1 Preamble

This chapter has been published as a paper: Vuckovic, D., Cudjoe, E., Hein, D. & Pawliszyn, J. Automation of solid-phase microextraction in high-throughput format and applications to drug analysis. *Anal. Chem.* 80, 6870-6880 (2008). Tables and figures are reprinted from this publication with permission from American Chemical Society (Copyright 2008 American Chemical Society). The full procedure for automated SPME developed in this original work was also described in step-by-step fashion for future users in Vuckovic, D., Cudjoe, E., Musteata, F. M. & Pawliszyn, J. Automated solid-phase microextraction and thin-film microextraction for high-throughput bioanalytical applications and ligand-receptor binding studies. *Nat. Protocols* 5, 140-161 (2010). Table 2.7 and Figures 2.8 and 2.19 are reprinted from this work with permission from Nature Publishing Group according to Nature Publishing Group policy whereby the ownership of the copyright remains with the authors and permission “to reproduce the Contribution in whole or in part in any printed volume (book or thesis) of which they are the author(s)” is automatically granted. The application of automated system to ligand-binding studies is beyond scope of this research thesis, so this material is not included in the chapter. On this basis, the permission of Marcel Florin Musteata who developed the theory of ligand-receptor binding by SPME regardless of the degree of depletion is considered to not be required.

The contribution of co-author, Erasmus Cudjoe to the work described within this chapter was in the development of 96-SPME device (the design of the device described in section 2.2.4) and the improvement of prototype PAS Concept 96 autosampler including programming of Concept software. Dietmar Hein designed and built PAS Concept 96 autosampler which was used to perform the experimental work described herein.

I, Erasmus Cudjoe, authorize Dajana Vuckovic, to use the material for her thesis.

I, Dietmar Hein, authorize Dajana Vuckovic, to use the material for her thesis.

### **2.1.2 Introduction**

SPME is easily coupled to gas chromatography due to its solvent-free nature and syringe device format both of which permit direct introduction of device into GC injector. Commercial autosamplers capable of performing all steps of SPME extraction and introduction into GC system have been available since 1990s and permit application of SPME for unattended analysis of large number of samples with sample throughput compatible with GC analysis times.<sup>126</sup> The first coupling of SPME to LC was reported in 1995<sup>127</sup> and involved manual introduction of SPME device into the path of mobile phase using a simple desorption chamber. All of the extracted analytes are swept onto the analytical column, so high analytical sensitivity can be achieved, and the process is analogous to thermal desorption used successfully in GC. This strategy was subsequently commercialized by Supelco, but all steps of the process are performed manually, and this format has not been successfully automated to date. Furthermore, high pressures typically encountered during LC analysis can cause inadvertent leaks at the interface and thus accidental loss of sample during the desorption step. Existing commercially available coatings for HPLC also swell considerably using aqueous solvent mixtures typically employed as mobile phases in LC. For example, commonly used commercial coating Carbowax/template resin (CW/TPR) was found to swell 36-40% after 15-min exposure to water/methanol or water/acetonitrile mixtures.<sup>128</sup> Such swelling significantly increases overall diameter of the device, so the coating can be accidentally stripped during removal from the interface due to the increase in dimensions. A second strategy for coupling of SPME to LC is called in-tube SPME because this strategy relies on the use of coated capillary rather than the more common fibre geometry. This strategy has been fully automated, and the main principle involves the placement of this coated capillary within the path of LC system, for example in lieu of sample injection loop or transfer tube. The sample is then drawn into and ejected from this capillary using appropriate software program that can be written for any commercial HPLC autosampler. During each draw cycle, analyte can partition into the extraction phase, and the process of drawing/ejecting provides agitation in the system in order to enhance mass transfer. Once extraction is completed, mobile phase is directed through the capillary and the analytes are desorbed and swept onto the analytical column for LC separation and analysis. The main advantages of this approach are full automation and high sensitivity because all of the analyte extracted is introduced onto the analytical column. However, the

use of capillary geometry means that sample pre-treatment such as filtration, centrifugation or dilution, is necessary to remove any particulate matter in order to avoid clogging of the capillary. Furthermore, sample throughput is relatively low, because samples are processed serially, and each extraction and desorption step can be time consuming due to slow mass transfer kinetics in liquid phase. One way to achieve high sample throughput when coupling SPME is to perform offline solvent desorption of many samples in parallel using regular HPLC vials, vial inserts or 96-well plates. In addition to lack of automation, the main disadvantage of this approach is decrease in sensitivity as all of the extracted analyte is not introduced into analytical system. For example, minimum desorption volume of 100  $\mu\text{L}$  is typically used to ensure complete immersion of the coating within the solvent, although volumes as low as 40-50  $\mu\text{L}$  have also been reported.<sup>129</sup> Thus, to date, none of the three main desorption strategies used in combination with LC, was capable of simultaneously providing both high sample throughput and high desorption efficiency.

The main goal of research described in this section was to evaluate and improve new autosampler designed to fully automate SPME in 96-well plate format using offline solvent desorption. The initial idea for a device consisting of 96 fibres which fit into the centres of a commercial 96-well plate was described in 2005<sup>126</sup>, and a simple semi-automated proof-of-concept study using an array of eight commercial PDMS-DVB fibres was carried out to investigate the feasibility of SPME in bioanalysis by comparison against accepted automated 96-well plate liquid-liquid extraction (LLE) method.<sup>130</sup> Good performance of SPME was reported with following figures of merit for a candidate drug molecule: linear range of 1-500 ng/mL for both methods, accuracy of 95.2-103.7% for SPME versus 98.0-101.8% for LLE, and method precision of 0.5-6.9% for SPME versus 0.8-3.3% for LLE. However, due to the high cost of a single commercial SPME fibre building a 96-fibre array with such commercial devices was very cost-prohibitive, so alternative configurations were explored by Hutchinson *et al.*<sup>131</sup> This work proposed the use of pins found in commercial 96-pin-tool replicator device as the metal support for immobilization of SPME coating. Hollow PDMS tubing (medical grade) was found to work well for the extraction of semi-volatile polyaromatic hydrocarbons. Among different agitation methods, orbital agitation while fibres are kept stationary was found to provide more uniform agitation than sonication or magnetic stirring. Based on the results of this study, Dietmar Hein and PAS technology designed and built prototype SPME autosampler, named Concept 96, which consisted of two orbital agitators, one arm capable of positioning 96-pin-tool replicator device, syringe arm (to dispense desorption solvent, internal standard) and a 96-well plate nitrogen blowdown device to permit incorporation of evaporation/reconstitution step for applications requiring

additional sensitivity. The availability of such system was deemed important for both bioanalytical and metabolomics applications of SPME as it would enable for the first time the use of SPME in laboratories needing to process large number of samples.

For the evaluation of Concept 96 autosampler, several benzodiazepines shown in Figure 2.1 were selected as target analytes because of their widespread use as tranquilizers, hypnotics, muscle relaxants, and anticonvulsants and their amenability to analysis by electrospray LC-MS. PDMS coating proposed by Hutchinson *et al.*<sup>131</sup> was found unsuitable for drug analysis due to very slow kinetics and poor intra-fibre reproducibility, so an alternative simple and reproducible fibre preparation procedure based on SPE-type sorbents was investigated and optimized for multi-fibre SPME.<sup>132</sup> The performance of the system was evaluated with respect to following parameters: selection of coating, carryover of analyte in the extraction phase, well cross-talk, fibre robustness, selection of optimal calibration method, uniformity of agitation in all wells, suitability for pre-equilibrium SPME, and fibre-to-fibre reproducibility. After full optimization, multi-fibre SPME-LC-MS/MS method was fully validated for high-throughput analysis of benzodiazepines in whole blood to show an example application in a complex heterogeneous matrix.

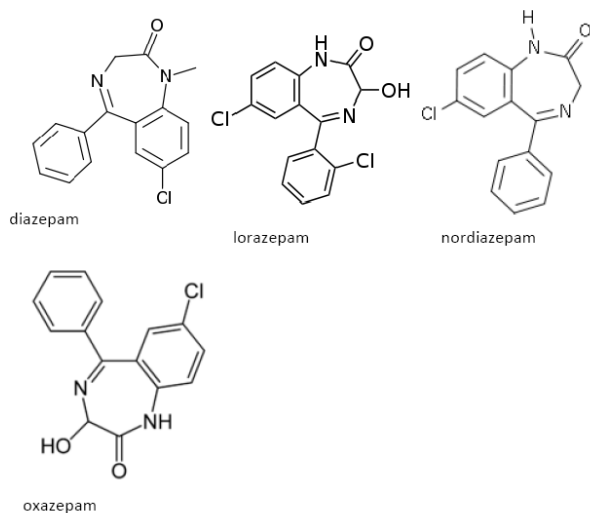


**Figure 2.1 Structures of selected benzodiazepines included in evaluation of Concept 96 autosampler.**



## **2.2 Experimental**

### **2.2.1 Chemicals and materials**

Diazepam, nordiazepam, oxazepam, and diazepam-d5 were purchased from Cerilliant (Round Rock, TX, USA) as 1 mg/mL methanolic solutions, while lorazepam was purchased as a 1 mg/mL solution in acetonitrile. Acetonitrile (HPLC grade), methanol (HPLC grade), and glacial acetic acid were purchased from Fisher Scientific (Ottawa, Canada). Sodium chloride, potassium chloride, and potassium phosphate were purchased from EMD Chemicals (Gibbstown, NJ, USA). Sodium phosphate and human serum albumin were purchased from Sigma-Aldrich (Oakville, Canada). Polypropylene 96 deep multi-well plates and BD K<sub>2</sub>EDTA 18 mg Plus Vacutainer blood collection tubes were purchased from VWR International (Mississauga, Canada). Nanopure water ( $\geq 18.0$  M $\Omega$ ) was obtained from water purification system (Barnstead, Thermo Fisher, San Jose, CA, USA).

### **2.2.2 Preparation of buffers and standard solutions**

Instrument calibration was performed using a set of calibration standards prepared in desorption solvent (acetonitrile/water, 1/1, v/v). These standards were injected in duplicate at the beginning and end of each sample run, and one quality control (QC) standard was also injected periodically throughout the run to ensure suitable instrument performance. These standards were stored refrigerated, and fresh standards were prepared monthly.

Phosphate-buffered saline (PBS) solution pH 7.4 was prepared by dissolving 8.0 g of sodium chloride, 0.2 g of potassium chloride, 0.2 g of potassium phosphate, and 1.44 g of sodium phosphate in 1 L of purified water and adjusting the pH to 7.4, if necessary. For all SPME optimization and evaluation experiments, standard solutions were prepared at appropriate concentration (typically 100 ng/mL unless otherwise indicated in text) in PBS buffer in such a way to keep the organic solvent concentration at exactly 1% (v/v) methanol. Fresh standards were prepared in PBS daily.

For the application of optimized method to whole blood samples, calibration standards and validation samples were prepared by spiking an appropriate amount of each drug standard in whole blood (final concentration range from 1 ng/mL to 1000 ng/mL) in such a way as to keep the organic solvent concentration at exactly 1% methanol. After spiking, samples were left standing for a minimum of 1 hr to ensure sufficient time for drug-protein binding to take place prior to extraction.

### **2.2.3 Preparation of 96-SPME device using pin-tool replicator and PDMS coating**

The initial design of the device was based on the work described by Hutchinson *et al.* who used a commercially available pin-tool replicator as the support to immobilize SPME coatings.<sup>131</sup> Pin-tool replicator (model AFIX96FP3) and floating pins (FP8, 0.356 mm diameter) were purchased from V&P Scientific (San Diego, CA, USA). The coating used for this device was HelixMark polydimethylsiloxane-based hollow tubing with 0.31 mm ID and 0.64 mm OD and was made from PDMS and proprietary filler (Helix Medical, Carpinteria, CA, USA). This tubing was cut into 2 mm pieces and placed directly over floating replicator pins. The thickness of the extraction phase for these fibres was 165  $\mu\text{m}$ , as determined by the thickness of the tubing. Pin-tool replicator was directly attached to PAS autosampler arm using appropriate screws.

### **2.2.4 Preparation of 96-SPME device using 1.55 mm diameter stainless steel wire and coated silica particles**

Based on the results of the coating optimization procedure (discussed in Section 2.3.1.9), thick 1.55 mm solid supports were found to perform better than thin solid supports. In order to house these new solid supports in a 96-SPME device, a simple prototype device was designed and built by Machine Shop at the University of Waterloo. This device consisted of top and bottom plates. Bottom plate was drilled with holes to fit 1.55 mm solid support. The spacing of the holes was chosen to match the centre of each well of commercial 96-well plates. The two plates were held together with screws in the four corners. 96-plate Silicone PCR-Mat was purchased from Ultident Scientific (St. Laurent, Canada) and placed between the two plates to ensure that the solid supports are sufficiently immobilized. The device is shown in Figure 2.2 (a). The attachment of the device to PAS autosampler is shown in Figure 2.2 (b) and was designed by E. Cudjoe and D. Hein.

To prepare thin SPME coatings on 1.55 mm support (stainless steel wire, type 316, Small Parts Inc. Miami Lakes, FL, USA), the procedure reported by Mullett and Pawliszyn was used.<sup>132</sup> This procedure involves the immobilization of coated silica particles using strong adhesive, and was previously shown to be suitable for solvent desorption. In current work, the procedure was further optimized to improve inter-fibre reproducibility. The overview of optimized procedure is shown in Figure 2.3. The main changes included optimization of the solid support diameter and an increase in acid etching time from 20 min to 2 hr.

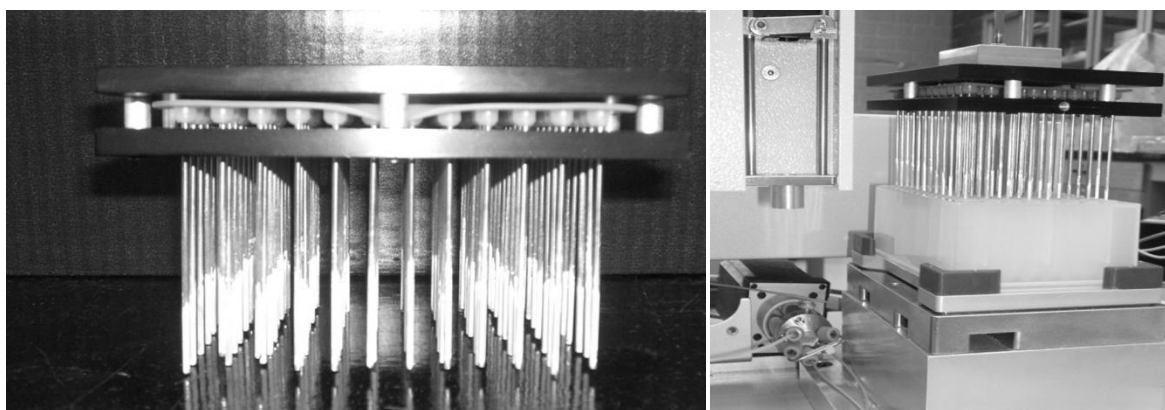


**Figure 2.2 (a) Custom-made multi-fibre SPME device constructed using 1.55 mm stainless steel wires and RPA extraction phase. (b) Photo showing the details of SPME multi-fibre device, 96 multi-well plate and agitator employed in PAS robotic system.**

Briefly, stainless steel wire was cut into 10 cm pieces using special metal cutter from Small Parts Inc. to obtain clean cut. The ends of wires were then sanded using aluminum oxide sand paper, followed by 20 min sonication in acetone and 2 hr sonication in 6M nitric acid. The wires were rinsed thoroughly with purified water and then methanol, and then allowed to air dry. A thin layer of Loctite 349 glue (modified methacrylate ester adhesive, R.S. Hughes Company, Plymouth, MI, USA) was placed on the wires by filling 2 mL HPLC vial with glue, capping it and passing the wire through the septum. The fibres were then rolled in 5-10  $\mu\text{m}$  coated silica particles ( $\text{C}_{18}$  or  $\text{C}_{16}$  amide particles obtained as research samples from Supelco, Bellefonte, PA, USA) to obtain good surface coverage. Coating length was 1.5 cm. Coated fibres were then cured under an ultraviolet lamp for 1 hour. During UV curing, fibres were rotated every 10 min to ensure all sides were cured.

Before initial use, the fibres were conditioned by overnight exposure to a methanol/water (1/1, v/v) solution using 850 rpm agitation, followed by a 30 min exposure to purified water and a 30-min exposure to acetonitrile/water (1/1, v/v) mixture. The long overnight conditioning with agitation was found important to remove any loosely bound particles from the surface. For subsequent uses, the fibres were only conditioned for 30 min using methanol/water (1/1, v/v) mixture.

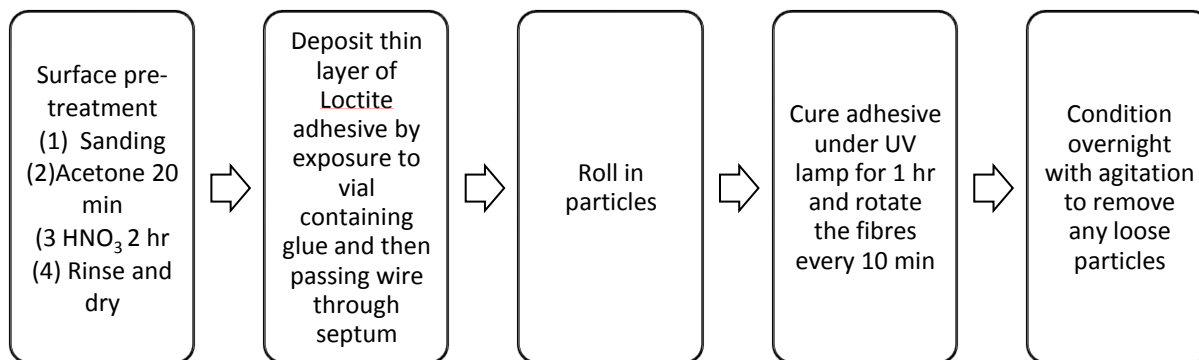


**Figure 2.3 Overview of optimized coating procedure using 5- $\mu$ m coated silica particles.**

### **2.2.5 Description of PAS autosampler for automated SPME**

The automated SPME system was designed and obtained from PAS (Magdala, Germany) as research prototype. The unit was designed to automate all sample preparation steps of SPME procedure, including the addition of an internal standard, multi-fibre SPME extraction and desorption for a preset amount of time with controlled agitation, evaporation of the solvent, reconstitution, and injection of the final sample solution from individual wells into the HPLC injection port. To achieve this, the unit consisted of a three-arm robotic autosampler, HPLC injection port and two orbital agitators. It was fully controlled with Concept software. One XYZ arm of the autosampler was used to hold, transport, and position the 96-fibre SPME device for the extraction and desorption steps of SPME. The second arm was equipped with a N<sub>2</sub> blow-down device in order to perform solvent evaporation and analyte pre-concentration steps if enhanced sensitivity was required. This feature was not used in current work and it was evaluated in separate research by E. Cudjoe. The third arm consisted of an XYZ arm equipped with a 250  $\mu$ L syringe and was designed to dispense preset volumes of reconstitution/desorption solvents or internal standard solutions into the individual wells of the 96-well plate, as well as to perform sample injection into the HPLC port of the analytical system. The desorption volume used in current work was 800–1000  $\mu$ L, which exceeded the syringe capacity. Thus, the desorption solvent was either dispensed manually using an air displacement Fisherbrand 200–1000  $\mu$ L pipette or using an automated 96/384-well microplate reagent dispenser (Ultrasense 2000, KD Scientific, Halliston, USA) in order to further increase automation and throughput.

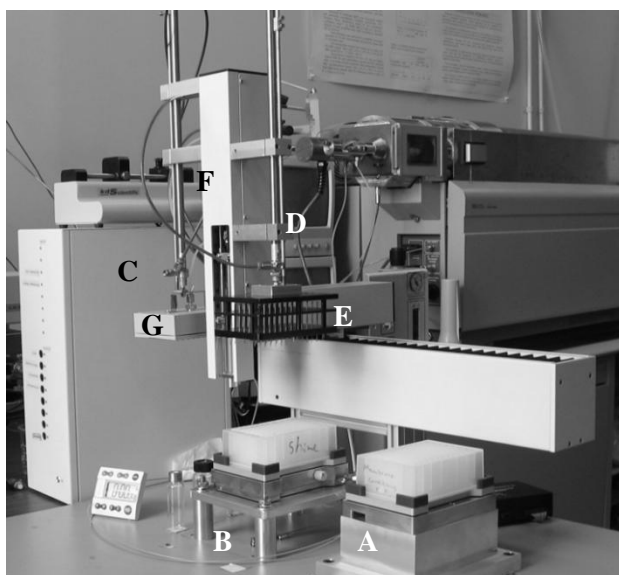


**Figure 2.4** Photo showing PAS Concept 96 robotic system. A and B are orbital agitators used for extraction and desorption, C is system controller, D is the arm used to manipulate SPME multi-fibre device, E depicts SPME multi-fibre device, F is syringe arm and G is the arm used for simultaneous nitrogen evaporation from all wells.

### **2.2.6 LC-MS/MS analysis**

Benzodiazepines were analyzed using a LC-MS/MS system consisting of CTC-HTS PAL autosampler with cooled sample tray, Shimadzu 10AVP LC with dual pumps (Shimadzu LC10ADvp) and system controller (SCL10Avp) and API3000 triple quadrupole mass spectrometer equipped with TurboIonspray source (Applied Biosystems/MDS Sciex, Concord, Canada). The flow of column effluent was diverted to waste for the first 1.0 min of chromatographic run time using bypass pump and a Waters switching valve. Analyst software version 1.4.1 was used for data acquisition and processing. Analytes were separated using Symmetry Shield RP18 column with dimensions of 2.1 x 50 mm and 5  $\mu$ m particles (Waters, Millford, MA, US) using chromatographic conditions previously developed by Lord *et al.*<sup>133</sup> Samples (20  $\mu$ l) were injected in duplicate and kept at 5 °C on the autosampler while waiting for analysis. Mass spectrometric conditions used were: nebulizer gas = 6, curtain gas = 10, CAD gas = 12, ionspray voltage 5300 V, and source temperature set to 400°C. The analysis was performed using positive ESI in multiple reaction monitoring (MRM) mode using instrument settings described in Table 2.1. These parameters were obtained by direct infusion of 1  $\mu$ g/mL benzodiazepine standard solution using syringe pump, followed by manual optimization of

each parameter until maximum signal was obtained. Dwell time of 200 msec was used for monitoring of each ion.

**Table 2.1 Summary of MS/MS parameters for the analysis of benzodiazepines.**

Analyte	Q1 Mass (amu)	Q3 Mass (amu)	Declustering Potential (V)	Focusing Potential (V)	Entrance Potential (V)	Collision Energy (V)	Cell Exit Potential (V)
Diazepam	285.0	153.9	92	120	7.5	39	10
Lorazepam	321.1	275.1	101	360	10	31	20
Oxazepam	287.1	241.1	61	160	10	31	18
Nordiazepam	271.1	140.0	66	170	10	39	10
Diazepam-d5	290.2	154.1	92	120	7.5	39	10

### 2.2.7 SPME procedure during optimization/evaluation experiments

SPME was performed using 1000  $\mu$ L aliquots of appropriate benzodiazepine standard prepared in PBS buffer, pH 7.4. Extraction time was varied depending on the experiment as stated in text. Extraction and desorption were performed using 850 rpm agitation. The desorption was performed using 1000  $\mu$ L of desorption solvent (acetonitrile/water, 1/1, v/v) for stated amount of time (60 min for PDMS coating and 30 min for C<sub>18</sub> and RPA coatings). The carryover was evaluated by performing a second desorption using fresh portion of desorption solvent. These extracts were then analyzed directly using LC-MS/MS.

### 2.2.8 SPME procedure for high-throughput analysis of benzodiazepines in whole blood

Whole blood was collected from a healthy volunteer using BD K<sub>2</sub> EDTA 18 mg Plus Vacutainer tubes and kept on ice until use. Whole blood was processed within 24 hr from collection, and stored refrigerated when not in use. The internal standard (diazepam-d5) dissolved in methanol was added to all samples and standards at the final concentration of 400 ng/mL. SPME procedure was performed using PAS autosampler and following extraction conditions: 800  $\mu$ L sample volume, 30 min extraction, 850 rpm agitation. Immediately after extraction, fibres were rinsed manually for 30 seconds using purified water in order to eliminate any blood droplets or red blood cells from the fibre surface. Initial design of PAS autosampler did not incorporate the possibility of wash step, but based on the results of this work, subsequent improved design of the unit incorporated a wash station where fibres could be rinsed by dipping in and out several times from multi-well plate containing purified

water. The desorption was performed using 800  $\mu\text{L}$  of desorption solvent (acetonitrile/water, 1/1, v/v) for 30 min at 850 rpm. These extracts were then analyzed directly using LC-MS/MS.

### **2.2.9 Data analysis and calculations**

Calibration was performed using 1/y weighted linear regression in SigmaPlot 2004 for Windows version 9.0 software. Weighted regression was found to perform better than simple linear regression by improving the accuracy of low concentration standards. Extraction efficiency (or absolute recovery) was calculated by dividing the amount of analyte extracted by the coating (in ng) with the total amount of analyte originally present in the spiked sample (in ng), and multiplying this result by 100% to convert it to percentage. The amount of analyte extracted was determined using instrument calibration curve for each analyte prepared directly in desorption solvent (single standard per concentration level, minimum of 6 levels to cover the entire linear range of the instrument). Relative recovery (or accuracy) was calculated by dividing experimentally determined sample concentration (in ng/mL, determined using calibration curve prepared in whole blood) by true sample concentration (in ng/mL), and multiplying this result by 100% to convert it to percentage. Whole blood calibration was performed by SPME of each standard in duplicate, and a minimum of six concentration levels across the entire linear range were used as described in Section 2.2.2.

## **2.3 Results and discussion**

### **2.3.1 Optimization and evaluation of automated 96-SPME system and PAS autosampler**

Research prototype PAS autosampler was designed on the basis of the concept initially proposed by O'Reilly *et al.*<sup>126</sup> and further supported by the results of a proof-of-concept study<sup>131</sup>. In this study, orbital agitation while fibres are held stationary was found to provide the best results when compared to sonication and magnetic stirring.<sup>131</sup> The authors also found that commercially available pin-tool replicator could successfully be used to immobilize an array of 96 SPME fibres. In this study, polyaromatic hydrocarbons were used as analytes and the analysis was performed using gas chromatography after solvent desorption.

The first objective of current research was to build on the study performed by Hutchinson *et al.* and evaluate the performance of new PAS Concept 96 autosampler for drug analysis with respect to factors such as (i) selection of the best fibre coating, (ii) optimization of the fibre coating procedure

(iii) selection of the best stainless steel support, (iv) examination of the need for fibre pre-conditioning and/or rinsing, (v) selection of the optimal calibration method, (vi) evaluation of fibre carryover, (vii) evaluation of well cross-talk and (vi) confirmation of uniform agitation in all wells. Additional factors such as agitation speed, optimization of extraction phase geometry and the influence of the exact position of the SPME extraction phase within the wells were also studied and are reported elsewhere.<sup>134</sup>

PDMS coating, recommended by Hutchinson *et al.*, was initially evaluated for use with PAS autosampler.<sup>131</sup> However, the performance of this coating for drug analysis was found to be inadequate as described in detail subsequent sections, so new coatings based on C<sub>18</sub>- and RPA-coated silica particles were also incorporated into this evaluation in order to improve the overall performance of the system.

### 2.3.1.1 Optimization of desorption conditions for PDMS coating

Optimization of solvent desorption conditions during SPME method development involves testing of different solvent compositions and desorption times in order to achieve efficient desorption of the analyte while minimizing or eliminating carryover. Carryover is defined as the amount of analyte remaining in the coating after first desorption. It is determined experimentally by performing a second desorption using fresh portion of desorption solvent, and can be calculated using Equation 2.1.

$$\% \text{ carryover} = \frac{\text{amount of analyte extracted in desorption 2}}{\text{total amount of analyte extracted in desorptions 1 and 2}} \times 100\% \quad \text{Equation 2.1}$$

In current study, polar solvents such as methanol or acetonitrile were tested for their ability to desorb the analytes from the fibre. Non-polar solvents are not suitable for desorption since they swell or dissolve the PDMS extraction phase. The results obtained are shown in Figure 2.5. Two desorption solvent compositions were found to remove  $\geq 99\%$  of analyte from the coating when 60-min desorption time with agitation speed of 850 rpm was used: acetonitrile/water (1/1, v/v) mixture and pure acetonitrile. Under these conditions, the carryover was found to be less than 1%. In addition to desorption efficiency, two other factors play a role when selecting the most appropriate desorption solvent for this automated SPME system. These are desorption solvent compatibility for direct injection into LC-MS and potential for solvent evaporation during the desorption step. According to this criteria, acetonitrile/water (1/1, v/v) solution was chosen as the desorption solvent for all subsequent experiments using PDMS coating, because it was directly compatible for injection using



gradient reverse-phase LC-MS method for the analysis of benzodiazepines and less susceptible to evaporative losses during desorption step than pure acetonitrile.

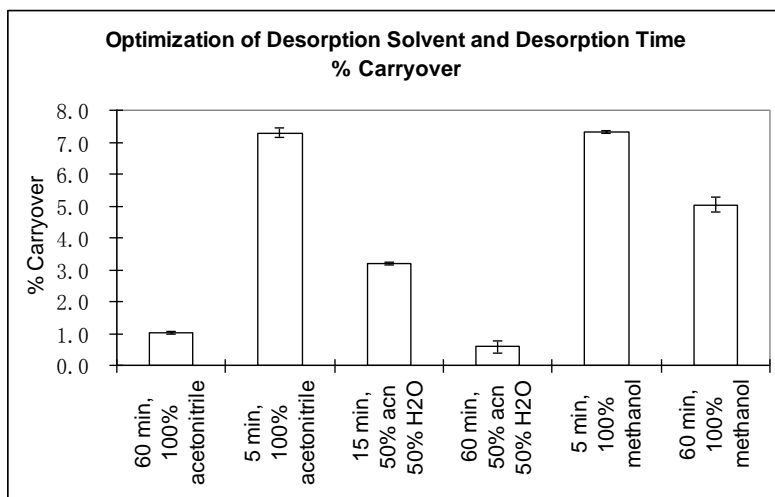


**Figure 2.5 Optimization of desorption conditions for diazepam using PDMS coating (n=3). Extraction was performed from 100 ng/mL diazepam standard in PBS buffer pH 7.4 for 60 min using agitation of 850 rpm.**

### 2.3.1.2 Determination of extraction time profile for PDMS coating

An extraction time profile was determined experimentally by measuring the amount of analyte extracted by the fibre as a function of time and is shown in Figure 2.6 (a). The equilibrium for diazepam was reached after 1200 min. As discussed in Section 1.4, the equilibration time is defined as the time after which the amount of analyte extracted remains constant within experimental error. The equilibration time is affected by coating thickness, sample temperature, agitation conditions and distribution constant, and the long equilibration time observed in current study was attributed to the thickness of extraction phase which is approximately 165  $\mu\text{m}$ . However, the coating thickness could not be further reduced using this method of constructing an array of 96-SPME devices, because this was the thinnest tubing commercially available with the appropriate dimensions. Such long extraction times are not suitable for high-throughput applications, and high sample throughput was the primary goal of this research. Therefore, in the next step, the suitability of Concept 96 system for pre-equilibrium SPME was examined.

For pre-equilibrium SPME methods, accurate timing of extraction step is very important in order to achieve good method precision because the amount of analyte extracted depends on the exact length

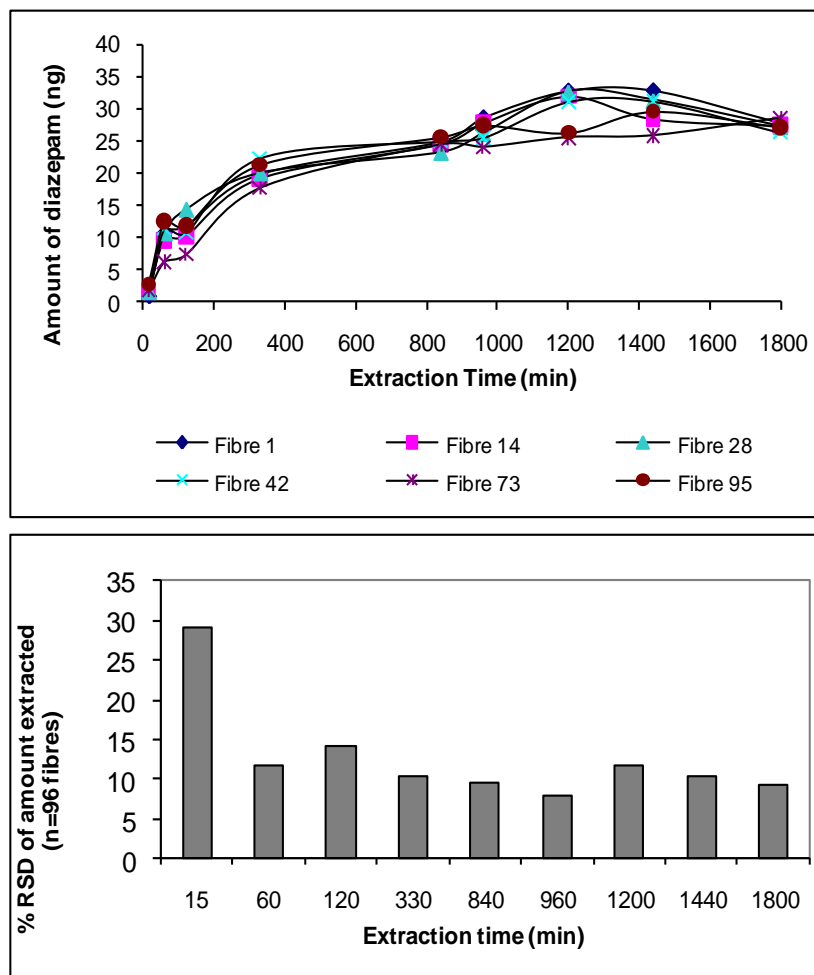


**Figure 2.6 (a) Representative extraction time profiles for the extraction of diazepam from 100 ng/mL standard solution for 6 different fibres and well positions (data for all 96 fibres was collected as discussed in text, but is shown for only 6 fibres for clarity) (b) Dependence of % RSD for the amount extracted of diazepam (n=96 fibres) on the extraction time.**

of extraction time as shown previously in Equation 1.6. Therefore, to examine the performance of Concept 96 robotic station for pre-equilibrium SPME, extraction was performed using all 96 fibres and the extraction time was varied from 15 min to 1800 min. The results of this experiment are shown in Figure 2.6 (b). Excellent method precision with RSD of 8-12% was found for all extraction times longer than 60 min, and there was no statistically significant difference between method precision

observed at pre-equilibrium times (60-960 min) *versus* equilibrium extraction times (1200 -1800 min). The main reason such good precision was observed at pre-equilibrium extraction times is that the extraction is performed in parallel for all samples and accurate timing and fibre positioning is achieved using software control via Concept software. However, using very short extraction time of 15 min, very poor method precision was observed with RSD of almost 30%. Possible reasons for this finding include that some time is required to establish uniform agitation in all of the wells and/or eliminate any air bubbles within the wells. Overall, the results show suitability of Concept 96 for pre-equilibrium SPME, but the use of short extraction times  $\leq 15$  min should be avoided to ensure uniform agitation can be established in all wells.

### 2.3.1.3 Evaluation of inter-fibre and intra-fibre reproducibility of PDMS fibres

Most SPME analyses rely on the use of a single fibre for extraction of all samples and standards in a given batch, rendering the issue of inter-fibre reproducibility not important for this type of analysis, as long as fibre is not damaged during the analysis. However, in current research, extraction of samples and standards is performed by an array of 96 fibres, so it is crucial for the reproducibility between the amount of analyte extracted by different fibres to be very good to ensure reliable quantitative analysis. To obtain good inter-fibre reproducibility of the amount extracted, it is important for the volume of the coating to be the same for all fibres. For hollow-tubing PDMS coating, the fibre-to-fibre reproducibility is thus limited by the uniformity of the tubing thickness and the ability to cut the tubing into pieces of equal length. The inter-fibre reproducibility of resulting PDMS coatings for the array of 96 fibres was evaluated using the extraction of diazepam from 100 ng/mL standard solution. Using equilibrium extraction and optimized desorption conditions, inter-fibre reproducibility (n=96 fibres) was found to be 10 and 11% RSD for each of two independent experiments as shown in Table 2.2. The results from a representative extraction are also shown in Figure 2.7 by plotting well position versus amount extracted. These plots were collected for several days and examined for any apparent trends. For example, a fibre with significantly lower volume of coating would be expected to extract smaller amounts of analyte on each day tested. However, no such trends in data were observed and no outlier fibres were detected, indicating that this coating could be made with satisfactory inter-fibre reproducibility.

It was previously reported that rinsing of the fibres between extraction and desorption steps can help further improve method precision by removing any small droplets from the surface of the fibres.<sup>133</sup> Thus, the incorporation of 30-second rinsing step with purified was examined. The results

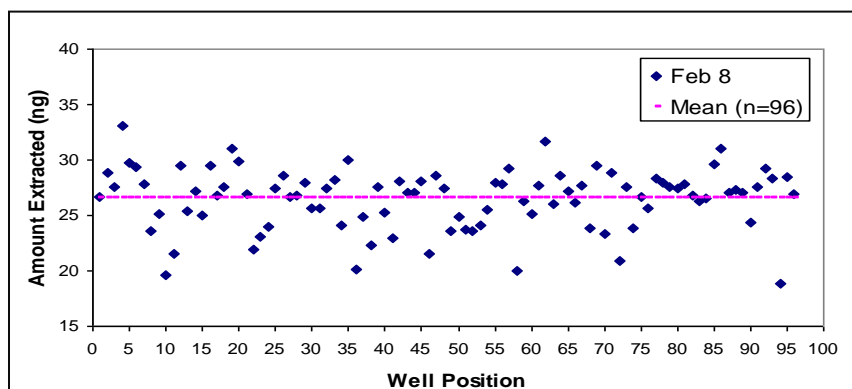


**Figure 2.7 Amount of diazepam extracted from 1 mL of 100 ng/mL diazepam standard solution using automated multi-fibre SPME (n=96 fibres).**

obtained are included in Table 2.2 and show that rinsing did not affect the amount of analyte extracted nor improve method precision. Therefore, the rinsing step could be omitted or added depending on the complexity of sample matrix. For example, in subsequent studies using whole blood (Section 2.3.2), presence of small blood droplets and/or red blood cells was found on the surface of the fibre after extraction, and addition of 30-second wash step helped eliminate these possible interferences prior to desorption resulting in clear particulate-free extracts.

**Table 2.2 The effect of fibre rinsing on the amount of diazepam extracted and inter-fibre reproducibility using multi-fibre SPME with PDMS coating.**

Rinse	Mean amount of diazepam extracted (ng) (n=96)	% RSD of extraction (n=96)
No	26.5	10
No	26.0	11
Yes	26.6	12
Yes	25.4	10
<b>Overall Mean (n=4):</b>	<b>26.1</b>	<b>NA</b>
<b>% RSD (n=4):</b>	<b>2.1</b>	<b>NA</b>

The intra-fibre reproducibility is defined as the reproducibility of the amount extracted when a single fibre is used to carry out repeated extractions. This parameter was evaluated using the data from five independent extractions of diazepam standard solution of known concentration (100 ng/mL). The average amount extracted by each fibre (n=5 extractions) and RSD were calculated individually for each of 96 fibres. The results for this evaluation are shown as histogram in Figure

2.8. The mean % RSD for the entire experiment was 9% (average RSD for all 96 fibres studied) which is acceptable for quantitative analysis by electrospray LC-MS. However, Figure 2.8 also shows that a significant number of fibres had unacceptably high RSDs ranging from 10-23%. Possible causes for the observed spread of RSD values were further investigated with the goal to further improve method performance.

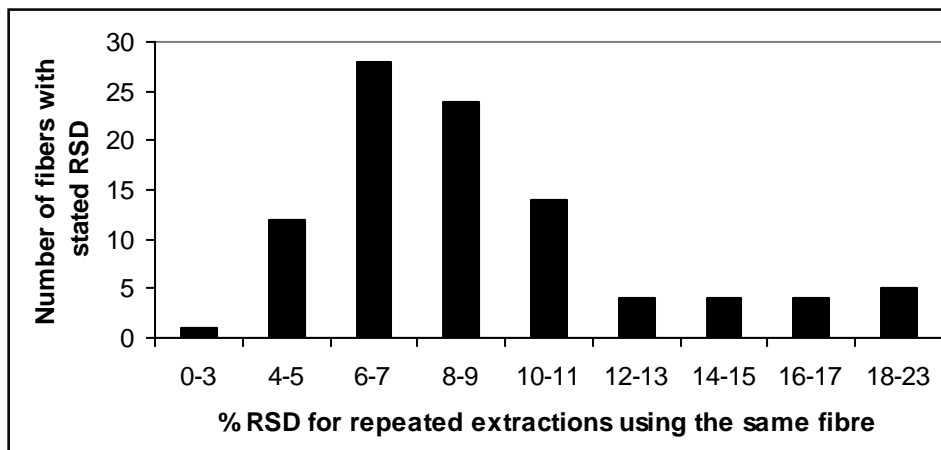


**Figure 2.8 Evaluation of intra-fibre reproducibility using PDMS coating. The distribution of fibres with given RSD for n=5 independent extractions using the same fibre is shown. The performance of fibres with % RSD exceeding 10 was deemed unacceptable for quantitative analysis. All of the extractions were performed using 100 ng/mL standard solution of diazepam in PBS and optimized SPME conditions.**

#### 2.3.1.4 Investigation of carryover using PDMS coatings

Although carryover was evaluated during the optimization of desorption conditions (Section 2.3.1.1), this evaluation was performed using only n=3 fibres. Furthermore, the initial carryover test was performed using only 60-min extraction time, so it was possible that carryover after equilibrium extraction is more significant, because higher amount of analyte is extracted at equilibrium. Furthermore, if the amount of carryover is not the same for all fibres, it could possibly cause poor intra-fibre reproducibility. This possibility was investigated by determining the carryover for all 96 fibres after 20 hr equilibrium extraction. The average carryover was found to be 0.3% using optimum desorption conditions (range observed was from none detected to 0.7%), thus confirming previous results. This indicated that carryover is not a significant contributing factor to poor intra-fibre reproducibility observed for some fibres.

### 2.3.1.5 Investigation of the uniformity of agitation using orbital shaking and PDMS coatings

A second possible explanation for poor reproducibility of repeated extractions using some fibres was that the agitation in all of 96 wells is not uniform. This possibility was examined by plotting the residual plots of the amount extracted *versus* well position over eight independent extractions using  $n=96$  fibres and equilibrium extraction conditions. Figure 2.9 shows two example plots obtained in this study, and illustrates that no apparent trends were observed. It was also examined whether the amount of analyte extracted by the wells in the centre of the plate was significantly different than the amounts extracted by the wells on the outside edges of the plate, due to differences in agitation. No such trends were observed. However, these plots were powerful enough to detect that the leveling of the system was not adequate after the movement of the unit from one lab to another. In this case, the residual plots showed consistently high positive residuals for rows A and B, indicating they were extracting higher amounts. During subsequent troubleshooting, improper leveling of the agitator was discovered and fixed. The subsequent residual plots became random in appearance. These experiments indicate that the use of residual plots is useful to evaluate the system performance and detect changes in agitation. More importantly, the results also indicate that the agitation within all wells is uniform and not likely cause of poor intra-fibre reproducibility observed for some fibres.

In a final set of experiments, the uniformity of agitation within wells was further confirmed by constructing extraction time profiles for all 96 fibres. The main hypothesis for performing these experiments was that any significant differences in agitation among the wells should result in longer extraction times for the equilibrium to be reached in some of the wells. Figure 2.6 (a) showed the results for six representative fibres, and the result for remaining 90 fibres were consistent with this, indicating no apparent differences in uniformity of agitation among the wells within the experimental error. Based on this study, agitation of 850 rpm using orbital shaking was found to be uniform and no well position correction factors needed to be applied to this automated multi-fibre SPME system.

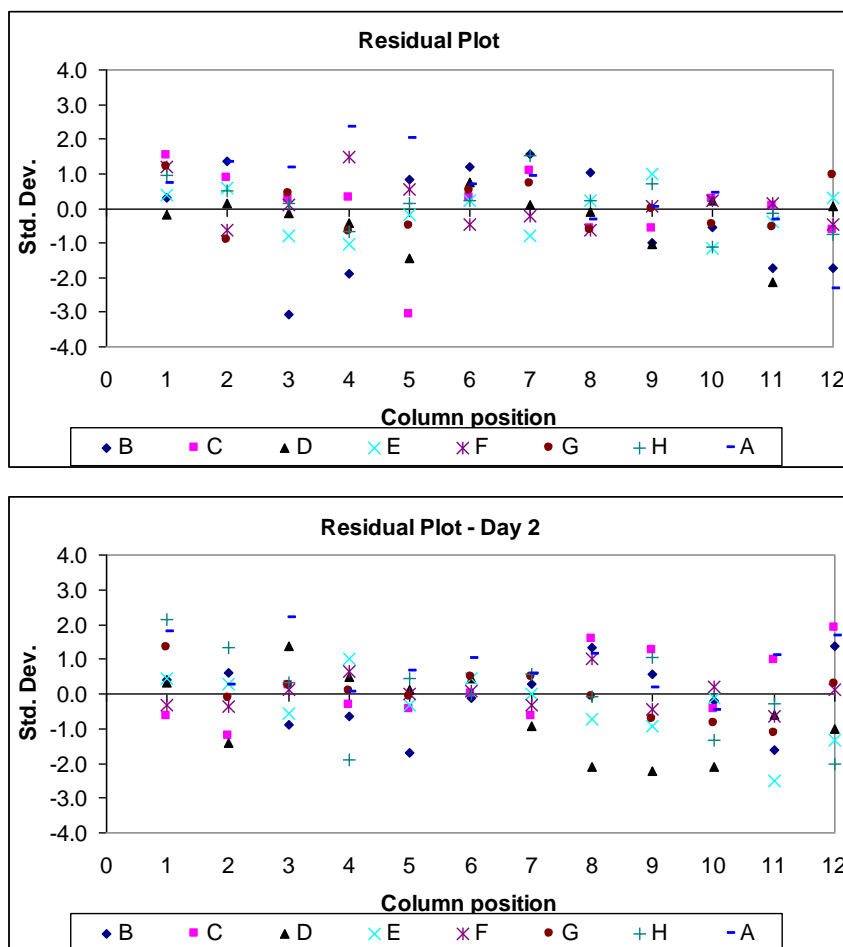


**Figure 2.9** Dependence of the amount extracted on well position in two typical experiments. The residual plots for the amount of diazepam extracted by each well of a 96-well plate are shown. Both figures are plotted using the same scale, and 0 position represents the overall mean amount of diazepam extracted (n=96) for the given extraction.

### 2.3.1.6 Investigation of well cross-talk using PDMS coatings

The cross-talk between wells is another important factor to examine during the evaluation of automated systems based on multi-well plate technology.<sup>135</sup> This issue was found particularly problematic for LLE methods based on multi-well plates as sealing of the plates during the mixing step may not be sufficient, and monitoring the performance with two or more contamination tracers is usually recommended to ensure good data quality.<sup>50</sup> In order to evaluate if there is any well cross-contamination for proposed SPME set-up, a blank buffer solution was placed in random well locations across the plate (27 locations shown in Figure 2.10), while the remaining wells contained a

high concentration of diazepam standard (300 ng/mL). After extraction and desorption, this plate was analyzed for the presence of any trace quantities of diazepam in the chromatograms obtained for the wells containing blank solution. No diazepam was found in these blank solutions confirming that the cross-contamination across the wells does not occur using optimum agitation conditions and sample volumes. If the agitation speed is further increased (for example >1000 rpm), this resulted in spilling and possible cross-contamination, indicating very high agitation speeds should be avoided. Furthermore, if the fibres are not properly centered within the wells, this was also found to cause inadvertent spilling and cross-contamination.

	1	2	3	4	5	6	7	8	9	10	11	12
A	S	S	B	S	S	B	S	S	B	S	B	S
B	S	B	S	S	B	S	S	B	S	S	S	S
C	B	S	B	S	S	B	S	S	S	B	S	B
D	S	S	S	S	B	S	S	B	S	S	S	S
E	S	B	S	B	S	S	B	S	S	S	B	S
F	B	S	S	S	S	S	B	S	B	S	S	S
G	S	S	S	B	S	B	S	S	S	S	S	B
H	B	S	S	S	S	S	S	B	S	S	S	S

**Figure 2.10 Plate map indicating well selection for cross-talk experiment. B denotes placement of blank PBS solution in the well and S denotes placement of 300 ng/mL diazepam standard solution in the well.**

### 2.3.1.7 Summary of overall performance of PDMS coatings

According to the results presented above, PDMS coating was found to perform well for drug analysis using Concept 96 system in terms of extraction efficiency, carryover, and inter-fibre reproducibility. The array of fibres was easy to prepare and affordable. The same set of fibres was used for all of the experiments described here indicating good coating reusability (> 50 times with no loss of extraction efficiency). However, two main issues were encountered with this coating: (i) very long extraction times and (ii) large range of RSD values observed during evaluation of intra-fibre reproducibility. The former impacts the analytical sensitivity, while the latter adversely affects quantitative analysis which is especially problematic for subsequent application development. Possible causes for poor intra-fibre reproducibility were investigated in detail, but no satisfactory explanation for the observed results was found after the examination of carryover, well cross-talk and uniformity of agitation. One possible explanation is that long extraction times result in slight and unpredictable variations in room temperature (for example, laboratory temperature during the day *versus* night), which affect the



magnitude of distribution constant and the amount of analyte extracted. The addition of internal standard (lorazepam) before extraction did not improve the observed results, so further use of this coating was discontinued and research efforts focused on finding a more suitable coating for this automated multi-fibre SPME system.

#### 2.3.1.8 SPME coatings based on coated silica particles: influence of particle type on coating properties

The new coating needed to satisfy four main criteria: (i) good extraction efficiency for drugs (ii) low cost of preparation (iii) thin to facilitate mass transfer of analytes and (iv) good intra- and inter-fibre reproducibility. Polypyrrole coatings were previously found to meet the first three criteria, but exhibited poor inter-fibre reproducibility (>30% RSD) despite extensive efforts to optimize the coating preparation procedure.<sup>136</sup> Materials that are typically used as stationary phases in reverse-phase liquid chromatography such as octadecyl (C<sub>18</sub>) porous silica particles were previously shown to perform well as SPME extraction phases due to their good extraction capacity and reasonable extraction kinetics for more polar analytes such as drugs and metabolites.<sup>86, 87, 132, 137-139</sup> The optimization of coating procedure based on coated silica particles was also attractive for future work in metabolomics, as the properties of the coating could be modified by changing the type of particles employed in the coating procedure. Thus, based on good potential of these coatings for both bioanalytical and metabolomics applications, their suitability for use with the automated multi-fibre SPME system was investigated.

Previous work within our research group recommended a simple coating procedure on the basis of the attachment of the coated silica particles to the stainless steel surface using a strong adhesive (Loctite commercially-available UV-curing adhesive based on methacrylate ester) with good chemical resistance.<sup>132</sup> However, no extensive data regarding inter-fibre reproducibility of this coating existed, so the first step of coating development focused on the evaluation of this parameter using benzodiazepines as model analytes. First experiment compared the performance of five different types of coated silica particles for coating preparation. Two main types of coated particles were considered: (i) C<sub>18</sub> and (ii) C<sub>16</sub> with an embedded amide group (reverse phase amide or RPA). The comparison focused on three main parameters: inter-fibre reproducibility, extraction efficiency and adhesion of the coating upon repeated use. Figure 2.11 shows the results of this comparison for diazepam, but the results for lorazepam, oxazepam, and nordiazepam showed similar trends. Two consecutive extractions were performed using 12 fibres of each coating type. Among different C<sub>18</sub>

particles tested, C<sub>18</sub> silica particles of 10 µm diameter had the highest extraction efficiency for benzodiazepines. However, the results for the second extraction using this coating show noticeable decrease in the amount extracted and significant deterioration of inter-fibre reproducibility. This indicates significant loss of coating upon repeated use. In contrast, SPME coatings based on 5 µm particles showed improved adhesion and the results for two consecutive extractions show excellent agreement. Among these coatings, Ascentis® RPA coating had the best inter-fibre reproducibility, so this particle type was selected for all further experiments.

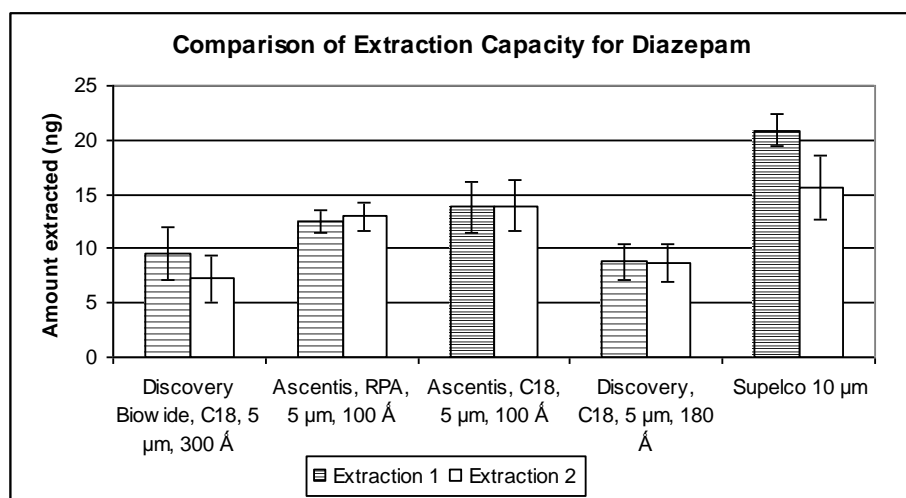


**Figure 2.11 Evaluation of different coated silica particles for use as SPME extraction phases. The amount shown is the mean amount extracted by 12 fibres tested. The error bars show one standard deviation from the mean. The results for two consecutive extractions are shown as an indication of coating adhesion.**

### 2.3.1.9 Evaluation of inter-fibre and intra-fibre reproducibility for C<sub>18</sub> and RPA coatings

Considering the poor intra-fibre reproducibility observed with PDMS coating, the next step of the evaluation focused on this parameter prior to proceeding any further with the coating development. A total of 14 experiments was performed on three consecutive days using 15 fibres with RPA 5 µm particle coating in order to evaluate both intra-day and inter-day reproducibility of the amount extracted by each individual fibre. The results obtained are summarized in Table 2.3. Mean %RSD ranged from 9-19% for intra-day reproducibility experiments, and 11-18% for all 14 experiments. Furthermore, the use of lorazepam as internal standard improved intra-fibre reproducibility

**Table 2.3 Summary of intra-fibre reproducibility results for 15 fibres coated with RPA 5  $\mu$ m extraction phase and using 0.81 mm stainless steel support. The results are shown as intra-day and inter-day reproducibility. The effect of the use of lorazepam as internal standard to improve reproducibility is also shown.**

	Mean % RSD Diazepam	Mean % RSD Oxazepam	Mean % RSD Nordiazepam	Mean % RSD Lorazepam
<b>INTRA-DAY REPRODUCIBILITY - no internal standard</b>				
Day 1 ( n=6 experiments)	9	15	10	15
Day 2 (n=3 experiments)	14	15	12	19
Day 3 (n=5 experiments)	12	16	12	12
<b>INTRA-DAY REPRODUCIBILITY - using lorazepam as internal standard</b>				
Day 1 ( n=6 experiments)	7	5	5	NA
Day 2 (n=3 experiments)	11	8	8	NA
Day 3 (n=5 experiments)	4	6	3	NA
<b>INTER-DAY REPRODUCIBILITY – no internal standard</b>				
All data (n=14 experiments)	11	17	11	18
<b>INTER-DAY REPRODUCIBILITY – using lorazepam as internal standard</b>				
All data (n=14 experiments)	7	10	8	NA

NA = not applicable since lorazepam was used as internal standard

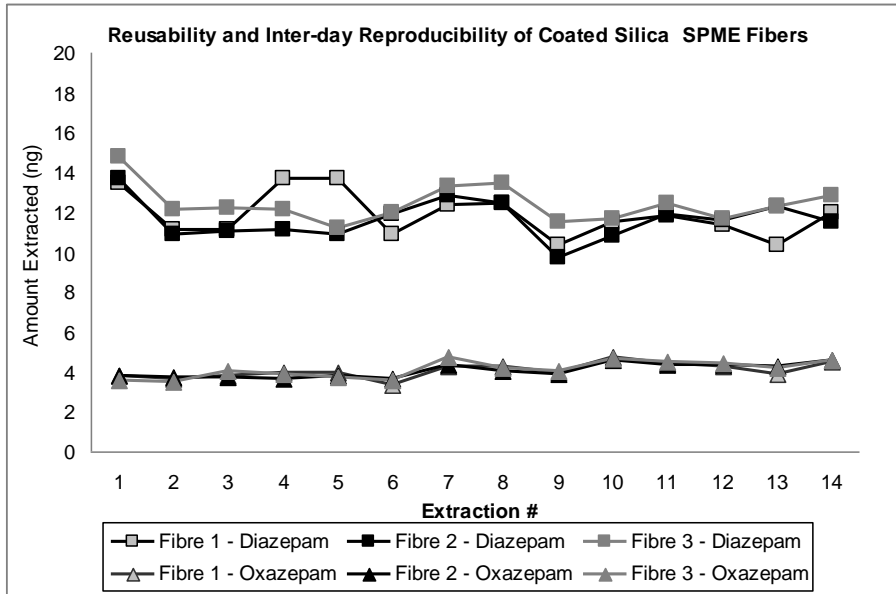


**Figure 2.12 Diagram showing reusability of RPA 5  $\mu$ m coatings over 14 extractions. The amount extracted of diazepam and oxazepam is shown over time for three representative fibres. Data points for lorazepam and nordiazepam are omitted for clarity.**

considerably with all intra- and inter-day mean %RSD  $\leq$ 11%. This showed that all of the factors during extraction could be well-controlled and that this coating was a good candidate for further development. Figure 2.12 shows the results for repeated extraction of diazepam and oxazepam for three representative fibres. The results show good reusability of coating and no loss of coating upon repeated use, indicating strong adhesion of the coating to the metal support.

Although the fibres based on coated silica particles showed acceptable intra- and inter-fibre reproducibility, further optimization of coating procedure was performed to investigate if the performance of the fibres could be further improved. The results of the experiment comparing the performance of stainless steel wires of different dimensions are shown in Figure 2.13 in order to determine the most suitable dimensions for use with automation. As predicted by SPME theory, the extraction efficiency of the fibres increased as the surface area of the solid support increased. Further increases in diameter beyond 0.061-inch (or 1.55 mm) were not considered because of the limitations of well dimensions in order to prevent scratching of the coatings by contact with the sides of the well during agitation. Increasing solid support diameter also resulted in improved inter-fibre reproducibility as indicated by lowest RSD in Figure 2.13 (b) for the thickest stainless steel wires. This indicates it was easier to achieve more uniform surface coverage with thicker fibre cores. Finally, increasing the diameter of stainless steel support was found beneficial to improve the mechanical robustness of the fibres and their compatibility with Concept 96 system. For PDMS coatings, the use of thin pins as solid support occasionally resulted in accidental bending of some fibres during the positioning step, but this problem was completely eliminated with the use of proposed 1.55 mm solid support. A custom-made multi-fibre SPME device was built to hold these 1.55-mm fibres as described in Experimental section with the help of the University of Waterloo machine shop. This new device was used for all subsequent experiments.

After the selection of optimum solid support, inter-fibre reproducibility was examined for all 96 fibres as shown in Table 2.4. The results showed that the fibres could be coated reproducibly with RSD values ranging from 13-17%, which is quite good for a lab-made coating. In agreement with previous results, internal standard was able to compensate well for variations in extraction efficiency for each fibre and to improve overall method precision to  $\leq$ 10% RSD which is acceptable for regulated bioanalysis.

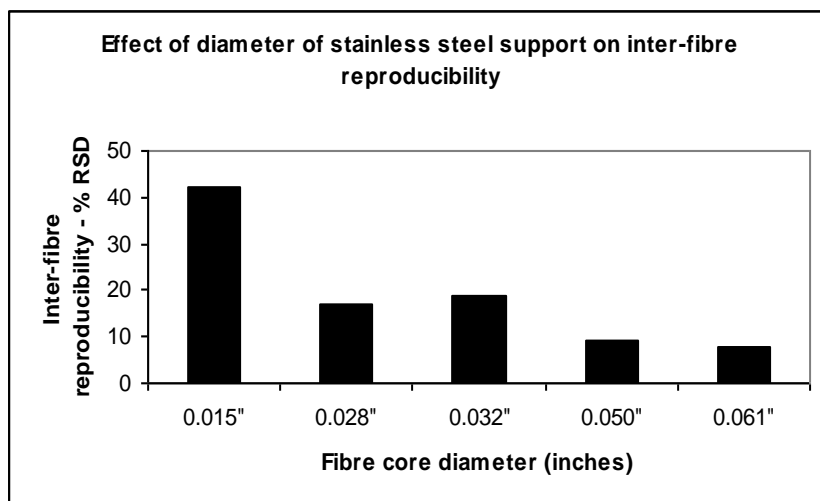
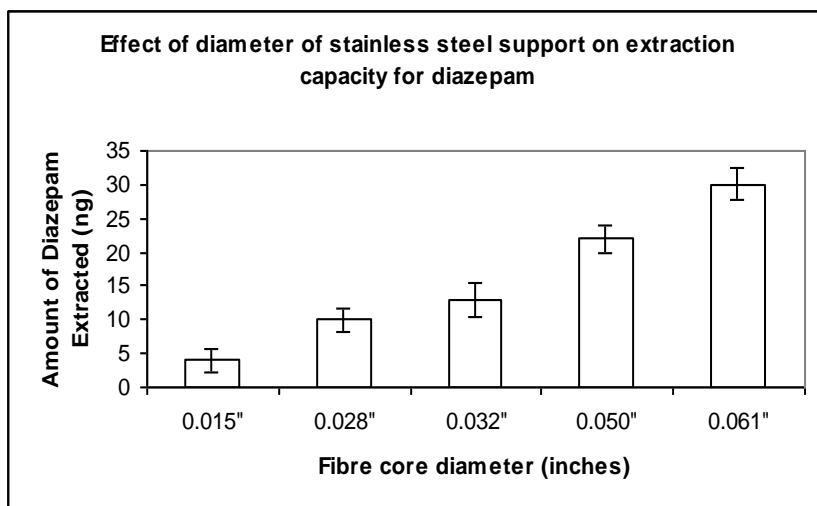


**Figure 2.13 (a) Evaluation of the effect of the diameter of stainless steel support on extraction efficiency for diazepam. The bars show the mean amount extracted by batch of 12 fibres, and the error bars show one standard deviation of results (b) Comparison of inter-fibre reproducibility (% RSD for the amount extracted) of batches of 12 fibres prepared using different dimensions of stainless steel support.**

**Table 2.4 Summary of inter-fibre reproducibility results for 96 fibres coated with RPA 5  $\mu$ m extraction phase and using 1.55 mm stainless steel support. The effect of the use of lorazepam as internal standard to improve reproducibility is also shown.**

Analytical Parameter	Diazepam	Nordiazepam	Oxazepam
Mean amount extracted, n=96 fibres, no internal standard (ng)	35.9	28.2	9.8
% RSD, no internal standard, n=96 fibres	15	13	17
Mean amount extracted, n=96 fibres, with internal standard (ng)	37.9	28.7	9.8
% RSD, with internal standard, n=96 fibres	9	6	6

#### 2.3.1.10 Optimization of acid etching time

During coating preparation, acid etching step helps to improve adhesion of the coating to stainless steel wire. The effect of varying acid etching time on inter-fibre reproducibility was examined. Figure 2.14 shows that increasing acid etching time to 2 hr significantly improved coating procedure.

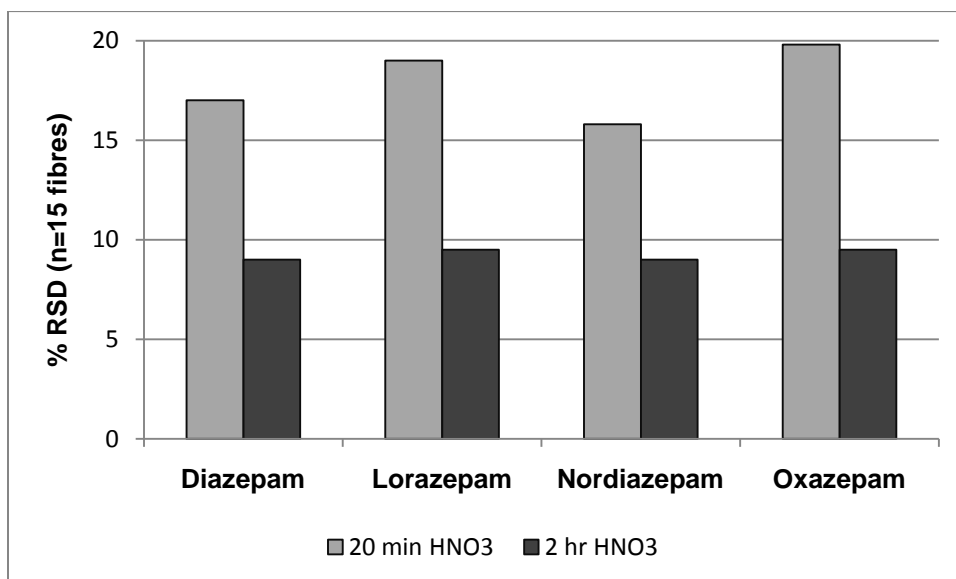


**Figure 2.14 Optimization of nitric acid etching time. Batches of 15 fibres (1.55 mm diameter) were prepared using coating procedure described in Experimental except acid etching time was increased from 20 min to 2 hr. The extraction was performed from 100 ng/mL benzodiazepine standard solution using optimized SPME conditions.**

### 2.3.1.11 Examination of coating surface using scanning electron microscopy (SEM)

The surface of the optimized coatings was examined using scanning electron microscope (LEO 1530 field emission SEM, Carl Zeiss NTS GmbH, Oberkochen, Germany). SEM images were acquired by trained operator Francois Breton using an acceleration voltage of 15 kV and are shown in Figure 2.15. Carbon conductive tape and specimen mounts (Ted Pella, Redding, CA, USA) were used to hold the samples. Prior to analysis, fibres were cut into 1-mm pieces, dried for 1 hr in oven at 140°C, and then sputtered with ~10 nm of gold. The images show that very uniform coverage of particles was achieved, with tight packing of spherical silica particles. Furthermore, a portion of the surface was removed on purpose to estimate the coating thickness. The coating consisted of a single layer of particles and estimated coating thickness was 5.7  $\mu\text{m}$  which is in line with particle dimensions of 5  $\mu\text{m}$ . It is interesting to note in the 600x magnification image that the particle size is not uniform. This large variability in particle size is expected to be an important contributing factor to observed inter-fibre variability in extraction efficiency. In future, this factor could possibly be explored to further improve inter-fibre reproducibility by finding a supply of more uniformly sized coated silica particles or to extend the procedure to the use of nanoparticles.

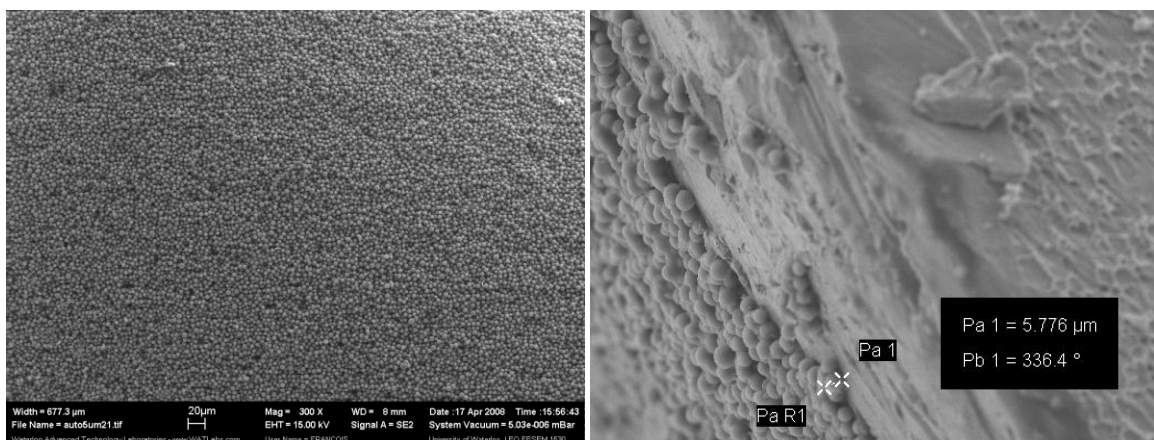


**Figure 2.15 SEM images of 1.55 mm SPME fibre coated with 5  $\mu\text{m}$  RPA particles and prepared according to procedure described in Experimental. (a) surface morphology using 300x magnification (b) estimation of coating thickness using 600x magnification.**

### 2.3.1.12 Optimization of automated SPME method for benzodiazepines

Using optimized fibres, the extraction time profiles were constructed for all four benzodiazepines using extraction times ranging from 1 to 120 min. The equilibrium was reached in 30 min for all

benzodiazepines tested, as shown in Figure 2.16. This confirms that the kinetics of the extraction for these SPME fibres are much faster than those for PDMS-based fibres due primarily to significant reduction in coating thickness (165  $\mu\text{m}$  versus 5  $\mu\text{m}$ ). The optimized desorption conditions were determined to be acetonitrile/water (1/1, v/v), with 30 min desorption time using 850 rpm agitation. These desorption conditions resulted in the carryover of 1-2% for the four benzodiazepines. However, the presence of carryover did not affect subsequent analysis, because the observed carryover was completely eliminated during pre-conditioning step. Therefore, the 30- min preconditioning step in methanol/water (1/1, v/v) served a dual purpose of : (i) wetting the fibre surface in preparation for the extraction and (ii) eliminating any carryover of analyte remaining in the extraction phase from a previous extraction.

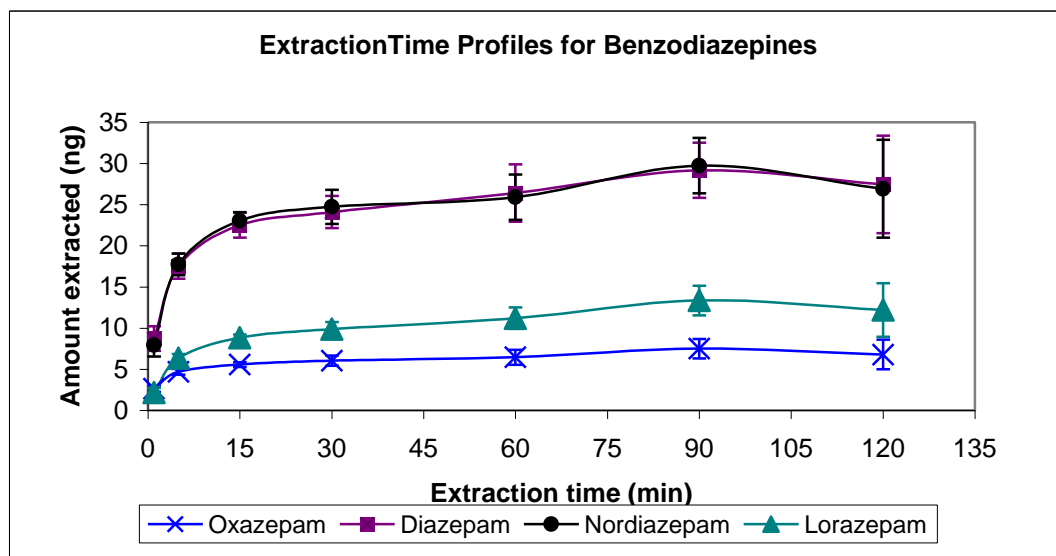


**Figure 2.16** Extraction time profile for diazepam, nordiazepam, oxazepam and lorazepam using RPA coating. Extraction conditions: 100 ng/mL benzodiazepine standard in PBS pH 7.4, 850 rpm agitation.

### 2.3.1.13 Summary of coating evaluation results: comparison of PDMS versus RPA coating

The summary of results obtained during evaluation of PDMS and RPA types of coatings is shown in Table 2.5. The experimental results clearly indicate better overall performance of thin RPA coating, with particular improvements observed in time required to reach equilibrium and improved intra-fibre reproducibility. Both coatings also had similar extraction efficiency for benzodiazepines tested, but lower carryover was observed with PDMS coating. However, the latter issue was successfully



resolved for RPA coating during preconditioning step, where any carryover is fully removed prior to next extraction as long as fresh portion of solvent is used each time precondition step is carried out. Therefore, RPA coating was selected for all subsequent experiments and evaluated in applications using more complex biological matrix as discussed in Section 2.3.2.

**Table 2.5 Comparison of performance of PDMS and RPA coatings for the extraction of diazepam.**

Analytical parameter	PDMS	RPA
Extraction efficiency for diazepam	30%	30%
Carryover	0.3%	1-2%
Intra-fibre reproducibility (n=5 extractions, mean of 96 fibres)	9% RSD	7% RSD
Intra-fibre reproducibility (n=5 extractions, RSD range for 96 fibres)	1-23% RSD	6-10% RSD
Inter-fibre reproducibility (n=96 fibres, no internal std)	10% RSD	12% RSD
Inter-fibre reproducibility (n=96 fibres, with internal std)	15% RSD	7 % RSD
Equilibration time	20 hr	30 min

#### 2.3.1.14 Comparison of method precision for manual *versus* automated dispensing of desorption solvent

The only step of the sample preparation procedure which was not automated with the proposed SPME-LC-MS/MS system was the placement of samples and desorption solution into wells. Although the original prototype unit of Concept 96 included a syringe arm for desorption solvent dispensing, the arm could only be used to dispense volumes of up to 250  $\mu$ L which was not sufficient in current work. Furthermore, the dispensing step was time consuming due to serial nature of dispensing. To address this issue, an automated multi-well plate dispensing unit (for example, Ultraspense 2000) can be used to dispense solutions into the wells instead of manual pipetting. The dispensing is performed in parallel for a row of wells, so the entire plate can be filled within 1 min. The effect of the use of automated 96/384 well microplate reagent dispenser (Ultraspense 2000) on overall method precision was examined (Table 2.6). Both methods of dispensing offered equivalent accuracy and precision, but the use of automated dispensing enhanced automation and reduced the amount of time required to prepare the entire plate about 10-fold.

**Table 2.6 Comparison of method precision (n=96 fibres) of manual pipetting *versus* automated dispensing. For manual pipetting, standard solution and desorption solvent were placed into wells using air displacement Fisherbrand 100-1000  $\mu$ L pipette. For automated dispensing experiment, standard solution and desorption solvent were placed into wells using Ultraspense2000.**

Analyte	Analytical parameter	Manual pipetting	Automated dispensing
Diazepam	Mean amount extracted (ng)	24.9	24.4
	RSD (%)	(10)	(11)
Oxazepam	Mean amount extracted (ng)	9.2	9.4
	RSD (%)	(5)	(6)
Nordiazepam	Mean Amount extracted (ng)	12.4	12.4
	RSD (%)	(9)	(9)

### 2.3.1.15 Comparison of calibration methods

The use of lorazepam as internal standard was found to improve overall method precision significantly as previously shown in Tables 2.3, 2.4 and 2.5. A more detailed study was then conducted to evaluate whether the use of deuterated internal standard provides additional improvements, and whether other calibration approaches such as fibre constant calibration and on-fibre standardization can also be employed when developing automated multi-fibre SPME methods. Briefly, using the on-fibre standardization calibration approach (see also Section 1.4), a known amount of calibrant (usually a deuterated analogue) is preloaded into the extraction phase prior to performing an extraction.<sup>84, 85, 140, 141</sup> The process of desorption of calibrant from the extraction phase into the system can be used to calibrate the simultaneous and symmetric process of analyte extraction into the coating. This calibration approach is particularly useful for calibration of pre-equilibrium SPME methods because it successfully corrects for non-uniform agitation conditions. For automated SPME methods with Concept 96, this means that sample throughput could be further improved by using very short pre-equilibrium extraction times. Fibre constant calibration is a simple method where the magnitude of  $K_{fs}V_f$  product is determined for each fibre for a given analyte using a standard solution of known analyte concentration and the relationship shown in Equation 1.1. The magnitude of  $K_{fs}$  is constant for a given analyte and extraction conditions, so the variations in magnitude of  $K_{fs}V_f$  product are reflective of small variations in the amount of coating deposited on each fibre. This correction factor derived for each individual fibre can then be applied to all subsequent extractions and used to eliminate inter-fibre variability from the data.

Figure 2.17 (a) shows the effect on method precision obtained using each of five calibration methods tested: (i) external calibration (ii) lorazepam as internal standard (iii) diazepam-d5 as internal standard (iv) on-fibre standardization and (v) calibration using fibre constant. The comparison was performed using the same set of 12 randomly selected fibres for the extraction of diazepam. The results shown for external calibration correspond to the true variability of the 12 fibres used for the experiment, as no correction to compensate for variation in  $V_f$  has been applied. The best results were obtained with internal standard calibration or the calibration using fibre constants. Among these two calibration methods, internal standard calibration is simpler and less time-consuming because it does not require any additional experiments. Both lorazepam and deuterated diazepam were found to perform equally well when used as internal standards for the quantitation of diazepam. More surprisingly, on-fibre standardization did not improve overall method precision when compared to the results obtained using external calibration. One possible explanation for the observed result is the compounding of experimental uncertainty because multiple parameters must be determined experimentally in order to apply on-fibre standardization. Both the amount of analyte extracted and the amount of calibrant remaining in the extraction phase must be determined experimentally. The performance of on-fibre standardization was further examined by investigating whether it can be used to correct for intra-fibre reproducibility for repeated extractions using the same fibre. This test was performed using a subset of five fibres and the results were compared to internal standard calibration as shown in Figure 2.17 (b). The results show equivalent performance of both methods. These results show that on-fibre standardization is suitable to use to correct for variation in extraction conditions and can improve inter-fibre reproducibility. Poor performance for the correction of inter-fibre reproducibility can possibly be caused by insufficient optimization of calibrant loading procedure. In other experiments described in Section 3.3.9, preloading of standard from methanol/water was found to provide improved performance. However, such approach for 96-array of fibres would be cost-prohibitive because it would consume large quantity of calibrant. Based on the results obtained, the internal standard calibration method was selected as the best and simplest calibration method for automated multi-fibre SPME.

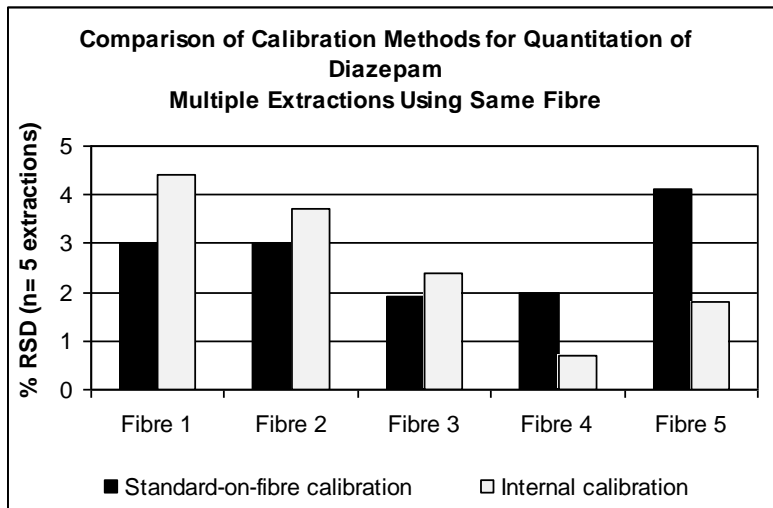
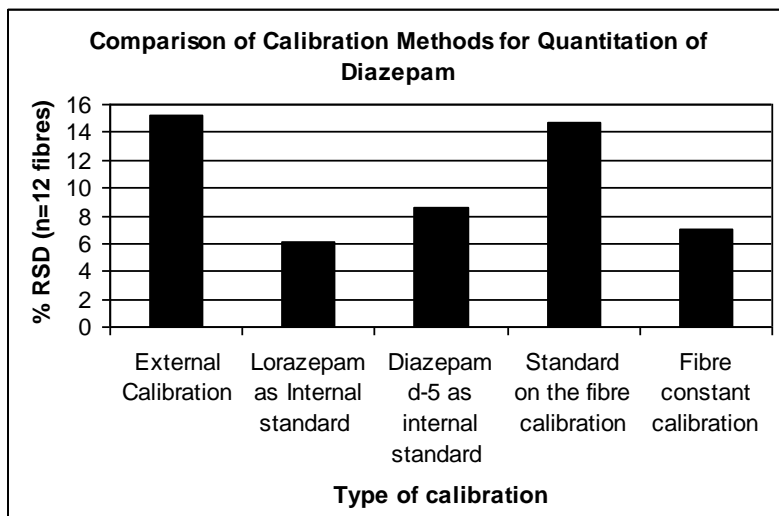


**Figure 2.17 (a) Comparison of external standard, internal standard and on-fibre standardization (standard-on-the fibre) calibration methods for the use with automated multi-fibre SPME. The dependence of % RSD (n=12 fibres) of the amount extracted on the choice of calibration method is shown. All extractions were performed from 100 ng/mL diazepam standard solution in PBS buffer pH 7.4 using optimal SPME conditions. (b) Comparison of standard-on-fibre *versus* internal standard calibration for improving intra-fibre reproducibility. The dependence of % RSD (n=5 extractions using each fibre) on the choice of calibration method is shown.**

### 2.3.1.16 SPME method development using Concept 96: general considerations

In conclusion, the performance of Concept 96 autosampler was found satisfactory, and the use of this robotic station provides high sample throughput with high degree of automation. Figure 2.18 shows an overview of the parameters that can be optimized during method development of such automated SPME methods. The main parameters whose optimization is mandatory is the type of coating and corresponding optimum preconditioning procedure, optimization of wash procedure to ensure no loss of analyte occurs between extraction and desorption step and the optimization of desorption conditions. Depending on the nature of analyte, sample matrix and overall analytical sensitivity required for a particular application, optimization of additional parameters such as pH, ionic strength, sample volume and addition of evaporation/reconstitution step can also be considered. Finally, the overall workflow of an automated SPME procedure using Concept 96 is shown in Figure 2.19 to show the recommended sequence of steps. Based on the results of this research, the prototype design of initial Concept 96 system was changed by PAS Technology to incorporate three orbital agitators: one for preconditioning, one for extraction and one for desorption. Furthermore, a wash station was added to the design to enable automation of the wash step. No agitator is used for this step to prevent any inadvertent desorption of the analyte(s). The option of temperature control during agitation was also added to enable temperature-controlled ligand-receptor binding studies. Finally, Concept software was revised to enable simple user-programming of all steps described in Figure 2.19.

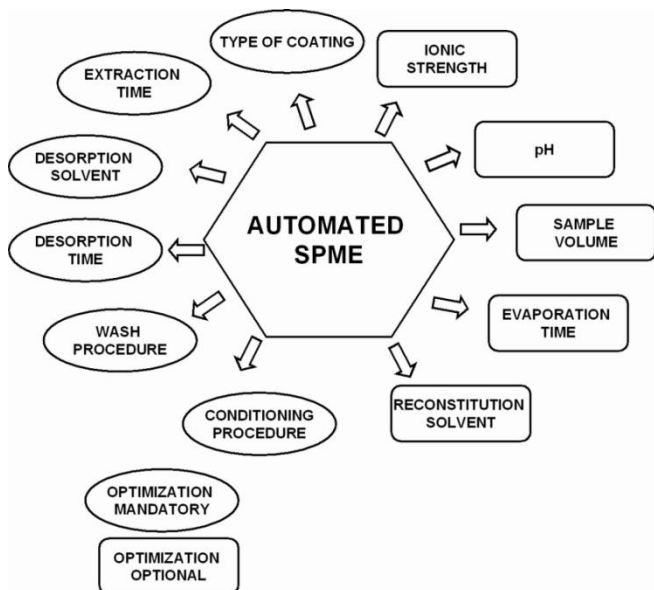


**Figure 2.18 Overview of parameters which may require optimization during method development of an automated SPME method using Concept 96 robotic station.**

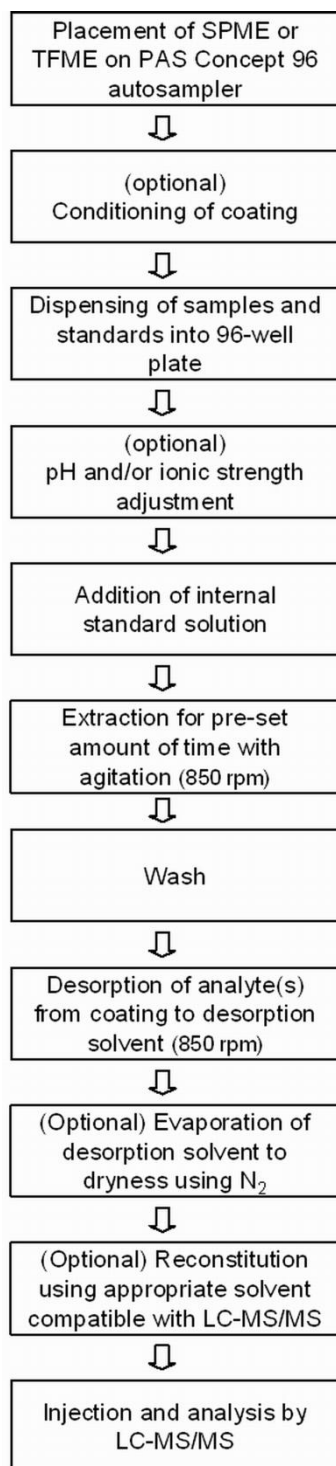


**Figure 2.19 Overview of automated SPME procedure using Concept 96 robotic station**

### **2.3.2 Example application of PAS autosampler: high-throughput analysis of benzodiazepines in whole blood**

Once the performance of Concept 96 was found satisfactory, full validation of the optimized SPME-LC-MS/MS method for the high-throughput analysis of benzodiazepines in whole blood was carried out according to Food and Drug Administration (FDA) guidelines for the method validation of bioanalytical methods.<sup>142</sup> These guidelines are used extensively in pharmaceutical industry, and any useful sample preparation method in regulated bioanalysis must be able to meet these stringent regulatory guidelines. The main aspects of validation included selectivity, linearity, limit of quantitation (LOQ), stability, matrix effects, method precision and accuracy. The latter two parameters require validation over minimum of three concentration levels and over minimum of three days, to establish both intra-day and inter-day method performance.

The selectivity of the method was evaluated by analyzing two lots of blank whole blood samples and no interferences at the retention time of analytes (2.0-2.5 min) were detected in any of the chromatograms. Example extracted ion chromatograms (XIC) of blank whole blood and 50 ng/ml benzodiazepine standard in whole blood are shown in Figure 2.20. Post-preparative stability of samples was demonstrated up to 72 hours when stored in refrigerated autosampler by re-analysis against the freshly acquired calibration curve. Longer times were not evaluated as the analysis of all samples was expected to be completed within this time window.

#### **2.3.2.1 Evaluation of matrix effects**

The widespread use of LC-MS/MS in bioanalysis is mainly due to the excellent sensitivity and selectivity achievable by this method of analysis when dealing with complex mixtures such as biological fluids. However, one of the issues that complicates accurate and precise analysis in LC-MS methods is the susceptibility of ESI to matrix effects. These matrix effects can be defined as the change in the signal of the analyte in the presence of matrix components due to competition for ionization, and can result in signal increase (ionization enhancement) or signal decrease (ionization suppression). As such, regulatory guidelines recommend the determination of matrix effects using various lots of biological fluids in order to evaluate how robust method is to such effects.<sup>142</sup> The main approaches to minimize/eliminate matrix effects are to develop sample preparation methods with efficient clean-up in order to remove as many matrix components as possible and to ensure good chromatographic retention and chromatographic resolution of analytes whenever possible.<sup>143</sup> Among sample preparation methods, plasma protein precipitation methods provide the poorest sample clean-

up and can result in largest degree of ionization suppression. Solid-phase extraction and liquid-liquid extraction generally provide much improved sample clean-up. Due to equilibrium extraction nature of SPME, it can provide even better sample clean-up than SPE because only a limited amount of sorbent is used and the amount of extraction is governed by the magnitude of distribution coefficient for both analytes of interest and other sample components.

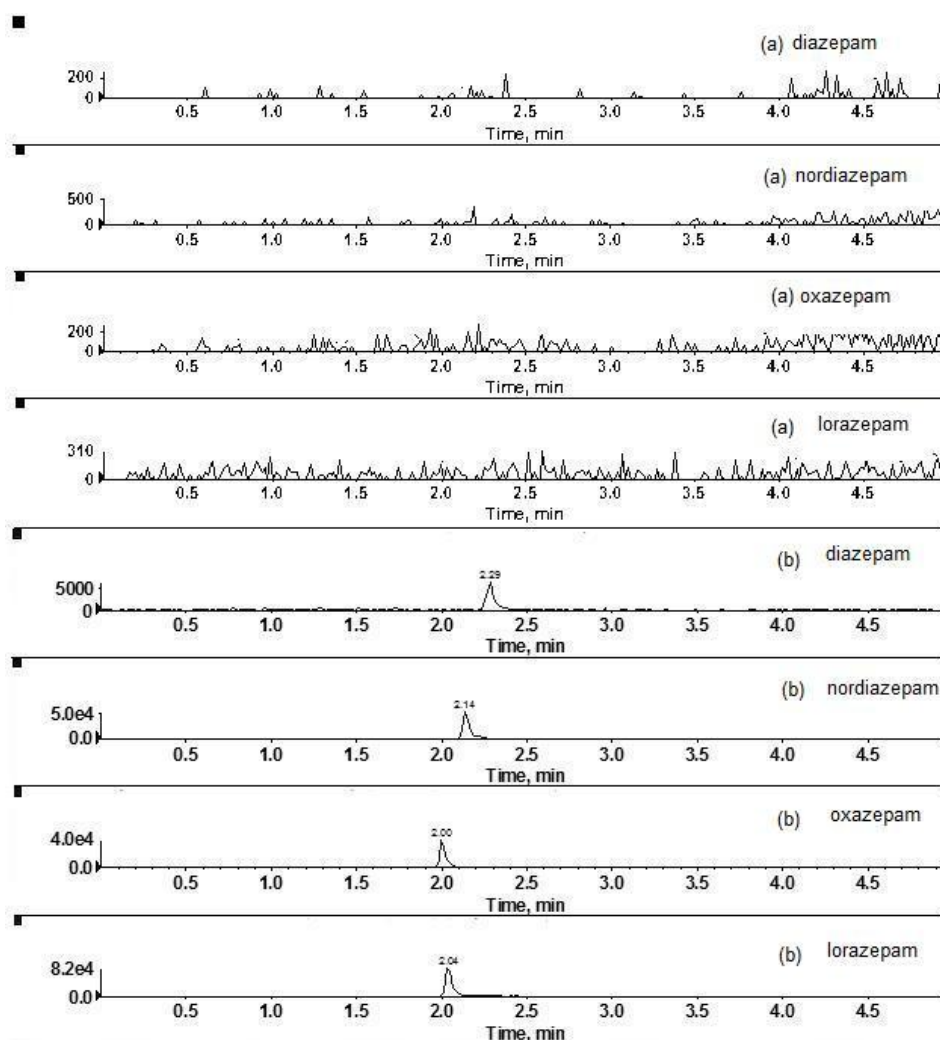


**Figure 2.20** Example extracted ion chromatograms (XIC) of diazepam, nordiazepam, oxazepam and lorazepam in (a) blank whole blood sample and (b) 50 ng/mL benzodiazepine standard in whole blood.

Therefore, as part of method validation, proposed SPME-LC-MS/MS method was evaluated in terms of absolute matrix effects. This test is performed by comparing signal intensity of blank



biological fluid sample spiked post-extraction with analytes *versus* signal intensity for neat standard prepared directly in desorption solvent at the same concentration level. In absence of any matrix effects, the two standard solutions should result in the same signal intensity within experimental error, and differences of  $\pm 20\%$  are generally acceptable. The results for this experiment are shown in Table 2.7. A set of duplicate standard solutions was prepared at concentration level of 1  $\mu\text{g/mL}$  and directly infused into mass spectrometer. The results show that no matrix effects were observed for lorazepam, while the remaining analytes showed significant degree of ionization suppression. This example highlights the importance of incorporating an LC separation step in overall workflow. Once entire LC-MS/MS method was evaluated, no matrix effects were observed for any of the analytes as indicated by the relative signal response ranging from 95-102%. Acceptable range is considered 80-120% which takes into account typical precision of electrospray LC-MS/MS methods.

**Table 2.7 Results of the evaluation of absolute matrix effects for the analysis of benzodiazepines in whole blood. % signal represents the ratio of the signal of blank whole blood extract spiked post-extraction *versus* neat standard prepared directly in desorption solvent at the same concentration level.**

Analyte	Direct infusion into MS (1 $\mu\text{g/mL}$ ) % Signal post-extraction spike <i>versus</i> neat standard	LC-MS/MS (20 $\text{ng/mL}$ ) % Signal post-extraction spike <i>versus</i> neat standard
Lorazepam	97	95
Oxazepam	79	101
Nordiazepam	46	100
Diazepam	49	102
Diazepam <i>d5</i> (IS)	45	102

### 2.3.2.2 Linearity, limit of detection (LOD) and limit of quantitation (LOQ)

The limit of detection (LOD) for the proposed method was determined according to 3x signal-to-noise criteria and was found to range from 0.8  $\text{ng/mL}$  for oxazepam to 3  $\text{ng/mL}$  for diazepam. Limit of quantitation (LOQ) for the proposed method was determined according to FDA guidelines.<sup>142</sup> In this definition, LOQ is the lowest concentration of the analyte in given matrix which meets the following acceptance criteria: (i) accuracy of  $\pm 20\%$  from the nominal concentration and (ii) precision  $\leq 20\%$  RSD for five replicate determinations. The lowest concentration tested (4  $\text{ng/mL}$ ) of all four benzodiazepines met this criteria, and the results are presented in Table 2.8. This sensitivity was sufficient for assaying clinically relevant concentrations of benzodiazepines. For example, expected therapeutic range of diazepam and nordiazepam is 0.15-0.8  $\mu\text{g/mL}$ <sup>144</sup>, whereas the therapeutic

concentration of more potent lorazepam is about 0.03 µg/mL.<sup>145</sup> Therefore, the strategies for further improving LOQ, such as addition of evaporation/reconstitution step were not further explored.

The method was linear in the range of 4-1000 ng/mL for diazepam and nordiazepam and in the range of 4-500 ng/mL for oxazepam and lorazepam, making it amenable for therapeutic drug monitoring of these drugs. Linearity was evaluated by constructing six independent calibration curves using independent sets of fibres, to investigate if calibration curves acquired using single point per calibration standard were sufficient for quantitative analysis. The results showed excellent agreement. For instance, the average slope of six calibration curves in two different lots of whole blood was found to be 0.00243±0.00005 for diazepam, while the linear regression coefficients ( $r^2$ ) ranged from 0.997-0.999. This linearity data further confirms the ability of internal standard to compensate properly for inter-fibre variation, and good overall performance of SPME method. It should be noted that the upper limit of linear dynamic range reported in Table 2.8 is limited by the linear dynamic range of the instrument due to detector saturation or ESI droplet surface saturation<sup>146, 50</sup>, and not by SPME procedure itself. This means that samples exceeding the upper limit can still be successfully analyzed after appropriate dilution.

**Table 2.8 Automated SPME-LC-MS/MS method validation results: LOQ and linear range.**

Analytical parameter	Diazepam	Oxazepam	Nordiazepam	Lorazepam
LOQ (ng/mL)	4	4	4	4
Mean % accuracy (n=5):	102	111	105	102
% RSD (n=5)	11	17	9	14
Signal-to-Noise Ratio	5	19	16	16
Dynamic Linear Range (ng/mL)	4-1000	4-500	4-1000	4-500

### 2.3.2.3 Method accuracy and precision: intra- and inter-day results

The accuracy and intra-day precision of the proposed method was evaluated at four concentration levels (10, 25, 100 and 500 ng/mL) using five replicate samples at each level (Table 2.9). For all compounds and all levels, the precision of the results does not exceed acceptance criteria of 15% RSD (range 2-14% RSD). Mean accuracy of 87-109%, also meets requirements of 85-115%. One suspected outlier (recovery of 121%) for oxazepam was detected in the results presented in Table 2.9 and is marked with asterisk (\*). More robust statistics, median and median absolute difference were used for this concentration level as recommended by Analytical Methods Committee when dealing with small data sets containing a suspected outlier.<sup>147</sup> The significant difference observed between

**Table 2.9 Automated SPME-LC-MS/MS method validation results: summary of intra-day accuracy and precision.**

Concentration	Relative recovery (%) Diazepam	Relative recovery (%) Oxazepam	Relative recovery (%) Nordiazepam	Relative recovery (%) Lorazepam
10 ng/mL	116	93	86	98
	103	81	89	88
	105	114	106	123
	120	94	117	115
	100	82	94	101
<b>Mean (n=5):</b>	<b>109</b>	<b>93</b>	<b>98</b>	<b>105</b>
<b>% RSD (n=5):</b>	<b>8</b>	<b>14</b>	<b>13</b>	<b>13</b>
25 ng/mL	84	75	103	84
	102	79	99	113
	96	92	102	94
	99	87	113	93
	87	121*	114	100
<b>Mean (n=5):</b>	<b>94</b>	<b>87*</b>	<b>106</b>	<b>97</b>
<b>% RSD (n=5):</b>	<b>8</b>	<b>9*</b>	<b>6</b>	<b>11</b>
100 ng/mL	102	108	97	99
	103	98	99	109
	109	94	100	105
	108	104	108	116
	92	86	95	99
<b>Mean (n=5):</b>	<b>103</b>	<b>98</b>	<b>100</b>	<b>106</b>
<b>% RSD (n=5):</b>	<b>6</b>	<b>9</b>	<b>5</b>	<b>7</b>
500 ng/mL	97	87	106	83
	101	102	96	102
	97	96	96	94
	100	100	92	110
	101	87	99	100
<b>Mean (n=5):</b>	<b>99</b>	<b>94</b>	<b>98</b>	<b>98</b>
<b>% RSD (n=5):</b>	<b>2</b>	<b>8</b>	<b>5</b>	<b>10</b>

mean-based and median-based statistics (20% RSD *versus* 9% RSD) supports the presence of outlier in this data set. This is further supported by the results collected for the evaluation of inter-day method accuracy and precision and shown in Table 2.10. This experiment was performed using five independent extractions of the same spiked whole blood standard solution at four different concentration levels. Five fibres were used at each level to submit the method to even more stringent evaluation than required by the regulatory guidance (five independent extractions for n=1 fibre at n=3 concentration levels is sufficient according to the guidance). Method accuracy ranged from 89-115%,

while intra-day method precision ranged from 1-12% RSD, both of which meet acceptance criteria for quantitative bioanalysis.

**Table 2.10 Automated SPME-LC-MS/MS method validation results: summary of accuracy and inter-day reproducibility results.**

Concentration (ng/mL)	Mean relative recovery (%) (n=5 analyses) Diazepam	Mean relative recovery (%) (n=5 analyses) Oxazepam	Mean relative recovery (%) (n=5 analyses) Nordiazepam	Mean relative recovery (%) (n=5 analyses) Lorazepam
10 ng/mL	115 (1)	99 (8)	89 (6)	94 (11)
	102 (2)	89 (10)	91 (6)	85 (12)
	115 (1)	112 (7)	115 (4)	115 (10)
	104 (2)	101 (8)	108 (5)	109 (10)
	99 (2)	90 (10)	96 (6)	96 (11)
25 ng/mL	113 (3)	97 (8)	100 (4)	99 (7)
	97 (3)	98 (8)	93 (1)	87 (9)
	102 (4)	107 (8)	106 (4)	103 (8)
	96 (4)	101(8)	104 (4)	107 (10)
	100 (3)	96 (7)	95 (4)	96 (8)
100 ng/mL	112 (5)	115 (10)	101 (4)	109 (12)
	104 (6)	96 (10)	100 (3)	100 (11)
	97 (5)	106 (10)	101 (4)	115 (11)
	101 (5)	113 (10)	101 (4)	91 (11)
	113 (5)	101 (10)	107 (3)	115 (9)
500 ng/mL	105 (6)	104 (12)	103 (4)	103 (10)
	97 (5)	95 (10)	92 (2)	94 (8)
	102 (3)	103 (11)	94 (4)	106 (10)
	99 (5)	104 (10)	90 (3)	97 (10)
	95 (5)	91 (12)	96 (3)	104 (8)

#### 2.3.2.4 Summary of method performance

The performance of proposed SPME-LC-MS/MS method was found satisfactory for the analysis of benzodiazepines in whole blood, and the method meets all regulatory requirements. The proposed sample preparation procedure is simple, automated and applicable to the extraction of whole blood samples without any sample pretreatment steps required. The validated method requires about 100 minutes (30 min preconditioning, 30 minute extraction, 30 minute desorption, ~10 min for dispensing of samples/wash solvent/desorption solvent) for the preparation of 96 samples. This translates into sample throughput of >1000 samples/day in labs where robotic plate feeder and liquid dispensing station is available to permit completely unattended operation, and represents highest SPME throughput reported to date. Table 2.11 gives an overview of various SPME method reported for the

analysis of diazepam in blood, plasma or serum. The results show that LOQ (4 ng/mL) achieved in current work is similar or better than obtained for other SPME methods, while the achieved sample throughput is considerably improved due to parallel nature of extraction. Furthermore, through the optimization of coating and the geometry of the extraction phase (by increasing fibre diameter), the disadvantages of offline desorption with no evaporation/reconstitution step could be successfully overcome (only 20  $\mu\text{L}$  out of 800  $\mu\text{L}$  was injected in current study), so that analytical sensitivity in current work is comparable to that achieved by in tube SPME, thermal or manual desorption methods where all of the extracted analyte is introduced onto analytical column.

**Table 2.11 Summary of SPME methods reported for analysis of diazepam in plasma, serum or whole blood.**

Method type	LC-UV	LC-MS	GC-MS	LC-MS	LC-MS/MS	LC-MS/MS
<b>Interface</b>	In-tube	In-tube	Thermal	Manual	Manual	Offline desorption + reconstitution/evaporation
<b>Biological fluid</b>	serum	serum and urine	plasma	blood	whole blood and <i>in vivo</i>	whole blood and <i>in vivo</i>
<b>SPME coating</b>	RAM diol silica	Supel-Q plot	PDMS 100 $\mu\text{m}$	RAM alkyl diol silica	polypyrrole	C <sub>18</sub> /PEG
<b>Precision</b>	5.0%	NR	6-15%	12%	NR	NR
<b>LOD (ng/mL)</b>	24	1	0.3	20	7	1.7
<b>Linear Range (ng/mL)</b>	50-50000	1-500	1-1000	25-1000	1-1000 <sup>a</sup>	4-2000
<b>Extraction time</b>	4 draw/eject cycles	10 draw/eject cycles	30 min	30 min	30 min	5 min
<b>Reference</b>	148,132	149	150	139	133	138

NR = not reported, <sup>a</sup> Linear range reported in the manuscript was 1-1000 ng/mL, but this contradicts LOD of 7 ng/mL also stated in the manuscript. Based on the data provided it is not clear which figure of merit is correct.

## 2.4 Conclusions and future directions

The optimized automated SPME system (Concept 96) was found to perform very well for the analysis of biological fluids and provided highest sample throughput reported to date with typical sample preparation times of  $\leq 1$  min/sample for the applications developed to date.<sup>151, 152</sup> Furthermore, parallel extraction format allows very accurate timing of extraction and desorption steps and reproducible computer-controlled positioning of fibres within the wells. These characteristics allow the use of pre-equilibrium extraction times with no sacrifice in method precision. SPME sample

throughput is now for the first time comparable to sample throughput achievable by automated SPE and LLE methods in 96-well plate format and is better than online SPE methods. Furthermore, in comparison to traditional methods employed for bioanalytical sample preparation, several features of SPME make it particularly attractive for analysis of biological fluids using LC-MS. First of all, SPME can provide improved sample clean-up, which can minimize/eliminate the occurrence of ionization suppression effects. This is achieved mainly through the use of small volume of extraction phase, which leads to the extraction of smaller amounts of analytes and potential interferences. This reduces potential for competitive ionization effects, which can be concentration-dependent, although the underlying mechanisms are not well-understood.<sup>146</sup> Secondly, SPME is fully compatible with the extraction of heterogeneous samples such as whole blood or tissue homogenates without the need for any sample pretreatment (filtration, centrifugation). This minimizes the overall number of sample handling steps, increases overall sample throughput and eliminates potential sample losses due to sample transfer between various devices (for example, adsorption to centrifuge tube walls or filter materials). The analysis of whole blood is also attractive for the determination of drug partitioning into red blood cells, and such experiments can easily be carried out using SPME (refer to Chapter 4 for an example using carbamazepine). Finally, SPME allows the determination of both unbound and total drug concentrations using a single sample by employing two different calibration strategies (matrix-free for unbound concentration and matrix-matched for total concentration). Traditional methods do not offer such flexibility, so the sample needs to be re-prepared using a different sample preparation method if both pieces of information are required, thus increasing the overall cost of analysis and adversely impacting sample throughput.

One of the limitations of proposed SPME automated system is that it is applicable only to non-volatile analytes because the wells are not sealed during extraction and desorption processes. Some data exists on using the system with semi-volatile polyaromatic hydrocarbons, however even with the use of appropriate internal standard to help correct for any evaporative losses, method precision worsens considerably as the volatility of analyte increases (RSD 14-40% depending on the analyte volatility).<sup>131</sup> A second limitation of proposed system is that the amount of analyte extracted by SPME is typically very small, especially when using biological fluids with high amount of protein (such as plasma, serum or whole blood) and/or when dealing with analytes with high-degree of protein binding (for example, >90% binding of diazepam). Thus, absolute recoveries for SPME in such cases are typically 1-2%, so highly sensitive analytical instrumentation is necessary to ensure adequate LOD/LOQ for a given application. This limitation has largely been addressed over the last

few years with the development of highly sensitive MS instrumentation. The MS instrument used in current work (API3000) already provided sufficient analytical sensitivity for therapeutic drug monitoring without need for further preconcentration through addition of evaporation/reconstitution step. Newer triple quadrupole instruments currently available (such as API5500 from Applied Biosystems or TSQ Vantage from Thermo) provide additional 10- to 100-fold improvement in sensitivity, thus enabling easy implementation of microextraction methods for a variety of clinically relevant applications. Finally, for the best method performance using any type of microextraction method, it is important to keep extraction conditions exactly the same for both standards and samples, so careful attention should be paid to extraction parameters such as pH, ionic strength, temperature and exact matrix composition as discussed in Section 1.4.

Beyond the work described in this chapter, Erasmus Cudjoe further developed Concept 96 robotic system by modifying the geometry of SPME device from fibre geometry described herein to thin-film geometry.<sup>134</sup> The main advantages of the thin-film geometry are improvement in extraction efficiency due to increased surface area, improved agitation as the new device acts like a stirring blade, and improvement in the extraction rate when using very short pre-equilibrium extraction times because analyte uptake by the coating in this linear portion of extraction time curve is directly proportional to the surface area of the device. Based on these improvements (up to 2-fold improvement in analytical sensitivity and extraction rate), commercial SPME device of Concept 96 incorporates thin film geometry. Currently, further modifications of Concept 96 are underway in order to enable the use of this system for parallel, automated desorption of *in vivo* SPME samplers thus increasing throughput of *in vivo* SPME methods such as described in Chapter 4.

## **2.5 Addendum**

The text of this chapter was rewritten in comparison to published research article. The author expresses sincere gratitude to Francois Breton for the acquisition of SEM images. The loan of Ultraspense 2000 unit by KD Scientific is also gratefully acknowledged.

## Chapter 3

### *In vitro* evaluation of *in vivo* SPME devices

#### 3.1 Preamble and introduction

##### 3.1.1 Preamble

This chapter has been published as a paper: Vuckovic D., Shirey B., Chen Y., Sidisky L., Aurand C., Stenerson K., & Pawliszyn J., *In vitro* evaluation of new biocompatible coatings for solid-phase microextraction: implications for drug analysis and *in vivo* sampling applications. *Anal. Chim. Acta* 638, 175-185 (2009). The figures and tables are reprinted from this manuscript with the permission of Elsevier (Copyright Elsevier 2009).

The contributions of co-authors Bob Shirey, Yong Chen, Len Sidisky, Craig Aurand and Katherine Stenerson, were the production and coating development of all prototype SPME devices used in this work. Furthermore, Bob Shirey performed the experimental work to evaluate the degree of swelling of these new coatings on exposure to common solvents.

I, Bob Shirey, authorize Dajana Vuckovic to use the material for her thesis.

I, Yong Chen, authorize Dajana Vuckovic to use the material for her thesis.

I, Len Sidisky, authorize Dajana Vuckovic to use the material for her thesis.

I, Craig Aurand, authorize Dajana Vuckovic to use the material for her thesis.

I, Katherine Stenerson, authorize Dajana Vuckovic to use the material for her thesis.

##### 3.1.2 Introduction

Presently, applications of SPME in combination with GC predominate in literature over SPME-LC applications. Two main reasons behind this trend are: (i) the lack of automation of SPME-LC



methods (addressed in Chapter 2) and (ii) the availability of a limited number of extraction phases suitable for use with LC applications.<sup>153, 154</sup> Figure 3.1 gives an overview of properties desired for LC applications with particular focus on the analysis of biological fluids including *in vivo* SPME sampling applications. Currently, only four coatings are available commercially: polydimethylsiloxane (PDMS), polydimethylsiloxane/divinylbenzene (PDMS/DVB), polyacrylate (PA) and Carbowax-templated resin (CW-TPR). These coatings do not possess sufficient mechanical robustness for use with *in vivo* applications. Furthermore, they exhibit poor extraction efficiency towards polar analytes and are expensive (>\$100 per fibre) which makes the use of multiple fibres during an animal study cost-prohibitive. As these coatings are meant for multiple uses, the issue of inter-fibre reproducibility has not been adequately documented for these fibres. Finally some of these coatings are not biocompatible. Although PDMS is generally considered biocompatible, it is not the first choice for use in medical devices that will be exposed directly *in vivo*.

Recent research efforts into the development of improved SPME coatings resulted in reports of monolithic silica coatings<sup>155, 156</sup> and polymer monolithic coatings<sup>157, 158</sup> which improve extraction kinetics and/or extraction of polar compounds by incorporation of appropriate functional groups. Various tailor-made sol-gel coatings have also been reported in literature as the means of improving chemical and mechanical stability and extraction efficiency, but these have predominantly been used in GC applications.<sup>159</sup> Finally, different types of coatings have been proposed in literature to address the biocompatibility requirement for *in vivo* SPME applications and include polypyrrole coatings<sup>133, 136, 160-162</sup>, coatings based on restricted access materials<sup>132, 139, 163, 164</sup>, and coatings based on mixtures of SPE sorbents (coated silica particles) with biocompatible polymers<sup>86, 137, 138</sup>. Among these, the latter type was recently selected by Supelco for commercialization and further development.

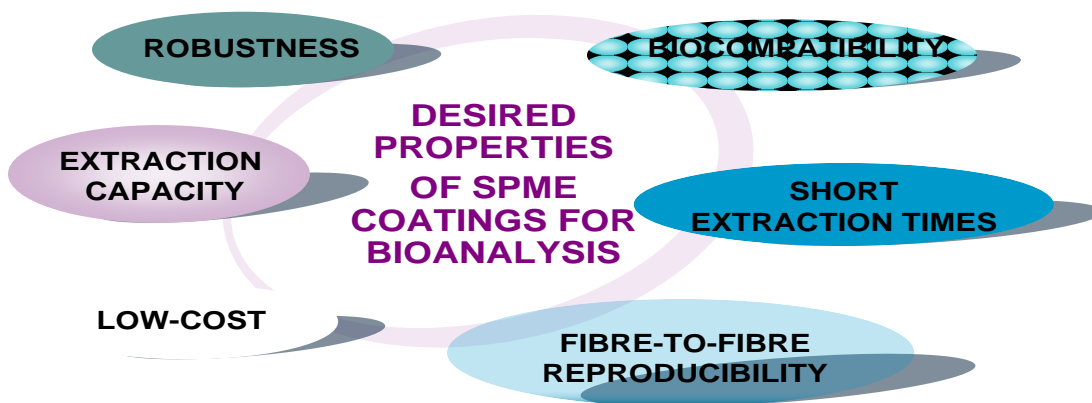


**Figure 3.1 Overview of desired properties for SPME coatings in bioanalysis.**

The main objective of this work was to evaluate *in vitro* the performance of a new line of biocompatible coatings produced by Supelco for the extraction of drugs from biological fluids. The model drugs evaluated in this work were diazepam, carbamazepine, ranitidine, pseudoephedrine and propranolol. Their structures are shown in Figure 3.2 and an overview of their properties is given in Table 3.1. The performance of these coatings with other classes of compounds commonly analyzed in biological fluids by LC such as riboflavin (water-soluble vitamin), adenosine (nucleoside) and hydrocortisone and progesterone (hormones) is also briefly reported. The proposed coatings were immobilized on a 200  $\mu\text{m}$  metal fibre core and consisted of a mixture of proprietary biocompatible binder and various types of porous coated silica (octadecyl, polar embedded RP-Amide and cyano) particles whose structures are shown in Figure 3.3.

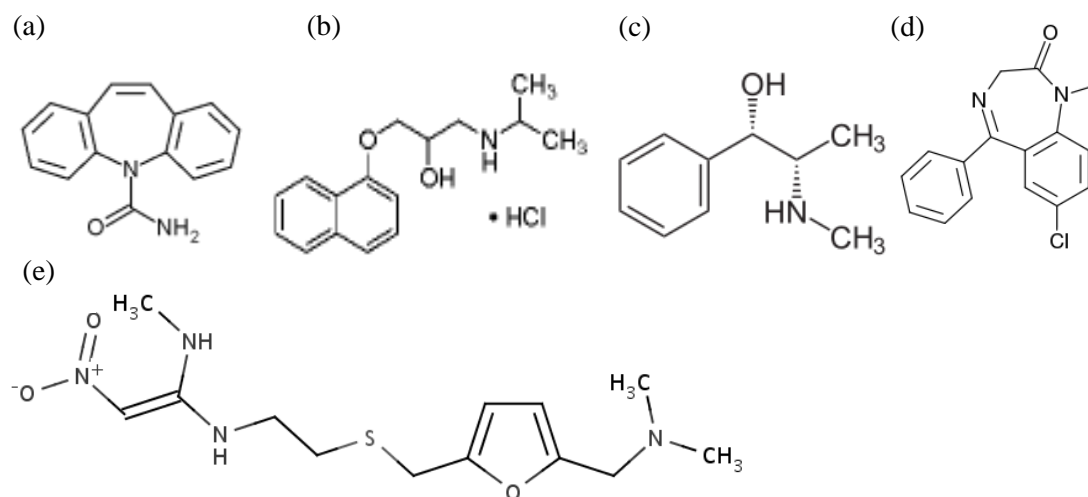


**Figure 3.2 Chemical structures of model drugs used in the evaluation of biocompatible coatings (a) carbamazepine, (b) propranolol (c) pseudoephedrine (d) diazepam (e) ranitidine.**

## 3.2 Experimental

### 3.2.1 Chemicals and materials

All drug standards were purchased as solids of highest purity from Sigma-Aldrich (Oakville, ON, Canada), except diazepam (Cerilliant, Round Rock, TX, USA) and carbamazepine-d10 (CBZ-d10, Alltech, Deerfield, IL, USA) which were purchased as 1 mg/mL and 100  $\mu\text{g}/\text{mL}$  methanolic solutions respectively. Acetonitrile (HPLC grade), methanol (HPLC grade), and glacial acetic acid were purchased from Fisher Scientific (Ottawa, ON, Canada), while human plasma with EDTA as anti-

coagulant was purchased from Cedarlane Laboratories Limited (Burlington, ON, Canada). Drug-free human urine was collected in sterile collection flasks from healthy volunteer and stored frozen at -20°C until use. All commercial (Carbowax-templated resin, CW-TPR, 50 µm thickness) and prototype SPME coatings were obtained as research samples from Supelco (Bellefonte, PA, USA). Research prototype biocompatible SPME coatings for HPLC use included (i) Discovery™ C<sub>18</sub> 15 µm thickness (ii) Discovery™ C<sub>18</sub> 30 µm thickness (iii) Discovery™ C<sub>18</sub> 45 µm thickness (iv) Discovery™ C<sub>18</sub> 60 µm thickness (v) Ascentis™ RP-Amide (RPA) 45 µm thickness and (vi) Discovery™ Cyano 45µm thickness. Chemical structure of coatings is shown in Figure 3.3. Discovery™ silica has 180 Å pore size and 200 m<sup>2</sup>/g surface area, while Ascentis™ silica has 100 Å pore size and 450 m<sup>2</sup>/g surface area. The length of coating was 15 mm for all prototypes. The coatings were prepared by mixing appropriate coated porous silica particles of 5 µm size with proprietary biocompatible binder, followed by immobilization on an inert, flexible metal alloy wire (200 µm diameter). Prototype fibres were housed inside *in vivo* SPME assembly based on 22-gauge hypodermic needle as shown in Figure 3.4. This design of *in vivo* SPME device is based on work by Musteata *et al.*<sup>88</sup>, but was modified as appropriate to accommodate the fibres immobilized on 200 µm flexible wire in current work.

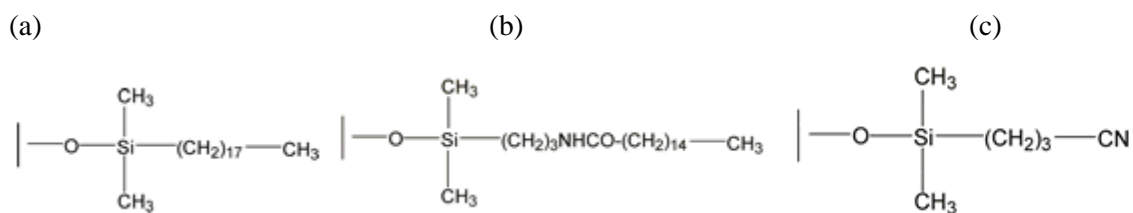


**Figure 3.3 Chemical structures of coatings evaluated in this chapter (a) octadecyl (C<sub>18</sub>) (b) C<sub>16</sub> with an embedded amide group (reverse-phase amide, RPA) and (c) cyanopropyl coating.**

### 3.2.2 Preparation of standard solutions

Instrument calibration was performed daily before and after each sample set using a set of standard solutions prepared with known drug concentrations (0.5 - 250 ng/mL, minimum of n=6 standards) in desorption solvent. These standard solutions were prepared by serial dilution of stock standard solution prepared in methanol at the concentration of 10 µg/mL. Phosphate-buffered saline (PBS) solution pH 7.4 was prepared as described previously (Section 2.2.2). Spiked biological standards were prepared in three different matrices: PBS pH 7.4, human urine and human plasma at the concentrations ranging from 1 to 1000 ng/mL depending on the experiment. Organic content of all

spiked standards used for extraction was kept constant at 1% v/v methanol. Spiked analytes in biological fluids (urine and plasma) were pre-incubated for 60 min prior to the extraction to allow for drug-protein binding to occur. For carbamazepine, this incubation time was found insufficient as discussed in text, so pre-incubation time for this drug was increased to a minimum of 12 hours in subsequent experiments.

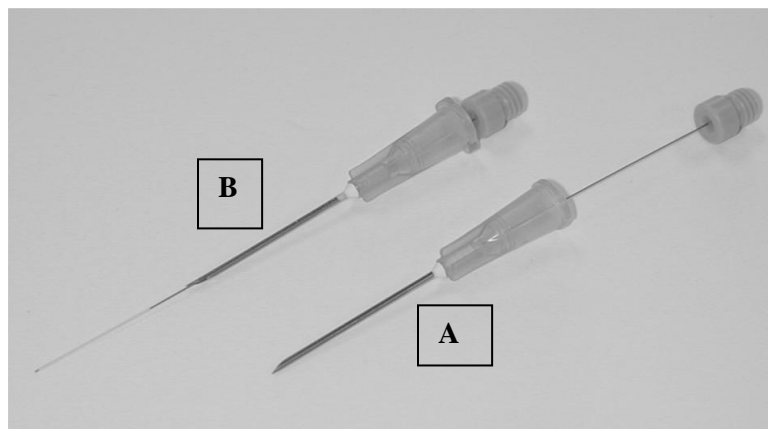


**Figure 3.4** Prototype *in vivo* SPME probe obtained from Supelco Inc. (A) SPME fibre is housed inside commercial hypodermic syringe for protection and for piercing living system or septum of sampling device. (B) Pushing on the plunger exposes SPME coating during extraction and desorption steps.

### 3.2.3 SPME procedure

Prior to each use, fibres were preconditioned for minimum of 30 min in methanol/water (1/1, v/v) at 1000 rpm agitation. Extraction was performed at room temperature ( $24 \pm 2^\circ\text{C}$ ) from 1.5 mL sample solution contained within 2 mL amber HPLC vial, except for sample volume experiments where extraction was performed from 0.25 mL sample contained within 0.3 mL amber polypropylene vial. For pre-equilibrium experiments, extraction times of 2 min (PBS buffer and urine) and 5 min (plasma) were used, unless otherwise stated in text. No agitation was employed during extraction, unless otherwise specified in text. Fibres were desorbed for 5 min using 2400 rpm vortex agitation using 100  $\mu\text{L}$  of desorption solvent (acetonitrile/water, 1/1, v/v) spiked with 100 ng/mL carbamazepine d10. Desorption was carried out in 0.15 mL capacity tapered polypropylene HPLC inserts (Supelco) and using multi-tube vortexer with foam insert of 50-vial capacity (model DVX-2500, VWR International, Mississauga, ON, Canada). Carbamazepine d10 was used as internal

standard primarily to correct for slight variations in the injection volume during LC-MS analysis. For ranitidine and pseudoephedrine, the use of weaker desorption solvent (water/acetonitrile, 9/1, v/v) ensured solvent strength was suitable for direct injection into LC-MS/MS system.

### 3.2.4 LC-MS/MS analysis

LC-MS/MS analysis was performed using instrument consisting of 500 ion trap MS, 430 autosampler, 212 LC pumps and MS Workstation Version 6.6 software (Varian, Walnut Creek, CA, USA). Injection volume for all experiments was 20  $\mu$ l. Analytes were separated using Varian Pursuit 5  $\mu$ m C<sub>18</sub>, 50 x 2.0 mm column. Mobile phase A consisted of acetonitrile/water/acetic acid (10/89.9/0.1) and mobile phase B of acetonitrile/water/acetic acid (90/9.9/0.1). Analytes were eluted using 300  $\mu$ L/min flow rate and simple gradient program which included a short hold at 100% A for 0.5 min, followed by linear increase to 90% B over 4.5 min, and short hold of 0.5 min at 100% B. Total run time per sample was 8.0 min, including column re-equilibration time of 2.5 min. Higher flow rates were explored but could not be used successfully due to insufficient desolvation at flow rates > 300  $\mu$ L/min based on the limitations of the design of this ion source.

MS parameters were optimized using direct infusion of 1  $\mu$ g/mL of individual analyte standard solutions prepared in acetonitrile/water. Analytes were ionized using positive ESI, with ion source temperature set to 400 °C. Chromatographic run time was divided into two MS timed events. During the first event (0-3.0 min), pseudoephedrine and ranitidine were monitored, and needle voltage of 3300V was used. Second timed event (3.0-8.0 min) was used to monitor diazepam, propranolol, carbamazepine and carbamazepine d10, and needle voltage of 5600 V was employed. The rest of MS/MS parameters are summarized in Table 3.1.

**Table 3.1 Summary of analyte properties, MS/MS parameters and LC retention times.**

Analyte	pKa <sub>165-167</sub>	Log P <sub>165</sub>	t <sub>R</sub> (min)	Parent m/z	Daughter m/z	Capillary voltage (V)	RF loading (%)	Excitation amplitude (V)
Diazepam	3.4	2.82	4.9	285.0	257.0	76	79	1.31
Pseudoephedrine	10.3	0.89	1.5	166.1	148.0	37	60	1.23
Ranitidine	2.3, 8.2	0.27	0.8	315.0	176.0	51	85	1.20
Propranolol	9.42	3.48	3.7	260.1	183.0	66	77	0.70
Carbamazepine	7	2.45	4.1	237.0	194.0	65	71	1.20
Carbamazepine d10	NA	NA	4.1	247.0	204.0	65	71	1.05

### 3.2.5 Data analysis and calculations

Extraction efficiency and relative recovery were calculated according to procedures previously described in detail in section 2.2.9. In current study, calibration curves in PBS, urine and plasma were acquired. Each point of each calibration curve in each matrix was acquired using a different fibre, and a minimum of six concentration levels were used in all experiments.

### 3.2.6 SEM procedure

In preparation for SEM, the coatings were cut into 2-3 mm pieces, dried for 1 hr at 140°C, and sputtered with ~10 nm of gold. SEM images of the coating (mounted using carbon conductive tape and specimen mounts Ted Pella, Redding, CA, USA) were acquired using LEO 1530 field emission SEM (Carl Zeiss NTS GmbH, Oberkochen, Germany) and an acceleration voltage of 15 kV. The images were collected by trained SEM operator, Francois Breton.

## 3.3 Results and discussion

The goal of this study was to evaluate the performance of a new line of biocompatible coatings prepared by Supelco using appropriate *in vitro* experiments. Any suitable coatings evaluated using this procedure could then be further evaluated *in vivo*, and the results of such experiments are described in Chapter 4. Commercial availability of single-use fibres with biocompatible coating would be advantageous for *in vivo* SPME studies, and the use of well-controlled commercial production process was expected to improve inter-fibre reproducibility for such devices. The coatings were prepared using a semi-automated batch manufacturing procedure by depositing multiple layers of a mixture of proprietary biocompatible polymer and coated porous silica particles typically used as stationary phases in LC or as SPE sorbents. The biocompatible nature of polymer was important to eliminate any adverse/toxic *in vivo* reactions such as clot formation as well as to reduce adsorption of proteins to the surface in order to avoid problems with analyte uptake into the coating. Three types of coatings were included in this comparison: C<sub>18</sub>, RPA and cyano. Example SEM image with 300× magnification shows the surface of the RPA biocompatible fibre (Figure 3.5), and shows the coverage of particles with a layer of biocompatible polymer. The surface of the coating is also smoother than previously reported for lab-made coatings which can help minimize interactions with the living system (for example, hemolysis).<sup>138</sup>

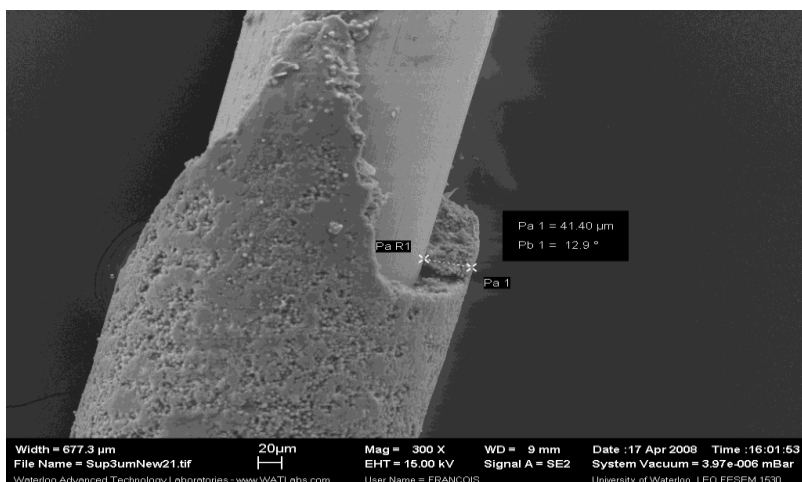


**Figure 3.5 Example SEM image acquired using 300x magnification of the surface of biocompatible RPA coating (3 µm particle size). Upper portion of coating was removed on purpose to facilitate the determination of coating thickness as shown in the image (41.4 µm).**

The selection of the experiments to carry out for this evaluation was based on the primary end-use of these coatings, which was *in vivo* SPME sampling. The main parameters investigated included mechanical robustness, extraction efficiency, carryover, extent of sample clean-up and inter-fibre reproducibility. In addition, the performance of coatings upon exposure to solvent was investigated by Supelco as reported elsewhere.<sup>128</sup> The new coatings were found not to swell upon the exposure to common LC solvents such as acetonitrile, methanol and aqueous combinations of these solvents. This presents an advantage over existing commercial coatings such as Carbowax TPR (CW-TPR) which swelled 36-40% upon 15-min exposure to common desorption solvents such as methanol/water or acetonitrile/water (1/1, v/v). Such high degree of swelling is highly problematic as it can cause inadvertent stripping of coating (and corresponding loss of sample) when retracted into SPME device and/or accidental stripping of coating within manual SPME-LC interface.<sup>129, 168</sup> The fibres were aimed for single-use so long-term reusability of coatings after exposure to biofluids was not investigated. Matrix modifications which can be used to improve extraction efficiency during *in vitro* experiments, such as pH adjustment and addition of salt, were not examined because they are not applicable to *in vivo* sampling of living systems. Many of the evaluation experiments were performed in PBS buffer because it is a good and simple alternative to use for *in vitro* SPME optimization experiments in order to avoid unnecessary exposure to human biological fluids and avoid lot-to-lot differences in the composition and pH of urine or plasma during SPME method development experiments. In addition, it does not contain any binding matrix so it is often used to perform matrix-free calibration in order to

determine free (unbound) analyte concentration in bioanalytical SPME methods.<sup>86</sup> More complex matrices such as urine and plasma were investigated when necessary to evaluate the fibre performance for complex matrices.

### 3.3.1 Evaluation of extraction efficiency and comparison to commercial CW-TPR coating

The extraction efficiency of new cyano, C<sub>18</sub> and RPA coatings was compared to that of the most commonly used existing commercial coating (CW-TPR). The experiment was performed using extraction of drug standard prepared in PBS buffer and short extraction time of 2-min was employed to mimic a typical *in vivo* sampling situation. The performance of C<sub>18</sub> and RPA coatings was found to be better than cyano coatings for the model drugs tested, and similar to the performance of commercial CW-TPR fibre as shown in Figure 3.6. The only exception to this trend was diazepam, where the commercial fibre extracted significantly higher amounts of diazepam in comparison to the new proposed coatings. Overall, some dependence of extraction efficiency on analyte log P values (Table 3.1) was observed, with more polar compounds (ranitidine and pseudoephedrine) exhibiting lower extraction efficiencies than more hydrophobic analytes.

To enable direct comparison of CW-TPR coating and the new biocompatible coatings such as shown in Figure 3.6 and Table 3.2, different dimensions of the two coating types needed to be taken into account. Commercial CW-TPR fibre was available only with the coating dimensions of 1 cm coating length, 160 µm diameter of fibre core and 50 µm coating thickness, while the dimensions of biocompatible coatings tested herein were 1.5 cm coating length, 200 µm diameter of fibre core and 45 µm thickness. Direct comparison is further complicated by the fact that the new coatings use coated porous spherical silica particles as the sorbent, so it is difficult to estimate exact volume of the coating. If both types of coatings are treated simply as cylinders and it is assumed the entire volume of immobilized phase could act as sorbent, an estimated correction factor of 1.6 can be applied to CW-TPR data to correct for the differences in coating volume. This correction factor was calculated by treating fibres as cylinders. According to this approach, the volume of two cylinders can be calculated: (i) the volume of fibre core cylinder only (radius = core diameter/2) and (ii) the volume of entire fibre (radius = fibre core diameter/2 + coating thickness). The volume of the coating is then determined by the subtraction of fibre core volume (i) from the total volume of entire fibre (ii). Full calculation is shown in Table 5.3. This comparison is only an approximation because it is expected to overestimate coating volume for biocompatible coatings because the biocompatible binder and the



core of silica particles which are present within the coating do not act as a sorbent. Despite of this, the approximation is useful to give an estimate of how the performance of new coatings compares to existing coatings.

CW-TPR coatings were previously found to perform poorly for the extraction of very polar analytes, but this was not reflected in the data collected using model drugs within this experiment. Therefore, the performance of the coatings was further tested by increasing the polarity range of analytes to include some even more polar species such as adenosine and riboflavin. The results obtained are shown in Table 3.2 for an equilibrium extraction from 5 µg/mL standard solution prepared in PBS pH 7.4 buffer. In general, the results confirm that the new RPA and C<sub>18</sub> coatings have better extraction efficiency for more hydrophilic compounds such as riboflavin and hydrocortisone than CW-TPR. However, this is general trend only and extraction efficiency is very analyte dependent, so for adenosine all coatings had similar extraction efficiencies, and no improvement was observed for new coatings. For more hydrophobic analyte such as progesterone, the extraction efficiency of proposed biocompatible coatings is approximately the same as that of CW-TPR. As expected, the RPA coating had improved extraction efficiency than C<sub>18</sub> coating towards more polar compounds because its structure incorporates a polar embedded functional group. However, the observed improvement was <2-fold even at equilibrium, and no noticeable differences could be observed within experimental error for short extraction times of 2-min.

**Table 3.2 Comparison of extraction efficiency at equilibrium of proposed biocompatible coatings *versus* existing commercial CW-TPR coating for compounds of varying polarity.**

Analyte	log P <sup>165</sup>	CW-TPR % Extracted*	Cyano % Extracted	RPA % Extracted	C <sub>18</sub> % Extracted
riboflavin	-1.46	0.02	0.18	2.3	1.3
adenosine	-1.05	0.20	0.16	0.27	0.18
hydrocortisone	1.61	1.34	0.85	19	20
progesterone	3.87	24	12	30	30

\* Correction factor of 1.6 was applied to CW-TPR % extracted data in order to account for different thickness and dimensions of CW-TPR fibre.

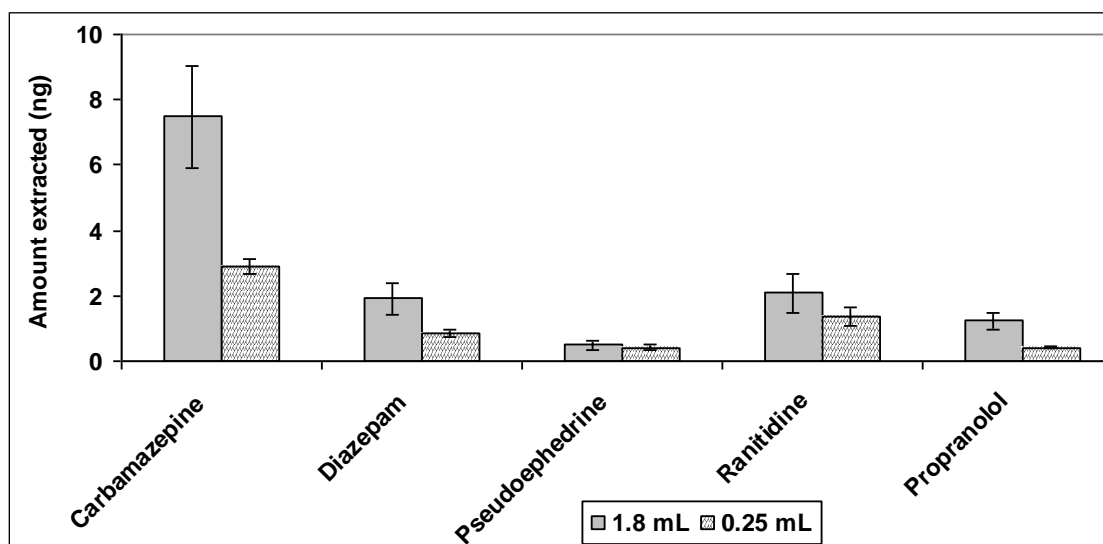
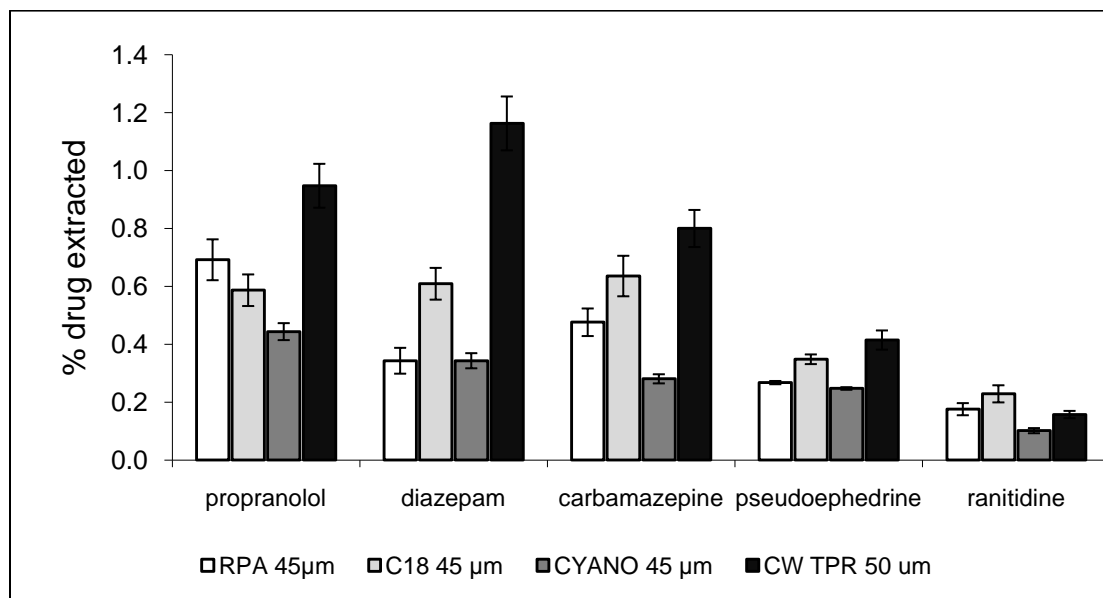


**Figure 3.6 (a)** Comparison of the extraction efficiency of RPA, C<sub>18</sub> and cyano coatings (45 µm thickness, n = 10 fibres of each type) for the extraction of various drugs. Extraction conditions: 2 min without agitation from 100 ng/mL drug standard in PBS buffer pH 7.4. Correction factor of 1.6 was applied to CW-TPR data in order to account for different thickness and dimensions of CW-TPR fibre as discussed in text. **(b)** Effect of sample volume (1.8 mL *versus* 0.25 mL) on the amount of drug extracted from plasma using 45 µm C<sub>18</sub> SPME coating (n=3 fibres per sample volume). Extraction conditions: equilibrium extraction from human plasma spiked with 100 ng/mL drug standard.

Equation 1.1 shows that at equilibrium, the amount extracted by SPME exhibits non-linear dependence on sample volume. This distinguishes SPME from traditional exhaustive techniques where linear dependence is encountered, and a reduction in sample volume results in linear decrease in analytical sensitivity. For SPME as shown in Figure 3.6 (b), the use of smaller sample volume (0.25 mL) *versus* 1.8 mL resulted in an approximately 2-fold decrease in the amount extracted. This feature makes SPME particularly attractive for analyses where limited amount of biofluids is available, for example in neonatal screening or rodent studies. The exact magnitude of the effect of sample volume depends on the magnitude of  $K_{fs}$ , so more hydrophilic analytes with lower  $K_{fs}$  values (ranitidine and pseudoephedrine) were not affected at all by the 7.2-fold reduction in sample volume, indicating the extraction takes place under negligible depletion conditions described by Equation 1.7.

### **3.3.2 Evaluation of coating thickness: effect on extraction time and inter-fibre reproducibility**

The effect of fibre thickness on coating performance was evaluated using C18 biocompatible coating prepared at four different thicknesses: 15, 30, 45 and 60  $\mu\text{m}$ . The coatings of increasing thickness were prepared by Supelco by depositing additional layers of extraction phase until the desired thickness was achieved. The actual coating thickness of each fibre was determined experimentally using optical measurement and coating thickness variation was <3% RSD for all coating thicknesses. Increasing coating thickness increases  $V_f$  and results in higher amounts extracted by SPME as shown by the relationship in Equation 1.1. However, increasing coating thickness also adversely affects the time required to reach equilibrium, as the analytes need to diffuse through longer distances with thicker coatings as shown in Equation 1.5.

The extraction time profiles were evaluated for all available coating thicknesses. They were constructed by extraction from 100 ng/mL carbamazepine standard solution and varying the extraction times from 1 min to 19 hr. During *in vivo* SPME sampling, agitation conditions are often unknown or changing, so two main approaches can be used during method development to find the time required to reach equilibrium for this type of application: (i) a flow-through system set at the expected flow rate in the system (for example, blood flow rate of the animal) or (ii) using static (no agitation) conditions.<sup>80, 136</sup> The latter case represents the worst-case scenario, as the only mass transfer occurs via diffusion. This time can then be selected as the *in vivo* sampling time and this approach ensures that equilibrium is reached regardless of whether agitation is present in the system under

study. The amount of analyte extracted at equilibrium is independent of agitation<sup>136</sup>, thus permitting quantitative analysis in conditions with unknown agitation rates. However, addition of any agitation increases mass transfer rates, so the resulting time needed to achieve equilibrium is shortened.

The average extraction time profiles under static conditions for all coating thicknesses (n=3 fibres) are shown in Figure 3.7 (a). From these results it can be concluded that the equilibrium was reached for 15  $\mu\text{m}$  fibres after 60 min. For all other coatings the extraction time required to reach equilibrium was  $\geq 300$  min. For *in vitro* testing, agitation can be used in order to significantly decrease the equilibration times for these fibres as shown in Figure 3.7 (b). However, for *in vivo* testing, thin coatings with very short equilibrium times are preferred (<5 min) in order to obtain acceptable temporal resolution and enable equilibrium sampling for improved overall method precision. For instances when equilibrium sampling is not feasible, such as the case with these new coatings, short extraction times can still be employed *in vivo* as long as appropriate kinetic calibration method is used. An overview of all available kinetic methods and their main principles is provided in recent review article<sup>80</sup>, and the reader is also referred to relevant discussion for on-fibre standardization calibration method presented in Chapter 1.

Table 3.3 shows the results of 2-min and 60-min static extractions for n=20 fibres, in order to investigate the impact of coating thickness on fibre variability. The results for both extractions show improved method precision as fibre thickness is increased. The result for 15  $\mu\text{m}$  fibres is particularly informative as 2-min extraction represents pre-equilibrium sampling time, whereas 60-min extraction time represents equilibrium sampling. Method precision using equilibrium sampling is typically better than using 2-min short sampling times as the small errors in accuracy of timing are much more significant contributors to overall error as the sampling time is decreased. However, current results show deterioration of method precision with increase in RSD from 7 to 13%. On the timescale of 2-min analytes typically only interact with the surface of the coating, as the time is too short for the analyte to diffuse within the entire thickness of the coating, and the variations in coating thickness would not be detected. However, as the extraction time is increased the analytes can diffuse further into the coating, and the variations in coating thickness can become more apparent. Small variation in coating thickness (for example  $\pm 1 \mu\text{m}$ ) contributes more to the overall inter-fibre variability for thin fibres *versus* thicker fibres, and is the main factor for the observed deterioration in precision observed for 15 and 30  $\mu\text{m}$  coatings, as the extraction time is increased.

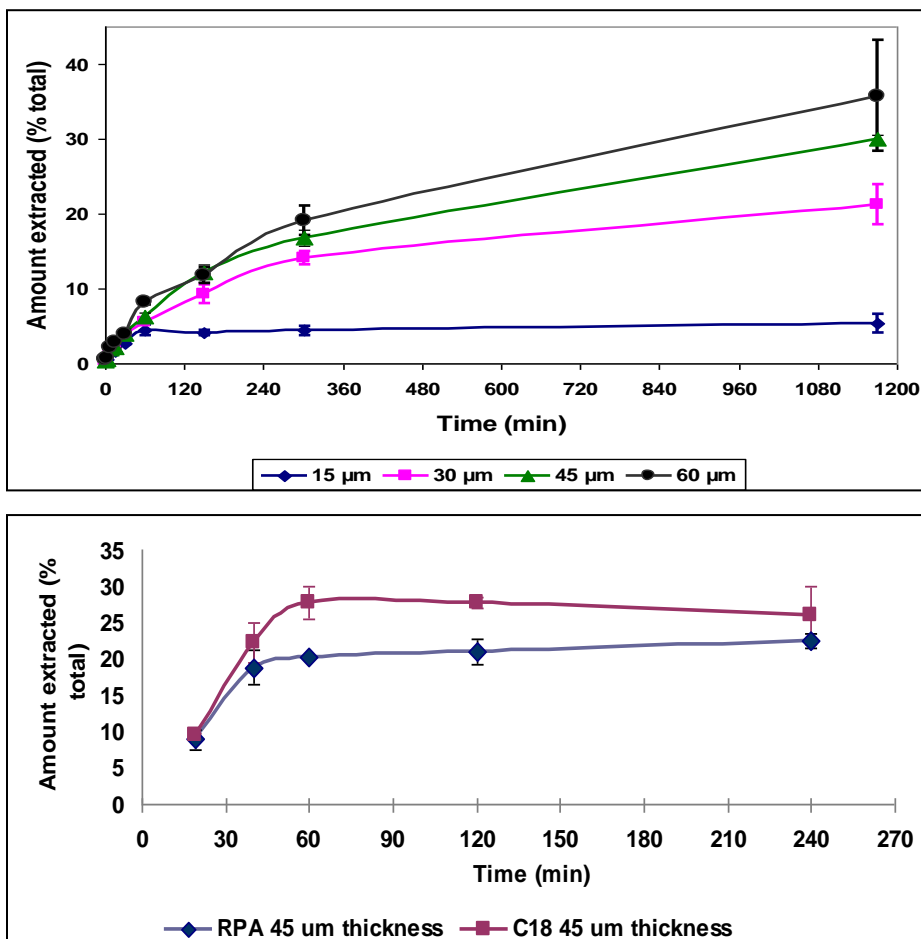


Figure 3.7 Example extraction time profiles for carbamazepine (a) using C<sub>18</sub> coatings (n = 3 fibres) of 15 μm, 30 μm, 45 μm and 60 μm thickness without agitation (b) using C<sub>18</sub> and RPA coatings of 45 μm thickness (n=3 fibres) using 2400 rpm vortex agitation to enhance mass transfer rates of analyte.

Table 3.3 Effect of increasing extraction time on the amount extracted and inter-fibre variability.

Extraction time	2 min extraction (static)				60 min extraction (static)			
	15 μm	30 μm	45 μm	60 μm	15 μm	30 μm	45 μm	60 μm
Coating thickness	15 μm	30 μm	45 μm	60 μm	15 μm	30 μm	45 μm	60 μm
% extracted (mean, n=20)	0.49	0.60	0.62	0.78	4.2	5.8	6.5	8.0
% RSD (n=20)	7	8	4	5	13	12	6	7

### 3.3.3 Evaluation of carryover

The carryover was evaluated using the thinnest (15  $\mu\text{m}$ ) and the thickest (60  $\mu\text{m}$ ) coatings to provide the best and worst case carryover scenarios respectively. To facilitate rapid mass transfer, 2400 rpm vortex agitation was chosen for this study, because this is the highest agitation method currently available in our lab. The composition of the desorption solvent was not varied in this experiment in order to keep desorption solvent composition directly compatible with LC-MS/MS method.

Therefore, the effect of two main parameters was investigated: desorption time and the volume of desorption solvent used. Figure 3.8 shows that the carryover was found to be negligible ( $\leq 0.2\%$ ) at all conditions tested for 15  $\mu\text{m}$  fibres. For 60  $\mu\text{m}$  fibres, carryover was found to be  $\sim 1\%$  for all desorption times when 100  $\mu\text{L}$  of desorption solvent was used, indicating that increasing the desorption time beyond 5 min was not beneficial. In contrast, increasing the desorption solvent volume to 1.5 mL reduced carryover to negligible levels ( $<0.1\%$ ). Overall, the results show that efficient desorption was achievable for all fibre thicknesses in reasonable amount of time. The volume of desorption solvent can be selected based on analytical sensitivity required for a particular application. The method developed in this research was aimed for subsequent application for *in vivo* study, so maximum sensitivity is desirable and the smallest desorption volume was selected. For *in vivo* studies, the fibres are meant for single-use, so carryover is not problematic as long as it is sufficiently negligible to enable quantitative analysis. If coatings are re-used, the small amount of analyte remaining in the coating can be completely removed prior to next extraction during the solvent pre-conditioning step. High carryover ( $>10\%$ ) was cited as one of the most significant problems encountered with existing PDMS-DVB commercial coatings<sup>130</sup>, and the results show that these new coatings can offer significant improvement in this parameter.

In a follow-up study, carryover was evaluated after equilibrium extraction using 45  $\mu\text{m}$  C<sub>18</sub> and RPA coatings and was found to be 0.9% and 1.4% respectively, which agrees with above results. A small amount of internal standard (CBZ d10) was also found in the carryover solution indicating that the coatings absorbed a small amount of internal standard during the desorption step (0.2 and 0.3% respectively for C<sub>18</sub> and RPA coatings). This is negligible amount for current study. However, if lower proportion of organic solvent is used as the desorption solvent, the amount of internal standard extracted can potentially become significant and this factor should be examined during method development.

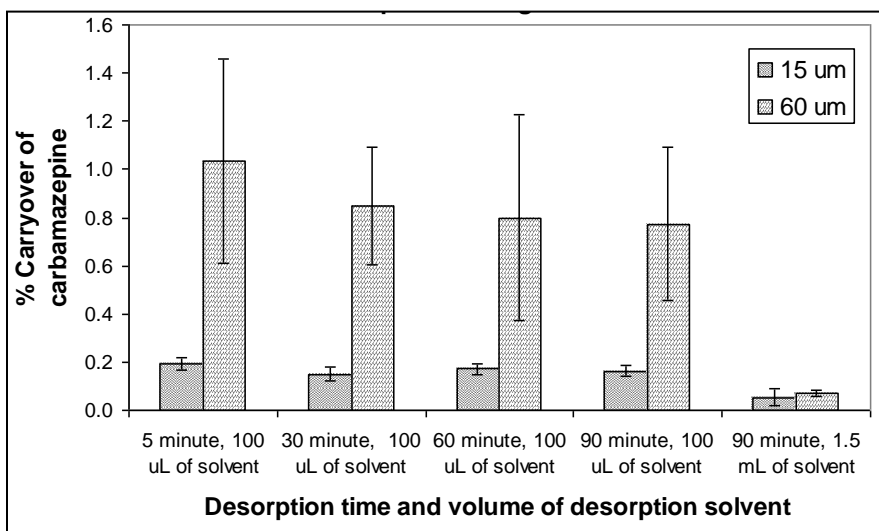


**Figure 3.8 Comparison of carryover results for carbamazepine using 15 µm and 60 µm C<sub>18</sub> coatings. Extraction conditions: 90 min extraction of 250 ng/mL carbamazepine standard in PBS buffer (n=3 fibres). Desorption conditions: two serial desorptions using conditions stated in figure.**

### 3.3.4 Selection of coating thickness

Based on the results presented in previous section, several trends were observed. Among the coating thicknesses evaluated in this study (15, 30, 45, 60 µm), none of the coatings were thin enough to permit *in vivo* applications with good temporal resolution using equilibrium sampling. For example, 60-min extraction time was needed to reach equilibrium for 15 µm coating, whereas concentrations of drugs and metabolites can be expected to change rapidly within this time window in a typical pharmacokinetic study. Thinner coatings than tested in current study (<15 µm) could not be reliably made by Supelco using semi-automated batch coating procedure as they exhibited unacceptable variation in coating thickness, which would in turn result in large variation in the amount extracted by individual fibres and overall poor inter-fibre reproducibility. Therefore, kinetic calibration methods need to be employed for *in vivo* studies requiring good temporal resolution. As expected according to theoretical consideration, the extraction efficiency increases with the increase in coating thickness, because of the corresponding increase in the volume of the fibre coating from Equation 1.1. Furthermore, slight improvement in inter-fibre reproducibility was observed for 45 and 60 µm coatings *versus* thinner 15 and 30 µm coatings especially as extraction times were increased. Carryover in the extraction phase was found to be acceptable regardless of the coating thickness

employed ( $\leq 1\%$ ). Based on all of these results, 45  $\mu\text{m}$  thickness was selected as the optimum choice balancing both extraction efficiency, good inter-fibre reproducibility and reasonable equilibrium extraction times when agitation is employed. All subsequent studies and subsequent prototype fibre production by Supelco focused on coatings of 45  $\mu\text{m}$  thickness.

### 3.3.5 Evaluation of inter-fibre reproducibility

In the next step of the evaluation, the performance of coatings in biological matrices of increasing complexity was examined: PBS, urine and plasma. The results obtained are shown in Table 3.4. As a general trend the amount of analyte extracted in urine was approximately the same or slightly higher than the amount of analyte extracted in PBS. Ionic strength and pH of the urine used in this study were not adjusted prior to the experiment, so the slight differences in the amount extracted by the two matrices can likely be attributed to the variation in these parameters and its impact on the magnitude of  $K_{fs}$  for a given analyte-coating combination. As expected, the amount of analyte extracted from plasma was significantly lower than from PBS and urine for diazepam and propranolol. This is expected because these drugs are known to bind to a significant extent to proteins within this matrix, which lowers free analyte concentration available for the extraction. No increase in RSD was observed with increasing complexity of matrix for propranolol and diazepam with RSD values  $\leq 13\%$  for all coatings and all matrices. However, the results for carbamazepine were unexpected. For carbamazepine, extraction efficiency appeared to be the same as observed for urine matrix, even though about 85% binding is expected to occur for carbamazepine in plasma. Furthermore, method precision for carbamazepine in plasma was very poor, and significantly higher than in other matrices or for the other model compounds studied (28, 18, 29% RSD for cyano, RPA and  $C_{18}$  coatings respectively). One possible explanation for the observed results was that pre-incubation time of 60 min used to establish binding between analyte and matrix of interest, was not sufficient for carbamazepine to establish binding equilibrium with plasma proteins. The variations in the free concentration of carbamazepine in plasma samples would subsequently lead to the variations in the amount extracted by SPME. Therefore, the plasma experiment was repeated for carbamazepine using  $C_{18}$  coating but pre-incubation time was increased to overnight incubation (12 hr) with refrigeration. The mean amount of carbamazepine extracted was found to be 0.18% with RSD of 11%. These results confirm the initial hypothesis. The amount extracted of carbamazepine decreased when pre-incubation time was increased, which indicates that additional binding of carbamazepine to plasma proteins took place. Achieving equilibrium between drug and plasma proteins eliminated any



variability in free concentration, so overall method precision was improved and consistent with the results for other matrices. This result shows that during method development of bioanalytical methods using SPME, it is very important to use a sufficient pre-incubation time in order to establish binding equilibrium between drug spiked into the plasma (serum or whole blood) in order to obtain acceptable accuracy and precision. The length of pre-incubation time needed is analyte-dependent, so this parameter should be carefully examined during method development. Obviously, the length of incubation time can be reduced by employing agitation if overnight incubation is not feasible for given application. The need for incorporation of pre-incubation time is in contrast to traditional exhaustive sample preparation methods which usually incorporate a step to disrupt plasma protein binding with the drug, so the performance of such methods does not depend on whether binding equilibrium was established or not.

The results in Table 3.4 show that good overall method precision was achieved with new coatings, and the results are in line with regulatory requirements for bioanalytical methods. The main contributing factor to the observed method precision is the slight variation in the amount of coating deposited on each fibre. Other contributions to overall experimental variance are variability of instrumental response (RSD for injections of quality control standard <5% RSD for all analytes in these sample sets), accuracy of sample and solvent dispensing step, accuracy of timing, and any evaporative and/or adsorptive losses of analyte during the entire procedure. Because the objective of the experiment was the evaluation of inter-fibre variability, internal standard was not added to the samples prior to extraction to remove this variation from the data, and was only added to the desorption solvent to correct for any variation in injection volume. Furthermore, during *in vivo* experiments, the use of internal standard is not feasible, so this approach mimics the situation that would be encountered during *in vivo* use of these fibres (Chapter 4) and shows that the inter-fibre variability is sufficiently low to permit such applications. In fact, the inter-fibre variability of proposed coatings is significantly better than that reported for polypyrrole coatings (~47–52% RSD for linezolid with single-use fibres), thus permitting single fibre use for the first time with suitable performance for quantitative analysis.<sup>136</sup> Due to poor inter-fibre reproducibility, *in vivo* experiments with polypyrrole probes were carried out using three probes for each animal for each time point to allow for data averaging.<sup>133</sup> Good inter-fibre reproducibility of new probes addresses this issue and permits the use of single probe for each sampling point. For routine *in vitro* use, method precision can be further improved by employing internal standard calibration to compensate for inter-fibre variability in the results, as previously shown in Section 2.3.1.15. However, considering that the

variability of instrumental response for bioanalytical LC-MS/MS methods is typically around 5-10% RSD, further correction of inter-fibre reproducibility may not be necessary.

**Table 3.4 Evaluation of inter-fibre reproducibility for three model drugs in three matrices of increasing complexity: PBS, urine and plasma. All extractions were performed using n=10 fibres with 45 µm thickness coating.**

CYANO COATING						
	Carbamazepine		Diazepam		Propranolol	
	% Extracted	% RSD	% Extracted	% RSD	% Extracted	% RSD
PBS	0.28	5.6	0.34	7.6	0.44	6.6
Urine	0.46	4.2	0.46	5.2	0.69	3.4
Plasma	0.42*	28*	0.12	4.4	0.29	7.9
RPA COATING						
	Carbamazepine		Diazepam		Propranolol	
	% Extracted	% RSD	% Extracted	% RSD	% Extracted	% RSD
PBS	0.48	10	0.34	13	0.69	10
Urine	0.65	3.5	0.56	3.8	0.78	3.6
Plasma	0.67*	18*	0.20	4.2	0.31	7.7
C <sub>18</sub> COATING						
	Carbamazepine		Diazepam		Propranolol	
	% Extracted	% RSD	% Extracted	% RSD	% Extracted	% RSD
PBS	0.64	11	0.61	9.0	0.59	9.3
Urine	0.64	9.4	0.60	8.4	0.80	7.0
Plasma	0.66*	29*	0.20	3.2	0.30	6.6

\* Pre-incubation time of 60-min was found insufficient for carbamazepine. Experiment was repeated as discussed in text.

### 3.3.6 Evaluation of method linearity

LOQ in urine using short 2-min extraction time was 1-5 ng/mL for all of the drugs tested. LOQ in plasma using 5-min extraction was 5-10 ng/mL for all of the drugs tested which is sufficient for therapeutic drug monitoring of these drugs. Furthermore, LOQ for diazepam of 5 ng/mL in plasma (5 min pre-equilibrium sampling time) which was obtained in current study is significantly better than that obtained for polypyrrole probes (LOD of 7 ng/mL, 30 min sampling time) illustrating the potential of new coatings for *in vivo* sampling of drugs with good temporal resolution.<sup>133</sup> The extraction time in plasma was increased *versus* 2-min time used for urine and PBS to ensure sufficient amount of analyte was extracted for accurate quantitation, because a significant portion of spiked

drugs was expected to bind to plasma proteins, thus lowering free drug concentration and reducing the amount extracted.

Linear range of proposed method was also evaluated and is summarized in Table 3.5. Only C<sub>18</sub> and RPA coatings were considered in this test because extraction efficiency of cyano fibres was lower for all analytes tested, so their use was discontinued. Each point of each calibration curve in Table 3.5 was obtained using a different fibre (n=1 determination per concentration level). Excellent results in terms of model fit and regression coefficient were observed in all cases. This gives further confirmation of the suitability of fibres for single use for *in vivo* applications, because no internal standard was spiked in the samples to eliminate inter-fibre reproducibility from the data set, thus mimicking situation that would be encountered *in vivo*. Internal standard was only spiked in desorption solvent to compensate for any variability in injection volume. An example calibration curve for carbamazepine in PBS buffer is shown in Figure 3.9. The method linear range is primarily limited by the linear dynamic range of ion trap instrument used in the study and ESI droplet surface saturation at high analyte concentrations. High concentration samples exceeding upper limit of linear dynamic range can be accurately analyzed after dilution to ensure their signal intensity does not saturate MS detector. This approach was successfully used during *in vivo* pharmacokinetic study reported in Chapter 4, where wide range of concentrations is encountered over the time course of the experiment.

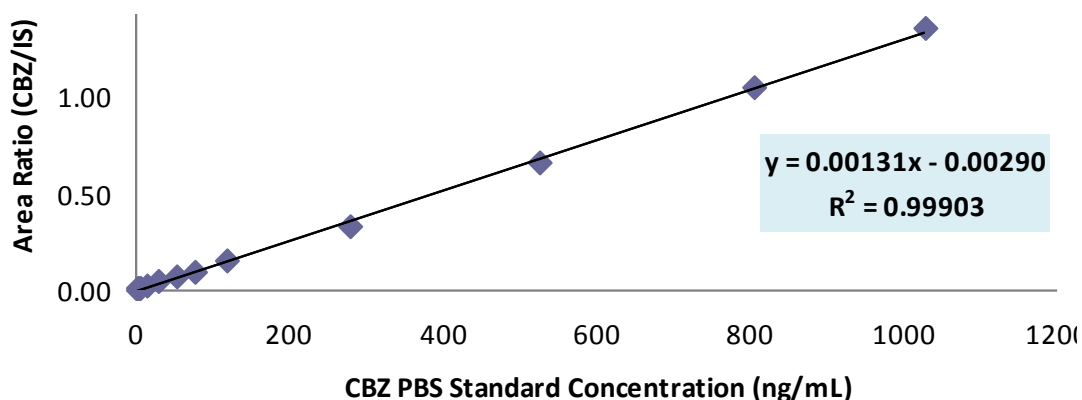


**Figure 3.9** Example calibration curve obtained for extraction of carbamazepine in PBS buffer pH 7.4 in concentration range 1-1000 ng/mL. LOQ of the method was 1 ng/mL. Extraction conditions: 2 min static, C<sub>18</sub> coating.

**Table 3.5 Summary of linearity results obtained for C<sub>18</sub> and RPA coatings in human urine and plasma for diazepam and propranolol. Each point of each calibration set was obtained using different fibre (n=1 determination for each concentration level).**

Matrix	Coating	No. of stds	Linear range (ng/mL)	Slope	Standard error - slope	Y-intercept	Standard error - Y intercept	r
<b>CARBAMAZEPINE</b>								
Urine	C <sub>18</sub>	7	1-250	1.08E-03	3.5E-5	6.5E-3	1.2E-3	0.9981
Plasma	C <sub>18</sub>	7	5-700	8.4E-4	4.9E-5	3.4E-2	1.1E-2	0.9986
Urine	RPA	7	1-250	1.14E-3	3.1E-5	5.8E-3	1.6E-3	0.9995
Plasma	RPA	7	5-700	7.7E-4	8.9E-5	5.8E-2	2.0E-2	0.9949
<b>DIAZEPAM</b>								
Urine	C <sub>18</sub>	7	1-250	9.88E-04	3.0E-06	-2.9E-04	3.0E-04	1.0000
Plasma	C <sub>18</sub>	7	5-700	3.15E-04	3.1E-06	-1.7E-03	8.3E-04	0.9999
Urine	RPA	7	1-250	8.6E-04	3.0E-05	-2.7E-03	3.1E-03	0.9980
Plasma	RPA	7	5-700	2.64E-04	7.8E-06	1.5E-03	2.1E-03	0.9986
<b>PROPRANOLOL</b>								
Urine	C <sub>18</sub>	6	5-250	2.3E-4	1.9E-5	2.5E-3	1.2E-3	0.9948
Plasma	C <sub>18</sub>	6	10-700	6.5E-5	3.7E-6	4.0E-3	3.2E-4	0.9989
Urine	RPA	6	5-250	2.8E-4	1.2E-5	2.7E-3	6.7E-4	0.9990
Plasma	RPA	6	10-700	7.9E-5	4.9E-6	3.6E-3	6.5E-4	0.9960

### 3.3.7 Evaluation of absolute matrix effects

Absolute matrix effects were evaluated using human plasma matrix, as it is the most complex among the three matrices studied in this research and most likely to be susceptible to high degree of ionization effects. The experiment was performed according to procedures described in detail in 2.3.2.1, and involves the comparison of signal intensity in plasma extract spiked post-extraction *versus* neat standard prepared at the same concentration directly in desorption solvent. The resulting solutions were evaluated both using direct infusion and full LC-MS/MS method. The direct infusion experiment provides true indication of all matrix components that are co-extracted by SPME and their overall influence on analyte ionization, whereas LC-MS/MS experiment evaluates the ability of chromatographic method to separate these species from analytes of interest. The results obtained are summarized in Table 3.6. According to direct infusion results, no ionization suppression or enhancement was observed for carbamazepine and diazepam, indicating any co-extracted interferences did not affect ionization for these model analytes. Ranitidine, propranolol and pseudoephedrine exhibited significant ionization enhancement when spiked in blank plasma extract.

However, once chromatographic step was added, ranitidine and pseudoephedrine no longer showed any signal enhancement, indicating they were sufficiently separated from co-extracted interferences that affected their ionization in direct infusion experiment. This result is quite interesting because, ranitidine and pseudoephedrine were not well-retained in reverse-phase method employed for the analysis, with retention times of 0.8 and 1.5 min respectively. The degree of matrix effects is usually the highest in this region with traditional sample preparation methods, so these results show that sample extracts obtained by SPME are much cleaner than usually observed for plasma protein precipitation and solid-phase extraction method. It can also be concluded that co-extracted species from plasma extract are likely to be hydrophobic in nature, as they did not impact the early-eluting species, implying they were well-retained on the chromatographic column employed in this analysis.

**Table 3.6 Evaluation of absolute matrix effects for the analysis of model drugs in human plasma. % signal represents the ratio of the signal of blank plasma extract spiked post-extraction versus neat standard prepared directly in desorption solvent at the same concentration level.**

Analyte	% Signal (direct infusion of 1 µg/mL individual drug standard)	Conclusion	% Signal LC-MS/MS (20 µL injection of 100 ng/mL mixed drug standard)	Conclusion
Carbamazepine	94	No effect	94	No effect
Ranitidine	274	Enhancement	107	No effect
Pseudoephedrine	377	Enhancement	92	No effect
Propranolol	154	Enhancement	76	Suppression
Diazepam	114	No effect	100	No effect

More surprisingly, significant degree of ionization suppression was observed for propranolol which is well-retained and chromatographically resolved from the other analytes in this method. To investigate the underlying cause for the observed ionization suppression, blank desorption solvent and blank plasma extracts were re-analyzed using full scan mode in m/z range of 100-500 (Figure 3.10). In comparison to desorption solvent, plasma extract showed additional peaks in the region of ~0.5 min, 1-2 min, and 6-7 min but these did not interfere with the analysis of analytes, as shown by the results for ranitidine and pseudoephedrine which elute within 0.5-2.0 min window. However, the presence of two large contamination peaks (main contributing m/z of 453, 340 and 277 Da) was found at the retention time of propranolol. Considering these peaks were present in blank desorption solvent, the observed ionization suppression of propranolol did not originate from poor sample clean-

up by SPME. Further experiments confirmed that the unknown contamination peaks originated from purified Nanopure water collected from in-house Barnstead purification system. Therefore, for accurate quantitative analysis of propranolol, another source of purified water or the use of deuterated internal standard for this compound is required. Alternatively, LC method could be re-developed in order to separate these impurity peaks from propranolol and eliminate the observed matrix suppression effect. These results also show that purity of chromatographic solvents is extremely important for successful LC-MS analysis.

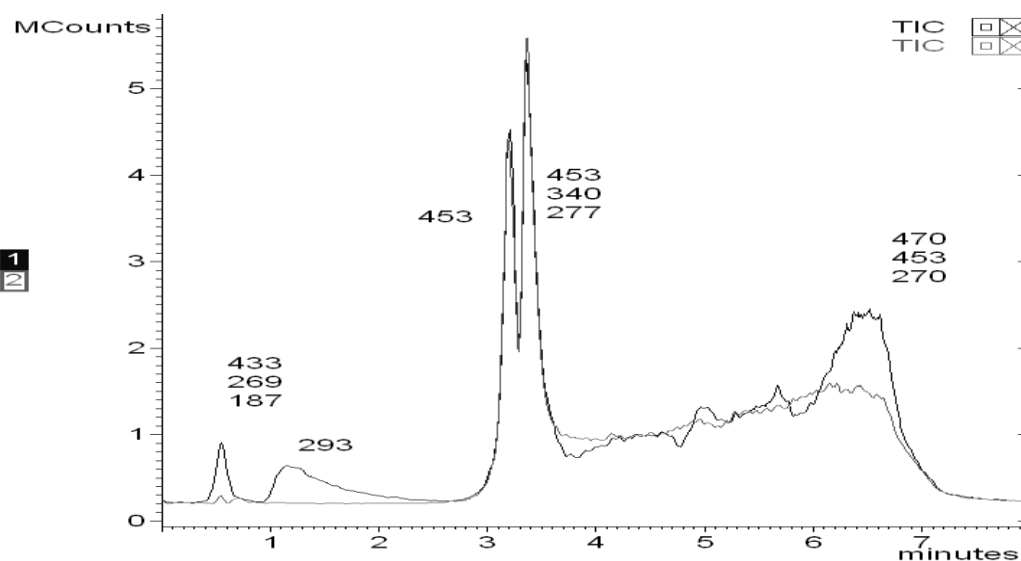


**Figure 3.10 Overlaid TIC chromatograms obtained for 20  $\mu$ L injection of desorption solvent and blank plasma extract in the region of  $m/z$  100-500. The main ions contributing to the peaks observed are marked directly on the chromatogram. Two large peaks with retention times 3-4 min arose from purified water and interfered with the analysis of propranolol.**

### 3.3.8 Optimization of preconditioning procedure

Preconditioning of reverse-phase sorbents such as  $C_{18}$  with an organic solvent such as methanol is important to wet hydrophobic chains and facilitate their interaction with the analytes. However, for kinetic calibration of SPME, standard pre-loading step must be incorporated prior to extraction step. To date, standard pre-loading step was primarily performed using purified water as diluent because the presence of organic solvent decreases significantly the amount of standard pre-loaded on fibre.<sup>86</sup> However, long exposure to purified water during standard pre-loading step could potentially cause the

collapse of C<sub>18</sub> chains and poor extraction efficiency, although such effects were not reported previously<sup>86</sup> nor observed in calibration comparison experiments performed in Chapter 2 (Section 2.3.1.15). However, preliminary experiments with carbamazepine indicated poor extraction efficiency when standard pre-loading step was included, so this issue was further investigated in a systematic experiment. The extraction efficiency of C<sub>18</sub> SPME coatings for diazepam and carbamazepine was compared when (i) no preconditioning (ii) 30 minute conditioning in purified water or (iii) 30 minute conditioning in methanol/water (1/1, v/v) was performed. The results obtained are shown in Figure 3.11. Preconditioning using methanol/water was found to be very important for the extraction of carbamazepine, and omission of preconditioning resulted in 12-fold decrease in extraction efficiency. The effect for diazepam was much less pronounced with less than 2-fold decrease. The difference in behaviour for the two analytes can be explained by poor aqueous solubility of carbamazepine in comparison to diazepam. However, these results also explain why standard pre-loading in purified water was acceptable for applications dealing with diazepam<sup>86</sup>, and found unacceptable in current work. To address this problem, the optimization of standard pre-loading procedure was investigated as the next step in this research.

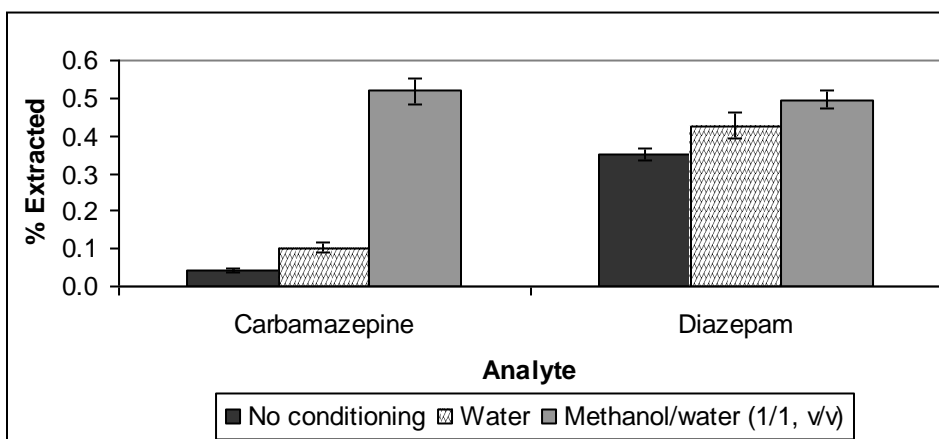


**Figure 3.11 Investigation of the effect of fibre preconditioning on the amount of analyte extracted using carbamazepine and diazepam as model analytes. Effect of no preconditioning is compared *versus* 30 min preconditioning in purified water *versus* 30 min preconditioning in methanol/water mixture. Extraction conditions: C<sub>18</sub> coating of 45  $\mu$ m thickness, 2 min static extraction from 100 ng/mL standard in PBS buffer, n=6 fibres per each condition.**

### 3.3.9 Optimization of standard loading procedure

The loading of standard from purified water may have adverse effect on the extraction efficiency of the new coatings, so pre-loading from standard solutions containing organic solvent is required. For these applications it is advantageous to combine fibre conditioning and standard loading in one step, in order to streamline sample preparation procedure and decrease total sample preparation time required for each sample. Therefore, loading of carbamazepine d10 from methanol/water (1/1, v/v) solution was investigated as shown in Table 3.7. The data shows that it is possible to combine fibre pre-conditioning and standard loading into one step as long as relatively high concentrations of loading standard are used. For example, using 100 ng/mL concentration of loading standard, only 0.17 ng of standard was preloaded on the fibre even when equilibrium extraction was used (60 min with 2400 rpm vortex). This is not sufficient quantity because successful application of kinetic method requires differentiation between amount loaded and remaining on fibre, and the amount remaining on fibre after exposure *in vivo* may not be sufficient to be detected. However, the use of 1000 ng/mL solution is able to load a sufficient quantity of standard, and was subsequently employed for *in vivo* study (Chapter 4). Furthermore, Table 3.7 shows that sample volume does not play a factor in the amount of standard loaded, because the amount of carbamazepine d10 loaded into C<sub>18</sub> fibre was the same regardless of whether 0.25 mL or 1.7 mL standard volume was used for loading. This situation is expected to occur when  $V_s \gg V_f K_{fs}$  according to Equation 1.1. The use of high amount of organic solvent in loading standard solution reduces the distribution constant between fibre and sample matrix ( $K_{fs}$ ), so that the amount of standard loaded is independent of sample volume in the range of volumes tested. This means that the smallest volume tested can be used to reduce overall consumption of deuterated standard. It is also interesting to note, without addition of organic modifier, the magnitude of  $K_{fs}$  is much higher as shown by higher % extracted of carbamazepine and its dependence on sample volume in Figure 3.6 (b).

**Table 3.7 Effect of sample volume and standard concentration on success of loading procedure.**

Concentration (ng/mL)	Volume used for loading (mL)	Amount loaded - CBZ d10 (ng)	% loaded - CBZ d10
100	0.25	0.17	0.67
100	1.7	0.17	0.10
1000	0.25	1.68	0.67
1000	1.7	1.65	0.10



### 3.3.10 Studies of coating performance: comparison between lots

Once 45  $\mu\text{m}$  biocompatible  $\text{C}_{18}$  coatings were selected as the best prototype coating for further production, multiple batches of the fibres with this coating were prepared. A typical batch of coating can produce total of 100-200 fibres. Ten fibres were randomly selected from each batch for quality control testing. These ten fibres were analyzed using equilibrium extraction times for four model benzodiazepines, and two main parameters were considered: the dependence of the amount extracted on the lot of coating and inter-fibre variability within each lot. Good agreement between the amount extracted was observed for all lots and all analytes tested as shown in Figure 3.12. Excellent inter-fibre reproducibility was found for all lots with all RSD values ranging from 2-7% for all analytes tested.

However, if the results for extractions performed simultaneously on the same day for five different lots (lot 75, 90, 93, 94, 96) are evaluated using single-factor ANOVA, the lot of coating is found to be significant factor at 95% confidence level for all analytes except nordiazepam. Based on these results, it is recommended to use fibres from a single batch of coating in a given experiment (for both samples and calibration standards), rather than mixing fibres from different lots.

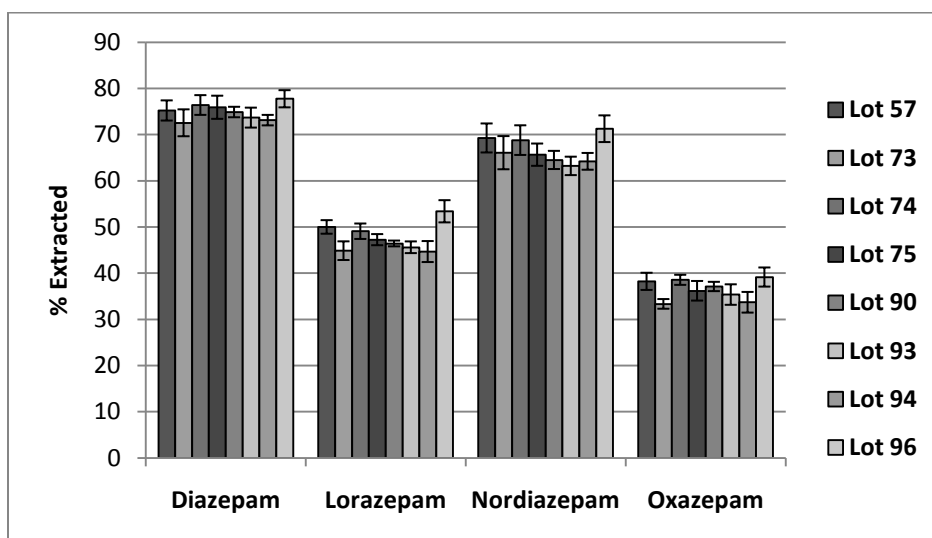


**Figure 3.12 Comparison of the extraction efficiency obtained for eight independent Supelco  $\text{C}_{18}$  lots of coating (n=10 fibres per lot) prepared on different days in April-May 2009. The results for four model analytes: diazepam, lorazepam, nordiazepam and oxazepam are shown. Extraction conditions: equilibrium, extraction from 100 ng/mL drug standard in PBS buffer pH 7.4.**

One other interesting aspect was encountered during experiments comparing different lots of coating. In initial studies, equilibrium extraction was performed using 60-min extraction time with 2400 rpm vortex as shown in Figure 3.7 in the example of extraction of carbamazepine. However, in subsequent experiments with large number of fibres (n=10 or 20), poor method precision (20-30% RSD) was observed in some experiments. Further troubleshooting experiments showed that the agitation in all positions of multi-tube vortexer was not uniform, and that equilibrium was not reached within 60-min period for some fibres, while for others it would. Furthermore, replicate extractions using the same set of fibres and exactly the same extraction conditions (but only varying the position of fibres in the multi-tube vortexer) did not show good agreement in the amount extracted by individual fibres indicating agitation may not be uniform and reproducible even when the exact same rpm setting is used. This was further confirmed by performing equilibrium extraction with no agitation and by increasing extraction time when vortex agitation was employed to ensure all wells have sufficient time to reach equilibrium. In these experiments, excellent precision was observed for all lots and all compounds (<5% RSD), and the amount extracted further increased (over 60-min extraction) for some fibres indicating that equilibrium was not successfully achieved using 60-min extraction time. Based on the results of this study, the extraction time was increased from current 60-min to 120-min to ensure equilibrium is achieved in all vials. This provided consistent results for all experiments, and poor precision results were not observed. The results show that even commercial agitation devices, may not provide sufficiently uniform agitation for use with SPME, and can be the cause of poor method precision. Uniformity of agitation should be considered in any experiment where extraction is performed in parallel for multiple samples. These results further highlight the utility of Concept 96 system described in Chapter 2, where factors such as uniformity of agitation were fully evaluated and found satisfactory. During this research on the performance of *in vivo* SPME devices, Concept 96 could not be used due to different device geometry. However, efforts are currently under way in our laboratory to build attachment for Concept 96 in order to successfully house an array of 96 *in vivo* SPME probes for the automation of desorption step.

### **3.4 Conclusions and future directions**

The research presented in this chapter investigated the performance of new prototype biocompatible SPME fibres from Supelco for bioanalysis. In the first stage of the work, 45  $\mu\text{m}$  coating was found to perform the best in terms of inter-fibre reproducibility and good extraction capacity, and was selected for further development and evaluation. Overall, the fibres were found to have good inter-

fibre reproducibility permitting single fibre use, which is one of the important requirements necessary for successful *in vivo* studies where separate fibres are used at each sampling point. In fact, proposed coatings met all of the criteria presented in Figure 3.1 except for short extraction times. Previous studies have also highlighted difficulties in reproducible preparation of very thin coatings on very thin solid supports<sup>136, 138</sup> and robustness of C<sub>18</sub>/polyethylene glycol thin coatings was not satisfactory<sup>138</sup>. Until this issue of coating preparation is resolved, thicker coatings with long equilibration times can still be successfully used for *in vivo* sampling applications by using kinetic calibration methods.<sup>80</sup> For this purpose, the effect of conditioning and sample preloading was examined in the current study, and successfully combined in a single step. The recommended workflows for *in vitro* and *in vivo* SPME using these new biocompatible SPME coatings are summarized in Figure 3.13. The availability of commercial *in vivo* SPME device is particularly important outcome of this work, as it enables the use of *in vivo* SPME in laboratories without in-house capability of making reproducible coatings and devices. However, current study only evaluated probe performance *in vitro*, so the subject of a follow-up study was a detailed investigation of *in vivo* performance of the probes as discussed in Chapter 4.

### **3.5 Addendum**

The text of this chapter was rewritten in comparison to published research article. The author gratefully acknowledges Francois Breton for the acquisition of SEM images.

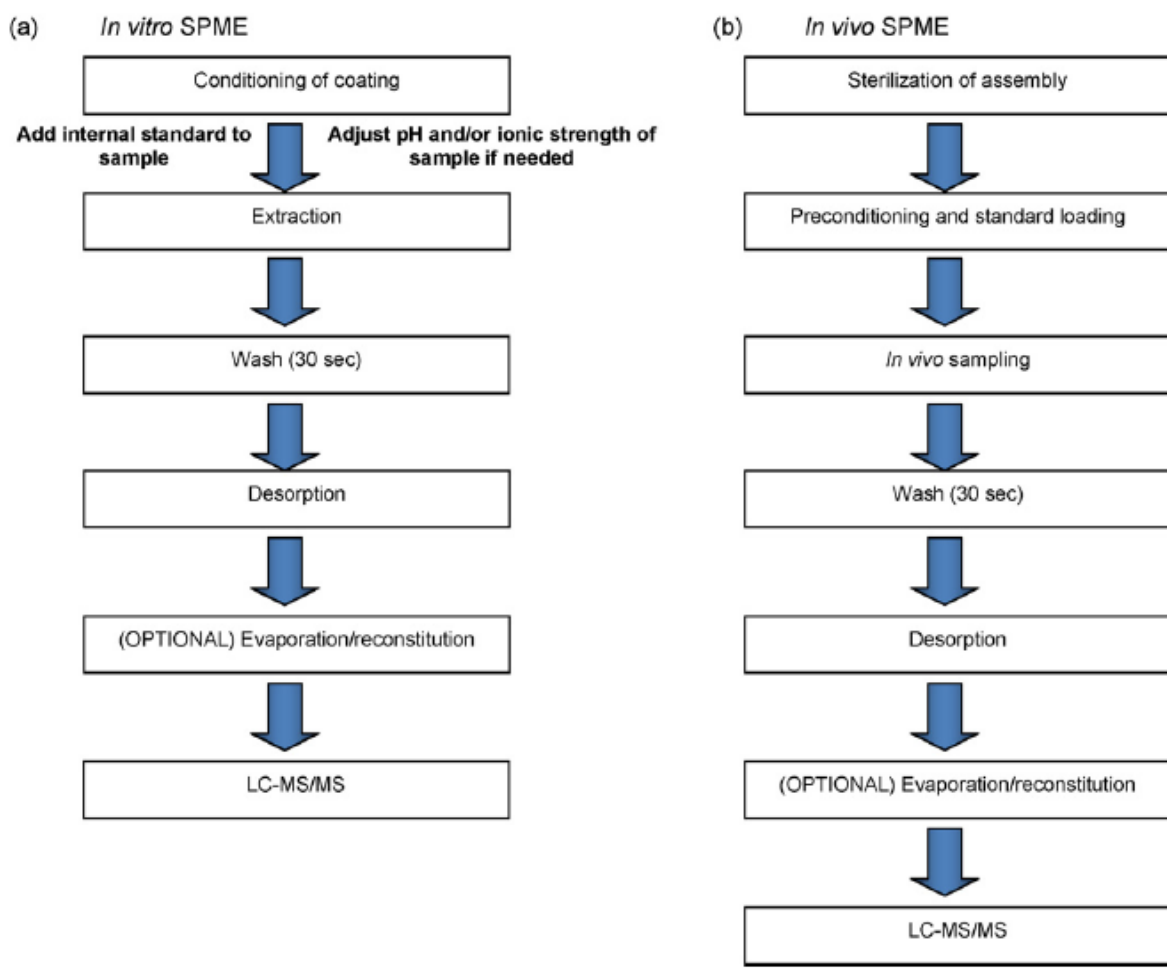


**Figure 3.13 Recommended workflow for (a) *in vitro* and (b) *in vivo* SPME procedure using prototype biocompatible SPME fibres.**

## Chapter 4

### ***In vivo* SPME sampling of mice: application to pharmacokinetic studies of carbamazepine and its metabolite**

#### **4.1 Preamble and introduction**

##### **4.1.1 Preamble**

*In vivo* experiments described in this chapter are currently submitted for publication: Vuckovic D., de Lannoy I., Gien B., Yang Y, Musteata F. M., Shirey B., Sidisky L, Pawliszyn J., *In vivo solid-phase microextraction for single rodent pharmacokinetics studies of carbamazepine and carbamazepine-10,11-epoxide in mice*, (2010).

*In vivo* experiments were performed in collaboration with Brad Gien and Ines de Lannoy from NoAB BioDiscoveries using their animal facility. The contributions of co-author, Brad Gien included the development of *in vivo* SPME sampling procedure for mice, the design and development of interface for sampling of mice as well as performing of entire *in vivo* sampling procedure including animal surgery to insert the interface and blood collection. Dr. Ines de Lannoy was involved in experimental planning and design of these *in vivo* experiments, performed data processing in order to estimate pharmacokinetic parameters using all three methods tested and co-wrote the manuscript. This data is summarized in Table 4.8 and Table 4.9, and is included with Ines's permission in order to show that the proposed *in vivo* SPME sampling procedure yielded results equivalent to traditional methods, indicating the validity of proposed approach. Yingbo Yang from NoAB BioDiscoveries performed LC-MS analysis on plasma samples collected both using terminal and serial sampling approaches using NoAb's in-house validated LC-MS/MS method. The detailed description of these methods is available in the manuscript. Only the final concentrations are shown here with permission of the authors in order to facilitate the comparison with *in vivo* SPME data. Florin Marcel Musteata was involved in experimental design and initial *in vivo* experiments performed on mice. Bob Shirey and Len Sidisky from Supelco Inc. prepared and further developed all *in vivo* SPME probes used in this study.

Section 4.3.7 presented within this chapter has been incorporated in manuscript entitled: Vuckovic, D., de Lannoy, I., Gien, B., Shirey, R.E., Sidisky, L., Dutta, S., Pawliszyn, J. *In vivo solid-phase microextraction: a new sample preparation tool in metabolomics*, (2010) which is currently

submitted for publication. The contributions of the authors are the same as described above. The contribution of S. Dutta is the LC-MS analysis of *in vivo* SPME samples using full hybrid Orbitrap system at Thermo facility in San Jose, while the relevant processing of this data set was performed by myself at the University of Waterloo.

I, Brad Gien, authorize Dajana Vuckovic to use the material for her thesis.

I, Ines de Lannoy, authorize Dajana Vuckovic to use the material for her thesis.

I, Yingbo Yang, authorize Dajana Vuckovic to use the material for her thesis.

I, Florin Marcel Musteata, authorize Dajana Vuckovic to use the material for her thesis.

I, Bob Shirey, authorize Dajana Vuckovic to use the material for her thesis.

I, Len Sidisky, authorize Dajana Vuckovic to use the material for her thesis.

I, Sucharita Dutta, authorize Dajana Vuckovic to use the material for her thesis.

#### **4.1.2 Introduction**

A typical pharmacokinetic study (PK) involves the dosing of multiple animals orally or intravenously with a drug compound, and monitoring the concentration of this compound (and possibly its metabolites) in plasma over time. Resulting drug concentrations are plotted against time, and this curve is used to estimate various PK parameters such as half life, clearance and availability. One recent trend in the analysis of biological samples, especially in the context of pharmacokinetic studies is a reduction in sample volume available for analysis, because increased number of samples are

collected from the same animal to ensure better data quality and greater number of sampling points.<sup>50</sup> There is also increased interest in single rodent pharmacokinetic studies, because collection of the data from single animal can result in improved estimation of PK parameters, and also considerable reduction in animal use and corresponding cost-savings.

Mice are the most difficult species for serial sampling experiments due to small body size and corresponding total blood volume (~1.85 mL total blood volume/25 g mouse). It is not recommended to exceed 20% of total blood volume during any 24-hr experiment, which poses strict limitations on the amount of blood that can be collected during each time point unless fluid replacement is performed. Traditional approach for performing PK studies on mice involves sacrifice of several mice per each time point. This results in significant overall animal use as typically 3-6 mice are employed per each time point and typical studies can have in excess of 10 time points. Furthermore, dosing errors are likely to occur when dosing such large cohort of animals, and these errors are included in resulting PK data derived from such studies. Such datasets also reflect inter-animal variability in drug absorption, distribution, metabolism and elimination, and the differences in drug metabolism can be particularly significant. PK data is used for important decisions during drug discovery process about whether or not to continue with a particular drug entity, so data quality is extremely important to avoid reaching erroneous conclusions. For example, Ingelse *et al.* show significant differences in PK parameters obtained using terminal sampling of 21 mice *versus* serial data collected for 2 mice, indicating that single rodent studies are likely to provide truer representation of *in vivo* kinetics.<sup>169</sup> In one crossover study in rats, the choice of sampling approach significantly influenced the results indicating that stress during sampling can exert an influence over the observed pharmacokinetic parameters.<sup>170</sup> In particular, a significant difference in  $t_{MAX}$  values was obtained by the two sampling approaches and attributed to physical stress which influenced blood flow and consequently drug absorption, distribution and metabolism. This comparison was facilitated by the ability to perform cross-over studies using the same animals, thus eliminating inter-animal variation from the results and clearly showing that sampling approach can have impact on the acquired pharmacokinetic data. In contrast, another study shows that PK data obtained from serial sampling was equivalent to the data obtained using multiple animals and terminal sampling.<sup>171</sup> This indicates that the effect of sampling on PK data is still not fully understood, and merits further research. Other advantages of single rodent pharmacokinetic studies include reduction in animal use which is particularly important when using rare/expensive strains of mice, decrease in the amount of compound needed to perform the study which is particularly advantageous in early drug discovery stages where the amount of pure drug is

limited, elimination of the effects of anesthesia from pharmacokinetics data, the ability to study inter-animal variation and the opportunity to perform multiple and/or simultaneous pharmacokinetic/pharmacodynamic investigations of mice.<sup>171-174</sup>

There are currently few successful approaches for serial sampling of mice reported in literature. One approach involves manual withdrawal of small blood volume (4-10  $\mu$ l) from tail vein followed by plasma protein precipitation.<sup>172, 173</sup> Other approaches include withdrawal of 30  $\mu$ L blood volume using external jugular vein cannulation followed by plasma protein precipitation<sup>175</sup> or serial sampling of 30  $\mu$ L of whole blood using lateral saphenous vein puncture in combination with plasma protein precipitation.<sup>171</sup> The withdrawal of 50-70  $\mu$ L blood volume using external jugular vein cannulation followed by turbulent flow chromatography on 2  $\mu$ L aliquot has also been successfully employed.<sup>176</sup> To avoid difficulties in handling small blood volumes (steps such as filtration, centrifugation, protein precipitation) Ingelse *et al.* suggest the use of sorbent trapping for collection of small whole blood volumes of 5-10  $\mu$ L, followed by protein precipitation, online SPE and LC-MS/MS analysis.<sup>169</sup> However, the proposed technique is considerably different from *in vivo* SPME sampling because (i) blood is withdrawn using established procedures of serial tail bleeding, (ii) sorbent device is designed not to interact with analytes of interest and is only used to physically hold the sample within the cartridge, (iii) exhaustive recovery is desired and (iv) sorbent trapping device does not provide sample clean up necessitating the subsequent use of SPE, which reduces overall sample throughput. Furthermore, problems with increased column back pressure were observed indicating insufficient sample clean-up even after application of SPE for sample clean-up. The main challenges with proposed serial sampling approaches were that the withdrawal of higher blood volumes limited the number of time points that could be collected and sometimes exceeded recommended blood volume sampling guideline. Furthermore, hemolysis was observed for tail vein bleeding during later time points, which caused overestimation of analyte concentrations.<sup>175</sup> The use of *in vivo* SPME could address both of these shortcomings, as no blood is withdrawn.

To date, *in vivo* SPME has been successfully applied for sampling of circulating blood in various animals such as dogs<sup>86, 87, 133, 138</sup>, pigs<sup>177</sup> and rats<sup>88</sup>. In addition to sampling of blood, *in vivo* SPME has also been successfully applied for sampling of tissue in freely moving animals within the past few years. For example, successful sampling of brain tissue of mice was reported for the estimation of toluene levels post-exposure to a single toluene dose.<sup>178, 179</sup> *In vivo* SPME sampling of muscle and adipose tissue of fish was used for environmental monitoring in order to detect trace bioaccumulation



of pharmaceuticals.<sup>180, 181</sup> Such studies are important for monitoring fate of various pollutants and its impact on aquatic wildlife, and the sensitivity of SPME was sufficient to detect diphenhydramine and diltiazem in wild fish without requiring lethal sampling.<sup>180</sup> In comparison to the well-established *in vivo* sampling method of microdialysis, SPME was simpler to apply and did not require any pumps or other hardware, thus making it more amenable to field sampling.<sup>182</sup> It was also found to provide better sensitivity and method precision, and eliminated adsorptive losses which are sometimes encountered with microdialysis.

For sampling of circulating blood in larger animals such as dogs and pigs, an SPME fibre can be directly inserted into an appropriate peripheral vein using an in-dwelling catheter.<sup>86, 87, 133, 138</sup> The catheter was then sealed using PRN adapter, and SPME probes were inserted with the aid of a hypodermic needle through the septum of PRN adapter. However for rodent sampling, the size of the blood vessels is too small to permit direct insertion of the current size of the probes without significant obstruction of the blood flow. To overcome this issue, the use of specially designed interface was proposed by Musteata *et al.*<sup>88</sup> Two main approaches were considered after surgical implantation of carotid artery catheter: (i) recirculation of blood to the catheter through the out tube of interface using pumping action of the heart or (ii) connection of the out tube to a syringe for manual recirculation of blood using low push/pull rate. The first approach resulted in clotting problems and sufficient pressure for blood flow through the interface over extended time period could not be maintained, whereas the second approach was more amenable to repeated serial sampling. After evaluation of various interface designs for rat sampling, polyurethane interface was found to minimize issues with blood clotting within the interface and was successfully employed in PK study. However, the internal volume of this interface was still too large for successful use in mice, so one of the goals of the research reported in this study was to modify sampling procedure to enable its use for sampling of mice. Once successful sampling protocol was established, the *in vivo* SPME sampling approach was validated against the established techniques to study pharmacokinetics of carbamazepine (CBZ) and its main metabolite, carbamazepine-10,11-epoxide (CBZEP): (i) terminal sampling using cardiac puncture of 3 mice/time point and (ii) serial sampling of 3 mice using Culex® automated sampling unit. CBZ was selected for this study because of its widespread use as treatment for epilepsy, and because it is one of the drugs where therapeutic drug monitoring of unbound (free) concentration is recommended because of significant inter-individual variation of free drug fraction while total drug concentration remains within therapeutic range.<sup>183, 184</sup> The latter feature makes CBZ a particularly interesting model drug for *in vivo* SPME studies because the amount of drug extracted

by SPME is proportional to unbound fraction. CBZEP is obtained through hepatic oxidation of CBZ. It is clinically its most important metabolite because its pharmacological activity is similar to the parent drug and it possibly contributes to the appearance of side effects.<sup>170, 185</sup> Finally, this research project was also used to evaluate the performance of commercial prototype *in vivo* SPME assemblies during *in vivo* studies, after satisfactory probe performance using biocompatible C<sub>18</sub> probes with 45 µm thickness was achieved during *in vitro* tests as previously described in Chapter 3.

## 4.2 Experimental

### 4.2.1 Chemicals and materials

CBZEP was obtained from Sigma-Aldrich (Oakville, ON, Canada). The sources of all other chemicals and materials were the same as stated in Chapters 2 and 3.

### 4.2.2 *In vivo* SPME procedure

The day before *in vivo* SPME sampling, prototype *in vivo* SPME probes housed within 22-gauge hypodermic needle as described in Chapter 3 and consisting of biocompatible C<sub>18</sub> coating (45 µm thickness, 5 µm particle size, Supelco, Bellefonte, PA, USA), were preconditioned and pre-loaded with deuterated carbamazepine internal standard. The conditioning and loading was performed at equilibrium from 300 µL of 1 µg/mL standard solution of carbamazepine-d10 (CBZ-d10, Alltech, Deerfield, IL, USA) dissolved in methanol/water (1/1, v/v) using vortex agitation of 1000 rpm. The development of this procedure was described in more detail in Chapter 3. The probes were kept in this conditioning/loading solution until each *in vivo* sampling time point in order to ensure that the coating does not dry out prior to sampling. Five extra probes were pre-loaded and used to determine the amount of calibrant loaded as described in Section 4.2.3.

*In vivo* SPME sampling was performed in seven conscious male CD-1 mice (Charles River Labs, St. Constant, PQ, Canada) weighing 20 to 30 g. Prior to experiments, mice were acclimatized for a minimum of five days, and were provided with food and water *ad libitum*. One day prior to *in vivo* SPME experiments, a catheter was implanted surgically in the carotid artery and the mice were allowed to recover from surgery and anesthesia overnight. On the day of sampling, custom-made sampling interface, consisting of small volume tubing and a PRN adapter was connected by a stainless steel connector to the implanted catheter. The main difference between the interface used in current work and the interface used previously by Musteata *et al.* to sample rats was the reduction in

overall internal volume of the interface.<sup>88</sup> The blood (~100  $\mu$ L) was drawn in and out of the interface manually using a syringe. Conditioned *in vivo* SPME probes were inserted into the interface through PRN adapter and held within the interface for 2 min. Approximately 10 pull/push cycles using syringe were accomplished during each 2-min sampling period. This assisted agitation was used to increase the amount extracted by SPME, and thus improve overall method sensitivity. The photo of the entire sampling set-up is shown in Figure 4.1.

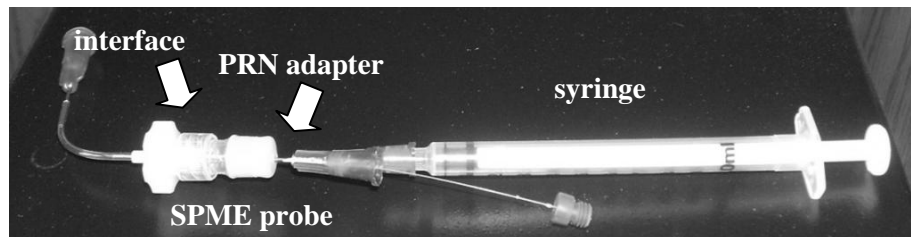


**Figure 4.1 Photograph of the mouse sampling interface shown with an SPME probe assembly inserted through the PRN adapter.**

The dosing of mice (2 mg/kg CBZ) was performed by injection into the lateral tail vein using CBZ dosing solution prepared in ethanol/propylene glycol/saline (1/1/3, v/v/v). *In vivo* SPME sampling was performed immediately prior to dosing and at 5, 15, 30, 60, 90, 120, 180 and 240 min post-dose. Between sampling points, catheter was periodically flushed with heparin-containing saline solution in order to prevent coagulation. For each sampling period, a new *in vivo* SPME probe was inserted into the blood-filled sampling interface 1 min before the stated time and held in the interface 1 min after the stated time (total sampling time of 2 min). Immediately after the probe removal from the interface, the SPME probe was rinsed for 30 sec using purified water to remove any cells or salts from the probe surface. The probes were stored in the freezer ( $-20^{\circ}\text{C}$ ) or on ice until analysis and LC-MS/MS analysis was performed within 24 hr of sampling.

The desorption of analytes from SPME probes was accomplished using 300  $\mu$ L of desorption solvent (acetonitrile/water, 1/1, v/v) spiked with 50 ng/mL diazepam using 0.3 mL amber polypropylene HPLC vials (Labsphere, Brossard, PQ, Canada). Diazepam was used as internal standard in this study in order to correct for injection volume variability. The desorption was performed for 60 min on multi-tube vortexer at 1000 rpm. The resulting sample solutions were injected directly into LC-MS/MS. A second desorption using a fresh portion of desorption solvent was also performed in order to evaluate the desorption efficiency and carryover.

### 4.2.3 *In vivo* SPME calibration procedure for determination of both free and total CBZ and CBZ-EP concentrations

The concentration of CBZ and CBZEP was determined using kinetic on-fibre standardization method. The theoretical basis of this method is described in Section 1.4. As part of kinetic on-fibre standardization procedure it is necessary to determine the product of  $K_{fs} \cdot V_f$  by performing equilibrium extraction in a set of calibration standards of known analyte concentration prepared in appropriate matrix. The choice of appropriate matrix depends on whether free (unbound) or total (bound + unbound) concentration of analyte is of interest in a given study. In current study, both concentrations were of interest so two independent calibration curves were constructed. One matrix-free calibration curve was constructed in PBS pH 7.4 buffer and used to determine unbound CBZ and CBZEP concentrations. Second matrix-matched calibration curve was constructed in mouse whole blood and used to determine total concentrations of CBZ and CBZEP. The plot of the amount extracted *versus* standard concentration is then used to determine  $K_{fs} \cdot V_f$  product using the slope of the linear regression line and known sample volume (using Equation 1.1). In cases of negligible depletion, the calculations are even simpler as the slope of the line is approximately equal to the  $K_{fs} \cdot V_f$  product as presented in Equation 1.7.

#### 4.2.3.1 Determination of $q_0$

In current study, the amount of standard pre-loaded on the fibre ( $q_0$ ) was determined by immediate desorption of five probes (without performing *in vivo* sampling), preconditioned and preloaded as described in Section 4.2.2 followed by LC-MS/MS analysis. The main considerations that were met when selecting the amount of standard to preload is that (i) sufficient quantity of calibrant should be preloaded to ensure some calibrant (sufficient for quantitative analysis) remains in the coating after *in vivo* sampling and (ii) there should be significant difference (within experimental error) between the amount of calibrant pre-loaded and remaining on the coating to facilitate the use of Equation 1.8. In current work, the amount of CBZ-d10 pre-loaded onto the fibres ( $q_0$ ) was ~1.6 ng and excellent precision was obtained as indicated by 7% RSD (n=5). The amount of calibrant remaining on the fibre ( $Q$ ) was ~0.96 with 18% RSD (n=50). The alternative method for determination of  $q_0$  is to experimentally determine the amount of CBZ-d10 remaining in each loading solution. In this case,  $q_0$  is then calculated as the difference in the amount initially present in each vial of loading solution minus the amount of calibrant remaining in the vial after loading procedure is finished. This approach is much more work-intensive as it requires the analysis of large number of loading solutions.

Furthermore, the concentration of loading standard employed in this study is very high (1  $\mu\text{g/mL}$ ) and exceeds linear dynamic range of LC-MS/MS method employed so serial dilution of these loading standard solutions is required prior to injection. This is the reason why the simpler approach described above was employed. The use of this simpler approach is further supported by extensive characterizations of various lots of Supelco biocompatible  $\text{C}_{18}$  fibres presented in Chapter 3 which show that at equilibrium intra-lot variability of the amount extracted by the probes is very low (typically <5% RSD). For other type of *in vivo* SPME fibres such as polypyrrole, where intra-lot variability is very high<sup>136</sup>, the simple approach employed here would not be adequate, and the alternative approach should be used instead.

#### 4.2.3.2 Determination of n and Q

The amount of analytes extracted during *in vivo* SPME sampling (n) and the amount of calibrant remaining on the fibre (Q) were calculated using CBZ, CBZEP and CBZ-d10 calibration curves (0.1 ng/mL – 100 ng/mL, n=9 standards dissolved directly in desorption solvent and covering the entire linear dynamic range of the instrument).

#### 4.2.3.3 Matrix-free and matrix-matched calibration: determination of $K_{fs} \cdot V_f$ product

Blank mouse blood (~ 10 mL in total) was collected from a group of non-dosed animals by NoAB BioDiscoveries, pooled and mixed immediately with heparin as anticoagulant. Calibration standards were then prepared by spiking this pooled mouse blood with an appropriate volume of stock CBZ and CBZEP standard solutions (prepared in methanol) in such a way as to keep the organic concentration in final calibration standard solution at exactly 1% methanol (v/v). These spiked whole blood samples were incubated overnight with refrigeration to permit protein binding to take place, as 1 hr incubation was previously found to be insufficient for CBZ as described in Chapter 3. After incubation, calibration standards (0.3 mL sample volume in 0.3 mL capacity amber HPLC vial) were subjected to equilibrium SPME sampling procedure in parallel (16 hr extraction, 200 rpm orbital agitation) using individual *in vivo* SPME probes for each standard. Vortex agitation at 1000 rpm could not be used for whole blood samples due to possibility of disruption of red blood cells. Thus, more gentle orbital shaking was employed and extraction time was extended to ensure equilibrium was reached. Fibres were rinsed for 30 sec using purified water and desorbed as described in Section 4.2.2. The calibration curve was obtained by 1/y weighted linear regression analysis using SigmaPlot 2004 for Windows (version 9.0) software.

For free concentration determination, calibration standards were prepared in PBS pH 7.4 buffer. Organic solvent concentration was kept at exactly 1% (v/v) for all standard concentrations, and overnight pre-incubation step was omitted for this calibration set as no binding matrix was present. The rest of the procedure was exactly the same as described for whole blood calibration standards. Example calibration curves obtained in different matrices for CBZ and CBZEP are shown in Table 4.1. It should be noted that the slope of the calibration curve in PBS buffer cannot be used as the indication of the magnitude of  $K_{fs}V_f$  product because the extraction is not negligible. Therefore, sample volume used for calibration must be taken into account according to Equation 1.1. For whole blood and plasma calibration, the extraction is negligible as shown by good agreement between fibre constant and slope for 0.3 mL sample volume used during calibration. For best accuracy of results, the more exact  $K_{fs}V_f$  was used to calculate total concentrations. However, this data shows that despite small total blood volume in mice (1.8 mL), the main assumption for application of *in vivo* SPME holds and the amount extracted is independent of sample volume.

**Table 4.1 Example calibration curves obtained for CBZ and CBZEP in PBS, blood and plasma.**

Analyte	Matrix	Linear range (ng/mL)	Number of calibration standards	Slope $\pm$ SD	Y-Intercept $\pm$ SD	$r^2$	$K_{fs}V_f$
CBZ	PBS	0.4-300	8	0.199 $\pm$ 0.006	0.01 $\pm$ 0.07	0.995	0.591
	Blood	1-2000	9	0.00641 $\pm$ 0.0002	-0.001 $\pm$ 0.01	0.992	0.00654
	Plasma	1-2000	9	0.00746 $\pm$ 0.0003	0.001 $\pm$ 0.02	0.991	0.00765
CBZEP	PBS	0.3-100	7	0.131 $\pm$ 0.007	-0.02 $\pm$ 0.04	0.988	0.233
	Blood	1-150	6	0.00287 $\pm$ 0.0002	0.002 $\pm$ 0.004	0.985	0.00290
	Plasma	1-150	6	0.00448 $\pm$ 0.00008	0.0002 $\pm$ 0.001	0.999	0.00455

The reason PBS buffer is often used to perform free concentration calibration is because it is easily available and it models well physiological conditions including pH and ionic strength. The suitability of PBS buffer to be used as artificial substitute for protein-free plasma was verified experimentally as follows: mouse protein-free plasma (n=2) was obtained by ultrafiltration of freshly collected mouse plasma using 3K MW cut-off Nanosep centrifugal devices (Pall, Port Washington, NY, USA) for 20 min at 13000 rpm at 4°C as recommended by the manufacturer. These samples were then spiked with

known concentration of CBZ, allowed to incubate overnight, and then subjected to SPME extraction. The amount of CBZ extracted from protein-free plasma was compared *versus* the amount of CBZ extracted from PBS buffer pH 7.4 (n=2).

#### 4.2.3.4 Determination of blood to plasma concentration ratios

Some compounds can preferentially partition into red blood cells, thus causing different drug concentrations to be measured in plasma *versus* whole blood samples. Drugs which do not exhibit preference for plasma *versus* red blood cells have blood to plasma concentration ratio of unity, and for such drugs direct comparison of the results for whole blood *versus* plasma analysis is possible. The ratios <1 show the exclusion of the drug from the red blood cells and the ratios >1 show the partitioning of the drug into red blood cells. For either of these types of drugs the knowledge of blood to plasma concentration ratio is crucial to accurately compare whole blood *versus* plasma analysis results. One of the goals of current study was the comparison of *in vivo* SPME results obtained in whole blood to the results obtained by traditional plasma analysis after terminal cardiac puncture, so it was necessary to experimentally determine blood to plasma concentration ratios for CBZ and CBZEP. This ratio can be determined using *in vitro* SPME by performing equilibrium SPME on two aliquots of same spiked whole blood sample: (i) whole blood aliquot as is and (ii) plasma aliquot obtained after centrifugation (4°C, 15000 rpm, 15 min) of the same spiked whole blood sample to isolate plasma sample. These samples were prepared exactly as described in Section 4.2.3.3 including overnight incubation period prior to SPME. Blood to plasma concentration ratio drug concentration dependent, so this experiment was performed over the entire range of CBZ concentrations observed *in vivo*. The total concentration of analyte in each matrix was determined using independent calibration curves prepared in whole blood and plasma at known analyte concentrations. The results for this experiment are shown in Table 4.2. The first time the experiment was performed, one possible outlying value (2.73) was observed as highlighted in the table. This caused large uncertainty in the experimentally determined ratio, so the experiment was subsequently repeated and these results are also included in the same table. The second experiment confirmed that the value of 2.73 was an experimental outlier. The experimental blood to plasma concentration ratio for CBZ ( $1.10 \pm 0.28$ ) for the combined data sets excluding the outlying value is not statistically different from unity as determined by a paired t-test ( $t=0.80$ ,  $t_{\text{CRITICAL}}=2.16$ ,  $p=0.44$ ). In an independent experiment, blood to plasma concentration ratio of  $1.32 \pm 0.35$  was determined for CBZEP ( $t=0.98$ ,  $t_{\text{CRITICAL}}=4.30$ ,  $p=0.43$ ). Based on these results, the concentrations measured by *in*

*in vivo* SPME sampling of whole blood were compared directly to conventional plasma analysis without application of a correction factor. Mouse whole blood to plasma ratio for CBZ and CBZEP has not been reported in literature to date, but the results obtained in this study agree well with ratios of  $1.06 \pm 0.21$  and  $1.53 \pm 0.45$  obtained in humans<sup>186</sup>, and  $1.37 \pm 0.125$  and  $1.32 \pm 0.134$  obtained in rats<sup>187</sup>, for CBZ and CBZEP, respectively.

**Table 4.2 Determination of whole blood to plasma concentration ratio for CBZ using equilibrium *in vitro* SPME.**

Total CBZ Concentration (ng/mL)		Whole Blood/Plasma Concentration Ratio
Whole Blood	Plasma	
<b>Experiment 1</b>		
25.0	15.5	1.61
39.0	27.9	1.40
131	48.0	2.73*
188	145	1.30
304	347	0.88
499	835	0.60
1921	2393	0.80
4060	3386	1.20
6767	5696	1.19
	<b>Mean (n=9)</b>	<b>1.30</b>
	<b>S.D. (n=9)</b>	<b>0.62</b>
	<b>% RSD (n=9)</b>	<b>48</b>
<b>Experiment 2</b>		
1.19	1.19	1.00
11.7	14.8	0.79
83.4	72.1	1.16
439	323	1.36
769	643	1.20
1367	1436	0.95
	<b>Mean (n=6)</b>	<b>1.08</b>
	<b>S.D. (n=6)</b>	<b>0.20</b>
	<b>% RSD (n=6)</b>	<b>19</b>

\*Potential outlier as described in text

#### 4.2.4 *In vitro* SPME validation

Prior to *in vivo* experiments, the entire SPME-LC-MS/MS method was validated in order to evaluate its accuracy and precision. The validation samples (n=4 at three concentration levels) were prepared as described above for preparation of mouse whole blood calibration standards and incubated



overnight with refrigeration to permit protein binding to take place (Section 4.2.3.3). These validation samples were allowed to equilibrate to room temperature. Then, the catheter end of the interface was placed directly into the vial containing spiked blood and the entire SPME procedure (2-min sampling, rinse and desorption) was carried out exactly as described for *in vivo* samples in section 4.2.3. SPME probes preloaded with calibrant were used for this experiment, and kinetic on fibre standardization was used to determine the total concentration of CBZ and CBZEP. Accuracy (% relative recovery) was calculated as the ratio of the experimentally determined amount of analyte to the true spiked amount x 100%.

#### **4.2.5 Terminal cardiac puncture sampling and automated serial sampling using Culex®**

The results of *in vivo* SPME were compared to two traditional sampling methods: (i) terminal cardiac puncture (n=3 mice per time point) and (ii) serial blood sampling (n=3 mice) using an automated *in vivo* sampling system (Culex®, BASi, West Lafayette, IN, USA). Sample collection and analysis for these two methods were performed entirely at NoAb BioDiscoveries, so only a brief overview of relevant procedures is given below. Additional details are included in the manuscript.<sup>188</sup>

For automated sampling, 2 mg/kg CBZ dosing of mice was performed using the jugular vein catheter and for terminal cardiac puncture sampling the mice were dosed through the tail vein. Blood samples were collected prior to dosing and at 5, 15, 30, 60, 90, 120, 180, 240 and 270 min post-dose.

For automated sampling method, 50 µL blood sample was automatically drawn via the carotid artery catheter from each of three mice at each time point, immediately diluted (1/1, v/v) with heparin-containing saline (20 IU/mL) and stored refrigerated until analysis. To enable serial sampling of the same animal for all of time points, it was necessary to replace the blood volume withdrawn at each time point using an equal volume of heparin-containing saline (20 IU/mL). Prior to LC-MS/MS analysis, blood samples were centrifuged to isolate plasma (6500 rpm for 5 min at 4°C), followed by plasma protein precipitation with acetonitrile (1/3, v/v) and evaporation/reconstitution in mobile phase as described in detail elsewhere. For terminal sampling method, 600 to 800 µL of blood was collected into heparinized tubes by direct cardiac puncture while mice were under CO<sub>2</sub>/O<sub>2</sub> anesthesia. Plasma was immediately isolated by centrifugation at 6800 rpm for 5 min at 4°C and stored frozen until analysis. Immediately, prior to LC-MS/MS analysis, thawed plasma samples were subjected to plasma protein precipitation using acetonitrile (1/4, v/v) followed by evaporation/reconstitution in mobile phase and dilution (1/10, v/v) as described in detail elsewhere.

#### 4.2.6 LC-MS/MS analysis

For terminal puncture and automated sampling experiments, LC-MS/MS analyses were performed at NoAB using appropriate validated methods described elsewhere. For all LC-MS/MS methods (both at the University of Waterloo and NoAB BioDiscoveries), samples were diluted if necessary to ensure they fall within linear dynamic range of the instrument employed. Full calibration curves were run before and after samples, and injections of quality control sample of known CBZ and CBZEP concentrations were performed periodically to ensure good signal stability throughout the entire run. For SPME experiments, LC-MS/MS analyses were performed using a LC-MS system consisting of Accela autosampler with cooled sample tray, Accela LC pumps and TSQ Vantage triple-quadrupole mass spectrometer equipped with heated electrospray (HESI) source (Thermo Fisher Scientific, San Jose, CA, US). Xcalibur software (version 2.0.7. SP1) was used for all data acquisition and processing. Reverse-phase LC method using Symmetry Shield RP18 column (2.1 x 50 mm, 5  $\mu$ m, Waters, MA, US) was used to separate the analytes using gradient elution with mobile phases (A) acetonitrile/water/acetic acid (10/90/0.1, v/v/v) and (B) acetonitrile/water/acetic acid (90/10/0.1, v/v/v). The gradient included hold at 100% A for 0.5 min, linear increase to 90% B in 2.5 min, hold at 90% B for 0.5 min and re-equilibration of the column to initial conditions for 1.5 min for a total run time of 5 min. Flow rate was 0.5 mL/min and eluent was diverted to waste for initial 1.5 min of the run time.

MS conditions were set using direct infusion of standard solution containing all analytes using syringe pump and systematic optimization of all parameters. Optimized ESI conditions included: sheath gas = 50 arbitrary units, auxiliary gas = 10 arbitrary units, spray voltage = 4000 V, and capillary temperature = 275 °C. All of the compounds were analyzed in positive ion SRM mode using the following transitions 237.1→194.1 (CBZ), 247.1→204.2 (CBZ-d10), 253.1→180.1 (CBZEP) and 285.1→193.1 (diazepam). Capillary and S-lens voltages were set to 20 and 87 V for CBZ, 22 and 89 V for CBZ-d10, 31 and 167 V for CBZEP, 32 and 122 V for diazepam. Example chromatogram is shown in Figure 4.2 and demonstrates that baseline chromatographic separation of CBZ and CBZEP was achieved by this method. This was very important for accurate analysis of CBZEP because approximately 0.3% of in-source oxidative conversion of CBZ to CBZEP was detected. This conversion was detected in high concentration CBZ standards, where a distinct peak with the retention time of CBZEP was observed. In the absence of chromatographic separation of the two analytes, this could cause systematic bias when trying to simultaneously analyze low concentrations of CBZEP in presence of high concentrations of CBZ.

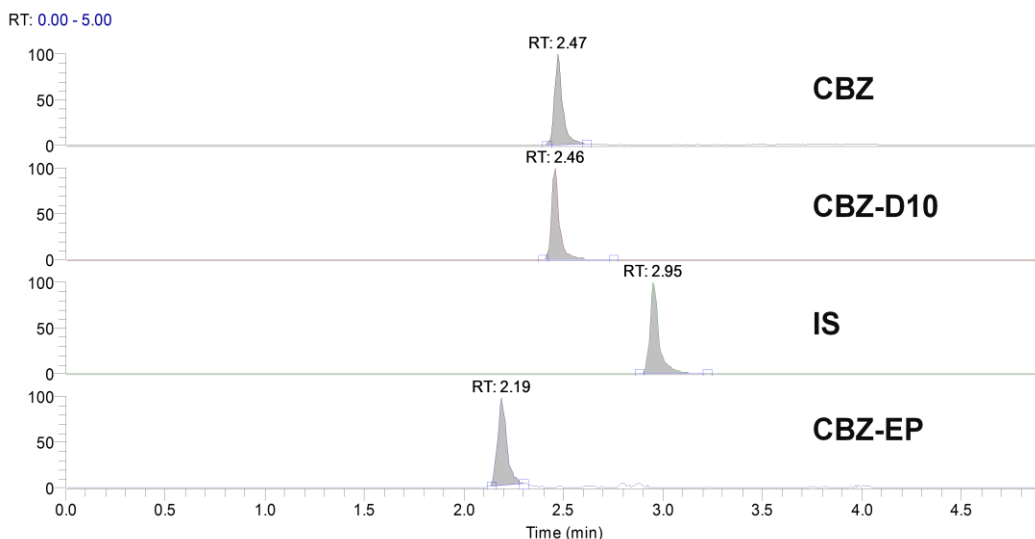


**Figure 4.2 Example selected reaction monitoring chromatogram of 5 ng/mL CBZ and CBZEP validation sample prepared in mouse whole blood with heparin as anticoagulant using SPME-LC-MS/MS method as described in Experimental.**

## 4.3 Results and discussion

### 4.3.1 Summary of SPME method development

SPME method for CBZ was developed as described in Chapter 3 simultaneously with the methods for other drugs. The desorption conditions were changed slightly from those presented in Chapter 3 to increase the volume of desorption solvent from 100  $\mu$ L to 300  $\mu$ L as this was found to decrease carryover to  $\leq 0.7\%$  even at the highest *in vivo* concentrations observed during early time points. The optimized CBZ method was then applied to CBZEP, and it was found that sufficient analytical sensitivity was achievable to observe this important metabolite directly *in vivo* without any further optimization necessary.

Initial *in vivo* studies used sampling approach proposed by Musteata *et al.* where blood is recirculated back to the animal using slow manual push and pull action using syringe.<sup>88</sup> These initial studies were performed using 4 push/pull cycles of 100  $\mu$ L of blood within 2-min sampling period, and the speed was selected on the basis of Musteata *et al.* study where 3 push/pull cycles were completed within each 2-min sampling interval. However, this initial data showed poor agreement between SPME and traditional sampling based on blood withdrawal at the early time points where concentrations are expected to change rapidly after intravenous dosing. One possible cause of this

observation was averaging of analyte concentrations during the sampling period or slow response of SPME coating to rapidly changing concentrations. Using a simple *in vitro* test, the effect of increasing the sampling speed on the amount extracted by SPME was investigated. As a control, fibre was placed in a 50 ng/mL CBZ standard solution in PBS buffer for 2 min with 10 push/pull cycles completed over the sampling period (10 push and pull cycles, no delay). The sampling was then repeated using the same fibre, but this time the fibre was first placed in blank PBS for 30 sec, then in 50 ng/mL CBZ standard solution in PBS for the remaining 90 sec sampling time (10 push and pull cycles with delay). The overall sampling speed was kept constant at 10 pull/push cycles over 2-min sampling period. A third experiment was performed with the same 30-s delay, but the agitation speed was lowered to 4 push/pull cycles. Agitation speeds above 10 push/pull cycles were not suitable for use *in vivo*, as they could cause animal shock and/or premature death. All determinations were performed in triplicate using the same fibre, and the results obtained are shown in Figure 4.3. The results show that using slower speed of 4 push/pull cycles, the amount of analyte extracted by SPME fibre was significantly lower *versus* 10 push/pull cycles and did not properly reflect the final concentration of 50 ng/mL. Instead, it represented time-weighted average concentration over the sampling time. However, when 10 push and pull cycles were employed, no significant difference in the amount extracted was observed whether sampling was performed in 50 ng/mL standard solution for the entire 2-min period or only for 1.5- min period with 0.5-min initial sampling period in blank solution. Based on these results, sampling speed of 10 push and pull cycles was employed for all subsequent *in vivo* experiments.

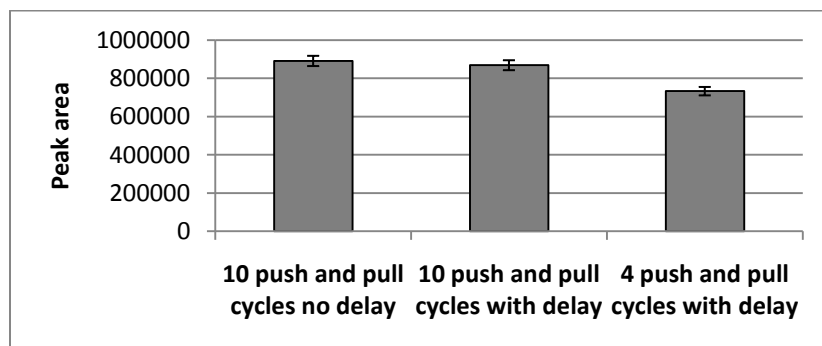


**Figure 4.3 Results of *in vitro* evaluation of assisted agitation speed. The dependence of the response (chromatographic peak area of CBZ, n=3 determinations) of SPME sampling to a rapid change in CBZ concentration (0 to 50 ng/mL as described in text) and influence of assisted agitation speed (4 *versus* 10 push/pull cycles).**

### 4.3.2 Investigation of suitability of PBS buffer for free concentration determination

During *in vivo* studies, it was desirable to monitor both free and total analyte concentrations. The determination of free concentration can be performed by preparing SPME calibration curve in matrix which does not contain any binding species. For this purpose, PBS buffer at pH 7.4 is often used because it is easier to obtain than protein-free plasma, especially for studies in mice where such limited blood volume is available. To investigate whether PBS buffer can serve as adequate surrogate matrix for current application, the amount of analyte extracted from PBS was compared to the amount extracted from protein-free plasma. Protein-free plasma was obtained using ultrafiltration through 3K ultrafiltration device. The mean absolute recovery of CBZ from protein-free plasma was  $29.3 \pm 7.8\%$  and in PBS was  $44.9 \pm 1.5\%$  using 0.22 mL sample volume. Using Student's t test at 95% confidence interval, there was no statistically significant difference between two matrices ( $t=-2.78$ ,  $t_{\text{critical}}=4.30$ ,  $p=0.11$ ) indicating PBS buffer can serve as good substitute for protein-free plasma. It should be noted that very small n was used for this test due to very limited availability of mouse plasma. For example, total blood volume that can be extracted during terminal sampling of mice is about 50% of total blood volume, or approximately 800-900  $\mu\text{L}$ . After centrifugation, only about 400  $\mu\text{L}$  of plasma is obtained from such sample. The amount of filtrate obtained after ultrafiltration further reduces the volume to about 200  $\mu\text{L}$ .

### 4.3.3 Summary of method validation results

The entire *in vivo* SPME procedure was validated by performing sampling from a vial of whole blood spiked with known CBZ concentration. Sampling was performed using interface and assisted agitation of 10 push/pull cycles in order to mimic *in vivo* situation as much as possible. The experiments were performed at three concentration levels using  $n=4$  independent determinations per level and on-fibre standardization method was used. A summary of the results is shown in Table 4.3 and shows acceptable accuracy and precision of the entire method including the on-fibre standardization approach.

Furthermore, extraction efficiency (or absolute recovery) was evaluated at equilibrium across the entire range of concentrations of interest using calibration standards prepared in different matrices as summarized in Table 4.4. Absolute recoveries of CBZEP were lower than for CBZ due to the slightly more polar nature of the compound. As noted in Section 3.3.10, extraction efficiency was dependent on the lot of the probes used, so for *in vivo* studies it was ensured that all *in vivo* samples and all calibration samples were extracted using probes from the same lot. The absolute recovery in plasma

**Table 4.3 Summary of validation results for CBZ using SPME with on-fibre standardization.**

CBZ concentration (ng/mL)	Accuracy Mean % relative recovery (n=4)	Precision % RSD (n=4)
5	96.8	17
200	109	14
2000	93.1	8

and whole blood was very low due to high degree of binding to plasma proteins. However, low absolute recoveries are permitted according to regulatory guidelines as long as it is shown that the absolute recovery is consistent across all concentration levels of the entire linear dynamic range of the method.<sup>142</sup> This is the case for the developed SPME methods as indicated by good precision of absolute recovery determination obtained using different concentration levels spanning the entire range of expected *in vivo* concentrations.

A 30-second washing step with purified water was incorporated between extraction and desorption steps in order to eliminate any salts from the surface of the fibre and/or any small blood droplets from *in vivo* assembly. These washing solutions were subsequently analyzed for the presence of CBZ, but no CBZ was detected in any of the chromatograms indicating no detectable loss of CBZ occurs during wash step.

**Table 4.4 Absolute recovery of CBZ and CBZEP at equilibrium in PBS, plasma and whole blood (n=10 concentration levels for CBZ, n=6 concentration levels for CBZEP).**

Analyte	Absolute recovery in PBS (%)	Absolute recovery in plasma (%)	Absolute recovery in whole blood (%)
CBZ	68±4	2.4±0.3	2.1±0.4
CBZEP	39±6	1.5±0.1	1.0±0.2

The lower limit-of-quantitation (LOQ) of proposed *in vivo* SPME procedure was 1 ng/ml for CBZ and CBZEP in whole blood, and was determined using 10x signal-to-noise ratio and exhibited acceptable precision (<20% RSD). The linear range evaluated in current study was 1-2000 ng/mL for CBZ and 1-150 ng/mL for CBZEP in whole blood because the expected concentrations of the drug and metabolite were not expected to exceed this range. The reported linear range is not limited by the probe capacity, and can be further extended depending on application requirements, as long as

samples are sufficiently diluted so that the signal falls within the linear range of the MS instrument employed. Example calibration curves in all matrices are shown in Table 4.1.

The effect of 1% methanol in plasma calibration standards was also examined by comparing the amount extracted from CBZ calibration standard with no methanol *versus* calibration standard prepared with 1% methanol. Due to poor solubility of CBZ in water, CBZ calibration standard without methanol was prepared by pipetting 10  $\mu$ L of appropriate CBZ stock standard prepared in methanol, allowing the solvent to evaporate completely to dryness and then reconstituting the residue using mouse plasma. The determination was performed in triplicate, and % extracted of CBZ was  $2.35 \pm 0.3$  and  $1.93 \pm 0.07$  for extraction of standard solution without and with 1% methanol, respectively. The results were compared using t test and no significant differences were found at 95% confidence interval ( $t_{\text{EXPTL}} = 2.34$ ,  $t_{\text{CRITICAL}} = 2.78$ ,  $p = 0.08$ ). Therefore, all subsequent whole blood and plasma calibration curves were prepared by keeping the proportion of methanol constant at 1% in all standard solutions.

Finally, the degree of overall plasma protein binding of CBZ in mouse plasma was also evaluated using equilibrium SPME and found to be  $97.1 \pm 0.1\%$  ( $n=3$  determinations). This is significantly higher than 76% binding typically reported for carbamazepine according to DrugBank data.<sup>189, 190</sup> This unexpected result was further investigated to verify if the presence of 1% methanol in spiked plasma samples affected the degree of binding. However, >90% binding was observed even when methanol was completely omitted from the preparation of spiked plasma samples. The binding of CBZ was then investigated in independent experiments using fluorescence spectroscopy and NMR by Dr. Barbara Bojko, and high degree of binding (>90%) was found using these methods for low CBZ concentrations such as the ones used in current SPME study, thus confirming the validity of SPME results.

#### **4.3.4 Evaluation of *in vivo* performance of prototype SPME assemblies**

Two main issues were encountered during early *in vivo* SPME experiments on mice and initial testing of *in vivo* SPME probes. First, it was necessary to completely eliminate any blood leaks during the entire sampling procedure as even minor leaks could result in premature animal death, and/or subsequent sample contamination during desorption step. In early studies, it was found that large number of *in vivo* SPME prototype probes (~20-50% depending on the study) leaked in the hub of the hypodermic needle due to inefficient sealing between the needle and SPME fibre using silicone glue used to prepare the probes. To address this issue, prototype *in vivo* SPME probes were modified by

the manufacturer as necessary until they were able to withstand expected blood pressure in mice. This was accomplished by reducing the gauge of needle from original 21-gauge to 22-gauge, changing the type of silicone glue used in the needle hub, and ensuring glue was properly filled within the hub and cured for sufficient amount of time during probe production. This resulted in the successful elimination of leaking problem and permitted *in vivo* SPME sampling on mice without adverse effects due to blood loss.

The second observed problem was that few probes during each *in vivo* experiment would exhibit outlying results (very low amount extracted as compared to adjacent time points). This problem was subsequently correlated to red appearance (by visual examination) of some of the probes which could not be eliminated using 30-second water rinse. The probes with good performance remained white in appearance after sampling and rinse steps, as long as rinse step was performed immediately after sampling without letting the probe dry out. The probes with poor performance, on the other hand, remained red after sampling and rinsing steps indicating hemolysis (1-2% of all the probes tested). Example results obtained during an example study on three mice are shown in Table 4.5. The fibres originally used for the time points shown in the table (mouse 3 time = 60 min, mouse 3 t = 120 min, mouse 2 time = 120 min and mouse 1 time = 30 min) remained red in appearance after rinsing step with purified water immediately post-extraction. The sampling was repeated using a new probe and these results are shown with label “repeat” in the table. The results show that three out of four red probes exhibited poor extraction efficiency. The use of such points would result in erroneous data points within PK curve with 5-10-fold underestimation of true CBZ amount. The red probe observed

**Table 4.5 Results obtained for repeated sampling: probes with red appearance versus new probes used for re-sampling.**

Mouse and sampling time point	CBZ d10 amount (ng)	CBZ Amount (ng)	$n_e$ (ng)	$C_{free}$ (ng/mL)	$C_{total}$ (ng/mL)
mouse 3 time 60	0.1916*	0.72	0.87	2.84	48.8
mouse 3 time 62repeat	0.6097	3.02	6.69	21.87	376
mouse 2 time 120	0.8593	0.28	1.24	4.04	69.5
mouse 2 time 122repeat	0.9065	0.24	1.30	4.25	73.0
mouse 3 time 120	0.3059*	0.27	0.37	1.22	20.9
mouse 3 time 122repeat	0.7561	0.87	2.72	8.90	153
mouse 1 time 30	0.3318*	2.25	3.21	10.51	181
mouse 1 time 32 repeat	0.7378	4.17	12.43	40.63	698

\*probes with poor performance can be identified by low amount of CBZ d10 calibrant on the probe



after sampling of mouse 2 at 120-min time point showed good extraction efficiency despite its red appearance. In this case, the results for the second sampling show excellent agreement. Based on the results of in Table 4.5, it is clear that it is valuable to repeat any samplings where coating remains red after rinsing. This means that few extra probes should be preloaded and preconditioned prior to *in vivo* study in case re-sampling needs to be performed. However, if re-sampling is not performed during the study for any reason, any poor quality data points can be found in raw data by checking for very low amount of CBZ d10 remaining in the coating (as marked with asterisk in Table 4.5).

This problem of occasional probe failure is currently under further investigation and is attributed to possible incomplete coverage of biocompatible binder on the surface of some probes. This hypothesis was confirmed by comparison of the surfaces of white *versus* red probes using scanning electron microscopy. The probes that were red showed cracked and jagged surface, in contrast to the relatively smooth surface observed for normal probes. The manufacturer is currently examining possible causes of poor probe surface properties and/or developing an appropriate quality control procedure to eliminate any such probes before shipping. Until this is accomplished, any probes that remained red after rinsing were discarded and the sampling was immediately repeated using a new probe (one incidence during entire *in vivo* experiment on n=7 mice described in section below).

#### **4.3.5 Results of *in vivo* study: pharmacokinetics of CBZ and CBZEP using *in vivo* SPME**

Single-dose full pharmacokinetic profiles for individual mice (n=7) were obtained using *in vivo* SPME after intravenous dosing of CBZ at 2 mg/kg. The results obtained for total concentration of CBZ and CBZEP are shown in Figure 4.4 and clearly demonstrate that *in vivo* SPME can be used effectively to study inter-animal variability as significant differences were observed in the amount of conversion of CBZ to CBZEP between individual mice. This is in agreement with previous studies in rats where inherent variability in clearance was estimated as 20-40%.<sup>187</sup> The total concentrations reported in Figure 4.4 were based upon calibration curve obtained in pooled mouse whole blood. Within-animal calibration is not feasible with mice due to limited blood volume – total extractable blood volume is insufficient to construct a full SPME calibration curve even if the mouse is sacrificed post-study. The exact amount of binding proteins varies from individual-to-individual, and any such variation can cause a small systematic error in the reported *in vivo* SPME results because the amount extracted by SPME is proportional to free fraction and free fraction is correlated to the amount of binding proteins present, especially for highly-bound drugs. However, this does not really represent a

major disadvantage of SPME, because it is the unbound drug concentration which is pharmacologically active. Considering that the amount of the drug extracted by SPME is directly proportional to unbound drug concentration, unbound drug concentration profiles obtained by *in vivo* SPME are much more accurate, regardless of the calibration strategy employed as they are independent of the amount of binding proteins present in particular individual. Unbound drug concentration also provides much more meaningful clinical information than total drug concentration. Table 4.6 and Table 4.7 show the results of free concentration determination for CBZ and CBZEP in current *in vivo* study. One assumption made in current study is that CBZ-d10 could be used as

**Table 4.6 Free concentration (ng/mL) of CBZ in circulating blood of n=7 mice obtained by *in vivo* SPME sampling.**

Time point (min)	M01	M02	M03	M04	M05	M06	M07	Mean (n=7)	SD (n=7)	% RSD (n=7)
0	ND	ND	ND	ND	ND	ND	ND	ND	ND	ND
5	151	166	200	110	91	111	115	135	39	29
15	140	202	177	78	112	62	77	121	54	44
30	170	72	109	71	39	57	55	82	45	54
60	61	32	49	47	16	38	18	37	17	44
90	10	11	27	36	2	16	42	21	15	72
120	8	6	23	11	1	5	2	8	7	93
180	2	3	ND	ND	ND	ND	ND	3	1	28

**Table 4.7 Free concentration (ng/mL) of CBZEP in circulating blood of n=7 mice obtained by *in vivo* SPME sampling.**

Time point (min)	M01	M02	M03	M04	M05	M06	M07	Mean (n=7)	SD (n=7)	% RSD (n=7)
0	ND	ND	ND	ND	ND	ND	ND	ND	ND	ND
5	0.48	0.33	0.56	0.25	0.86	1.7	0.79	0.71	0.49	69
15	0.71	0.63	0.86	0.4	2.08	1.7	1.24	1.09	0.61	56
30	1.02	0.33	0.79	0.48	1.17	2.85	1.4	1.15	0.84	73
60	0.48	0.25	0.4	0.33	0.71	2.24	0.56	0.71	0.69	97
90	0.25	0.21	0.33	0.33	0.25	1.17	1.55	0.58	0.54	93
120	0.25	0.19	0.25	0.25	0.25	0.48	0.25	0.27	0.09	34
180	ND	ND	ND	ND	ND	ND	ND	ND	ND	ND

calibrant for kinetic calibration for CBZEP or in other words that the time constants  $a$  for the two compounds were similar. This is reasonable assumption considering the two structures are very similar, and structural analogues were previously found as useful calibrants in absence of appropriate deuterated compound.<sup>89</sup>

#### **4.3.6 Results of *in vivo* study: comparison of *in vivo* SPME to automated serial and discrete terminal sampling of mice**

The results obtained for automated serial sampling of  $n=3$  mice in combination with traditional plasma analysis are shown in Figure 4.5 for individual mice. SPME results follow the same general profile as obtained for traditional analysis, showing rapid decrease in carbamazepine concentrations over the course of study as expected after i.v. dosing. Average concentration-time profiles obtained for CBZ and CBZEP using all three sampling methods are overlaid in Figure 4.6. No correction factors to account for red blood cell partitioning were applied to either analyte according to the results reported in Section 4.2.3.4. The total drug concentrations for CBZ and CBZEP obtained by three methods were also used to calculate PK parameters such as peak blood concentration ( $C_0$ ), terminal half-life, clearance (CL) and area under the curve (AUC). This calculation of PK parameters was performed by Dr. de Lannoy and Table 4.8 and Table 4.9 are included with her permission for method comparison purposes. It is clearly shown that the results obtained by *in vivo* SPME agree with the results obtained by both serial and terminal sampling approaches for both CBZ and CBZEP. The comparison of the data using t test also showed no significant differences in determined PK parameters. This validates the proposed *in vivo* SPME sampling approach in mice.

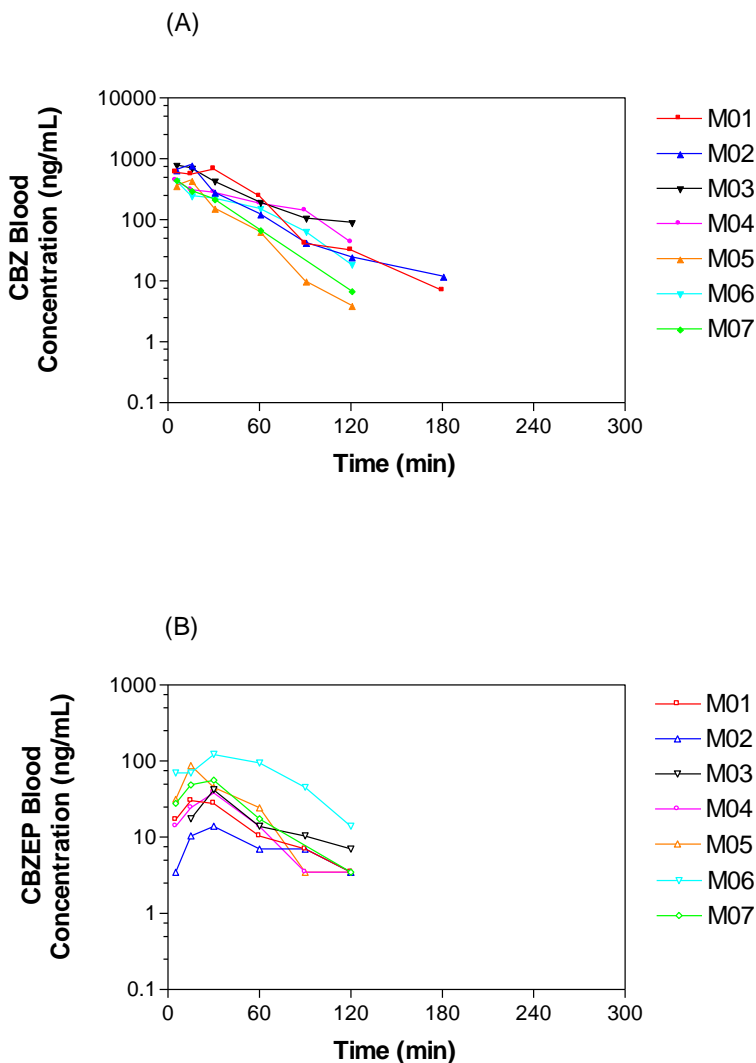


**Figure 4.4 Whole blood concentration *versus* time profiles obtained by *in vivo* SPME sampling for CBZ (A) and its formed metabolite, CBZEP (B), in seven individual mice (M01 to M07) following the administration of a single *i.v.* dose of 2 mg/kg CBZ. Samples were collected up to 240 min, but CBZ and CBZEP were not detected in some of the late time point samples as shown in the figure. Y-scale is shown on logarithmic scale.**

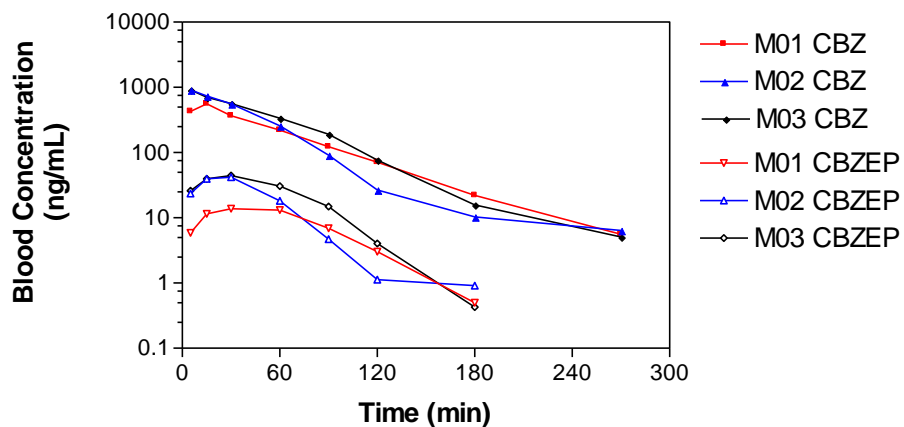


**Figure 4.5** Whole blood concentration *versus* time profiles obtained by automated serial sampling for CBZ and its formed metabolite, CBZEP, in three individual mice (M01 to M03) following administration of a single *i.v.* dose of 2 mg/kg of CBZ. This data was collected by NoAB BioDiscoveries and is included for comparison purposes only with permission of authors.

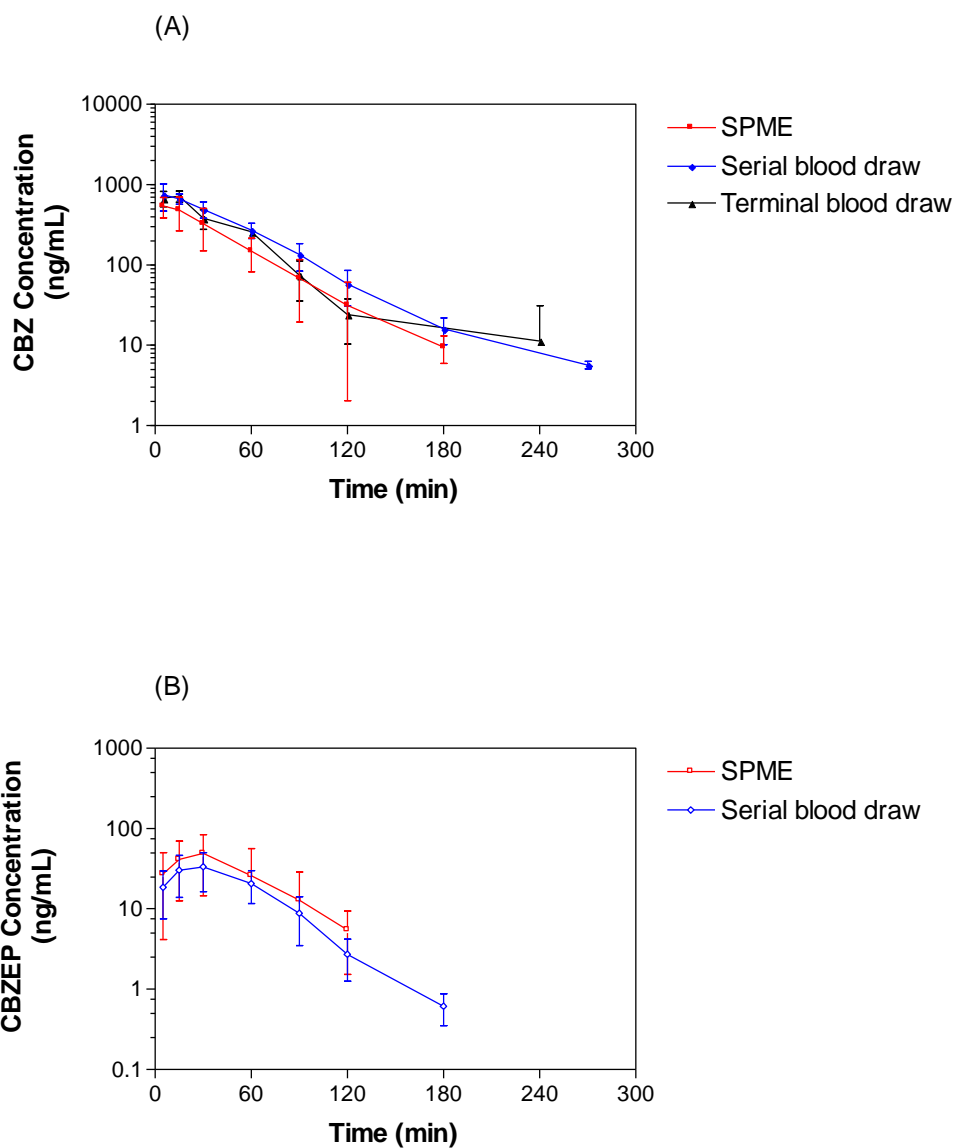


**Figure 4.6 Mean ( $\pm$ SD) concentration *versus* time profiles of CBZ (A) and CBZEP metabolite (B), following 2 mg/kg *i.v.* administration of CBZ to mice. Samples were taken by serial SPME sampling (n=7 mice), by serial automated blood draws (n=3 mice) or by terminal blood draws (3 mice/time point). SPME and serial blood sampling measured whole blood concentrations whereas terminal sampling measured plasma concentrations. SPME analysis was performed at the University of Waterloo, while serial and terminal analysis were performed by NoAB BioDiscoveries and are included only for comparison purposes with permission of authors.**

**Table 4.8 Mean ( $\pm$  SD) estimated PK parameters for CBZ following 2 mg/kg *i.v.* administration of CBZ to mice. Blood was sampled by SPME sampling (n=7 mice) and by serial automated blood draws (n=3 mice) and plasma was sampled by terminal blood draws (n=3 mice/time point). SPME analysis was performed at the University of Waterloo, while serial and terminal blood draw analyses were performed by NoAB BioDiscoveries and are included only for comparison purposes with permission of authors.**

Parameter	Units	SPME sampling <sup>a</sup>	Serial Blood draws <sup>a</sup>	Terminal blood draws <sup>b</sup>
C <sub>0</sub>	ng/mL	600 $\pm$ 100	800 $\pm$ 300	680
Terminal t <sub>1/2</sub>	min	32 $\pm$ 12	50 $\pm$ 23	45
AUC <sub>0-inf</sub>	min*ng/mL	26600 $\pm$ 10000	42700 $\pm$ 8000	36500
CL	mL/min/kg	87 $\pm$ 35	48 $\pm$ 9	55
MRT <sub>0-inf</sub>	min	40 $\pm$ 11	50 $\pm$ 7	47
V <sub>ss</sub>	mL/kg	3200 $\pm$ 800	2400 $\pm$ 800	2600

<sup>a</sup> Parameters are estimated from individual whole blood concentration *versus* time profiles for each animal. <sup>b</sup> Parameters are estimated from the mean plasma concentration *versus* time profiles.

**Table 4.9 Mean ( $\pm$  SD) estimated PK parameters in blood for the formed metabolite, CBZEP, following 2 mg/kg *i.v.* bolus administration of CBZ to mice. Blood was sampled by SPME sampling (n=7 mice) and by serial automated blood draws (n=3 mice). SPME analysis was performed at the University of Waterloo, while serial blood draw analysis was performed by NoAB BioDiscoveries and is included only for comparison purposes with permission of authors.**

Parameter	Units	SPME sampling <sup>a</sup>	Serial blood Draws <sup>a</sup>
t <sub>max</sub>	min	34 $\pm$ 26	30 $\pm$ 0
C <sub>max</sub>	ng/mL	57 $\pm$ 37	33 $\pm$ 17
Apparent t <sub>1/2</sub>	min	36 $\pm$ 17	23 $\pm$ 5
AUC <sub>0-inf</sub>	min*ng/mL	3400 $\pm$ 2600	2200 $\pm$ 1000
MRT <sub>0-inf</sub>	min	62 $\pm$ 20	52 $\pm$ 9

<sup>a</sup> Parameters are estimated from individual whole blood concentration *versus* time profiles for each animal.

The precision of SPME results obtained in current study is about 60% for CBZ (mean RSD for all time points of 60%, RSD range of 39-109%, n= 7 mice). This is higher than that for serial sampling

(mean RSD 29%, RSD range 11-47%, n=3 mice) and terminal sampling (mean RSD 50%, RSD range 4-173%, n=3 mice/sampling point) approaches. The data for traditional approaches obtained in current study is in good agreement with literature report of precision of <35% for serial sampling in mice and <50% for discrete terminal sampling in mice.<sup>171</sup>

The overall method precision reported for SPME includes inter-probe variability, the experimental error inherent in the determination of the amount of on-probe calibrant as well as the analytes of interest, the variability in dosing and probably, the most significant factor, which is inter-animal variability in both the extent of metabolism as well as plasma protein binding. The magnitude of the contribution of the first two factors was estimated during method validation by repeated sampling of known CBZ concentrations *via* interface and was found to be <20% RSD for all concentrations tested (Section 4.3.3). Therefore, it appears that inter-animal variability is significant factor contributing to overall method precision. This variability in plasma-protein binding, which can result in significant differences in unbound fraction, is not included in plasma analysis data, because the traditional analysis is based on the total concentration determination (unbound + bound), which would not be affected by the differences in binding. In humans, the variability of unbound fractions was reported as 0.15 to 0.3 for CBZ and from 0.33 to 0.67 for CBZEP, and no significant relationship was established between unbound and total CBZ concentrations indicating that degree of binding can vary significantly *in vivo*.<sup>191</sup> Furthermore, a recent report based on serial miniscule bleeding in mice and traditional sample preparation found inter-animal variation as high as 200% at any given time point indicating that inter-animal variability can be very significant.<sup>192</sup> The extent of inter-animal variability can be verified in follow-up experiments using inbred strains of mice and larger cohorts of animals, as both the study by Watanabe *et al.* and current study used small number of animals. Both *in vivo* SPME and automated sampling experiments were performed over three days, so the results also reflect inter-day variability. For example, slight variations in preparation of dosing solution are reflected in the data. If only the data for n=3 mice collected on the same day and dosed with the same dosing solution is considered, SPME method precision shows improvement (mean RSD of 49%, RSD range of 12-104%). This method precision is in agreement with the findings of an earlier independent study on three mice performed on the same day by *in vivo* SPME (mean RSD for all time points of 42%, RSD range of 2-77%, n=3 mice). Regardless of the sampling method employed, all the method precision data shows a general trend towards higher RSD values for later time points *versus* early time points. This can be attributed to the differences in the rate of metabolism and elimination of CBZ. Based on the data of this study, it appears that the analytical variability of SPME is less than

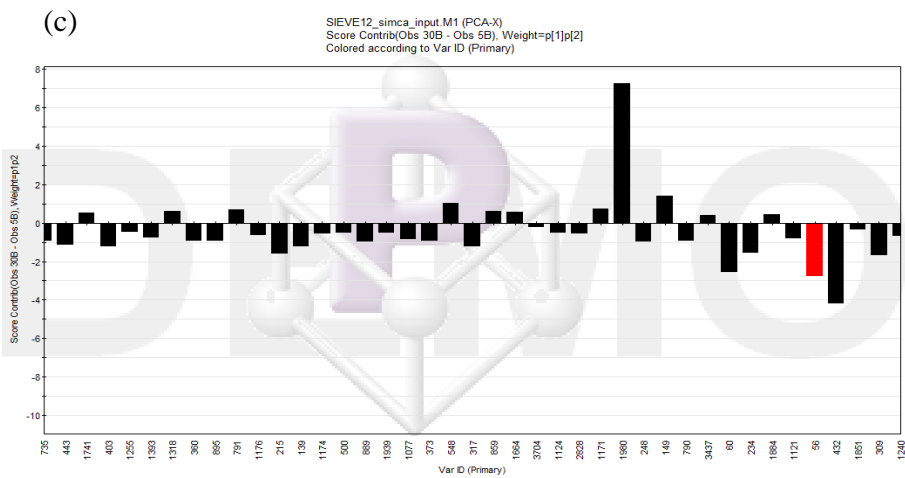
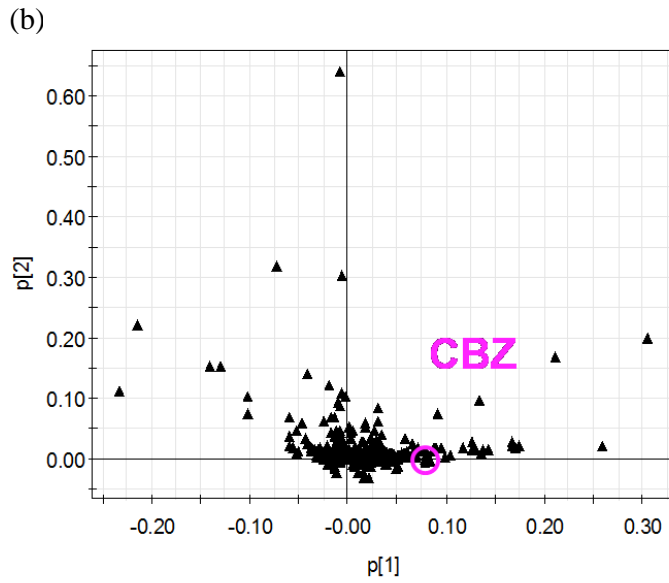
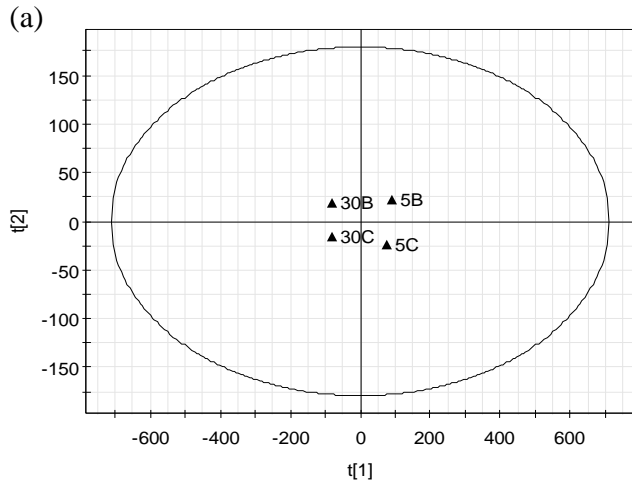


inter-animal variability, thus permitting the use of SPME to study factors such as differences in binding and metabolism.

#### **4.3.7 Preliminary investigation of suitability of *in vivo* SPME for global metabolomics**

As a proof of concept study, the potential of *in vivo* SPME sampling for global metabolomic studies was investigated using the same experimental procedure described in Section 4.2.2, but the mice were dosed with 4 mg/kg of carbamazepine. The profiles obtained at 5 and 30-min post-dose were compared after analysis using a HILIC method in positive ESI mode as described elsewhere<sup>193</sup> (LC-MS analysis performed by S. Dutta at Thermo Fisher facility, data processing performed by D. Vuckovic at the University of Waterloo according to procedures described in detail in Chapter 7). The results obtained after principal component analysis with Pareto scaling are depicted in Figure 4.7 and show clear clustering of the two sets of samples. First principal component was found to describe 93.7% of variance, and second principal component described an additional 5.9% of variance. The data was further examined to select the peaks most responsible for the observed clustering, and the pairwise comparisons of the intensity observed for these metabolites are also shown in Figure 4.7. Among the metabolites shown to contribute to clustering (Figure 4.7c), peak 56 was identified as carbamazepine with an exact mass of 237.1030 and confirmed against the authentic standard. CBZ was expected to contribute to the observed differences in the 5 min *versus* 30 min post-dose samples according to PK study results presented earlier.

These results gave preliminary indication of the utility of *in vivo* SPME in global metabolomic studies. However, they were not further processed for several reasons: very small sample size was used so any conclusions drawn from the data would be of limited utility. Furthermore, biocompatible C<sub>18</sub> coating was used for the extraction while HILIC LC-MS was employed for global analysis. This resulted in <500 observed metabolites peaks, and most of the peaks observed were not well-retained using HILIC method indicating their hydrophobic nature. Therefore, further research efforts focused on the development of SPME coatings suitable for metabolomics (Chapter 5) and LC-MS method development for global metabolomic studies (Chapter 6).



(d)

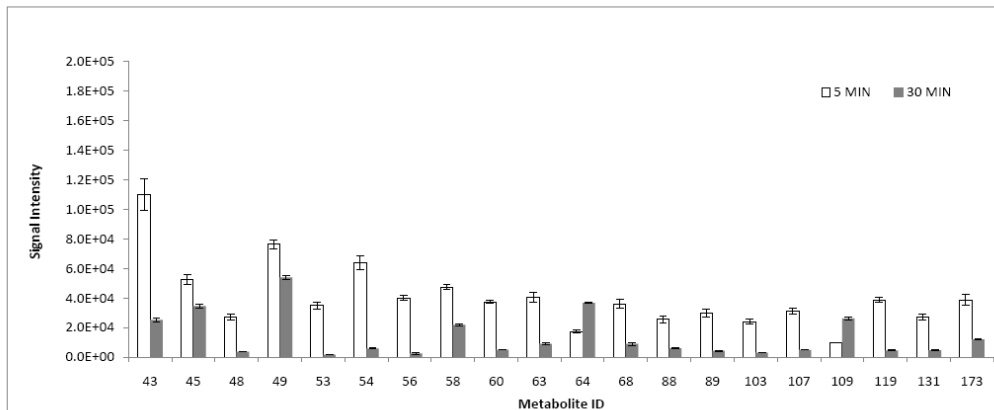


**Figure 4.7 Representative results from a proof of concept *in vivo* SPME metabolomics study. (a) Scores scatter plot indicating good clustering of two sample types 5 min post-dose samples (labelled as 5B and C) and 30 min post-dose samples (labelled as 30 B and C). (b) Loadings scatter plot of PC1 versus PC2 illustrating the peaks contributing most to the observed clustering. (c) Example of a score contribution plot showing 30 representative metabolites. In this metabolite subset, metabolites with IDs of 56, 60, 432 and 1980 contribute the most to the observed clustering. (d) pair-wise comparison of selected differentiating peaks based on PCA analysis including observed signal intensity and RSD.**

#### 4.4 Conclusions

*In vivo* SPME sampling in mice provides advantages over established sampling methods. The use of SPME permits simultaneous determination of both total and unbound analyte concentrations as described in this chapter, whereas traditional methods require two separate sample analyses to obtain both parameters, increasing both time and cost of analysis and requiring additional volume of biofluids. This determination of unbound fraction of analytes is an important factor in bioavailability and intrinsic clearance calculations.<sup>194</sup> In comparison to terminal sampling approaches, *in vivo* SPME significantly reduces animal use by 5-10-fold or more depending on the number of animals used per sampling point and the total number of sampling points. For example, in study described herein 33 mice were used (11 time points x 3 mice/time point) versus 7 mice sampled using *in vivo* SPME method. In comparison to serial sampling approaches, *in vivo* SPME enables the sampling of unlimited number of points as no blood is withdrawn and the total circulating blood volume remains constant throughout the study leading to more accurate PK data. Furthermore, automated serial

sampling requires expensive robotic equipment with the cost of \$20,000 per machine, while *in vivo* SPME can be carried out with much simpler apparatus (*in vivo* SPME probes and interface), for overall reduction in the cost of analysis. *In vivo* SPME can also be used for simultaneous sampling of different compartments, for example blood and brain, and such studies are currently underway within our laboratory, while Culex® sampling unit is limited to sampling of blood. The ability for multi-compartment studies and reduced animal use can be particularly important for precious expensive animals such as genetically modified mice for human cancer research.<sup>22</sup> Furthermore, serial sampling approaches (whether by SPME or Culex®) provide opportunity for longitudinal studies, for example in metabolomic studies of aging, recovery from an illness or systems biology. For example, a recent global metabolomics study measuring internal body time using diurnal variability of selected metabolites, relied on terminal sampling procedures and resulted in the sacrifice of numerous mice and introduction of inter-animal variation into collected data.<sup>17</sup> The availability of *in vivo* SPME for mice for the first time can provide a useful tool for similar studies in future and extend such studies from urine analysis<sup>125</sup> to plasma analysis.

#### **4.5 Addendum**

The text of this chapter was rewritten in comparison to submitted research article.

## **Chapter 5**

# **Systematic evaluation of SPME extraction phases for metabolomics**

### **5.1 Preamble and introduction**

#### **5.1.1 Preamble**

This work has not yet been published. HiSep and polyethylene glycol (PEG) coatings were prepared by Francois Breton and submitted for inclusion in the evaluation. Biocompatible prototype coatings described in Chapter 3 (cyano, C<sub>18</sub> and RPA) were obtained as research samples from Supelco to be included in the evaluation. I am the sole author of all other experimental work reported herein.

#### **5.1.2 Introduction**

The focus of this chapter is to describe the development of suitable SPME coatings for the simultaneous extraction of polar and non-polar metabolites suitable for use in metabolomic studies. This coating development was necessary because the existing commercial coatings do not perform well for the direct extraction of polar compounds as previously discussed in Chapter 3. The choice of sorbent is very important in SPME methods because it determines the magnitude of distribution constants for a given analyte and/or interferences and therefore impacts both extraction efficiency and selectivity.

For global metabolomics, it is desirable to find the least selective coating in order to enable simultaneous extraction of as many metabolites as possible, both hydrophilic and hydrophobic. The experimental approach first focused on the development of suitable LC-MS methods for metabolomics using a standard mixture of known metabolites. This metabolite test mixture consisted of a diverse range of compounds including amino acids, amines, organic acids, hormones, sugars, nucleosides and small peptides. The metabolites were selected based on (i) their amenability to electrospray ionization, (ii) commercial availability of authentic standards, (iii) wide molecular weight range (80-777 Da) and (iv) wide polarity range (log P range of -5 to 7.4). This standard mixture and LC-MS methods were subsequently used to perform systematic evaluation of 40 types of commercially-available sorbents for their usefulness in metabolomic studies. It was desirable to test as wide range of sorbents as possible, so silica-based, carbon-based and polymer-based sorbents were included in this systematic evaluation. Polymeric sorbents typically have several advantages over

silica-based sorbents including higher surface area, improved pH working range, and minimal requirements in terms of preconditioning prior to use.<sup>195, 196</sup> These polymeric sorbents were also developed to improve extraction efficiency towards polar compounds, which was achieved through introduction of polar functional groups within the polymer and/or increasing surface area in order to increase the number of interactions between analyte and sorbent. The primary mechanism of interaction using chemically bonded silica-based sorbents are van der Waals forces, although some sorbents also incorporate other mechanisms such as ion-exchange due to the addition of appropriate functional groups. The primary mechanism of carbon-based sorbents is adsorption, but one of the problems that can be encountered using this type of sorbent is excessive or even irreversible retention. In SPME methods, this translates into poor desorption efficiency. Polymeric sorbents interact with analytes primarily through pi-pi interactions, although additional interactions are possible depending on the nature of functional groups introduced during polymer modification (for example, hydrogen bonding or ion-exchange). A variety of mixed-mode sorbents, both silica-based and polymer-based was included in the study because of the potential to extract a wide range of analytes, including both ionizable and neutral species. For mixed-mode anion-exchange sorbents, positively charged groups on the sorbent interact with negatively charged functional groups on the analytes, while hydrophobic interactions between hydrophobic portions of the molecule and hydrophobic portions of the sorbent can also occur. For mixed-mode cation-exchange sorbents, negatively charged groups of the sorbent interact with positively charged groups of the analytes. In the final stage of the study, the influence of pH on extraction capability was also evaluated to verify if it can further improve metabolite coverage. pH range selected for use in this study was 3.0, 5.0, 7.4 and 9.5. Higher and lower pH values were not examined as silica-based sorbents are not stable beyond this range.<sup>197</sup>

#### 5.1.2.1 Overview of LC-MS methods for metabolomics

The majority of global metabolomics methods described in literature rely on a reverse-phase LC separation using C<sub>18</sub> stationary phase.<sup>12, 17, 26, 33, 38, 51, 54, 67, 124, 198-210</sup> Most of these reverse-phase methods with C<sub>18</sub> columns rely on simple linear gradient of acetonitrile/water or methanol/water with formic or acetic acid used as the additive to help the ionization process. However, this is somewhat surprising as many metabolites are polar species which are not sufficiently retained on C<sub>18</sub> columns. Thus, the observed trend may be indicative that insufficient attention is paid in some studies to the analytical method employed in the analysis. Despite the prevalence of C<sub>18</sub> methods in literature, inadequate evidence exists that they are the best platform for global metabolomics. For example,

Bruce *et al.* compared the performance of C<sub>18</sub>, C<sub>8</sub> and phenyl column for UHPLC-MS method for global metabolomics analysis of human plasma.<sup>211</sup> They found that C<sub>18</sub> and C<sub>8</sub> columns performed better for separation of lipophilic components of plasma than phenyl column. However, C<sub>18</sub> column exhibited carryover effects of lipophilic species and baseline drifts which could not be eliminated even with the use of extended gradient times, so C<sub>8</sub> stationary phase was recommended as the best choice for metabolomic studies. In another study, Evans *et al.* proposed the use of two complementary mobile phase conditions (pH 3 for acidic analytes using positive ESI and pH 8 for basic analytes using negative ESI) in order to improve the coverage of acidic and basic analytes.<sup>205</sup>

The use of ion-pairing strategies in combination with LC-MS is usually avoided because these additives are often not sufficiently volatile and can cause significant ionization suppression and adduct formation. As such relatively few ion-pairing methods have been reported for global metabolomic studies. For instance, Coulier *et al.* proposed the use of hexylamine as ion-pair agent for the analysis of nucleotides, coenzyme A esters, sugar nucleotides and sugar biphosphates.<sup>70</sup> The optimized elution conditions using C<sub>18</sub> column included both a pH gradient (pH 6.3 to pH 8.5) and ion pair reagent gradient (5 to 0 mM). The method was documented to have good inter- and intra-day precision. However, the use of ion pair gradient is unusual as the variation in the amount of ion pair reagent can cause differences in retention and poor reproducibility of retention times. Closer examination of the paper does in fact reveal that authors observed retention time variation of ~0.5 min over long run times (>1 day) and <0.1 min over 12-hr run time. Most global metabolomic studies require analysis times in excess of 24 hr, so this retention time drift makes the proposed method very problematic in terms of chromatographic alignment necessary during data processing stage. In a similar approach, Büscher *et al.* used tributylamine for the global metabolomics analysis of yeast cell extracts.<sup>45</sup> However, considering the potential for ionization suppression and drifting retention times, ion pairing strategy was not explored in current research. This strategy seems to be more suitable for the analysis of well-defined targeted set of analytes with a particular objective. For example, Gu *et al.* proposed an ion pair strategy with perfluoroheptanoic acid for the analysis of twenty amino acids for large-scale screening of metabolic phenotypes and one of the advantages of this method was chromatographic resolution between isobaric species such as leucine and isoleucine.<sup>212</sup>

A more promising method to increase metabolite coverage appears to be the use of hydrophilic interaction chromatography (HILIC). The main advantages reported in literature of HILIC *versus* reverse-phase methods include better retention of polar compounds such as sugars and phosphates

and improved analytical sensitivity when using MS detection due to the use of mobile phases with high organic content. The main disadvantages include the need for long re-equilibration times when gradient elution is employed<sup>213</sup> which decreases overall sample throughput and poor retention of acidic compounds. The mechanism of HILIC separation mainly relies on the partitioning of analytes into hydrated layer existing on the surface of the stationary phase. Gradient elution in HILIC method begins with a mobile phase with low polarity and high organic content (such as acetonitrile), and analyte elution is achieved by increasing aqueous content of the mobile phase. Volatile buffer salts are used as additives to reduce any electrostatic interactions between analytes and stationary phase.<sup>64</sup> Several recent studies document the usefulness of HILIC in order to improve metabolite coverage in global metabolomic studies, similar to what is proposed in this chapter.<sup>31, 213-215</sup> For example, Mohamed *et al.* used the combination of (i) reversed-phase method with C<sub>16</sub> column embedded with sulfonamide group and (ii) HILIC methods to enhance the metabolite coverage.<sup>215</sup> Kamleh *et al.* used Zic-HILIC column with formic acid/acetonitrile mobile phase and 32 min analysis time.<sup>216</sup> Jankevics *et al.* proposed the use of HILIC method with ammonium acetate 10 mM buffer/acetonitrile mobile phases<sup>217</sup>, while Cubbon *et al.* proposed the use of 5 mM ammonium acetate buffer/acetonitrile phases, with typical analysis times of 30 min.<sup>64</sup> Chen *et al.* used the combination of C<sub>18</sub> reversed-phase method and HILIC method using unmodified silica.<sup>214</sup> Their HILIC method using ultra-high pressure liquid chromatography (UHPLC) relied on a very slow gradient of 95 to 80% acetonitrile with run time of 35 min, whereas typical UHPLC analysis times are 10-15 min and rely on much steeper gradients. The use of these two complementary LC-MS methods increased the information content of the acquired data. Using reversed-phase method, oxidation of fatty acids was detected as the important contribution for the differentiation between healthy and liver cancer patients. Using HILIC methods, improved separation of the groups was achieved and compounds related to arginine and proline metabolism, alanine and aspartate metabolism, lysine degradation, and nicotinamide metabolism were found to be significantly changed in the two populations. Two acylcarnitines were found as differentiating metabolites using both methods.

In addition to reversed-phase and HILIC methods, the use of silica hydride stationary phases using aqueous normal phase chromatography has also been proposed for the analysis of polar metabolites.<sup>53,</sup>

218



## 5.2 Experimental

### 5.2.1 Materials and coatings preparation

For this evaluation, all SPME coatings suitable for direct extraction and commercially available from Supelco Inc. (Bellefonte, PA, USA) were included. These were polyacrylate coating (PA, 85  $\mu\text{m}$ ), polydimethylsiloxane (PDMS, 100  $\mu\text{m}$ ) coating, polydimethylsiloxane/divinylbenzene coating (PDMS/DVB, 60  $\mu\text{m}$ ) and Carbowax/template resin coating (CW/TPR, 50  $\mu\text{m}$ ). New prototype Supelco biocompatible coatings whose development and evaluation was discussed in Chapter 3 were also obtained as research samples and included in this evaluation: C<sub>18</sub>, RPA and cyano coatings (1.5 cm coating length, 45  $\mu\text{m}$  coating thickness, prepared using porous coated silica particles of 5  $\mu\text{m}$  size). The remaining coatings were prepared by immobilization of commercially available SPE sorbents using Loctite adhesive on stainless steel wire of 1.55 mm diameter (0.061 inch, Small Parts Inc., Florida, USA) using optimized procedure described in Chapter 2 (coating length 1.5 cm). All sorbents utilized in this work were obtained as research samples in the format of SPE cartridges from their respective manufacturers as outlined in Table 5.1. Additional carbon tape coating, previously found to perform well for extraction of polar Ochratoxin A, was also prepared by the immobilization of one adhesive side of the tape on the stainless steel wire (coating length 12 mm).<sup>152</sup> Self-adhesive carbon tape was obtained from TAAB Laboratories Equipment (Calleva Park, Reading, UK) with dimensions of 12 mm wide x 20 m long.

All coatings were prepared in triplicate. Prior to each extraction, coatings were evaluated visually for uniformity of particle coverage. If any particle loss was noted, coatings were discarded and new coatings were prepared. The problem of particle loss occurred primarily for coatings with very large sorbent particles (>80  $\mu\text{m}$ ), and these coatings could be used only for 2-3 times prior to requiring replacement. The coating reusability and robustness were not the main concerns in current study, because the coating procedure would be changed to use biocompatible binder, smaller particle size and smaller solid support diameter after the most promising sorbents were isolated in current study.

### 5.2.2 Materials and metabolite standard mixture preparation

All metabolites and buffer reagents were obtained from Sigma-Aldrich (Oakville, Canada). All metabolites and their properties are listed in Table 5.2 and their structures are shown in Figure 5.1. Stock standard solutions were prepared in water/methanol/ethanol and diluted as appropriate. Protoporphyrin and  $\beta$ -carotene had poor solubility, so the stock solutions of these analytes were

prepared separately in acetonitrile and chloroform, respectively and spiked (100  $\mu\text{L}$ ) into combined stock standard solution. Stock standard solutions were kept frozen ( $-20^{\circ}\text{C}$ ), protected from light and were prepared fresh weekly.

Buffer solutions at pH 3.0, 5.0, 7.4 and 9.5 were prepared using formate, acetate, phosphate and carbonate salts and pH was verified to be within  $\pm 0.05$  pH units experimentally. Sodium chloride (8 g) was added to all buffers to keep ionic strength constant and close to physiological levels. For extraction, metabolite standard solutions were prepared at 1  $\mu\text{g}/\text{mL}$  concentration level by dilution of stock standard in such a way to keep the organic content of all extraction standards at 1% organic solvent (v/v).

For instrument calibration, working standard solutions with known concentration of metabolites were prepared by dilution of stock standard with desorption solvent. This calibration set was analyzed before and after each sample set and mid-level standard was also periodically analyzed as QC sample every 12 injections to ensure method and instrument stability. Sample batches could be run for 3-4 days without interruption with QC standard showing RSD  $<20\%$  over this time period for most analytes.

### **5.2.3 SPME procedure**

All coatings were preconditioned in solution of methanol/water (1/1, v/v) for a minimum of 1 hr prior to extraction. All extractions were performed for 16 hr at room temperature with no agitation using 1.5 mL sample volume contained in amber 2-mL HPLC glass vials. The desorption procedures differed depending on whether metabolites were analyzed using reverse phase or HILIC LC-MS method as described below.

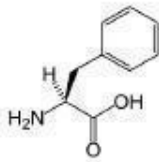
Table 5.1 Summary of SPE sorbents and their properties.

Sorbent	Manufacturer	Support	Type	Functional group	Particle size (µm)	Surface area (m <sup>2</sup> /g)	Pore size (Å)
Clean Screen DAU	UCT	silica	reverse phase+ SCX	proprietary and benzenesulfonic acid	40-63	NA	NA
Clean Screen GHB	UCT	silica	proprietary mixed-mode		NA	NA	NA
SSBCX	UCT	silica	SCX	benzenesulfonic acid	40-63	NA	NA
C18+B	UCT	silica	reverse phase+ SCX	C <sub>18</sub> and benzenesulfonic acid	40-63	NA	NA
C8+B	UCT	silica	reverse phase+ SCX	C <sub>8</sub> and benzenesulfonic acid	40-63	NA	NA
RPA	Supelco	silica	reverse phase	C <sub>16</sub> with embedded amide	3	450	100
HiSEP	Supelco	silica	reverse phase	surface modified with hydrophilic polymer	5	NA	120
PEG	Supelco	silica	reverse phase	polyethylene glycol	5	NA	120
Discovery MCAX	Supelco	silica	reverse phase+ SCX	C <sub>8</sub> and benzenesulfonic acid	50	480	70
DPA 6S	Supelco	polymer	adsorption of compounds containing -OH and -COOH groups	polyamide resin	50-120	NA	NA
Oasis MCX	Waters	polymer	reverse phase + SCX	N-vinylpyrrolidone divinyl benzene copolymer + sulfonic acid	30	810	80
Oasis WAX	Waters	polymer	reverse phase + WAX	N-vinylpyrrolidone divinyl benzene copolymer + piperazine	30	810	80
Oasis WCX	Waters	polymer	reverse phase + WCX	N-vinylpyrrolidone divinyl benzene copolymer + carboxylic acid	30	810	80
Oasis MAX	Waters	polymer	reverse phase + SAX	N-vinylpyrrolidone divinyl benzene copolymer + quaternary amine	30	810	80
HRP	Macherey Nagel	polymer	reverse phase	highly porous styrene divinylbenzene polymer	50-100	1200	NA
HRX	Macherey Nagel	polymer	reverse phase	hydrophobic styrene divinylbenzene polymer	85	1000	55-60
Carboxen-1016	Supelco	carbon	adsorption	graphitized carbon, 60/80 mesh	177-250	NA	NA

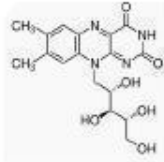
Sorbent	Manufacturer	Support	Type	Functional group	Particle size (µm)	Surface area (m <sup>2</sup> /g)	Pore size (Å)
<b>Diamino</b>	Macherey Nagel	silica	special	primary and secondary amine	45	500	60
<b>Easy</b>	Macherey Nagel	polymer	reverse phase + WAX	polar-modified styrene divinylbenzene polymer + unknown WAX group	80	650-700	50
<b>AccuCAT</b>	Varian	silica	SAX + SCX	sulfonic acid and quaternary amine	40	NA	60
<b>Spe-ed Advanta</b>	Applied Separations	polymer	reverse phase + WCX	polar-modified styrene divinylbenzene polymer (carboxylic acid modification)	NA	NA	NA
<b>Certify</b>	Varian	silica	reverse phase + SCX	C <sub>8</sub> and benzenesulfonic acid	40	NA	60
<b>Certify II</b>	Varian	silica	reverse phase + SAX	C <sub>8</sub> and quaternary amine	40	NA	60
<b>CH</b>	Applied Separations	silica	reverse phase	cyclohexyl	40	NA	60
<b>Focus</b>	Varian	polymer	normal + reverse phase	polar-modified styrene divinylbenzene polymer	NA	NA	NA
<b>Screen A</b>	Phenomenex	silica	reverse phase + SAX	C <sub>8</sub>	55	500	70
<b>Screen C</b>	Phenomenex	silica	reverse phase + SCX	C <sub>8</sub> and benzenesulfonic acid	55	500	70
<b>Strata X</b>	Phenomenex	polymer	reverse phase	surface modified styrene divinylbenzene polymer with pyrrolidone group	33	800	85
<b>Strata XAW</b>	Phenomenex	polymer	reverse phase + WAX	surface modified styrene divinylbenzene polymer + diamine group	33	800	85
<b>Strata XCW</b>	Phenomenex	polymer	reverse phase + WCX	surface modified styrene divinylbenzene polymer + carboxylic acid	33	800	85
<b>PBA</b>	Varian	silica	covalent	phenylboronic acid	40	NA	60
<b>PH</b>	Applied Separations	silica	reverse phase	phenyl	40	NA	60
<b>Plexa</b>	Varian	polymer	reverse phase	proprietary highly polar hydroxylated polymer	NA	NA	NA
<b>Plexa PCX</b>	Varian	polymer	reverse phase + SCX		NA	NA	NA

**Table 5.2 Physicochemical properties of metabolites included in standard metabolite mixture.**

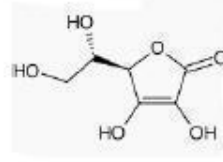
Analyte	Formula	Molecular Weight (MW)	pKa <sup>159</sup>	Log P <sup>159</sup>
3-hydroxybutyric acid (HBA)	C <sub>4</sub> H <sub>8</sub> O <sub>3</sub>	104.1	4.41	-0.47
Adenine	C <sub>5</sub> H <sub>5</sub> N <sub>5</sub>	135.1	4.15	-0.09
Adenosine	C <sub>10</sub> H <sub>13</sub> N <sub>5</sub> O <sub>4</sub>	267.2	NA	-1.05
Adenosine diphosphate (ADP)	C <sub>10</sub> H <sub>15</sub> N <sub>5</sub> O <sub>10</sub> P <sub>2</sub>	427.2	NA	-2.64
Adenosine monophosphate (AMP)	C <sub>10</sub> H <sub>14</sub> N <sub>5</sub> O <sub>7</sub> P	347.2	NA	-1.68
Ascorbic acid	C <sub>6</sub> H <sub>8</sub> O <sub>6</sub>	176.1	4.7	-1.85
Adenosine triphosphate (ATP)	C <sub>10</sub> H <sub>16</sub> N <sub>5</sub> O <sub>13</sub> P <sub>3</sub>	507.2	NA	-3.61
β-carotene	C <sub>40</sub> H <sub>56</sub>	536.9	NA	17.62
β-Estradiol	C <sub>18</sub> H <sub>24</sub> O <sub>2</sub>	272.4	NA	4.01
β-NAD	C <sub>21</sub> H <sub>27</sub> N <sub>7</sub> O <sub>14</sub> P <sub>2</sub>	663.4	NA	-3.68
Cholic acid	C <sub>24</sub> H <sub>40</sub> O <sub>5</sub>	408.6	4.98	2.02
Choline	C <sub>5</sub> H <sub>14</sub> NO <sup>+</sup>	104.1	NA	-5.16
Citric acid	C <sub>6</sub> H <sub>8</sub> O <sub>7</sub>	192.1	2.79	-1.64
Folic acid	C <sub>19</sub> H <sub>19</sub> N <sub>7</sub> O <sub>6</sub>	441.4	NA	-2.81
Fructose	C <sub>6</sub> H <sub>12</sub> O <sub>6</sub>	180.2	12.1	-1.55
Fructose-6-phosphate	C <sub>6</sub> H <sub>13</sub> O <sub>9</sub> P	262.2	NA	-2.14
Fumaric acid	C <sub>4</sub> H <sub>4</sub> O <sub>4</sub>	116.1	3.03	0.46
Glucose	C <sub>6</sub> H <sub>12</sub> O <sub>6</sub>	180.2	12.9	-3.24
Glucose 6-phosphate	C <sub>6</sub> H <sub>13</sub> O <sub>9</sub> P	260.1	1.11	-3.79
Glutamic acid	C <sub>5</sub> H <sub>9</sub> NO <sub>4</sub>	147.1	2.23	-3.69
Glutathione (oxidized)	C <sub>20</sub> H <sub>32</sub> N <sub>6</sub> O <sub>12</sub> S <sub>2</sub>	612.6	NA	-7.89
Glutathione (reduced)	C <sub>10</sub> H <sub>17</sub> N <sub>3</sub> O <sub>6</sub> S	307.3	NA	-5.41
Histamine	C <sub>5</sub> H <sub>9</sub> N <sub>3</sub>	111.1	9.8	-0.7
Histidine	C <sub>6</sub> H <sub>9</sub> N <sub>3</sub> O <sub>2</sub>	155.2	2.76	-3.32
Hydrocortisone (cortisol)	C <sub>21</sub> H <sub>30</sub> O <sub>5</sub>	362.5	NA	1.61
Linoleic acid	C <sub>18</sub> H <sub>32</sub> O <sub>2</sub>	280.4	4.77	7.05
Lysine	C <sub>6</sub> H <sub>14</sub> N <sub>2</sub> O <sub>2</sub>	146.2	3.12	-3.05
Maleic acid	C <sub>4</sub> H <sub>4</sub> O <sub>4</sub>	116.1	1.83	-0.48
Nicotinamide	C <sub>6</sub> H <sub>6</sub> N <sub>2</sub> O	122.1	3.35	-0.37
Phenylalanine	C <sub>9</sub> H <sub>11</sub> NO <sub>2</sub>	165.2	1.24	-1.38
Progesterone	C <sub>21</sub> H <sub>30</sub> O <sub>2</sub>	314.5	NA	3.87
Protoporphyrin IX	C <sub>34</sub> H <sub>34</sub> N <sub>4</sub> O <sub>4</sub>	562.7	NA	7.43
Pyruvic acid	C <sub>3</sub> H <sub>4</sub> O <sub>3</sub>	88.1	2.45	-1.24
Retinal	C <sub>20</sub> H <sub>30</sub> O	286.5	NA	7.6
Riboflavin	C <sub>17</sub> H <sub>20</sub> N <sub>4</sub> O <sub>6</sub>	376.4	10.2	-1.46
Ribose-5-phosphate	C <sub>5</sub> H <sub>11</sub> O <sub>8</sub> P	230.1	NA	-2.65
Sucrose	C <sub>12</sub> H <sub>22</sub> O <sub>11</sub>	342.3	12.6	-3.7
Taurocholic acid	C <sub>26</sub> H <sub>45</sub> NO <sub>7</sub> S	515.7	NA	0.01
Thyroxine	C <sub>15</sub> H <sub>11</sub> I <sub>4</sub> NO <sub>4</sub>	776.8	NA	4.12
Tryptophan	C <sub>11</sub> H <sub>12</sub> N <sub>2</sub> O <sub>2</sub>	204.2	7.38	-1.06
Uridine diphosphate (UDP)	C <sub>9</sub> H <sub>14</sub> N <sub>2</sub> O <sub>12</sub> P <sub>2</sub>	404.2	NA	-3.12
Uridine diphosphate glucose (UDPG)	C <sub>15</sub> H <sub>24</sub> N <sub>2</sub> O <sub>17</sub> P <sub>2</sub>	566.3	NA	-5.8



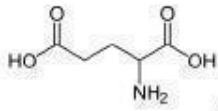
phenylalanine



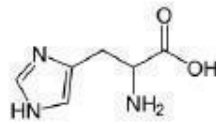
riboflavin



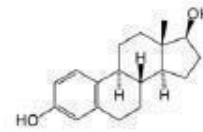
ascorbic acid



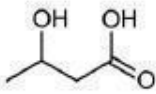
glutamic acid



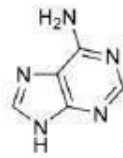
histidine



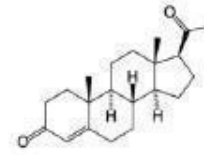
β-estradiol



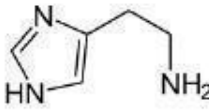
3-hydroxybutyric acid



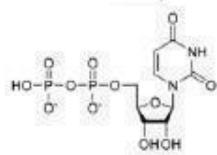
adenine



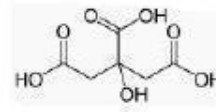
progesterone



histamine



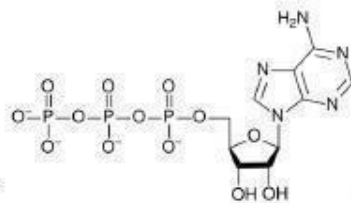
UDP



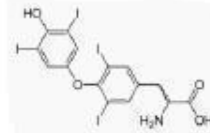
citric acid



adenosine



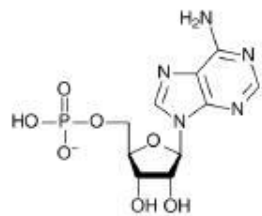
ATP



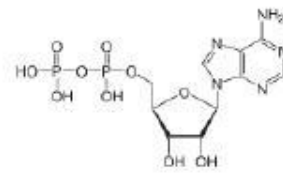
thyroxine



UDPG



AMP



ADP

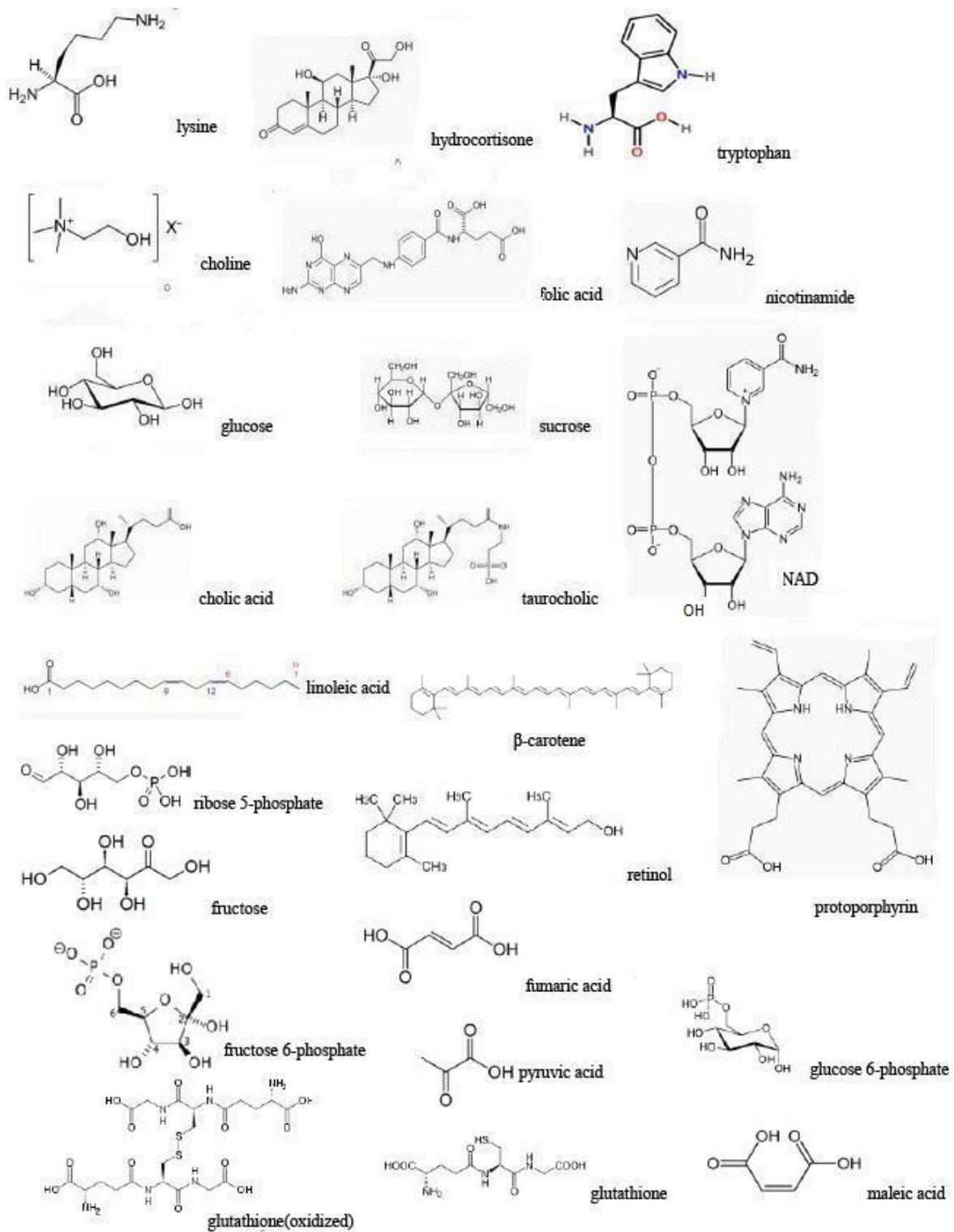


Figure 5.1 Structures of metabolites included in metabolite standard test mixture.

Due to long LC-MS analysis times, coatings were sub-divided into several batches, and independent extractions were performed for metabolites amenable to reverse phase chromatography *versus* metabolites amenable to HILIC chromatography. This ensured that all samples would be analyzed within 48 hr of preparation to eliminate potential issues with analyte degradation while waiting for analysis.

#### 5.2.3.1 SPME desorption prior to reverse phase LC-MS (used for analytes of low to intermediate polarity)

Fibres were desorbed immediately after extraction using 250  $\mu$ L of desorption solvent (acetonitrile/water, 1/9, v/v) for 120 min. Three additional desorptions (120 min each) were then performed using fresh 250  $\mu$ L aliquots of acetonitrile/water (1/1, v/v) as the desorption solvent to ensure complete removal of all analytes for the comparison. All desorption steps were performed in 0.3 mL capacity amber polypropylene HPLC microvials. After desorption, vials were manually vortexed for a minimum of 1 min. Samples (20  $\mu$ L) were injected directly using reverse phase LC-MS method described in Section 5.2.5.

#### 5.2.3.2 SPME desorption prior to HILIC LC-MS (used for polar analytes)

Fibres were desorbed immediately after extraction using 250  $\mu$ L of desorption solvent (acetonitrile/water, 9/1, v/v) for 120 min. Three additional desorptions (120 min each) were then performed using fresh 300  $\mu$ L aliquots of acetonitrile/water (3/2, v/v) as the desorption solvent to ensure complete removal of all analytes for the comparison. All desorption steps were performed in 0.3 mL capacity amber polypropylene HPLC microvials. Vials were manually vortexed for a minimum of 1 min. Samples (20  $\mu$ L) were injected directly using reverse phase LC-MS method described in Section 5.2.5.

### 5.2.4 Calculation of correction factors to account for different coating dimensions

To prepare coatings with commercial sorbents, particles of different size were immobilized because of limited commercial availability. Coating length and solid support core were kept constant at 15 mm and 1.55 mm, respectively. However, to facilitate the comparison of different sorbent types, particle size needed to be taken into account. Furthermore, the coatings obtained from Supelco (both commercial and prototype) had different dimensions than lab-made coatings, so appropriate correction factors were needed to account for different dimensions of all fibres used in this comparison. Coating volume was estimated by simply treating all types of coatings as cylinders and



assuming the entire volume of immobilized phase could act as sorbent. Based on SEM results, it was determined that a single layer of sorbent particles was immobilized using the described procedure for lab-made coatings for all particle sizes  $\geq 5 \mu\text{m}$ . Therefore, particle size was used as an approximation of coating thickness. However, particle size of  $3 \mu\text{m}$  resulted in multiple layer coverage with estimated coating thickness of  $10 \mu\text{m}$ , so this was used as coating thickness for this particular type of coating. In the next step, the volume of two cylinders was calculated: (i) the volume of fibre core cylinder only (radius = core diameter/2) and (ii) the volume of entire fibre (radius = fibre core diameter/2 + coating thickness). The volume of the coating is then determined by the subtraction of fibre core volume (i) from the total volume of entire fibre (ii). Full calculations for all types of coatings used in current study are shown in Table 5.3. For sorbents where a range of particle sizes was given, the mean size was used as coating thickness for volume estimation. For example, for HR-P sorbent where size was reported as  $50\text{-}100 \mu\text{m}$ , the value of  $75 \mu\text{m}$  was used to estimate the coating volume. Clearly, the correction factors shown in Table 5.3. are only approximate because they assume (i) tight packing of spherical particles within the coating (ii) uniform size of all particles (iii) same extraction efficiency for sorbent and binder and (iv) do not take into account different surface areas and porosity of particles. Despite of this, the approximation is useful to give an estimate of how the performance of new coatings compares to existing coatings and to ensure coatings are not accidentally rejected simply based on different dimensions. Particle size information for Plexa, Plexa PCX and Focus sorbents from Varian and for Speed Advanta sorbent from Applied Separations could not be obtained as shown in Table 5.1 so no correction factor was applied to these coatings. This is in agreement with visual examination ( $< 50 \mu\text{m}$ ), so  $40 \mu\text{m}$  particle size appears to be a reasonable assumption for these coatings. Finally, no correction factor was applied for carbon tape coatings as the proportion of carbon was unknown. Therefore, the results for this coating are reported “as is”, whereas the results for all other coatings are reported with respect to performance of  $40 \mu\text{m}$  particle size which was arbitrarily selected as the reference point as shown in Table 5.3.

**Table 5.3 Determination of correction factors to use during coating comparison.**

	Thickness (µm)	Length (cm)	Core (µm)	Fibre diameter (µm)	Fibre radius (µm)	Core radius (µm)	Total volume (µm <sup>2</sup> cm)	Core volume (µm <sup>2</sup> cm)	Coating volume (µm <sup>2</sup> cm)	Correction factor
lab-made	213.5	1.5	1550	1977	988.5	775	4.60E+07	2.83E+07	1.77E+07	0.17
lab-made	85	1.5	1550	1720	860	775	3.49E+07	2.83E+07	6.55E+06	0.46
lab-made	80	1.5	1550	1710	855	775	3.44E+07	2.83E+07	6.14E+06	0.49
lab-made	51	1.5	1550	1652	826	775	3.22E+07	2.83E+07	3.85E+06	0.78
lab-made	55	1.5	1550	1660	830	775	3.25E+07	2.83E+07	4.16E+06	0.72
lab-made	75	1.5	1550	1700	850	775	3.40E+07	2.83E+07	5.74E+06	0.52
lab-made	40	1.5	1550	1630	815	775	3.13E+07	2.83E+07	3.00E+06	1.00
lab-made	45	1.5	1550	1640	820	775	3.17E+07	2.83E+07	3.38E+06	0.89
RPA 3 µm	10	1.5	1550	1570	785	775	2.90E+07	2.83E+07	7.35E+05	4.08
lab-made	5	1.5	1550	1560	780	775	2.87E+07	2.83E+07	3.66E+05	8.18
lab-made	33	1.5	1550	1616	808	775	3.08E+07	2.83E+07	2.46E+06	1.22
lab-made	30	1.5	1550	1610	805	775	3.05E+07	2.83E+07	2.23E+06	1.34
lab-made	50	1.5	1550	1650	825	775	3.21E+07	2.83E+07	3.77E+06	0.80
CW TPR	50	1.0	160	260	130	80	5.31E+05	2.01E+05	3.30E+05	9.09
biocompatible prototypes	45	1.5	200	290	145	100	9.91E+05	4.71E+05	5.20E+05	5.77
PA	85	1.0	160	330	165	80	8.55E+05	2.01E+05	6.54E+05	4.58
PDMS	100	1.0	160	360	180	80	1.02E+06	2.01E+05	8.17E+05	3.67
PDMS DVB	60	1.0	160	280	140	80	6.16E+05	2.01E+05	4.15E+05	7.23

### 5.2.5 LC-MS analysis

All samples were analyzed according to one of the two optimized LC methods described in Table 5.4 using LC-MS system consisting of Varian pumps (212-LC), Prostar 430 Autosampler and 500-MS ion trap mass spectrometer using positive electrospray ionization (ESI) mode unless otherwise specified. While waiting for analysis, samples were stored refrigerated at 4°C in the lab refrigerator in order not to exceed 12 hr storage on autosampler tray at room temperature (no cooling option available on autosampler). The analysis of metabolite standard mixture of known concentrations was performed at the beginning, end and throughout each sample batch, and was used for quality control and calibration purposes. An example chromatogram of metabolite standard analyzed using reverse phase PFP method is shown in Figure 5.2.

**Table 5.4 Summary of optimized LC-MS parameters**

LC parameter	Reverse phase LC method	HILIC LC method
<b>Analytical column</b>	HS F5 Pentafluorophenyl (Supelco)	Ascentis Si (Supelco)
<b>Column dimensions</b>	2.1 x 10 mm	2.1 x 10 mm
<b>Particle size</b>	3 µm	3 µm
<b>Mobile phase A</b>	Water/acetic acid (99.9/0.1, v/v)	ammonium formate/acetonitrile (5/95, 2 mM total)
<b>Mobile phase B</b>	water/acetonitrile/acetic acid (89.9/10/0.1)	ammonium formate/acetonitrile (40/60, 2 mM total)
<b>Flow rate</b>	200 µL/min	200 µL/min
<b>Injection volume</b>	20 µL	20 µL
<b>Run time</b>	35 min	30 min
<b>Gradient program</b>	0-3 min 100% A, 3-20 min linear gradient to 10%A, 20-30 min hold at 10% A, 5 min re-equilibration at 100% A	0-2 min 100% A, 2-14 min linear gradient to 65%A, 14-18 min hold at 65% A, 12 min re-equilibration at 100% A
<b>Nebulizer pressure</b>	60 psi	60 psi
<b>Drying gas pressure</b>	22 psi	22 psi
<b>Temperature</b>	400°C	400°C

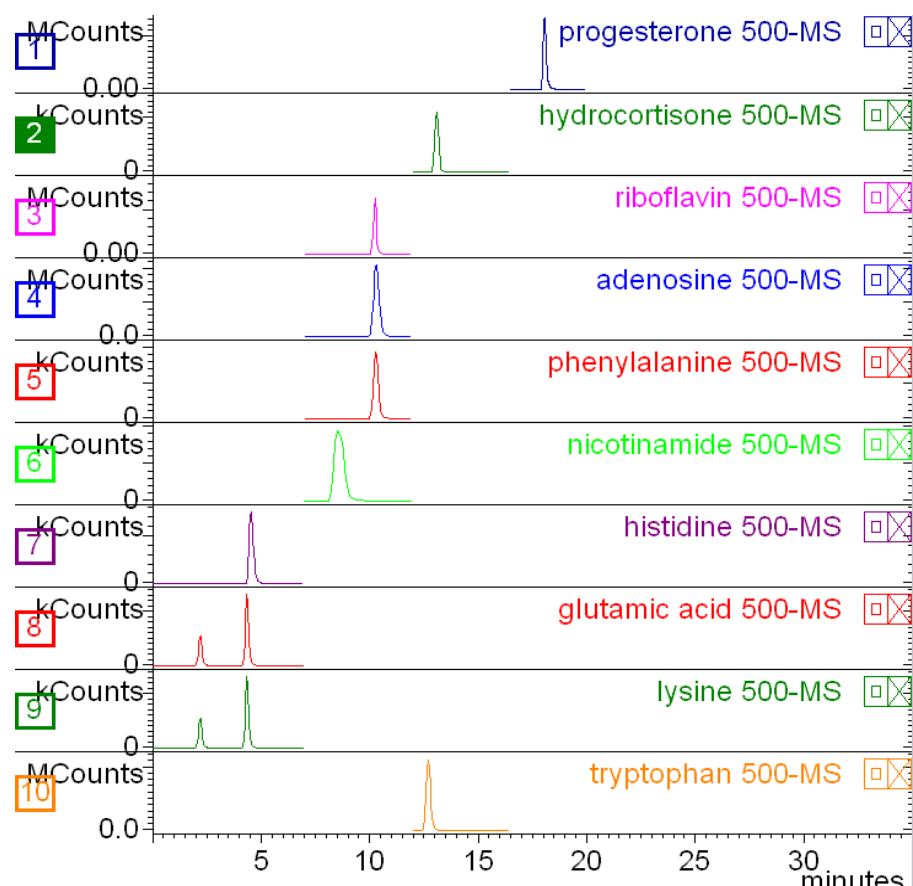


**Figure 5.2 Example chromatogram using reverse phase pentafluorophenyl LC-MS method.**

Optimum MS parameters for each analyte were initially determined using direct introduction of 1  $\mu\text{g/mL}$  single component standard solution into mass spectrometer. These optimum parameters are summarized in Table 5.5, Table 5.6 and Table 5.7. Using this data, general parameters for full scan methods were set by selecting the parameters that will provide the best performance across the range of analytes. The following settings were used based on the data presented in tables. Using positive ESI for analytes with  $\text{MW} < 500$ , needle, capillary and RF voltage were set to 6000 V, 45V and 60V respectively in full scan mode. Using positive ESI for analytes with  $\text{MW} > 500$ , needle, capillary and RF voltage were set to 6000 V, 80V and 80V respectively in full scan mode. Using negative ESI for analytes with  $\text{MW} < 500$ , needle, capillary and RF voltage were set to 5000 V, 45V and 60V respectively in full scan mode. Furthermore, it was decided to run the methods using two scan ranges:  $m/z$  100-500 and  $m/z$  500-1000 because the optimum parameters differed greatly for low MW species *versus* high MW species and good sensitivity could not be achieved simultaneously for all compounds regardless of MW. However, despite the extensive optimization, analytical sensitivity for

some analytes was very poor (analytes for which optimum voltages deviated from set voltages had extremely poor sensitivity indicating ion transmission was very sensitive to selected parameters) as determined during preliminary column evaluation experiments, so MS/MS mode with optimized capillary and RF voltage parameters for each analyte was used during coating evaluation experiments. This minimized the number of analytes that could be successfully monitored during each analysis because of slow acquisition rates in MS/MS mode which permitted monitoring of 4-5 analytes per each retention time window with adequate number of data points across peak.

**Table 5.5 Optimization of MS parameters (a) needle voltage, (b) capillary voltage and (c) RF voltage in positive ESI mode for compounds with MW<500.**

Analyte	Needle voltage (V)	Capillary voltage range (V)		RF voltage range (V)	
3-hydroxybutyric acid	4800	85	100	40	55
Cholic acid	6000	50	110	55	65
Glucose-1-phosphate	5250	100	120	65	72
Folic acid	5200	75	160	63	70
Glucose	5230	30	60	50	60
Hydrocortisone	5577	30	60	85	100
Estradiol ( $\beta$ )	6000	30	80	70	85
Histidine	4300	30	50	50	65
Progesterone	6000	60	72	80	90
Adenine	6000	55	65	50	60
Riboflavin	6000	40	90	85	100
Phenylalanine	6000	20	50	55	65
Glutamic acid	6000	20	45	50	60
Histamine	6000	30	50	45	55
Tryptophan	6000	30	50	60	75
Lysine	6000	20	45	50	60
Nicotinamide	6000	40	70	48	55
Choline	6000	30	60	45	55
$\beta$ -NAD	5200	75	90	77	85
Retinol	6000	65	75	77	85
Adenosine	2800	40	60	70	80
Sucrose	6000	50	90	85	95
Maleic acid	5500	20	60	50	85
Pyruvate	6000	20	60	48	65
ADP	6000	25	80	60	70
AMP	6000	30	70	85	95
Fumarate	6000	50	150	60	70
Glutathione reduced	4300	40	60	80	95
Ribose 5-phosphate	6000	40	100	75	85
Fructose 6-phosphate	4500	40	80	80	92
Glucose-6-phosphate	6000	30	75	75	90

**Table 5.6 Optimization of MS parameters (a) needle voltage, (b) capillary voltage and (c) RF voltage in negative ESI mode for compounds with MW<500.**

Analyte	Needle voltage (V)	Capillary voltage range (V)		RF voltage range (V)	
Citric acid	5000	40	60	40	60
Ascorbic acid	4700	20	40	40	60
3-hydroxybutyric acid	6000	20	35	35	60
Cholic acid	6000	140	200	45	55
Folic acid	6000	40	60	50	60
Glucose-1-phosphate	5250	30	60	60	100
Linoleic acid	6000	75	100	120	140
UDP	6000	20	70	45	55
Folic acid	5500	70	90	68	75
Glucose	6000	20	40	50	60
Estradiol ( $\beta$ )	6000	80	150	140	160
Adenine	6000	40	60	90	110
Riboflavin	4000	40	80	70	80
D-phenylalanine	6000	30	60	45	100
Glutamic acid	5000	25	55	40	75
Tryptophan	4000	40	70	40	70
Lysine	5000	40	60	75	85
Pyruvate	6000	20	40	115	128
ADP	4500	40	90	65	80
AMP	4000	40	80	95	110
Maleic acid	6000	20	40	55	65
Fumarate	6000	15	35	60	75
Glutathione reduced	3800	45	55	90	100
Ribose 5-phosphate	5000	30	50	80	90
Fructose 6-phosphate	5000	25	50	80	95
Glucose-6-phosphate	4500	20	70	82	95

**Table 5.7 Optimization of MS parameters (a) needle voltage, (b) capillary voltage and (c) RF voltage in positive ESI mode for compounds with MW>500.**

Analyte	Needle maximum (V)	Capillary voltage range (V)		RF voltage range (V)	
ATP	6000	60	80	60	75
Taurocholic acid	4600	100	220	70	78
Beta-NAD	5200	75	90	77	85
Protoporphyrin IX	6000	80	180	70	80
UDPG	3900	75	110	70	90
Beta-CAROTENE	6000	70	110	70	80
Glutathione oxidized	6000	80	120	75	90
Thyroxine	6000	50	90	87	95

## 5.3 Results and discussion

### 5.3.1 Development of pentafluorophenyl (PFP) reverse-phase method

In initial work, the performance of reverse phase methods with C<sub>18</sub>, C<sub>16</sub> amide (RPA) and pentafluorophenyl (PFP) stationary phases was evaluated for their ability to retain metabolites within standard metabolite mixture. Alkyl stationary phases with embedded polar groups such as C<sub>16</sub> amide used in this evaluation, tend to improve retention of some poorly retained compounds on C<sub>18</sub> column and have improved wettability which allows their use in 100% aqueous mobile phases without alkyl chain collapse which is observed with traditional C<sub>18</sub> columns.<sup>218</sup> PFP column was incorporated in this evaluation because it relies on different retention mechanism *versus* those employed for alkyl stationary phases. Among the columns tested, PFP column provided the best retention for the largest number of metabolites tested. PFP column was able to adequately retain 22 analytes with one analyte exhibiting unacceptable peak shape. In comparison, C<sub>18</sub> column was able to retain 13 analytes among which three had unacceptable peak shape. Overall, RPA column had very similar performance to C<sub>18</sub> column and did not sufficiently retain more polar analytes. Examples of retained analytes on PFP column which were not well-retained on C<sub>18</sub> column included adenine, adenosine, lysine, histidine, nicotinamide, phenylalanine and histamine (Figure 5.2). Excellent performance of PFP column *versus* typical C<sub>18</sub> column is attributed to the ability to use 100% aqueous phase and to the different retention mechanism of PFP column that is more likely to incorporate some aromatic interactions. These results are in agreement with recent report in literature, where a comparison of C<sub>18</sub> *versus* PFP columns for LC-MS metabolomics of food also showed superior performance of PFP column to retain more polar metabolites.<sup>219</sup> This improved metabolite coverage subsequently resulted in better class separation of fermentation samples during statistical analysis, and is therefore highly important for global metabolomic studies.

### 5.3.2 Evaluation of extraction reproducibility

To ensure the comparison of coatings was meaningful, the reproducibility of extractions using n=3 fibres of all types for all metabolites was regularly documented. Example results for pH 7.4 extraction followed by reverse-phase LC analysis are shown in Figure 5.3 (a) with average RSD of 8% for all coatings and metabolites tested within this set. The RSD for glutamic acid is higher than for other compounds because the extraction capacity is poor so the signal intensity is close to LOQ of this

compound. Figure 5.3 (b) shows the results for pH 9.5 extraction followed by HILIC analysis with average RSD of 20%.

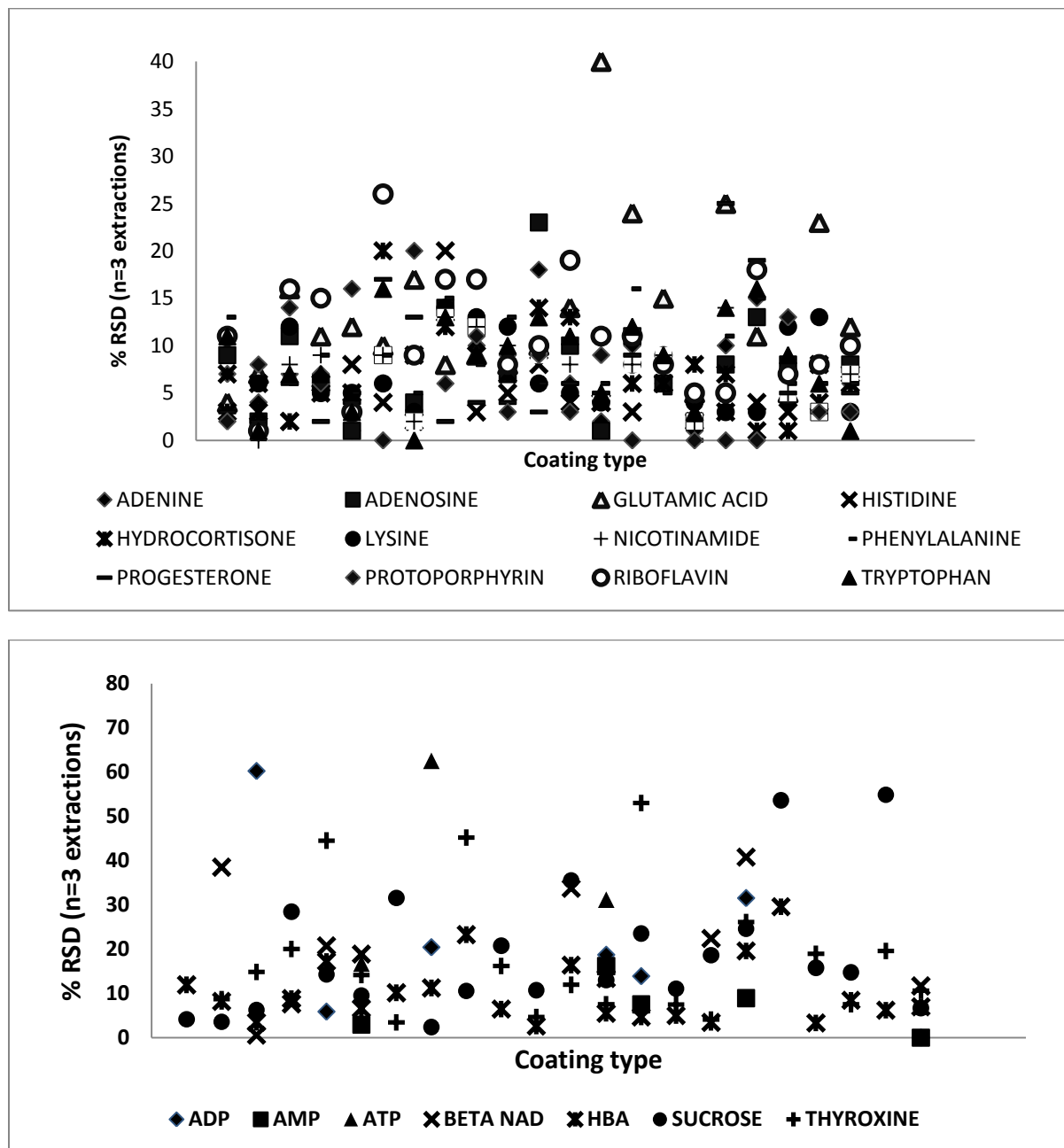
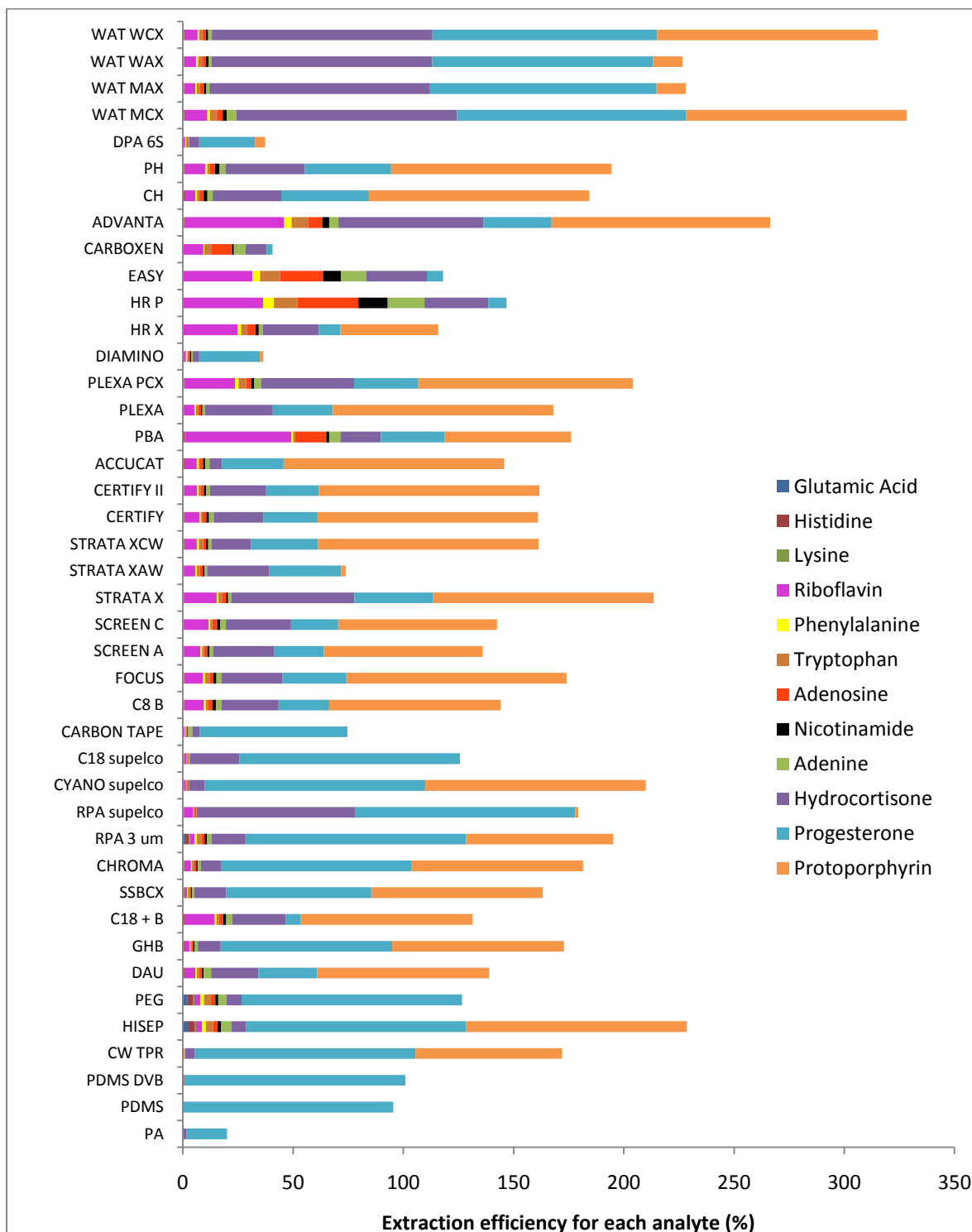
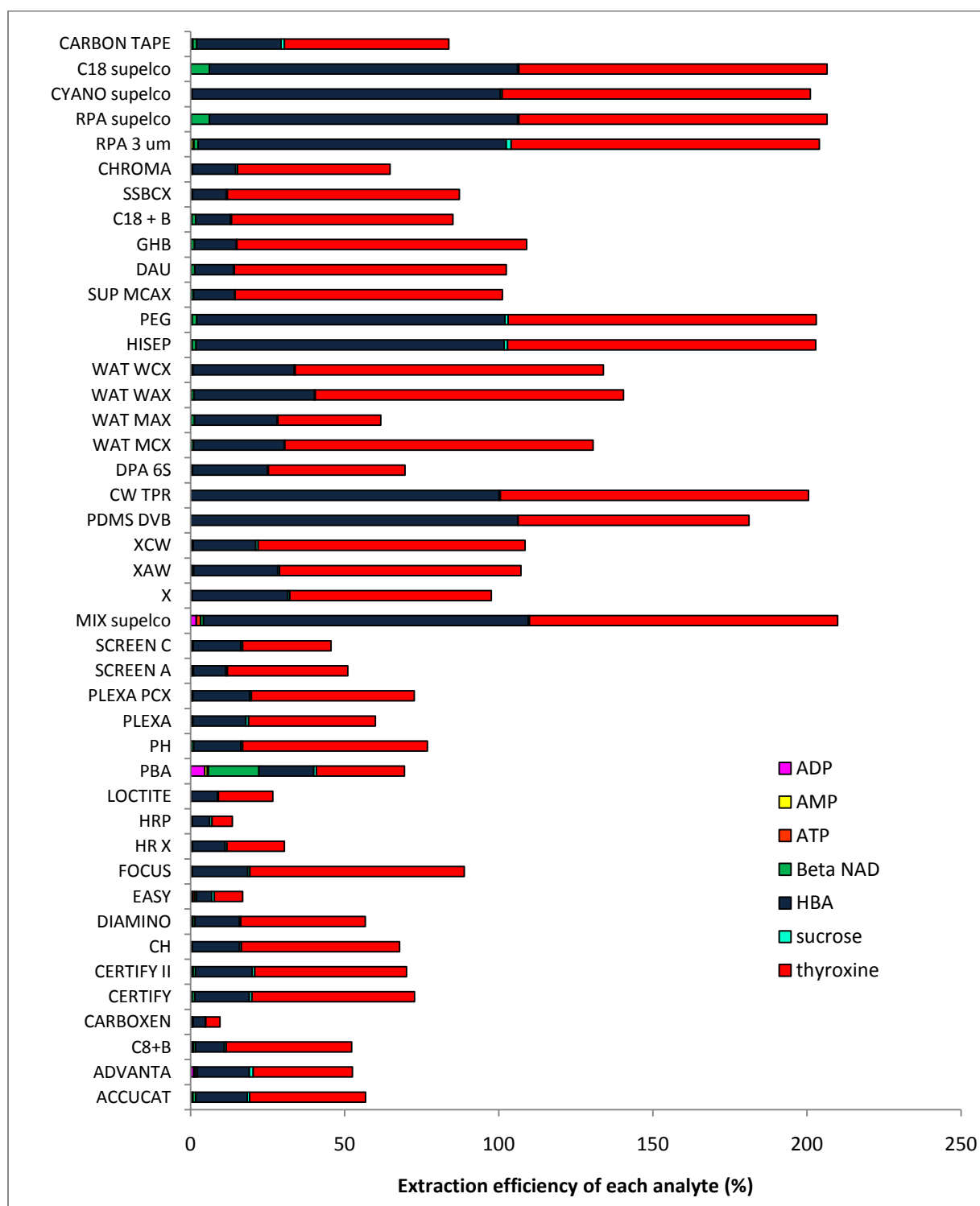


Figure 5.3 Example of extraction reproducibility (a) at extraction pH of 7.4 and analysis using reverse phase LC-MS method and (b) at extraction pH of 9.5 and analysis using HILIC LC-MS.





**Figure 5.4 Comparison of the extraction efficiency of all sorbents for the extraction of 12 selected metabolites at pH 7.4 analyzed using PFP reverse phase method.**



**Figure 5.5 Comparison of the extraction efficiency of all sorbents for the extraction of seven selected metabolites at pH 7.4 analyzed using HILIC method.**

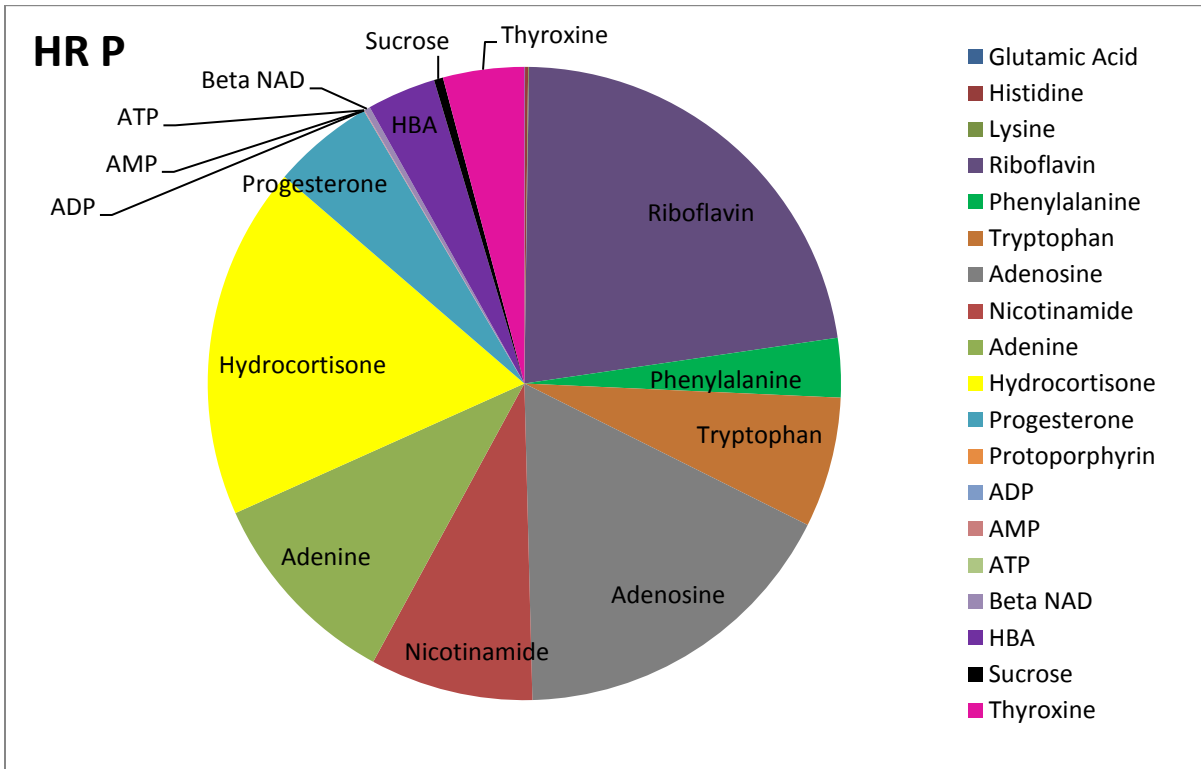
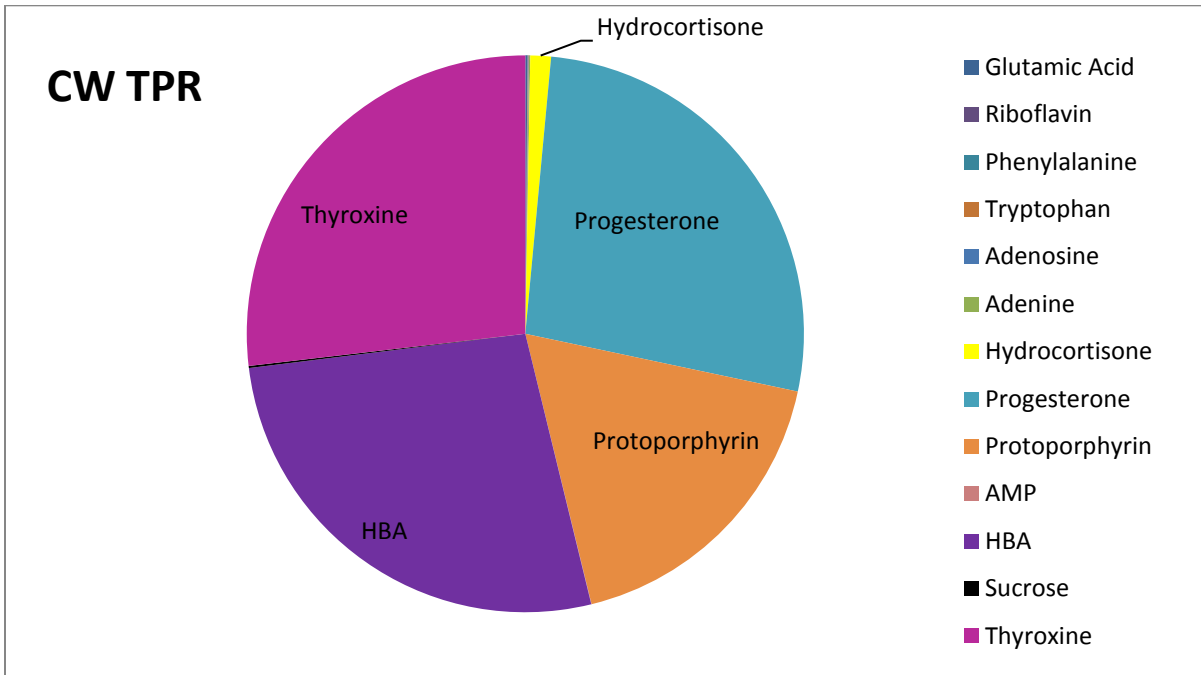
### 5.3.3 Comparison of extraction efficiency of various sorbents at pH 7.4

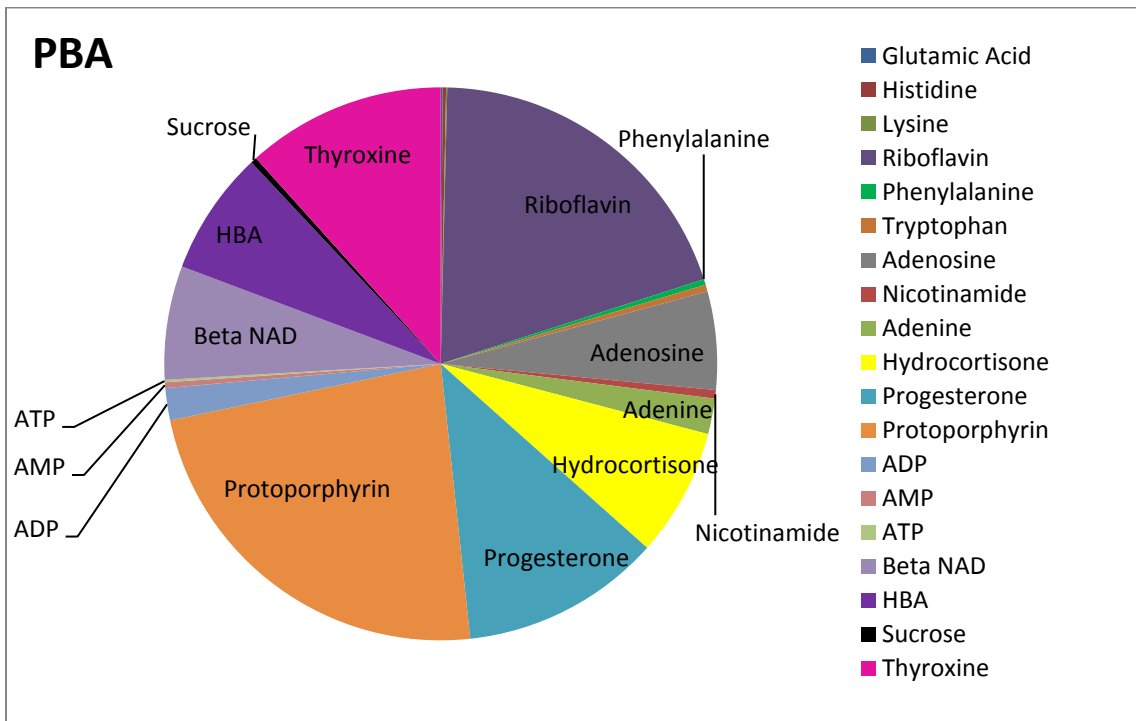
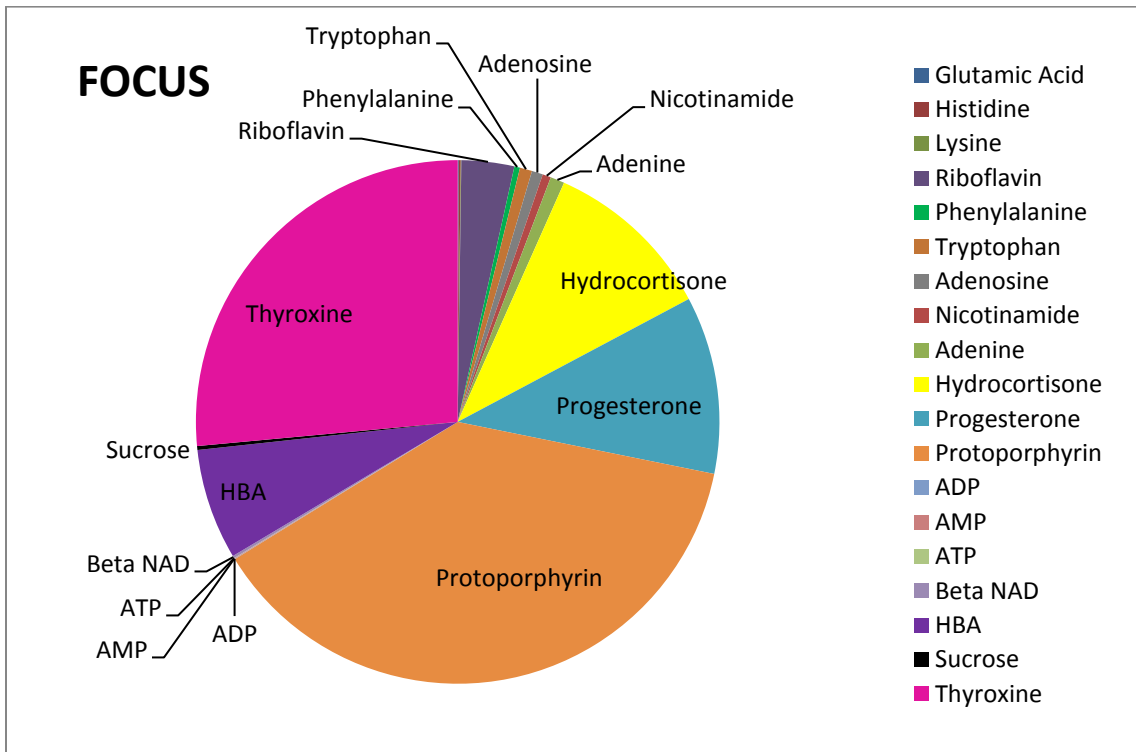
The performance of various sorbents was compared for the extraction from PBS buffer at physiological pH. The results of these studies are summarized in Figure 5.4 for the metabolites analyzed using reverse-phase method and in Figure 5.5 for the analytes analyzed using HILIC method. Several trends are easily apparent. Commercial coatings performed extremely poorly for the extraction of polar metabolites, and the data clearly demonstrates why coating development was necessary. Mixed-mode coatings significantly improve the extraction of polar species, while polymeric polystyrene divinylbenzene sorbents with and without modification (for example, Easy and HRP from Macherey Nagel and Advanta from Applied Separations) perform even better than mixed-mode coatings of any type. A third type of coating that performed very well is phenylboronic acid (PBA) coating. PBA forms reversible covalent interaction with compounds containing 1,2- or 1,3-diols. Many compounds of biological interest contain this functionality, so it is not surprising PBA coating performed so well for the analysis of these type of metabolites. Most stable binding is observed at alkaline pH, but in our study good results were observed at physiological pH as well. To disrupt the binding, it is necessary to include acid in the desorption solvent and in current study 1% formic acid was added to the desorption solvent for this purpose.

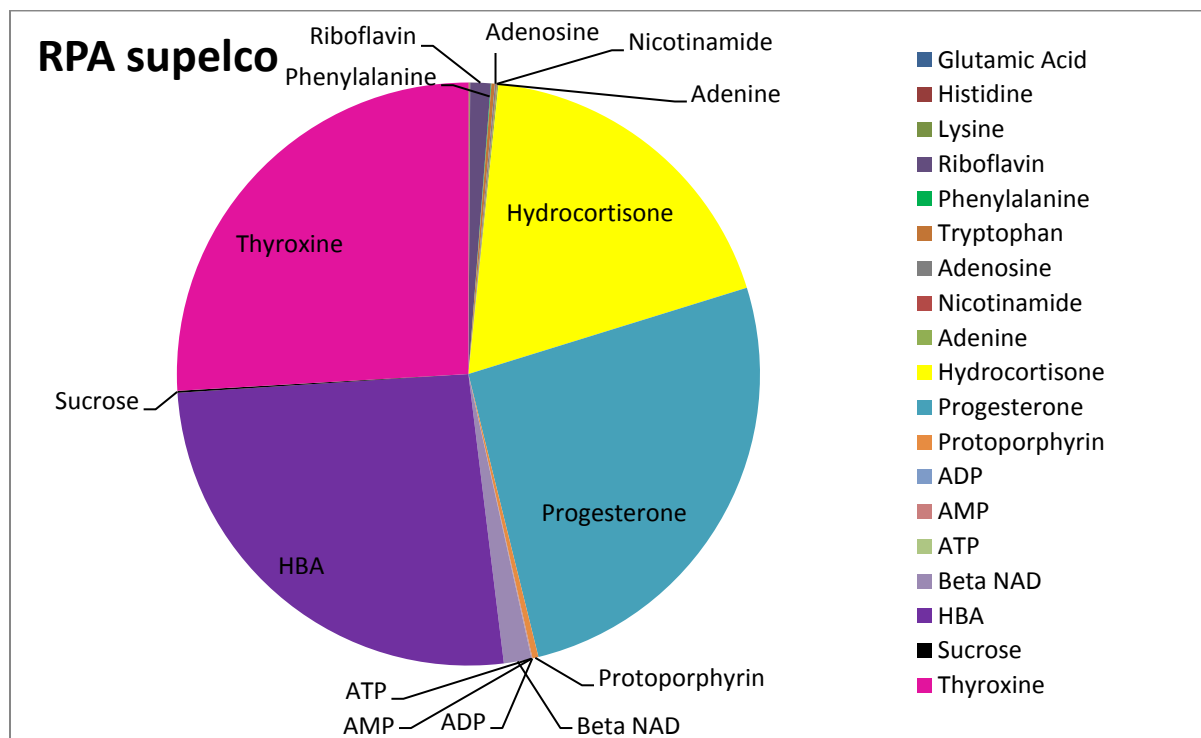
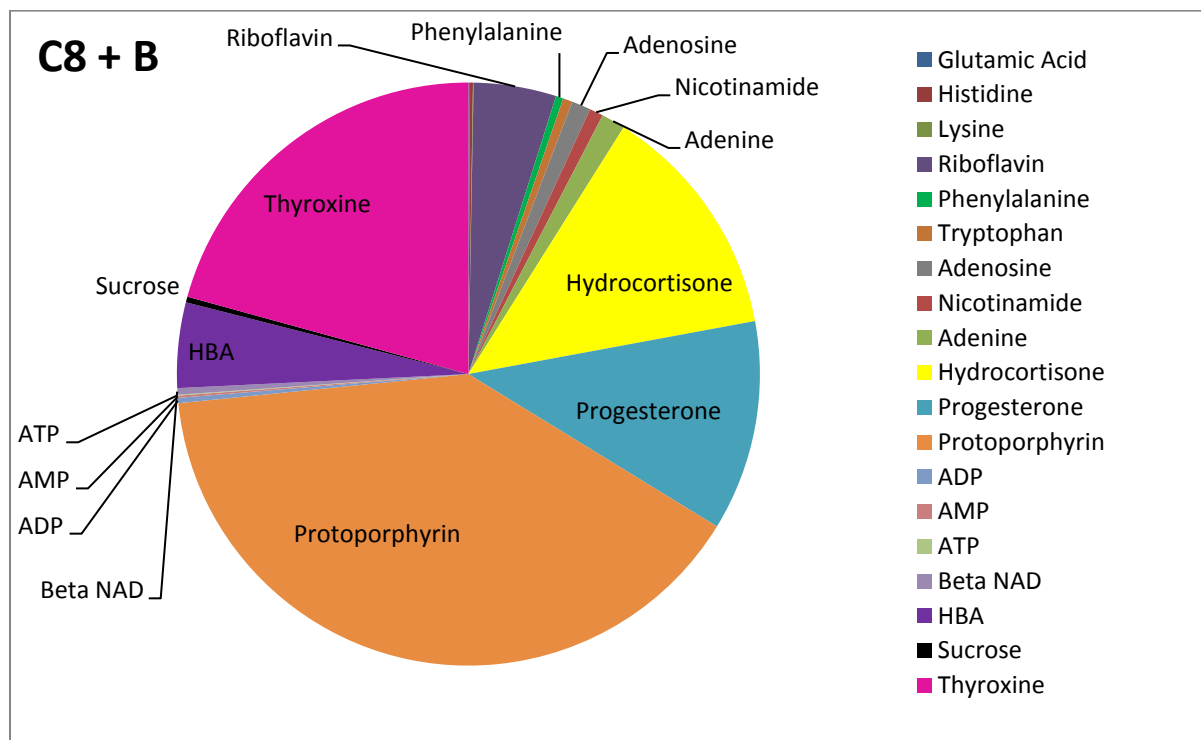
Figure 5.6 shows in more detail the performance of six selected coatings including commercial CW-TPR and prototype RPA coating discussed in Chapter 3. The results clearly illustrate that mixed-mode, PS-DVB and PBA coatings show better and more balanced performance across the wide polarity range which makes them more suitable for global metabolomic studies. Figure 5.7 shows the extraction performance of all sorbents for several selected metabolites of varying MW and polarity to further illustrate the described trends. The examination of all data for all analytes showed that the extraction of very polar species ( $\log P < -2$ ) is typically very poor for all coatings. The only exception to this trend is if the said polar analyte can be extracted by PBA coating (for example,  $\beta$ -NAD in Figure 5.7).

### 5.3.4 Dependence of extraction efficiency on pH

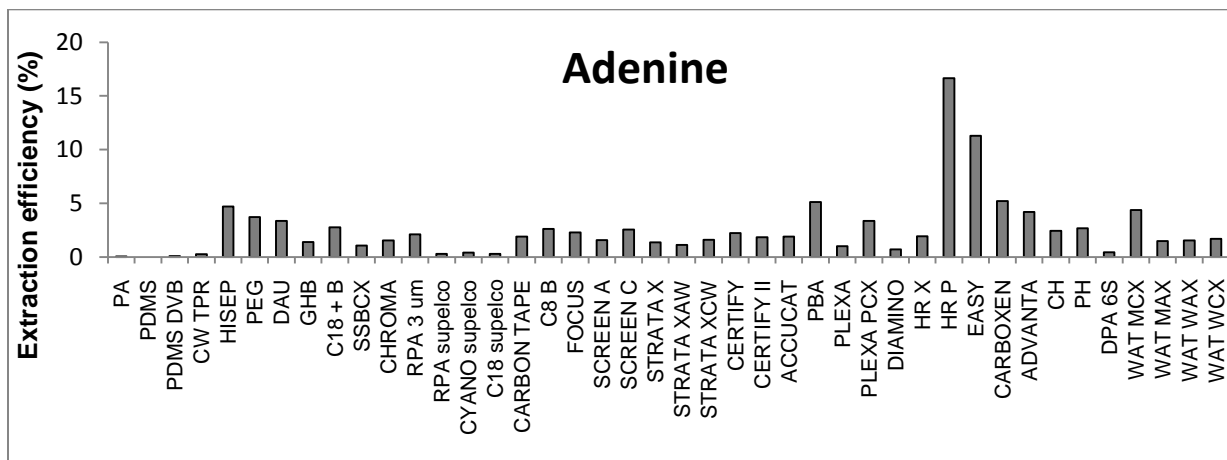
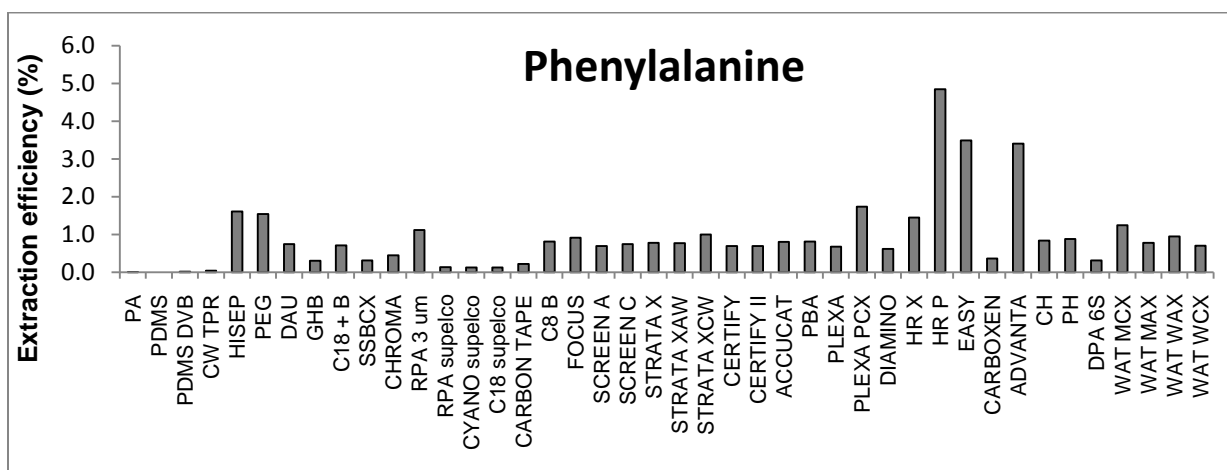
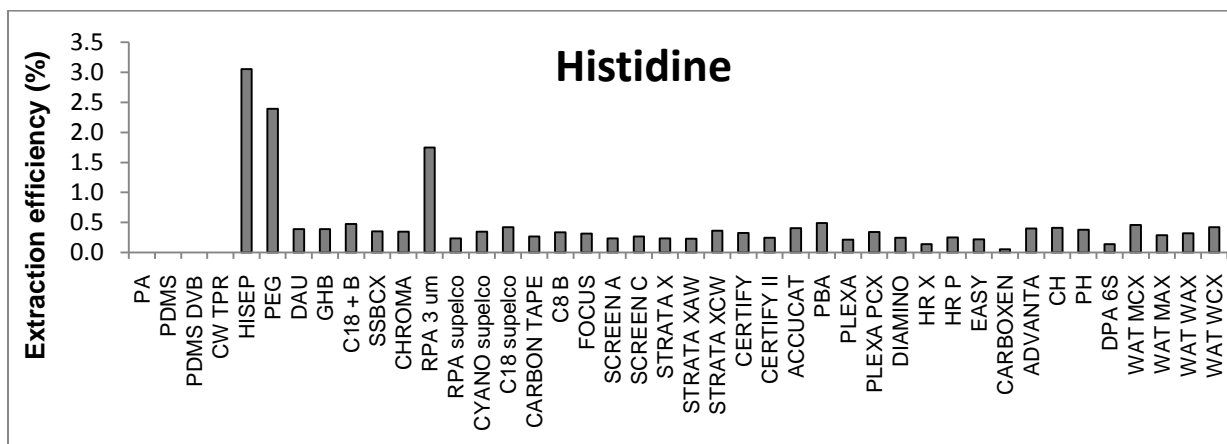
The results of extraction performed at pH 9.5 for all sorbents are included in Figure 5.8 and show very similar trends to what was observed at pH 7.4. Similar trends were observed for pH 3.0 and 5.0. The dependence of extraction efficiency on pH is shown for selected metabolites for three most promising coating types in Figure 5.9. The results show that generally physiological pH works well for the majority of metabolites, and no significant improvements would be achieved by adding a pH







**Figure 5.6 Comparison of extraction efficiency of CW-TPR, HRP, FOCUS, PBA, C<sub>8</sub>+B and RPA SPME coatings for the extraction of selected metabolites at pH 7.4.**



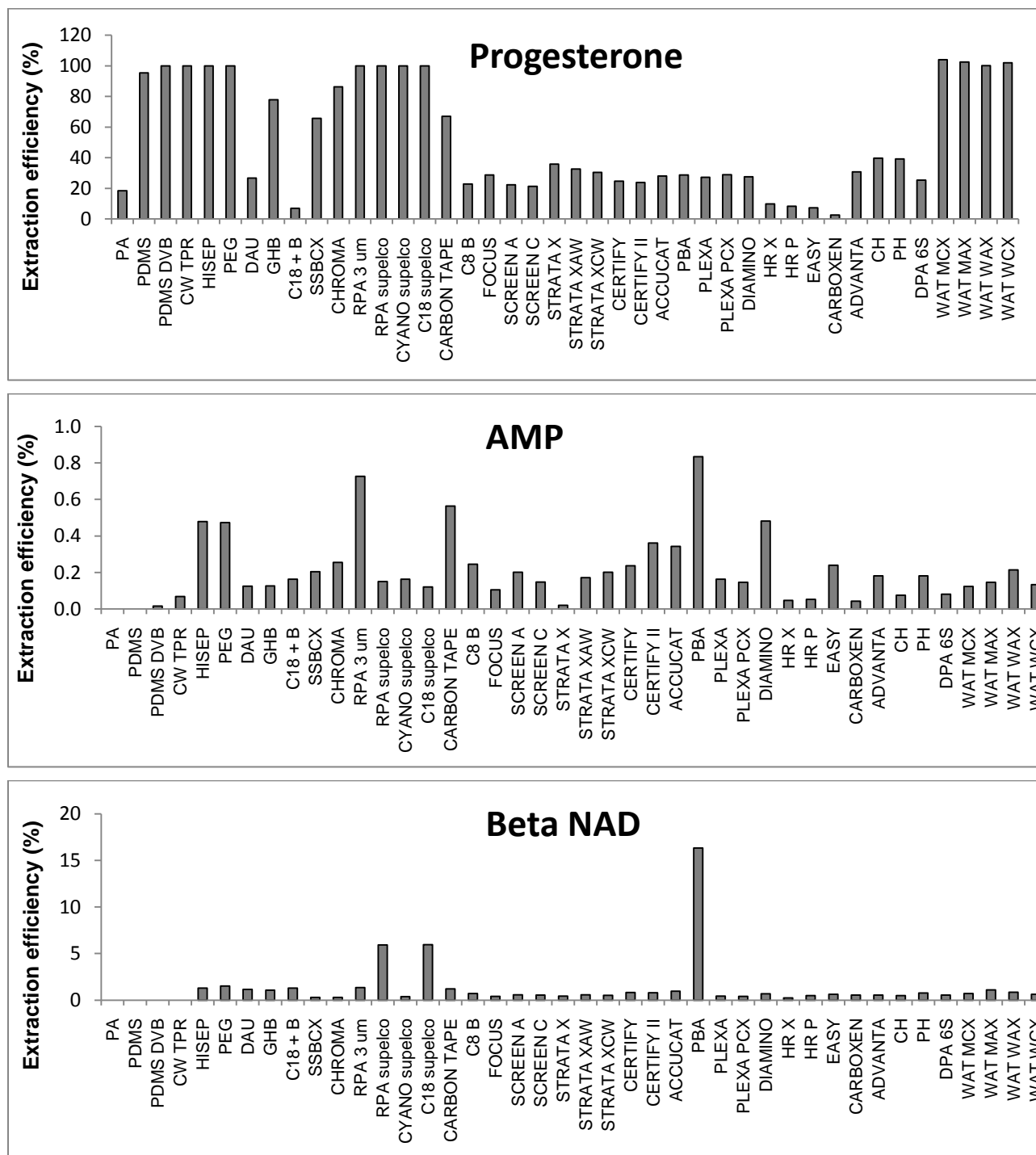
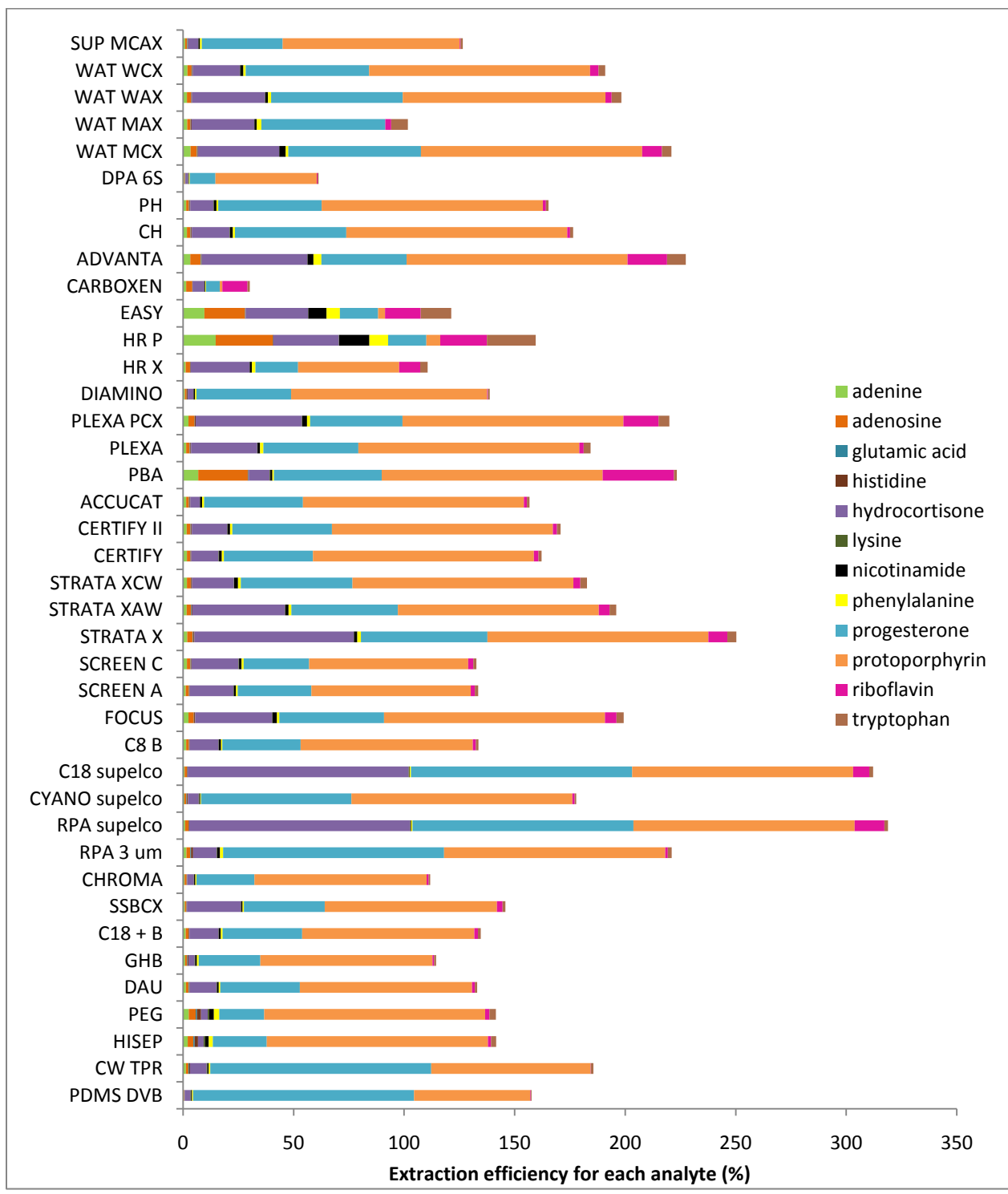


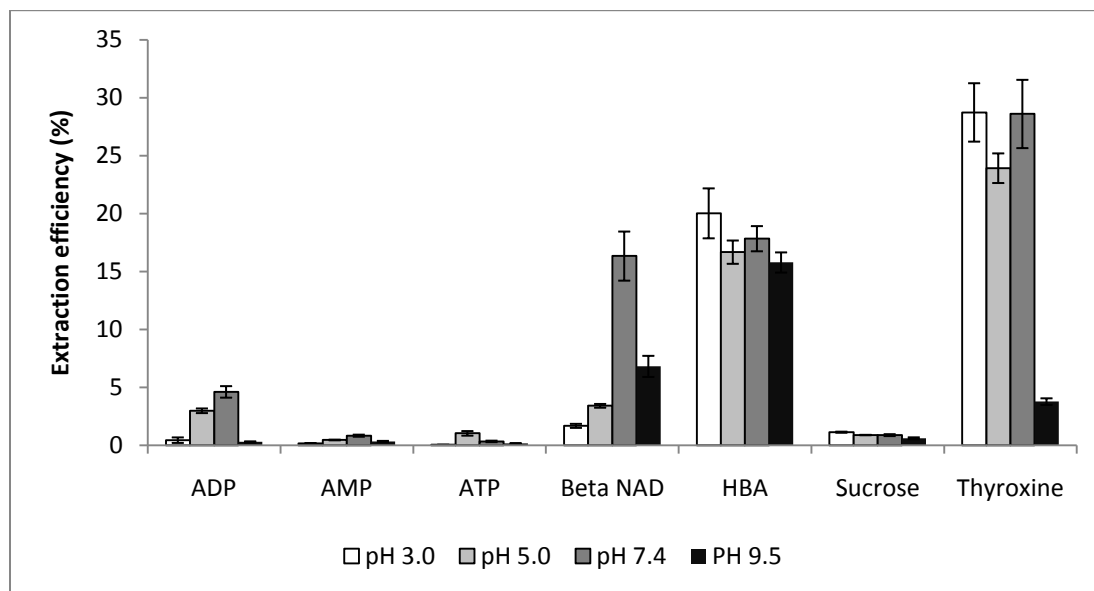
Figure 5.7 Extraction efficiency of selected individual metabolites (histidine, phenylalanine, adenine, progesterone, AMP and  $\beta$ -NAD) at pH 7.4 using all coatings tested.



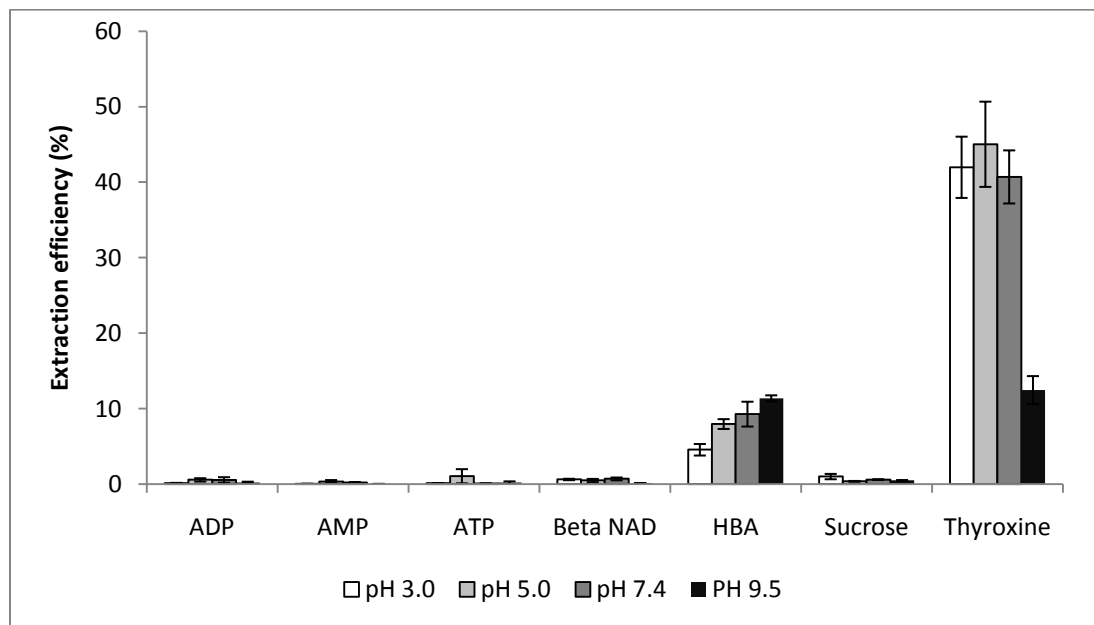


**Figure 5.8 Comparison of the extraction efficiency of all sorbents for the extraction of 12 selected metabolites at pH 9.5 analyzed using PFP reverse phase method.**

(a)



(b)



(c)

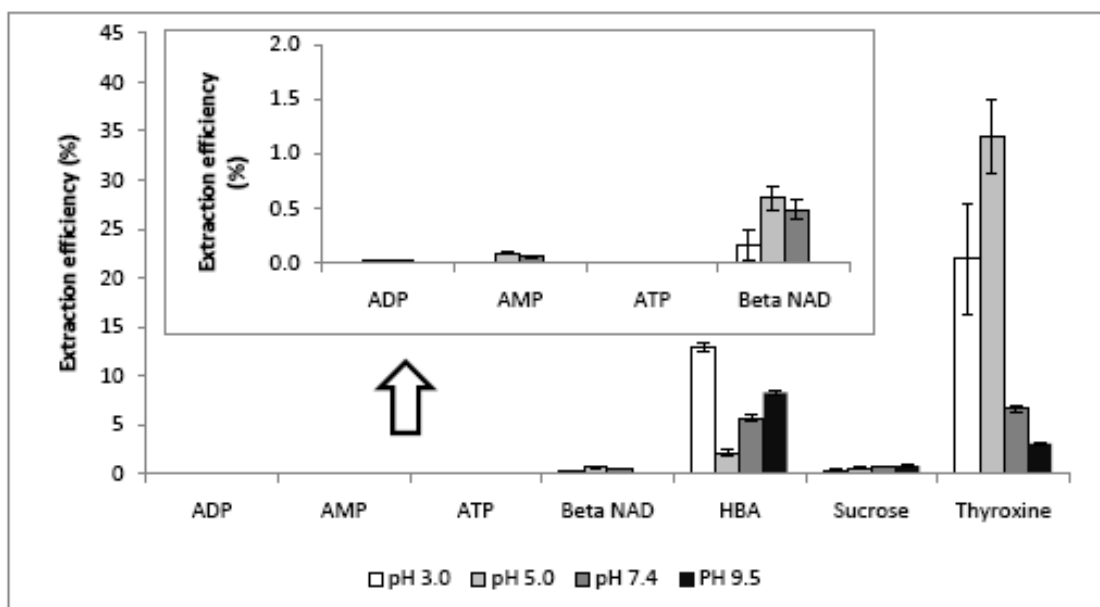


Figure 5.9 Dependence of the extraction efficiency of selected metabolites on pH using (a) PBA coating (b) mixed-mode C<sub>8</sub>+B coating and (c) HRP coating.

Table 5.8 Dependence of the extraction efficiency of Waters Oasis MAX, MCX, WAX and WCX coatings on sample pH.

pH	Coating type	ADP	AMP	ATP	Beta NAD	HBA	Sucrose
pH 3.0	WAT MAX	ND	0.01	ND	0.13	23	0.54
	WAT MCX	ND	0.04	ND	0.38	32	0.55
	WAT WAX	ND	0.01	ND	0.15	24	0.48
	WAT WCX	ND	0.01	ND	0.15	30	0.53
pH 5.0	WAT MAX	ND	0.19	ND	ND	39	0.22
	WAT MCX	0.03	0.16	ND	ND	35	0.30
	WAT WAX	ND	0.19	ND	ND	48	0.28
	WAT WCX	ND	0.15	ND	ND	49	0.29
pH 7.4	WAT MAX	ND	0.15	ND	1.1	27	0.31
	WAT MCX	0.05	0.12	ND	0.72	29	0.26
	WAT WAX	ND	0.21	ND	0.86	39	0.29
	WAT WCX	0.02	0.13	ND	0.64	33	0.32
pH 9.5	WAT MAX	0.05	0.32	ND	8.7	2.2	0.78
	WAT MCX	0.09	0.27	0.05	2.8	2.5	0.41
	WAT WAX	0.17	0.74	ND	7.5	0.78	0.91
	WAT WCX	0.31	0.62	0.15	5.8	1.4	0.87

adjustment step within the global metabolomics workflow. Interestingly, the results of different types of mixed-mode coatings (SCX, SAX, WCX, WAX) also do not show strong dependence on pH (Table 5.8).

### 5.3.5 Summary of coating selection and performance

Figure 5.10 compares the performance of three best types of coatings identified in this study: (i) mixed-mode coating ( $C_{18}$  or  $C_8$  with benzenesulfonic acid from any manufacturer), (ii) polystyrene-divinylbenzene polymeric coatings (HR-P, EASY or Advanta) and (iii) PBA coating. The ability to extract basic, neutral and acidic compound simultaneously at physiological pH without pH adjustment using modified and non-modified polystyrene-divinylbenzene was also shown in other studies for the extraction of pharmaceuticals from aqueous samples using solid-phase extraction.<sup>220</sup> In this comparison, Chromabond EASY showed better performance for majority of analytes (log P range

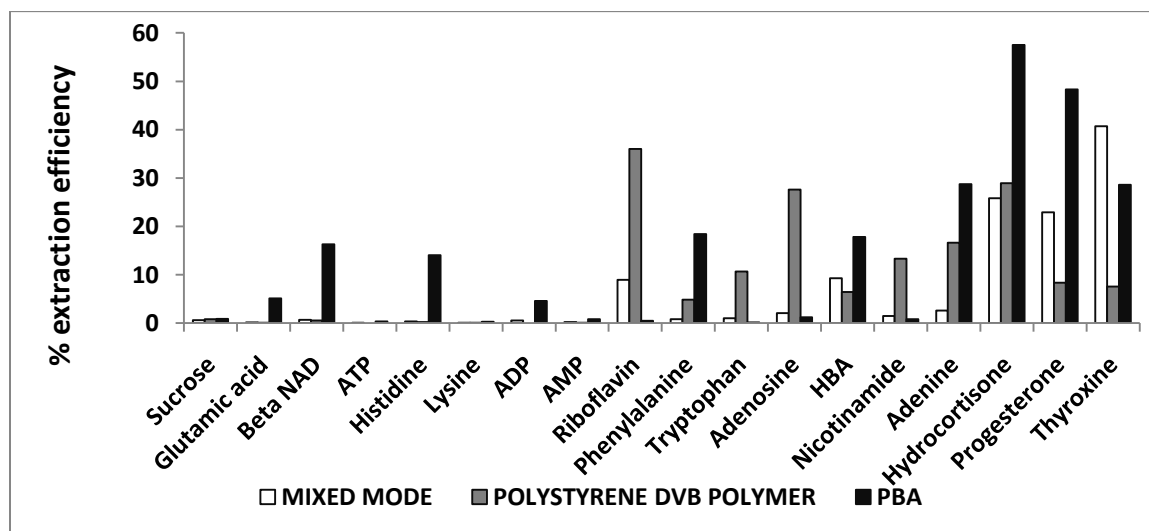


**Figure 5.10 Comparison of three most promising types of coatings for global metabolomic studies for the extraction of representative metabolites at pH 7.4: mixed mode coating, polystyrene divinylbenzene polymer and PBA coating. For mixed mode coating, experimental results for  $C_8$  with benzenesulfonic acid coating from UCT is shown as example. For polystyrene divinylbenzene polymer coating, the results for HRP coating from Macherey Nagel are shown. Correction factor to account for differences in particle size was applied as discussed in text to facilitate the comparison between various coatings. The metabolites are arranged in the order of decreasing polarity (increasing log P value) from left to right to illustrate any trends with respect to analyte polarity.**

tested -1.3 to 4.1) *versus* HR-P sorbent, but Oasis HLB sorbent showed the best overall performance and was selected for further use. This sorbent is similar to Oasis sorbents included in current comparison, but without addition of an ion-exchange group. Low recoveries were observed for acidic compounds using EASY and HR-P sorbents but this was attributed to poor desorption efficiency due to the use of unoptimized elution protocol, and recoveries were improved with subsequent elution steps. Recoveries for acidic compounds have been reported to be lower using Easy sorbent than hydrophobic sorbents such as Chromabond HR-P.<sup>195</sup> For EASY sorbent, the effect of preconditioning was previously evaluated. Addition of preconditioning step was important for acidic species, while extraction efficiency for basic and neutral compounds remained the same regardless of the inclusion of preconditioning step.<sup>196, 220</sup>

Phenylboronate resins and phenylboronic acid sorbents were previously successfully used for targeted metabolomics analysis of urinary nucleosides due to selective binding of cis-diol groups available on ribose sugar group under basic conditions.<sup>221</sup> However, for the latter sorbent type, selectivity for cis-diol groups can be modified by using aprotic conditions which enables the extraction of Lewis base containing compounds, especially amino species. Their data indicates suitability of phenylboronic sorbents for more generic screens, similar to results obtained in our study. However, our results were not obtained under aprotic conditions so a further study of the mechanism involved would be interesting for the compounds not expected to bind to phenylboronic acid.

In another study focused on developing SPE method for metabolomics analysis of urine by NMR, the authors propose the use of two SPE cartridge system C<sub>18</sub> and Hysphere strong hydrophobic polystyrene divinylbenzene resin.<sup>56</sup> In this method, hydrophobic species are trapped on C<sub>18</sub> cartridge, while non-retained polar species are subsequently trapped on Hysphere polystyrene-divinylbenzene sorbent, results which are in good agreement with our findings. In contrast to our study, these authors recommend extraction at pH 3. Among 72 observed metabolites, 28 were retained on C<sub>18</sub>, 23 on PS-DVB, and 21 metabolites were retained by both types of sorbent. Overall the use of SPE methodology was found to work well and allowed identification of various amino acids, organic acids, osmolytes, polyols, methylamines, saturated and unsaturated fatty acids and their derivatives, aromatic compounds and bile acids.

## 5.4 Conclusions

In this study, the coatings suitable for the simultaneous extraction of polar and hydrophobic species at physiological pH were identified. The results indicate that good metabolite coverage can be achieved using these new coatings, and this was explored further for the extraction of human plasma reported in Chapter 6. In preparation for *in vivo* global metabolomic studies it is important to produce the identified best coatings in biocompatible format. On the basis of this research, Supelco produced biocompatible prototype mixed-mode coatings using the same procedure they developed for C<sub>18</sub> and RPA coatings as described in Chapter 3. The production of polar-modified PS-DVB and PBA coatings in biocompatible format is currently under development. Some of the preliminary results of this study indicate the coating coverage with the biocompatible layer can have some impact on the extraction efficiency of polar species in particular (for example, comparing the results of RPA 3  $\mu\text{m}$  *versus* RPA Supelco). This could be a potential further area of study to select a biocompatible polymer with minimum impact on extraction of polar metabolites.

## Chapter 6

# Development and evaluation of global SPME-LC-MS metabolomics methods on benchtop Orbitrap instrument

### 6.1 Preamble and introduction

#### 6.1.1 Preamble

This work has not yet been published. Biocompatible mixed-mode prototype coatings were obtained as research samples from Supelco on the basis of the findings reported in Chapter 5. These new coatings were prepared using the same semi-automated batch coating procedures previously described in Chapter 3. I am the sole author of all other experimental work reported herein.

#### 6.1.2 Introduction: metabolomics and high-resolution mass spectrometry

Various LC-MS platforms have been successfully employed to date for global metabolomics analysis including triple quadrupole<sup>212, 222</sup>, ion trap<sup>43, 44, 70, 205</sup>, time-of-flight (TOF)<sup>12, 45, 211</sup>, quadrupole time-of-flight (QTOF)<sup>17, 51, 208, 214, 215, 223</sup>, Orbitrap<sup>36, 216, 224</sup> and Fourier transform ion cyclotron resonance (FTICR)<sup>38, 39, 205</sup> instrument. Instruments with low mass resolution (quadrupole and ion trap) are not ideally suited for this type of analysis, as many metabolites can have exactly the same nominal mass. Considering the complexity of LC chromatograms it is not feasible to assume that chromatographic resolution is sufficient to separate all possible metabolites with the same nominal mass. As such the use of higher mass resolution instrument such as TOF, Orbitrap and ICR is preferred as it can resolve peaks with the same nominal mass in mass dimension, and provide very accurate metabolite mass and isotope ratio information which can aid in tentative identification by assigning or narrowing down the possible chemical formulas that could give rise to this mass. Among these instruments, TOF and QTOF type of instruments have the advantage of very fast data acquisition times, while the resolution achievable is approximately 10,000-20,000 depending on the exact instrument design. Orbitrap instruments can have resolution up to 100,000, but data acquisition speeds are lower than for TOF instruments. ICR instruments offer the highest mass resolution (up to 1,000,000), but data acquisition speeds are lower and they can be difficult to couple with LC methods and often require use of nano-LC.<sup>38</sup> With the improvement of the duty cycles of triple quadrupole instruments, they can also be used for targeted monitoring of selected metabolites with high sensitivity and specificity, but the main disadvantages of this approach are that only a finite number of transitions can be monitored. This

means that the data on only selected metabolites are collected, thus losing the advantage of global metabolomics methods.

In current work, new type of benchtop Orbitrap instrument (Exactive, Thermo Fisher, San Jose, CA, USA) was employed and the metabolomics methods previously reported in Chapter 5 using ion trap instrument, were transferred onto this high resolution instrument. The main reason for the change in platforms was an increased mass resolution (100,000), improved mass accuracy (<5 ppm for most compounds with external calibration), improved sensitivity and ability to use higher LC flow rates *versus* ion trap instrument due to better design of ESI source. In addition to the collection of full scan high-resolution data, the use of this instrument was also reported to enable simultaneous quantitative analysis of selected analytes by isolation of narrow mass windows around monoisotopic  $m/z$  of interest.<sup>225</sup> The isolation of such narrow mass windows eliminates significant amount of noise and permits quantitation with similar figures of merit to what has traditionally been obtained on triple-quadrupole instruments.

In Exactive, which is the benchtop single stage MS used in current study, the ions are transferred from ion source to heated capillary to tube lens to skimmer to RF lens to lens L0 through analyzer ion optics in order to reach the C-trap. The ions are then accumulated in C-trap, their energy is dampened using nitrogen gas and they are then injected in a short burst into Orbitrap. The main operating principle of Orbitrap detector involves trapping of ions in an electric field around a central spindle-shaped electrode.<sup>226</sup> The movement of ions induces an image current on the outer barrel-like electrode, and  $m/z$  of ions is determined based on their oscillation frequency after performing Fourier transformation. The resolution of the analysis is determined by the length of oscillating time, and maximum resolution achievable is 100,000 at full width half-maximum of reference  $m/z$  of 200. This means that higher resolution is typically achievable for masses lower than  $m/z < 200$  and lower resolution is achievable for  $m/z > 200$ .<sup>227</sup>

### 6.1.3 Strategies for improving metabolite coverage in LC-MS metabolomics

The main strategies reported to date in order to improve metabolite coverage in global metabolomics methods by LC-MS include: using both positive and negative electrospray ionization modes, use of complementary LC methods relying on different separation mechanisms (see Chapter 5), use of different ionization sources (atmospheric pressure chemical ionization, atmospheric pressure photoionization) and the use of ultra-high performance liquid chromatography (UHPLC) or capillary liquid-chromatography with nanospray ionization.<sup>30, 31, 55, 205, 228</sup> Capillary methods are



ideally suited for coupling with ESI because of slow flow rates, and have been demonstrated to improve metabolite coverage. However, run times for these methods can be very long, for example 60-min run time was used in a recent study with 25-min wash step between each injection, for a total run time of 85 min/sample using only a single ionization mode<sup>67</sup>, although run times as long as 2000 min/sample have also been reported<sup>31</sup>. This low throughput is a major disadvantage for large-scale metabolomic studies, so the use of capillary methods is currently not widespread. Previous studies comparing the performance of HPLC (LC performed on columns with particles with 3-10  $\mu\text{m}$  size) *versus* ultra-high performance liquid chromatography UHPLC (LC performed on columns with sub 2  $\mu\text{m}$  particle size) showed improved performance of UHPLC methods in terms of sample throughput, analytical sensitivity and metabolite coverage.<sup>30, 205</sup> For example, Evans *et al.* were able to reduce run time from 32 min to 12 min per sample by switching from HPLC to UHPLC, while obtaining narrower chromatographic peaks (increased peak height translates into increased analytical sensitivity) and improved chromatographic resolution due to the decrease in particle size.<sup>197</sup> However, these studies were performed on TOF MS instrument or linear ion trap instruments capable of high acquisition rates. In our study, although Accela U-HPLC system is capable of operating under both HPLC and UHPLC conditions, HPLC mode was selected in order to ensure sufficient number of data points can be obtained across chromatographic peak using Exactive scan rates of 1 Hz at maximum 100,000 resolution. Bateman *et al.* previously demonstrated that at 1 Hz data acquisition rate, too few data points are collected when coupling UHPLC with Exactive Orbitrap instrument.<sup>199, 225</sup> The selection of HPLC *versus* UHPLC in current study means that longer analysis times were required and that some analytical sensitivity and metabolite coverage may have been lost in comparison to UHPLC methods. However, this choice was made to ensure good method precision and sufficient number of points across the peak to permit semi-quantitative differential analysis of the obtained profiles.

Finally, fast polarity switching is available on Exactive instrument (1 second switch between positive and negative ionization modes) and although successful use of this type of feature was reported<sup>26, 44</sup>, this feature was not utilized in current work because it is impossible to find ion transmission conditions which will simultaneously give stable electrospray in both positive and negative mode. Also, polarity switching would further reduce the number of points across the peak, which could worsen overall method precision even further for some peaks. Data quality was deemed more important than sample throughput, so all samples were analyzed separately in positive and negative ionization modes using each of proposed LC-MS methods. The importance of

performing analysis in both positive and negative ESI modes was demonstrated using recent metabolomics study on human serum, where the use of negative ESI was found to increase metabolite coverage by >90%.<sup>124, 228</sup> The use of APCI in positive mode, MALDI and desorption ionization on silicon (DIOS) mass spectrometry further enhanced metabolite coverage but the gains in metabolite coverage over electrospray methods were more modest (~20%). However, the cited study was performed using low resolution MS, giving rise to possibility of incorrect ion assignments, so the number of unique ions may be somewhat underestimated for each method.

The main objectives of the research presented in this chapter were to set-up and evaluate the performance of reverse-phase and HILIC LC-MS methods on Exactive with the goal of developing very robust methods with optimum analytical sensitivity. Furthermore, mixed-mode coating identified in Chapter 5 and subsequently produced by Supelco in the biocompatible format and housed within an *in vivo* device such as described in Chapter 3 was evaluated for the extraction of selected metabolites in human plasma, with particular focus being paid to parameters such as ionization suppression, extraction time and analyte carryover. Prior to their use in metabolomic studies as described below, the extraction efficiency of these new Supelco biocompatible coatings was evaluated using targeted extraction of benzodiazepines according to the procedures described in Section 3.3.10. The inter-fibre reproducibility was found to be <5% RSD before proceeding with the metabolomics applications.

## **6.2 Experimental**

### **6.2.1 Materials and reagents**

All reagents used for mobile phase preparation were of LC-MS grade. LC-MS grade solvents and LC-MS grade formic acid (1 mL glass ampoules) were obtained from Fisher Scientific. LC-MS grade salts were obtained from Sigma-Aldrich (Oakville, Canada).

### **6.2.2 LC-MS analysis**

LC analysis was performed using Accela U-HPLC system and Accela autosampler (Thermo Scientific, San Jose, CA, USA). Injection volume for all analyses was 10 µL. Autosampler trays were cooled to 4°C.

### 6.2.2.1 Reverse-phase LC method using pentafluorophenyl stationary phase

Chromatographic separation was performed using Discovery HS F5 column, 2.1 x 100 mm, 3  $\mu\text{m}$  particle size (Supelco, Bellefonte, PA, USA) using method previously described in Chapter 5. Guard column with same stationary phase and dimensions of 2.1 mm x 20 mm was used to extend column lifetime. Flow rate was 300  $\mu\text{L}/\text{min}$ . Mobile phase A consisted of water/formic acid (99.9/0.1, v/v) and mobile phase B consisted of acetonitrile/formic acid (99.9/0.1, v/v). The gradient conditions employed for the analysis were 100% A from 0 to 3.0 min, linear gradient to 10% A from 3.0 to 25.0 min and isocratic hold at 10% A until 34.0 min. The column was re-equilibrated to starting mobile phase conditions for 6 min, for a total run time of 40 min per sample.

### 6.2.2.2 HILIC LC method using aminopropyl stationary phase

Bajad *et al.* compared the performance of different reverse-phase and HILIC methods for their ability to retain water-soluble cellular metabolites.<sup>222</sup> Based on the results of this study, amino column, pH 9 and 50 min total analysis time were identified as the best chromatographic conditions to analyze highly polar water-soluble species. In current work, similar conditions were found to work the best after comparison of mobile phases pH 3, 7 and 9. In comparison to literature method, the run time in current work was shortened to 30 min, and salt concentration decreased to 2 mM to avoid ionization suppression and improve analytical sensitivity. The LC column used for this separation was Nucleodur 100-5  $\text{NH}_2$  RP, 2 mm x 250 mm column from Macherey Nagel (Duren, Germany). Gradient elution was used with total flow rate of 500  $\mu\text{L}/\text{min}$ . The composition of mobile phases A and B was ammonium formate-hydroxide buffer, pH 9.0/acetonitrile with proportions of 9/1 (v/v) and 1/9 (v/v), respectively. The total concentration of buffer was kept at 2 mM. The gradient program used was 100% B from 0 to 3.0 min, linear change to 100% A from 3.0 to 8.0 min and hold at 100% A until 22.9 min. The column was re-equilibrated to starting conditions for 7.0 min prior to next injection, thus making the total run time of 30 min per sample.

### 6.2.2.3 HILIC LC method using underivatized silica stationary phase

The LC column used for this separation was Luna HILIC Si, 2 mm x 100 mm column with 3  $\mu\text{m}$  particle size obtained from Phenomenex (Torrance, CA, USA). Analytical column was protected using a guard column with same stationary phase and dimensions of 4 mm x 2 mm obtained from the same manufacturer. Total flow rate was 400  $\mu\text{L}/\text{min}$ . Mobile phase A consisted of acetonitrile/ammonium acetate buffer (9/1, v/v, effective salt concentration 20 mM) and mobile phase

B consisted of acetonitrile/ammonium acetate buffer (1/1, v/v, effective salt concentration 20 mM). Starting mobile phase composition was 100% A held for 3.0 min, with linear ramp to 100% B in 5 min, followed by a 4-min hold at 100% B. The column was re-equilibrated for 8 min prior to next injection, thus making the total run time of 20 min per sample.

#### 6.2.2.4 Summary of optimized MS conditions for all LC methods

MS analysis was performed on Exactive benchtop Orbitrap instrument (Thermo Scientific, San Jose, CA, USA). Only one literature report to date utilized this second-generation Orbitrap instrument for metabolomics/lipidomics studies and the authors do not adequately describe how they selected MS parameters for analysis (capillary voltage 51 V, spray voltage 4.2 kV).<sup>199</sup> Thus, in current study, various parameters were systematically investigated as discussed in Sections 6.3.3 to 6.3.5 in order to ensure suitable full scan parameters were used for the analysis. Based on these results, optimized MS parameters for each method employed are summarized in Table 6.1. The stability of proposed ESI conditions was verified by monitoring spray current and ensuring it was stable at all mobile phase conditions and <1  $\mu$ A for reverse-phase methods and <5  $\mu$ A for all HILIC methods. All experiments were performed at maximum resolution (100,000 resolution, 1 Hz data acquisition) with AGC target set to Balanced (1,000,000 ions). In positive mode, scan range was m/z 100 -1000 for both reverse-phase and HILIC methods. In negative mode, m/z scan range was 80-1000 for reverse-phase and HILIC method using amino column. For HILIC method using underivatized Si column, the scan range was reduced to m/z of 125-1000 in order to eliminate the influence of large intensity m/z 117 background ion.

**Table 6.1 Summary of Exactive MS parameters used for metabolomics.**

LC method	ESI mode	Sheath gas (arb)	Aux gas (arb)	ESI voltage (kV)	Capillary voltage (V)	Capillary temperature (°C)	Tube lens voltage (V)	Max. Inject time (ms)
PFP	Positive	40	25	4.0	27.5	275	100	100
PFP	Negative	50	25	-2.7	-67.5	325	-85	100
Amino	Negative	50	25	-2.5	-55	275	-110	100
Si	Positive	60	30	2.8	90	325	155	250
Si	Negative	50	25	-2.5	-55	275	-110	250

### 6.2.3 Data processing

Known metabolites were processed using Xcalibur software version 2.1 (Thermo Fisher) by extraction of theoretical monoisotopic mass with 5 ppm (for positive ESI) and 10 ppm (for negative ESI) window tolerance and subsequent integration of the resulting extracted ion chromatograms.

Mass accuracy of the measurement is defined as the ratio of mass error (difference between experimentally measured mass and true mass of given analyte) and the theoretical mass, and can be calculated using Equation 6.1.

$$\text{mass accuracy (ppm)} = \frac{m_{\text{exptl}} - m_{\text{theoretical}}}{m_{\text{theoretical}}} \times 1000000 \quad \text{Equation 6.1}$$

### 6.2.4 Evaluation of absolute matrix effects

For this test, human plasma samples were extracted using C<sub>18</sub> or mixed mode (C<sub>18</sub> + benzenesulfonic acid) SPME fibres (n=2 of each type, 45 µm thickness, housed in *in vivo* SPME assembly). The resulting extract was divided into two aliquots: one aliquot was analyzed as is to determine the amount of known endogenous metabolites present. The second aliquot was spiked with known concentration of the metabolites. The signal obtained for this post-extraction spike was compared *versus* neat standard prepared at the same concentration directly in the desorption solvent after taking into account any endogenous level of each metabolite using the simple formula of Equation 6.2. Relative signal intensity of 80-120% were deemed to be free from absolute matrix effects.

$$\% \text{ signal} = 100\% \times \frac{(\text{signal}_{\text{postextraction spike}} - \text{signal}_{\text{blank extract}})}{\text{signal}_{\text{neat standard}}} \quad \text{Equation 6.2}$$

## 6.3 Results and discussion

### 6.3.1 Comparison of instrumental sensitivity: ion trap *versus* triple quadrupole *versus* benchtop Orbitrap

Prior to setting up metabolomics methods on Exactive, a preliminary evaluation of its performance in comparison to existing ion trap and triple quadrupole instruments was carried out using benzodiazepine standard solutions. The benzodiazepine method for each instrument was optimized using direct infusion of individual standard and the parameters were systematically varied to select the optimum value for each. LOQ on each instrument was first estimated using 10x signal-to noise ratio by injecting progressively more dilute standard solutions. LOQ was then further verified according to Food and Drug Administration method validation guidance to ensure RSD observed at

LOQ level does not exceed 20%.<sup>142</sup> A summary of the results for four benzodiazepines is shown in Table 6.2. It is shown that for these analytes the sensitivity of Exactive in full scan mode is approximately equal to that of API 3000 triple quadrupole instrument in MS/MS mode and even better than sensitivity of Varian 500 ion trap instrument in MS/MS mode. This was very promising result for *in vivo* metabolomics as we were previously able to successfully use API 3000 for analysis of benzodiazepines and carbamazepine after *in vivo* sampling. Full scan mode on either ion trap or triple quadrupole instrument is typically 50-100x fold less sensitive than MS/MS mode (and also less selective), so the overall results show excellent performance of Exactive in full scan mode even when large full scan range is utilized (100-1000 m/z). In another study, the authors compared performance of TOF instrument in MS mode with QTOF instrument in MS/MS mode and found 10-1000-fold improvement in analytical limits of detection.<sup>45</sup>

**Table 6.2 Comparison of instrumental sensitivity for benzodiazepines based on injections of neat standards using reverse phase C<sub>18</sub> method and positive ESI mode.**

Compound	Varian 500 LOQ in MS/MS mode* (pg)	API 3000 LOQ in MS/MS mode (pg)	Exactive LOQ in full scan mode 100-1000 m/z (pg)	Exactive LOQ in full scan mode 250-350 m/z (pg)
Oxazepam	30	1.2	4.2	4.2
Lorazepam	30	1.8	4.7	4.7
Diazepam	12	6	4.3	0.9
Nordiazepam	15	3.6	4.7	0.9

\*full scan mode about 100x less sensitive

### 6.3.2 Development of MS methods on Exactive

In the first step of MS method development, individual standard mixtures of all metabolites described in Chapter 5 were infused directly into Exactive MS using a syringe pump at 5  $\mu$ L/min. The ions observed for each compound in both negative and positive ESI were documented and MS parameters individually optimized for each compound and recorded. All compounds in positive ESI exhibited mass accuracy < 5 ppm except for  $\beta$ -carotene, with poor mass accuracy of 9 ppm (Table 6.3), similar to what was documented elsewhere<sup>229</sup>. A possible explanation for this observation is that fragile or metastable molecular ions such as  $\beta$ -carotene can dissociate according to the following mechanism where  $[M+^1H]^+$  ion loses  $^1H$  resulting in  $M^{++}$  ion. When this reaction occurs in Orbitrap, it decreases the time for mass assignment of  $[M+^1H]^+$  ions, thus resulting in less accurate mass assignment. As a general trend in Tables 6.3 and 6.4, the largest errors are observed for relatively fragile ions which

**Table 6.3 Summary of ions observed and mass accuracy in positive ESI mode during direct infusion of metabolite standard mixture using 5  $\mu$ L/min flow rate.**

Analyte	Theoretical		Observed positive mode			
	MW Pos H	MW Pos Na	MW Pos H	Mass accuracy	MW Pos Na	Mass accuracy
Lysine	147.1128	169.0947	147.1127	-0.68	169.0946	-0.59
Histidine	156.0768	178.0587	156.0767	-0.34	178.0586	-0.55
Maleic acid	117.0182	139.0002	no	no	no	no
Fumaric acid	117.0182	139.0002	no	no	no	no
Citric acid	193.0343	215.0162	no	no	215.0161	-0.58
Hydrocortisone	363.2166	385.1985	363.216	-1.65	no	no
Progesterone	315.2319	337.2138	315.2314	-1.45	no	no
Phenylalanine	166.0863	188.0682	166.0862	-0.33	188.0706	no
Glutamic acid	148.0604	170.0424	148.0604	-0.23	no	no
Tryptophan	205.0972	227.0791	205.0971	-0.26	227.0789	-0.88
Nicotinamide	123.0553	145.0372	123.0554	0.90	no	no
$\beta$ -estradiol	273.1849	295.1669	273.1843	-2.22	no	no
Taurocholic acid	516.2989	538.2809	no	no	538.2803	-1.10
Folic acid	442.1470	464.1289	442.1458	-2.62	464.1277	-2.59
Cholic acid	409.2949	431.2768	no	no	431.2756	-2.77
Ascorbic acid	177.0400	199.0219	no	no	no	no
Glucose	181.0707	203.0526	no	no	203.0522	-2.02
Sucrose	343.1235	365.1054	343.1225	-2.88	365.1043	-3.10
Fructose	181.0707	203.0526	no	no	203.0522	-2.02
Glutathione ox	613.1592	635.1412	613.1587	-0.88	635.1404	-1.23
Adenine	136.0618	158.0437	136.0617	-0.53	none	no
Adenosine	268.1040	290.0860	268.1037	-1.23	290.0854	-1.98
HBA	105.0546	127.0366	no	no	127.0366	0.27
Pyruvic acid	89.0233	111.0053	no	no	no	no
Glutathione red	308.0911	330.0730	308.0902	-2.86	330.0719	-3.41
Protoporphyrin	563.2653	585.2472	563.2651	-0.32	no	no
Retinol	287.2369	309.2189	287.2361	-2.93	no	no
$\beta$ -carotene	537.4455	559.4274	537.4406	-9.08	no	no
Histamine	112.0869	134.0689	112.0872	2.46	no	no
Choline	104.1070	127.0968	104.1073	2.97	no	no
Linoleic acid	281.2475	303.2295	no	no	no	no
AMP	348.0704	370.0523	348.0703	-0.17	370.0523	-0.01
Riboflavin	377.1456	399.1275	377.1453	-0.69	399.1272	-0.77
ADP	428.0367	450.0186	428.0366	-0.21	450.0179	-1.63
Fructose 6-phosphate	261.0370	283.0189	no	no	283.0188	-0.49
Glucose 6-phosphate						
Glucose 1-phosphate						
Ribose 5-phosphate	231.0264	253.0084	no	no	253.0083	-0.30
ATP	508.0030	529.9850	no	no	529.9847	-0.50
UDP	405.0095	426.9914	no	no	no	no
$\beta$ -NAD	665.1242	687.1061	665.1246	0.60	687.1071	1.46
Thyroxine	777.6940	799.6759	777.6940	0.00	no	no

**Table 6.4 Summary of ions observed and mass accuracy in negative ESI mode during direct infusion of metabolite standard mixture using 5  $\mu$ L/min flow rate.**

Analyte	Theoretical	Observed in negative mode	
	MW Neg	MW [M-H] <sup>-</sup>	Mass accuracy
Lysine	145.0983	145.0968	-9.99
Histidine	154.0622	154.0607	-9.76
Maleic acid	115.0037	115.0022	-12.9
Fumaric acid	115.0037	115.0022	-12.9
Citric acid	191.0197	191.0182	-8.00
Hydrocortisone	361.2021	no	no
Progesterone	313.2173	no	no
Phenylalanine	164.0717	164.0704	-7.95
Glutamic acid	146.0459	146.0445	-9.48
Tryptophan	203.0826	203.0814	-5.93
Nicotinamide	121.0407	no	no
$\beta$ -estradiol	271.1704	271.1702	-0.58
Taurocholic acid	514.2844	514.2842	-0.39
Folic acid	440.1324	440.1338	3.16
Cholic acid	407.2803	407.2811	1.96
Ascorbic acid	191.0197	175.0233	no
Glucose	179.0561	179.0547	-7.90
Sucrose	341.1089	341.1092	0.77
Fructose	179.0561	179.0547	no
Glutathione oxidized	611.1447	611.1443	-0.64
Adenine	134.0472	134.0458	-10.61
Adenosine	266.0895	no	no
Hydroxybutyric acid	103.0401	103.0387	-13.30
Pyruvic acid	87.0088	87.0075	-14.60
Glutathione reduced	306.0765	306.0766	0.22
Protoporphyrin	561.2507	no	no
Retinol	285.2224	no	no
$\beta$ -carotene	535.4309	no	no
Histamine	110.0724	no	no
Choline	no	no	no
Linoleic acid	279.2330	279.2332	0.87
Riboflavin	375.1310	no	no
Fructose 6-phosphate	259.0224	259.0225	0.21
Glucose 6-phosphate	See above	see above	no
Glucose 1-phosphate	See above	see above	no
Ribose 5-phosphate	229.0119	229.0114	-2.10
AMP	346.0558	346.0567	2.57
ADP	426.0221	426.0237	3.66
ATP	505.9885	505.9888	0.65
UDP	402.9949	402.9963	3.42
$\beta$ -NAD	662.1018	662.1030	1.74
Thyroxine	777.6951	no	no



can dissociate early. This can occur in Orbitrap as a result of ion energy deposition during the injection of ions from C-trap into the Orbitrap detector. All compounds in negative ESI mode exhibited mass accuracy <15 ppm (Table 6.4). Mass accuracy was particularly poor (10-15 ppm) for compounds with  $m/z < 200$  indicating that Orbitrap mass calibration procedure in this region may use further improvement by inclusion of an ion with  $m/z < 100$  during the mass calibration process. A useful approach for further increasing mass accuracy using Orbitrap instrument is to use background ions to perform internal calibration during each sample run, and resulting mass accuracy was improved from 1-2 ppm to 0.2 ppm.<sup>230</sup>

Therefore, among the compounds tested 25 were observed in positive mode and 31 in negative mode. Total of 21 compounds were observed in both modes, but the method sensitivity is not the same in both modes. These results show significant overlap in the metabolite coverage by both modes using the selected metabolite test mixture, but the best coverage and analytical sensitivity is obtained when the data from two modes is combined. According to literature, the complementary nature of the two modes has also been documented with Giavalisco reporting only 10% overlap between the two modes in plant metabolomics study<sup>38</sup> and 14% overlap reported in the analysis of human plasma<sup>205</sup>. In contrast Xie *et al.* used only positive ESI mode on the basis of greater number of total metabolites observed during their metabolomics study on urine to study acute toxicity of melamine.<sup>204</sup>

Table 6.5 shows that the combination of chromatographic and ionization conditions can have significant impact on the analytical sensitivity of a given metabolite. For example, the LOQ of taurocholic acid can be improved 275-fold by performing analysis in negative ESI mode (using reverse phase LC-MS method). On the other hand, analytical sensitivity for folic acid is improved by 50-fold by the use of HILIC method and negative ESI. These differences can be important as a metabolite may not be detected by one method, but successfully detected by another. The use of complementary methods provides improved metabolite coverage.

### **6.3.3 Evaluation of reverse-phase LC-MS method using pentafluorophenyl column**

The effect of capillary and tube lens voltages was evaluated, while spray voltage and capillary temperature were kept constant at 4000V and 275°C respectively. Example results are shown for positive ionization mode in Figure 6.1. No significant differences between methods 1 (capillary voltage 27.5 and tube lens voltage 100 V) and 2 (capillary voltage 57.5 and tube lens voltage 110 V) were observed. Positive method 3 (capillary voltage 90 V, tube lens voltage 170 V) showed 2-fold decrease in sensitivity for analytes with lower MW, but no significant improvement for higher MW

**Table 6.5 Summary of LOQs obtained for various metabolites using proposed LC-MS methods on Exactive instrument.**

Analyte	LOQ - Amount injected on-column (pg)			
	Positive ESI – reverse phase	Positive ESI – HILIC	Negative ESI – reverse phase	Negative ESI – HILIC
Phenylalanine	1.3	700	26	5.0
Histidine	1.9	85	76	85
Lysine	2.1	105	NA	11
Tryptophan	2.1	117	41	12
Progesterone	2.9	119	NA	NA
Hydrocortisone	3.5	2430	NA	7.3
Riboflavin	4.0	37	NA	NA
Adenosine	8.2	11	NA	109
Glutamic acid	9.0	840	5.4	9.2
Adenine	9.3	5.5	9.3	5.5
Nicotinamide	28	12	NA	NA
Protoporphyrin	28	NA	NA	NA
Thyroxine	39	286	NA	286
AMP	55	110	NA	110
Histamine	155	NA	NA	NA
Glutathione reduced	203	97	20	97
Taurocholic acid	550	89	2.0	8.9
Cholic acid	673	827	6.7	9.1
Glutathione oxidized	1800	418	540	418
Folic acid	2100	42	NA	42
Ascorbic acid	9900	NA	990	130
Sucrose	13550 (Na)	19 (Na)	NA	189
Glucose+fructose	24200	4260	24	35-116
Citric acid	25850 (Na)	NA	860	2350
Choline	0.03	NA	NA	NA
Ribose phosphate	NA	3610	24	107
β-NAD	NA	124	693	124
Glucose-or-fructose phosphate	NA	2610	30	19
Pyruvic acid	NA	NA	269	5650
Maleic and fumaric acid	NA	NA	285	NA
Hydroxybutyric acid	NA	NA	19	NA
β-estradiol	NA	NA	NA	1610
Linoleic acid	NA	NA	2390	NA
ATP	NA	540	NA	540
UDP	NA	630	NA	630
ADP	NA	128	NA	1170

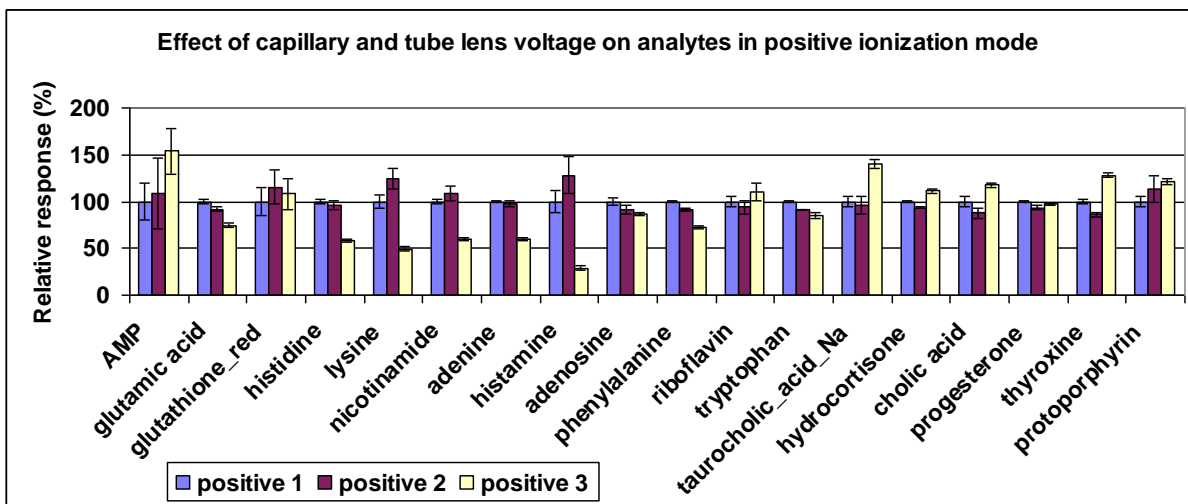


**Figure 6.1** Effect of capillary and tube lens voltage on signal intensity of selected analytes using positive ESI PFP LC-MS method. The capillary and tube lens settings for methods positive 1, 2 and 3 were 27.5 and 100 V, 57.5 and 110 V and 90 and 170 V, respectively.

analytes *versus* methods 1 and 2. Based on this data, capillary and tube lens voltages of 27.5 V and 100 V, respectively, were selected for future studies. Similar evaluation was performed in negative ESI mode and capillary and tube lens voltages of -67.5 V and -85 V were selected as optimum for the chosen metabolite mixture. These results are in agreement with Brown *et al.* who investigated the effect of tube lens voltage in negative ESI mode on the number of metabolites detected and the propensity of ions to fragment or form adducts under different electrospray conditions.<sup>33</sup> It was found that higher voltages (100 V *versus* 20 V) showed increased number of peaks without significant amounts of fragmentation. However, no evaluation of sensitivity similar to that performed in current study was carried out.

One of the problems that is commonly observed in LC-MS analysis is ionization suppression or enhancement caused by co-eluting matrix components. For targeted analysis, the goal of sample preparation is to remove as many of these matrix components as possible. Isotopically labeled standards are also used in order to compensate for any remaining matrix effects due to incomplete removal of possible interferences.<sup>50</sup> In metabolomics, the situation is much more complicated as the analysis of all compounds is desired, so the goal of sample preparation is to be as unselective as possible. In this case, great issues with matrix effects can be expected. To evaluate SPME performance in terms of this parameter, the absolute matrix effects were evaluated. The results obtained in this experiment are shown in Figure 6.2. In positive ESI, significant absolute matrix

effects were observed only for citric acid using both coatings tested (C<sub>18</sub> and mixed mode). In negative ESI, the majority of metabolites showed no ionization suppression or enhancement, indicating satisfactory performance of SPME method. However, significant ionization suppression was considered as % signal <80% and was observed for ascorbic acid using C<sub>18</sub> coating. Significant

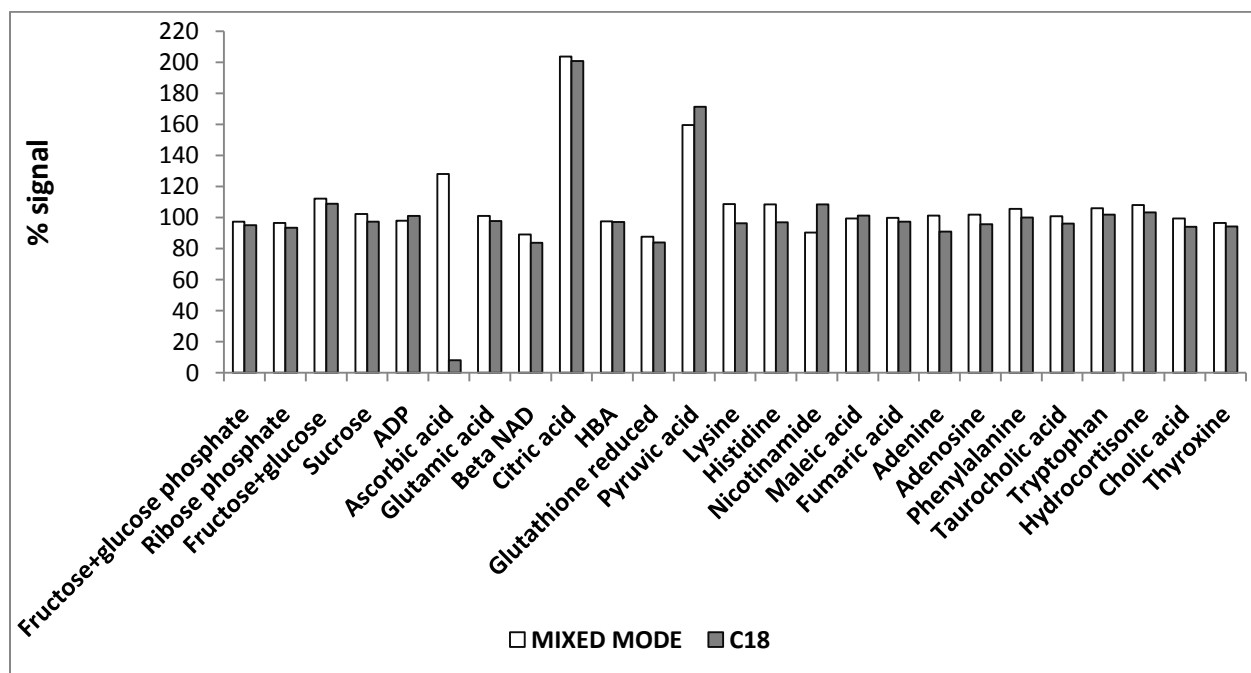
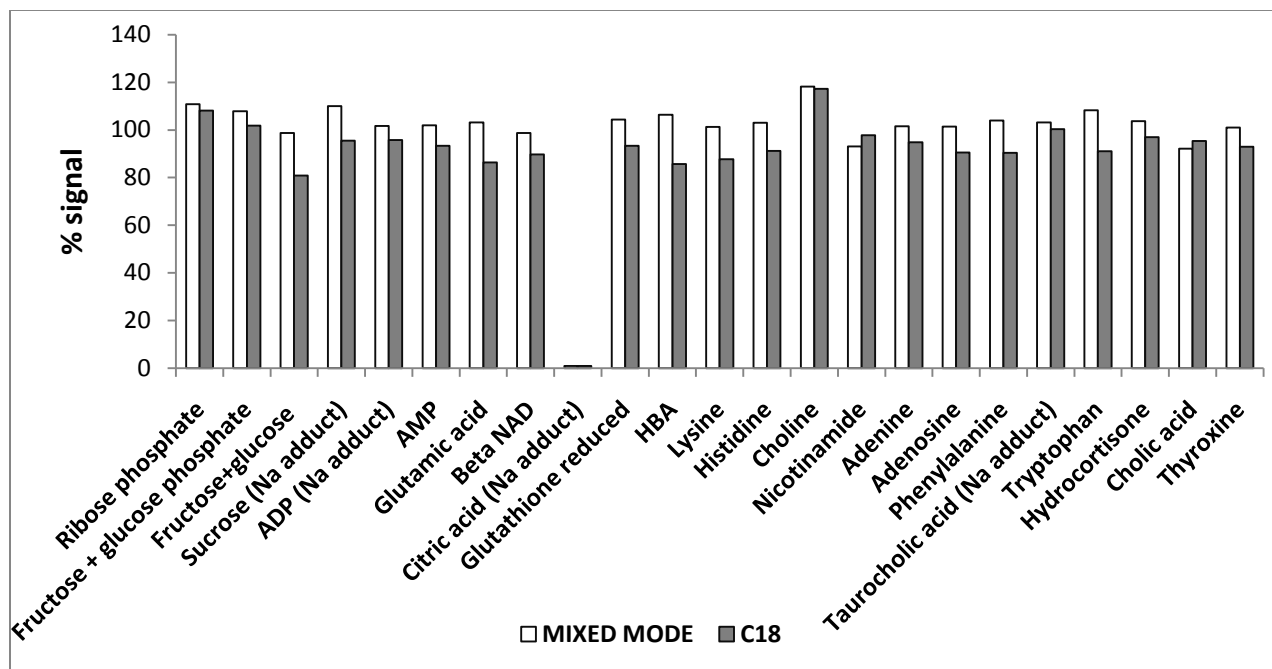


**Figure 6.2 Evaluation of absolute matrix effects using (a) positive and (b) negative ESI reverse-phase LC-MS method with PFP column. Percent signal was calculated as the area obtained in human plasma extract spiked post-extraction versus neat standard at the same concentration level prepared directly in desorption solvent. Percent signal >120% represents ionization enhancement for a given metabolite and % signal <80% represents ionization suppression for a given metabolite. The results are shown for two types of Supelco biocompatible coatings: mixed mode and C<sub>18</sub> coatings.**

ionization enhancement (% signal >120%) was observed for citric and pyruvic acid (both coatings). The result for citric acid was not surprising in this particular test as this analyte was present in large concentrations since it was used as anti-coagulant in human plasma sample used for the study. Citric acid peak was the most intense peak in the entire chromatogram in either ionization modes (taking into account both known and unknown metabolites). Ascorbic acid and maleic acid were not chromatographically resolved from large citric acid peak, which affected their ionization properties. Interestingly, hydroxybutyric acid,  $\beta$ -NAD and reduced glutathione also eluted within the same retention time window and exhibited no significant suppression or enhancement, indicating the effect was analyte dependent, not only retention time dependent. In positive ESI mode, no metabolites which co-eluted with citric acid showed any significant ionization suppression or enhancement. Finally, it should be noted for the cases where an apparent ionization enhancement was observed, this is not likely to be true enhancement of the signal. This unexpected increase in signal can most likely be attributed to fragmentation of other species within the complex matrix which contain the particular group (for example, citrate or pyruvate in current example).

#### **6.3.4 Evaluation of LC-MS method using amino column for improved separation of sugar compounds**

Using HILIC method employed in Chapter 5, it was not possible to achieve chromatographic separation of sugars such as glucose and fructose, or various sugar phosphates. Considering these species are also isobaric, they cannot be distinguished by mass spectrometric detector, which makes chromatographic resolution of these species highly desirable. To address this issue, the use of LC column with aminopropyl phase was investigated, as this column packing was reported to enable separation of various sugars under reverse phase conditions. The successful use of this column packing under HILIC conditions was also reported by Bajad *et al.* for separation of various polar metabolites of interest in current work.<sup>222</sup> In fact, in this study Bajad *et al.* tested nine different LC-

MS methods (both reverse phase and HILIC) and found that aminopropyl column in HILIC mode at pH 9 performed the best for separation of large number of polar metabolites.

Thus, in current study, the performance of aminopropyl column using both reverse phase and HILIC modes was tested. The particular focus was paid to polar metabolites containing sugar and/or phosphate moieties which were not well retained on pentafluorophenyl column. Using reverse phase mode, the retention of some sugar compounds was still not satisfactory while other compounds were too broad or suffered from excessive tailing. HILIC mode at pH 9 was found to provide best retention for the compounds of interest and an example chromatogram of selected metabolites is shown in Figure 6.4. Furthermore, this amino column based method was not as sensitive to high aqueous content of injection solvent as HILIC method based on underivatized silica making it more suitable for metabolomics. Based on these results, it was investigated whether this amino method can completely replace HILIC method proposed in Chapter 5 and the performance of the method using human plasma samples was evaluated.

As a first step, the absolute matrix effects were evaluated to ensure that a significant degree of ionization suppression or enhancement was not observed. The results obtained in this experiment are shown in Figure 6.3. Significant suppression was observed for taurocholic acid using both coatings, and for glucose, fructose and histamine using mixed-mode coating.

However, when it was attempted to use the method for a full sample set, two important problems were encountered. First, a significant loss of signal intensity over time was observed for all metabolites due to build-up of salt deposits in the ion source even though volatile salts were employed. This is illustrated in using the results of two QC samples. After ~ 10 hr of run time, significant loss of intensity was observed as shown by drop in intensity for most compounds (QC2) and after ~20 hr of run time the loss of signal intensity was so severe that 13 out of 21 compounds could no longer be observed. Based on these results, the method was not deemed suitable for further use. This lack of robustness is surprising considering that similar method was employed by Bajad *et al.* for the analysis of *Escherichia coli* extracts using similar design ion source as employed in our analysis.<sup>222</sup> The same method was also successfully employed in cross-platform comparison for quantitative metabolomics study of primary metabolism.<sup>45</sup> One possible explanation for this discrepancy is that Bajad *et al.* analyzed very small sample sets at a time with full source cleaning between sets, but this was not discussed in manuscript. For example, in our work, analysis of 15-20 samples at a time would yield acceptable results such as reported by Bajad *et al.* (intra- and inter-day

RSD <35% for 141 out of 144 compounds analyzed). However, such small sample sets are not feasible for metabolomic studies which typically require analysis of large number of samples as well as quality control samples to ensure data integrity. Another possible explanation is poor stability of stationary phase under high pH conditions resulting in phase bleed contaminating MS, as the columns used in our study and in literature studies were obtained from different manufacturers. This could be possibly addressed by using stationary phase bonded to a stable polymer rather than silica particles.<sup>55</sup>

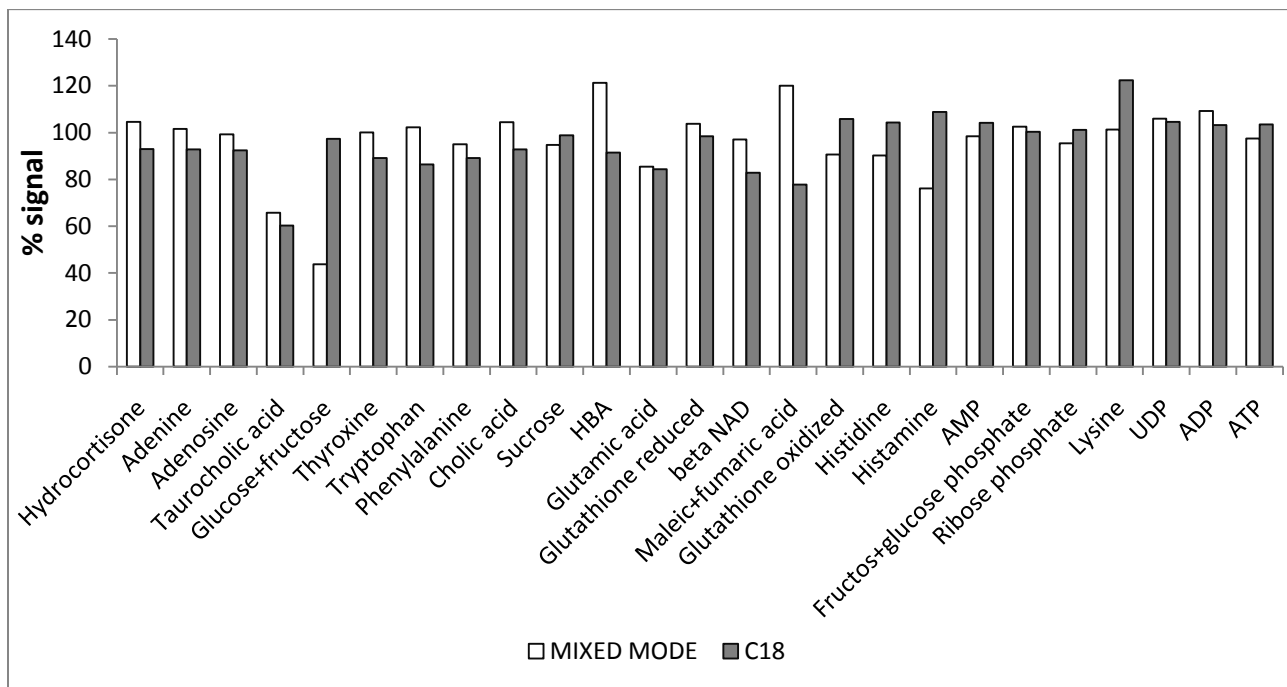


**Figure 6.3 Evaluation of absolute matrix effects using negative ESI HILIC LC-MS method with amino column. Percent signal was calculated as the area obtained in human plasma extract spiked post-extraction *versus* neat standard at the same concentration level prepared directly in desorption solvent. Percent signal >120% represents ionization enhancement for a given metabolite and % signal <80% represents ionization suppression for a given metabolite.**

### 6.3.5 Evaluation of HILIC LC-MS method on Exactive using underivatized Si column

HILIC method developed in Chapter 5 was transferred to Exactive instrument and its performance for metabolomics analysis of plasma was investigated. The minimum recommended buffer salt concentration for this column was 5 mM, so this was used as starting mobile phase *versus* 2 mM used in method developed in Chapter 5. However, the use of this mobile phase resulted in very broad peaks especially for phosphate-containing species such as AMP and ADP as well as oxidized glutathione as

shown in Figure 6.4 (b). Using these conditions, ATP and UDP were not detected at all. This finding agrees with the results reported by Kamleh *et al.* who did not detect ATP when only formic acid was used as additive in their proposed HILIC method.<sup>216</sup> Increasing pH to improve peak shape of phosphates while retaining chromatographic resolution was not possible due to working pH range of the column (up to pH 8). Chromatographic peak shape was improved by increasing salt concentration to 20 mM and modifying gradient conditions as shown in Figure 6.4 (a). Increasing buffer concentration helped the peak shape by reducing electrostatic interactions

**Table 6.6 Results of QC sample analysis for known metabolites using negative ESI mode HILIC LC-MS method with aminopropyl column. % signal intensity of QC2 and QC3 is shown with respect to signal intensity observed for QC1 with approximately 10 hr elapsed between each QC sample. Signal intensity observed for QC1 was set to 100%.**

Analyte	QC2 % signal	QC3 % signal
Hydrocortisone	ND	ND
Adenine	ND	ND
Taurocholic acid	135	ND
Glucose+fructose	17	ND
Thyroxine	124	20
Tryptophan	34	8
Phenylalanine	41	4
Cholic acid	27	ND
Sucrose	100	8
HBA	18	2
Glutamic acid	30	8
Maleic+fumaric cad	2	ND
Histidine	57	4
Histamine	113	ND
AMP	37	6
Fructose+glucose phosphate	6	ND
Ribose phosphate	ND	ND
Lysine	30	ND
UDP	ND	ND
ADP	ND	ND
ATP	ND	ND

between charged analytes and stationary phase. Further increases in salt concentration were not investigated because of possible ionization suppression effects as salt concentration is further increased. The results of this development indicate that the exact properties of HILIC columns can vary to a large extent between manufacturers and demand thorough method re-optimization even when a stationary phase of the same type is employed. Therefore, the proposed method resulted in



acceptable peak shapes and chromatographic resolution between metabolites, except for sugar phosphates which co-eluted. Lack of chromatographic resolution between eluting components can result in ionization suppression or enhancement, so matrix effects were investigated in detail.

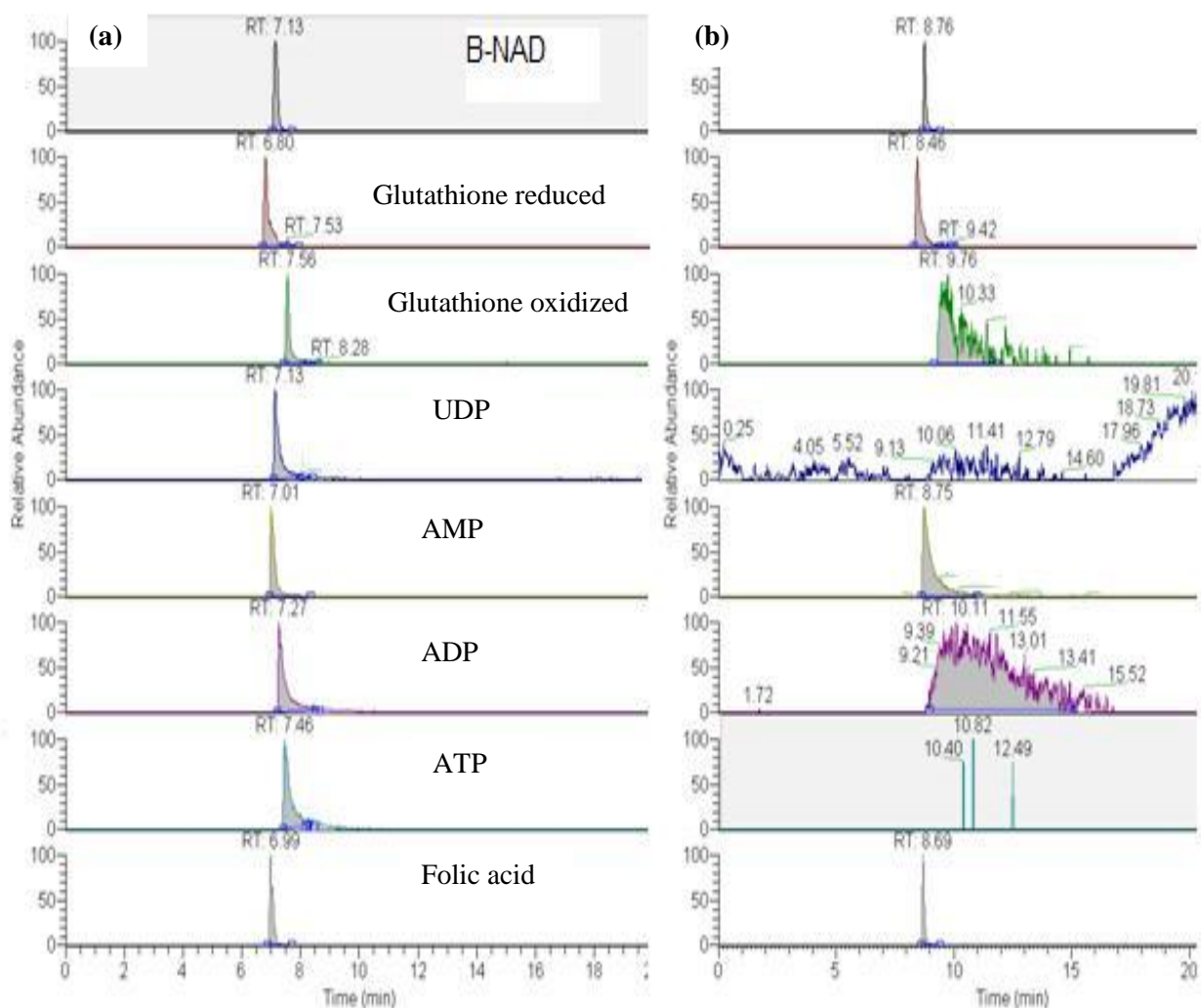


**Figure 6.4 Example XIC of metabolite standard solution prepared at 1  $\mu\text{g/mL}$  in 60% acetonitrile and analyzed using HILIC method with unmodified Si column in negative ESI mode (a) final method using 20 mM effective concentration of buffer and (b) initial method using 5 mM effective concentration of buffer. Only selected metabolites are shown for clarity.**

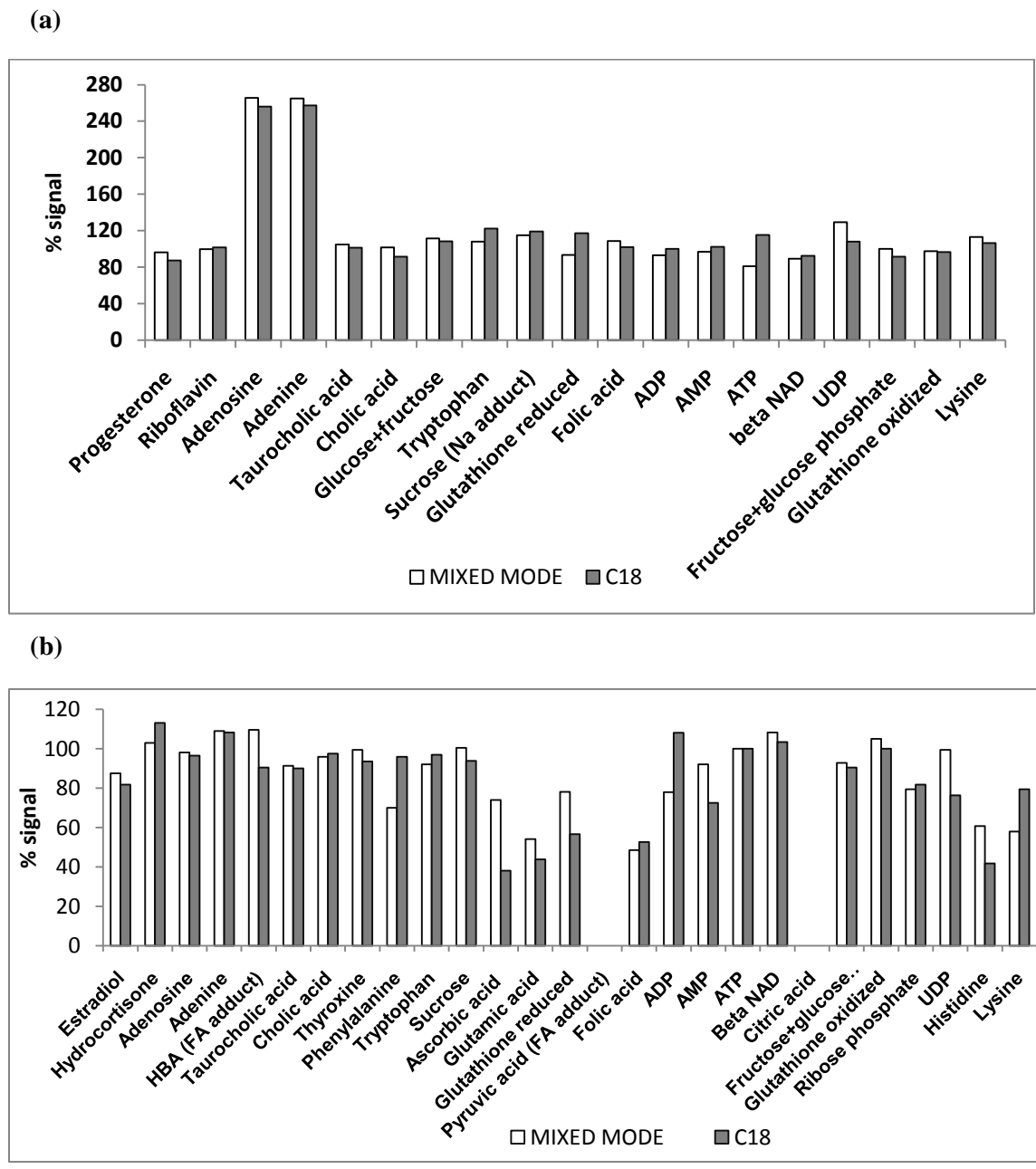


**Figure 6.5 Evaluation of absolute matrix effects using (a) positive and (b) negative ESI HILIC LC-MS method with underivatized Si column. Percent signal was calculated as the area obtained in human plasma extract spiked post-extraction *versus* neat standard at the same concentration level prepared directly in desorption solvent. Percent signal >120% represents ionization enhancement for a given metabolite and % signal <80% represents ionization suppression for a given metabolite.**

The results obtained in positive and negative ESI modes with proposed method are shown in Figure 6.5. Overall the results were satisfactory, except in the region of 3-4 min where significant ionization suppression was observed as indicated by the results for ascorbic acid, glutamic acid, pyruvic acid, folic acid and reduced glutathione in negative ESI mode. However, these species were well-retained on PFP column and most of these species (except ascorbic acid) did not show adverse ionization effects using reverse-phase LC-MS method. Thus, they should be analyzed using reverse-phase method. Furthermore, ionization suppression was observed for phenylalanine (mixed mode fibre) as well as histidine and lysine (both coatings). These species were also well-retained on reverse-phase method and could be suitably analyzed using that method with no adverse matrix effects. Citric acid also showed significant ionization suppression, due to its use as anti-coagulant in the batch of human plasma used for this analysis. The analytes of interest for HILIC separation such as phosphates did not show any ionization suppression or enhancement indicating suitability of the method for the metabolomics analysis of plasma as a complementary method to reverse-phase method.

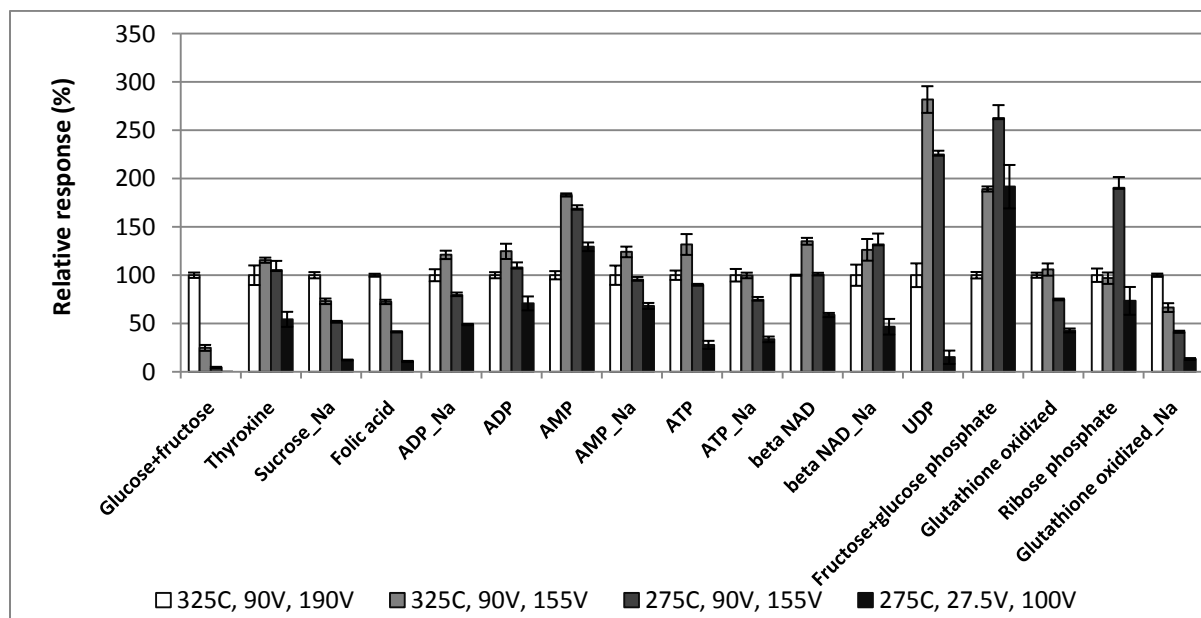
In a targeted metabolomics study employing mixed-mode extraction using Strata-XCAW significant absolute matrix effects for estrogens were encountered (all target estrogen species not detected when spiked in biological matrix) even though analysis was performed using reverse-phase method where estradiols have good retention and chromatographic resolution between different species can be achieved.<sup>231</sup> In our study we did not detect estradiol using reverse-phase method (below method LOD, presumably due to presence of acid in mobile phase as documented previously<sup>231</sup>). Using HILIC method estradiol peak was detected and was not subject to ionization suppression, even though it eluted with solvent front using HILIC column (retention time of 0.9 min), where matrix effects are expected to be the most predominant. The predominance of matrix effects using traditional exhaustive techniques has been well-documented in various targeted analysis, although it has been largely unreported in global metabolomic studies. For example, in a study examining levels of amino acids in plant seeds, ionization suppression of 31-65% was reported for all amino acids tested with worst performance for glutamic acid, aspartic acid and serine.<sup>212</sup>

Injection solvent with relatively high aqueous content is proposed for this method (60-75% acetonitrile) to ensure adequate solubility of polar species, nucleosides in particular. Poor solubility of nucleosides in acetonitrile *versus* water was demonstrated in other studies.<sup>221</sup> Cubbon *et al.* also successfully used 50% acetonitrile as injection solvent in their HILIC method for the analysis of urine.<sup>64</sup> This choice of desorption solvent comes with some deterioration in peak shape for early

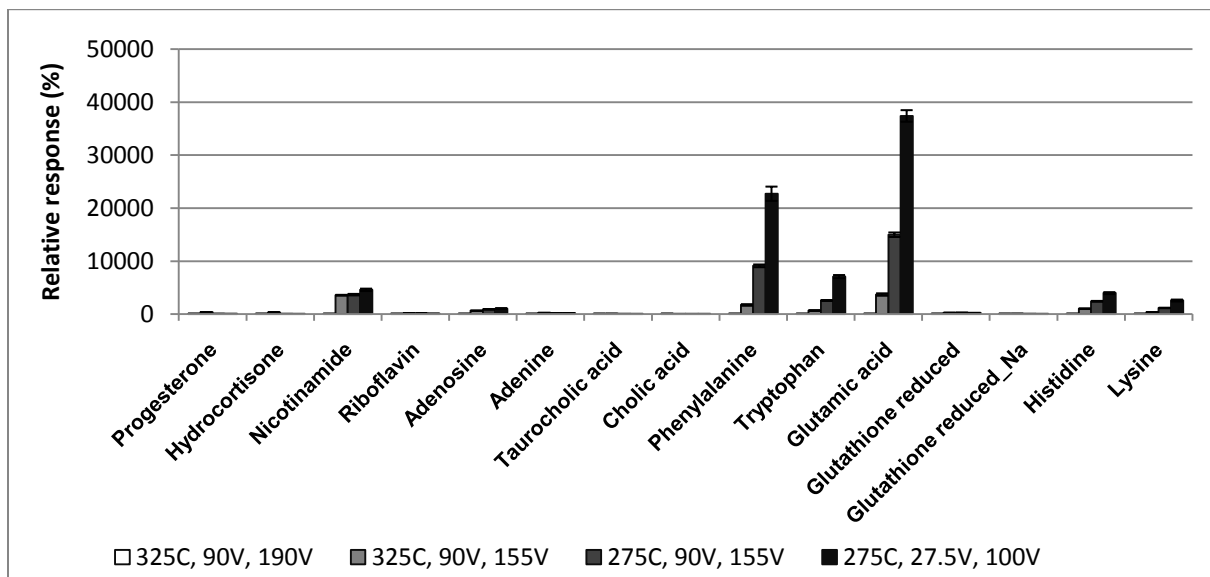
eluting compounds. However, these species can be reliably analyzed on reverse-phase method, whereas the more polar species are the focus of current study and can be successfully analyzed with 60-75% acetonitrile with good peak shape. In contrast, Gika *et al.* injected 100% aqueous urine sample with no solvent strength adjustment prior to analysis.<sup>213</sup> Such high aqueous content usually results in very poor chromatographic peaks shape, and it is not clear how this was overcome in their method.

The results for optimization of MS parameters for this method are shown in Figure 6.6. Part (a) of this figure shows the results for the most polar analytes which are not well-retained using reverse-phase method. These analytes are the focus of HILIC method so optimum analytical sensitivity was desirable for these species. Capillary voltage and tube lens voltage of 90V and 155V respectively were found to perform the best for the analysis of these species. Similar performance was achieved whether 275 or 325 °C capillary temperature was observed, so the lower temperature of 275 °C was selected. The particular settings selected for inclusion in this evaluation were chosen on the basis of direct infusion experiments. It is interesting to note the optimum settings for the polar analytes of interest resulted in considerable reduction in signal intensities of other metabolites such as phenylalanine, glutamic acid and tryptophan as shown in Figure 6.6 (b). This shows that simple optimization using total ion intensity of metabolite standard mixture may not be the best MS optimization method.

(a)



(b)



(c)

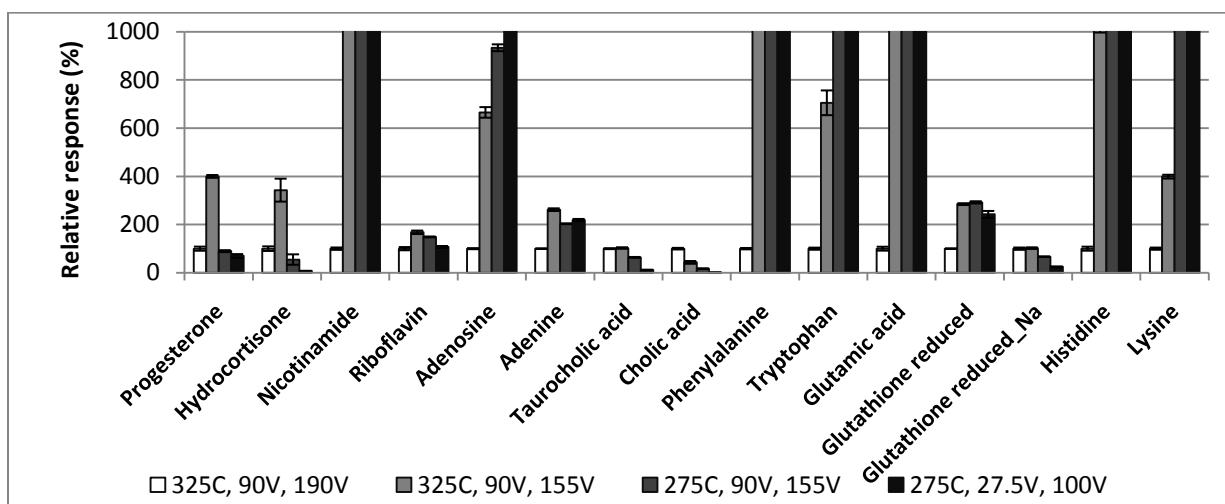


**Figure 6.6 Optimization of MS parameters (capillary temperature, capillary voltage and tube lens voltage) for metabolites using negative ESI HILIC LC-MS method (a) results for very polar metabolites (b) results for metabolites with sufficient retention using reverse phase method – full scale (c) same as in (b) but y-scale zoomed in to show trends for metabolites not well visible in (b).**

Finally, the robustness of the proposed method was evaluated, and the method was found to be very stable over long analysis times. Example results for repeated injection of QC sample are shown in Table 6.7.

**Table 6.7 Results of QC sample analysis for known metabolites using negative ESI mode HILIC LC-MS method with unmodified Si column. % signal intensity of QC2 and QC3 is shown with respect to signal intensity observed for QC1 with approximately 10 hr elapsed between each QC sample. Signal intensity observed for QC1 was set to 100%.**

Analyte	QC2 % signal	QC3 % signal
Estradiol	107	83
Hydrocortisone	105	102
Maleic + fumaric acid (FA adduct)	111	65
Adenosine	109	112
Adenine	115	113
Glucose	95	83
Fructose	111	88
HBA (FA adduct)	106	105
Taurocholic acid	98	108
Cholic acid	99	101
Thyroxine	101	107
Phenylalanine	118	107
Tryptophan	100	97
Sucrose	107	124
Ascorbic acid	86	79
Glutamic acid	86	86
Glutathione reduced	94	96
Pyruvic acid (FA adduct)	87	79
Folic acid	91	89
ADP	117	103
AMP	91	95
ATP	127	88
$\beta$ -NAD	103	103
Citric acid	106	84
Fructose+glucose phosphate	98	96
Glutathione oxidized	118	102
Ribose phosphate	99	97
UDP	130	116
Histidine	103	109
Lysine	104	116

### 6.3.6 Summary of proposed LC-MS methods on Exactive

The combination of reverse phase pentafluorophenyl and Si HILIC LC-MS method was found to provide good coverage of many metabolites of interest. In comparison to other complementary methods reported in literature, the reverse-phase and HILIC methods proposed by Mohamed *et al.* were unable to retain some of very important metabolites, for example ATP and glutathione.<sup>215</sup> These metabolites are very important as ATP is involved in energy metabolism, and glutathione ratio can be used as a measure of cellular toxicity. Thus, it was important to ensure in our methods that these important metabolites can be analyzed. It is suspected that Mohamed *et al.* did not observe ATP due to poor solubility in their chosen injection solvent for HILIC method (acetonitrile/methanol, 75/25). This highlights the importance of compromise when selecting an appropriate injection solvent for a global metabolomics method. For optimum chromatographic peak shape, final sample extract should be dissolved in solvent of weaker or equal strength to starting conditions. For HILIC chromatography, this means using acetonitrile/water (9/1) as injection solvent. However, many polar metabolites are not sufficiently soluble under these conditions as encountered in our work. The use of injection solvents with higher aqueous portion (75/25, or 3/2) improves solubility of such species so that they can be detected but sacrifices good peak shape for some of the early eluting analytes. In our work, the main reason for the use of HILIC method was to retain and separate very polar species such as AMP, ADP, UDP, and ATP, so injection solvent with higher aqueous proportions was selected. This did result in poor peak shape of some early eluting analytes such as taurocholic acid. However, these analytes could be analyzed with good peak shape and sensitivity on proposed reverse phase method, so this was not problematic.

The observed ionization suppression results show that when using SPME and proposed LC-MS methods, ionization suppression was mostly observed for high-intensity citric acid peak used as an additive in human plasma, and particularly in negative mode some acidic compounds eluting within the same retention time window were susceptible to ionization effects (about 2-fold suppression or enhancement). For *in vivo* SPME samples, this issue will be completely eliminated as no additives are added, and the extraction is performed directly in animal blood stream. In contrast to traditional methods, no significant matrix effects were observed in early parts of chromatogram either in HILIC or reverse-phase mode when SPME is used as sample preparation method. This is not the case for traditional methods, where 10-fold dilution of urine was shown to result in significant ionization suppression for 162 components, while acceptable results were achieved for 283 components using HILIC LC-MS method showing data quality is compromised for many species of potential

interest.<sup>215</sup> Using capillary LC-MS method which is less prone to matrix effects due to the use of low flow rates, significant absolute and relative matrix effects were observed for 3 out of 7 compounds tested in plant metabolomics study.<sup>232</sup> The observation of relative matrix effects, which could affect relative quantification in metabolomics study, is particularly problematic and was found to depend on the exact nature of matrix under study. For example, *A. Thaliana* leaf and root extracts were not susceptible to relative matrix effects while *A. Halleri* leaves exhibited significant relative matrix effects. The authors explain this observation by explaining that *A. Thaliana* plants were less diverse (grown under strict and identical conditions), while *A. Halleri* plants were independently grown in a greenhouse under less-controlled conditions, thus exhibiting more inter-individual variability. Another study on yeast extracts evaluated matrix effects using an ion-pair reverse-phase method and HILIC method, and significant matrix effects were observed for 75% of about 60 metabolites tested.<sup>45</sup> In another study on yeast cell extracts using direct introduction mass spectrometry which is the most susceptible to matrix effects, severe matrix effects were observed for 4 out of 10 studied metabolites with 5-fold loss in signal intensity observed even at lowest extract concentration.<sup>36</sup> No similar matrix effects evaluation for global metabolomic studies on human plasma have been reported to date using LC-MS methods, but based on the studies cited for other matrices it appears that significant absolute matrix effects can be expected for a minimum of 30-40% of analytes, whereas SPME appears to be less susceptible due to lower extraction efficiency (non-exhaustive nature of extraction) and the absence of highly intense ions that are likely to cause ionization suppression/enhancement. This can be an important finding as presence of ionization suppression can obscure weak signals, so their intensity is below limit of detection.<sup>232</sup>

In other studies, detector saturation was also observed for some species in urine including hippuric acid, betaine, creatine and creatinine,<sup>215</sup> but this effect was not observed for our SPME-LC-MS method for any metabolites as the extraction efficiency for polar compounds was relatively low.

Finally, it should be mentioned that the proposed combination of methods was not able to separate isobaric sugar phosphates (for example, glucose 1-phosphate and glucose 6-phosphate or fructose 1-phosphate and fructose 6-phosphate), so if these metabolites are of interest alternative methods need to be employed. For example, these species were successfully separated in recent targeted metabolomic studies using anion exchange chromatography<sup>48</sup> or using porous graphitic carbon column<sup>28</sup>, but are not applicable for more global metabolomics analyses. Alternatively, the reasons for poor robustness of HILIC method with aminopropyl column can be further examined.



### 6.3.7 Evaluation of global SPME-LC-MS method using pentafluorophenyl LC-MS method

#### 6.3.7.1 Evaluation of extraction time

An in-depth investigation of the influence of extraction time on the richness of the metabolite profile was carried out using pentafluorophenyl LC-MS method using both positive and negative ionization mode. The extractions were performed from human plasma using Supelco mixed-mode fibres and the extraction times were varied from 5 min to 24 hr. The dependence of the amount extracted was first evaluated for the known metabolites which were identified against the injection of authentic standard. It was found that for the more polar species equilibrium was reached by 5 min extraction time, and no further increases in the amount extracted were observed with subsequent increases in extraction time. These results are shown in Figure 6.7 (a) and (b). For example, the examination of Figure 6.7 (a) shows that glutamic acid, histidine, lysine, choline, phenylalanine, tryptophan and nicotinamide reached equilibrium using 5 min extraction time. Similar trend was observed for citric acid, but was not included in Figure 6.7 (a) since very large amounts of citric acid were extracted (3000 ng) so it could not be easily presented on the same scale as the other compounds. The main reason for the extraction of large amounts of citric acid is the fact that sodium citrate was used as anti-coagulant for the human plasma employed in this study. Taurocholic acid, hydrocortisone, cholic acid and progesterone, on the other hand, showed significant increases in the amount extracted with increasing extraction time, and in fact equilibrium was not reached even after 2 hr extraction time. Among the compounds showing improved extraction at the longer extraction times, some of the compounds were observed at all extraction times, indicating analytical sensitivity was sufficient for these compounds to detect small amounts extracted even at the shortest time. This was the case for hydrocortisone and progesterone in Figure 6.7 (a), for example. Other compounds in Figure 6.7 (a), such as cholic and taurocholic acid required longer time to ensure sufficient amount was extracted to be detectable by the instrumental method employed. For example, in positive ionization mode, cholic acid became detectable only using extraction time of 68 min or longer.

These results agree with expectations and show that richer metabolic profiles can be obtained using larger extraction times. In the example of Figure 6.7 (a), 9 out of 11 compounds could be detected using 5-min extraction time, whereas by increasing extraction time to 68 min, all 11 compounds could be analyzed. An interesting general trend was also observed. The more polar compounds, which have shorter retention times in reverse phase method, reached equilibrium very fast with Supelco mixed-

mode extraction phase employed in this study, as no further increases in the amount extracted was detected beyond 5-min extraction time. This finding is important from calibration perspective, as it means that equilibrium calibration can be used to determine the metabolite concentration in the system under study for any polar metabolites identified during data processing that are of interest, provided authentic standard of the identified compound is available (post-processing calibration of metabolites of interest identified in global study). This trend was further verified by processing the data of all unknown metabolites observed in human plasma as discussed in Section 7.3.5.

For the compounds which were detected using both positive and negative ESI mode, the results obtained using two modes at different extraction times show good agreement for all compounds with typical differences within  $\pm 30\%$ . Furthermore, this data was compared using paired t-test, and no significant differences were found in the amount extracted determined using each of two methods at 99% confidence interval ( $t = -2.25$ ,  $t_{\text{CRITICAL}} = 2.73$ ,  $p = 0.03$ ). This is an excellent result especially considering a very simple one-point calibration standard curve was used to estimate the total amount extracted of each known metabolite and the sample analysis occurred over relatively long-time period (4 days). This data indicates reliable quantitative analysis of selected metabolites can be performed using large metabolomics data sets such as collected in this study.

The extraction time trends were also evaluated using HILIC method after independent extractions of same pooled human plasma samples (Figure 6.8). The results show very good agreement between the two sets of data both in terms of extraction time trends and with regards to the amount of analyte extracted. The two data sets for overnight extraction (1440 min) for metabolites observed in both reverse and HILIC modes (negative ESI, total of 8 analytes observed in both modes) were further compared using paired t-test and no significant differences were found at 99% confidence ( $t = -1.03$ ,  $t_{\text{CRITICAL}} = 3.50$ ,  $p = 0.34$ ) indicating good data quality achievable by both methods. No additional identified metabolites were observed using HILIC *versus* reverse-phase method.

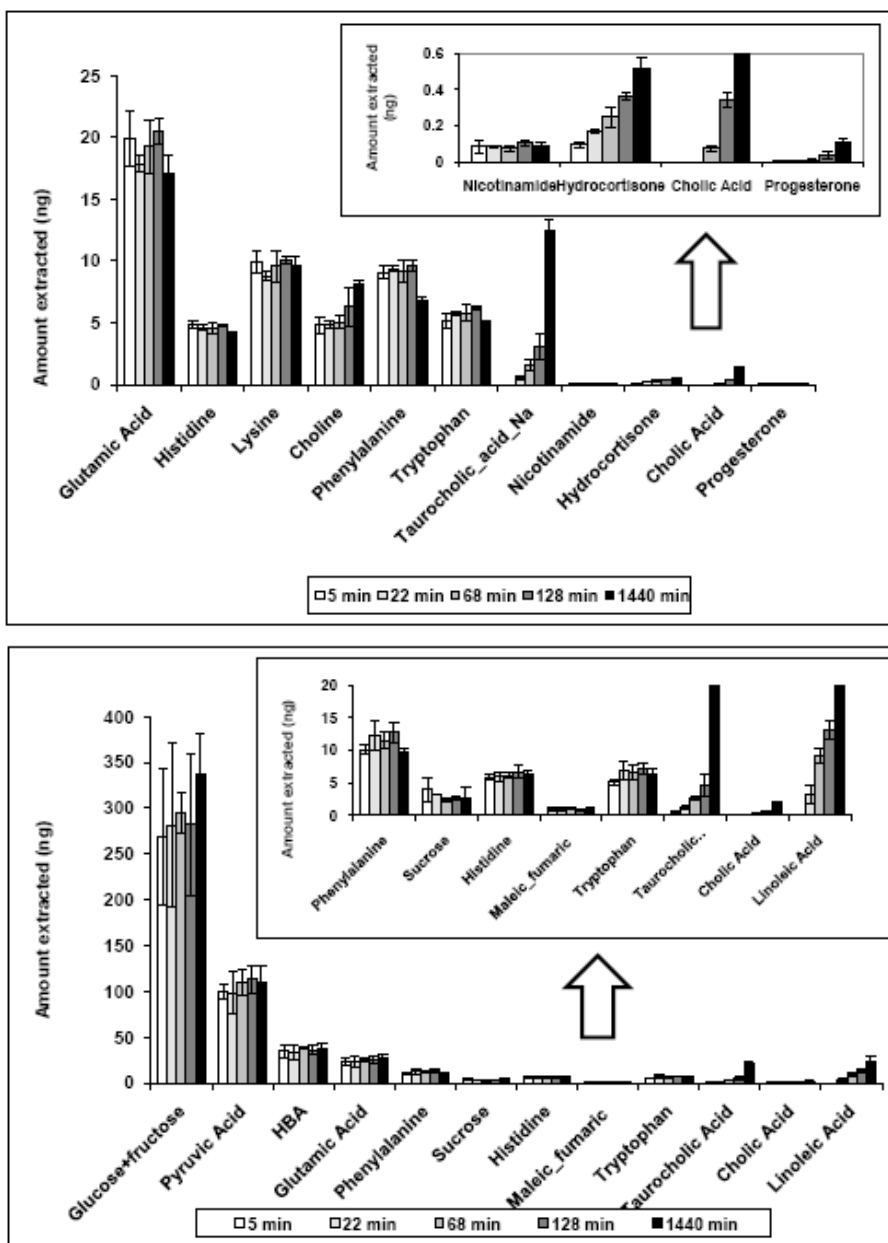
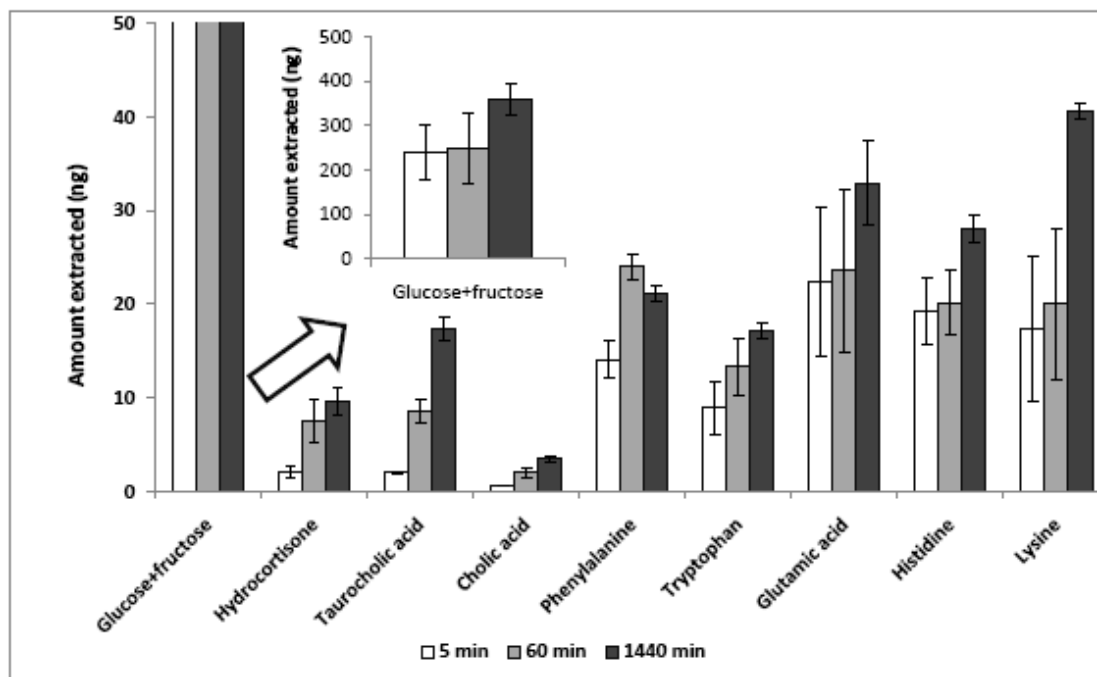


Figure 6.7 The dependence of the amount extracted of known metabolites on extraction time using Supelco mixed-mode fibres (n=3 at each time point). Samples were analyzed using pentafluorophenyl LC-MS method. (a) The results for analytes observed in positive ESI mode. The inset graph shows expanded region to facilitate the comparison of analytes with sub-ng amounts extracted (b) the results for analytes observed in negative ESI. The inset graph shows expanded region to facilitate the comparison of analytes with < 20 ng extracted.



**Figure 6.8** The dependence of the amount extracted of known metabolites on extraction time. All extractions were performed from human plasma using Supelco mixed-mode fibres (n=3 at each time point). Samples were analyzed using HILIC LC-MS method. The results for analytes observed in negative ionization mode. The inset graph shows full scale for glucose and fructose.

### 6.3.7.2 Evaluation of carryover of SPME method for metabolomics

The data shown in Chapter 5 demonstrated significant carryover of many metabolites when static desorption conditions were used and multiple desorption steps were necessary in order to ensure complete desorption of analytes for the comparison of different sorbents. During the evaluation of coatings it was not desirable to employ agitation to facilitate faster mass transfer during desorption step in order to avoid possible loss of particles from the coating (the coating procedure was not optimized for each particle type). Based on the results of that study, Supelco prepared research prototype mixed-mode (C<sub>18</sub>+benzenesulfonic acid, 45 μm thickness) biocompatible coatings using proprietary biocompatible polymer. The robustness of these coatings is very good, so it was possible to employ vortex agitation to speed up the desorption step. Desorption time of 60 min with 1000 rpm agitation was found sufficient to effectively desorb both polar and hydrophobic metabolites from the coatings. To ensure, the desorption was efficient and that no additional desorption steps were

necessary, carryover was evaluated after SPME extraction from plasma. Example results obtained using reverse-phase method are shown in Figure 6.9 and the dependence of % carryover on the length of extraction time is also illustrated. No significant carryover ( $\leq 2\%$ ) was detected for the majority of compounds. Only histidine, lysine and choline exhibited significant carryover. Possible explanation for the higher carryover of amines could be that at pH values above pKa of silanol groups (4.5-4.7), silanol groups can become ionized, which can lead to ionic interactions with positively charged species such as protonated amines, thus resulting in poor elution or desorption of these species.<sup>197</sup>

The carryover experiment was repeated for the known metabolites detected using HILIC LC-MS method. No carryover was found for the majority metabolites with the exception of glucose, phenylalanine and glutamic acid where carryover was found to be  $\leq 2\%$  in all cases. These results indicate that single desorption step is sufficient when using proposed mixed-mode coating for metabolomics. However, considering that it is impossible to evaluate the potential for carryover of all metabolites present in a biofluids sample and extracted by the coating, it cannot be verified with absolute confidence that the coating is absolutely clean prior to any subsequent extraction with absolutely no metabolites remaining within the coating. For this reason, it is recommended to use these coatings as single-use fibres to ensure no accidental contamination peaks are observed during subsequent sample analysis. This is not problematic, as these coatings are produced at low-cost and are already aimed as single-use devices during *in vivo* sampling as discussed in Chapter 4 due to sterility considerations.

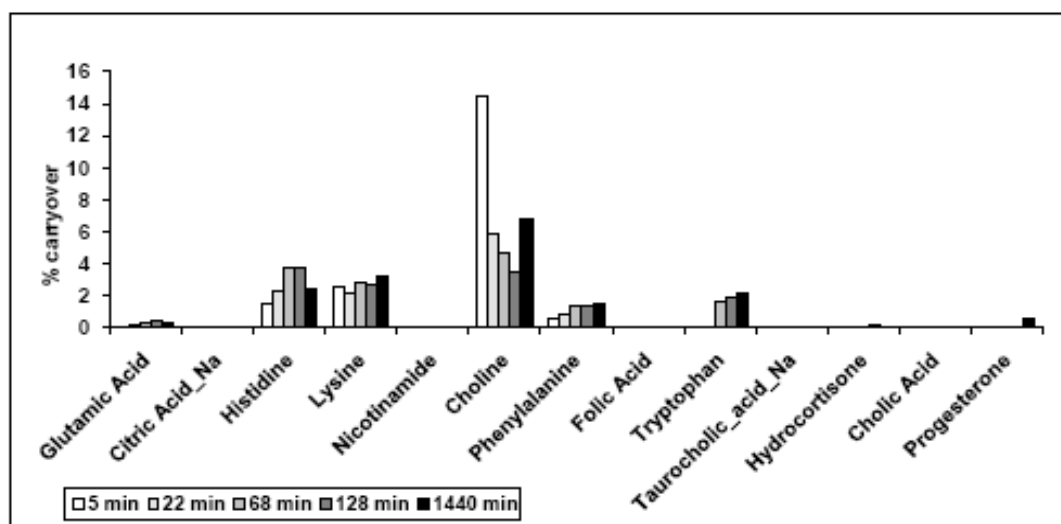
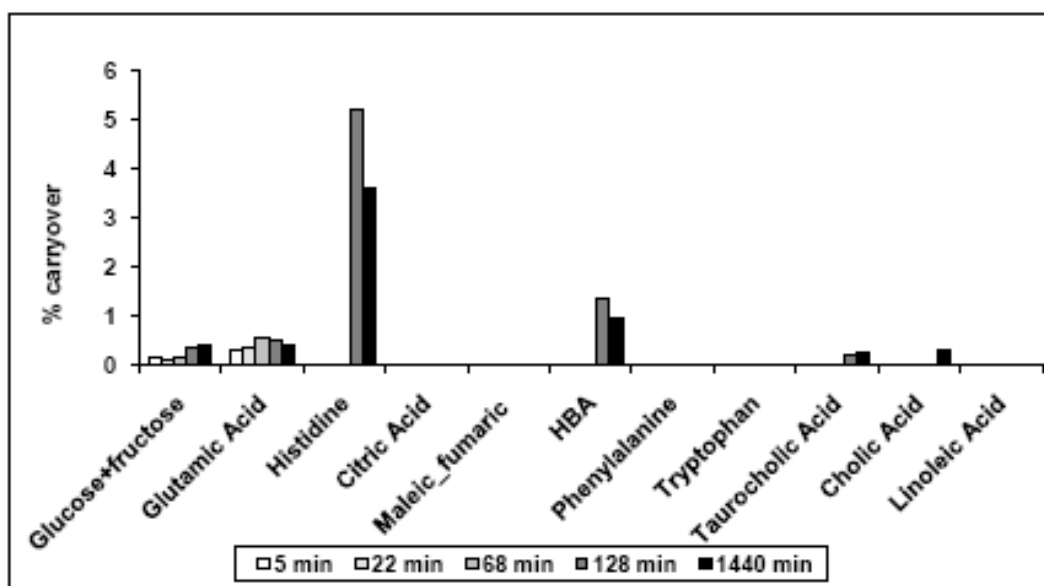


**Figure 6.9** The amount of carryover observed for known metabolites and its dependence on extraction time. All extractions were performed from human plasma using Supelco mixed-mode fibres (n=3 at each time point). Samples were analyzed using pentafluorophenyl LC-MS method. The carryover was evaluated by performing a second desorption using fresh 300  $\mu$ L portion of desorption solvent. The results for analytes observed in (a) positive and (b) negative ionization mode.

### 6.3.7.3 Evaluation of analyte stability in SPME coating

In the next experiment, the stability of selected metabolites in coating after 7-day storage in freezer (-20°C) was performed. The extraction was performed using a set of fibres on one day (time 0). Half of the fibres were analyzed immediately and the amount of analytes extracted was determined using a freshly-prepared standard. The remaining fibres were retracted in the hypodermic needle, wrapped in aluminum foil and stored frozen for exactly 1-week. They were analyzed on day 7 against a freshly-prepared standard. Two consecutive desorptions were performed on both days to evaluate the carryover as well. The results obtained are summarized in Figure 6.10. Overall, the stability on fibre was found to be acceptable as indicated by no statistically significant difference in the amount extracted for the analytes tested. However, it appears that during storage, the coating dries out as the amount desorbed during first desorption was significantly lower than for the freshly extracted fibres. Once the results for the first and second desorptions are taken into account, there are no significant differences in the amount extracted. These results imply that the initial desorption time for fibres stored in freezer should be extended or sufficient number of desorptions performed to ensure effective removal of all analytes.

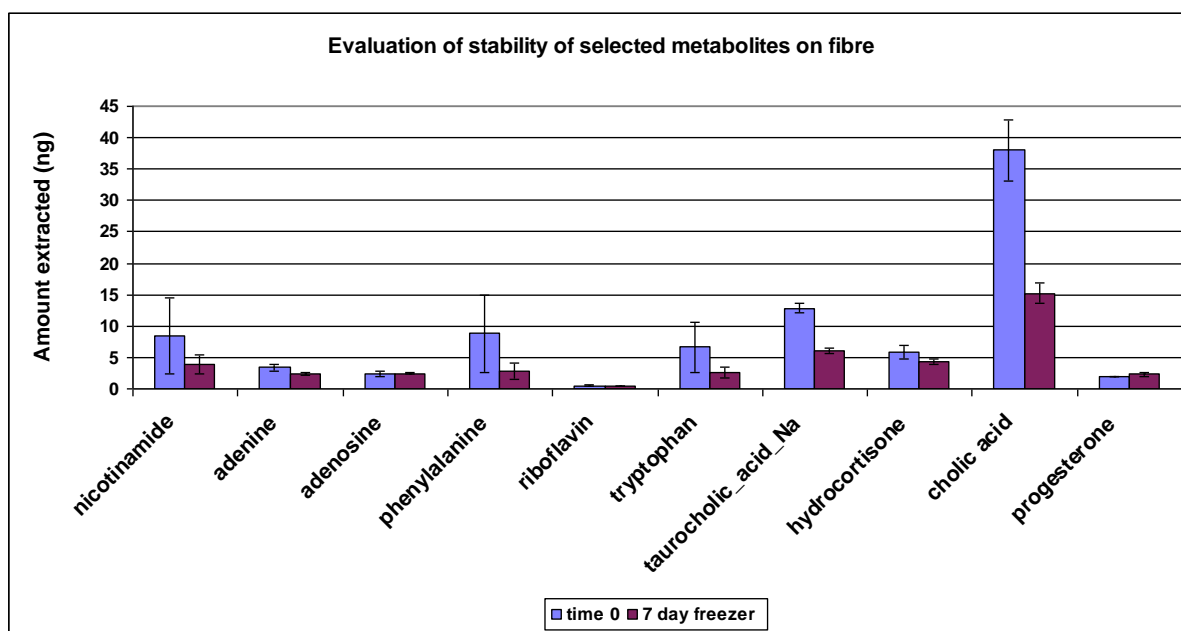


**Figure 6.10** The results of the evaluation of metabolite stability (1-week, -20°C storage) within SPME coating for selected metabolites using n=3 mixed-mode Supelco fibres.

#### 6.3.7.4 Comparison of coating performance for the extraction of human plasma for known metabolites

Using HILIC LC-MS method, the performance of mixed mode coating was compared to that of C<sub>18</sub> coating. The comparison was done using HILIC method to check the extraction efficiency of polar analytes. Example results for a set of known metabolites are depicted in Figure 6.11. Small improvement in the extraction efficiency of these compounds was consistently observed. Further processing of unknown metabolites was performed and gave consistent results. Metabolite coverage could be further enhanced by the use of other complementary coatings identified in Chapter 5.

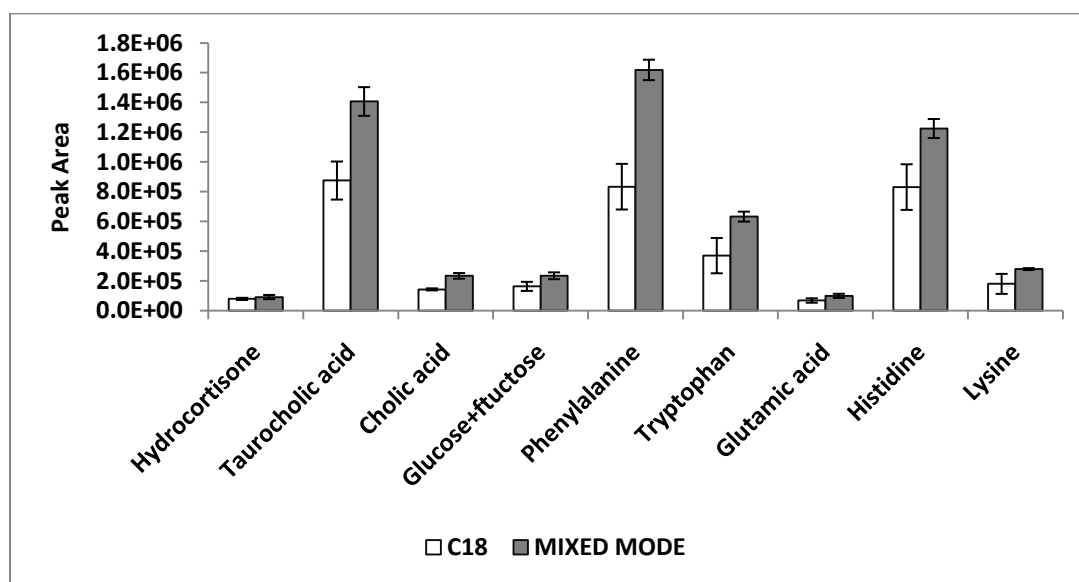


**Figure 6.11 Comparison of the performance of biocompatible C<sub>18</sub> versus biocompatible mixed-mode (C<sub>18</sub> + Benzenesulfonic acid) coating for extraction of human plasma. Extraction was performed using n=3 fibres of each type, for 1440 min and the analysis was performed using negative ESI HILIC LC-MS method. Coating dimensions and thickness were the same so no correction factor was applied. Error bars show one standard deviation from the mean.**

## 6.4 Conclusions

This chapter illustrates some of the difficulties in developing truly global LC-MS methods with adequate performance for metabolomic studies. No single LC method can sufficiently retain all compounds of interest, thus necessitating the use of complementary methods. Although proposed HILIC method with aminopropyl column was able to retain the vast majority of compounds not well retained with PFP method, further evaluation of the method showed it was not sufficiently robust for



metabolomic studies with 10-fold loss of signal intensity observed over 30-hr run time. Considering metabolomic studies typically require the analysis of large number of samples, methods with such poor robustness are not acceptable. Thus, the original HILIC method using underivatized silica was employed in all subsequent studies due to its demonstrated robustness over long run times.

In terms of the development of SPME method suitable for global metabolomic studies, the results presented herein show excellent performance of SPME in terms of matrix effects with <5% and <20% of metabolites exhibiting suppression and/or enhancement effects, and in most cases these effects were correlated to elution within the time window of highly intense sodium citrate peak which was used as anticoagulant. These results show another important advantage of *in vivo* SPME methods where the effect of anticoagulant can be completely eliminated from the data because no additives are required for direct in-vein extraction approaches. Furthermore, the use of short extraction times (5 min with no agitation) was sufficient to extract measurable quantities of various metabolites from a human plasma sample (non-spiked). Interestingly and surprisingly, it was possible to detect some very polar metabolites such as lysine and glutamic acid which exhibited very poor extraction efficiency during method development experiments in Chapter 5. Clearly, the concentrations of these metabolites in human plasma are sufficiently high so that low extraction efficiency (<0.5%) was still sufficient to detect these metabolites in plasma. Analyte carryover was also evaluated for the set of known metabolites and found to be  $\leq 2\%$  for majority of analytes except for selected amines. The use of desorption conditions of acetonitrile/water (1/1, v/v) presented a compromise between good solubility of metabolites of varying polarity, good desorption efficiency and reasonable chromatographic shapes upon direct injection into reverse-phase method. The same extract was also compatible with direct injection into HILIC method after slight adjustment of injection solvent strength by dilution with acetonitrile (1/1, v/v). Increasing the proportion of organic solvent in HILIC method even further was found to cause poor solubility of very polar species such as ADP and ATP, thus preventing analysis of these species, which was not desirable as the aim of this HILIC method was to analyze these very polar metabolites.

## Chapter 7

# Metabolomics of human plasma: comparison of *in vitro* SPME to traditional methods

### 7.1 Preamble and introduction

#### 7.1.1 Preamble

Some of the data presented within this chapter has been incorporated in manuscript entitled. Vuckovic, D., de Lannoy, I., Gien, B., Shirey, R.E., Sidisky, L., Dutta, S., Pawliszyn, J. *In vivo solid-phase microextraction: a new sample preparation tool in metabolomics*, (2010) which is currently submitted for publication. However, all of the work reported within this chapter has been performed solely by myself at the University of Waterloo, so permissions of other co-authors cited on the manuscript are not deemed necessary. The contributions of the authors as cited on manuscript are as follows: I. de Lannoy and B. Gien developed *in vivo* SPME procedure for mice which was previously described in Chapter 4 with appropriate permissions. The contributions of R.E. Shirey and L. Sidisky are the development of biocompatible prototype probes suitable for *in vivo* SPME sampling as described in Chapters 3 and 4 with appropriate permissions. The contribution of S. Dutta is the LC-MS analysis of *in vivo* SPME samples using full hybrid Orbitrap system at Thermo facility in San Jose as described in Chapter 4 with appropriate permission.

#### 7.1.2 Introduction: current sample preparation trends for global metabolomics of human plasma

The objective of the research presented in this chapter was to compare the optimized SPME method presented in Chapter 6 to some of traditional methods employed to in global metabolomic studies of human plasma. It was not feasible to compare SPME to all possible plasma protein precipitation methods reported in literature, so the two best candidate methods were selected from literature based on their performance in comparison studies which examined factors such as efficiency of protein removal and number of observed metabolites. For instance, Polson *et al.* compared the effectiveness of various protein precipitation methods (organic solvent, acid, salt and metal) for use with LC-MS.<sup>233</sup> Among the tested methods, acetonitrile, trichloroacetic acid and zinc sulfate were found to provide best protein removal efficiencies as determined using spectrophotometric method, but precipitation with acetonitrile was most compatible with subsequent LC-MS analysis. Protein removal efficiency

of acetonitrile was found to be slightly higher for acetonitrile (93.2±0.7%) *versus* ethanol (88.6±0.5%) and methanol (88.7±1.1) for all plasma species tested including human, mouse, rat and dog. Minimum plasma to precipitant ratio of 1 to 2.5 was recommended, and further increases in the amount of precipitant (for example 1 to 4 ratio) did not yield any further improvements in terms of protein removal efficiency. In contrast, a more recent study using Bradford assay for estimation of protein concentration, found that acetonitrile had poorest protein removal efficiency (94%) *versus* pure ethanol (96%) and pure methanol (98%).<sup>234</sup> The authors do not provide an explanation for this apparent discrepancy, but this could be caused by different errors inherent in two assays for the estimation of protein concentration. The examination of protein removal efficiency by gel electrophoresis indicated better performance of acetonitrile *versus* methanol supporting results by Polson *et al.*<sup>12</sup> Heat and acid treatment were also found to be efficient for protein removal (98%), but resulted in much fewer number of metabolite features *versus* organic solvent extraction.<sup>234</sup> Among the fourteen extraction methods tested, the precipitation with methanol was found to perform the best in term of metabolite coverage and method reproducibility. Pereira *et al.* compared the performance of three different plasma protein precipitation methods: methanol precipitation (1/2, v/v), methanol precipitation (1/4, v/v) and slow precipitation with acetonitrile (1/1.35, v/v) over 3 days.<sup>58</sup> In this study, best results were obtained using plasma protein precipitation with methanol in 1 to 2 ratio. However, this finding is in apparent disagreement with other reports claiming minimum ratio of 1 to 2.5 plasma-to-solvent ratio is needed for effective protein removal<sup>233</sup>, and shows there is no consensus in literature regarding the best plasma to precipitant ratio. In an early study, Bruce *et al.* compared the performance of plasma protein precipitation using various aqueous solutions of methanol or acetonitrile using 1 to 4 plasma to precipitant ratio for the analysis of human plasma.<sup>211</sup> Precipitation with pure methanol was found to be optimum method with the best metabolite coverage. However, the overall sample procedure was very long and demanding and incorporated 2-hr standing period, ultrafiltration step as well as evaporation/reconstitution step. Such long multi-step sample preparation procedure can be expected to result in significant loss of metabolites, and in fact only 516-735 features were observed which is quite low in comparison to other reported methods. The same group further refined their methodology in a more comprehensive study where performance of four different solvents (methanol, ethanol, acetonitrile and acetone) and combinations of solvents was tested.<sup>12</sup> The best method performance for the solvent precipitation of human plasma samples was obtained using methanol/ethanol (1/1, v/v) and methanol/acetonitrile/acetone (1/1/1, v/v/v) using 1 to 4 plasma to precipitant ratio. Protein removal efficiency was examined using gel electrophoresis and the best

performance was found for acetonitrile, acetone, acetonitrile/acetone and ethanol/acetonitrile/acetone precipitants. However, the number of metabolites observed for these solvents was the lowest. The reproducibility of precipitation methods with pure acetone and acetonitrile was also worse than for remaining methods. Thus, the authors propose precipitation with methanol/ethanol and methanol/acetonitrile/acetone as the two best options taking into account all three criteria.<sup>12</sup>

Michopoulos *et al.* evaluated the performance of precipitation with methanol, precipitation with acetonitrile and SPE in combination with reverse-phase UHPLC-MS method for global metabolomic studies on human plasma.<sup>51</sup> Precipitation with methanol was found to provide better results than acetonitrile, while SPE with C<sub>18</sub> cartridge was found to improve method precision over solvent protein precipitation methods, presumably due to improved sample clean-up. Tiziani *et al.* examined various deproteinization methods for human serum before NMR analysis.<sup>235</sup> After comparison of ultrafiltration *versus* plasma protein precipitation with perchloric acid, acetone, methanol/chloroform or acetonitrile, the authors found that ultrafiltration and acetone precipitation methods provided the best protein removal on the basis of NMR data. However, ultrafiltration provided better results for some of the polar species, due to better solubilization than acetone precipitation so it was recommended as the best method of sample preparation prior to NMR.

The above discussion shows that there is an increased interest in recent years in researching the effect of different sample preparation methods on global metabolomics LC-MS data, but there is still no consensus regarding the optimum method(s) to employ. However, certain trends are apparent from different studies comparing the performance of various plasma protein precipitation methods. The precipitation with acetonitrile appears to perform better in terms of protein removal<sup>12, 233</sup>, while the precipitation with methanol, ethanol or methanol/ethanol mixture results in better metabolite coverage and method precision<sup>12, 234</sup>. Based on these results, we selected (i) precipitation with pure acetonitrile and (ii) precipitation with methanol/ethanol (1/1, v/v) as two plasma protein precipitation methods to incorporate in our study. We selected plasma to precipitant ratio of 1 to 4 for the comparison which is in line with the recommendations in literature to use minimum ratios of 1 to 2 or 1 to 3. Not surprisingly, all of the above literature results show that none of the precipitation methods provides complete protein removal, with estimates of 2-10% of proteins remaining in final extract indicating incomplete sample clean-up.<sup>12</sup> This explains the observation of short column lifetimes for metabolomic studies<sup>51, 52</sup> as this protein portion can build up over time in the analytical column. The presence of proteins is very problematic because it can drastically affect properties of chromatographic column employed for analysis and reduce column lifetime. For example,

metabolomics analysis of urine resulted in an unusable data set because clear run order pattern was observed during principal component analysis.<sup>31</sup> This was subsequently attributed to an increase in column back-pressure over an analytical run, which can be caused by poor sample clean-up. In another study, Zelena *et al.* estimated column lifetime at approximately 400 samples in combination with plasma protein precipitation methods.<sup>52</sup> However, the inability to use a single column to collect an entire large metabolomics data set, can be very problematic from data processing perspective as it can be difficult/impossible to successfully align data from different columns due to small variations in column performance. Thus, one possible advantage of SPME over these methods is the extension of column lifetime. A second useful feature of SPME for metabolomic studies is that the amount extracted is proportional to the biologically-active free (unbound) concentration. Therefore, ultrafiltration was selected for inclusion in current study, as it is one of the most commonly used methods for the determinations of unbound concentration.

Table 7.1 gives an overview of the sample preparation methods employed for global metabolomics analysis of human serum or plasma, and shows large variations in methods employed. Among these applications, the most successful study to date is the identification of sarcosine as putative biomarker for prostate cancer.<sup>20, 44</sup> It is informative to note that the sample preparation workflow for this application is the most demanding among all reported methods and includes a four-step solvent extraction.<sup>44</sup> Further research and investigation is needed to directly compare this method *versus* more common plasma protein precipitation methods for its performance in global metabolomics.

**Table 7.1 Overview of global LC-MS metabolomic studies using human plasma or serum.**

Sample type	Purpose of study	Sample preparation method	Ref.
Serum	Recommended method for Human serum metabolome (HUSERMET) project	Thawing on ice, precipitation with methanol (1/3, v/v), 15 min centrifugation, lyophilization at 45°C for 16 hr, reconstitution in purified water (no pre-concentration)	52
Plasma	Evaluation of Exactive instrument of metabolomics and lipidomics	Precipitation with acetonitrile (1/4, v/v), 10 min centrifugation, 1/1 dilution with formic acid (0.1%)	199
Serum	Investigation of mechanism of acetaminophen hepatotoxicity in mice	Precipitation with 66% acetonitrile (1/20, v/v), 10 min centrifugation,	201
Plasma	Investigation of metabolic syndrome	Precipitation with methanol (ratio and centrifugation conditions not stated), evaporation to dryness, reconstitution (4-fold concentration)	205
Serum	Diagnosis of colorectal cancer and disease understanding	Dilution with water (1/1, v/v), precipitation with 62.5% methanol/ 37.5% acetonitrile (1/2 v/v), 10 min standing at room temperature, 20 min centrifugation, filtration of supernatant with 0.45 µm filter	206
Plasma	Diagnosis of prostate cancer	Four-step solvent extraction at 4°C: extraction with 50% ethyl acetate/50 % ethyl alcohol (1/4, v/v), extraction with methanol (1/2, v/v), extraction with 75% methanol/ 25% water (1/2,v/v) and extraction with 50% dichloromethane/ 50% methanol (1/2, v/v), pooling of all extracts, solvent evaporation, lyophilization, reconstitution in 10% methanol with 0.1% formic acid	20
	Investigation of normal variability in metabolomics with respect to age, sex and race		44
Plasma	Development of methodology for analysis of anionic metabolome	Ultrafiltration using 5k cutoff membrane	55
Serum	Investigation of metabolite coverage using different ionization methods	Precipitation with cold methanol (1/2, v/v), 20 min incubation at -20°C, 10 min centrifugation, evaporation/reconstitution in mobile phase	228, 234, 236
Plasma	Diagnosis of ankylosing spondylitis	precipitation with acetonitrile (1/3, v/v), 10 min standing at 4°C, 10 min centrifugation, lyophilization at -50°C, reconstitution in acetonitrile/water (3/1, v/v, no pre-concentration)	237
Serum	Diagnosis of intestinal fistulas	Precipitation with acetonitrile (1/4, v/v), 10 min standing at room temperature, 10 min centrifugation at 4°C, lyophilization, reconstitution in 75% acetonitrile (1.7-fold concentration)	223
Plasma	Investigation of analytical <i>versus</i> biological variability	Precipitation with cold methanol (1/4, v/v), 45 s vortex, 1 hr precipitation at -20°C, 2x15 min centrifugation, evaporation to dryness, reconstitution (2-fold concentration)	67

### 7.1.3 Challenges with existing sample preparation methods

For the preparation of plasma or serum samples, metabolism quenching step is often not employed or it is not clear how soon after sample collection it was performed.<sup>198</sup> This can be expected to have a significant impact on the composition of metabolome, but no global metabolomic studies currently discuss how well the analyzed metabolome represents the true metabolome at the time of sampling. A recent more targeted study using red blood cell lysate focused on the extraction of thiols and determination of reduced/oxidized glutathione ratio which can be used as an indicator of oxidative stress.<sup>238</sup> In this study, ultrafiltration was found to perform better than plasma protein precipitation because of significantly smaller amount of conversion of reduced glutathione to oxidized form during the sample preparation procedure ( $3.5\pm 0.2\%$  conversion for ultrafiltration *versus*  $21\pm 1\%$  conversion for plasma protein precipitation with acetonitrile).

Several studies incorporate evaporation/reconstitution step as part of sample preparation strategy, but this can result in poor solubilization of some metabolites.<sup>17, 51, 205, 223</sup> The composition of utilized reconstitution solvents varied greatly: for example, Michopoulos *et al.* used 5% acetonitrile as reconstitution solvent, Yin *et al.* 75% acetonitrile and Minami *et al.* used 100% acetonitrile. Evans *et al.* tested two reconstitution solvents (100% aqueous and 10% methanol).<sup>205</sup> Using 10% methanol poor peak shape was observed for early eluting compounds, but using either method relatively hydrophobic species such as diacylglycerols, triacylglycerols or diacylphospholipids could not be observed indicating ineffective solubilization of these species using sample preparation conditions employed. Bruce *et al.* on the other hand advocate the use of 80% methanol as reconstitution solvent, but no discussion of resulting chromatographic peak shapes is provided.<sup>12, 211</sup> Zelena *et al.* recommend lyophilization, followed by reconstitution in purified water, but this method appears likely to fail to solubilize more hydrophobic species, although this is not discussed in manuscript.<sup>52</sup>

Current initiatives aim to further define normal human metabolome through large-scale studies, such as human serum metabolome project which aims to analyze 7000 samples of healthy subjects, subjects with ovarian cancer and Alzheimer's disease.<sup>52</sup> Recent global metabolomics analysis of human plasma samples for effects of age, sex and race found that the most significant changes in the metabolome occurred as consequence of the aging process, but even in this case the majority of metabolites showed < 2-fold change with the exception of some xenobiotics such as caffeine and iminodiacetate.<sup>44</sup> This is in agreement with recent study examining normal biological variability of human plasma and cerebrospinal fluid which recommends  $\geq 2$ -fold as a statistically relevant threshold

with respect to inherent variability of healthy control group.<sup>67</sup> More efforts are also needed to accurately define normal concentration levels of various metabolites, as such information is currently not available for numerous known metabolites. Clearly, establishing a normal baseline of various metabolomes can aid in biological interpretation and is an important step in moving metabolomics forward. Studies, such as current study, which clearly document the performance of different methods are also crucial to aid in the appropriate method selection depending on the problem being studied.

The main goals of this study were to evaluate the performance of SPME *versus* existing methods commonly employed for global metabolomic studies of human plasma: (i) plasma protein precipitation with acetonitrile, (ii) plasma protein precipitation with methanol/ethanol and (iii) ultrafiltration. A particular focus within the study was paid to parameters such as metabolite coverage and method precision.

## **7.2 Experimental**

### **7.2.1 Materials**

Human plasma with sodium citrate as anticoagulant was obtained from Cedarlane Laboratories Limited (Burlington, ON, Canada). 3K Nanosep centrifugal device (molecular weight cutoff of 3000 Da) were obtained from Pall, Port Washington, NY, USA. The main component of the device is ultrafiltration membrane consisting of modified polyethersulfone on polyethylene substrate, while the remaining components were made of polypropylene. Ethanol (HPLC grade) was obtained from Fisher Scientific. Other materials and reagents are the same as described in Chapters 5-6.

### **7.2.2 SPME sample preparation**

SPME samples (n=7) were prepared according to the method developed and described in detail in Chapter 6. Briefly, 300  $\mu$ L of human plasma was extracted using Supelco prototype biocompatible mixed-mode fibre (C18 and benzenesulfonic acid, 45  $\mu$ m thickness, 5  $\mu$ m particle size) for 5 min under static conditions. The fibres were then desorbed in 300  $\mu$ L of desorption solvent for 60 min in acetonitrile/water (1/1, v/v) using vortex agitation at 1000 rpm. This extract was directly analyzed using pentafluorophenyl reverse-phase and amino HILIC methods in both negative and positive ESI modes using conditions described in Chapter 6.



### 7.2.3 Ultrafiltration (UF) sample preparation

Aliquots of human plasma (500  $\mu\text{L}$ ,  $n=7$ ) were placed in 3K Nanosep centrifugal device and centrifuged at 10000 rpm for 30 min at 4  $^{\circ}\text{C}$ . The resulting filtrate was diluted 30-fold in purified water prior to LC-MS analysis.

### 7.2.4 Plasma protein precipitation with acetonitrile (PP)

This procedure was adapted from study by Bruce *et al.*<sup>12</sup> Aliquots of human plasma (100  $\mu\text{L}$ ,  $n=7$ ) were precipitated by addition of 400  $\mu\text{L}$  of acetonitrile (LC-MS grade). The samples were then manually vortexed for minimum of 60 seconds, followed by centrifugation at 12000 rpm for 15 min at 4  $^{\circ}\text{C}$ . The resulting supernatant (150  $\mu\text{L}$ ) was transferred to amber polypropylene HPLC vials (0.3 mL capacity) and diluted with 150  $\mu\text{L}$  of purified water prior to LC-MS analysis.

### 7.2.5 Plasma protein precipitation with methanol/ethanol (PM)

This procedure was adapted from study by Bruce *et al.*<sup>12</sup> Aliquots of human plasma (100  $\mu\text{L}$ ,  $n=7$ ) were precipitated by addition of 400  $\mu\text{L}$  of methanol/ethanol (1/1, v/v). The samples were then manually vortexed for minimum of 60 seconds, followed by centrifugation at 12000 rpm for 15 min at 4  $^{\circ}\text{C}$ . The resulting supernatant (150  $\mu\text{L}$ ) was transferred to amber polypropylene HPLC vials (0.3 mL capacity) and diluted with 150  $\mu\text{L}$  of purified water prior to LC-MS analysis.

### 7.2.6 LC-MS analysis

All of the samples (SPME, PP, PM, and UF) were directly analyzed using pentafluorophenyl reverse-phase and unmodified silica HILIC methods in both negative and positive ESI modes using conditions described in Chapter 6. Prior to start of each sample set, mass calibration of Exactive instrument was performed using standard test mixture of caffeine, MRFA and Ultramark as recommended by manufacturer. Mass accuracy was within 1 ppm for all calibration peaks on all days. Negative calibration was found stable for a minimum of 48 hr, while positive calibration was found stable for minimum of 96 hr, so mass calibration was performed at 48-hr intervals and sample sets were arranged in batches not to exceed 48-hr analysis time. Sample sets for reverse-phase and HILIC methods were prepared as independent sets on different days to ensure sample degradation does not occur while waiting for analysis. For HILIC analysis, samples were diluted with acetonitrile to adjust the injection solvent strength. After preparation, samples were stored refrigerated on the autosampler while waiting for injection.

Samples were run in randomized order. Randomization of run order is extremely important in metabolomic studies in order to eliminate the factors such as small changes in sample concentration due to storage in autosampler while waiting for injection, solubility and adsorption issues with time, as well as change in instrument signal over time. If randomization is not performed, then the analysis of data sets can result in erroneous identification of potential biomarkers which are not relevant to treatment itself but rather stem from the inability to perfectly control all variables during an analysis.

QC sample was run at the beginning, the end and periodically throughout the sample batch (every 10-12 injections) to verify instrument performance. This QC sample was prepared by combining 10  $\mu$ L aliquots of each sample within entire sample set according to procedure proposed by Wilson *et al.* and is the leading approach adopted in metabolomic studies.<sup>239</sup> The reason for the preparation of this pooled sample is to ensure that this sample contains most of the potential metabolites within a given data set, whereas a prepared standard mixture of known metabolites would not sufficiently represent the sample complexity and could not adequately ensure good quality control for all metabolites. These repeated injections of the same QC sample can be checked during principal component analysis, and should cluster tightly together if instrument performance was acceptable for the run. Furthermore, the mass accuracy and precision obtained for selected metabolites of interest (for example, once differentiating metabolites are found during PCA analysis) can be further examined to provide further verification whether differences in given metabolite arise from samples or from analytical variability improving overall confidence in the results. Other quality control approaches reported in literature include reinjection of random study samples<sup>200</sup> and single point calibration using QC samples<sup>240</sup>. Former approach does not appear sufficient for quality control purposes as it does not provide sufficient number of replicates of any single sample, while the latter approach is very time and processing-intensive and assumes significant amount of instrumental drift and correlation of this drift with run-order. However, if the employed LC-MS method is sufficiently robust, this extent of instrumental drift should not be observed. Appropriate blank solutions and a known metabolite standard mixture were also analyzed throughout each sample set and subsequently used to identify relevant metabolites or to eliminate peaks originating from blank solution and not the plasma samples themselves. For each data set, the performance of QC sample was examined using both known metabolites and principal component analysis. Figure 7.1 shows example results for one QC set processed for known metabolites. The results were in line with reported results in literature of <20% RSD over 48-hour period for known metabolites and good clustering of QC samples was observed in PCA.<sup>215</sup> Sucrose consistently showed poor performance using PFP method with typical RSD >50% so

it was preferentially analyzed using HILIC method. RSDs for retinol and  $\beta$ -NAD were higher than for other compounds due to very low signal intensities observed for these compounds (Figure 7.2).

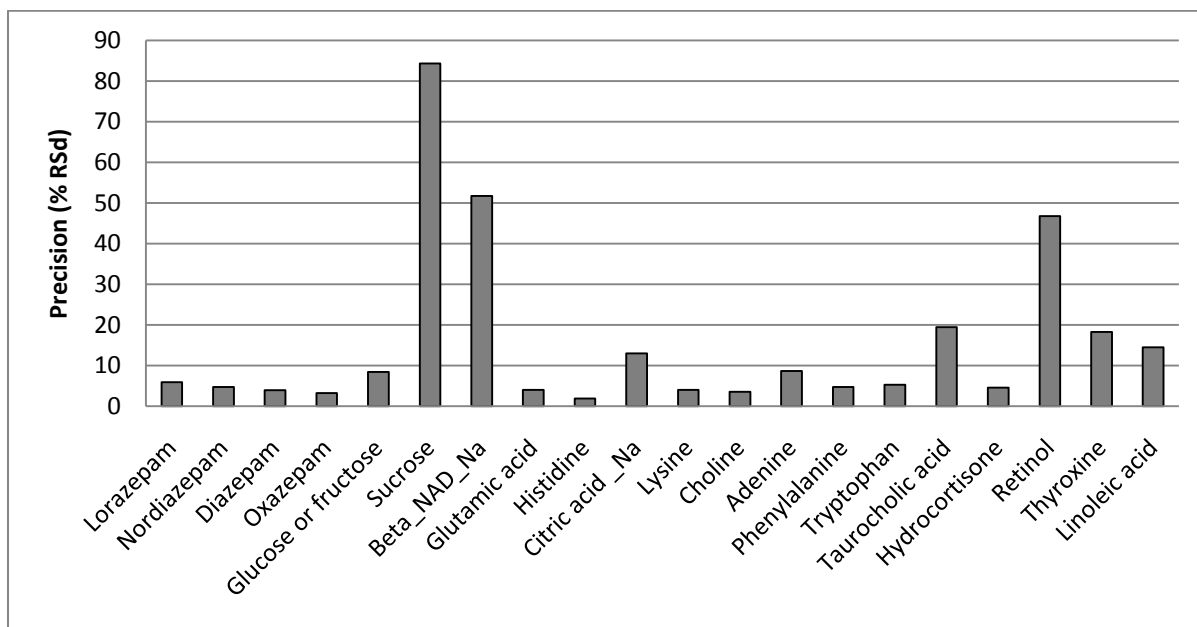


**Figure 7.1 Example results for QC sample analyzed using positive ESI PFP LC-MS method over 48-hr period.**

### 7.2.7 Data processing

Known metabolites in plasma samples were analyzed using Xcalibur software Version 2.1 (Thermo Fisher) by isolating extracted ion chromatograms (XIC) using 5 ppm (positive ESI mode) and 10 ppm (negative ESI mode) windows around the accurate mass of a given compound. These metabolites were identified in human plasma samples by comparison of retention time and accurate mass with that of the authentic metabolite standard mixture.

Global metabolomics analysis was performed using SIEVE software version 1.2.0 (Thermo Fisher). The main steps of SIEVE workflow include (i) alignment (ii) identification of frames meeting given criteria (also called peak picking or feature detection) (iii) comparison of signal abundances in control *versus* treatment groups for each peak to yield univariate statistical probability that the levels are different or not and (iv) tentative identification of features using ChemSpider database. Chromatographic alignment is performed during data processing, because small differences in retention time commonly occur during an analysis run (typical RSD of retention time <1 % RSD),

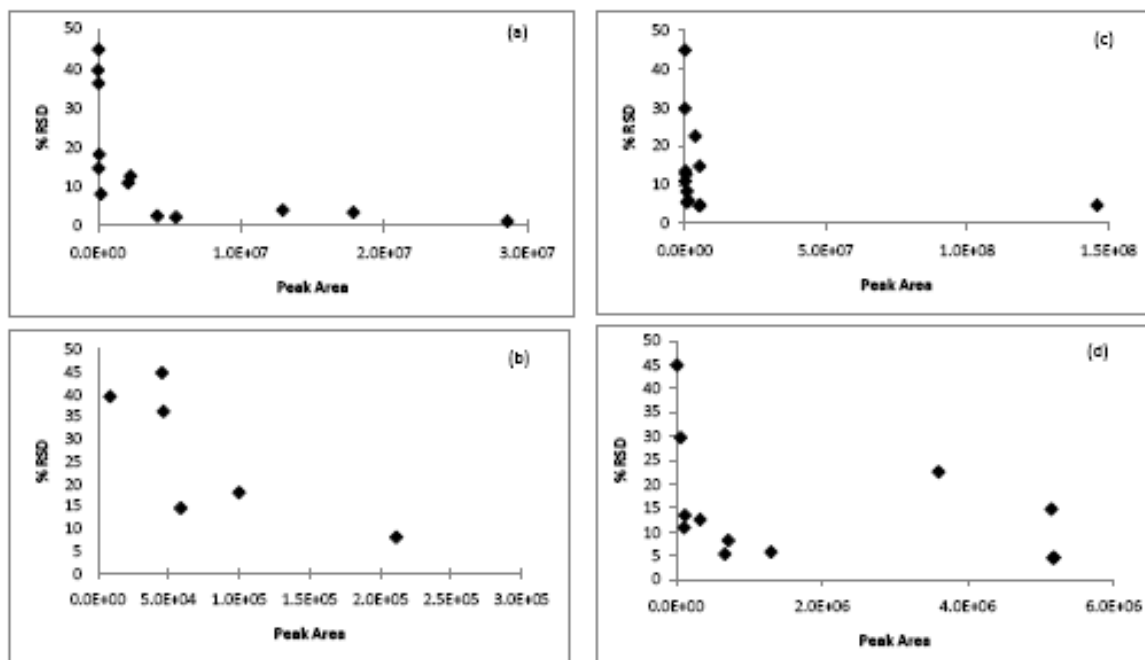


**Figure 7.2** Dependence of % RSD on signal intensity for  $n=7$  injections of QC sample prepared by mixing aliquots of each sample within the sample set. The sample set was SPME extraction from human plasma using different extraction times. The QC injections were made randomly throughout the sample run over 48-hour period using pentafluorophenyl LC-MS method. Each point represents known metabolite detected in human plasma. (a) results for positive ionization mode (b) results for positive ionization mode: expanded scale to enable comparison of RSD for low signal intensities. (c) results for negative ionization mode (d) results for negative ionization mode: expanded scale to enable comparison of RSD for low signal intensities.

and these differences can affect subsequent comparison across samples unless they are properly corrected.<sup>241</sup> The success of alignment was evaluated using likeness score provided by the software and values greater than 0.8 were found acceptable. Following parameters were used for framing: 0.005 mass window, 1.0 min retention time window, maximum number of frames =20000, minimum signal intensity of 10000. Initial 1.0-2.0 min and final 2.0 min of chromatographic run time were excluded from processing, as they represent column void and column re-equilibration time, respectively. The results obtained after framing were evaluated manually to eliminate any frames containing only background noise and no real chromatographic peaks (typically 50-70% of frames were rejected using this criterion as current version of SIEVE software was not able to distinguish

between chromatographic peak shape and random background noise if the noise exceeded the intensity threshold level. If the signal intensity threshold was increased, this resulted in omission of significant number of real peaks without resolving the problem of background noise, so manual verification of all SIEVE data sets was absolutely necessary. At this stage, any peaks which were also present in the corresponding blank injections were removed from the data set (~ 20% of peaks). According to this procedure, a typical SIEVE data set of 20000 frames would be reduced to a final data set of 1000-3000 real chromatographic peaks (and not present in blanks) depending on the sample preparation and LC-MS method employed. This data set also contained probability calculations that each frame is different in each set of samples, as well as integrated signal intensities for each sample and each frame, facilitating inter-sample comparison.

Relevant three-dimensional data sets (m/z, retention time and signal intensity) were also further subjected to PCA using SIMCA P+ Version 12.0.1 software (Umetrics, Sweden) using Pareto scaling as recommended for LC-MS data sets.<sup>214, 215, 223, 231</sup> Pareto scaling is a scaling method which uses square root of standard deviation as the scaling factor, and is used to ensure small-fold changes can be detected even in presence of large-fold changes (for example, to ensure several very high intensity peaks do not dominate PCA results).<sup>242</sup> In other words, this method reduces the importance of large values within a data set, while still keeping the underlying structure of data. PCA reduces the dimensionality of data, and isolates orthogonal components which contribute the most to observed variation in inputted data sets. It is blinded or unsupervised type of analysis, and it attempts to find natural clusters within the data set, which can be examined using a scores plot. In a properly-designed and executed metabolomics study, analytical variation should be smaller than biological variation due to specific treatment, so samples are expected to cluster according to the group they belong (for example, control *versus* disease). The variables contributing the most to a given principal component then can be further examined for their potential as biomarkers using a loadings plot. The overall processing workflow is illustrated in Figure 7.3. PCA is used extensively in metabolomic studies to help isolate potential variables of interest because univariate approaches would yield a high false discovery rate when dealing with data sets containing thousands of peaks. The main disadvantages of the technique are that it looks for global patterns in the data, so some fine underlying structure in the data may be lost and the interpretation of loading plots can be difficult if dealing with large number of variables.<sup>2</sup> Another problem is the input of large number of variables *versus* usually relatively limited number of samples, which reduces the power of statistical approaches employed. This means that a high false positive discovery rate can result unless high significance thresholds are used.<sup>19</sup> Structured

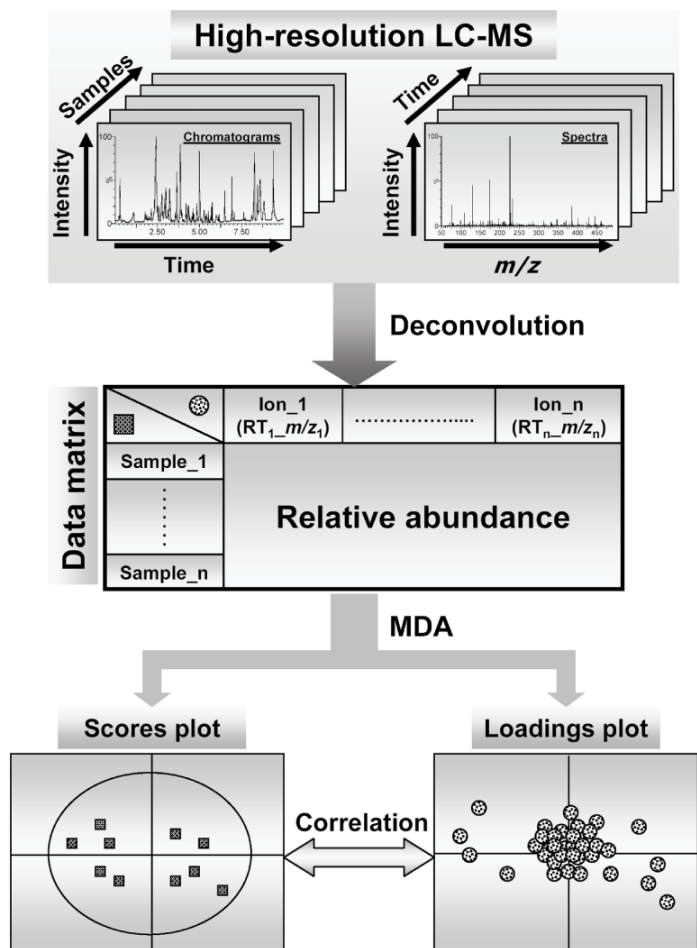


**Figure 7.3 Data processing procedures for LC-MS-based metabolomics. Chromatographic and spectral data are acquired by high-resolution LC-MS. Subsequent data processing, such as centroiding, deisotoping, filtering, peak recognition, yields a data matrix containing information on sample identity, ion identity (RT and  $m/z$ ) and ion abundance. With appropriate data transformation and scaling, a multivariate model can be established through unsupervised or supervised multivariate data analysis (MDA). The scores plot illustrates the principal or latent components of the model and sample classification, while the loadings plot presents the contribution of each ion to each principal component of the MDA model. Figure reprinted with permission from Taylor & Francis from review by Chen *et al.*<sup>27</sup>**

data sets may benefit from PLS-DA approaches, but the main disadvantage of these supervised methods is potential for overfitting of data resulting in overall poor model performance.<sup>2</sup> This is

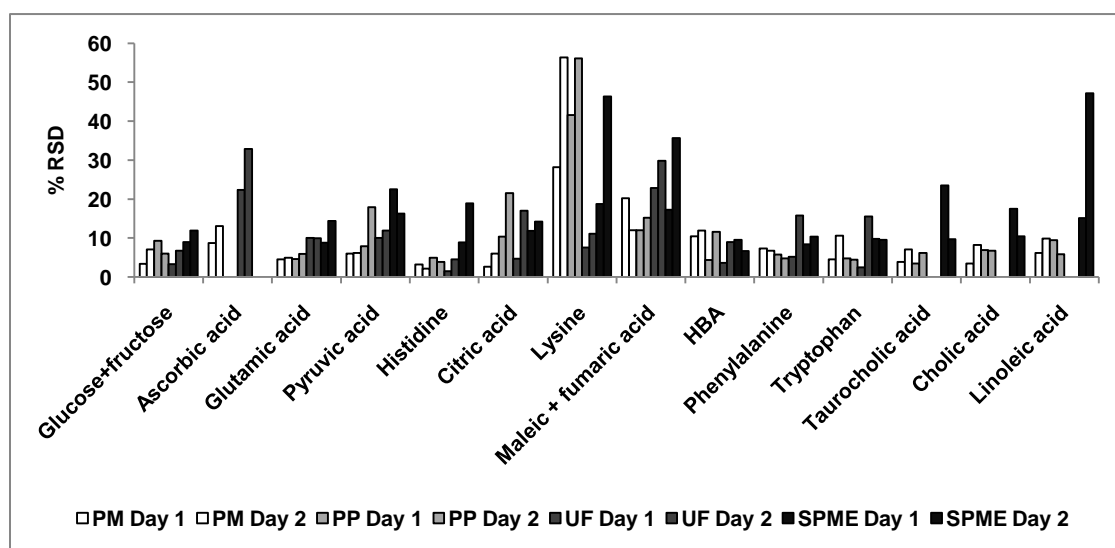
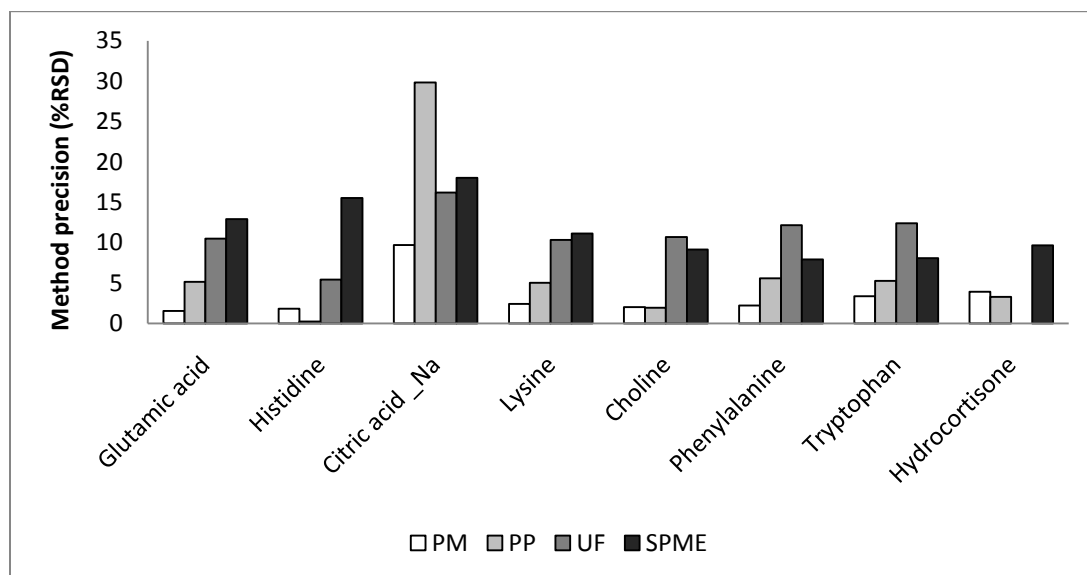
particularly likely when using small sample numbers such as used in current study so PLS approaches were not explored.

## 7.3 Results and discussion

### 7.3.1 Comparison of sample preparation methods for known identified metabolites

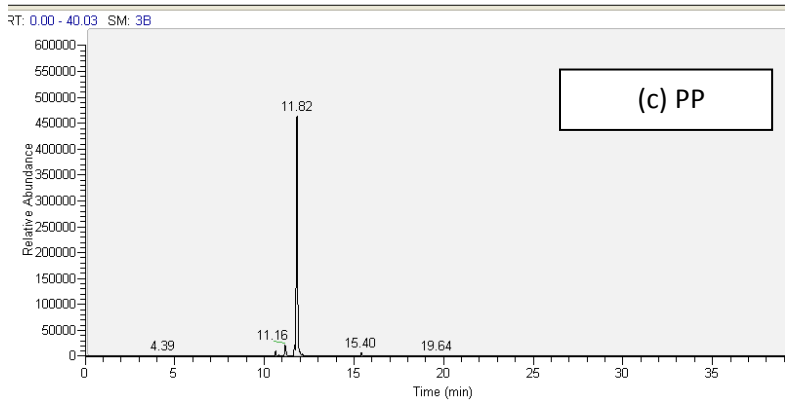
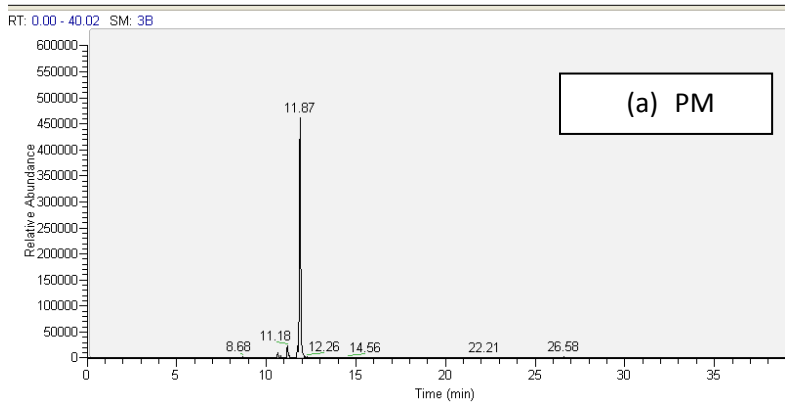
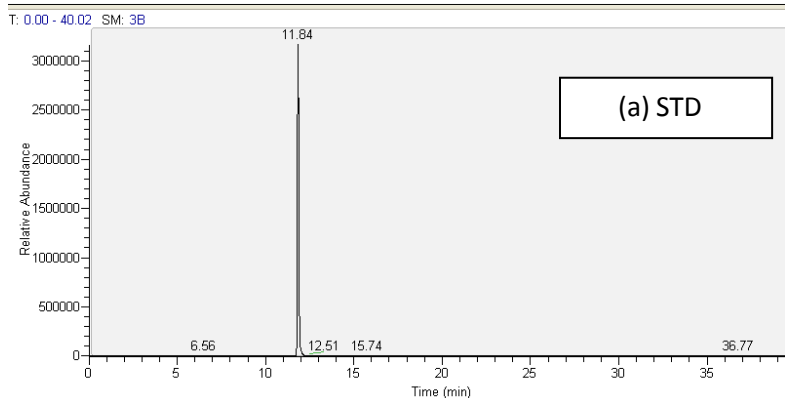
The authentic standards for the metabolites which were used for coating development (Chapter 5) were used to identify these metabolites in human plasma samples. Both accurate mass and retention time were used to assign the identity of these species in unspiked plasma samples. Method precision for each sample preparation procedure was determined on the basis of seven independent extractions of the same pooled human plasma sample and example results are shown in Figure 7.4. Overall the performance of SPME was similar to that of traditional methods with RSDs for most compounds  $\leq 30\%$ .

For ultrafiltration, an interesting trend was observed where more hydrophobic species such as cholic acid, taurocholic acid, linoleic acid and hydrocortisone were not detected at all as illustrated by missing bars in Figure 7.4. This is further illustrated in Figure 7.5 using taurocholic acid as an example. The same figure also shows another important trend. In general, the signal intensities for plasma protein precipitation methods shown in (b) and (c) for taurocholic acid example were much higher than observed for SPME as depicted in (d) for taurocholic acid. This was a general trend observed across the entire chromatographic space and is attributed to non-exhaustive nature of SPME whereby only a small portion of analyte is extracted depending on the magnitude of its  $K_{fs}$  value and the length of extraction time. However, despite lower signal intensities, the signal intensities were still sufficiently high for reliable detection and sufficient number of points across peaks could be acquired as illustrated in Figure 7.5 (f) for the taurocholic acid example.



**Figure 7.4 Comparison of method precision (expressed as % RSD for n=7 replicates) obtained for plasma protein precipitation with methanol/ethanol (PM), plasma protein precipitation with acetonitrile (PP), ultrafiltration (UF) and SPME. The samples were prepared using single pooled lot of human plasma with sodium citrate as anti-coagulant using procedures described in Experimental section. Missing bars denote peak not detected by a particular method. (a) Results for the analysis using pentafluorophenyl LC-MS method in positive ESI mode. (b) Results for the analysis using pentafluorophenyl LC-MS method in negative ESI mode. The results for two independent sample sets are shown and denoted as Day 1 and Day 2.**





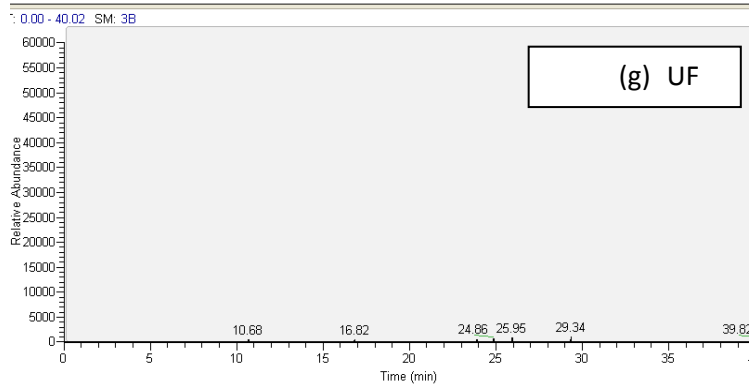
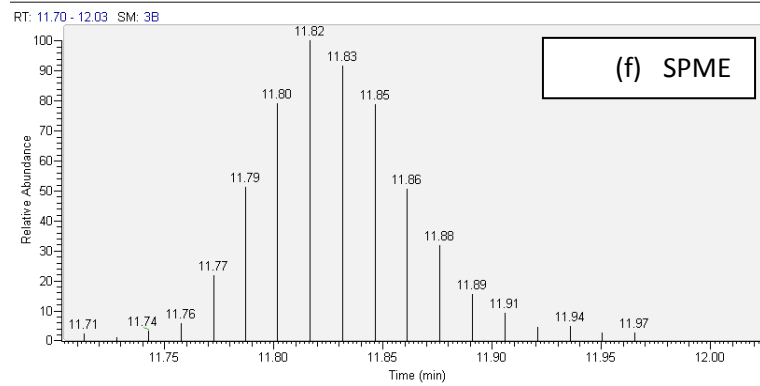
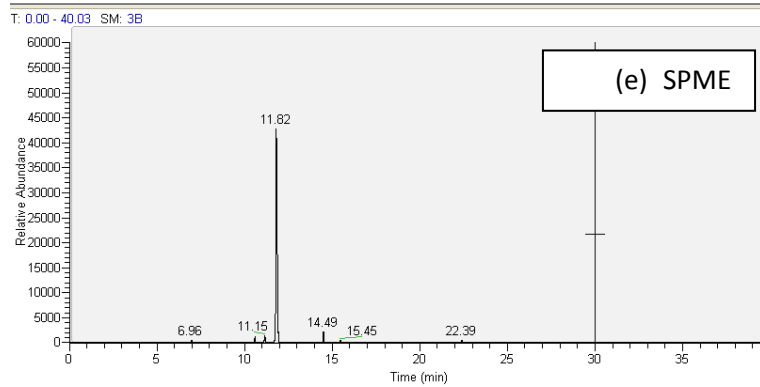
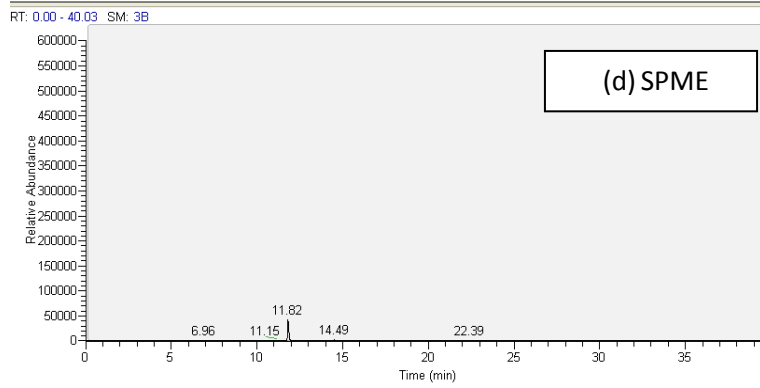
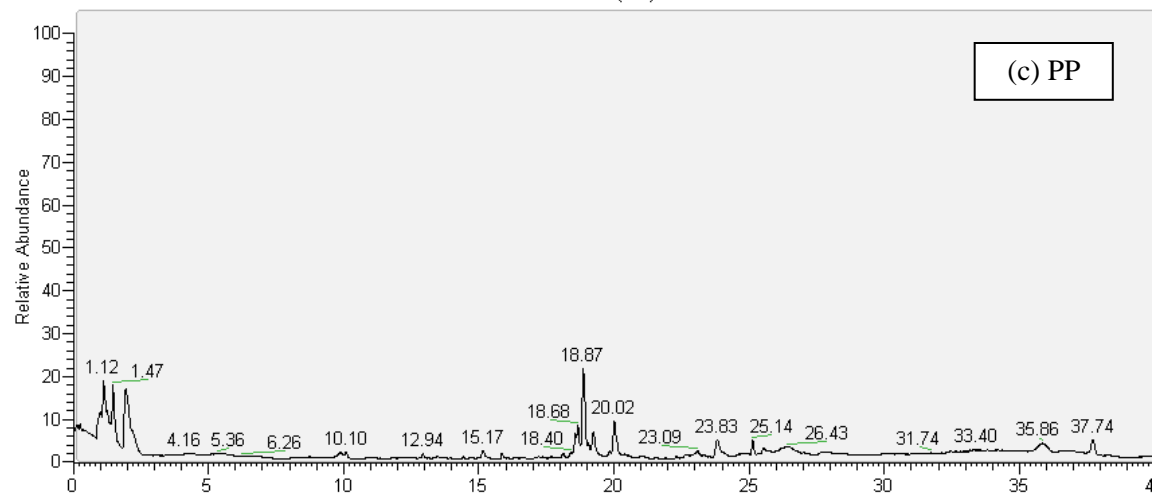
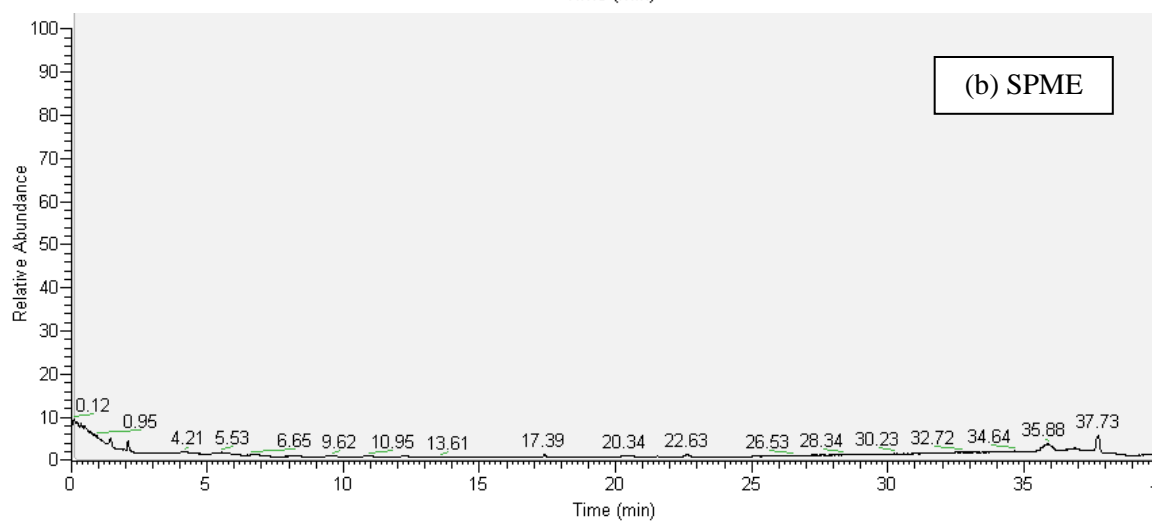
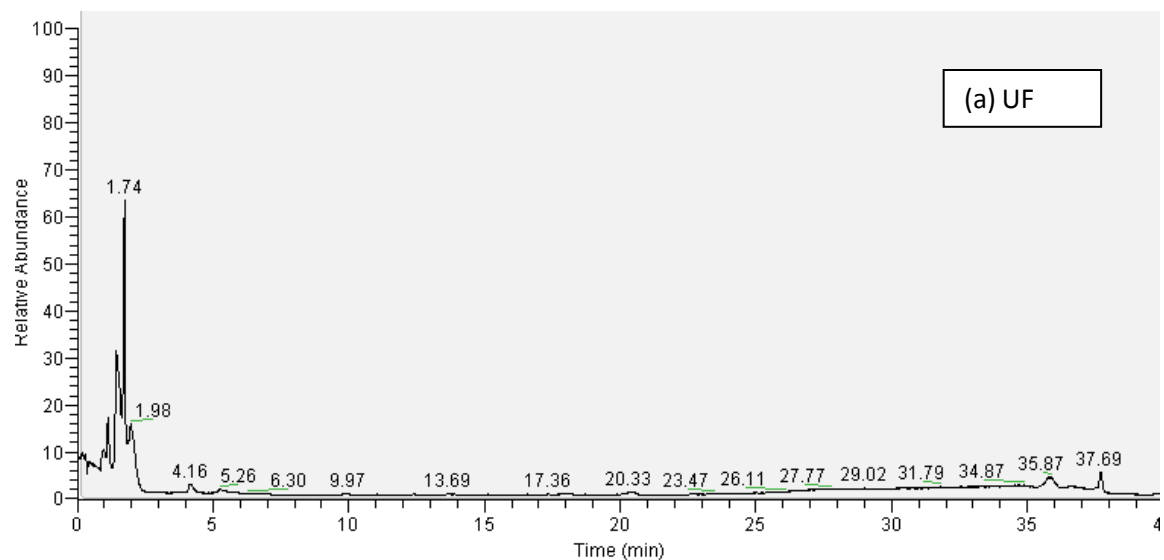


**Figure 7.5 Taurocholic acid example. Taurocholic acid peak detected using negative ESI pentafluorophenyl LC-MS method in (a) standard mixture (b) human plasma sample prepared using PM (c) human plasma sample prepared using PP (d) human plasma sample prepared using SPME shown on same scale as PM and PP methods (e) human plasma sample prepared using SPME but y-scale zoomed in to better see peak shape (f) number of points obtained across SPME peak (g) human plasma sample prepared using UF shown using y-scale zoomed to the same scale as shown in (e).**

For ultrafiltration, very high signal intensities were observed for early eluting metabolites (typically with retention times <5 min), while most late-eluting metabolites were completely missing. This is depicted in total ion chromatograms of Figure 7.6 for reverse phase method. Due to complementary nature of HILIC method, this trend was reversed when samples were analyzed using HILIC LC-MS as shown in Figure 7.7. In this case, ultrafiltration showed the highest signal intensity for mid-to-late eluting peaks, while precipitation methods had much higher signal intensities for more hydrophobic early eluting species. Figure 7.7 also shows example extracted ion chromatograms for tryptophan to illustrate that the trend of generally higher signal intensities for precipitation methods *versus* SPME is consistent for both reverse-phase and HILIC methods.

### **7.3.2 Global metabolomics - plasma protein precipitation with acetonitrile (PP) results**

The analysis of two data sets of the results obtained on human plasma after plasma protein precipitation with acetonitrile resulted in total of 2975 peaks (positive ESI) and 2082 peaks (negative ESI) mode with reverse-phase LC-MS method performed using pentafluorophenyl column. The results of these analyses are summarized in Figure 7.8 and Figure 7.9. A single metabolite can give rise to more than one ion observed in MS. These ions include protonated ions, sodium adducts, potassium adducts, ammonium adducts, multiply-charged ions, isotope peaks and ions corresponding to loss of neutral species such as carbon monoxide, carbon dioxide, water, ammonia or formic acid, although other more unusual species have also been documented.<sup>33</sup> Therefore, the observation of 2082 peaks in negative mode does not mean 2082 unique metabolites were observed. For example, a recent study on human serum using hybrid Orbitrap instrument investigated the occurrence of various ions originating from same species using both positive and negative ESI modes.<sup>33</sup> In negative ESI, among total of 4513 peaks observed, 18% of peaks detected were attributed to isotopes, 1.6% were attributed to Na and K adducts, 3.4% to doubly charged species and 8.1% to neutral loss fragments.



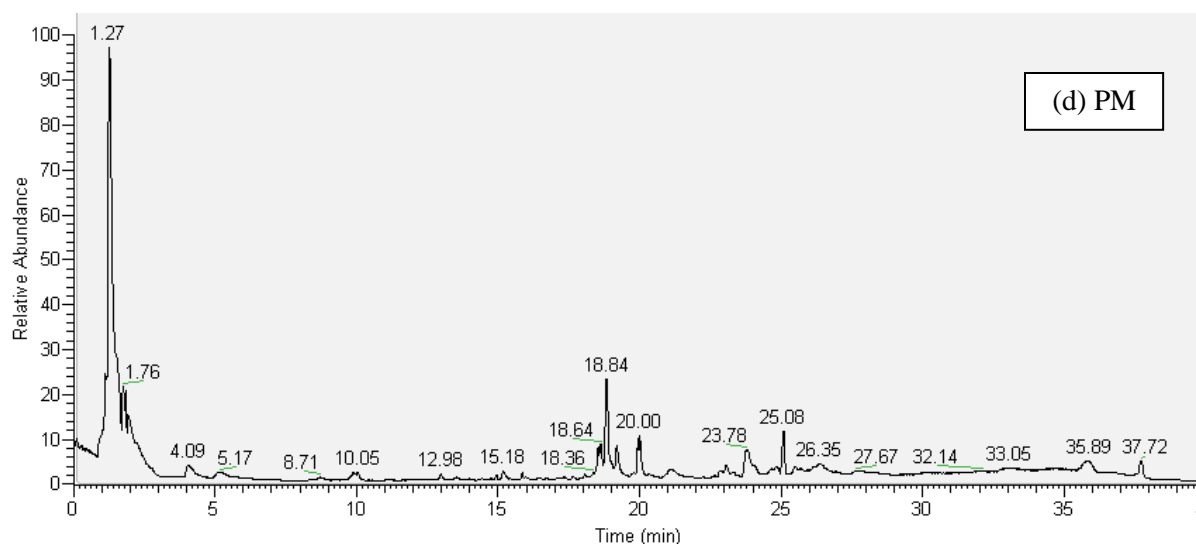


**Figure 7.6 Total ion count (TIC) chromatograms obtained using negative ESI pentafluorophenyl LC-MS method in (a) human plasma sample prepared using UF (b) human plasma sample prepared using SPME (c) human plasma sample prepared using PP (d) human plasma sample prepared using PM. All TICs are shown on the same scale ( $1 \times 10^8$ ) to facilitate comparison.**

In positive ESI, among total of 2079 detected peaks, 14% were attributed to isotope peaks, 3.4% to Na and K adducts, 8.1% to doubly charged species and 1.9% to neutral loss fragments. In other words, based on these results unique metabolite coverage can be estimated to be approximately 30% less than the total number of peaks reported. In a second study, the authors estimated approximately three m/z ions were observed for each compound in each ESI mode using UHPLC-nanospray FTICR, so the overall number of metabolites was approximately one third of the total number of peaks reported.<sup>38</sup> A third study by Evans *et al.* reported average of seven m/z ions observed for each unique metabolite during the building of their metabolite library.<sup>205</sup> However, a manual examination of our data for the known metabolites indicates the presence of isotope peaks, but very few adduct peaks. Sodium adducts were particularly observed for acids and phosphorylated species, but not often observed for other metabolites. Few metabolites showed very small intensities for formic acid adduct peaks. This is in line with the estimate of three ions per metabolite.<sup>38</sup> However, the examination of SIEVE data indicates that usually only the most abundant ion is entered in the feature table, although additional minor ions with small signal intensities may be present in the collected spectra. Therefore, based on the manual examination of known metabolites and SIEVE tables, the estimate of seven m/z

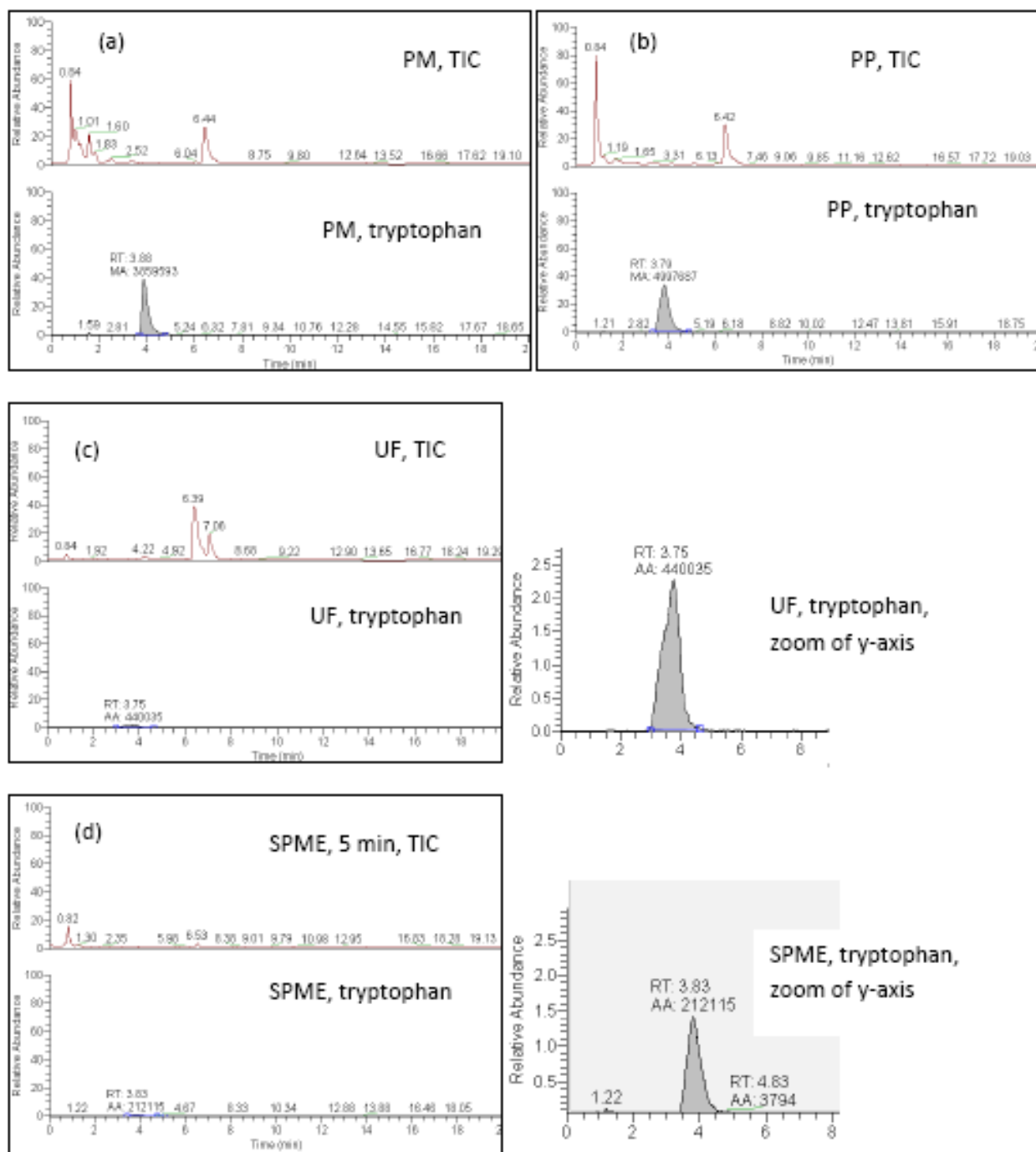


**Figure 7.7 Total ion count (TIC) and extracted ion chromatogram (XIC) for tryptophan obtained using negative ESI HILIC LC-MS method in (a) human plasma sample prepared using PM (b) human plasma sample prepared using PP (c) human plasma sample prepared**

**using UF (d) human plasma sample prepared using SPME. All TICs and XIC are shown on the same scale ( $1 \times 10^8$  and  $5 \times 10^5$ , respectively) to facilitate comparison across methods.**

ions per single metabolite appears to be an overestimate for the data collected/processed in current study. The likely number of unique metabolites appears to fall in line with estimates of Brown *et al.*<sup>33</sup> especially for SPME data where many peaks had very low signal intensity, and adducts and fragments, even if formed, may be below instrumental limit of detection. As can be seen from this discussion, the discrepancy in the reported percentage of unique metabolites may in fact arise from the data processing stage of the workflow where different software may treat minor ions differently in terms of inclusion in the feature table. The formation of multiple ions as observed in ESI also further complicates putative identification of metabolites because during global metabolomics analysis it is not known *a priori* what type of ion is formed. The development of software that can correlate the ions belonging to the same species is currently an active area of research in order to help address this issue. Standardization of data processing procedures and software can also help to reach consensus regarding the number of unique features reported in various studies.

Figure 7.8 and Figure 7.9 also show the histograms of the distribution of method precision observed for all unknown peaks when seven replicate independent extractions are considered. This type of representation is indicative of overall data quality. High metabolite coverage with poor method precision is not useful from the data interpretation perspective as biological variability cannot be confidently distinguished from analytical variability. Although currently there are no set requirements regarding acceptable precision of peaks in global LC-MS metabolomics analysis, RSD values of up to 20-30% should be acceptable<sup>29, 52</sup> considering that RSD values of 15% are allowed for targeted analysis by LC-MS/MS, and 20% RSD is allowed at LOQ level<sup>142</sup>. For plasma protein precipitation with acetonitrile, the distribution of % RSD for all peaks shows that 67% of all peaks had RSD of  $\leq 20\%$ , and 82% of the peaks had RSD of  $\leq 30\%$  in negative ESI mode. In positive ESI mode, 54% and 71% of peaks had RSD of  $\leq 20\%$  and  $\leq 30\%$  respectively. This is significantly better than recently reported for similar plasma protein precipitation method with acetonitrile in combination with positive ESI UHPLC-MS analysis on QTOF instrument where only 49% of peaks had RSD  $\leq 30\%$ .<sup>51</sup>

The metabolite coverage achieved in current study is typically better than reported in literature using other LC-MS platforms. For instance, in one study on mouse blood relying on the precipitation with acetonitrile and reverse-phase LC-MS analysis on QTOF system, the authors detected 938 and

695 peaks using positive and negative ESI.<sup>17</sup> This is significantly less than observed in our study and indicates that the selection and optimization of analytical platform plays an important role in metabolite coverage. It is interesting to note that among these peaks, 142 and 176 peaks respectively exhibited significant circadian oscillations, indicating significant influence of the time of day on observed metabolite profile. Among the identified metabolites, certain lysophosphatidylcholines and amino acids showed significant circadian rhythms. This study clearly shows that the sampling time is another important factor to standardize during the development of blood collection protocols.

Another study on human serum utilizing precipitation with acetonitrile followed by UHPLC-MS analysis with QTOF instrument reported detection of 4900 and 3600 peaks in positive and negative ESI modes, respectively.<sup>223</sup> However, this number is most likely an overestimation of true number found in human serum because the authors did not eliminate blank peaks from their data sets prior to reporting of overall number in this particular study. In our study, significant number of blank peaks (~20%) were observed even when the reagents of highest available purity were used for solvent and mobile phase preparation. Therefore, the studies which do not exclude these peaks from their reports tend to considerably overestimate true number of features detected.

### **7.3.3 Global metabolomics - plasma protein precipitation with methanol/ethanol (PM) results**

In positive ESI reverse-phase LC method, plasma protein precipitation using methanol/ethanol resulted in total of 3245 peaks observed. The results of this analysis are summarized in Figure 7.10. The analysis of two data sets of the results obtained on human plasma after plasma protein precipitation with methanol/ethanol resulted in total of 2252 peaks observed in negative ESI mode with pentafluorophenyl column. The results of this analysis are summarized in Figure 7.11 Overall, the results show that plasma protein precipitation method with methanol/ethanol performed better than precipitation with acetonitrile for the metabolomics analysis of human plasma, as it resulted in better metabolite coverage. Furthermore, method precision was better for PM method as shown by the results for distribution of % RSD shown in Figure 7.11 (b). In fact, 69% and 81% of peaks observed with PM method had % RSD  $\leq$ 20%, while 80% and 89% had % RSD  $\leq$ 30% in positive and negative ESI mode, respectively. Finally, the sensitivity of PM method was higher than for PP method as shown in Figure 7.12. 973 peaks exhibited higher signal intensity in PM method than in PP method as shown by area ratio of 1.2 and above. In contrast, only 274 peaks exhibited higher signal intensity in PP method than in PM method as shown by area ratio of 0.8 and below. Only 30 peaks were observed



in PP method and not present in PM method *versus* 176 peaks observed in PM method only (negative ESI). In positive ESI mode, only 6 unique peaks were observed for PP method *versus* 270 unique peaks observed for PM method.

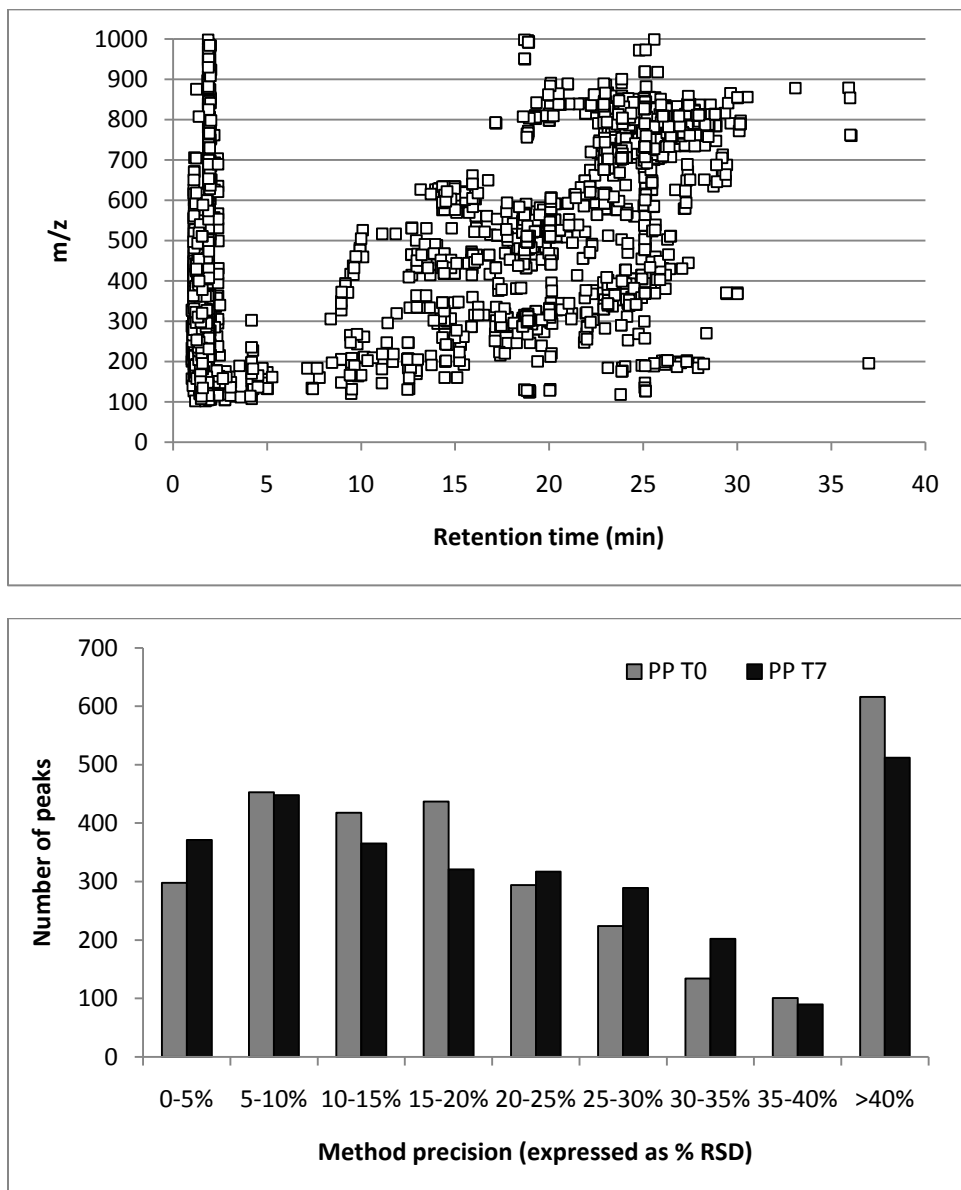


**Figure 7.8 (a) Ion map ( $m/z$  versus retention time) for human plasma sample prepared using plasma protein precipitation with acetonitrile (PP) and analyzed using positive ESI pentafluorophenyl LC-MS method. (b) Number of peaks with given % RSD obtained in two independent data sets.**

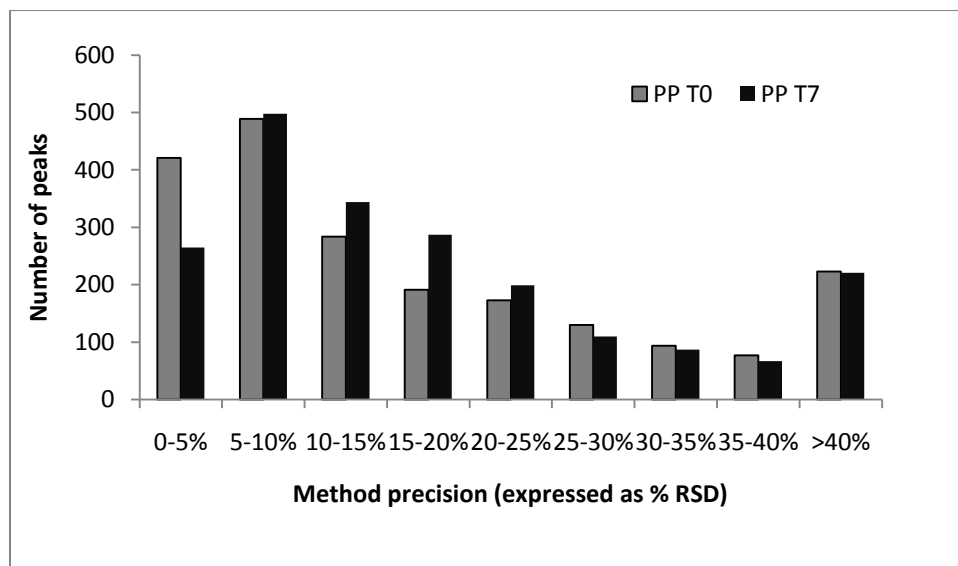
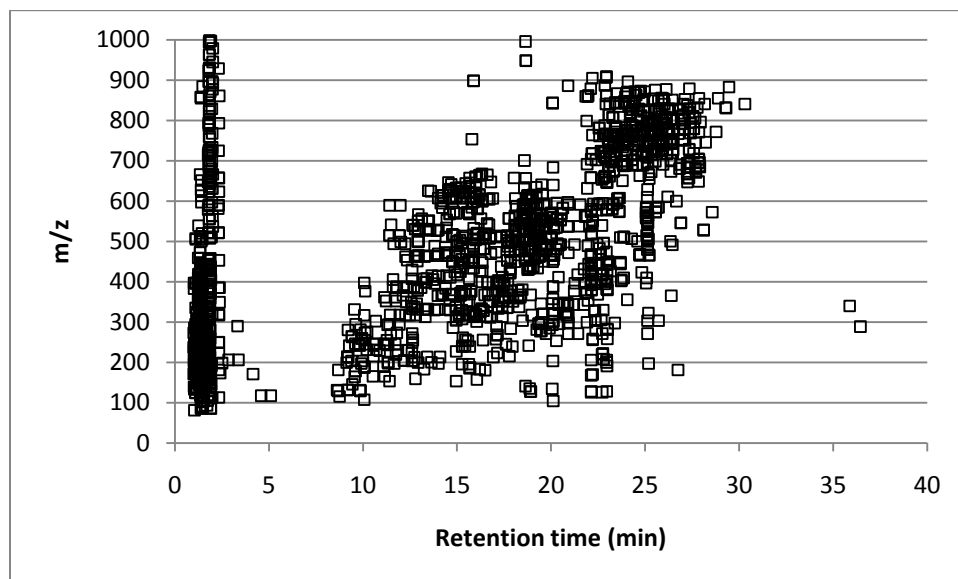


**Figure 7.9 (a) Ion map ( $m/z$  versus retention time) for human plasma sample prepared using plasma protein precipitation with acetonitrile (PP) and analyzed using negative ESI pentafluorophenyl LC-MS method. (b) Number of peaks with given % RSD obtained in two independent data sets.**

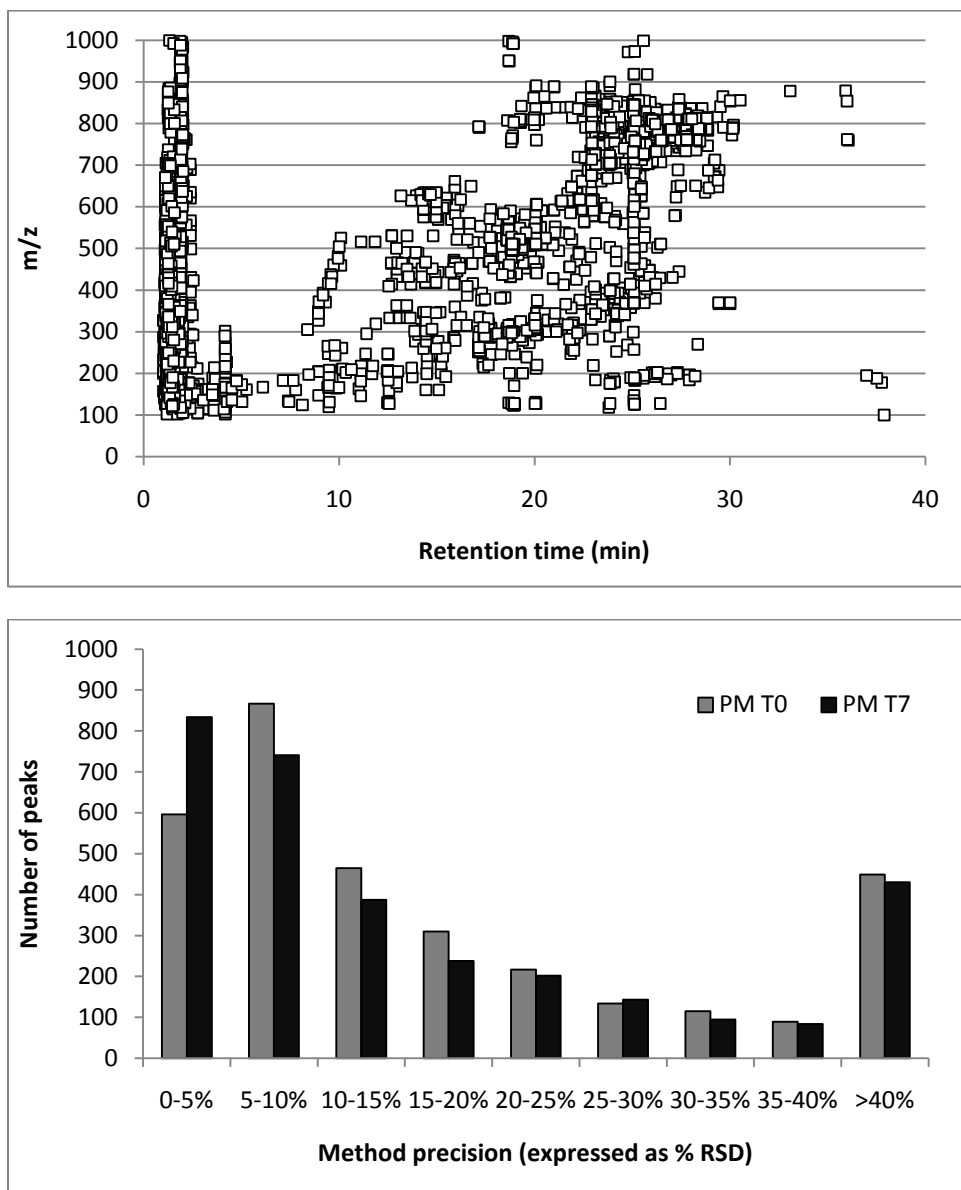


**Figure 7.10 (a)** Ion map ( $m/z$  versus retention time) for human plasma sample prepared using plasma protein precipitation with ethanol/methanol (PM) and analyzed using positive ESI pentafluorophenyl LC-MS method. **(b)** Number of peaks with given % RSD obtained in two independent data sets.

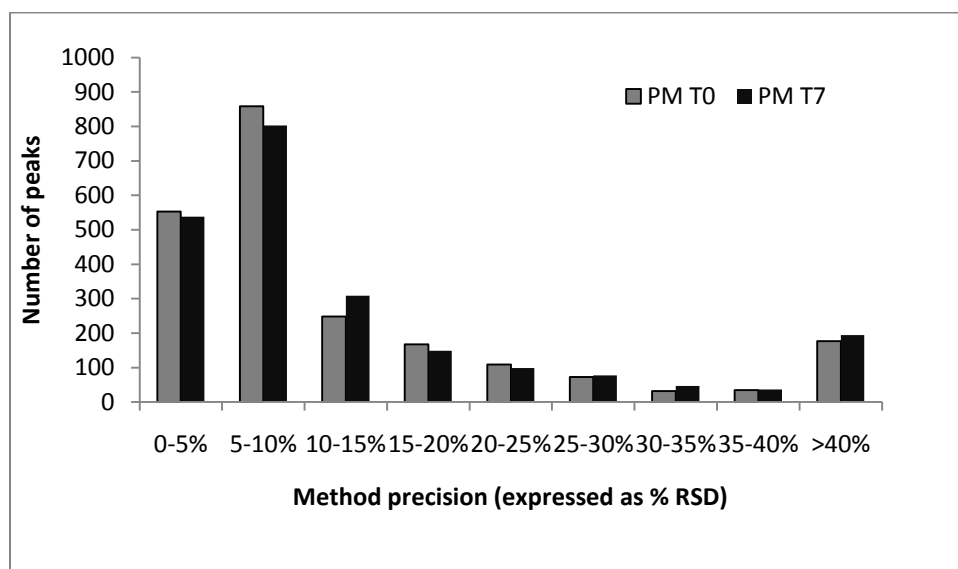
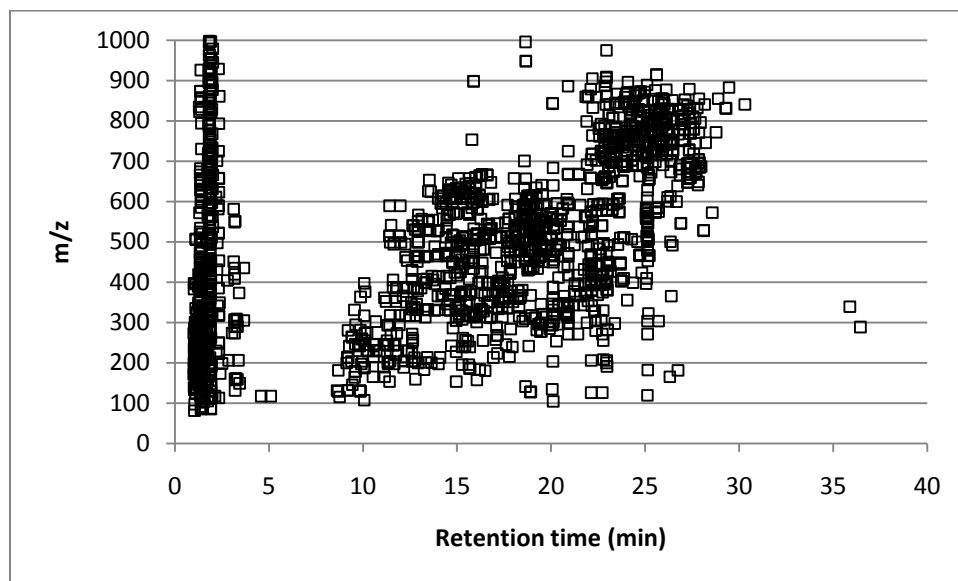


**Figure 7.11 (a) Ion map ( $m/z$  versus retention time) for human plasma sample prepared using plasma protein precipitation with ethanol/methanol (PM) and analyzed using negative ESI pentafluorophenyl LC-MS method. (b) Number of peaks with given % RSD obtained in two independent data sets.**

The improved results for plasma protein precipitation with methanol/ethanol are attributed to better solubility of some polar metabolites in methanol/ethanol *versus* acetonitrile mixture, while improved method precision is attributed to typically higher signal intensities observed in PM method *versus* PP method. In addition to solubility differences of some metabolites between the two solvents, additional

differences between the two methods can arise from factors such as difference in the amount and type of protein remaining after precipitation, degree of metabolite binding to proteins and degree of protein denaturation which causes disruption of metabolite binding.<sup>234</sup> Our results show significant overlap in metabolite coverage between the two plasma protein precipitation methods and higher overlap than reported previously (overlap of 1354 peaks for acetonitrile *versus* total of 2056 observed peaks in methanol in Want *et al.* study), but the reasons for this remain unclear at this time.<sup>234</sup>

The results obtained using PM method and pentafluorophenyl LC-MS method developed on Exactive compare favourably with UHPLC-MS method on C<sub>18</sub> column in combination with plasma protein precipitation using methanol proposed by Pereira *et al.*<sup>58</sup> In their approach, 1108 and 814 ions were observed in negative and positive ESI mode respectively. In another study on human serum after precipitation with methanol/acetonitrile (5/3, v/v) followed by analysis with UHPLC-MS method on C<sub>18</sub> column, 1570 peaks were observed in positive ESI and 450 peaks in negative ESI mode.<sup>206</sup> Want *et al.* reported detection of 2056 features using methanol precipitation *versus* 1606 features detected for acetonitrile precipitation using LC-MS method with ion trap.<sup>234</sup> Excellent results observed in our study (~2-fold increase in peaks observed) are attributed to good analytical sensitivity of Exactive instrument as well as the use of pentafluorophenyl reverse phase method rather than a simple C<sub>18</sub> reverse method. Increased separation/retention of polar analytes such as achieved by pentafluorophenyl column improves metabolite coverage. In another UHPLC-MS study with hybrid Orbitrap instrument by Brown *et al.*, the observed metabolite coverage was 2079 peaks in positive and 4513 peaks in negative mode. These results agree well with our findings, although better coverage in negative mode was observed using their method.<sup>33</sup> In contrast, 5300 peaks were reported in metabolomics study of human plasma using capillary LC-TOF MS method in positive ESI mode after precipitation with methanol.<sup>67</sup> However, this number includes any background contamination ions, as these features were not removed from the data by the authors so it represents a significant overestimation of metabolite coverage. The number of reliably identified features was further reduced to 3641 features upon examination of plasma from different individuals, which agree very well with our results using PM method. Therefore, based on the plasma protein precipitation results with both methanol/ethanol and acetonitrile, it can be concluded that Exactive provides an excellent LC-MS platform for metabolomics and achieved metabolite coverage is better or equivalent to what is reported in literature for other LC-MS platforms including TOF both in combination with conventional LC and UHPLC, as well as full hybrid Orbitrap instruments. Of course, the main shortcoming of the developed LC-MS methods on Exactive is the lack of MS/MS capability available

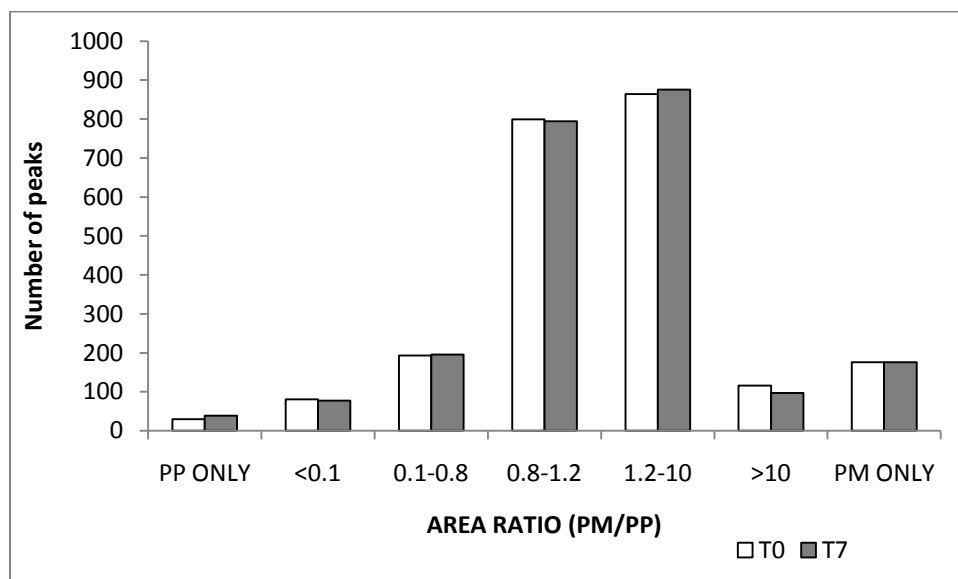
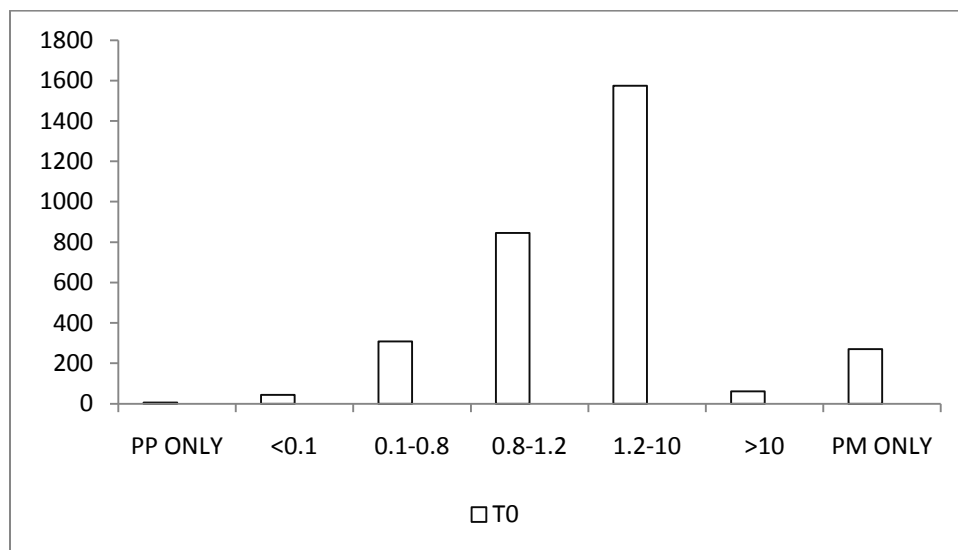


**Figure 7.12 Comparison of plasma protein precipitation methods using data collected with (a) positive and (b) negative ESI pentafluorophenyl LC-MS method. Two independent data sets are shown (T0 and T7) acquired a week apart on the same human plasma sample using n=7 independently prepared replicates. The graph shows number of peaks with given area ratio. For peaks with area ratios of 0.8-1.2, two methods can be considered to be equivalent. For peaks with area ratios <0.8 plasma protein precipitation with acetonitrile (PP) yielded better results. For peaks with area ratios >1.2 plasma protein precipitation with methanol/ethanol yielded better results.**

on instruments such as QTOF or hybrid Orbitrap which can be used to aid in identification of metabolites. However, for comparative global metabolomic studies, where identification is not routinely performed, Exactive provides an excellent choice in terms of high mass resolution, excellent analytical sensitivity and excellent signal stability and mass accuracy over long analysis times.

#### **7.3.4 Global metabolomics - ultrafiltration (UF) results**

The analysis of two independent data sets obtained on human plasma after ultrafiltration resulted in 2686 peaks in positive ESI mode using pentafluorophenyl LC-MS method. The ion map and the histogram of the distribution of RSD values are shown in Figure 7.13. The analysis of same samples using negative ESI resulted in total of 2093 peaks observed. The results of this analysis are summarized in Figure 7.14. Both ion maps show relatively poor metabolite coverage in the region of 5-30 min, indicating poor performance of UF method for more hydrophobic species. This is in line with the trends reported for the analysis of identified metabolites in Section 7.3.1. The observed poor coverage is attributed to poor solubility of some hydrophobic species in aqueous solution, possible high degree of protein-binding which would result in low analyte concentrations (below LOD) and possible adsorptive losses to ultrafiltration device. Poor performance of ultrafiltration for hydrophobic species was also previously shown in combination with NMR metabolomic studies.<sup>235</sup> To overcome this difficulty, the authors proposed an additional method for the extraction of hydrophobic species from the ultrafiltration membrane. However, the proposed method relied on multi-step time-consuming procedure, thus significantly reducing sample throughput. As shown in Figure 7.15 and Figure 7.16, SPME is able to successfully overcome this issue and provides balanced coverage of both hydrophilic and hydrophobic species.

Both Figure 7.13 and Figure 7.14 show that method precision for UF method was worse than the results obtained for either of plasma protein precipitation methods. In fact, only 52% of peaks observed in positive ESI mode had %RSD  $\leq$ 20% and only 69% had % RSD  $\leq$ 30%. In negative ESI mode, 48% of peaks observed with UF method had % RSD  $\leq$ 20%, and 64% had % RSD  $\leq$ 30%. This is attributed to the fact that large degree of co-elution was observed in 1-5 min retention time window, so there is likely to be large degree of competition for ionization which can result in large degree of ionization suppression and enhancement, and overall poor method precision.

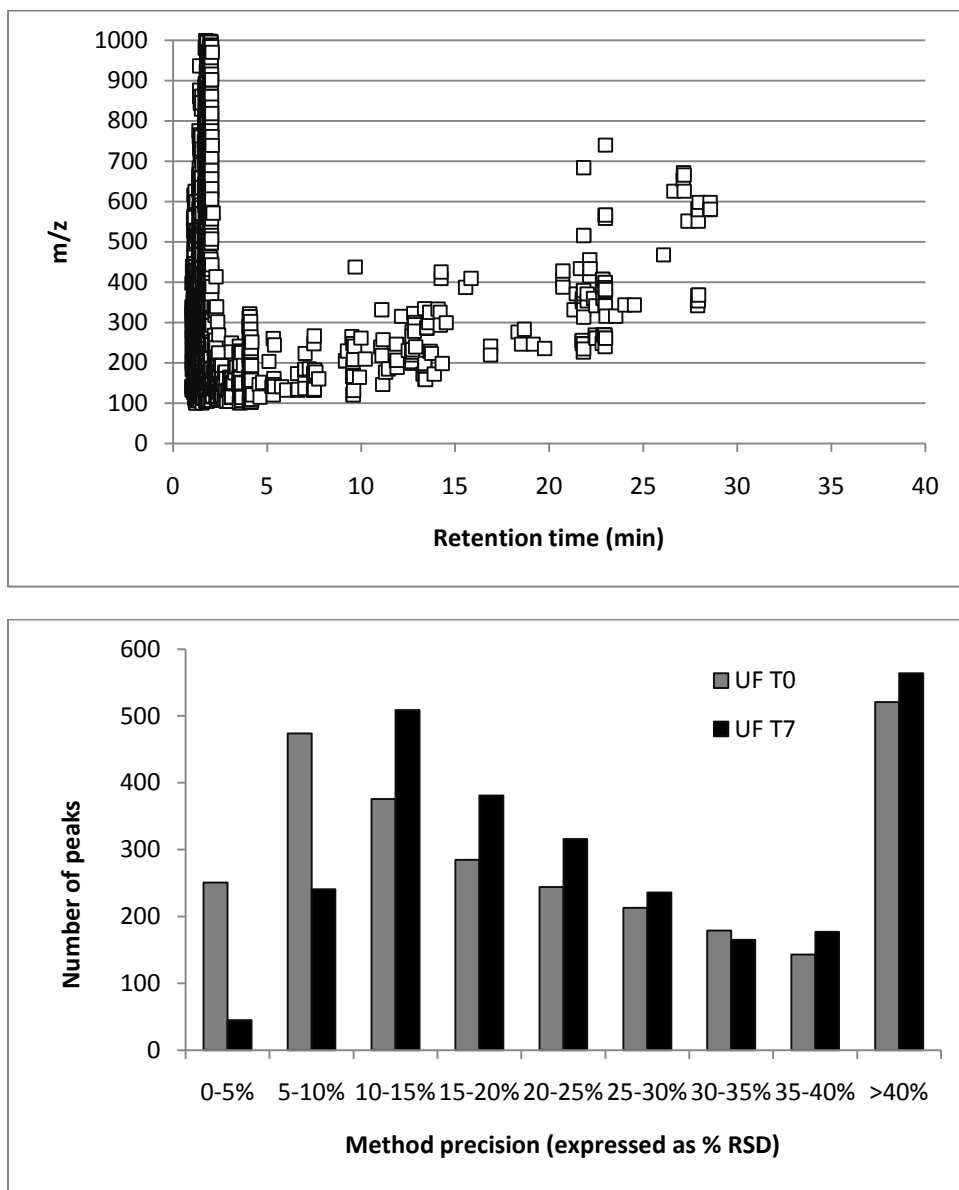


**Figure 7.13 (a) Ion map ( $m/z$  versus retention time) for human plasma sample prepared using ultrafiltration (UF) and analyzed using positive ESI pentafluorophenyl LC-MS method. (b) Number of peaks with given % RSD obtained in two independent data sets.**



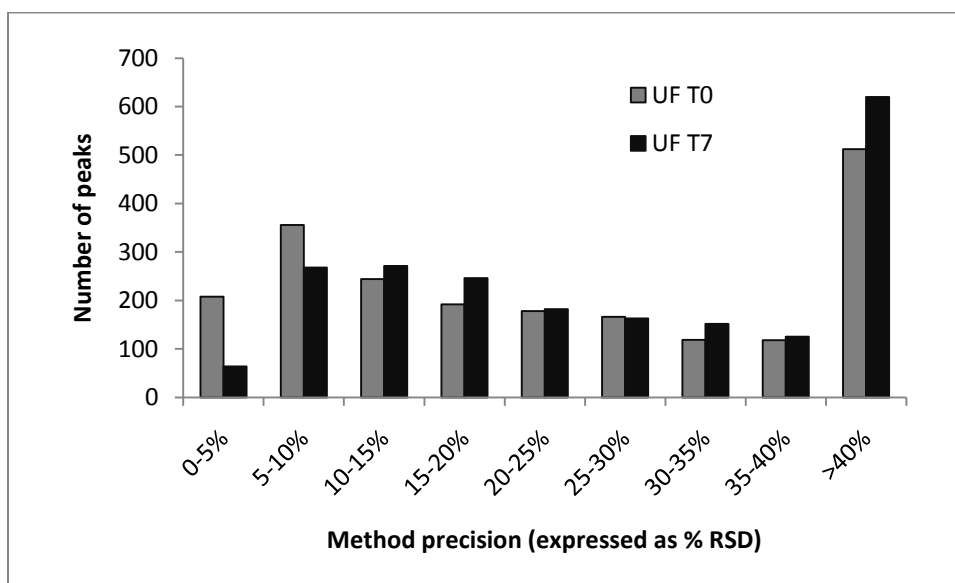
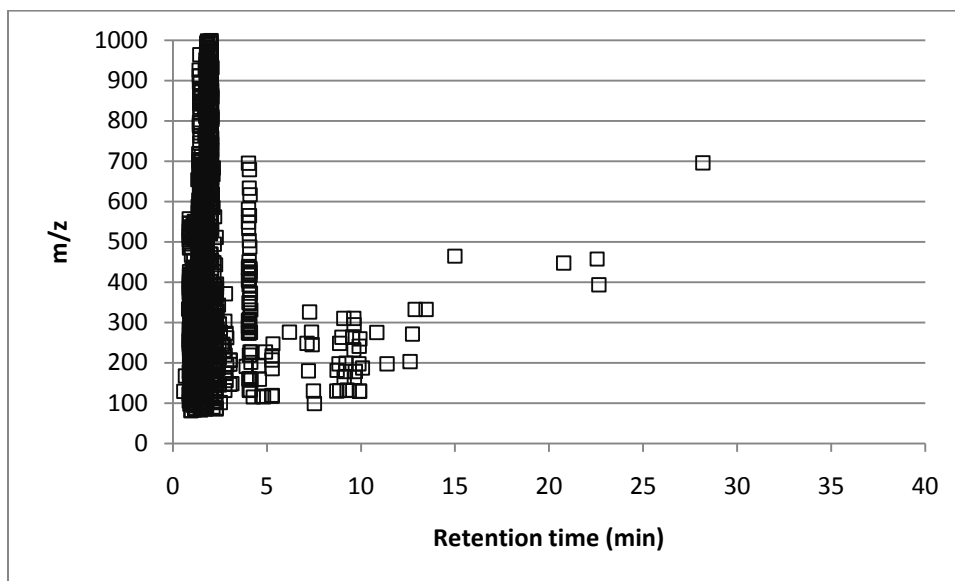


**Figure 7.14 (a) Ion map ( $m/z$  versus retention time) for human plasma sample prepared using ultrafiltration (UF) and analyzed using negative ESI pentafluorophenyl LC-MS method. (b) Number of peaks with given % RSD obtained in two independent data sets.**

### 7.3.5 Global metabolomics - SPME results using mixed-mode coating

The metabolite coverage and method precision observed for the extraction of human plasma using SPME is summarized in Figure 7.15 and Figure 7.16. The number of metabolites observed depended in part on the extraction time used and these effects are also illustrated in the figures. Namely, the

figures show all metabolites subdivided into three groups as illustrated with examples in Figure 7.17. The first group labelled as equilibrium reached, showed no further increase in the amount detected when the extraction time was incrementally increased from 5 min to 24-hr overnight extraction. Approximately 40-50% of all metabolites exhibited this trend. The second group, consisting of approximately 40-50% of all metabolites, showed an increasing trend in the amount extracted with the extraction time, indicating that the equilibrium was only reached using longer extraction times. Depending on the analytical sensitivity and extraction efficiency for a given individual analyte, majority of the metabolites from this group could be detected even using the shortest time tested of 5 min. For these metabolites, increasing extraction time only resulted in increasing of signal intensity. Some metabolites, however, only became detectable at longer extraction times. However, some care should be taken in the interpretation of the metabolites which were only observed when very long extraction times were used as these may be due to degradation or conversion of some metabolites during long extraction at room temperature in human plasma. Short extraction times are preferable for metabolomics to reduce the possibility of such conversion/degradation when using *in vitro* SPME and also from the perspective of sample throughput. The results clearly illustrate that although some gain in metabolite coverage can be observed using long extraction times, the metabolite coverage with very short times of 5 min already provides 84% and 60% of coverage achievable at equilibrium for positive and negative ESI reverse-phase method, respectively. Therefore, the best approach when using SPME for global metabolomic studies is to use very short extraction times and improve metabolite coverage by using complementary coatings such as recommended in Chapter 5 (polystyrene-divinyl benzene polymeric coating and phenylboronic acid silica-based coating).

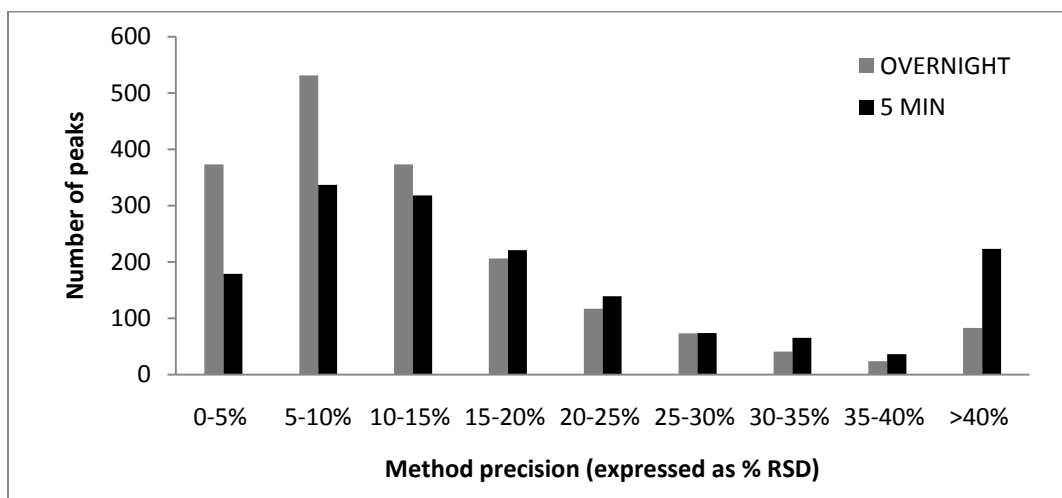
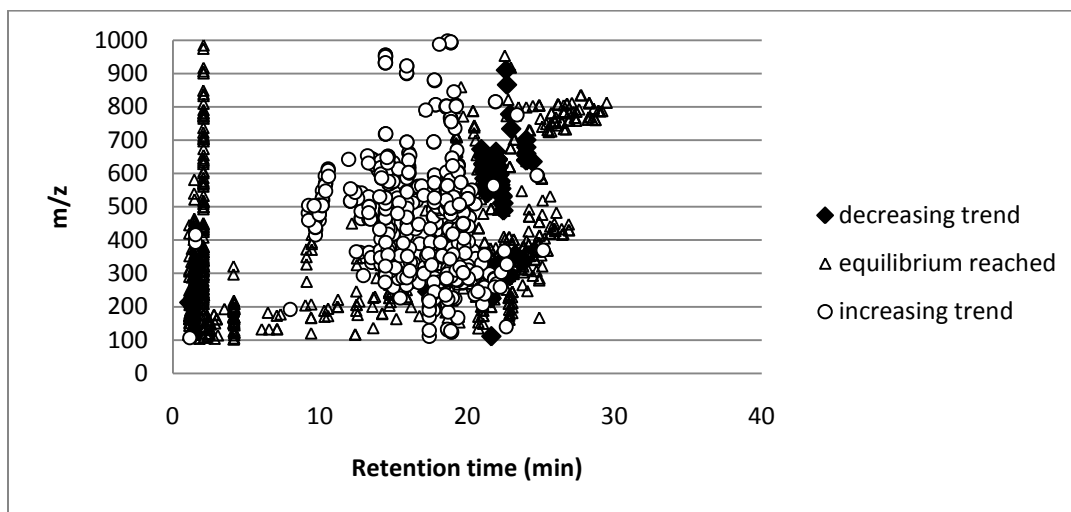


**Figure 7.15 (a) Ion map ( $m/z$  versus retention time) for human plasma sample prepared using SPME and analyzed using positive ESI pentafluorophenyl LC-MS method. (b) Number of peaks with given % RSD obtained in two SPME data sets where extraction time was varied from 5 min to overnight.**

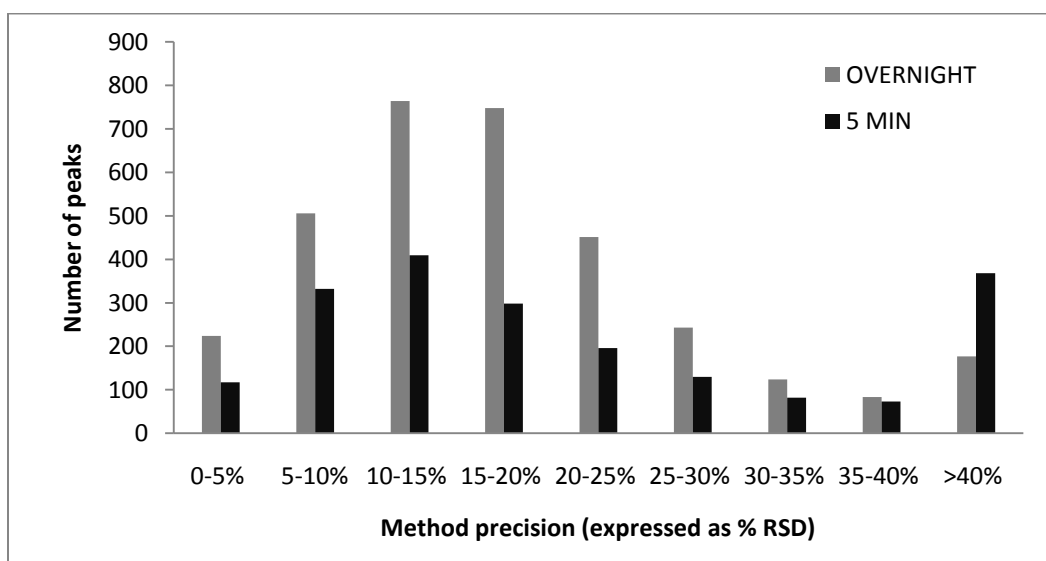
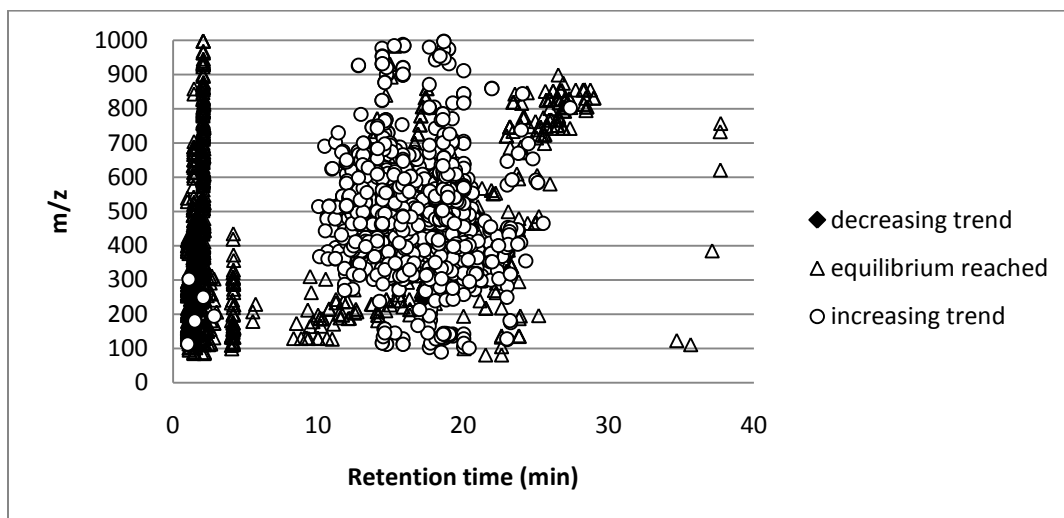
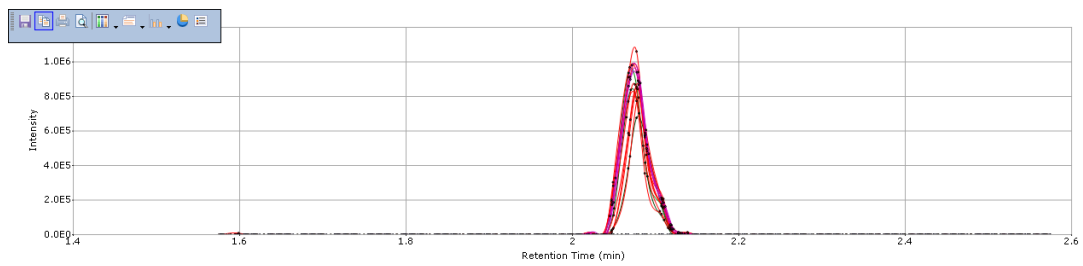


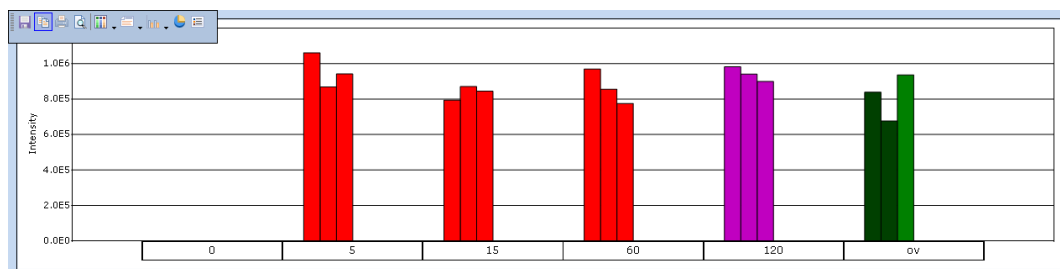
**Figure 7.16 (a) Ion map ( $m/z$  versus retention time) for human plasma sample prepared using SPME and analyzed using negative ESI pentafluorophenyl LC-MS method. (b) Number of peaks with given % RSD obtained in two SPME data sets where extraction time was varied from 5 min to overnight.**

The third group of metabolites was labelled as decreasing trend, where the amount extracted decreased with extraction time. Such trend can be observed for adsorptive coatings in case of competitive displacement effects when the number of binding sites becomes limited. In current study, this trend was attributed to the degradation of these metabolites over time as it was only

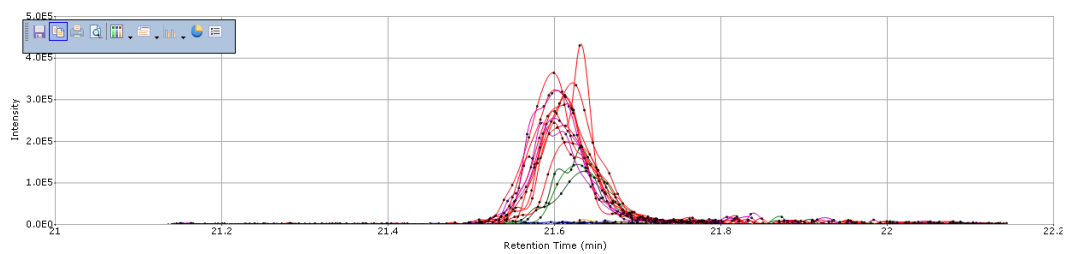
(a)



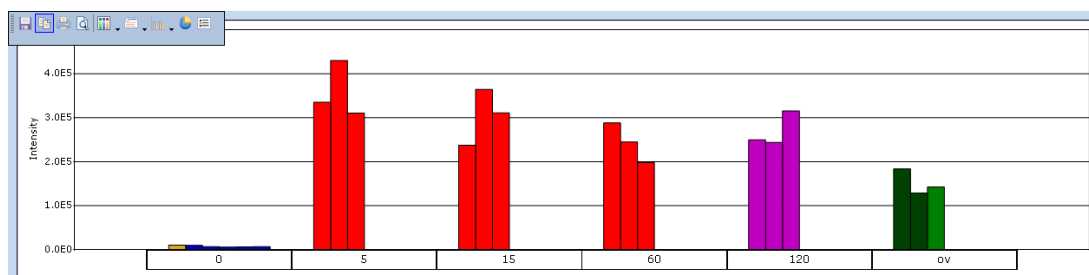
(b)



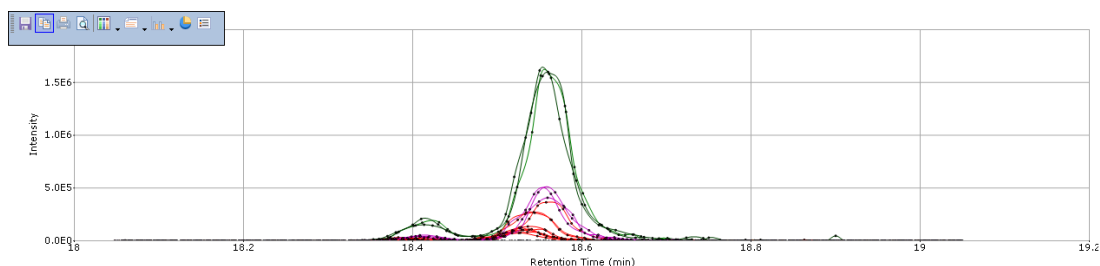
(c)



(d)



(e)



(f)

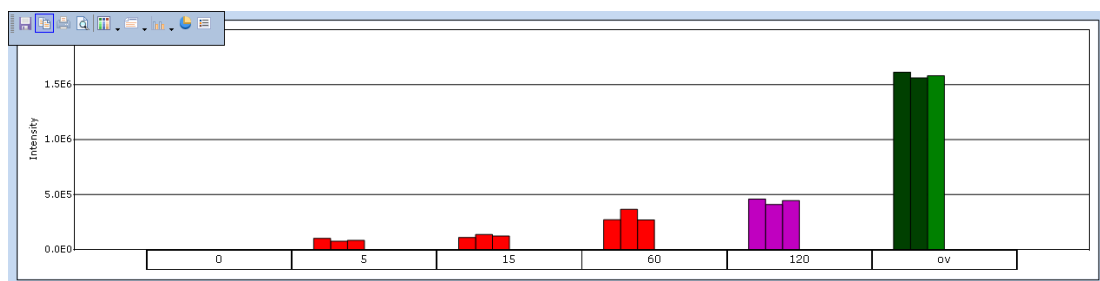


**Figure 7.17 Example of three metabolites processed using SIEVE software (a,b) peak showing equilibrium reached trend with no further increases in the amount extracted with increasing extraction time (c,d) peak showing decreasing trend where the amount extracted decreases with increasing extraction time (e,f) peak showing increasing trend where the amount extracted increases with increasing extraction time. The panels a, c, e show XIC for this metabolite and demonstrate good chromatographic alignment of the peaks. The panels b, d, f show the magnitude of integrated intensity for each extraction time (n=3 extractions per each time point), while label 0 shows the results for blank injection of desorption solvent.**

observed for very few metabolites (2 in negative ESI mode and <35 in positive ESI mode) as summarized in Table 7.2.

Both Figure 7.15 and Figure 7.16 show that method precision for SPME method was similar to the results obtained for plasma protein precipitation methods. In positive ESI mode, 66% and 80% of peaks had  $RSD \leq 20\%$  and  $\leq 30\%$  respectively using 5-min extraction time. Using overnight extraction times (equilibrium), method precision was even better with 81% having  $RSD \leq 20\%$  and 92% of peaks having  $RSD \leq 30\%$ . In negative ESI mode, 68% and 88% of peaks had  $RSD \leq 20\%$  and  $\leq 30\%$  respectively using overnight extraction time *versus* 58% and 74% for 5-min extraction time. It

**Table 7.2 List of features exhibiting decreasing trend with increasing SPME extraction time.**

Ionization mode	Retention time (min)	m/z	Tentative chemical formula according to HMDB	Mass accuracy (ppm)	Ion type
negative	1.42	289.9239	no hits	N/A	N/A
negative	17.35	243.1707	no hits	N/A	N/A
positive	17.29	245.1860	no hits	N/A	N/A
positive	17.83	387.1925	C <sub>21</sub> H <sub>32</sub> O <sub>4</sub>	-1.7	M+K[1+]
positive	20.96	672.4352	no hits	N/A	N/A
positive	21.06	650.4218	no hits	N/A	N/A
positive	21.11	628.4086	C <sub>28</sub> H <sub>52</sub> NO <sub>7</sub> P	0.1	M+2ACN+H [1+]
positive	21.11	628.9105	no hits	N/A	N/A
positive	21.11	625.9312	no hits	N/A	N/A
positive	21.15	606.3958	no hits	N/A	N/A
positive	21.15	606.8975	no hits	N/A	N/A
positive	21.17	584.4138	no hits	N/A	N/A
positive	21.17	603.9180	no hits	N/A	N/A
positive	21.23	562.4007	C <sub>24</sub> H <sub>50</sub> NO <sub>6</sub> P	5.0	M+2ACN+H [1+]
positive	21.23	584.3824	no hits	N/A	N/A
positive	21.28	562.3692	no hits	N/A	N/A
positive	21.30	562.8708	no hits	N/A	N/A
positive	21.64	287.2216	C <sub>16</sub> H <sub>30</sub> O <sub>4</sub>	-0.2	M+H [1+]
positive	21.64	224.6278	no hits	N/A	N/A
positive	21.64	111.1171	no hits	N/A	N/A
positive	21.64	225.1294	no hits	N/A	N/A
positive	22.24	573.9073	no hits	N/A	N/A
positive	22.25	328.3207	C <sub>20</sub> H <sub>38</sub> O <sub>2</sub>	-0.8	M+NH <sub>4</sub> [1+]
positive	22.40	529.8813	no hits	N/A	N/A
positive	22.70	865.6229	C <sub>50</sub> H <sub>90</sub> O <sub>7</sub> P <sub>2</sub>	-0.6	M+H [1+]
positive	22.88	291.1954	no hits	N/A	N/A
positive	23.79	338.2278	C <sub>52</sub> H <sub>99</sub> NO <sub>13</sub>	4.1	M+3Na [3+]
positive	23.84	339.3963	C <sub>63</sub> H <sub>118</sub> O <sub>6</sub>	-2.7	M+H+2Na [3+]
positive	24.02	639.3123	no hits	N/A	N/A
positive	24.02	638.3095	no hits	N/A	N/A
positive	24.02	678.3326	no hits	N/A	N/A
positive	24.02	659.2878	no hits	N/A	N/A
positive	24.02	700.3145	no hits	N/A	N/A

is important to mention that all steps of extraction and desorption in current study were performed manually, which makes small errors in accurate timing likely for short 5-min extraction times. However, as previously shown in Chapter 2, precision of pre-equilibrium SPME methods can be improved to be in line with that of equilibrium methods when automated system such as Concept 96 is used. Therefore, future work for *in vitro* metabolomics using SPME can make use of this automated 96-well plate format for further improvement of method precision.

Another contributing factor to poor method precision observed for some peaks can be low signal intensity, where a peak is inconsistently detected either by detector or by data processing software. The effect of signal intensity on method precision is shown for SPME and PP methods in Figure 7.18. The figure clearly shows that signal intensity plays a major role in the number of peaks meeting acceptable RSD criteria. For example using SPME, only approximately 40% of peaks with integrated intensity < 1000 had acceptable precision, while for signal intensities in the range of  $1 \times 10^5$  to  $1 \times 10^6$  >90% of peaks showed acceptable precision. This is in agreement with other studies where similar trend was reported.<sup>208</sup> Interestingly, the number of peaks of given intensity that meet acceptable RSD criteria appears to be higher when SPME is used as sample preparation method *versus* plasma protein precipitation. One possible explanation for this observation could be ionization suppression which has been shown to adversely affect method precision especially for low-level signals in absence of adequate sample clean-up.<sup>143</sup>

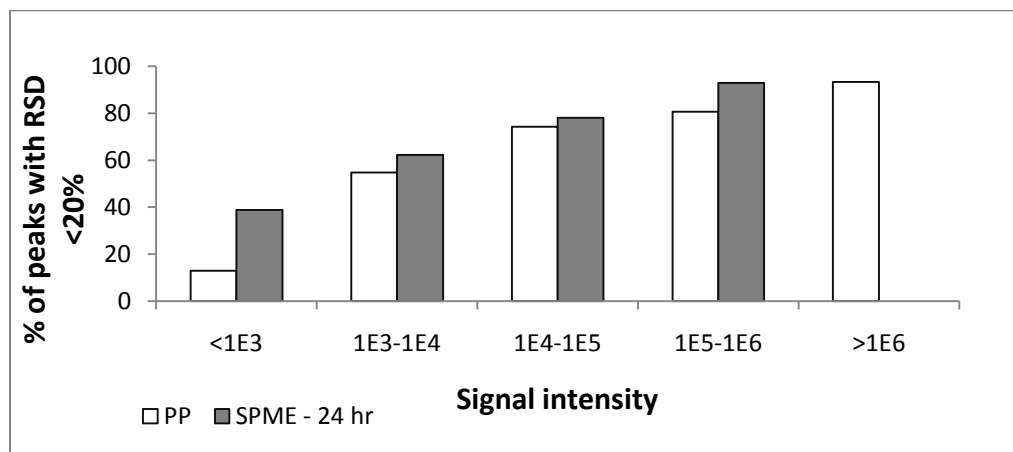


**Figure 7.18** Dependence of % RSD on signal intensity. Comparison of plasma protein precipitation with acetonitrile (PP) *versus* SPME using pentafluorophenyl method in negative ESI mode.



### 7.3.6 Results for semi-quantitative analysis of identified metabolites using traditional methods

The current goal of the global LC-MS metabolomic studies is not full identification and absolute quantitation of all metabolites because current analytical capability is not sufficiently advanced to permit this because of the difficulties such as lack of authentic standards and databases, inadequate resolution, matrix effects, issues with degradation and conversion, etc.<sup>15</sup> However, an acceptable global metabolomics method must be sufficiently quantitative to at least enable differential quantification of metabolites. Ionization suppression/enhancement effects are particularly problematic for any type of quantitative work as the observed changes in signal intensity for a particular metabolite may simply due to different composition of given sample which resulted in different ionization behaviour of that analyte, even if it is present at the same concentration in both samples.

The completeness of metabolite extraction for traditional methods and susceptibility to matrix effects can be verified by comparing the ability of each of three methods to extract metabolites from identical biological samples. This comparison was performed for a set of known metabolites and the results are reported in Table 7.3. The concentration in human plasma sample of each metabolite was determined using semi-quantitative approach where 100% recovery of metabolite was assumed for each method, and the concentration in human plasma was estimated in comparison to neat metabolite standard. Theoretically, if the quality of metabolomics data collected by each method was good with no matrix effects, the two plasma protein precipitation methods should give identical results. Ultrafiltration should give identical results to plasma protein precipitation methods for compounds that are not highly bound, and lower results for highly protein-bound compounds. Such results were observed for some of metabolites tested, for example maleic acid, fumaric acid, tryptophan and phenylalanine and are summarized by indicator good in the Data quality column of Table 7.3. However, the results shown in this table also illustrate problems with the analysis of some of metabolites. For example, for some of the polar analytes there was a large discrepancy observed between PM and PP results, for example citric acid and pyruvic acid. Not surprisingly, these results indicate that exhaustive extraction is not achieved for all metabolites. This can be caused by poor metabolite solubility in precipitant used and/or co-precipitation of metabolite. Precipitation with methanol/ethanol was found to perform better for these polar species, while more hydrophobic species performed well using either of the two precipitation approaches. For some metabolites, such as glucose, fructose, histidine, lysine, citric acid and hydroxybutyric acid (HBA), the results for UF method were significantly higher than for plasma protein-precipitation methods. In addition to poor

metabolite solubility and/or accidental co-precipitation, the observed results can be caused by very significant ionization suppression effects, as these compounds were eluting with relatively short retention times (<5 min) where many other co-eluting species were also present as shown in ion maps in Figure 7.9 and Figure 7.11. Although, large number of co-eluting species were also present in UF method, this extract was diluted 30-fold prior to injection (compared to 2-fold dilution for precipitation methods), so it would be expected to have less significant ionization suppression effects. It is important to mention that all methods and all compounds reported in Table 7.3 exhibited good method precision for n=7 replicates as discussed in Section 7.3.1. Signal-to-noise ratio and signal intensity precision are typically the only criteria used to include or exclude peaks from global metabolomics data sets prior to further processing. However, our results clearly show that this is not adequate approach. Issues with ionization suppression can lead to erroneous results and conclusions when comparing samples from different individuals due to inter-sample variation in composition and lead to false discovery of possible biomarkers. Furthermore, plasma protein precipitation data cannot be reliably used to estimate concentrations of metabolites in given biofluids for more polar species.

In addition to inter-method comparison, the results obtained for the three methods were also compared to known expected concentrations of each metabolite in normal human plasma as reported in Human Metabolome Database (HMDB).<sup>243-245</sup> For this comparison, only normal adult plasma concentrations were considered. The range shown in Table 7.3 presents minimum and maximum concentration of all ranges reported within HMDB. The results show reasonable agreement for majority of metabolites. The concentrations experimentally estimated for few metabolites are lower than expected (for example, ascorbic acid, cholic acid, glucose/fructose) but this can be attributed to the fact that no metabolism quenching for this plasma sample was not performed upon collection, as this was commercially purchased pooled human plasma sample. Also, this plasma sample was stored for approximately 6 months at -20°C prior to analysis, which could have resulted in the observed changes of unstable metabolites. This is especially likely for metabolite such as ascorbic acid which is known to oxidize easily.

**Table 7.3 Summary of metabolite concentrations in human plasma determined using traditional sample preparation methods and comparison to normal concentrations expected in plasma according to the ranges reported in Human Metabolome Database.**<sup>243-245</sup>

Metabolite	Plasma concentration estimated in current study			Normal concentration in plasma according to HMDB ( $\mu\text{M}$ )	Data quality
	PM method ( $\mu\text{M}$ )	PP method ( $\mu\text{M}$ )	UF method ( $\mu\text{M}$ )		
Glucose+fructose	73	88	667	3300-6100 glucose, 32-64 fructose	Poor
Ascorbic acid	0.84	ND	0.71	11-114	Good
Glutamic acid	47	33	44	21-151	Good
Pyruvic acid	921	61	1593	22-258	Poor
Histidine	7.4	6.7	38	55-120	Poor
Lysine	8.7	3.5	342	130-467	Poor
Citric acid	9193	10	342103	Anticoagulant in current study	Poor
Maleic+fumaric acids	3.3	1.8	4.2	0-4 fumaric, N/A maleic	Good
HBA	321	255	604	0-700	Poor
Phenylalanine	34	30	40	38-169	Good
Tryptophan	36	33	4.4	36-130	Good
Taurocholic acid	0.09	0.10	ND	0.2-0.6	Good
Cholic acid	0.02	0.02	ND	0.5-2.0	Good
Linoleic acid	51	36	ND	10-370	Good

Above example shows that the reliance on good method precision (as indicated by acceptable RSD for a given peak in QC sample) cannot be used as the only criteria for ensuring good data quality in comparative metabolomics experiments. New approaches to address such problems are currently under development to ensure only signals with adequate performance are included in data interpretation. For example, Croixmarie *et al.* recently proposed injection of series of pooled samples rather than single QC pooled sample (for example 3/1, 1/1, 1/3). During data processing, the signal for each metabolite was then examined for linearity and any signals not meeting criteria were eliminated.<sup>71</sup> This included the elimination of blank peaks, peaks with erratic profiles, peaks that exceed linear dynamic range of the instrument and so on. Using this method, 5296 initial peaks in negative ESI mode and 8937 peaks in positive ESI mode were reduced to 1286 and 2095 peaks using correlation cutoff value of 0.8. Using this reduced data set improved the clustering during PCA

analysis as well as separation between treatment and controls, thus leading to more reliable interpretation. These examples illustrate that there is still significant amount of research needed to improve data processing workflows for metabolomic studies and ensure only good quality data is used in the search for biomarkers. This example also illustrates that high metabolite coverage (for example >5000 peaks in the cited study) is not the only parameter to consider during the development of global metabolomic studies, as high number of peaks of poor quality contribute nothing to the improved understanding of living systems.

### **7.3.7 Comparison of methods: summary**

The main results obtained for each of four methods discussed in previous sections are summarized in Table 7.4. Median RSD is included in Table 7.4 rather than mean RSD, because median is more robust estimator and less significantly influenced by presence of outliers.<sup>72</sup> In general, the precision of SPME method was similar to that observed for plasma protein precipitation methods, and better than precision observed for ultrafiltration. However, this result is somewhat surprising as signal intensities using traditional methods were significantly higher than for SPME method, so improved method precision would be expected. In fact, equilibrium SPME using overnight extraction time exhibited the best method precision among all methods tested in positive ESI mode, whereas in negative ESI mode it provided the highest metabolite coverage. These results indicate that SPME is a useful sample preparation method for global metabolomic studies. In terms of metabolite coverage in positive ESI mode, SPME performed more poorly than other methods tested, so alternative coatings to further improve metabolite coverage should be explored in future. Another interesting aspect for future studies is to begin the characterization of metabolites observed by SPME and not by other methods, to see if any previously unknown or unreported metabolites can be discovered. One such example is shown in Figure 7.19. This metabolite was detected by SPME using mixed mode coating and 5-min short extraction time, as well as by ultrafiltration and SPME using different coatings such as phenylboronic acid coating. The accurate mass of this unknown metabolite was submitted to database search using HMDB for tentative identification of possible chemical formula. Five possible metabolites in HMDB were identified as possible matches for this unknown peak as listed in the figure.

**Table 7.4 Summary of results (metabolite coverage and median RSD) observed for the analysis of technical replicates (n=7) of the same human plasma sample prepared using different sample preparation methods as discussed in experimental and analyzed using reverse-phase PFP LC-MS method.**

	Number of peaks or features		Median RSD of signal intensity	
	Positive ESI	Negative ESI	Positive ESI	Negative ESI
<b>PP</b>	2975	2082	19	12
<b>PM</b>	3245	2252	12	8
<b>UF</b>	2686	2093	20	22
<b>SPME (5 min)</b>	1592	2005	16	18
<b>SPME (overnight)</b>	1821	3320	11	17

In terms of method precision, our results show good agreement with literature reports. For example median RSD of 16% was observed for the analysis of technical replicates of human plasma sample, and similar method precision distribution as obtained in Figure 7.11.<sup>67</sup> SPE using C<sub>18</sub> sorbent was found to result in 1500 features using UHPLC-MS platform<sup>51</sup>, which is in line with the results we observed for SPME using positive ESI reverse-phase method. However, using SPE only 48% of detected peaks had acceptable RSD of  $\leq 30\%$  indicating better performance of SPME method developed in current study. In HUSERMET project study which uses plasma protein precipitation with methanol followed by lyophilization, method precision was similar to what was observed in our methods, but metabolite coverage was significantly less (1600 and 1100 in positive and negative ESI, respectively).<sup>52</sup> The results shown in Table 7.4 are better than results reported in other studies in human plasma or serum. For example, Want *et al.* reported mean RSD values of 36% for acetonitrile precipitation and 25% for methanol precipitation which is ~2-fold worse than our results.<sup>234</sup>

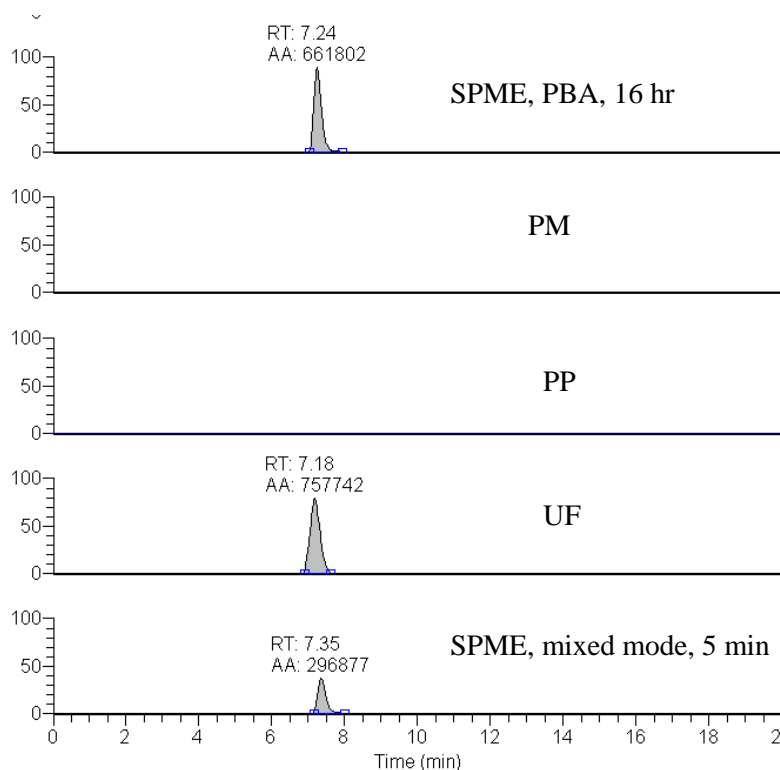


**Figure 7.19** Example metabolite detected ( $m/z$  of 411.0783) by SPME and UF methods, but not by plasma protein precipitation methods. All XICs are shown on the scale of  $5 \times 10^4$  to facilitate comparison between methods. The analysis was performed using negative ESI HILIC LC-MS method. Search of HMDB resulted in four possible hits with mass accuracy of 0.8 ppm (HMDB 00379, 06471, 06355 and 03518) and one hit with mass accuracy of -3.6 ppm (HMDB ID 01451).

This may be attributed to use of low resolution instrument (ion trap), so species with same nominal mass could not be distinguished. Another possible explanation is that their method used lower plasma to precipitant ratio of 1 to 2 while our study employed 1 to 4 ratio, possibly resulting in lower extent of ionization suppression. The number of features observed by precipitation with acetonitrile (2200) reported by UHPLC-MS analysis using QTOF system in positive ESI mode<sup>51</sup> is less than found in current study using conventional LC and single-stage Orbitrap system, indicating that a powerful LC-MS platform for metabolomics was developed in current study. Similar to what was observed in current study, HILIC LC-MS methods resulted in fewer features than reverse-phase methods.<sup>64, 213</sup> For example, Gika *et al.* observed 3284 features after analysis of rat urine using reverse-phase method *versus* 2098 of features observed using HILIC method.<sup>213</sup> However, due to complementary nature of HILIC and reverse-phase mechanism, the metabolites identified by each of two methods are likely to

be different thus providing additional insight into metabolic processes over the use of reverse-phase methods only.<sup>64</sup>

Furthermore, the results obtained in our study compare well to the results obtained in the study which compared various plasma protein precipitation methods with ultrafiltration.<sup>235</sup> Ultrafiltration with 3K membrane similar to the one used in our study was found to provide efficient protein removal and good solubilization of highly abundant polar metabolites (for example, citrate, lactate, alanine and succinate) observed by NMR. The loss of hydrophobic species, similar to what was observed in our study, was also documented. To overcome this disadvantage of ultrafiltration, the authors propose the extraction of membrane material with methanol/water mixture followed by liquid-liquid extraction with chloroform, followed by evaporation and reconstitution step. This was found to efficiently recover hydrophobic species. However, this adds extra steps to the sample preparation method, so the use of SPME as proposed in current work provides a simpler and faster alternative with fewer steps and less potential for accidental contamination/analyte loss. Furthermore, the same study also shows that precipitation with acetonitrile leaves a considerable amount of lipoprotein. This can have adverse effect on the lifetime of chromatographic columns used in LC-MS studies, and the methods with more efficient protein removal should preferably be used.

From ion maps shown for all methods it can be seen that the region of 3-10 min has relatively fewer peaks, and any peaks that are present are of low molecular weight. The raw data files were subsequently manually examined to verify whether this was an artifact of data processing, but no additional metabolite peaks were found beyond those reported in figures. The bias towards low molecular weight species in this region of chromatogram can be attributed to the fact that larger molecular weight species are expected to have more hydrophobic character in at least some portions of the molecule, which would result in their increased retention under reverse-phase conditions and elution in later portions of chromatogram.

Brown *et al.* recently reported an instrument-specific artifact for Orbitrap mass analyzer which causes reporting of Fourier artifact peaks within 0.3 Da window of true peak, situation which occurs if there is overabundance of ions of certain  $m/z$  which causes the detector to overload and clipping of associated oscillation signal.<sup>33</sup> For study of serum, 0.8% of peaks and 1.6% of total peaks detected using positive and negative ESI were assigned to be Fourier artifact peaks after examination of Fourier data. Considering the intensities of some abundant peaks using traditional methods were very high in current study, plasma protein precipitation and ultrafiltration methods can be considered to be

more susceptible to this type of artifact than SPME. For example, intensity distribution plot shown previously in Figure 7.18 shows that signal intensity using PP method exceeded  $1 \times 10^6$  for some peaks, while no peaks in SPME exceeded this intensity.

Some of the factors that must be taken into account during the design of metabolomics study include number of samples to be collected, proper selection of controls and quality/robustness of the overall analytical method employed for the analysis. Other experimental factors impact the quality of the data collected and include: autosampler carryover, sample degradation while awaiting analysis, background ions originating from solvents, columns and glassware/plasticware used during sample preparation, contamination buildup that can elute and change intensity, sensitivity changes in MS during the run, saturation of the detector by exceeding linear dynamic range of instrument, and of course ionization suppression/enhancement due to co-eluting components.<sup>203</sup> Croixmarie *et al.* found that the main source of variation in their data set was the origin of liver hepatocytes (46% of variance), while the treatment with drug only accounted for 13% of variation and run order accounted for 11% of variation.<sup>71</sup> The biological variability was found to be 35% and 46% RSD for cerebrospinal fluid and human plasma respectively, *versus* analytical variability of 15-16% RSD for both matrices.<sup>67</sup> In animal, plant and cell studies it can be easier to control biological variation as the study can be designed in such a way to minimize variability due to genetic makeup, environmental factors, diet or growth conditions, etc. When dealing with human samples, biological variability is much greater as it is impossible to control many of these factors. However, the results of current study on human plasma show that analytical reproducibility of proposed SPME-LC-MS methods is sufficient to be able to detect biological variability with 2-fold changes in signal intensity of metabolites as proposed fold change cutoff to interrogate differences between treatment and control groups.<sup>67</sup>

### **7.3.8 Global metabolomics: data processing and identification challenges**

Current versions of SIEVE software do not employ any normalization strategy, and other metabolomics software such as XCMS also does not employ any normalization. Few LC-MS metabolomic studies do employ normalization strategies, but there is currently no consensus in literature regarding the optimum (and if any) normalization strategy to use. Burton *et al.* report that normalization is not necessary for relatively small batches of data acquired on the same instrument at the same time.<sup>203</sup> This was the situation in current work, so no normalization was employed. One potential drawback of this is that large intensity peaks could obscure some important low intensity



peaks. However, in samples prepared by SPME there were no peaks observed with very high intensity, so this approach should be adequate.

Among the studies that do employ normalization, there is no consensus regarding the most appropriate normalization process to use during data processing, and both statistical (for example, normalization by median intensity) and internal standard normalization methods are employed.<sup>241</sup> Van der Kloet *et al.* advocate the use of normalization to single internal standard selected from cocktail of internal standards.<sup>240</sup> The selection is based on which internal standard results in the lowest RSD for the unknown metabolite. However, the assumption these authors make prior to application of their proposed method, is that no ionization suppression or enhancement is observed for any analyte. This assumption is clearly not realistic for a practical data set. Also, it is not practical to include internal standards for each of hundreds or thousands of potential metabolites present in a given sample, while the use of few, selected internal standards does not cover the entire expected chemical diversity and would not be expected to perform equally well for all metabolites. Several reports use normalization by dividing each peak with sample median on particular run-day, with each run-day containing exactly balanced number of samples from each treatment group.<sup>20, 44, 205</sup> Other reports used normalization by total peak intensity observed for each sample<sup>64, 206, 214, 218</sup>, or normalization to constant total signal intensity arbitrarily set to a single value as the most effective normalization for LC-MS data.<sup>214, 217</sup> Such total area normalization, also often employed in NMR studies, assumes that decreases in certain metabolites are balanced by increases in other metabolites, thus keeping the total number of metabolites nearly constant. However, in LC-MS analysis, this is not a feasible assumption as the intensity of signal observed is dependent on the identity of analyte. Furthermore, exogenous species ingested through diet or originating from environmental exposure are also present in untargeted LC-MS chromatograms. These species are expected to vary from individual-to-individual, for example signal intensity for caffeine peak will depend on the individual's consumption of beverages containing caffeine. This means that the total signal intensity would not be expected to be constant, so this type of normalization may not be suitable for LC-MS data.<sup>241</sup>

Burton *et al.* advocate the use of artifact detection prior to using multivariate statistical approaches on data and that the data should be checked for background ions (constant across all runs), suppression/enhancement that occurs at specific retention times and trends dependent on acquisition order.<sup>203</sup> Typically, if the exact same sample preparation procedure is used for all samples within the batch, the background ions do not need to be removed prior to statistical analysis, because they are

present at the same levels in all samples and will not cause differentiation of samples during principal component analysis. However, depending on what type of normalization is used on data, it may change the apparent levels of background ions leading to statistically relevant differences, so for improved data quality the removal of these peaks is recommended although it is not often performed in studies reported in literature.<sup>203</sup> In our case, it was desired to compare the performance of several sample preparation methods and the exact sample treatment and solvent composition varied between these different techniques. In this case, to enable any meaningful comparison, it was absolutely necessary to remove any blank peaks from all data sets using appropriate blank controls for that method, in order to facilitate the accurate comparison across methods.

Another area in need of further research is an improvement in the identification of metabolites. Current version of HMDB database contains about 6500 entries, but often does not contain compounds after phase I and II metabolism (such as glucuronides, sulfates, amino acid conjugates, etc.) For example, the search for unknown metabolites presented in Table 7.2 resulted in many metabolites with no known matches within the database. Other approaches reported in literature to improve the identification part of metabolomics workflow include the use of in-house library of a large number of authentic compounds collected using particular methods employed in metabolomics study and the use of retention time indices such as routinely employed in GC-MS.<sup>205</sup> However, the use of retention indices in LC is complicated by the variation in retention index caused by the factors such as column aging and/or slight changes in mobile phase pH with time. This means that if the chromatographic behaviour of retention marker differs from that of the analyte of interest, a drift can be observed in metabolite retention index. The authors addressed this issue by using larger retention index windows for compounds that showed such drift experimentally. Finally, existing public databases currently do not provide any retention time information, so the addition of such information could aid in tentative identification of metabolites.

## **7.4 Conclusions**

The data presented within this chapter support the use of SPME in global metabolomic studies of human plasma. In comparison to ultrafiltration, SPME provided more comprehensive simultaneous coverage of both hydrophilic and hydrophobic species, while ultrafiltration performed very poorly for hydrophobic species. Plasma protein precipitation methods performed poorly for many polar metabolites, indicating that the results for such species may not be reliable and method precision cannot be the only measure of ensuring good data quality in metabolomic studies. SPME also reduced

potential for ionization effects and provided unbound concentration information which is not achievable by plasma precipitation methods. The developed LC-MS methods on Exactive were found to perform as well or better than most methods reported in literature and provided excellent metabolite coverage and method precision.

## **7.5 Addendum**

The text of this chapter was rewritten in comparison to submitted research article.

## Chapter 8

### ***In vivo* SPME sampling for global metabolomic studies in mice**

#### **8.1 Preamble and introduction**

##### **8.1.1 Preamble**

This work has not yet been published. Animal experiments were performed in collaboration with Brad Gien and Ines de Lannoy from NoAB BioDiscoveries using their animal facility. The contributions of Brad Gien included the development of *in vivo* SPME sampling procedure for mice, the design and development of interface for sampling of mice as well as performing of entire *in vivo* sampling procedure including animal surgery to insert the interface and blood collection. Dr. Ines de Lannoy was involved in experimental planning and design of these *in vivo* experiments.

I, Brad Gien, authorize Dajana Vuckovic to use the material for her thesis.

I, Ines de Lannoy, authorize Dajana Vuckovic to use the material for her thesis.

##### **8.1.2 Introduction**

In pharmaceutical industry, global LC-MS metabolomic studies can be used to investigate drug mechanism, distribution, metabolism and toxicity of existing drugs as well as drugs under development.<sup>27</sup> Experimental designs for such clinical and/or pharmaceutical metabolomic studies vary depending on the main objective of the study. One common design includes the investigation of the effect of xenobiotic on the whole animal by studying changes in metabolism over time via monitoring of single or multiple biofluids.<sup>209</sup> The main approaches for identifying xenobiotic metabolism include the comparison of animals dosed with drug (or other xenobiotic) versus animals dosed only with vehicle, and this type of experimental design would permit investigation of both endogenous and exogenous metabolism.<sup>210</sup> If the objective of the study is primarily xenobiotic metabolism, then a better experimental design involves the dosing of one group of animals with xenobiotic versus second group which is treated with stable isotopically-labelled form of the same xenobiotic. In this case, the main difference between data sets should stem from xenobiotic metabolites as they would show mass shift between two groups due to isotopic labelling, and would

largely eliminate effect of endogenous metabolism from the data. A third type of study can be employed to reveal inter-species differences in metabolism, for example by comparing response of normal strains of mice versus genetically modified strains of mice (for example, humanized mouse lines or mouse lines with particular genes knocked-out).<sup>27</sup> For example, Liu et al. used this methodology to discover four new metabolites of fenofibrate indicating new Phase II taurine conjugation pathway of this drug.<sup>202</sup> In another study, the mechanism of hepatotoxicity of existing drugs was successfully classified using UHPLC-MS metabolomics approach, and can in future enable classification of drug candidates during discovery stage.<sup>71</sup>

The main objectives of current experiment were (i) to perform full metabolomic study on mice after *i.v.* dosing with 2 mg/kg carbamazepine and (ii) to investigate any advantages of *in vivo* SPME sampling versus *ex vivo* approaches based on blood withdrawal. This study was selected to expand on the preliminary data shown in 4.3.7 using larger number of mice (n=4 control and n=4 dosed) and using optimized coatings (Chapter 5) and LC-MS methods on Exactive (Chapter 6). Furthermore, the advantages of *in vivo* mode of sampling were investigated whereby the results obtained using *in vivo* SPME were compared versus *ex vivo* SPME, ultrafiltration and plasma protein precipitation using methanol/ethanol. As such, this chapter complements data presented in Chapter 7 using human plasma but further expands the discussion in order to include the role and benefits of *in vivo* sampling within the context of animal global metabolomic studies.

## **8.2 Experimental**

### **8.2.1 Materials**

Same materials and reagents as described in Chapters 3-7 were utilized for this study. L-phenylalanine-d5 (99.3 % purity) was obtained from CDN Isotopes (Pointe-Claire, PQ, Canada) and D-glucose 1,2,3,4,5,6,6-d7 (98% purity) was obtained from Cambridge Isotope Laboratories (Andover, MA, USA).

### **8.2.2 Summary of overall experiment design**

Animal experiments were performed on eight male CD-1 mice (Charles River Labs, St. Constant, PQ, Canada) weighing 20 to 30 g. All procedures followed were reviewed by the NoAb BioDiscoveries' animal care committee and were performed in accordance with the principles of the Canadian Council on Animal Care. Prior to experiments, mice were acclimatized for a minimum of five days, and were

provided with food and water *ad libitum*. One day prior to *in vivo* SPME experiments, a catheter was implanted surgically in the carotid artery and the mice were allowed to recover from surgery and anesthesia overnight. On the day of sampling, custom-made sampling interface, consisting of small volume tubing and a PRN adapter was connected by a stainless steel connector to the implanted catheter using the procedure and devices described in detail in 4.2.2. *In vivo* SPME sampling was performed on all eight conscious mice without any dosing of carbamazepine (n=1 sampling per mouse). One mouse (M3) was selected randomly in order to estimate intra-animal variability and the reproducibility of *in vivo* SPME sampling. For this mouse, five independent consecutive *in vivo* SPME samplings were performed using five individual SPME probes.

For traditional analysis based on blood withdrawal, four of the above mice were designated as control mice (M1, M2, M3, M4) and no CBZ dosing was performed for these mice. Immediately following the completion of *in vivo* SPME sampling, these mice underwent direct cardiac puncture while under CO<sub>2</sub>/O<sub>2</sub> anesthesia in order to collect the blood. The collected blood for each individual mouse was centrifuged immediately upon collection at 4°C to obtain plasma. Resulting plasma was stored on dry ice for transportation and to minimize metabolism. The processing of plasma was completed within 6 hr post-collection according to the procedures described below.

The remaining four mice (M5, M6, M7, M8) were dosed (2 mg/kg CBZ) by injection into the lateral tail vein using CBZ dosing solution prepared in ethanol/propylene glycol/saline (1/1/3, v/v/v). *In vivo* SPME sampling was performed 30-min post-dose using the procedures described below. Immediately following the completion of *in vivo* SPME sampling, each mouse underwent direct cardiac puncture while under CO<sub>2</sub>/O<sub>2</sub> anesthesia in order to collect its blood for traditional analysis. The collected blood for each individual mouse was centrifuged immediately upon collection at 4°C to obtain plasma. Resulting plasma was stored on dry ice for transportation and to minimize metabolism. The processing of plasma was completed within 6 hr post-collection according to the procedures described below.

The overview of the entire animal study employed in this research is provided in Figure 8.1. To summarize, using *in vivo* sampling it was possible to evaluate the effects of CBZ dosing using the same mice as samples before and after dosing were collected (t<sub>0</sub> and t<sub>30</sub> samples for M5, M6, M7, M8). Using traditional methods requiring relatively large blood volumes, the comparison could not be performed on the same mice so n=4 mice were used as controls (M1, M2, M3, M4) and compared against does mice (M5, M6, M7, M8). During 30-min sampling of M6, a significant blood clot was

found, which prevented proper sample collection. Therefore, the only data point available for this mouse is *in vivo* SPME sampling at t=0. For traditional experiment based on plasma, sufficient amount of plasma (300  $\mu\text{L}$ ) could not be collected for M1 and M7, so *ex vivo* SPME was performed using 150  $\mu\text{L}$  aliquot. These samples were used only for confirmation of the presence and absence of certain metabolites of interest and were not included in general data processing due to the dependence of the amount extracted by SPME on sample volume.

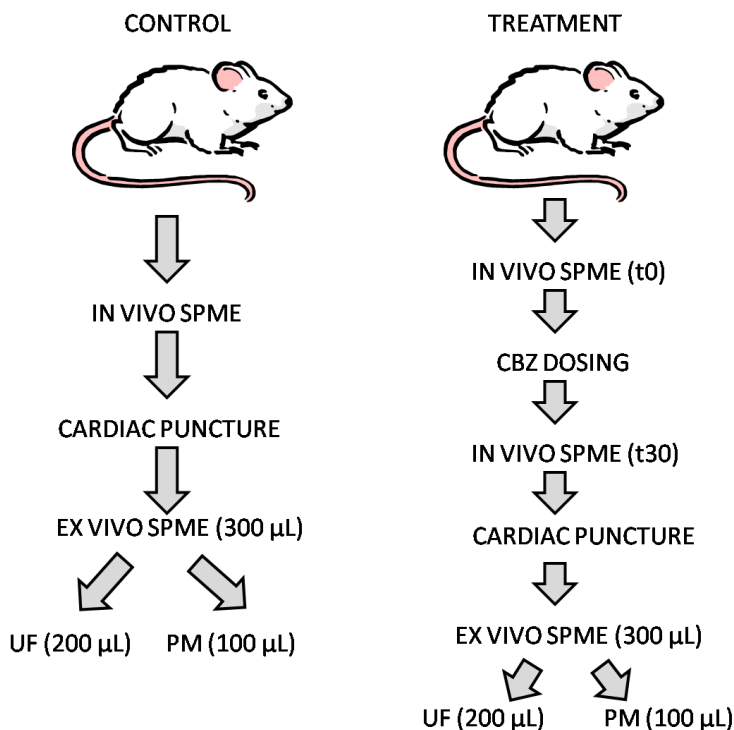


**Figure 8.1 Overview of animal study employed for comparison of *in vivo* SPME to traditional methods based on blood withdrawal.**

#### 8.2.2.1 *In vivo* SPME sampling

The day before *in vivo* SPME sampling, prototype *in vivo* SPME probes housed within 22-gauge hypodermic needle as described in Chapter 3 and consisting of biocompatible mixed-mode coating ( $\text{C}_{18}$  with benzenesulfonic acid, 45  $\mu\text{m}$  thickness, 3  $\mu\text{m}$  particle size, Supelco, Bellefonte, PA, USA), were preconditioned and pre-loaded with deuterated carbamazepine internal standard. The conditioning and loading was performed at equilibrium from 300  $\mu\text{L}$  of 1  $\mu\text{g}/\text{mL}$  standard solution of carbamazepine-d10 (CBZ-d10, Alltech, Deerfield, IL, USA) dissolved in methanol/water (1/1, v/v) using vortex agitation of 1000 rpm. The development of this procedure was described in more detail

in Chapter 3. The probes were kept in this conditioning/loading solution until each *in vivo* sampling time point in order to ensure that the coating does not dry out prior to sampling. Three extra probes were pre-loaded and used to determine the amount of calibrant loaded according to similar procedures as described in Section 4.2.3.

For each sampling period, a new conditioned *in vivo* SPME probe was inserted into the blood-filled sampling interface 1 min before the stated time and held in the interface 1 min after the stated time (total sampling time of 2 min). Immediately after the probe removal from the interface, the SPME probe was rinsed for 30 sec using purified water to remove any cells or salts from the probe surface. The probes were stored on dry ice until desorption which was carried out within 6-hr post-collection. The desorption of analytes from SPME probes was accomplished using 300  $\mu$ L of desorption solvent (acetonitrile/water, 1/1, v/v) spiked with two internal standards 1450 ng/mL glucose-d7 and 300 ng/mL phenylalanine-d5 using 0.3 mL amber polypropylene HPLC vials (Labsphere, Brossard, PQ, Canada). The desorption was performed for 60 min on multi-tube vortexer at 1000 rpm.

#### 8.2.2.2 *Ex vivo* SPME

*Ex vivo* SPME was performed on 300  $\mu$ L of mouse plasma obtained after cardiac puncture as described above, except for M1 and M7 where 150  $\mu$ L plasma aliquot was used due to limited sample availability. SPME was performed according to the method developed and described in detail in Chapter 6. Briefly, SPME was performed using Supelco prototype biocompatible mixed-mode fibre (C<sub>18</sub> and benzenesulfonic acid, 45  $\mu$ m thickness, 3  $\mu$ m particle size) for 5 min with 1000 rpm vortex agitation. The fibres were then desorbed using 300  $\mu$ L of desorption solvent (acetonitrile/water, 1/1, v/v, containing glucose-d7 and phenylalanine-d5 internal standards) for 60 min in using vortex agitation at 1000 rpm.

#### 8.2.2.3 Ultrafiltration (UF) sample preparation

After completion of *ex vivo* SPME experiment, 200  $\mu$ L aliquot of mouse plasma used in 8.2.2.2 was placed in 3K Nanosep centrifugal device and centrifuged at 10000 rpm for 30 min at 4 °C. The resulting filtrate was diluted 10-fold in purified water prior to LC-MS analysis.

#### 8.2.2.4 Plasma protein precipitation with methanol/ethanol (PM)

This procedure was adapted from study by Bruce *et al.*<sup>12</sup>. Experiments performed in Chapter 7 confirmed better performance of solvent precipitation with methanol/ethanol versus solvent



precipitation with acetonitrile, so in this study only solvent precipitation with methanol/ethanol was used. Aliquots (100  $\mu$ L) of mouse plasma from Section 8.2.2.2 were precipitated by addition of 400  $\mu$ L of methanol/ethanol (1/1, v/v). The samples were then manually vortexed for minimum of 60 seconds, followed by centrifugation at 12000 rpm for 15 min at 4 °C. The resulting supernatant (150  $\mu$ L) was transferred to amber polypropylene HPLC vials (0.3 mL capacity) and diluted with 150  $\mu$ L of purified water prior to LC-MS analysis.

### **8.2.3 LC-MS analysis**

Aliquots (100  $\mu$ L) of *in vivo* SPME, *ex vivo* SPME, UF and PM sample solutions were analyzed directly using pentafluorophenyl positive ESI LC-MS method (Section 6.2.2.1 and 6.2.2.4 for conditions) according to same general procedures described in Section 7.2.6. The remaining sample solutions were stored frozen (-30°C) for subsequent analysis to be described in follow-up studies.

### **8.2.4 Data processing**

Same data processing scheme as described in Section 7.2.7 was used in current study. For framing using SIEVE, the following parameters were used: 0.005 mass window, 1.0 min retention time window width, maximum number of frames =20000, minimum signal intensity of 5000, retention time 1.0-33.0 min.

## **8.3 Results and discussion**

### **8.3.1 Blank controls**

One important aspect to consider during the design of global metabolomic studies using SPME is to collect the appropriate blank controls to ensure peaks detected by SPME are real and belong to the biological sample under study. With this goal in mind, it is not sufficient to only run injections of blank desorption solvent, but it is necessary to analyze blank fibres which have undergone the same preconditioning and desorption procedures as the probes used in the study. Figure 8.2 shows TIC traces obtained for blank fibre and for direct injection of blank desorption solvent. Although, the chromatograms generally have the same appearance and TIC intensity, the blank fibre does show higher intensity in the region of 21-23 min and 10-15 min. Full examination of the data after SIEVE

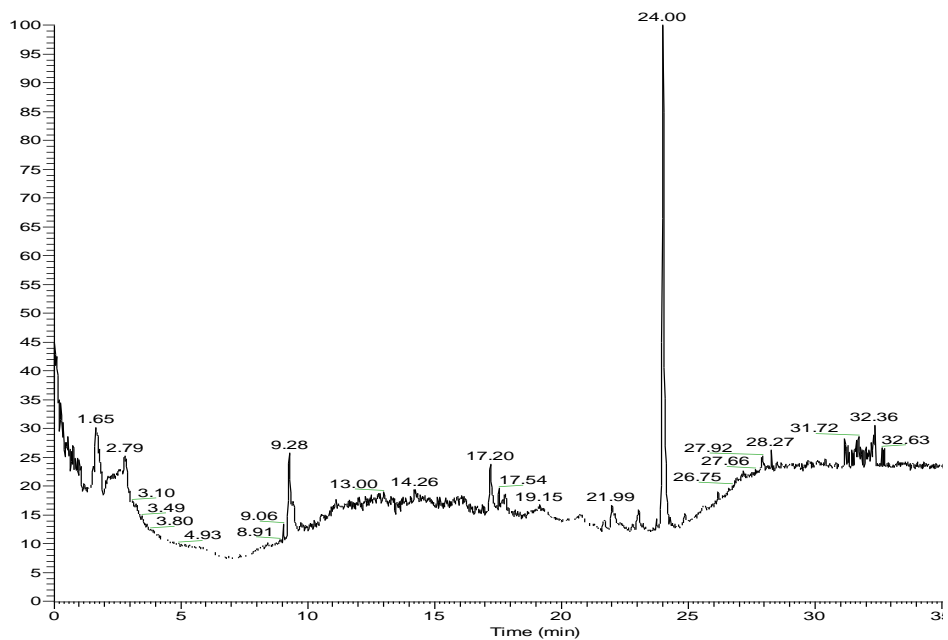
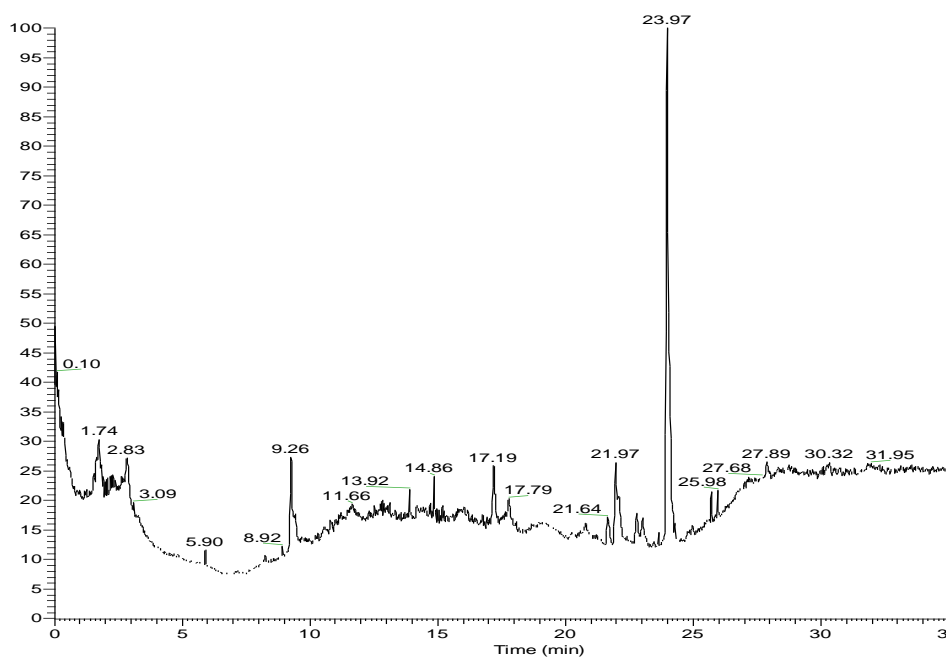


**Figure 8.2 TIC of (a) blank SPME fibre (absolute intensity  $9.3 \times 10^7$  counts, run order 66) and (b) blank desorption solvent (absolute intensity  $1.1 \times 10^8$  counts, run order 81) collected using positive ESI LC-MS method with pentafluorophenyl column.**

processing ( $n=3$  of each blank type) shows that 430 features have higher intensities than observed in direct injection of blank desorption solvent. These peaks can occur due to preconcentration of the

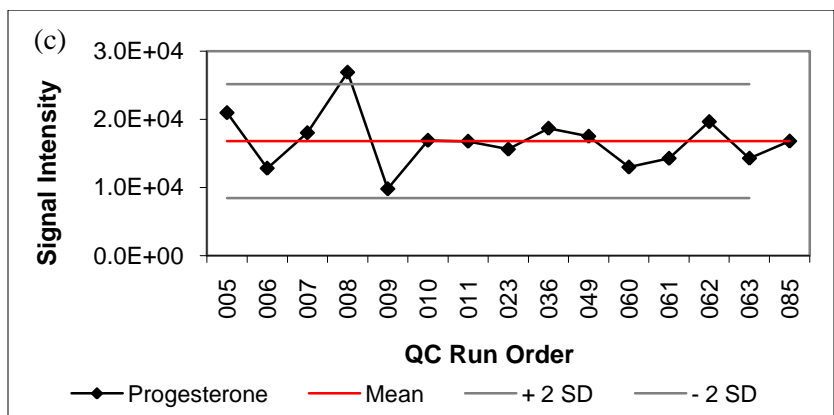
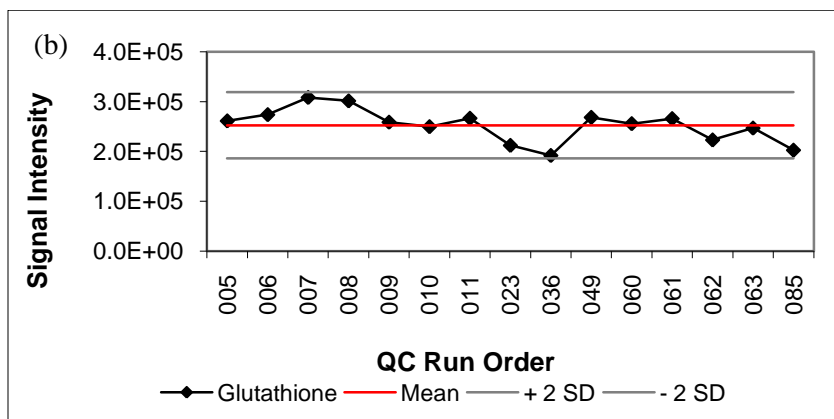
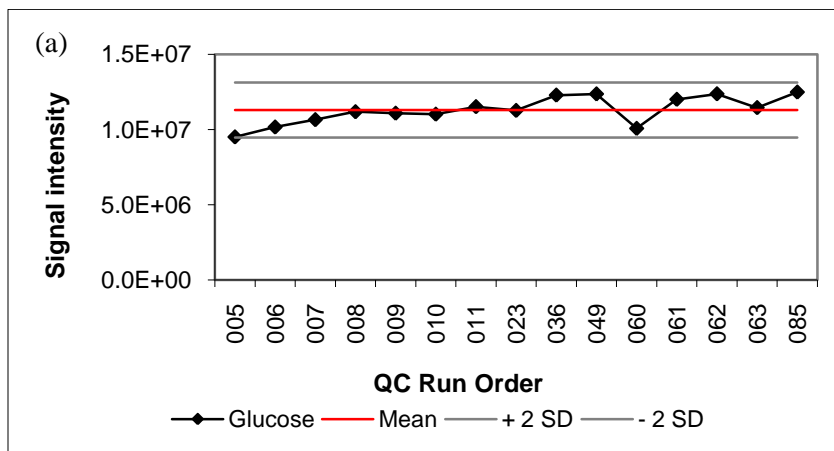
contaminant species present in conditioning solvent by the fibre (for example, any contaminants present in purified water or methanol). Additional sources of these species can be fibre production process itself or possibly vessels (such as vials or well-plates) used during the conditioning procedure. For traditional methods, appropriate blank controls were prepared by taking an aliquot of purified water through the entire sample preparation procedure and injecting the resulting sample. As one of the goals of current study was comparison of different methods, samples obtained using each method were processed in SIEVE together with the corresponding blank controls in order to ensure all peaks used for subsequent PCA were real peaks originating from the biological system rather than artifacts of the sample preparation procedure.

### 8.3.2 Quality control (QC) results

In current study, quality control sample was prepared by combining aliquots of all samples (*in vivo* SPME, *ex vivo* SPME, UF and PM) within the sample set. This QC was run at the beginning of the sample set to ensure system is properly conditioned, throughout the sample set after every 12 sample injections and at the end of the sample set. The results for this QC are used to ensure no systematic drift occurred throughout the entire run time. Plots of signal intensity *versus* run order for several identified metabolites are shown in Figure 8.3. The metabolites were selected to cover a wide range of signal intensities and the entire chromatographic space in terms of retention time. Injections 005 to 008 were considered part of the preconditioning procedure and are included to show that the system was adequately pre-conditioned. Figure 8.4 shows RSD results for all QC injections for all known metabolites observed using *in vivo* SPME. The results indicate good performance of the entire LC-MS system with mean RSD of 16% for all known metabolites in QC sample. Two internal standards glucose-d7 and phenylalanine-d5 had RSD of 7 and 12% for all QC injections and RSD of 23% and 2% for *in vivo* SPME injections (n=8 animals). Carbamazepine d10 which was used as on-fibre calibrant for CBZ had RSD of 12% in all QC injections and 17% for *in vivo* SPME injections (n=8 animals) indicating no problems with any of the probes used during the study.

Furthermore, in addition to targeted processing of selected metabolites confirmed using authentic standards, QC samples can also be used to evaluate the quality of global metabolomics data. This is performed by subjecting these QC samples to SIEVE processing followed by PCA together with the actual samples. The results of PCA analysis for current study including QC samples are shown in Figure 8.6 (a, b and d). All QC injections (shown in red) cluster tightly together with no evident outliers indicating good quality of the data set indicating that further processing and interpretation of

the dataset is worthwhile as analytical variability was properly kept in check during the run. This is further illustrated in Figure 8.7 which shows the dependence of the same data on the run order.



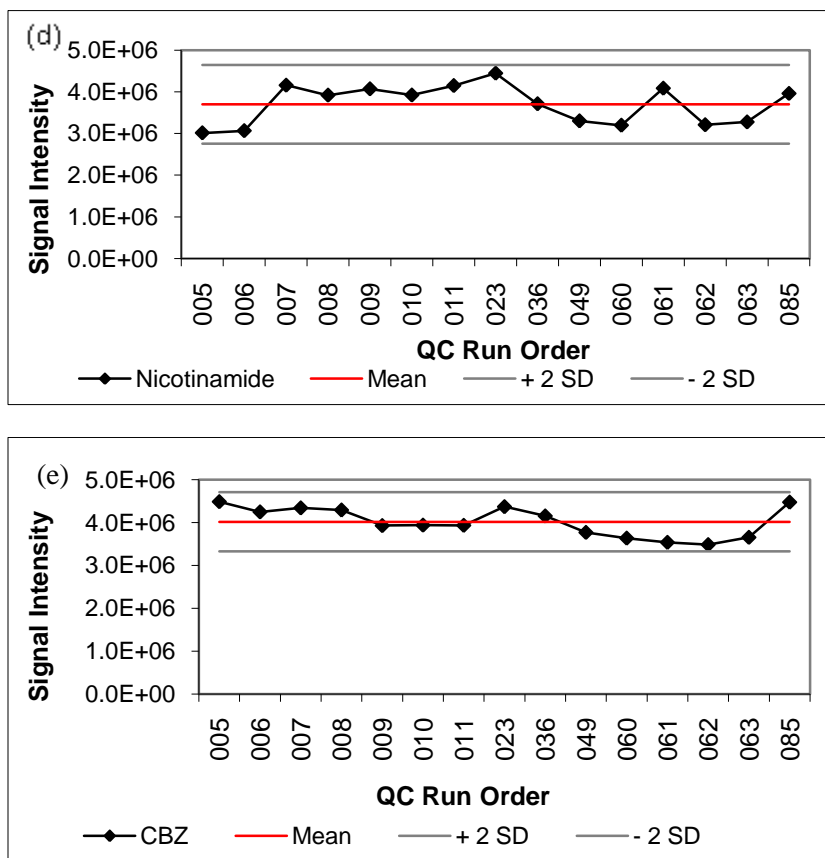


**Figure 8.3** Signal intensity versus QC run order for selected compounds (a) glucose (b) reduced glutathione (c) progesterone (d) nicotinamide and (e) carbamazepine.

### 8.3.3 Evaluation of intra-animal variability and reproducibility of *in vivo* SPME sampling

One of the goals of current study was to evaluate the reproducibility of *in vivo* SPME sampling for global metabolomics on one mouse (n=5 consecutive samplings prior to dosing). Although some temporal variability in metabolite concentrations can be expected over the time scale of the experiment, some of the metabolites should remain effectively unchanged permitting an approximate evaluation of *in vivo* SPME procedure. The results of this experiment are shown in Figure 8.4 for the set of known metabolites and compared against the inter-animal variability (n=8 mice) for the same set of metabolites. The reproducibility of QC injections is also included in the figure as a reference point. For the majority of the metabolites inter-animal variation is significantly higher than within-animal variation, with some of the metabolites such as reduced and oxidized glutathione exhibiting >3-fold higher inter-animal variability. These results are in line with the study by Crews *et al.* who

reported biological variability of 35% and 46% RSD for cerebrospinal fluid and human plasma respectively, *versus* analytical variability of 15-16% RSD for both matrices.<sup>67</sup> One exception to this general trend was adenosine where inter-animal variation was similar to within-animal variation. This can perhaps be attributed to extremely short half life of this species which may contribute to rapidly changing concentrations on the timescale of the experiment.

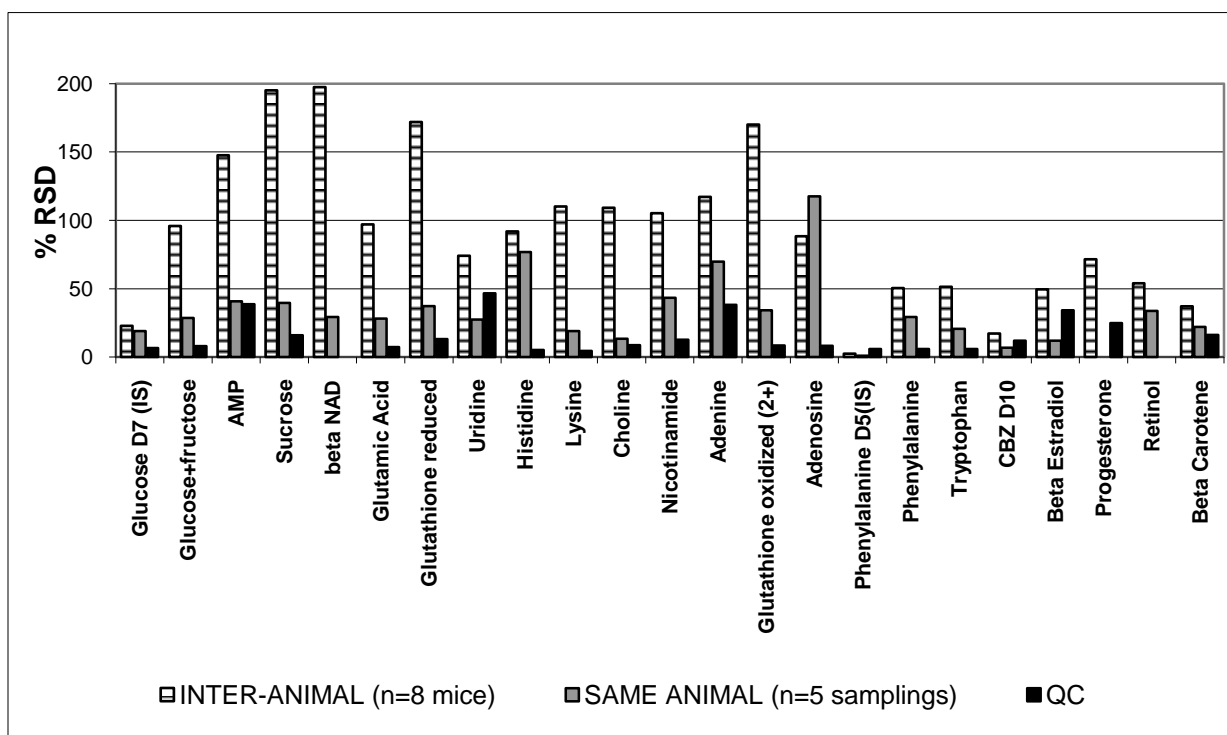
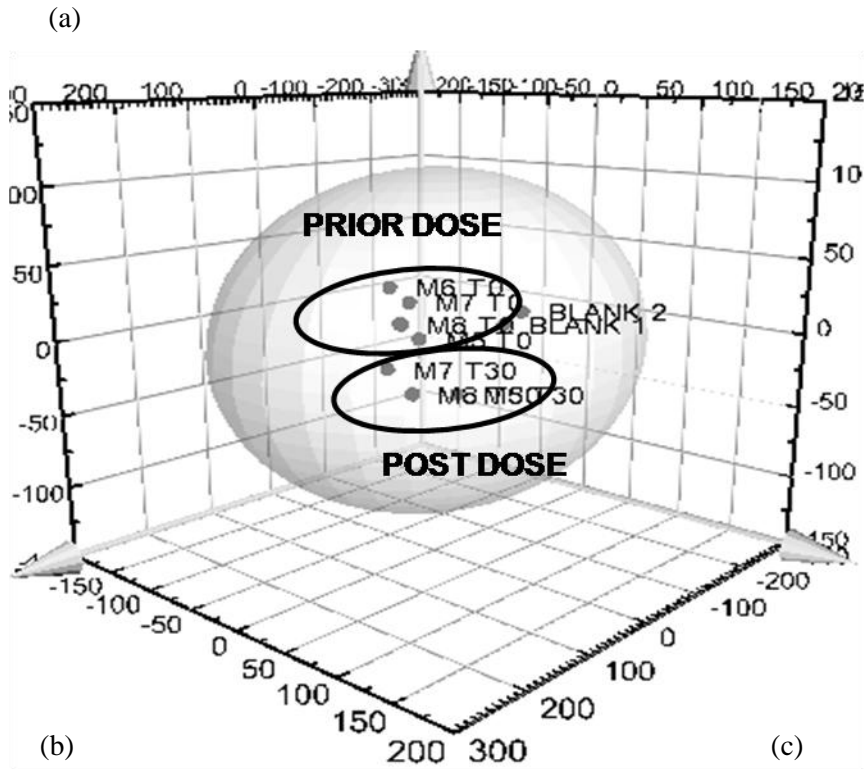


**Figure 8.4 Comparison of inter-animal versus intra-animal variability (expressed as %RSD) for the set of known metabolites detected using *in vivo* SPME sampling.**

### 8.3.4 Principal component analysis: effect of CBZ dosing

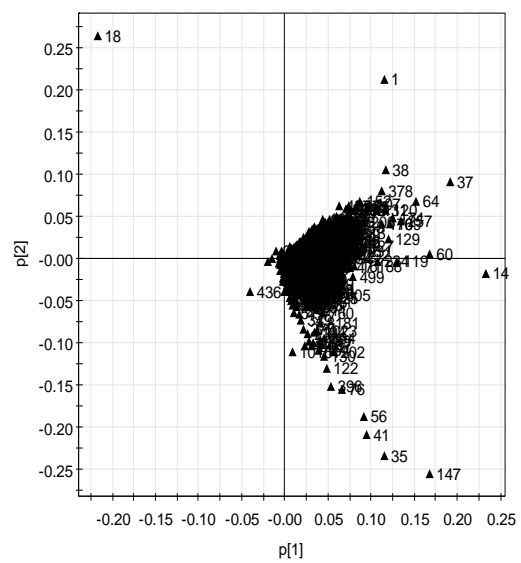
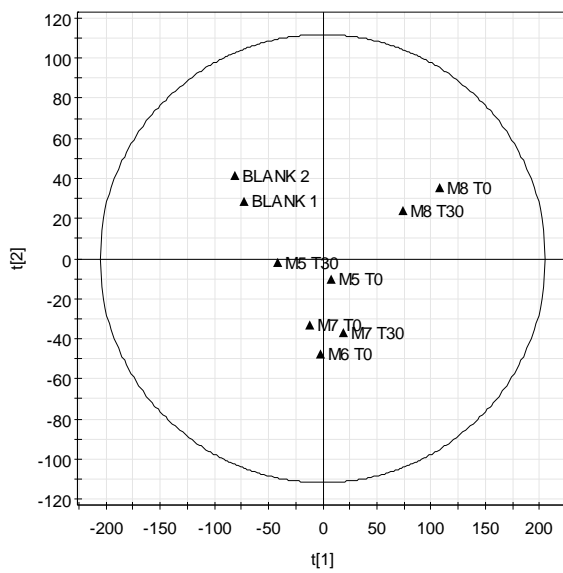
Using *in vivo* SPME, it was possible to sample the same n=4 mice before and after dosing with carbamazepine. The data set consisted of 1845 features detected using short 2-min sampling time which is in agreement with our previous studies on human plasma (see Table 7.4). The results of PCA for this data set are shown in Figure 8.5. First three components described 87.9% of variance and the differentiation of mice according to dosing was immediately apparent as shown in Figure 8.5 (a). The main source of variation was biochemical individuality of animals as shown in 2D scores plot of principal components 1 and 2 (Figure 8.5 (b)), with the two components contributing to 60.2 and 17.8% of variance respectively. Principal component 3 accounted for 9.9% of variance and allowed

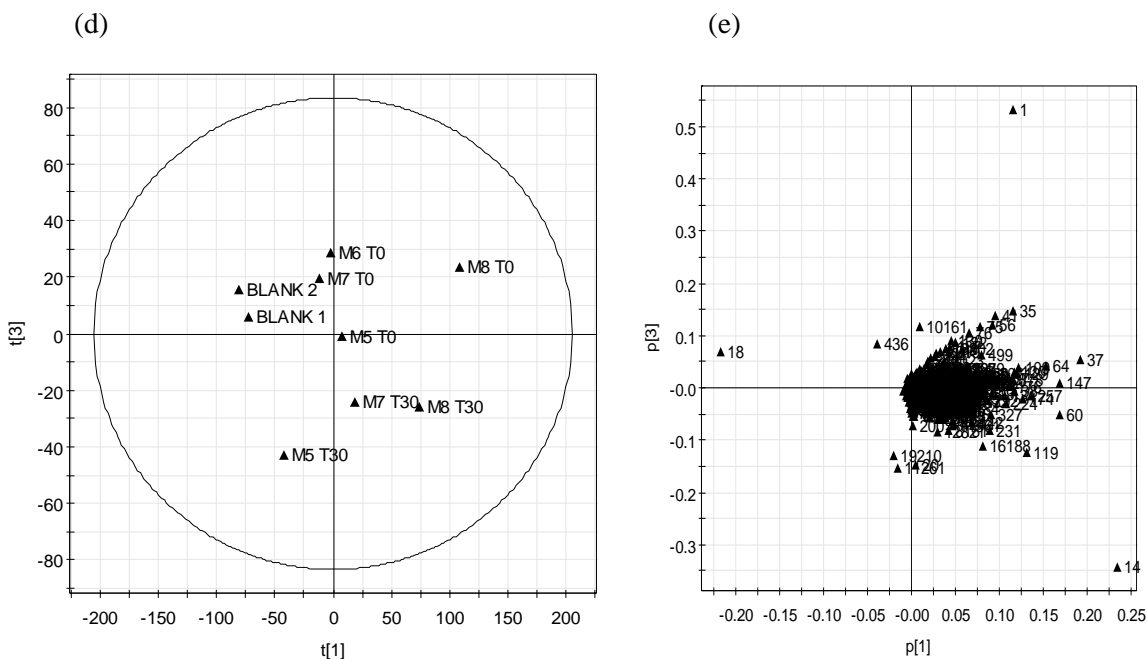
the differentiation of this data set according to CBZ dosing. These results are in agreement with the study performed by Croixmarie *et al.* who found that the main source of variation in their data set was the origin of liver hepatocytes (46% of variance), while the treatment with drug only accounted for 13% of variation and run order accounted for 11% of variation.<sup>71</sup>



(b)

(c)





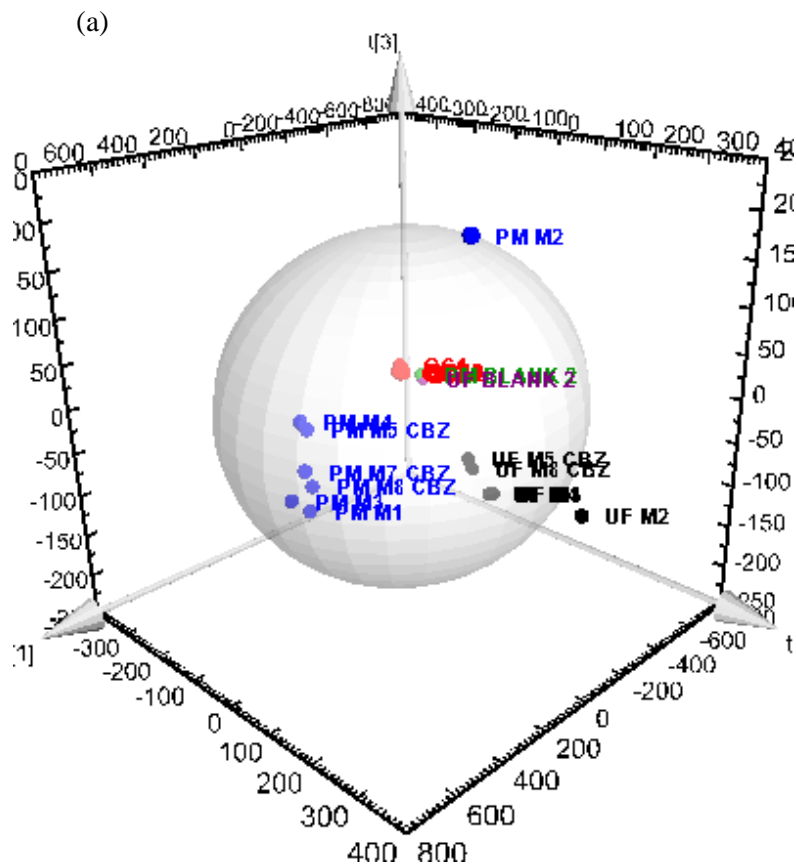
**Figure 8.5 (a) 3D scores plot obtained for *in vivo* SPME sampling of n=4 mice (M5, M6, M7, M8) prior to (T0) and 30-min (T30) post dose. (b) 2D scores plot of the same dataset showing PC1 versus PC2 (c) Loadings scatter plot of PC1 versus PC2 illustrating the peaks contributing most to the observed clustering (d) 2D scores plot of the same dataset showing PC1 versus PC3 (e) Loadings scatter plot of PC1 versus PC3 illustrating the peaks contributing most to the observed clustering. Blank injections are shown, while QC injections are omitted for clarity in all plots.**

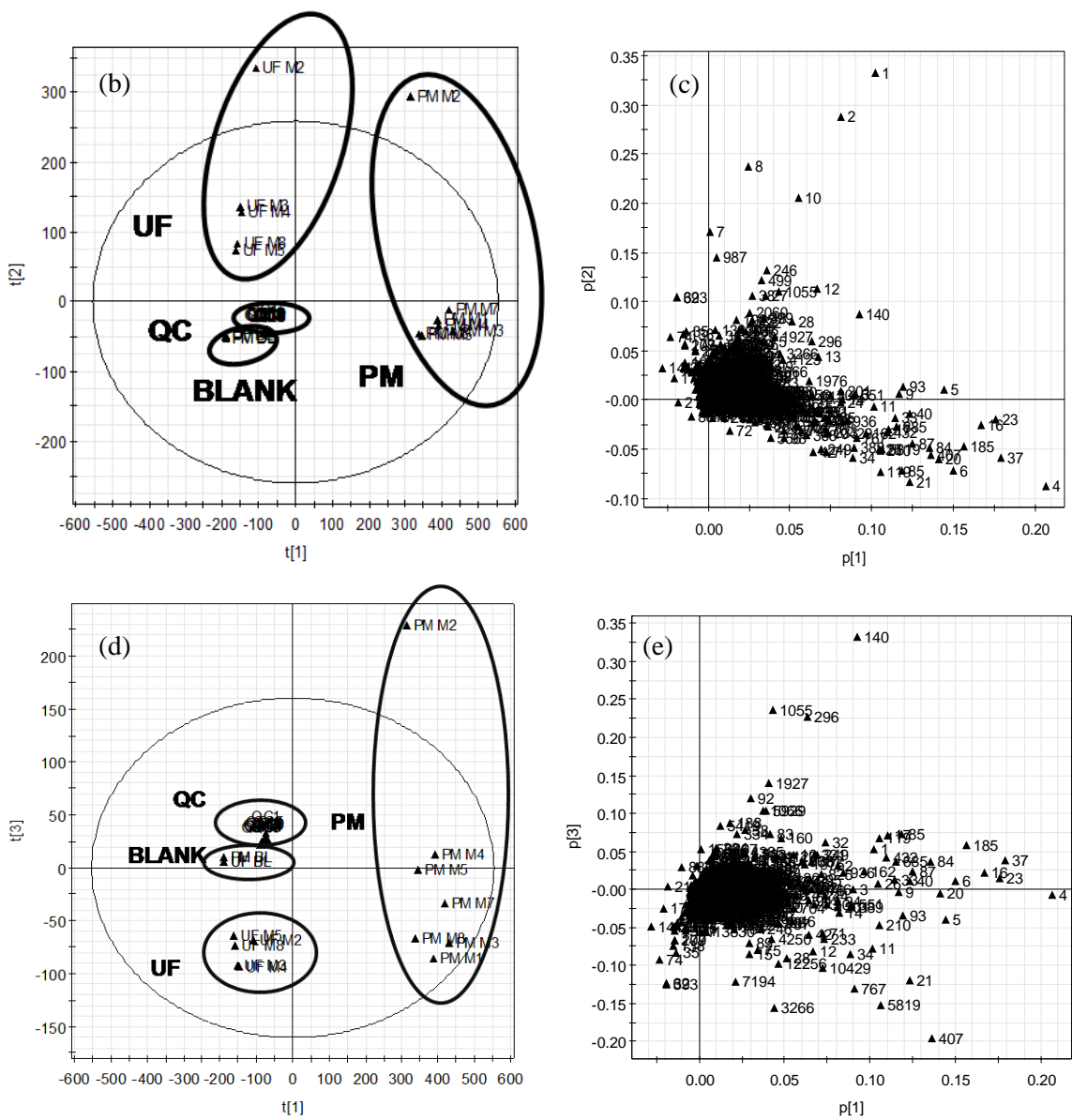
Figure 8.6 shows the results of PCA for samples obtained using ultrafiltration (UF) and solvent precipitation with methanol/ethanol (PM). The results indicate large influence of the sample preparation method on the data collected. This is the result of vastly different metabolite coverage achievable by the two methods as discussed in detail in Chapter 7 using human plasma example. Differentiation according to dosing is observed only for UF samples, and no such differentiation is observed for PM samples using three principal components which contribute 66.2, 14.5 and 5.6% of variance respectively. Clearly one disadvantage of the traditional analysis employed here was the fact that different mice were sampled as control *versus* treatment groups. This was necessary in order to collect sufficient blood volume to perform the analysis using all methods. The results show that the use of small sample set (n=4 mice/group) may or may not permit acceptable differentiation of samples according to dosing as inter-animal variability is included within the data set. Inter-animal variability can be very high (estimated at 78% using *in vivo* SPME method) thus making it very easy



to obscure the effect of dosing as was found for PM method in current study. Thus, if the only objective of the study was a classical metabolomics study to the effects of xenobiotic dosing, PM data set would be virtually unusable and would require a new study with much larger number of animals. In contrast, both SPME and UF were able to clearly differentiate the samples based on dosing even when such small data set was used. Both of these methods provide a response which is proportional to biologically active free concentration. The fact that both methods were able to differentiate the samples indicates that free concentration information can be extremely valuable in the context of metabolomic studies.

Furthermore, the data was examined for known CBZ metabolites which include 10,11-carbamazepine epoxide (m/z 253.0972 for protonated ion), 2-hydroxycarbamazepine (m/z 253.0972

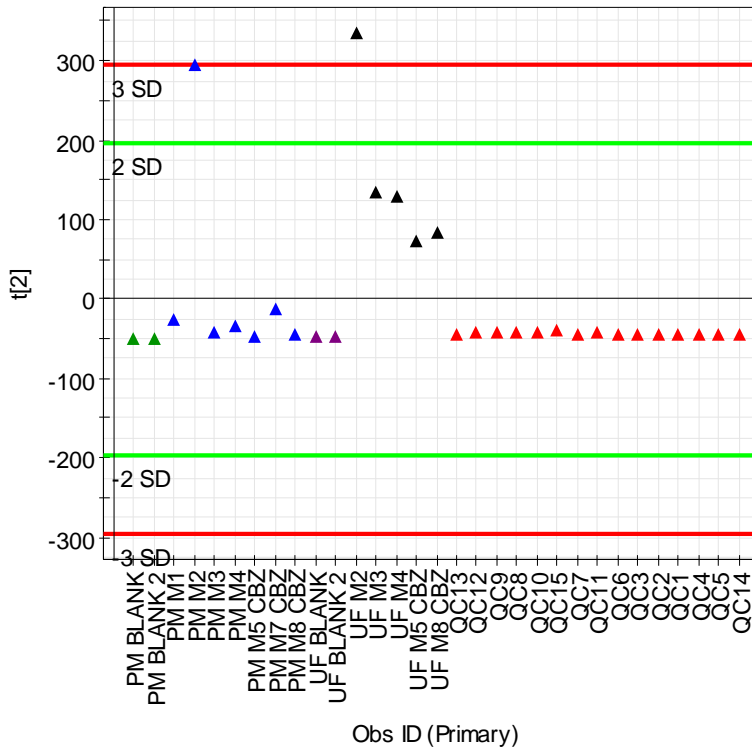
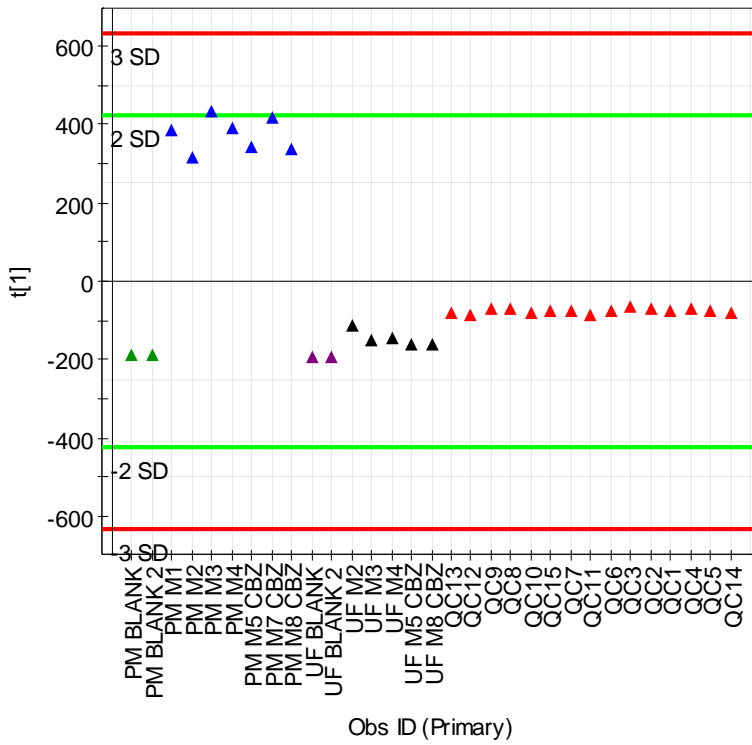




**Figure 8.6(a)** 3D scores plot obtained using ultrafiltration (UF, black spheres) and solvent precipitation (PM, blue spheres) for  $n=4$  mice prior to CBZ dosing (PM and UF) and  $n=4$  mice 30-min post dose (PM CBZ and UF CBZ). (b) 2D scores plot of the same dataset showing PC1 versus PC2 (c) Loadings scatter plot of PC1 versus PC2 illustrating the peaks contributing most to the observed clustering (d) 2D scores plot of the same dataset showing PC1 versus PC3 (e) Loadings scatter plot of PC1 versus PC3 illustrating the peaks contributing most to the observed clustering. Blank and QC injections are also shown.

for protonated ion), 3-hydroxycarbamazepine (m/z 253.0972 for protonated ion), 10,11-dihydrocarbamazepine (m/z 239.1179 for protonated ion), 10,11-dihydro-10-hydroxycarbamazepine (m/z 255.1128 for protonated ion) and 10,11-dihydro-10,11-dihydroxycarbamazepine (m/z 271.1077 for protonated ion).<sup>246</sup> The main CBZ metabolite, 10,11-carbamazepine epoxide was detected using all sample preparation methods employed in current study, while other metabolites were only detected in samples prepared using solvent precipitation (PM) and had relatively low signal intensity. In other words, the detection of these species by SPME and UF failed due to very low concentrations in blood at the time point of analysis. The low concentration of these metabolites may be due to the fact that samples were analyzed only 30-min post-dose, and perhaps monitoring of longer times would be useful in this situation. Thus, from the perspective of monitoring very low level exogenous drug metabolites PM data was invaluable even though it failed to differentiate mice according to dosing using the global metabolomics approach. Therefore, this study clearly shows the advantages of using set of complementary methods during an animal study to further enhance the understanding of the biological processes and shows that each method can contribute an important piece of the puzzle.

Figure 8.6 depicts another interesting finding. Mouse 2 (labelled as M2) is shown as an outlier using both UF and PM methods as shown by this point falling outside Hotelling's 95% confidence interval. This result is not simply an analytical outlier as shown in Figure 8.7, as QC standards, blanks and other samples do not exhibit significant trends with respect to run order. Furthermore, *ex vivo* SPME results also indicate M2 as an outlier, whereas *in vivo* SPME results show reasonable clustering of M2 with other mice (Figure 8.9). This data seems to indicate that important metabolic changes occurred for blood collected from M2 during sampling or sample storage procedures, which resulted in a significantly changed composition of this sample. From experimental viewpoint, blood from M2 was treated in exactly the same way as for the rest of the mice, so it is not clear what additional precautions could be taken to ensure sample integrity for this particular blood sample. This data therefore indirectly indicates an advantage of *in vivo* SPME sampling – the ability to properly capture the metabolome composition at the time of sampling without inadvertent changes in composition occurring during or post-sample collection.



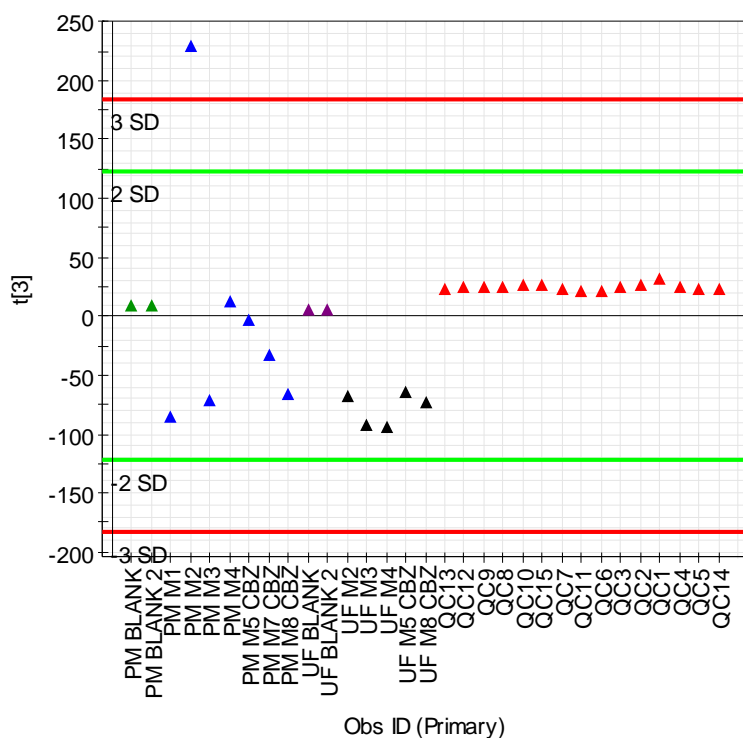


**Figure 8.7** Plot of principal component 1 (a), 2 (b) and 3 (c) versus observation ID for data set shown in Figure 8.6.

No global metabolomic studies on the dosing of carbamazepine have been reported in literature, so the current study also presented an interesting model to examine CBZ effects on endogenous metabolites, whereas CBZ exogenous metabolites are well-characterized in literature. The most relevant metabolites detected after PCA analysis were subjected to database search using HMDB for tentative identification of possible chemical formula. Current version of HMDB database contains about 6500 entries, but often does not contain compounds after phase I and II metabolism (such as glucuronides, sulfates, amino acid conjugates, etc.) . In current study, the tentative identification was performed by comparing the accurate mass obtained for unknown peak with database entries within 5 ppm accuracy. Furthermore, possible matches were examined according to the compound polarity and ion type. For example, compounds with higher log P values would be expected to have longer retention times – if the unknown peak eluted with the retention time of 1.5 min, this

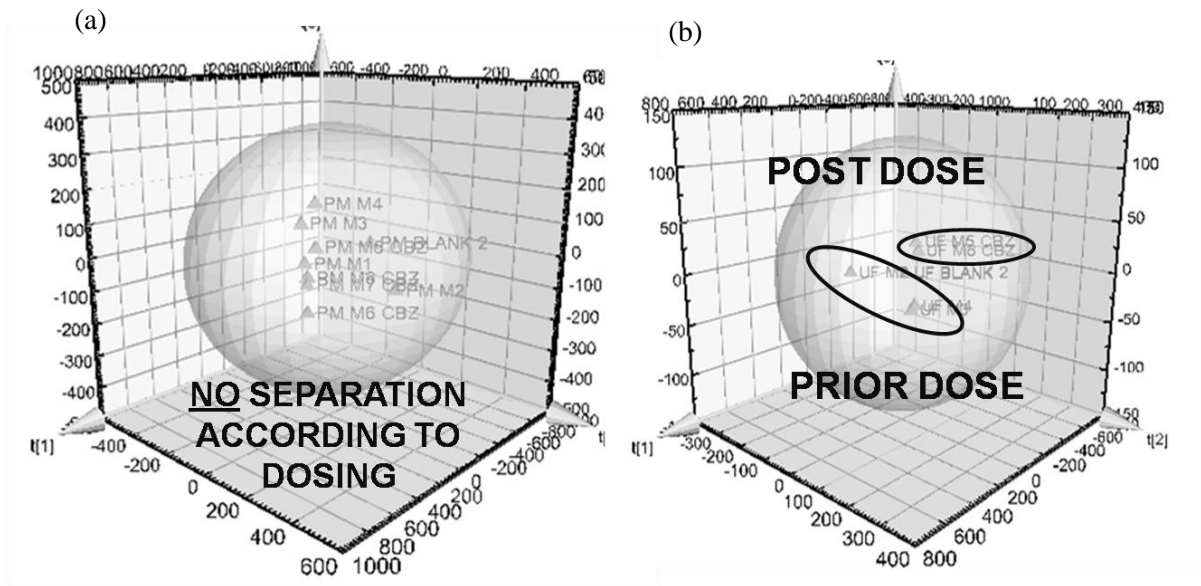


Figure 8.8 Individual 3D scores plot obtained using (a) ultrafiltration (UF) and (b) solvent precipitation (PM) for n=4 mice prior to CBZ dosing (PM and UF) and n=4 mice 30-min post dose (PM CBZ and UF CBZ).

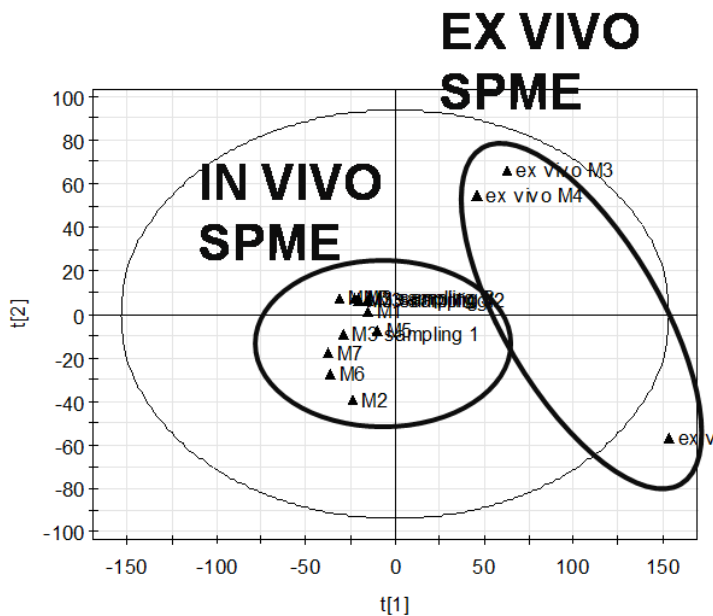


Figure 8.9 Results of PCA comparing *in vivo* versus *ex vivo* SPME sampling (no CBZ dosing) shown as 2D scores plot of 2 main principal components contributing 51.2% and 19.0% of variance respectively.

would not represent a likely match and would be omitted from the table. Likely matches were also examined according to ion type, with protonated and sodiated ions being more likely than other adducts. Finally, expected concentration in blood of tentative matches was also considered with more abundant species being more likely to be observed using this global metabolomics workflow. For unknown peaks, where no suitable ions were identified using database according to the described criteria, the entry was marked as no hits. For unknown species with many possible chemical formulas, the entry was marked accordingly as it was not possible to further narrow down chemical identity of the compounds.

Table 8.1 summarizes the tentative identification of top 20 metabolites observed using ultrafiltration which contributed to the differentiation of samples according to the dosing. The majority of these species are very polar metabolites with retention times  $\leq 3.5$  min, and one of the entries likely corresponds to propylene glycol which was used as dosing vehicle and only present in mice receiving CBZ treatment. Interestingly, both carbamazepine and carbamazepine 10,11-epoxide were observed in UF samples, but were not identified as the main contributors according to PCA so they are not listed within this table. Table 8.1 also shows whether each particular metabolite was observed by other methods employed in current study (SPME and PM). The results show that one of differentiating metabolites is unique to UF only, while others were observed by other methods as well. As mentioned previously, differentiation of samples after solvent precipitation could not be performed successfully, so no such list of features could be collected based on PM data.

Table 8.2 lists top 20 features obtained using *in vivo* SPME after PCA. It is immediately apparent that the differentiating metabolites observed by *in vivo* SPME are completely different than those observed for UF (Table 8.1) indicating the techniques are complementary in nature due to the differences in metabolite coverage achievable by the two techniques. In contrast to UF data, carbamazepine (both protonated and sodiated forms) were detected by PCA as important differentiating metabolites. One potentially interesting finding is tentative identification of oleamide. According to HMDB, oleamide interacts with multiple neurotransmitter systems, although its mode of action is not fully understood. An indication of seizure-limiting properties of this compound was previously reported in literature, although exogenous dosing of this compound did not result in statistically significant attenuation of full epileptic episodes when compared to dosing of known anti-epileptics such as CBZ due possibly to potency and/or dosage selection.<sup>247</sup> The current study is the

**Table 8.1 List of features contributing to differentiation of UF samples according to CBZ dosing**

Retention time (min)	m/z	Tentative chemical formula according to HMDB	Mass accuracy (ppm)	Ion type	Observed by SPME	Observed by PM
1.65	158.9612	no hits	N/A	N/A	no	yes
1.25	203.0527	C <sub>6</sub> H <sub>12</sub> O <sub>6</sub>	0.53	M+Na[1+]	yes	yes
1.28	153.0869	no hits	N/A	N/A	no	yes
1.34	115.0366	multiple formulas	0.33	M+Na[1+]	yes	yes
1.36	169.0582	C <sub>5</sub> H <sub>10</sub> N <sub>2</sub> O <sub>3</sub>	-0.91	M+Na[1+]	no	yes
1.36	147.0763	C <sub>5</sub> H <sub>10</sub> N <sub>2</sub> O <sub>3</sub>	-0.83	M+H[1+]	yes	yes
1.45	118.0863	multiple formulas including propylene glycol	0.39-0.45	M+H [1+]	yes	yes
1.41	120.0657	C <sub>4</sub> H <sub>9</sub> NO <sub>3</sub>	1.5	M+H [1+]	yes	yes
1.45	148.0603	Glutamic acid*	-0.93	M+H[1+]	yes	yes
1.47	176.1030	C <sub>6</sub> H <sub>13</sub> N <sub>3</sub> O <sub>3</sub>	0.18	M+H[1+]	yes	yes
1.85	115.0366	multiple formulas	0.33	M+Na[1+]	yes	yes
1.93	118.0862	multiple formulas including propylene glycol	0.39-0.45	M+H[1+]	yes	yes
1.93	147.0757	C <sub>5</sub> H <sub>10</sub> N <sub>2</sub> O <sub>3</sub>	-4.8	M+H[1+]	yes	yes
2.16	148.0426	no hits	N/A	N/A	no	yes
2.55	102.034	no hits	N/A	N/A	no	no
3.50	150.0582	C <sub>5</sub> H <sub>11</sub> NO <sub>2</sub> S methionine	-0.92	M+H[1+]	yes	yes
7.65	182.0809	C <sub>19</sub> H <sub>11</sub> NO <sub>3</sub>	-1.5	M+H[1+]	yes	yes
9.51	166.0863	Phenylalanine*	0.28	M+H[1+]	yes	yes
12.26	205.0966	Tryptophan*	-2.7	M+H[1+]	yes	yes
17.58	207.1490	no hits	N/A	N/A	yes	yes

\*confirmed with authentic standard

first report to tentatively link oleamide to the *in vivo* action of carbamazepine, and clearly merits further exploration. Another interesting compound tentatively identified in Table 8.2 is thromboxane. Thromboxane is one of the products of arachidonic acid cascade, and this cascade within brain is under discussion as putative drug target of common mood stabilizers such as carbamazepine according to current literature.<sup>248</sup> It is interesting to note that this simple study resulted in two possible links to known or putative endogenous metabolites involved in carbamazepine mechanism. In future studies, it would be interesting to further characterize and interpret the unknown metabolites reported



in Table 8.2, as it could provide additional information regarding biological processes affected by CBZ administration.

**Table 8.2 List of features contributing to differentiation of *in vivo* SPME samples according to CBZ dosing**

Retention time (min)	m/z	Tentative chemical formula according to HMDB	Mass accuracy (ppm)	Ion type	Observed by PM	Observed by UF
1.90	158.9640	no hits	N/A	N/A	no	no
1.90	226.9513	no hits	N/A	N/A	no	no
2.88	102.0340	no hits	N/A	N/A	yes	no
10.47	156.1380	C <sub>14</sub> H <sub>28</sub> O <sub>2</sub>	-1.8	M+2ACN+2H[2+]	yes	yes
14.31	259.0836	Carbamazepine*	-1.9	M+Na[1+]	yes	yes
14.32	237.1017	Carbamazepine*	-2.1	M+H[1+]	yes	yes
17.22	409.1510	no hits	N/A	N/A	yes	yes
18.71	520.3394	C <sub>26</sub> H <sub>50</sub> NO <sub>7</sub> P lysophospholipid	-0.82	M+H[1+]	yes	yes
18.75	544.3395	C <sub>28</sub> H <sub>50</sub> NO <sub>7</sub> P lysophospholipid	-0.56	M+H[1+]	yes	no
18.87	568.3394	C <sub>30</sub> H <sub>50</sub> NO <sub>7</sub> P lysophospholipid	-0.64	M+H[1+]	yes	no
19.26	520.3400	C <sub>26</sub> H <sub>50</sub> NO <sub>7</sub> P lysophospholipid	0.46	M+H[1+]	yes	yes
21.64	256.2733	no hits	N/A	N/A	yes	no
21.96	282.2786	C <sub>18</sub> H <sub>35</sub> NO oleamide	-1.9	M+H[1+]	yes	yes
21.96	283.2719	no hits	N/A	N/A	yes	no
21.96	282.3002	no hits	N/A	N/A	yes	no
22.05	282.2584	no hits	N/A	N/A	yes	no
24.02	338.3409	C <sub>20</sub> H <sub>40</sub> O thromboxane	-2.4	M+ACN+H[1+]	yes	yes
19.94	303.2313	C <sub>20</sub> H <sub>30</sub> O <sub>2</sub>	-1.8	M+H[1+]	yes	no
24.98	391.2838	C <sub>24</sub> H <sub>38</sub> O <sub>4</sub>	1.2	M+H[1+]	yes	yes
12.57	413.1332	C <sub>8</sub> H <sub>13</sub> NO <sub>4</sub> 2-Keto-6-acetamidocaproate	2.7	2M+K[1+]	yes	yes

\*confirmed with authentic standard

### 8.3.5 Principal component analysis: biochemical individuality

As shown in 2D scores plot presented in Figure 8.5(b) principal component 1 and 2 corresponded to biochemical individuality: individual mice clustered closely together regardless of CBZ dosing. Table 8.3 lists 20 most important features contributing to this differentiation as extracted from the loadings

**Table 8.3 List of features contributing to differentiation of *in vivo* SPME samples according to biochemical individuality**

Retention time (min)	m/z	Tentative chemical formula according to HMDB	Mass accuracy (ppm)	Ion type	Observed by PM	Observed by UF
1.63	308.0905	Glutathione*	-1.8	M+H [1+]	yes	no
1.90	294.9385	no hits	N/A	N/A	no	no
1.90	362.9258	no hits	N/A	N/A	no	no
1.90	430.9131	no hits	N/A	N/A	no	no
1.92	105.0425	C <sub>5</sub> H <sub>5</sub> N <sub>5</sub> O <sub>2</sub> , 2,8-Dihydroxyadenine or 8-Hydroxyguanine	-2.0	M+ACN+2H[2+]	no	no
1.92	136.9821	no hits	N/A	N/A	no	no
2.87	184.9854	C <sub>3</sub> H <sub>5</sub> O <sub>7</sub> P Phosphohydroxypyruvic acid	4.5	M+H[1+]	yes	no
2.90	226.0119	C <sub>3</sub> H <sub>5</sub> O <sub>7</sub> P Phosphohydroxypyruvic acid	3.5	M+ACN+H[1+]	no	no
2.90	131.5334	C <sub>6</sub> H <sub>9</sub> N <sub>2</sub> O <sub>5</sub> P Imidazole acetol-phosphate	3.0	M+ACN+2H[2+]	no	no
6.45, 7.28	132.1019	C <sub>6</sub> H <sub>13</sub> NO <sub>2</sub> leucine isomers	-0.10	M+H[1+]	yes	yes
9.36	166.0862	Phenylalanine*	-0.37	M+H[1+]	yes	yes
10.47	156.1383	C <sub>14</sub> H <sub>28</sub> O <sub>2</sub>	0.20	M+2ACN+2H[2+]	yes	yes
11.70	116.1435	no hits	N/A	N/A	yes	yes
17.55	207.1491	no hits	N/A	N/A	yes	yes
19.06	496.3388	C <sub>29</sub> H <sub>47</sub> NO <sub>4</sub>	-1.8	M+Na[1+]	yes	yes
20.24	524.371	C <sub>26</sub> H <sub>54</sub> NO <sub>7</sub> P lysophospholipid	-0.12	M+H[1+]	yes	yes
21.64	256.2733	no hits	N/A	N/A	yes	no
21.96	282.2786	C <sub>18</sub> H <sub>35</sub> NO oleamide	-1.9	M+H[1+]	yes	yes
24.02	338.3409	C <sub>20</sub> H <sub>40</sub> O thromboxane	-2.4	M+ACN+H[1+]	yes	yes
26.68	806.5693	C <sub>46</sub> H <sub>80</sub> NO <sub>8</sub> P phosphatidylcholine	-0.16	M+H[1+]	yes	no

\*confirmed with authentic standard

plot shown in Figure 8.5(c). The list includes glutathione and several amino acids, tentative identification of hydroxylated base and several lipids and seven unknown features. Some of these features are detected only using *in vivo* SPME and not by any other method (PM or UF) further indicating complementary nature of the tested methodologies.

Compound identification remains a bottleneck of metabolomics analysis, and the tentative identification performed in current study represents at best only an educated guess – further work is absolutely necessary to confirm the identity of discussed species. As shown in Tables 8.1 to 8.3, numerous features could not even be tentatively identified with a likely chemical formula, showing concerted global effort is needed to further characterize and catalogue mammalian metabolites in various specimens.

### 8.3.6 Advantages of *in vivo* sampling versus blood withdrawal approaches

Table 8.4 shows 83 features which were detected using *in vivo* SPME sampling, and not detected using *ex vivo* SPME after blood withdrawal. The majority of these peaks (all except 9) were also not detected using solvent precipitation and ultrafiltration methods. This data was compiled by comparing *in vivo* SPME results versus *ex vivo* SPME results for the mice which were not dosed (n=8 mice for *in vivo* SPME, n=4 mice for *ex vivo* SPME), so it represents endogenous metabolites, rather than CBZ metabolites. The fact that *in vivo* SPME is capable to capture this many unique features not observed by any other methods presents a unique advantage of *in vivo* sampling approaches as the metabolome at the time of analysis is better representative of the true metabolome at the time of sampling. Efforts are currently underway in our laboratory to further characterize these species, but preliminary data indicates that many of the species are energy metabolites with fast turnover rates. For example, *in vivo* SPME was able to capture  $\beta$ -NAD which was not observed using the *in vitro* methodology post-blood withdrawal (SPME, UF or PM) as shown in Figure 8.10 and Figure 8.11. These results are shown in Figures 8.10 and 8.11 for one mouse but are consistent for the entire cohort of eight mice sampled within the study. The figure shows the detection of  $\beta$ -NAD using reversed-phase negative ESI method, but the same finding was also confirmed in reversed-phase positive ESI method.

Tentative database identification of few additional species seem to indicate the presence of hydroxylated bases as well as some phosphorylated species such as phosphohydroxypyruvic and imidazole acetol-phosphate, but this requires further confirmation against authentic standards or using fragmentation patterns on a full Orbitrap. For the nine species in Table 8.4 which were also found using solvent precipitation method, the fact they were not observed using *ex vivo* SPME on the same plasma sample seems to indicate that the free (unbound) concentration of these species decreased in the collected blood samples in comparison with the true *in vivo* concentration. This is supported by the fact that these species have relatively long retention times, indicative of relatively hydrophobic species which generally exhibit higher degree of binding. The time delay between blood collection

and sample preparation could indicate slow-binding kinetics. Alternatively, it is possible that the total concentrations of these species decreased after blood withdrawal due to other processes occurring such as degradation or enzymatic conversion, but the total concentration remained sufficiently high to still be detectable by PM method.

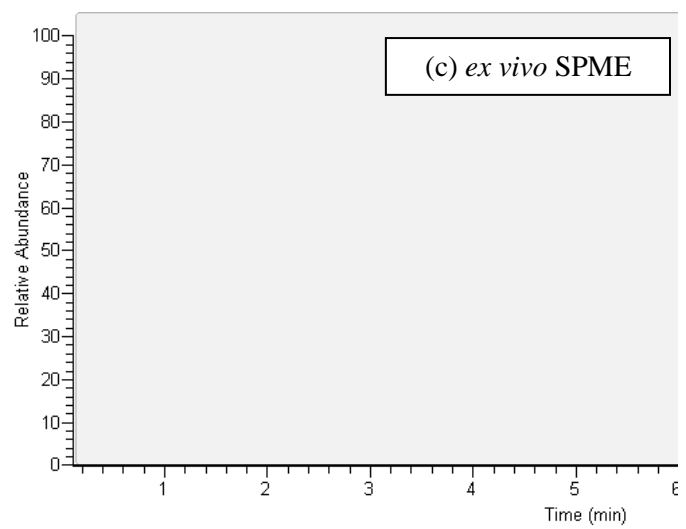
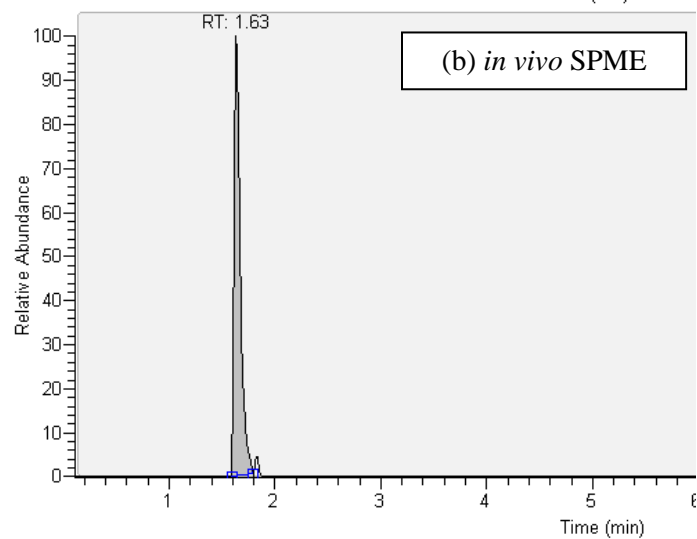
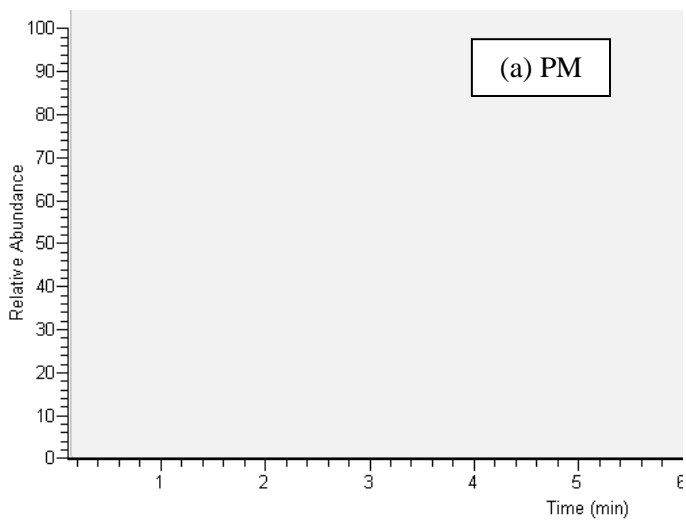
**Table 8.4 List of features observed using *in vivo* SPME and not observed using *ex vivo* SPME**

Time (min)	m/z	Observed by PM	Observed by UF	Observed by <i>in vivo</i> SPME	Observed by <i>ex vivo</i> SPME
1.60	232.0913	no	no	yes	no
1.62	349.0733	no	no	yes	no
1.63	359.5208	no	no	yes	no
1.63	665.1195	no	no	yes ( $\beta$ -NAD)	no
1.63	380.0340	no	no	yes	no
1.63	310.0972	no	no	yes	no
1.63	309.0939	no	no	yes	no
1.63	332.5612	no	no	yes	no
1.90	498.8875	no	no	yes	no
1.91	704.3677	no	no	yes	no
1.92	881.8183	no	no	yes	no
1.95	658.8367	no	no	yes	no
1.97	472.8165	no	no	yes	no
2.86	174.9391	no	no	yes	no
2.86	338.9091	no	no	yes	no
2.87	334.9113	no	no	yes	no
10.33	216.0663	no	no	yes	no
10.46	132.0808	no	no	yes	no
11.44	455.1882	no	no	yes	no
11.64	290.1706	no	no	yes	no
12.21	329.2295	no	no	yes	no
12.21	307.2476	no	no	yes	no
12.26	383.1205	no	no	yes	no
12.65	213.1597	no	no	yes	no
13.47	379.3050	no	no	yes	no
13.48	401.2866	no	no	yes	no
13.79	585.2098	no	no	yes	no
13.80	753.3840	no	no	yes	no
14.73	263.1725	no	no	yes	no
14.82	214.1799	yes	no	yes	no

Time (min)	m/z	Observed by PM	Observed by UF	Observed by <i>in vivo</i> SPME	Observed by <i>ex vivo</i> SPME
15.56	837.4057	no	no	yes	no
15.64	247.0880	yes	no	yes	no
17.43	226.1225	no	no	yes	no
17.50	269.1280	no	no	yes	no
17.55	279.1814	no	no	yes	no
17.56	300.1600	no	no	yes	no
17.91	302.1207	no	no	yes	no
18.11	476.2348	no	no	yes	no
18.22	346.1468	no	no	yes	no
18.62	266.1536	no	no	yes	no
18.86	252.1250	no	no	yes	no
18.86	250.1292	no	no	yes	no
19.11	263.2116	no	no	yes	no
21.27	590.4322	no	no	yes	no
21.40	757.3939	no	no	yes	no
21.51	730.5676	no	no	yes	no
21.60	686.5406	no	no	yes	no
21.69	642.5152	no	no	yes	no
21.72	657.3538	no	no	yes	no
21.79	643.8542	no	no	yes	no
21.79	581.4620	no	no	yes	no
21.80	599.4922	no	no	yes	no
21.91	537.4360	no	no	yes	no
21.91	555.4663	no	no	yes	no
21.91	560.4216	no	no	yes	no
22.00	516.3995	no	no	yes	no
22.01	511.4394	no	no	yes	no
22.02	493.4092	no	no	yes	no
22.12	449.3831	no	no	yes	no
22.12	472.3685	no	no	yes	no
22.26	428.3424	no	no	yes	no
22.46	791.4290	no	no	yes	no
22.46	781.9151	no	no	yes	no
22.50	339.2866	no	no	yes	no
22.67	727.8665	no	no	yes	no
22.78	693.8612	no	no	yes	no
22.86	685.1505	no	no	yes	no

Time (min)	m/z	Observed by PM	Observed by UF	Observed by <i>in vivo</i> SPME	Observed by <i>ex vivo</i> SPME
23.16	896.4543	no	no	yes	no
23.88	717.8722	no	no	yes	no
24.15	911.4509	no	no	yes	no
24.18	480.1591	no	no	yes	no
24.33	866.9233	no	no	yes	no
24.58	738.5066	yes	no	yes	no
24.60	813.5258	yes	no	yes	no
24.62	385.2452	no	no	yes	no
24.72	788.5220	yes	no	yes	no
24.80	388.3417	no	no	yes	no
24.81	764.6094	yes	no	yes	no
24.81	763.6062	no	no	yes	no
25.43	788.5201	yes	no	yes	no
25.45	744.5446	yes	no	yes	no
25.81	762.5433	yes	no	yes	no
26.69	796.5851	no	no	yes	no

Table 8.5 shows 24 compounds which were found in *ex vivo* SPME samples and not found in *in vivo* samples, indicating these species were likely formed during or after blood collection. In majority of cases (18 out of 24), the presence of these species was also confirmed in samples obtained after PM method, and two of these species were also found using ultrafiltration. For six species which were not confirmed in solvent precipitation samples, it is possible that significant ionization suppression occurred within the retention time window of these species.



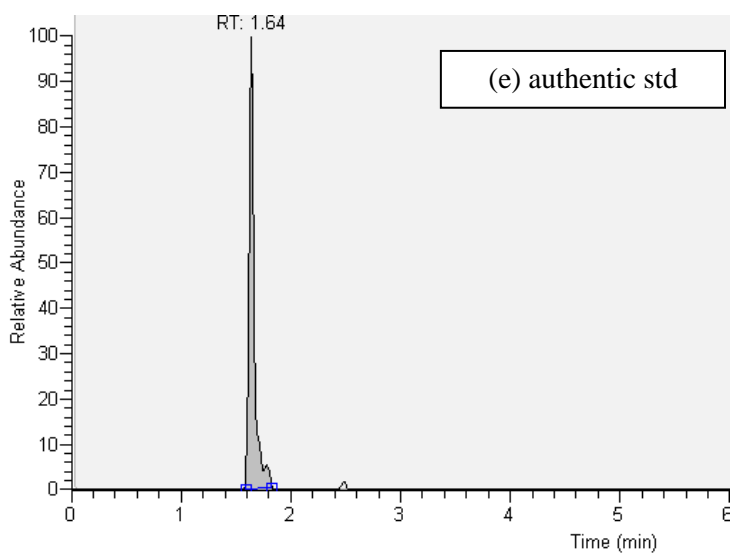
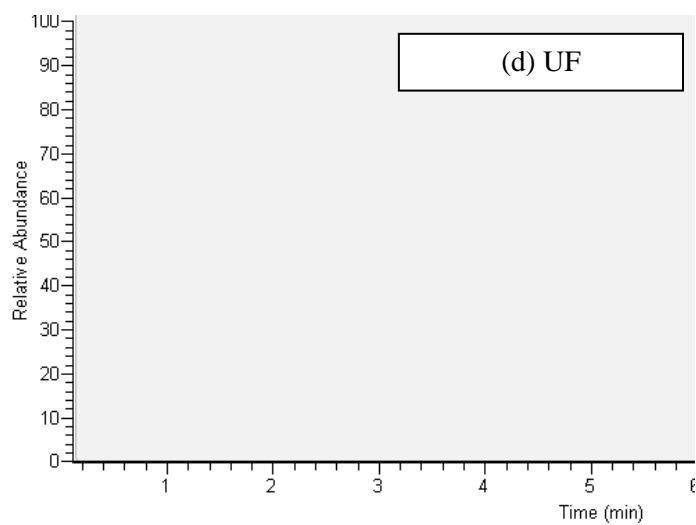


**Figure 8.10** XIC of  $m/z$  662.1019 corresponding to  $\beta$ -NAD for the same mouse sample analyzed using negative ESI reverse phase PFP LC-MS method by (a) PM (b) *in vivo* SPME (c) *ex vivo* SPME (d) UF and (e) injection of authentic metabolite standard containing  $\beta$ -NAD.



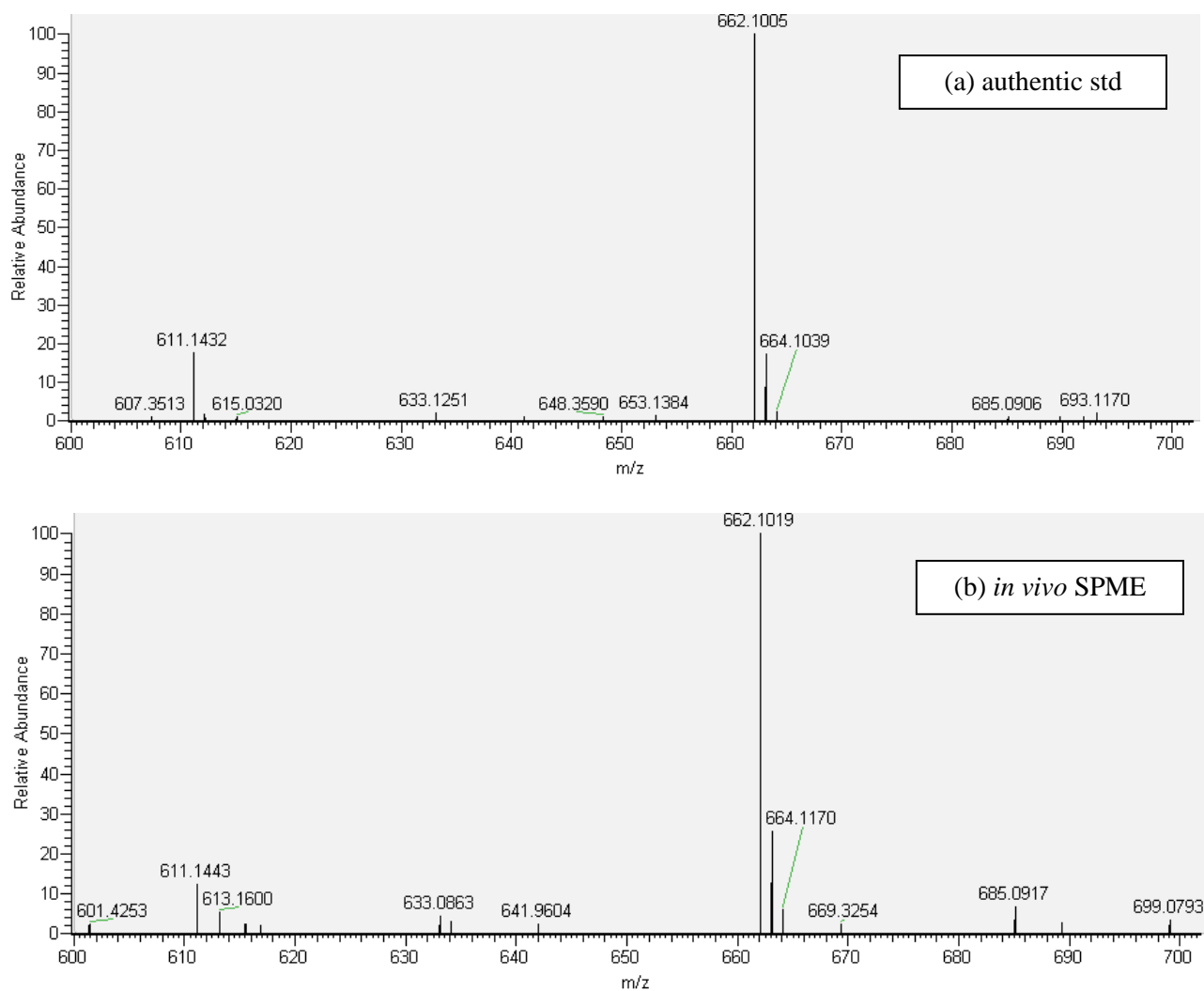


**Figure 8.11** Mass spectrum of (a) authentic  $\beta$ -NAD standard solution dissolved directly in desorption solvent (mass accuracy -2.1 ppm) (b) unknown peak identified for *in vivo* SPME sample shown in Figure 8.10 (mass accuracy 0 ppm). Mass accuracy is calculated using expected accurate mass of  $\beta$ -NAD of 662.1019 for  $[M-H]^-$  in negative ESI mode.  $m/z$  of 685.0916 corresponds to  $[M+Na-2H]^-$  ion of NAD while 664.1174 ion corresponds to  $[M-H]^-$  ion of NADH.

**Table 8.5** List of features observed using *ex vivo* SPME and not observed using *in vivo* SPME

Time	m/z	Observed by PM	Observed by UF	Observed by <i>in vivo</i> SPME	Observed by <i>ex vivo</i> SPME
1.63	192.9099	no	no	no	yes
1.90	835.8282	no	no	no	yes
10.23	427.2228	yes	yes	no	yes
13.29	381.1538	yes	yes	no	yes
13.42	347.2210	yes	no	no	yes
14.73	345.2052	yes	no	no	yes
18.27	480.2990	yes	no	no	yes
18.65	282.6229	yes	no	no	yes
18.71	520.2381	yes	no	no	yes
18.71	520.2143	yes	no	no	yes
18.71	547.2985	yes	no	no	yes
18.71	520.4332	yes	no	no	yes
18.71	520.4213	yes	no	no	yes
18.71	520.4647	yes	no	no	yes
18.71	551.3123	yes	no	no	yes
18.73	591.3254	yes	no	no	yes
18.73	544.2952	yes	no	no	yes
18.73	539.8147	yes	no	no	yes
19.08	880.8452	no	no	no	yes
19.99	539.2618	no	no	no	yes
20.23	759.3737	no	no	no	yes
21.17	337.2733	yes	no	no	yes
21.20	439.2361	yes	no	no	yes
29.32	925.2700	no	no	no	yes

In conclusion, both Table 8.4 and Table 8.5 present convincing evidence that observable changes occur in metabolome during and/or after blood collection. Additional studies to further elucidate the nature of compounds captured by *in vivo* SPME can help further establish this technique as an important tool in metabolomics.

## 8.4 Conclusions

This chapter presents an important addition to global metabolomics data of human plasma presented in Chapter 7. Primarily, it shows distinct advantages of *in vivo* SPME sampling approach over

traditional methods based on blood withdrawal. Firstly, *in vivo* SPME is capable of capturing numerous metabolites not observed by other techniques including some important energy metabolites. This means that the true metabolome at the time of sampling is captured more accurately and can help lead to more accurate biological data interpretation in future. Secondly, the ability to repeatedly sample the same animals permits the use of small cohort of animals while still obtaining highly relevant data, which may not be the case when animal sacrifice per each experiment data point is utilized as the underlying data structure may be obscured by inherent inter-animal variability in metabolic processes. Thirdly, *in vivo* SPME can be a very promising tool to study inter-animal variation with the information on unbound concentration providing an important dimension for biological data interpretation. Finally, the results for mouse 2 in current study indicate significant changes in sample composition *versus in vivo* SPME sample collected for the same mouse, indicating sample composition can unpredictably change after biofluid collection despite the precautions taken. From the perspective of CBZ metabolism, two seemingly important links to oleamide and thromboxane have emerged from SPME data, but further characterization of all potentially differentiating metabolites is needed.

## Chapter 9

### Summary and future directions

#### 9.1 Summary

Increasing the number of steps involved in sample preparation for metabolomics applications results in the narrowing of chemical diversity of captured metabolome, as each step can contribute some degree of selectivity and/or inadvertent metabolite losses can occur during sample handling due to adsorption, degradation, etc.<sup>34</sup> The use of solid-phase microextraction, in particular *in vivo* SPME, completely streamlines the process and reduces the overall number of steps as well as eliminates the need for metabolism quenching while ensuring captured metabolome is a good representation of true metabolome at the time of sampling. In comparison to the traditional methods, SPME is characterized by lower amounts extracted due to its non-exhaustive nature, which translates into lower MS signal intensities and overall lower analytical sensitivity. However, despite this apparent shortcoming, method precision of SPME was found equivalent or better than traditional methods, indicating that the small amounts of metabolites extracted are still sufficient for reliable quantitative analysis. In fact, non-exhaustive nature of SPME resulting in small amounts extracted is of utmost importance for *in vivo* sampling using SPME as it minimizes the disturbance to the system under study and permits the use of small probe dimensions making the technique less invasive than other more traditional approaches. Furthermore, lower overall signal intensities encountered in SPME methods resulted in additional two significant benefits: (i) reduced ionization suppression which improves quantitation and data quality and (ii) improved metabolite coverage as low intensity peaks are not obstructed by the presence of highly intense peaks. In fact, highest metabolite coverage among all methods tested was achieved by SPME in combination with negative ESI LC-MS method, indicating that SPME can be a powerful tool for metabolomics analysis. One important aspect of SPME is that the amount extracted is proportional to unbound concentration which is biologically active, so it is possible that SPME metabolomics data may be more easily correlated to the observed biological effect, but this aspect demands further investigation. The current study does clearly show that SPME performs better than ultrafiltration in terms of improving the coverage of hydrophobic species. These species tend to be more highly protein-bound, so information on the unbound concentration of these analytes becomes extremely valuable for biological interpretation. In fact, for some xenobiotics such as carbamazepine, significant inter-individual variability of unbound

concentrations has been documented even when total concentration is effectively the same, and similar situation can be envisioned for some of endogenous metabolites.

The success of current study also relied heavily on detailed optimization of LC-MS methods in order to achieve optimum analytical sensitivity. Interestingly, when a generic method on a full hybrid instrument was used <500 features were observed in positive ESI mode, which is significantly less than minimum of 1500 features observed in current study using a single-stage Orbitrap MS. The use of complementary HILIC and reverse phase methods, as well as positive and negative ionization modes also significantly increased metabolite coverage. The obtained SPME extract was compatible for direct injection using both methods after appropriate dilution with acetonitrile prior to HILIC method. The step of evaporation/reconstitution was completely avoided in current workflow in order to avoid possible issues with metabolite solubility in a given reconstitution solvent.

The results of this thesis clearly show that SPME can be a very useful sample preparation method for global metabolomic studies in order to improve/complement metabolite coverage, to provide information on biologically active free concentration and to improve quantitative information of the collected metabolomics data. However, the true promise of SPME for metabolomic studies lies in its potential for use during *in vivo* sampling. The *in vivo* mouse study described in Chapter 8 clearly demonstrates the utility of *in vivo* SPME sampling and shows improved metabolism quenching of *in vivo* SPME versus traditional approaches based on blood withdrawal. Clearly, *in vivo* SPME presents an important step towards the development of sampling methodology that can properly capture the true metabolome at the time of sampling. Further investigation of all metabolites that are preferentially extracted using *in vivo* SPME and not observed using other methods is currently underway using the preliminary data reported in Section 8.3.6. At this point in time, it appears that SPME is very useful for capture of short-lived and unstable metabolites such as energy metabolites and anti-oxidants such as glutathione species. In addition to the capture of unique metabolites not accessible by common metabolomic methods, another advantage of *in vivo* SPME is the ability to repeatedly sample the same animal to further increase reliability of analytical results. This permits the use of smaller animal data sets while still collecting appropriate data. As shown in the example of Chapter 8, *in vivo* SPME was able to differentiate mice based on carbamazepine dosing using only n=4 mice, whereas same size cohort (n=4 control and treatment animals) was insufficient for solvent precipitation method presumably due to the confounding influence of underlying inter-animal variability when sampling different mice in control *versus* treatment groups. This seriously limited

the usability of such dataset. Of course, further opportunities for improvement of *in vivo* SPME methodology in the context of metabolomics do exist, and one limitation encountered in the study described in Chapter 8 is the fact that some known CBZ metabolites could not be detected using SPME samples, while they were detected in solvent precipitation samples. This is likely due to low concentration of these species, and can be addressed in future with further improvements in sensitivity of LC-MS instrumentation. With currently available technology, this can be addressed by performing animal studies with higher doses of drug (relatively low 2 mg/kg dose) or increasing the sampling time further from the short 2-min time used in the study reported herein. In terms of understanding the effects of carbamazepine dosing, current study provided interesting links between carbamazepine and endogenous metabolites such as (i) oleamide which was previously reported to have seizure-reducing effects and (ii) thromboxane which is one of the species in cascade regarded as putative drug target of carbamazepine and similar medicines. Both of these links merit further and more detailed exploration.

Some of the research outcomes presented within this thesis are relevant not only for the use of SPME in metabolomics, but for the analysis of any non-volatile and/or polar species, such as drugs or pesticides in biological fluids. Firstly, the issue of low sample throughput for SPME-LC methods was successfully addressed through the development and evaluation of 96-well plate SPME system described in Chapter 2. Although, the current study only evaluated the system in terms of targeted analysis and found its performance satisfactory, efforts are already underway in our laboratory to extend its use to metabolomic studies. Secondly, the feasibility of *in vivo* SPME sampling in mice was demonstrated for the first time, and is valuable to permit longitudinal or multiple studies on the same mice, thus reducing animal use which is especially important when genetically-modified or other rare strains of mice are used. Finally, this work addressed several limitations of existing commercial SPME coatings and devices. In collaboration with Supelco, new line of biocompatible SPME coatings housed inside a hypodermic needle was evaluated. The availability of such single-use devices with good-inter fibre reproducibility is extremely important to make *in vivo* SPME technology available to any user rather than confined to specialized laboratories capable of producing their own coatings. Furthermore, new types of coatings including mixed-mode, polar-modified polystyrene-divinyl benzene and phenylboronic acid were found to drastically improve extraction of polar compounds using SPME. Mixed-mode coating was already successfully incorporated into biocompatible *in vivo* SPME assemblies by Supelco, and efforts are currently under way to produce the other two types of coatings (phenylboronic acid and polar-enhanced polystyrene-divinylbenzene

polymers) in biocompatible format. However, it is important to mention that some challenges in terms of SPME coating do remain. In particular, there is a lack of suitable coating procedures to produce very thin coatings on very thin solid supports. Another opportunity in improvement of coatings and SPME devices lies in further miniaturization of the device dimensions. Such research is particularly important from miniaturization perspective in order to further decrease invasiveness of SPME procedures and increase spatial resolution when studying heterogeneous systems, such as tumor and surrounding tissue, for example. For some applications such as high-throughput bioanalysis, coating reusability plays an important role in overall cost of analysis, so further evaluation and improvement of long-term coating robustness is beneficial.

## 9.2 Future directions

The field of metabolomics provides interesting opportunities for in-depth study of living systems. Some of the driving forces for the interest in metabolomics is that (i) the complexity of metabolome of a given organism is expected to be lower than that of proteome/genome in terms of number of components, (ii) changes in metabolites can be amplified and easier to detect *versus* correlated changes in transcriptome/proteome, and (iii) metabolomics experiments are more cost-effective than their genomic/proteomic counterparts.<sup>14</sup> The research presented herein supports the use of solid-phase microextraction as an effective sample preparation method for global metabolomic studies of biofluids. In future, this metabolomics workflow can also be extended to *in vivo* SPME sampling of tissues. For example, Zhou *et al.* and Zhang *et al.* have successfully sampled adipose and muscle tissue of fish.<sup>180, 181, 249</sup> The methodology was validated for targeted analysis of pharmaceuticals, but global metabolomic studies can be envisioned as a next logical step. Tissue metabolomics is particularly interesting for the study of damaged tissues such as tumors in search of novel biomarkers because the concentration of such biomarkers is expected to be higher in such tissue than in surrounding areas.<sup>22</sup> For this type of studies, *in vivo* SPME presents a less-invasive sampling method over traditional methods that typically rely on invasive biopsy followed by solvent extraction. SPME also provides improved spatial resolution sampling which is important when dealing with such heterogeneous specimens, and coatings with 1 mm and 2 mm dimensions have already been successfully employed by our research group. Other interesting areas for exploration include single cell studies pending further miniaturization of SPME devices or the use of special coatings to trap known reactive metabolites and intermediates (for example, using glutathione or methoxylamine trapping agents).<sup>194, 250</sup> From SPME perspective, it is also important to further characterize additional

unknown metabolites observed by SPME in current study and not detected by other methods in the hope of identifying new or previously undetected components of human and/or mouse plasma. This will further enhance understanding of advantages and disadvantages of this new methodology for global metabolomic studies.

From technical perspective, LC-MS-based metabolomic studies would greatly benefit from improved data processing workflows, especially in terms of peak detection and identification. The former aspect was found particularly problematic in current study when using commercial SIEVE software, as large number of noise features was reported as peaks. This demanded manual verification of all reported peaks in order to exclude the noise peaks and retain only the true analyte peaks. This step presented the bottleneck of the entire workflow, with a typical dataset of 20,000 peaks requiring 5-10 hr unattended computer processing time and > 20 hr of manual verification. The issue of rapid peak identification can be addressed in part by building of comprehensive databases, and such efforts are currently underway worldwide as exemplified by HMDB database used extensively in current work. However, the metabolite coverage of such databases is still inadequate as large proportion of peaks cannot be even tentatively matched with a chemical formula using this approach. Furthermore, more efforts into standardization of LC methods and inclusion of LC retention times within such databases are needed. From MS instrument perspective, Orbitrap instruments present a great advance to improve mass resolution and are easily compatible with conventional LC analysis. In future, further increases in acquisition speeds can help couple these instruments with UHPLC for increased chromatographic resolution, sensitivity and sample throughput. Further increases in instrumental sensitivity are also greatly beneficial in order to detect metabolites present at very low concentrations, which may remain undetected using current workflows. It is also important to remember that electrospray LC-MS is simply one suitable platform for global metabolomics, and introduces systematic bias towards metabolites that are amenable to electrospray ionization. Other platforms and ionization methods play important role to achieve the goal of comprehensive metabolite coverage.

The study of inter-animal variability is a fascinating topic and the availability of *in vivo* SPME to sample various compartments of freely moving animals (for example, blood, bile and tissue such as liver, muscle and adipose tissue) opens up new possibilities to investigate fate of xenobiotics and metabolites in living system. Such integrative multi-compartmental studies are particularly important when studying fate and distribution of xenobiotics<sup>198</sup>, and the availability of *in vivo* SPME would provide more opportunity to longitudinal studies over time, as no sacrifice of animals is required.



Numerous studies to establish the variability of endogenous metabolites and their normal concentrations are currently ongoing, and some of the discrepancies in literature can be attributed to inadequate performance of analytical approach selected for the study. For well-designed studies, great degree of inter-animal variability can provide fascinating insight in biology of various processes. For example, in a recent study Coen *et al.* used metabolomics of various compartments (using both NMR and LC-MS approach) to understand toxic response of rats to the administration of galactosamine.<sup>198</sup> Even within the same strain, age and sex of rats, about 25% of rats were found to be non-responders (no liver toxicity was observed due to differences in distribution and metabolism of this compound) *versus* 75% of rats which suffered from various degrees of hepatotoxicity. This study provided interesting insight into mechanism of galactosamine toxicity and inter-individual variation in response to xenobiotics. It effectively illustrates the power of metabolomic studies to study the differences in individual response rather than overall population response and opens up many new areas of investigation.

In contrast to hypothesis-driven approaches, global metabolomics data is collected without prior assumptions or hypotheses, so it allows testing of multiple hypotheses as well as *a posteriori* hypothesis generation. Furthermore, the holistic approach for simultaneous analysis of large number of metabolites has promise in the area of personalized health and nutrition, where metabolic profiles are expected to provide a snapshot of homeostasis within giving individual, and any departures from such homeostasis when monitored over time can be addressed by nutritional or medical intervention to attempt and restore global homeostasis before the actual onset of a medical condition.

## References

- (1) Ceglarek, U.; Leichtle, A.; Brügel, M.; Kortz, L.; Brauer, R.; Bresler, K.; Thiery, J.; Fiedler, G. M. *Mol. Cell. Endocrinol.* **2009**, *301*, 266-271.
- (2) van der Greef, J.; Smilde, A. K. *J. Chemom.* **2006**, *19*, 376-386.
- (3) Fiehn, O. *Comp. Funct. Genomics* **2001**, *2*, 155-168.
- (4) Ryan, D.; Robards, K. *Anal. Chem.* **2006**, *78*, 7954-7958.
- (5) Novotny, M. V.; Soini, H. A.; Mechref, Y. *J. Chromatogr. B* **2008**, *866*, 26-47.
- (6) Williams, R. J. In *Biochemical Individuality*; Wiley and Sons: New York, 1956.
- (7) Horning, E. C.; Horning, M. G. *J. Chromatogr. Sci.* **1971**, *9*, 129-140.
- (8) Horning, E. C.; Horning, M. G. *Methods Med. Res.* **1970**, *12*, 369-371.
- (9) Jellum, E. *J. Chromatogr.* **1977**, *143*, 427-462.
- (10) Pauling, L.; Robinson, A. B.; Teranishi, P.; Cary, P. *Proc. Natl. Acad. Sci. U. S. A.* **1971**, *68*, 2374-2376.
- (11) Villas-Bôas, S. G.; Mas, S.; Åkesson, M.; Smedsgaard, J.; Nielsen, J. *Mass Spectrom. Rev.* **2005**, *24*, 613-646.
- (12) Bruce, S. J.; Tavazzi, I.; Parisod, V.; Rezzi, S.; Kochhar, S.; Guy, P. A. *Anal. Chem.* **2009**, *81*, 3285-3296.
- (13) Nielsen, J.; Oliver, S. *Trends Biotechnol.* **2005**, *23*, 544-546.
- (14) Dunn, W. B.; Ellis, D. I. *TrAC, Trends Anal. Chem.* **2005**, *24*, 285-294.
- (15) Orešič, M. *Nutrition, Metabolism and Cardiovascular Diseases*, **2009**, *19*, 816-824.
- (16) Bernini, P.; Bertini, I.; Luchinat, C.; Nepi, S.; Saccenti, E.; Schäfer, H.; Schütz, B.; Spraul, M.; Tenori, L. *J. Proteome Res.* **2009**, *8*, 4264-4271.
- (17) Minami, Y.; Kasukawa, T.; Kakazu, Y.; Iigo, M.; Sugimoto, M.; Ikeda, S.; Yasui, A.; Van Der Horst, G. T. J.; Soga, T.; Ueda, H. R. *Proc. Natl. Acad. Sci. U. S. A.* **2009**, *106*, 9890-9895.

- (18) Ackermann, B. L.; Hale, J. E.; Duffin, K. L. *Curr. Drug. Metab.* **2006**, *7*, 525-539.
- (19) Koulman, A.; Lane, G. A.; Harrison, S. J.; Volmer, D. A. *Anal. Bioanal Chem.* **2009**, *394*, 663-670.
- (20) Sreekumar, A.; Poisson, L. M.; Rajendiran, T. M.; Khan, A. P.; Cao, Q.; Yu, J.; Laxman, B.; Mehra, R.; Lonigro, R. J.; Li, Y.; Nyati, M. K.; Ahsan, A.; Kalyana-Sundaram, S.; Han, B.; Cao, X.; Byun, J.; Omenn, G. S.; Ghosh, D.; Pennathur, S.; Alexander, D. C.; Berger, A.; Shuster, J. R.; Wei, J. T.; Varambally, S.; Beecher, C.; Chinnaiyan, A. M. *Nature* **2009**, *457*, 910-914.
- (21) Griffin, J. L. *Curr. Opin. Chem. Biol.* **2006**, *10*, 309-315.
- (22) Griffin, J. L.; Kauppinen, R. A. *J. Proteome Res.* **2007**, *6*, 498-505.
- (23) Robertson, D. G.; Reily, M. D.; Baker, J. D. *J. Proteome Res.* **2007**, *6*, 526-539.
- (24) Lee, S. H.; Woo, H. M.; Jung, B. H.; Lee, J.; Kwon, O. S.; Pyo, H. S.; Choi, M. H.; Chung, B. C. *Anal. Chem.* **2007**, *79*, 6102-6110.
- (25) Rezzi, S.; Ramadan, Z.; Fay, L. B.; Kochhar, S. *J. Proteome Res.* **2007**, *6*, 513-525.
- (26) Idborg-Bjorkman, H.; Edlund, P. -.; Kvalheim, O. M.; Schuppe-Koistinen, I.; Jacobsson, S. P. *Anal. Chem.* **2003**, *75*, 4784-4792.
- (27) Chen, C.; Gonzalez, F. J.; Idle, J. R. *Drug Metab. Rev.* **2007**, *39*, 581-597.
- (28) Buchholz, A.; Takors, R.; Wandrey, C. *Anal. Biochem.* **2001**, *295*, 129-137.
- (29) Koulman, A.; Cao, M.; Faville, M.; Lane, G.; Mace, W.; Rasmussen, S. *Rapid Commun. Mass Spectrom.* **2009**, *23*, 2253-2263.
- (30) Griffiths, W. J.; Wang, Y. *Chem. Soc. Rev.* **2009**, *38*, 1882-1896.
- (31) Theodoridis, G.; Gika, H. G.; Wilson, I. D. *TrAC Trends. Anal. Chem.* **2008**, *27*, 251-260.
- (32) Graca, G.; Duarte, I. F.; Goodfellow, B. J.; Carreira, I. M.; Couceiro, A. B.; Domingues, M. D. R.; Spraul, M.; Tseng, L. -.; Gil, A. M. *Anal. Chem.* **2008**, *80*, 6085-6092.
- (33) Brown, M.; Dunn, W. B.; Dobson, P.; Patel, Y.; Winder, C. L.; Francis-Mcintyre, S.; Begley, P.; Carroll, K.; Broadhurst, D.; Tseng, A.; Swainston, N.; Spasic, I.; Goodacre, R.; Kell, D. B. *Analyst* **2009**, *134*, 1322-1332.

- (34) Moco, S.; Vervoort, J.; Moco, S.; Bino, R. J.; De Vos, R. C. H.; Bino, R. *TrAC Trends Anal. Chem.* **2007**, *26*, 855-866.
- (35) Blow, N. *Nature* **2008**, *455*, 697-700.
- (36) Madalinski, G.; Godat, E.; Alves, S.; Lesage, D.; Genin, E.; Levi, P.; Labarre, J.; Tabet, J. -.; Ezan, E.; Junot, C. *Anal. Chem.* **2008**, *80*, 3291-3303.
- (37) Bedair, M.; Sumner, L. W. *TrAC Trends Anal. Chem.* **2008**, *27*, 238-250.
- (38) Giavalisco, P.; Köhl, K.; Hummel, J.; Seiwert, B.; Willmitzer, L. *Anal. Chem.* **2009**, *81*, 6546-6551.
- (39) Giavalisco, P.; Hummel, J.; Lisec, J.; Inostroza, A. C.; Catchpole, G.; Willmitzer, L. *Anal. Chem.* **2008**, *80*, 9417-9425.
- (40) Miura, D.; Fujimura, Y.; Tachibana, H.; Wariishi, H. *Anal. Chem.* **2009**.
- (41) Sun, G.; Yang, K.; Zhao, Z.; Guan, S.; Han, X.; Gross, R. W. *Anal. Chem.* **2007**, *79*, 6629-6640.
- (42) Kaplan, K.; Dwivedi, P.; Davidson, S.; Yang, Q.; Tso, P.; Siems, W.; Hill Jr., H. H. *Anal. Chem.* **2009**, *81*, 7944-7953.
- (43) Boudonck, K. J.; Mitchell, M. W.; Németh, L.; Keresztes, L.; Nyska, A.; Shinar, D.; Rosenstock, M. *Toxicol. Pathol.* **2009**, *37*, 280-292.
- (44) Lawton, K. A.; Berger, A.; Mitchell, M.; Milgram, K. E.; Evans, A. M.; Guo, L.; Hanson, R. W.; Kalhan, S. C.; Ryals, J. A.; Milburn, M. V. *Pharmacogenomics* **2008**, *9*, 383-397.
- (45) Büscher, J. M.; Czernik, D.; Ewald, J. C.; Sauer, U.; Zamboni, N. *Anal. Chem.* **2009**, *81*, 2135-2143.
- (46) Lindon, J. C.; Nicholson, J. K.; Holmes, E.; Keun, H. C.; Craig, A.; Pearce, J. T. M.; Bruce, S. J.; Hardy, N.; Sansone, S. -.; Antti, H.; Jonsson, P.; Daykin, C.; Navarange, M.; Beger, R. D.; Verheij, E. R.; Amberg, A.; Baunsgaard, D.; Cantor, G. H.; Lehman-McKeeman, L.; Earll, M.; Wold, S.; Johansson, E.; Haselden, J. N.; Kramer, K.; Thomas, C.; Lindberg, J.; Schuppe-Koistinen, I.; Wilson, I. D.; Reily, M. D.; Robertson, D. G.; Senn, H.; Krotzky, A.; Kochhar, S.; Powell, J.; Van Der Ouderaa, F.; Plumb, R.; Schaefer, H.; Spraul, M. *Nat. Biotechnol.* **2005**, *23*, 833-838.
- (47) Teahan, O.; Gamble, S.; Holmes, E.; Waxman, J.; Nicholson, J. K.; Bevan, C.; Keun, H. C. *Anal. Chem.* **2006**, *78*, 4307-4318.

- (48) Rammouz, R. E.; Létisse, F.; Durand, S.; Portais, J.; Moussa, Z. W.; Fernandez, X. *Anal. Biochem.* **2010**, *398*, 169-177.
- (49) Bolten, C. J.; Kiefer, P.; Letisse, F.; Portais, J. -.; Wittmann, C. *Anal. Chem.* **2007**, *79*, 3843-3849.
- (50) Chang, M. S.; Ji, Q.; Zhang, J.; El-Shourbagy, T. A. *Drug Dev. Res.* **2007**, *68*, 107-133.
- (51) Michopoulos, F.; Lai, L.; Gika, H.; Theodoridis, G.; Wilson, I. *J. Proteome Res.* **2009**, *8*, 2114-2121.
- (52) Zelena, E.; Dunn, W. B.; Broadhurst, D.; Francis-McIntyre, S.; Carroll, K. M.; Begley, P.; O'Hagan, S.; Knowles, J. D.; Halsall, A.; Wilson, I. D.; Kell, D. B. *Anal. Chem.* **2009**, *81*, 1357-1364.
- (53) Pesek, J. J.; Matyska, M. T.; Loo, J. A.; Fischer, S. M.; Sana, T. R. *J. Sep. Sci.* **2009**, *32*, 2200-2208.
- (54) Courant, F.; Pinel, G.; Bichon, E.; Monteau, F.; Antignac, J. -.; Le Bizec, B. *Analyst* **2009**, *134*, 1637-1646.
- (55) Khin, T. M.; Uehara, T.; Aoshima, K.; Oda, Y. *Anal. Chem.* **2009**, *81*, 7766-7772.
- (56) Rezzi, S.; Vera, F. A.; Martin, F. - J.; Wang, S.; Lawler, D.; Kochhar, S. *J. Chromatogr. B: Anal. Tech. Biomed. Life Sci.* **2008**, *871*, 271-278.
- (57) Tuck, M. K.; Chan, D. W.; Chia, D.; Godwin, A. K.; Grizzle, W. E.; Krueger, K. E.; Rom, W.; Sanda, M.; Sorbara, L.; Stass, S.; Wang, W.; Brenner, D. E. *J. Proteome Res.* **2009**, *8*, 113-117.
- (58) Pereira, H.; Martin, J. F.; Joly, C.; Sébédio, J. L.; Pujos-Guillot, E. *Metabolomics* **2009**, *10.1007/s11306-009-0188-9*.
- (59) Deprez, S.; Sweatman, B. C.; Connor, S. C.; Haselden, J. N.; Waterfield, C. J. *J. Pharm. Biomed. Anal.* **2002**, *30*, 1297-1310.
- (60) Rosenling, T.; Slim, C. L.; Christin, C.; Coulier, L.; Shi, S.; Stoop, M. P.; Bosman, J.; Suits, F.; Horvatovich, P. L.; Stockhofe-Zurwieden, N.; Vreeken, R.; Hankemeier, T.; van Gool, A. J.; Luider, T. M.; Bischoff, R. *J. Proteome Res.* **2009**, *8*, 5511-5522.
- (61) van de Merbel, N. C. *Trac Trends Anal. Chem.* **2008**, *27*, 924-933.

- (62) Kraut, A.; Marcellin, M.; Adrait, A.; Kuhn, L.; Louwagie, M.; Kieffer-Jaquinod, S.; Lebert, D.; Masselon, C. D.; Dupuis, A.; Bruley, C.; Jaquinod, M.; Garin, J.; Gallagher-Gambarelli, M. *J. Proteome Res.* **2009**, *8*, 3778-3785.
- (63) Thongboonkerd, V.; Saetun, P. *J. Proteome Res.* **2007**, *6*, 4173-4181.
- (64) Cubbon, S.; Bradbury, T.; Wilson, J.; Thomas-Oates, J. *Anal. Chem.* **2007**, *79*, 8911-8918.
- (65) Gu, H.; Chen, H.; Pan, Z.; Jackson, A. U.; Talaty, N.; Xi, B.; Kissinger, C.; Duda, C.; Mann, D.; Raftery, D.; Cooks, R. G. *Anal. Chem.* **2007**, *79*, 89-97.
- (66) Lenz, E. M.; Bright, J.; Wilson, I. D.; Hughes, A.; Morrisson, J.; Lindberg, H.; Lockton, A. *J. Pharm. Biomed. Anal.* **2004**, *36*, 841-849.
- (67) Crews, B.; Wikoff, W. R.; Patti, G. J.; Woo, H. -.; Kalisiak, E.; Heideker, J.; Siuzdak, G. *Anal. Chem.* **2009**, *81*, 8538-8544.
- (68) Williams, J.; Wood, J.; Pandarinathan, L.; Karanian, D.; Bahr, B.; Vouros, P.; Makriyannis, A. *Anal. Chem.* **2007**, *79*, 5582-5593.
- (69) Canelas, A. B.; Ten Pierick, A.; Ras, C.; Seifar, R. M.; Van Dam, J. C.; Van Gulik, W. M.; Heijnen, J. J. *Anal. Chem.* **2009**, *81*, 7379-7389.
- (70) Coulier, L.; Bas, R.; Jespersen, S.; Verheij, E.; Van Der Werf, M. J.; Hankemeier, T. *Anal. Chem.* **2006**, *78*, 6573-6582.
- (71) Croixmarie, V.; Umbdenstock, T.; Cloarec, O.; Moreau, A.; Pascussi, J. -.; Boursier-Neyret, C.; Walther, B. *Anal. Chem.* **2009**, *81*, 6061-6069.
- (72) Smilde, A. K.; Van Der Werf, M. J.; Schaller, J. -.; Kistemaker, C. *Analyst* **2009**, *134*, 2281-2285.
- (73) Weckwerth, W.; Morgenthal, K. *Drug Discovery Today* **2005**, *10*, 1551-1558.
- (74) Belardi, R. G.; Pawliszyn, J. *Water Pollut. Res. J. Can.* **1989**, *24*, 179.
- (75) Arthur, C. L.; Pawliszyn, J. *Anal. Chem.* **1990**, *62*, 2145.
- (76) Kumar, A.; Ashok, G.; Malik, A. K.; Matysik, F. M. *Bioanal. Rev.* **2009**, *1*, 35-55.
- (77) Vas, G.; Vekey, K. *J. Mass. Spectrom.* **2004**, *39*, 233-254.

- (78) Pragst, F. *Anal. Bioanal. Chem.* **2007**, 388, 1393-1414.
- (79) Ai, J. *Anal. Chem.* **1997**, 69, 1230-1236.
- (80) Ouyang, G.; Pawliszyn, J. *Anal. Chim. Acta* **2008**, 627, 184-197.
- (81) Zhou, S. N.; Zhao, W.; Pawliszyn, J. *Anal. Chem.* **2008**, 80, 481-490.
- (82) Ouyang, G.; Cai, J.; Zhang, X.; Li, H.; Pawliszyn, J. *J. Sep. Sci.* **2008**, 31, 1167-1172.
- (83) Zhang, X.; Es-haghi, A.; Cai, J.; Pawliszyn, J. *J. Chromatogr. A* **2009**, 1216, 7664-7669.
- (84) Chen, Y.; O'Reilly, J.; Wang, Y.; Pawliszyn, J. *Analyst* **2004**, 129, 702-703.
- (85) Chen, Y.; Pawliszyn, J. *Anal. Chem.* **2004**, 76, 5807-5815.
- (86) Zhang, X.; Es-Haghi, A.; Musteata, F. M.; Ouyang, G.; Pawliszyn, J. *Anal. Chem.* **2007**, 79, 4507-4513.
- (87) Musteata, F. M.; Musteata, M. L.; Pawliszyn, J. *Clin. Chem.* **2006**, 52, 708-715.
- (88) Musteata, F. M.; de Lannoy, I.; Gien, B.; Pawliszyn, J. *J. Pharm. Biomed. Anal.* **2008**, 47, 907-912.
- (89) Zhang, X.; Cudjoe, E.; Vuckovic, D.; Pawliszyn, J. *J. Chromatogr. A* **2009**, 1216, 7505-7509.
- (90) Soini, H. A.; Bruce, K. E.; Klouckova, I.; Brereton, R. G.; Penn, D. J.; Novotny, M. V. *Anal. Chem.* **2006**, 78, 7161-7168.
- (91) Xu, Y.; Gong, F.; Dixon, S. J.; Brereton, R. G.; Soini, H. A.; Novotny, M. V.; Oberzaucher, E.; Grammer, K.; Penn, D. J. *Anal. Chem.* **2007**, 79, 5633-5641.
- (92) Xu, Y.; Dixon, S. J.; Brereton, R. G.; Soini, H. A.; Novotny, M. V.; Trebesius, K.; Bergmaier, I.; Oberzaucher, E.; Grammer, K.; Penn, D. J. *Metabolomics* **2007**, 3, 427-437.
- (93) Riazanskaia, S.; Blackburn, G.; Harker, M.; Taylor, D.; Thomas, C. L. P. *Analyst* **2008**, 133, 1020-1027.
- (94) Zhang, Z. -.; Cai, J. -.; Ruan, G. -.; Li, G. -. *J. Chromatogr. B: Anal. Tech. Biomed. Life Sci.* **2005**, 822, 244-252.

- (95) Gallagher, M.; Wysocki, C. J.; Leyden, J. J.; Spielman, A. I.; Sun, X.; Preti, G. *Br. J. Derm.* **2008**, *159*, 780-791.
- (96) Zimmermann, D.; Hartmann, M.; Moyer, M. P.; Nolte, J.; Baumbach, J. I. *Metabolomics* **2007**, *3*, 13-17.
- (97) Gaspar, E. M.; Lucena, A. F.; Duro da Costa, J.; Chaves das Neves, H. *J. Chromatogr. A* **2009**, *1216*, 2749-2756.
- (98) Curran, A. M.; Ramirez, C. F.; Schoon, A. A.; Furton, K. G. *J. Chromatogr. B* **2007**, *846*, 86-97.
- (99) Buszewski, B.; Ulanowska, A.; Ligor, T.; Jackowski, M.; Kłodzińska, E.; Szeliga, J. *J. Chromatogr. B* **2008**, *868*, 88-94.
- (100) Chen, X.; Xu, F.; Wang, Y.; Pan, Y.; Lu, D.; Wang, P.; Ying, K.; Chen, E.; Zhang, W. *Cancer* **2007**, *110*, 835-844.
- (101) Yu, H.; Xu, L.; Wang, P. *J. Chromatogr. B* **2005**, *826*, 69-74.
- (102) Xue, R.; Dong, L.; Zhang, S.; Deng, C.; Liu, T.; Wang, J.; Shen, X. *Rapid Commun. Mass Spectrom.* **2008**, *22*, 1181-1186.
- (103) Halasz, A.; Hawari, J. *J. Chromatogr. Sci.* **2006**, *44*, 379-386.
- (104) Halasz, A.; Groom, C.; Zhou, E.; Paquet, L.; Beaulieu, C.; Deschamps, S.; Corriveau, A.; Thiboutot, S.; Ampleman, G.; Dubois, C.; Hawari, J. *J. Chromatogr. A* **2002**, *963*, 411-418.
- (105) Hawari, J.; Halasz, A.; Paquet, L.; Zhou, E.; Spencer, B.; Ampleman, G.; Thiboutot, S. *Appl. Environ. Microbiol.* **1998**, *64*, 2200-2206.
- (106) MacPherson, T.; Greer, C. W.; Zhou, E.; Jones, A. M.; Wisse, G.; Lau, P. C. K.; Sankey, B.; Grossman, M. J.; Hawari, J. *Env. Sci. Tech.* **1998**, *32*, 421-426.
- (107) Whyte, L. G.; Hawari, J.; Zhou, E.; Bourbonniere, L.; Inniss, W. E.; Greer, C. W. *Appl. Environ. Microbiol.* **1998**, *64*, 2578-2584.
- (108) Mirata, M. -.; Wüst, M.; Mosandl, A.; Schrader, J. *J. Agric. Food Chem.* **2008**, *56*, 3287-3296.
- (109) Mallouchos, A.; Komaitis, M.; Koutinas, A.; Kanellaki, M. *J. Agric. Food Chem.* **2002**, *50*, 3840-3848.



- (110) Demyttenaere, J. C. R.; Morriña, R. M.; De Kimpe, N.; Sandra, P. *J. Chromatogr. A* **2004**, *1027*, 147-154.
- (111) Witte, V.; Abrell, L.; Attygalle, A. B.; Wu, X.; Meinwald, J. *Chemoecology* **2007**, *17*, 63-69.
- (112) Augusto, F.; Luiz Pires Valente, A. *TrAC Trends Anal. Chem.* **2002**, *21*, 428-438.
- (113) Crewe, R. M.; Moritz, R. F. A.; Lattorff, M. G. *Chemoecology* **2004**, *14*, 77-79.
- (114) Prudic, K. L.; Khera, S.; Solyom, A.; Timmermann, B. N. *J. Chem. Ecol.* **2007**, *33*, 1149-1159.
- (115) Hurd, L. E.; Prete, F. R.; Jones, T. H.; Singh, T. B.; Co, J. E.; Portman, R. T. *J. Chem. Ecol.* **2004**, *30*, 155-166.
- (116) Tentschert, J.; Kolmer, K.; Holldobler, B.; Bestmann, H. -.; Delabie, J.; Heinze, J. *Naturwissenschaften* **2001**, *88*, 175-178.
- (117) Tentschert, J.; Bestmann, H. J.; Heinze, J. *Chemoecology* **2002**, *12*, 15-21.
- (118) Cai, L.; Koziel, J. A.; O'Neal, M. E. *J. Chromatogr. A* **2007**, *1147*, 66-78.
- (119) Monnin, T.; Malusse, C.; Peeters, C. *J. Chem. Ecol.* **1998**, *24*, 473-490.
- (120) Colazza, S.; Aquila, G.; De Pasquale, C.; Peri, E.; Millar, J. G. *J. Chem. Ecol.* **2007**, *33*, 1405-1420.
- (121) Stashenko, E. E.; Martínez, J. R. *J. Sep. Sci.* **2008**, *31*, 2022-2031.
- (122) Verdonk, J. C.; De Vos, C. H. R.; Verhoeven, H. A.; Haring, M. A.; Van Tunen, A. J.; Schuurink, R. C. *Phytochemistry* **2003**, *62*, 997-1008.
- (123) Beck, J. J.; Smith, L.; Merrill, G. B. *J. Agric. Food Chem.* **2008**, *56*, 2759-2764.
- (124) Wilson, I. D.; Plumb, R.; Granger, J.; Major, H.; Williams, R.; Lenz, E. M. *J. Chromatogr. B: Anal. Tech. Biomed. Life Sci.* **2005**, *817*, 67-76.
- (125) Murdoch, T. B.; Fu, H.; MacFarlane, S.; Sydora, B. C.; Fedorak, R. N.; Slupsky, C. M. *Anal. Chem.* **2008**, *80*, 5524-5531.
- (126) O'Reilly, J.; Wang, Q.; Setkova, L.; Hutchinson, J. P.; Chen, Y.; Lord, H. L.; Linton, C. N.; Pawliszyn, J. *J. Sep. Sci.* **2005**, *28*, 2010-2022.

- (127) Chen, J.; Pawliszyn, J. B. *Anal. Chem.* **1995**, *67*, 2530-2533.
- (128) Vuckovic, D.; Shirey, R.; Chen, Y.; Sidisky, L.; Aurand, C.; Stenerson, K.; Pawliszyn, J. *Anal. Chim. Acta* **2009**, *638*, 175-185.
- (129) Lord, H. L. *J. Chromatogr. A* **2007**, *1152*, 2-13.
- (130) Xie, W.; Pawliszyn, J.; Mullett, W. M.; Matuszewski, B. K. *J. Pharm. Biomed. Anal.* **2007**, *45*, 599-608.
- (131) Hutchinson, J. P.; Setkova, L.; Pawliszyn, J. *J. Chromatogr. A* **2007**, *1149*, 127-137.
- (132) Mullett, W. M.; Pawliszyn, J. *Anal. Chem.* **2002**, *74*, 1081-1087.
- (133) Lord, H. L.; Grant, R. P.; Walles, M.; Incledon, B.; Fahie, B.; Pawliszyn, J. B. *Anal. Chem.* **2003**, *75*, 5103-5115.
- (134) Cudjoe, E.; Vuckovic, D.; Hein, D.; Pawliszyn, J. *Anal. Chem.* **2009**, *81*, 4226-4232.
- (135) Wells, D. A. In *High Throughput Bioanalytical Sample Preparation: Methods and Automation Strategies*; Elsevier: UK, 2003; , pp 610.
- (136) Schubert, J. K.; Miekisch, W.; Fuchs, P.; Scherzer, N.; Lord, H.; Pawliszyn, J.; Mundkowsky, R. G. *Clin. Chim. Acta* **2007**, *386*, 57-62.
- (137) Musteata, M. L.; Musteata, F. M.; Pawliszyn, J. *Anal. Chem.* **2007**, *79*, 6903-6911.
- (138) Es-haghi, A.; Zhang, X.; Musteata, F. M.; Bagheri, H.; Pawliszyn, J. *Analyst* **2007**, *132*, 672-678.
- (139) Walles, M.; Mullett, W. M.; Pawliszyn, J. *J. Chromatogr. A* **2004**, *1025*, 85-92.
- (140) Wang, Y.; O'Reilly, J.; Chen, Y.; Pawliszyn, J. *J. Chromatogr. A* **2005**, *1072*, 13-17.
- (141) Zhou, S. N.; Zhang, X.; Ouyang, G.; Eshaghi, A.; Pawliszyn, J. *Anal. Chem.* **2007**, *79*, 1221-1230.
- (142) Food and Drug Administration, *Guidance for Industry* **2001**.
- (143) Matuszewski, B. K.; Constanzer, M. L.; Chavez-Eng, C. M. *Anal. Chem.* **1998**, *70*, 882-889.
- (144) Divoll, M.; Greenblatt, D. J. *Psychopharmacology (Berl.)* **1981**, *75*, 380-382.

- (145) Muchohi, S. N.; Obiero, K.; Newton, C. R. J. C.; Ogutu, B. R.; Edwards, G.; Kokwaro, G. O. *Br. J. Clin. Pharmacol.* **2008**, *65*, 12-21.
- (146) Bakhtiar, R.; Majumdar, T. K. *J. Pharmacol. Toxicol. Methods* **2007**, *55*, 227-243.
- (147) Analytical Methods Committee, Royal Society of Chemistry *AMC Technical Brief #6* **2001**.
- (148) Mullett, W. M.; Levsen, K.; Lubda, D.; Pawliszyn, J. *J. Chromatogr. A* **2002**, *963*, 325-334.
- (149) Yuan, H.; Mester, Z.; Lord, H.; Pawliszyn, J. *J. Anal. Toxicol.* **2000**, *24*, 718-725.
- (150) de Oliveira, M. H.; Queiroz, M. E. C.; Carvalho, D.; Silva, S. M.; Lancas, F. M. *Chromatographia* **2005**, *62*, 215-219.
- (151) Vuckovic, D.; Cudjoe, E.; Hein, D.; Pawliszyn, J. *Anal. Chem.* **2008**, *80*, 6870-6880.
- (152) Vatinno, R.; Vuckovic, D.; Zambonin, C. G.; Pawliszyn, J. *J. Chromatogr. A* **2008**, *1201*, 215-221.
- (153) Zambonin, C. G. *Anal. Bioanal. Chem.* **2003**, *375*, 73-80.
- (154) Musteata, F. M.; Pawliszyn, J. *TrAC Trends Anal. Chem.* **2007**, *26*, 36-45.
- (155) Shintani, Y.; Zhou, X.; Furuno, M.; Minakuchi, H.; Nakanishi, K. *J. Chromatogr. A* **2003**, *985*, 351-357.
- (156) Hou, J.; Ma, Q.; Du, X.; Deng, H.; Gao, J. *Talanta*, **2004**, *62*, 241-246.
- (157) Wen, Y.; Feng, Y. *J. Chromatogr. A*, **2007**, *1160*, 90-98.
- (158) Wen, Y.; Fan, Y.; Zhang, M.; Feng, Y. *Anal. Bioanal. Chem.* **2005**, *382*, 204-210.
- (159) Dietz, C.; Sanz, J.; Cámara, C. *J. Chromatogr. A* **2006**, *1103*, 183-192.
- (160) Wu, J.; Lord, H. L.; Pawliszyn, J.; Kataoka, H. *J. Microcolumn Sep.* **2000**, *12*, 255-266.
- (161) Wu, J.; Lord, H.; Pawliszyn, J. *Talanta* **2001**, *54*, 655-672.
- (162) Wu, J.; Pawliszyn, J. *Anal. Chim. Acta* **2004**, *520*, 257-264.

- (163) Jarmalaviciene, R.; Szumski, M.; Kornysova, O.; Klodzinska, E.; Westerlund, D.; Krawczyk, S.; Mickevicius, D.; Buszewski, B.; Maruska, A. *Electrophoresis* **2008**, *29*, 1753-1760.
- (164) Musteata, F. M.; Walles, M.; Pawliszyn, J. *Anal. Chim. Acta* **2005**, *537*, 231-237.
- (165) Syracuse Research Corporation *PhysProp Database* .
- (166) Jjemba, P. K. *Ecotoxicol. Environ. Saf.* **2006**, *63*, 113-130.
- (167) Box, K.; Bevan, C.; Comer, J.; Hill, A.; Allen, R.; Reynolds, D. *Anal. Chem.* **2003**, *75*, 883-892.
- (168) Volmer, D. A.; Hui, J. P. M. *Arch. Environ. Contam. Toxicol.* **1998**, *35*, 1-7.
- (169) Ingelse, B. A.; Vogel, G.; Botterblom, M.; Nanninga, D.; Ooms, B. *Rapid Comm. Mass Spectrom.* **2008**, *22*, 834-840.
- (170) Zhu, Y.; Chiang, H.; Wulster-Radcliffe, M.; Hilt, R.; Wong, P.; Kissinger, C. B.; Kissinger, P. T. *J. Pharm. Biomed. Anal.* **2005**, *38*, 119-125.
- (171) Peng, S. X.; Rockafellow, B. A.; Skedzielewski, T. M.; Huebert, N. D.; Hageman, W. *J. Pharm. Sci.* **2009**, *98*, 1877-1884.
- (172) Chen, J.; Hsieh, Y.; Cook, J.; Morrison, R.; Korfmacher, W. A. *Anal. Chem.* **2006**, *78*, 1212-1217.
- (173) Bateman, K. P.; Castonguay, G.; Xu, L.; Rowland, S.; Nicoll-Griffith, D. A.; Kelly, N.; Chan, C. -. *J. Chromatogr. B: Biomed. Sci. App.* **2001**, *754*, 245-251.
- (174) Bundgaard, C.; Jørgensen, M.; Mørk, A. *J. Pharmacol. Toxicol. Methods* **2007**, *55*, 214-223.
- (175) Balani, S. K.; Li, P.; Nguyen, J.; Cardoza, K.; Zeng, H.; Mu, D. -.; Wu, J. -.; Gan, L. -.; Lee, F. W. *Drug Metab. Dispos.* **2004**, *32*, 1092-1095.
- (176) Long, J. M.; James, C. A.; Clark, B. J.; Castelli, M. G.; Rolando, S. *Chromatographia* , *55*, S31-S34.
- (177) Lord, H. L.; Mundkowski, R.; Miekisch, W.; Schubert, J.; Pawliszyn, J. *HTC-9, Ninth International Symposium on Hyphenated Techniques in Chromatography* **2006**, P110.

- (178) Nakajima, D.; Tin-Tin-Win-Shwe; Kakeyama, M.; Fujimaki, H.; Goto, S. *Neurotoxicol.* **2006**, *27*, 615-618.
- (179) Win-Shwe, T. -.; Mitsushima, D.; Nakajima, D.; Ahmed, S.; Yamamoto, S.; Tsukahara, S.; Kakeyama, M.; Goto, S.; Fujimaki, H. *Toxicol. Lett.* **2007**, *168*, 75-82.
- (180) Zhou, S. N.; Oakes, K. D.; Servos, M. R.; Pawliszyn, J. *Environ. Sci. Technol.* **2008**, *42*, 6073-6079.
- (181) Zhang, X.; Cai, J.; Oakes, K. D.; Breton, F.; Servos, M. R.; Pawliszyn, J. *Anal. Chem.* **2009**, *81*, 7349-7356.
- (182) Zhou, S. N.; Ouyang, G.; Pawliszyn, J. *J. Chromatogr. A* **2008**, *1196-1197*, 46-56.
- (183) Dasgupta, A. *Clin. Chim. Acta* **2007**, *377*, 1-13.
- (184) Dasgupta, A. *Clin. Chem. Lab. Med.* **2002**, *40*, 986-993.
- (185) Potter, J. M.; Donnelly, A. *Ther. Drug Monit.* **1998**, *20*, 652-657.
- (186) Bonneton, J.; Genton, P.; Mesdjian, E. *Biopharm. Drug Dispos.* **1992**, *13*, 411-416.
- (187) Remmel, R. P.; Sinz, M. W.; Cloyd, J. C. *Pharm. Res.* **1990**, *7*, 513-517.
- (188) Vuckovic, D.; Gien, B.; de Lannoy, I.; Musteata, F. M.; Shirey, R.; Sidisky, L.; Pawliszyn, J. *manuscript submitted* **2010**.
- (189) Wishart, D. S.; Knox, C.; Guo, A. C.; Cheng, D.; Shrivastava, S.; Tzur, D.; Gautam, B.; Hassanali, M. *Nucleic Acids Res.* **2008**, *36(Database issue)*; D901-D906.
- (190) Wishart, D. S.; Knox, C.; Guo, A. C.; Shrivastava, S.; Hassanali, M.; Stothard, P.; Chang, Z.; Woolsey, J. *Nucleic Acids Res.* **2006**, *34(Database issue)*, D668-D672.
- (191) Kodama, Y.; Kuranari, M.; Kodama, H.; Fujii, I.; Takeyama, M. *J. Clin. Pharmacol.* **1993**, *33*, 851-855.
- (192) Watanabe, T.; Schulz, D.; Morisseau, C.; Hammock, B. D. *Anal. Chim. Acta*, **2006**, *559*, 37-44.
- (193) Vuckovic, D.; de Lannoy, I.; Gien, B.; Shirey, R. E.; Sidisky, L. M.; Dutta, S.; Pawliszyn, J. *manuscript submitted* **2010**.
- (194) Tolonen, A.; Turpeinen, M.; Pelkonen, O. *Drug Discovery Today* **2009**, *14*, 120-133.

- (195) Fontanals, N.; Marcé, R. M.; Borrull, F. *J. Chromatogr. A* **2007**, *1152*, 14-31.
- (196) Fontanals, N.; Marcé, R. M.; Borrull, F. *TrAC Trends Anal. Chem.* **2005**, *24*, 394-406.
- (197) Majors, R. E. *LC-GC North America* **2008**, *26*, 1074-1090.
- (198) Coen, M.; Want, E. J.; Clayton, T. A.; Rhode, C. M.; Young, S. H.; Keun, H. C.; Cantor, G. H.; Metz, A. L.; Robertson, D. G.; Reily, M. D.; Holmes, E.; Lindon, J. C.; Nicholson, J. K. *J. Proteome Res.* **2009**, *8*, 5175-5187.
- (199) Koulman, A.; Woffendin, G.; Narayana, V. K.; Welchman, H.; Crone, C.; Volmer, D. A. *Rapid Commun. Mass Spectrom.* **2009**, *23*, 1411-1418.
- (200) Llorach, R.; Urpi-Sarda, M.; Jauregui, O.; Monagas, M.; Andres-Lacueva, C. *J. Proteome Res.* **2009**, *8*, 5060-5068.
- (201) Chen, C.; Krausz, K. W.; Shah, Y. M.; Idle, J. R.; Gonzalez, F. J. *Chem. Res. Toxicol.* **2009**, *22*, 699-707.
- (202) Liu, A.; Chen, Y.; Yang, Z.; Feng, Y.; Rui, W.; Luo, W.; Liu, Y.; Gonzalez, F. J.; Dai, R. *Xenobiotica* **2009**, *39*, 345-354.
- (203) Burton, L.; Ivosev, G.; Tate, S.; Impey, G.; Wingate, J.; Bonner, R. *J. Chromatogr. B: Anal. Tech. Biomed. Life Sci.* **2008**, *871*, 227-235.
- (204) Xie, G.; Zheng, X.; Qi, X.; Cao, Y.; Chi, Y.; Su, M.; Ni, Y.; Qiu, Y.; Liu, Y.; Li, H.; Zhao, A.; Jia, W. *J. Proteome Res.* **2009**.
- (205) Evans, A. M.; DeHaven, C. D.; Barrett, T.; Mitchell, M.; Milgram, E. *Anal. Chem.* **2009**, *81*, 6656-6667.
- (206) Qiu, Y.; Cai, G.; Su, M.; Chen, T.; Zheng, X.; Xu, Y.; Ni, Y.; Zhao, A.; Xu, L. X.; Cai, S.; Jia, W. *J. Proteome Res.* **2009**, *8*, 4844-4850.
- (207) Patterson, A. D.; Slanar, O.; Krausz, K. W.; Li, F.; Hofer, C. C.; Perlík, F.; Gonzalez, F. J.; Idle, J. R. *J. Proteome Res.* **2009**, *8*, 4293-4300.
- (208) Gika, H. G.; Macpherson, E.; Theodoridis, G. A.; Wilson, I. D. *J. Chromatogr. B* **2008**, *871*, 299-305.
- (209) Plumb, R. S.; Stumpf, C. L.; Gorenstein, M. V.; Castro-Perez, J. M.; Dear, G. J.; Anthony, M.; Sweatman, B. C.; Connor, S. C.; Haselden, J. N. *Rapid Commun. Mass Spectrom.* **2002**, *16*, 1991-1996.

- (210) Plumb, R. S.; Stumpf, C. L.; Granger, J. H.; Castro-Perez, J.; Haselden, J. N.; Dear, G. *J. Rapid Commun. Mass Spectrom.* **2003**, *17*, 2632-2638.
- (211) Bruce, S. J.; Jonsson, P.; Antti, H.; Cloarec, O.; Trygg, J.; Marklund, S. L.; Moritz, T. *Anal. Biochem.* **2008**, *372*, 237-249.
- (212) Gu, L.; Jones, A. D.; Last, R. L. *Anal. Chem.* **2007**, *79*, 8067-8075.
- (213) Gika, H. G.; Theodoridis, G. A.; Wilson, I. D. *J. Sep. Sci.* **2008**, *31*, 1598-1608.
- (214) Chen, J.; Wang, W.; Lv, S.; Yin, P.; Zhao, X.; Lu, X.; Zhang, F.; Xu, G. *Anal. Chim. Acta* **2009**, *650*, 3-9.
- (215) Mohamed, R.; Varesio, E.; Ivosev, G.; Burton, L.; Bonner, R.; Hopfgartner, G. *Anal. Chem.* **2009**, *81*, 7677-7694.
- (216) Kamleh, A.; Barrett, M. P.; Wildridge, D.; Burchmore, R. J. S.; Scheltema, R. A.; Watson, D. G. *Rapid Commun. Mass Spectrom.* **2008**, *22*, 1912-1918.
- (217) Jankevics, A.; Liepinsh, E.; Liepinsh, E.; Vilskersts, R.; Grinberga, S.; Pugovics, O.; Dambrova, M. *Chemometrics Intellig. Lab. Syst.* **2009**, *97*, 11-17.
- (218) Callahan, D. L.; De Souza, D.; Bacic, A.; Roessner, U. *J. Sep. Sci.* **2009**, *32*, 2273-2280.
- (219) Yoshida, H.; Yamazaki, J.; Ozawa, S.; Mizukoshi, T.; Miyano, H. *J. Agric. Food Chem.* **2009**, *57*, 1119-1126.
- (220) Weigel, S.; Kallenborn, R.; Hühnerfuss, H. *J. Chromatogr. A* **2004**, *1023*, 183-195.
- (221) Tuytten, R.; Lemiere, F.; VanDongen, W.; Witters, E.; Esmans, E. L.; Newton, R. P.; Dudley, E. *Anal. Chem.* **2008**, *80*, 1263-1271.
- (222) Bajad, S. U.; Lu, W.; Kimball, E. H.; Yuan, J.; Peterson, C.; Rabinowitz, J. D. *J. Chromatogr. A* **2006**, *1125*, 76-88.
- (223) Yin, P.; Zhao, X.; Li, Q.; Wang, J.; Li, J.; Xu, G. *J. Proteome Res.* **2006**, *5*, 2135-2143.
- (224) Dunn, W. B.; Broadhurst, D.; Brown, M.; Baker, P. N.; Redman, C. W. G.; Kenny, L. C.; Kell, D. B. *J. Chromatogr. B*, **2008**, *871*, 288-298.
- (225) Bateman, K. P.; Kellmann, M.; Muenster, H.; Papp, R.; Taylor, L. *J. Am. Soc. Mass Spectrom.* **2009**, *20*, 1441-1450.

- (226) Hu, Q.; Noll, R. J.; Li, H.; Makarov, A.; Hardman, M.; Cooks, R. G. *J. Mass Spectrom.* **2005**, *40*, 430-443.
- (227) Krauss, M.; Hollender, J. *Anal. Chem.* **2008**, *80*, 834-842.
- (228) Nordstrom, A.; Want, E.; Northen, T.; Lehtio, J.; Siuzdak, G. *Anal. Chem.* **2008**, *80*, 421-429.
- (229) Lanina, S. A.; Toledo, P.; Sampels, S.; Kamal-Eldin, A.; Jastrebova, J. A. *J. Chromatogr. A* **2007**, *1157*, 159-170.
- (230) Scheltema, R. A.; Kamleh, A.; Wildridge, D.; Ebikeme, C.; Watson, D. G.; Barrett, M. P.; Jansen, R. C.; Breitling, R. *Proteomics* **2008**, *8*, 4647-4656.
- (231) Flores-Valverde, A. M.; Hill, E. M. *Anal. Chem.* **2008**, *80*, 8771-8779.
- (232) Bottcher, C.; Roepenack-Lahaye, E.; Willscher, E.; Scheel, D.; Clemens, S. *Anal. Chem.* **2007**, *79*, 1507-1513.
- (233) Polson, C.; Sarkar, P.; Incedon, B.; Raguvaran, V.; Grant, R. *J. Chromatogr. B: Anal. Tech. Biomed. Life Sci.* **2003**, *785*, 263-275.
- (234) Want, E. J.; O'Maille, G.; Smith, C. A.; Brandon, T. R.; Uritboonthai, W.; Qin, C.; Trauger, S. A.; Siuzdak, G. *Anal. Chem.* **2006**, *78*, 743-752.
- (235) Tiziani, S.; Emwas, A. -.; Lodi, A.; Ludwig, C.; Bunce, C. M.; Viant, M. R.; Günther, U. L. *Anal. Biochem.* **2008**, *377*, 16-23.
- (236) Want, E. J.; Nordström, A.; Morita, H.; Siuzdak, G. *J. Proteome Res.* **2007**, *6*, 459-468.
- (237) Gao, P.; Lu, C.; Zhang, F.; Sang, P.; Yang, D.; Li, X.; Kong, H.; Yin, P.; Tian, J.; Lu, X.; Lu, A.; Xu, G. *Analyst* **2008**, *133*, 1214-1220.
- (238) Lee, R.; Britz-McKibbin, P. *Anal. Chem.* **2009**, *81*, 7047-7056.
- (239) Sangster, T.; Major, H.; Plumb, R.; Wilson, A. J.; Wilson, I. D. *Analyst* **2006**, *131*, 1075-1078.
- (240) Van Der Kloet, F. M.; Bobeldijk, I.; Verheij, E. R.; Jellema, R. H. *J. Proteome Res.* **2009**, *8*, 5132-5141.
- (241) Katajamaa, M.; Oresic, M. *J. Chromatogr. A* **2007**, *1158*, 318-328.



- (242) van den Berg, R. A.; Hoefsloot, H. C. J.; Westerhuis, J. A.; Smilde, A. K.; van der Werf, M. J. *BMC Genomics* **2006**, *7*.
- (243) Wishart, D. S.; Knox, C.; Guo, A. C.; Eisner, R.; Young, N.; Gautam, B.; Hau, D. D.; Psychogios, N.; Dong, E.; Bouatra, S.; Mandal, R.; Sinelnikov, I.; Xia, J.; Jia, L.; Cruz, J. A.; Lim, E.; Sobsey, C. A.; Shrivastava, S.; Huang, P.; Liu, P.; Fang, L.; Peng, J.; Fradette, R.; Cheng, D.; Tzur, D.; Clements, M.; Lewis, A.; de Souza, A.; Zuniga, A.; Dawe, M.; Xiong, Y.; Clive, D.; Greiner, R.; Nazyrova, A.; Shaykhtudinov, R.; Li, L.; Vogel, H. J.; Forsythe, I. *Nucleic Acids Res.* **2009**, *37*, D603-D610.
- (244) Wishart, D. S.; Tzur, D.; Knox, C.; Eisner, R.; Guo, A. C.; Young, N.; Cheng, D.; Jewell, K.; Arndt, D.; Sawhney, S.; Fung, C.; Nikolai, L.; Lewis, M.; Coutouly, M. -.; Forsythe, I.; Tang, P.; Shrivastava, S.; Jeroncic, K.; Stothard, P.; Amegbey, G.; Block, D.; Hau, D. D.; Wagner, J.; Miniaci, J.; Clements, M.; Gebremedhin, M.; Guo, N.; Zhang, Y.; Duggan, G. E.; MacInnis, G. D.; Weljie, A. M.; Dowlatabadi, R.; Bamforth, F.; Clive, D.; Greiner, R.; Li, L.; Marrie, T.; Sykes, B. D.; Vogel, H. J.; Querengesser, L. *Nucleic Acids Res.* **2007**, *35*.
- (245) Human Metabolome Database, Version 2.5. [www.hmdb.ca](http://www.hmdb.ca) (accessed Nov 29, 2009).
- (246) Miao, X.; Metcalfe, C. D. *Anal. Chem.* **2003**, *75*, 3731-3738.
- (247) Dougalis, A.; Lees, G.; Ganellin, C. R. *Neuropharmacology* **2004**, *46*, 541-554.
- (248) Bazinet, R. P. *Biochem. Soc. Trans.* **2009**, *37*, 1104-1109.
- (249) Zhang, X.; Cai, J.; Oakes, K. D.; Breton, F.; Servos, M. R.; Pawliszyn, J. *Anal. Chem.* **2009**, *81*, 7349-7356.
- (250) Ma, S.; Chowdhury, S. K.; Alton, K. B. *Curr. Drug. Metab.* **2006**, *7*, 503-523.